bulletin 10

fib
CEB-FIP

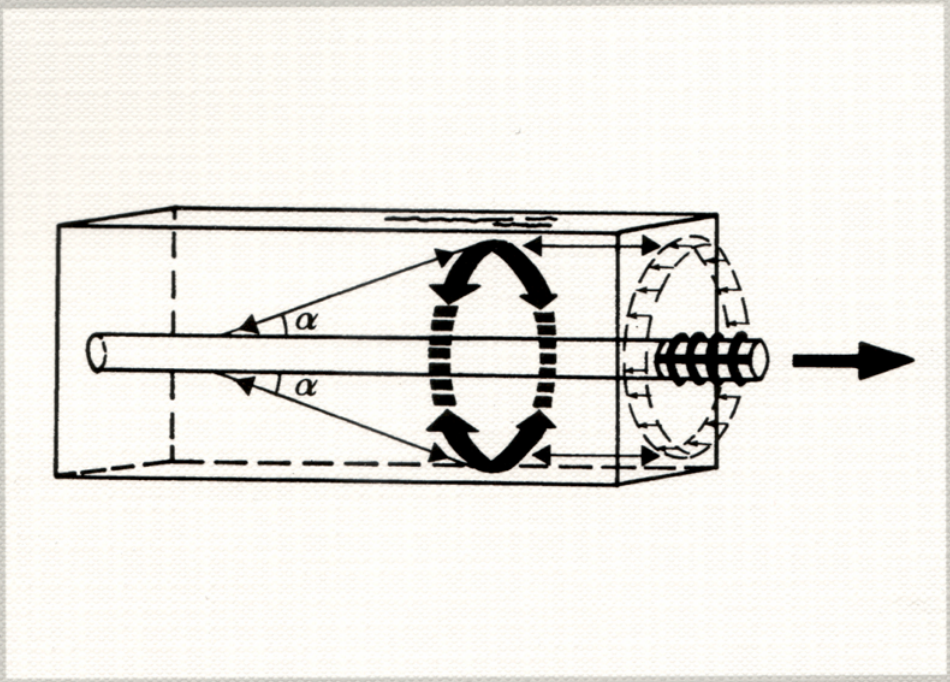

Bond of reinforcement in concrete

state-of-art report

Bond of reinforcement in concrete

State-of-art report prepared by

Task Group *Bond Models*

(former CEB Task Group 2.5)

August 2000

Subject to priorities defined by the Steering Committee and the Praesidium, the results of *fib*'s work in Commissions and Task Groups are published in a continuously numbered series of technical publications called 'Bulletins'. The following categories are used:

category	minimum approval procedure required prior to publication
Technical Report	approved by a Task Group and the Chairpersons of the Commission
State-of-Art report	approved by a Commission
Manual or Guide (to good practice)	approved by the Steering Committee of *fib* or its Publication Board
Recommendation	approved by the Council of *fib*
Model Code	approved by the General Assembly of *fib*

Any publication not having met the above requirements will be clearly identified as preliminary draft.

The work for this report having been started in former CEB (see preface), after the 1998 merger of CEB and FIP into *fib*, this state-of-art report was assessed and approved by experts chosen by the *fib* Steering Committee and is now published in the *fib* series of bulletins.

Members of the Task Group:

Ralejs Tepfers[⑦⑧] (Göteborg, Sweden, convener of Task Group), **Zenon Achillides** (Sheffield, UK), **Atorod Azizinamini**[②③] (Lincoln, Nebraska, USA), **György Balázs**[①③⑥] (Budapest, Hungary), **Agniezka Bigaj-van Vliet**[①②] (Stuttgart, Germany), **Joe Cabrera** (Leeds, UK), **John Cairns**[①④⑤⑧] (Edinburgh, UK), **Edoardo Cosenza**[⑦] (Naples, Italy), **Joop den Uijl**[②⑥⑧] (Delft, The Netherlands), **Rolf Eligehausen**[①②③] (Stuttgart, Germany), **Björn Engström**[①②⑥] (Göteborg, Sweden), **Lászlo Erdélyi** (Budapest, Hungary), **Pietro Gambarova**[①②] (Milano, Italy), **James Jirsa**[⑤] (Austin, Texas, USA), **Susan Lane** (McLean, Virginia, USA), **Roberto Leon**[①③] (Atlanta, Georgia, USA), **Jonas Magnusson**[②] (Göteborg, Sweden), **Utz Mayer**[①⑨] (Stuttgart, Germany), **Steven McCabe**[①⑤⑧] (Lawrence, Kansas, USA), **Claudio Modena** (Padova, Italy), **Janis Modniks**[⑦] (Riga, Latvia), **Toby J. Mottram** (Coventry, UK), **Keivan Noghabai**[①②④] (Luleå, Sweden), **Koji Otsuka**[⑥] (Sendai, Japan), **Josko Ozbolt**[③] (Stuttgart, Germany), **Stavrola J. Pantazopoulou**[④⑦⑧] (Xanthi, Greece), **Kypros Pilakoutas**[⑦] (Sheffield, UK), **Giovanni Plizzari**[①②] (Brescia, Italy), **Roberto Realfonzo**[⑦] (Naples, Italy), **Jesús Rodriguez**[④] (Madrid, Spain), **Gian Paolo Rosati**[①] (Milano, Italy), **Gaetano Russo**[①] (Udine, Italy), **Salvatore Russo** (Venice, Italy), **Hiroshi Shima**[①⑦] (Kochi, Japan), **Christiano Schumm†** (Milano, Italy), **Luc Taerwe**[⑦] (Ghent, Belgium), **Vitauts Tamuzs**[⑦] (Riga, Latvia), **Tamon Ueda**[①⑦] (Sapporo, Japan), **Lucie Vandewalle**[①⑥] (Heverlee, Belgium), **Elisabeth Vintzileou**[③] (Athens, Greece)

[①②③④⑤⑥⑦⑧]: Chapter number for which this Member was actively involved in the drafting Working Party.
Full affiliation details of Commission members may be found in the *fib* Directory.

Cover figure: Schematic representation of radial components of bond forces balanced by tensile stress rings in the concrete anchorage zone (Tepfers 1973)

© fédération internationale du béton (*fib*), 2000
Although the International Federation for Structural Concrete *fib* - fédération internationale du béton - created from CEB and FIP, does its best to ensure that any information given is accurate, no liability or responsibility of any kind (including liability for negligence) is accepted in this respect by the organisation, its members, servants or agents.
All rights reserved. No part of this publication may be reproduced, stored in a retrieval system, or transmitted in any form or by any means, electronic, mechanical, photocopying, recording, or otherwise, without prior written permission.

First published 2000 by the International Federation for Structural Concrete (*fib*)
Post address: Case Postale 88, CH-1015 Lausanne, Switzerland
Street address: Federal Institute of Technology Lausanne - EPFL, Département Génie Civil
Tel (+41.21) 693 2747, Fax (+41.21) 693 5884, E-mail fib@epfl.ch

ISSN 1562-3610
ISBN 2-88394-050-9

Printed by Sprint-Druck Stuttgart

Copyright fib, all rights reserved. This PDF copy of fib Bulletin 10 is intended for use and/or distribution only by National Member Groups of fib.

Preface

In 1993, the CEB Commission 2 *Material and Behavior Modeling* established the Task Group 2.5 *Bond Models*.

Its terms of reference were as follows: To write a state-of-art report concerning bond of reinforcement in concrete and later recommend how the knowledge could be applied in practice (Model Code like text proposal). This Bulletin 10 covers the first part of this work, the state-of-art report.

After the work with the bond clauses in CEB-FIP Model Code 1990 was finished, the former CEB Task Group VI/I "Anchorage Zones" arranged a conference "Bond in Concrete - from Research to Practice" in Riga, October 1992. From the contributions in the three volumes of proceedings it became evident that bond research had become extensive with wide spread directions. It was no longer possible that a few experienced researchers could cover the complete field of bond in a satisfactory way. So it was concluded that a new Task Group had to engage more researchers and especially young ones with fresh approaches and ideas. The development of the internet made it possible to start the work in a new way with fast electronic communication between the Task Group members. As the mailing and copying costs could be kept down, it was now possible to attach to the network all persons interested in the work. Especially young researchers were included in the network, and fresh ideas were brought to the *fib* community, formerly CEB, which is very important for the future of the international work on development of application of concrete in structures.

The use of the internet as communication base gave many advantages but also created some problems. These are related to the use and compatibility of different word processing software. Further there was a need for a rigorous discipline concerning the order of the manuscripts with successive improvements so that a mix up and parallel versions were avoided. A very important step forward was the setting up of a home page, thanks to the kindness of Sheffield University and support from EU TMR network ConFibreCrete. Here all document drafts were stored chronologically. However, this new system of working still needs to be developed further.

The work had to be started with updating the knowledge in form of a state-of -art report. As the theme now was very wide the work was organized in Working Parties (WP), every party having a convener responsible for one chapter of the state-of -art report.

The different fields of bond research are presented in the chapters of this report as follows:

Chapter 1 (WP 1, convenor Pietro Gambarova, Milano, Italy)
Bond mechanics including pull-out and splitting failures. The bond models are presented and compared, because they form the base for a possible new computerised code of practice.

Chapter 2 (WP 2, convener Björn Engström, Göteborg, Sweden)
Anchorage and bond in high strength concrete. Concretes have to day strengths far beyond C80, which is the strongest concrete mentioned in Model Code 90. The bond performance of reinforcement in HSC is more brittle and different from that in NSC.

Chapter 3 (WP 3, convener György Balázs, Budapest, Hungary)
Bond under repeated loading. The knowledge of bond under repeated loads is dispersed and had to be brought together to become an efficient source for code of practice development.

Copyright fib, all rights reserved. This PDF copy of fib Bulletin 10 is intended for use and/or distribution only by National Member Groups of fib.

Chapter 4 (WP 4, convener John Cairns, Edinburgh, UK)
Bond of corroded reinforcement. To be able to judge the durability of bond resistance of reinforcement, which has started to corrode, a condensation of knowledge in this field is important.

Chapter 5 (WP 5, convener John Cairns, Edinburgh, UK)
Bond of fusion bonded epoxy coated reinforcement. The knowledge of bond of epoxy coated bars has to be made covering and consistent to be correctly interpreted for use as firm base for codes in practice.

Chapter 6 (WP 6, convener Joop den Uijl, Delft, The Netherlands)
Bond of prestressing tendons. There is a development going on with thicker and stronger strands used for prestressing. Also deeper knowledge has been produced. All this has to be gathered for conclusions for an improved Code of Practice.

Chapter 7 (WP 7, convener Ralejs Tepfers, Göteborg, Sweden)
Bond of non-metallic reinforcement. New reinforcing materials for concrete with continuous carbon, aramid and glass fibers, FRP (Fiber Reinforced Polymers), have been developed. Wrapping techniques and external reinforcements have come into use. The bond problems of the new fiber composite reinforcement (FRP) are treated in order to provide a base for a new code of practice. Collaboration exists with ***fib*** TG 9.3 *FRP (Fiber Reinforced Polymer) Reinforcement for Concrete structures*. The EU TMR ConFibreCrete network also contributed to this chapter.

Chapter 8 (WP 8, convener Steven McCabe, Lawrence, Kansas, USA)
Innovative developments in the light of bond philosophy. This chapter aims to pull together the past and the future. It has turned out that students of today have little knowledge about the earlier developments. This because the older information is not always available in the computerised information bases of the libraries where search is done. It is important to know that the understanding of bond problems has grown gradually and is rather old and should not be lost and research done again. The necessary knowledge for the codes was produced with and for the existing materials and design techniques and thus may not be applicable to new materials. Further out-look is given for possible developments concerning bond.

The work of the Task Group *Bond Models* should continue with the development of recommendations for inclusion in Codes of Practice. All persons having participated in the preparation of this state-of-art report are mentioned on the copyright page. Those participating in the work actively have their names mentioned in front of the relevant chapter in this state-of-art report. To all members of the Task Group my sincere thanks are expressed for the extensive, intense and qualified work brought in on a free and voluntary basis.

Göteborg, in March 2000

Ralejs Tepfers
Convener of ***fib*** Task Group *Bond Models*

Copyright fib, all rights reserved. This PDF copy of fib Bulletin 10 is intended for use and/or distribution only by National Member Groups of fib.

CONTENTS

1 Bond mechanics including pull-out and splitting failures **1**

1.1 Introduction 3
1.2 Bond modeling for macroscopically uncracked concrete 31
1.3 Bond modeling for transversely-cracked concrete 45
1.4 Concrete splitting in bond modeling 55
1.5 Discrete models in bond analysis 74
1.6 Concluding remarks 87
References 89
Notation 97

2 Anchorage and bond in high strength concrete **99**

2.1 General considerations 100
2.2 Local bond behaviour 105
2.3 Behaviour and design of anchorage regions 122
2.4 Reinforced concrete ties 147
2.5 References 150
Notations 155

3 Bond under repeated loading **157**

3.1 Introduction 158
3.2 General 158
3.3 Cyclic bond behaviour 160
3.4 Reversed cyclic bond behaviour 167
3.5 Concrete under repeated loading 172
3.6 Numerical analysis of bond under repeated loading 175
3.7 Conclusions 180
3.8 References 183

4 Bond of corroded reinforcement **187**

4.1 Introduction 188
4.2 Corrosion of reinforcement 188
4.3 Review of test data on bond of corroded reinforcement 190
4.4 Analytical modeling of effects of corrosion 200
4.5 Conclusions 211
4.6 References 212

Copyright fib, all rights reserved. This PDF copy of fib Bulletin 10 is intended for use and/or distribution only by National Member Groups of fib.

5 Bond of fusion bonded epoxy-coated reinforcement **217**

5.1 Background to fusion bonded epoxy coated reinforcement (FBECR) 219
5.2 The importance of bond to structural performance 222
5.3 Review of parameters influencing anchorage performance of FBECR 224
5.4 Analytical models for bond strength of FBECR 230
5.5 Influence of FBECR on tension stiffening, deflection and cracking 231
5.6 Review of existing code rules for design with FBECR 235
5.7 Derivation of proposed additions to MC 90 for epoxy coated reinforcement 236
5.8 References 243

6 Bond of prestressing tendons **269**

6.1 Introduction 270
6.2 Bond mechanism 272
6.3 Modeling 275
6.4 Prestress transfer and anchorage of plain seven-wire strand 285
6.5 Prestress transfer and anchorage of wire and strand with increased surface roughness 296
6.6 Prestress transfer and anchorage of epoxy coated strand 298
6.7 Design rules for transmission length and anchorage length 303
6.8 Summary and conclusions 309
6.9 Notations 310
6.10 References 311

7 Bond of non-metallic reinforcement **315**

7.1 Characteristics of materials 317
7.2 Bond and anchorage of FRP reinforcing materials 322
7.3 Local bond stress-slip relationship 337
7.4 Anchorage of continuous fibre tendons for prestressing 359
7.5 Joints 363
7.6 Bond of continuous fibre sheets and plates 366
7.7 Conclusions 380
7.8 Design rules 381
7.9 References 387

8 Innovative developments in the light of bond philosophy **395**

8.1 Introduction 396
8.2 History of developments in bond 396
8.3 Codes: Where do we stand? 405
8.4 Lessons from and benefits of bond research 410
8.5 Current needs and future directions 419
8.6 References 422

Copyright fib, all rights reserved. This PDF copy of fib Bulletin 10 is intended for use and/or distribution only by National Member Groups of fib.

1 Bond mechanics including pull-out and splitting failures

Working Party 1:

Pietro Gambarova[①] (Convener, Milan University of Technology, Italy), **György Balázs**[②] (Technical University of Budapest, Hungary), **Agniezka Bigaj-van Vliet** (University of Stuttgart, Germany), **John Cairns**[②] (Heriot Watt University, Edinburgh, UK), **Rolf Eligehausen**[②] (University of Stuttgart, Germany), **Björn Engström**[②] (Chalmers University of Technology, Göteborg, Sweden), **Enzo Giuriani** (University of Brescia, Italy), **Roberto Leon** (Georgia Institute of Technology, Atlanta, USA), **Utz Mayer** (University of Stuttgart, Germany), **Steven McCabe** (University of Kansas, Lawrence, USA), **Keivan Noghabai** (Luleå University of Technology, Sweden), **Giovanni Plizzari**[①] (University of Brescia, Italy), **Gian Paolo Rosati**[①] (Milan University of Technology, Italy), **Gaetano Russo**[①] (University of Udine, Italy), **Hiroshi Shima** (Kochi University of Technology, Japan), **Tamon Ueda** (Hokkaido University, Sapporo, Japan), **Lucie Vandewalle** (Katholieke Universiteit Leuven, Heverlee, Belgium)

[①] principal author, [②] main contributing author

1.1 Introduction **3**
1.1.1 Bar-concrete interaction 3
1.1.2 Different factors influencing bond performances 7
1.1.2.1 Geometry and stress level of the reinforcing unit 7
1.1.2.2 Concrete quality and state of stress 9
1.1.2.3 Technological aspects and environmental effects 9
1.1.2.4 Load time-history 12
1.1.3 Influence of bond on structural behavior (ductility) 15
1.1.4 Pull-out and splitting failures 17
1.1.5 Active and passive confinement 18
1.1.6 Anchored bars and pretensioned tendons 19
1.1.7 Testing 19
1.1.7.1 Short specimens 21
1.1.7.2 Long specimens 27
1.1.8 Modeling 27

1.2 Bond modeling for macroscopically uncracked concrete **31**
1.2.1 Elastic models with nonlinear interface 34
1.2.2 Inelastic models with nonlinear interface 38

1.3 Bond modeling for transversely-cracked concrete **45**
1.3.1 Transient cracking 48
1.3.2 Stabilized cracking 50
1.3.3 Tension-stiffening 50

1.4 Concrete splitting in bond modeling **55**
1.4.1 Overview on partial and through splitting 55
1.4.2 Local bond-stress relationships 56
1.4.3 Models based on transverse reinforcement and concrete confining effects 58
1.4.4 Anchorage capacity after cover splitting 63
1.4.5 Splitting crack control 64
1.4.6 Hydraulic-pressure analogy 65
1.4.6.1 Nature of problem and previous literature 65

Copyright fib, all rights reserved. This PDF copy of fib Bulletin 10 is intended for use and/or distribution only by National Member Groups of fib.

1.4.6.2 Elastic-cracked model 66
1.4.6.3 Elastic-cohesive model 67
1.4.6.4 Elastic-plastic-cohesive model 69
1.4.6.5 Applications 70
1.4.6.6 Concluding remarks 73

1.5 Discrete models in bond analysis 74
1.5.1 Layer models 74
1.5.2 Fracture mechanics models 77
1.5.3 Dedicated finite elements 78
1.5.4 Damage mechanics models 80
1.5.5 Distributed/discrete-crack FE models 81
1.5.6 Micromechanics-based FE models 82
1.5.7 Element-embedded crack model - Inner Softening Band 83
1.5.8 Structural models 85

1.6 Concluding remarks 87

References 89

Notations 97

Copyright fib, all rights reserved. This PDF copy of fib Bulletin 10 is intended for use and/or distribution only by National Member Groups of fib.

1 Bond mechanics including pull-out and splitting failures

1.1 Introduction

1.1.1 Bar-concrete interaction

Steel-to-concrete bond is the many-faceted phenomenon which allows longitudinal forces to be transferred from the reinforcement to the surrounding concrete in a R/C or P/C structure. Due to this force transfer, the force in a reinforcing bar changes along its length, as does the force in the concrete embedment. Wherever steel strains differ from concrete strains, a relative displacement between the steel and the concrete (slip) does occur, but this lack of compliance is also the effect of the highly-localized strains in the concrete layer closest to the reinforcement (interface).

The resistant mechanisms upon which the steel-to-concrete bond is based are already well known, due to the many test results that have been gathered and analysed in the last thirty years by resorting to a variety of specimens and techniques. Because of the extension of bond-related literature, in the following reference is made mainly to the papers and reports published since the late Seventies and early Eighties, while the previous research activity is summarized in Section 8.2. Useful information can be found also in the literature review by Tassios, 1979, in the Proceedings "Bond in Concrete" (Bartos, 1982), and in CEB Bulletin No. 151, 1982.

The scientists who have contributed to the knowledge of the many aspects of bonding agree that the interaction between the concrete and a bar subjected to a pull-out force is characterized by four different stages (Fig. 1.1.1a):

Stage I (uncracked concrete): for low bond-stress values, $\tau \leq \tau_I = (0.2\text{-}0.8)\ f_{ct}$, bond efficiency is assured mostly by chemical adhesion, and no bar slip occurs, but highly localized stresses arise close to lug tips (Fig. 1.1.2a, elastic behavior). Chemical adhesion is also accompanied by the micromechanical interaction associated with the microscopically rough steel surface, but on the whole chemical and physical adhesion plays a minor role, as confirmed by the low bond performances of plain bars, where chemical adhesion and microinterlocking are soon followed by the sliding of the bars (dry friction, end of Stage IVa, which is highly affected by transverse pressure). Note that the relative displacement of the bar is always measured with reference to the undisturbed concrete and consists of two parts, the relative slip at the interface and the shear deformations in the concrete (Fig. 1.1.1b); therefore, even if there is no bar slip, a certain displacement occurs owing to the localized strains close to the interface. This explains the slip in stage I.

Stage II (first cracking): for higher bond stress values ($\tau > \tau_I$), the chemical adhesion breaks down; in deformed bars the lugs induce large bearing stresses in the concrete (p*, Fig. 1.1.2b) and transverse microcracks originate at the tips of the lugs allowing the bar to slip, but the wedging action of the lugs remains limited and there is no concrete splitting (Fig. 1.1.1c).

Stage III: for still higher bond stress values $\tau > \tau\ (1\text{-}3)\ f_{ct}$, the longitudinal cracks (splitting cracks, Figs. 1.1.1d, e and 1.1.2c) spread radially, owing to the wedging action which is enhanced by the crushed concrete stuck to the front of the lugs. The outward component of the pressure (p**, Fig. 1.1.2b) is resisted by the hoop stresses in the surrounding concrete (Tepfers, 1979): as a consequence, the surrounding concrete exerts a confinement action on the bar, and bond strength and stiffness are assured mostly by the interlocking among the reinforcement, the concrete struts radiating from the bar and the undamaged outer ring. In the case of light transverse reinforcement, this stage ends as soon as concrete splitting reaches the outer surface of the concrete member (through splitting τ_3). Afterwards, a more or less sudden failure occurs depending on transverse confinement (Stage IVb, splitting failure). However, in relatively-long anchorages with moderate confinement a pull-out failure usually occurs even after through splitting, owing to the simultaneous presence of different stages along the bonded length. Hence, bond failure may be defined as "splitting-induced pull-out failure". In the case of heavy transverse reinforcement or large concrete cover, through splitting is prevented by their confining action, and concrete splitting remains limited to a cracked core around the bar (Stage IVc, pull-out failure).

Stage IVa: in plain bars this stage immediately follows the breakage of adhesive bond; force transfer is provided by friction and is strongly affected by the transverse pressure; concrete shrinkage and bar roughness favor friction, while interface wear along the sliding plane reduces the radial compressive stresses, and - in the end - the bond stress is reduced too.

Copyright fib, all rights reserved. This PDF copy of fib Bulletin 10 is intended for use and/or distribution only by National Member Groups of fib.

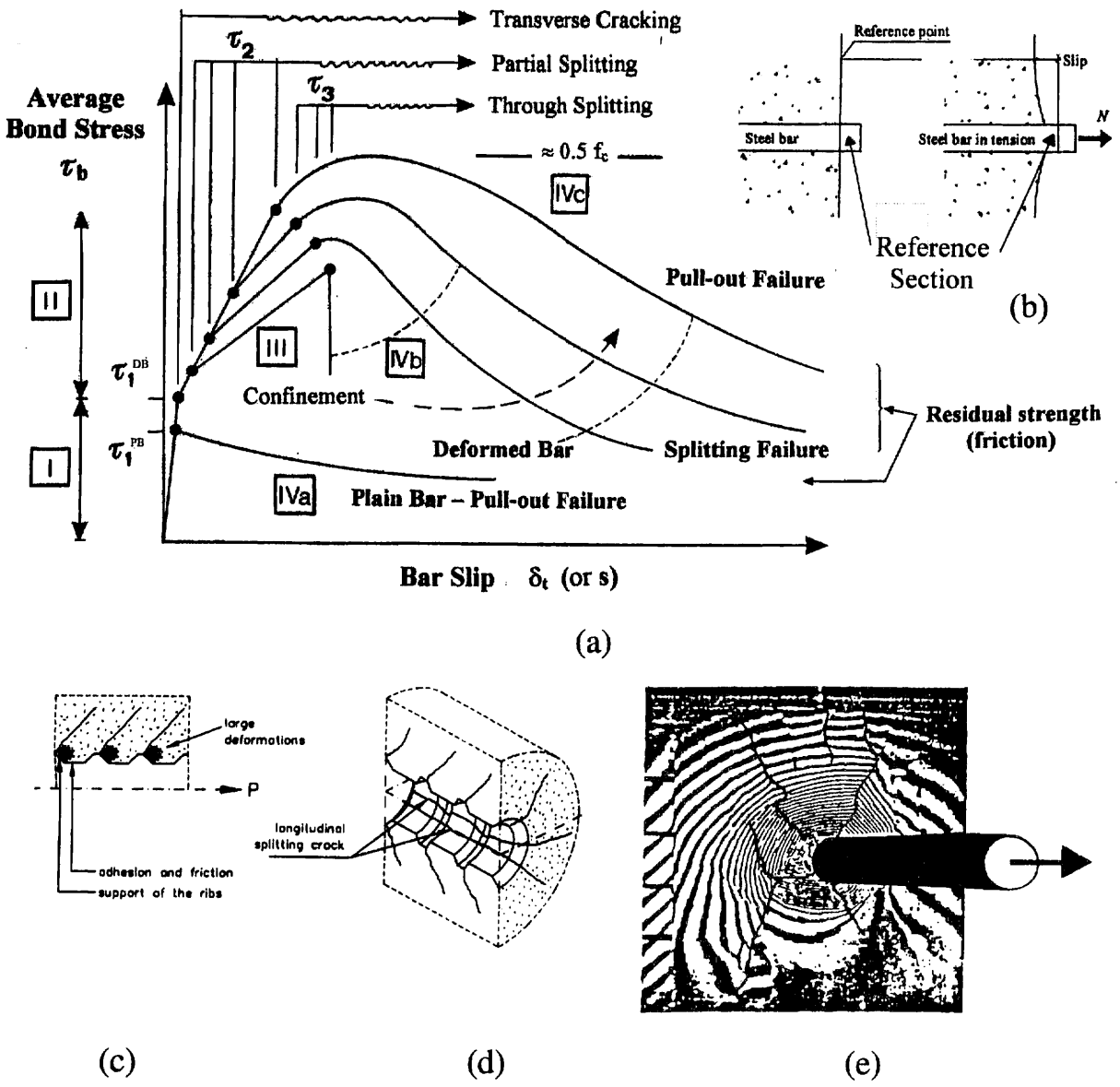

Fig. 1.1.1 - (a) Local bond stress-slip law (see also Tassios, 1979); (b) relative bar displacement (slip); (c) chemical adhesion, friction and bearing action (not all active at the same time); (d) transverse cracks and splitting; and (e) partial splitting (Baranek, 1980, moiré holography). In (a): PB = Plain Bar; DB = Deformed Bar.

<u>*Stage IVb*</u>: in the case of deformed bars confined by light-to-medium transverse reinforcement, the longitudinal cracks (splitting cracks) break out through the whole cover and bar spacing, and the bond tends to fail abruptly (Fig. 1.1.4c). On the other hand, a sufficient amount of transverse reinforcement (namely stirrups) can assure bond efficiency in spite of concrete splitting, because of the confinement action developed by the reinforcement. In Stage IVb, bond stress values as high as (1/3 - 1/2) f_c can be developed, with the unavoidable and often unacceptable side-effect represented by very high slip values (δ_t/d_b or $s/\phi \geq 0.05$, with δ_t or s = bar slip at the loaded end, and d_b or ϕ = bar diameter).

At increasing slip values, the bond strength reaches a peak and then starts decreasing (Fig. 1.1.1a), but still the bond strength remains significant even at very large slip values: τ_b/f_c = 0.15-0.30 (see for instance Gambarova et al., 1989; Gambarova and Rosati, 1996: $\delta_t/d_b \geq 1/3$, d_b = 18 mm). In the end, bond behavior tends to become of the dry-friction type (Coulomb type), since the concrete keys between the lugs are crushed or sheared off (Figs. 1.1.4a,b), and the tips of the lugs rub against the concrete without any appreciable increase in the wedging action. Fig. 1.1.3 shows the possible different bond stages along an anchorage (Fig. 1.1.3a) and a lapped splice (Fig. 1.1.3b).

Copyright fib, all rights reserved. This PDF copy of fib Bulletin 10 is intended for use and/or distribution only by National Member Groups of fib.

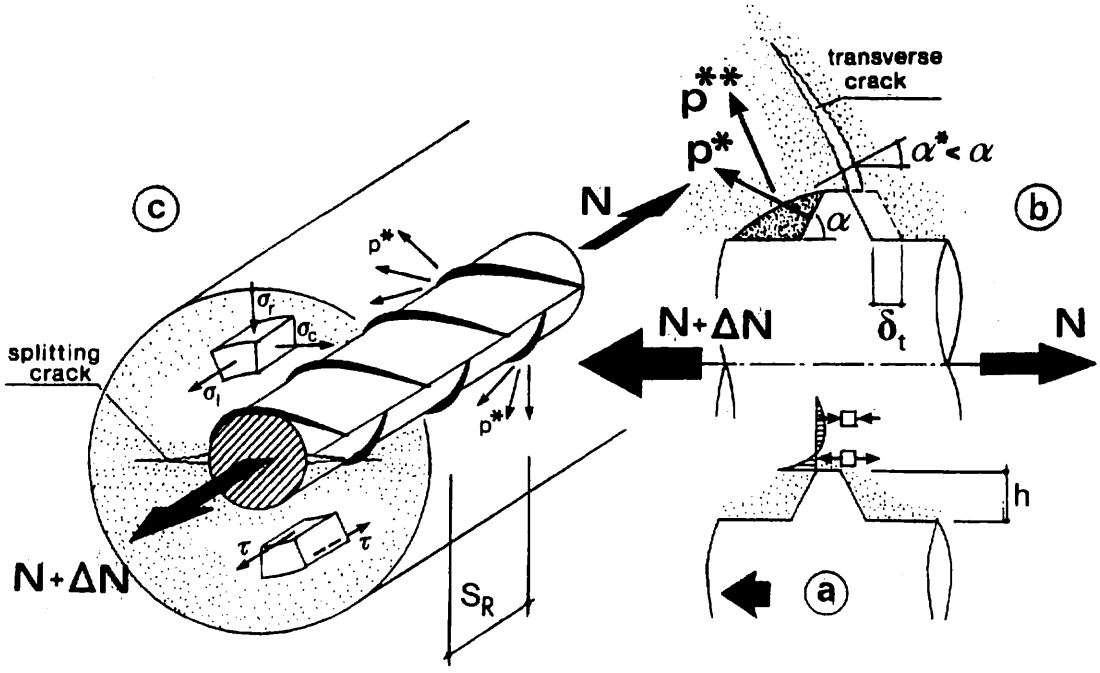

Fig. 1.1.2 - Bond and splitting in reinforced concrete (deformed bars): (a) typical stress peaks in the elastic phase; (b) bar-concrete slip and wedging action of the bar (Gambarova and Rosati, 1996); (c) main parameters.

Stage IVc: in the case of deformed bars confined by heavy transverse reinforcement, through splitting does not occur and bond failure is caused by bar pull-out. The force transfer mechanism changes from rib bearing to friction, and the shear resistance of the keys can be considered as a criterion for this transition (Figs. 1.1.4a). Under continued loading, the interface is smoothed due to wear and compaction, leading to a further decrease of bond stress.

As far as Stage III is concerned, due to the build-up of the wedging action exerted by the bars and to the propagation of the splitting cracks, all possible contributions to confinement are mobilized: as a matter of fact, the confinement efficiency depends on concrete cover and bar spacing (Ferguson, 1966; Edwards and Jannopoulos, 1978; Ferguson et al., 1954; Morita and Kaku, 1979), on transverse reinforcement (Ferguson, 1966; Chinn et al., 1955; Orangun et al., 1977; Losberg and Olsson, 1979; Kemp and Wilhelm, 1979; Skorogobatov and Edwards, 1979; Morita and Kaku, 1979; Morita and Fujii, 1982), on transverse pressure (Dörr, 1978; Robins and Standish, 1984) and - last but not least - on crack cohesion, which is one of the many aspects of concrete fracture behaviour (concrete toughness, see Reinhardt and van der Veen, 1990; Rosati and Schumm, 1992; Gambarova et al., 1994; Noghabai, 1995a; McCabe and Pantazopoulou, 1998).

Stage III is certainly the most typical both for anchorages and splices in the working load situation: for these reasons, special attention has been devoted so far to this stage, whilst Stage IVb has been investigated far less, although the outbreak of splitting cracks through the entire concrete cover and bar spacing may lead to a brittle collapse, which can be prevented only by means of an appropriate design of both concrete cover and transverse reinforcement.

With reference to splitting, the situation is even worse in lightweight concrete: since the cracks tend to spread through the aggregate particles (which no longer act as 'crack arrestors') the splitting cracks are blunter and smoother. A somewhat similar situation is also present in high-strength concretes (f_c = 60-120 MPa), where again the cracks spread across the aggregate particles, because of (a) the strong chemical bond between the aggregates and the mortar, and (b) the very good mechanical properties of the mortar itself.

Copyright fib, all rights reserved. This PDF copy of fib Bulletin 10 is intended for use and/or distribution only by National Member Groups of fib.

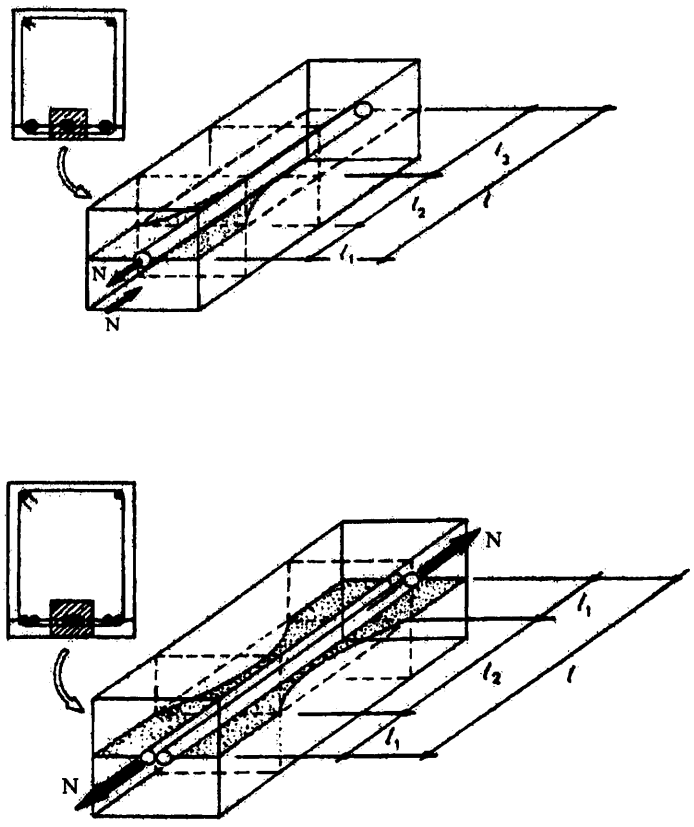

Fig. 1.1.3 – Typical bond behavior (a) in an anchorage and (b) in a lapped splice; complete splitting in l_1, partial splitting in l_2, transverse cracking or chemical adhesion in l_3 (Gambarova et al., 1989). Note that anchorages and lapped splices have the same basic behavior. The two examples sketched here represent as many limit situations and are aimed at showing the various bond aspects, which depend on the structural and material parameters.

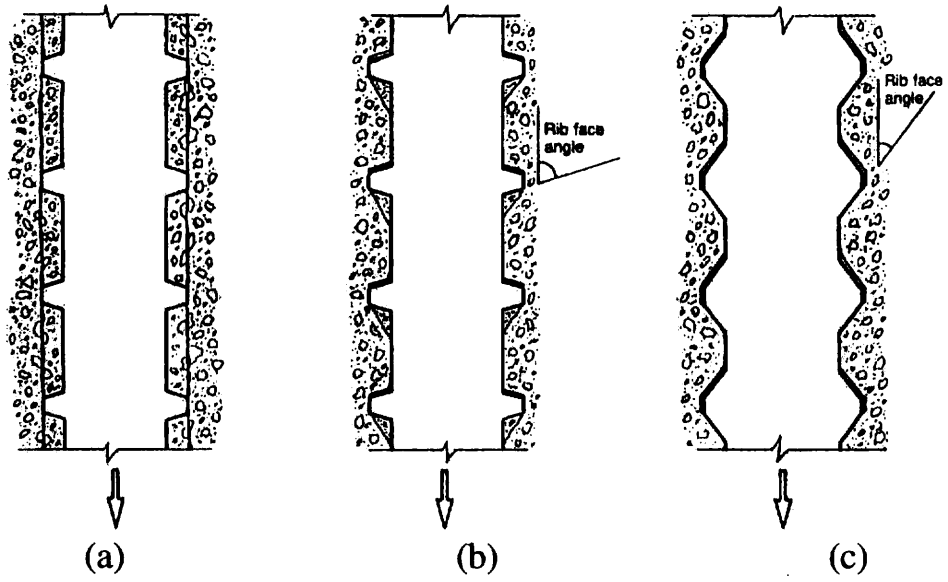

Fig. 1.1.4 - Modes of bond failure: (a) pull-out; (b) splitting-induced pull-out accompanied by crushing and/or shearing-off in the concrete below the ribs; and (c) splitting accompanied by slip on the rib faces (Cairns, 1992; Andreasen, 1992).

Copyright fib, all rights reserved. This PDF copy of fib Bulletin 10 is intended for use and/or distribution only by National Member Groups of fib.

Within this context, Stages I-to-IV refer to the "local" behavior of bond (Figs. 1.1.1, 1.1.2 and 1.1.4), while the "global" behavior results from the superimposition of the various stages. Since the local behavior applies to an ideal segment of a bar, and the global behavior to a whole bar, the two behaviors should be treated separately in principle. However, because of their strict interdependence, the two behaviors are dealt with side-by-side in the following, even if Sections 1.1 and 1.4 concern mostly the local behavior, Sections 1.2 and 1.3 the global behavior, and Section 1.5 both behaviors.

Finally, one has to remember that bond properties and behavior are often lumped into a set of relationships, which are considered as "constitutive laws" of the bar-concrete interface. As a matter of fact, these relationships represent a "structural" behavior and not a "constitutive" behavior, and generally they do not even consider all the aspects which make the real bar-concrete interaction more or less different from the idealized bond scholars are used to think of.

1.1.2 Different factors influencing bond performances

Bond behavior depends on a variety of factors and parameters, which refer basically to the reinforcing unit (bar, multi-wire strand, tendon), to the concrete and to the stress state in both the reinforcing unit and the surrounding concrete. Nevertheless, many technological aspects come into play too, such as concrete cover, clear space between the bars, number of bar layers and bundled bars, casting direction with respect to bar orientation, and bar position with respect to the free surface of the fluid concrete. Other less obvious parameters should also be considered, like the Poisson ratio (which - for instance - plays a relevant role in non-metallic reinforcement) and bar size, which is accompanied by not negligible size effects in smooth bars (bond strength diminishes in large-size bars, Bazant and Sener, 1988; Bazant and Desmorat, 1994; Bazant et al., 1995; Fig. 1.1.5e). However, size effects seem to be absent in well-confined deformed bars and barely noticeable in splitting-prone anchorages (Morita et al., 1993). Finally, the load time-history should be also taken into account.

Since the scope of this chapter is not to be a state-of-the-art work on bond, but to recall the physical behavior of bond and some experimental evidence, in order to emphasize the input data which are necessary for bond modeling, only a few lines will be devoted to the above-mentioned aspects, and some fundamental results will be quoted too, with no claim to be exhaustive.

1.1.2.1 Geometry and stress level of the reinforcing unit

Bar geometry, and more specifically rib geometry, governs bond behavior to a high degree and is instrumental in guaranteeing an adequate bond resistance.

In R/C members ribbed bars (often with a roughly circular section) are extensively used. In this case the best bond performances can be obtained by means of an appropriate combination of rib height (h), rib spacing (s_R), and bar diameter (d_b). The so-called "bond index" or "relative rib area" (f_R) is a coefficient that takes care of the 3 above mentioned parameters (Figs. 1.1.2a,c):

$$f_R = \frac{A_R}{\pi \cdot d_b \cdot s_R} \tag{1.1}$$

where A_R is the area of the projection of a single rib (consisting often of 2 lugs) on the cross-section of a bar. The experimental evidence proves that bond performances are pretty much the same, provided that the bond index and the surface conditions are the same, and that the rib face angle is greater than 30° (Fig. 1.4.2a). The generally accepted values 0.05-0.10 represent a good compromise for f_R, in terms of ultimate bond strength, splitting ability, industrial requirements, good service-load performances (limited crack opening and cover splitting). Rehm (1969) found that bond strength tends to be a linear function of f_R (Fig. 1.1.5a), but recent studies on highly-confined beam-end specimens (Darwin and Graham, 1993) and on weakly-reinforced simply-supported beams (Tholen and Darwin, 1998) lead to somewhat contradictory conclusions. In the former case, increases in the relative rib area resulted in significant increases in bond strength, while in the latter case the relative rib area did not affect the rotational capacity of the plastic hinge, which is significantly related to bond behavior (f_R = 0.069 and 0.119, A_s/bd = 1% and 1.4%, i.e. = 43% and 68% of the balanced reinforcement ratio). However, the importance of the confinement should be always kept in mind.

In P/C members, multi-wire strands are extensively used. Albeit smooth wires are the rule, indented wires guarantee better bond performances (with a smaller transfer length), but at the cost of a stronger splitting

Copyright fib, all rights reserved. This PDF copy of fib Bulletin 10 is intended for use and/or distribution only by National Member Groups of fib.

action (dangerous in thin P/C members). Generally speaking, higher bond strengths can be achieved by increasing the diameter of the outer wires (compared to that of the centre wire) and by reducing the pitch of the outer wires. The bond stress-slip responses of plain and indented 7-wire strands are shown in Fig. 1.1.5b (Karlsson, 1985).

In the discussion of the fundamentals of bond-slip behavior discussed above (Fig. 1.1.1a), it has been assumed that the non-linear behavior depends on the softening of the concrete surrounding the steel bar. This softening depends on cracking around the tips of the lugs, local crushing of concrete, successive development of radial and longitudinal splitting cracks, and formation of cracked shear planes (Figs. 1.1.4a and b). The local bond-slip behavior has often been studied in pull-out tests with a short embedment length (Section 1.1.6.1). Typical of these tests is that the steel stress is kept relatively small and cannot play any significant role. However, in long anchorages (that are the rule in R/C and P/C structures) the reinforcement stresses are definitely higher, but still their role can be neglected as long as rib bearing is the force transferring mechanism (with concrete crushing in front of the ribs and/or cover splitting). In fact, the transverse deformation coupled with the longitudinal steel stress is small in comparison with the rib height (Poisson effect). However, when the force transfer mechanism is based mostly on friction (as in smooth bars and pretensioned strands) the local transverse deformation of the bar cannot be disregarded, since the surface roughness and the transverse reduction of bar diameter may have the same magnitude. This transverse contraction may considerably reduce the radial compressive stress and, hence, the frictional bond stress.

For ribbed bars the influence of steel stress is small as long as the steel is in the elastic range. However, experimental results show that yielding has a drastic negative effect on the bond mechanism resulting in a non-linear descending branch in the bond-slip relationship at the very onset of yielding (Shima et al., 1987; Engström, 1992; Bigaj, 1995, see Stage II in Fig. 1.4.4a). Hence, the bond stress-slip relationship can be influenced not only by the softening of the surrounding concrete, but also by the softening of the steel at yielding. The effect on the bond-stress development is similar to the effect of splitting cracks through the concrete cover (IVb in Fig. 1.1.1 a). The influence of steel yielding is yet not well understood. In Stages II and III (Fig. 1.1.2a) the bond is transferred by a combination of bearing stresses under the lugs and friction. Due to the contraction of the steel bar at and beyond yielding, the outward component of the pressure p* or p** may decrease , resulting in a reduced contribution from macro friction. Furthermore, it is also possible that yielding in addition affects the geometry of the ribs, by reducing the area of the projection of the ribs and the relative rib area (bond index).To a certain extent MC90 implicitly takes the effect of bar contraction into account, by assuming the variable bond stress-slip relation along the transfer length (bond stress reduction in the vicinity of the crack).

In prestressing strands the Poisson effect has a considerable influence on the bond stress also when the steel is in the elastic range. As already mentioned, the transverse deformation of the prestressing tendon depends on the situation (transfer length of anchorage zone) and differs for pretensioned and post-tensioned reinforcement.

When the external force is released, the diameter of a pretensioned tendon increases. This generates radial compressive stresses and, hence, contributes to the frictional bond resistance. On the contrary, the bond resistance of a tendon is strongly reduced when the steel stress is increased, because of the transverse contraction of bar section. As a consequence, two different bond situations can be distinguished (see also Section 1.1.5, Fig. 1.1.14a, transfer-length region, push-in situation, and Fig. 1.1.14b, flexural-bond region, pull-out situation). Along the transfer length the steel stress is reduced when the pretensioned tendon is released. This causes an increase of the tendon diameter and contributes to a better bond resistance. On the other hand, under flexural loading the steel stress in a cracked section is increased, resulting in a reduction of the tendon diameter and a lower bond resistance.

As far as post-tensioned reinforcement is concerned, the influence of tendon contraction due to the Poisson effect can be explained in a similar way. Obviously the magnitude of this effect depends on the roughness of the tendon surface, that is usually considerably lower than in the case of ordinary ribbed reinforcement. It should be kept in mind, however, that the stress level in the prestressing steel (and, hence, the related transverse deformation) is normally much higher than in ordinary reinforcement.

The effect of the stress level in reinforcement on its bond behavior is explicitly recognized in MC90 by considering a higher bond strength along the transfer length of pretensioned tendons.

Copyright fib, all rights reserved. This PDF copy of fib Bulletin 10 is intended for use and/or distribution only by National Member Groups of fib.

1.1.2.2 Concrete quality and state of stress

Concrete quality is of paramount importance in bond, with reference not only to concrete strength, but also to certain technological aspects related to concrete casting, which are often more important than the strength itself.

Since bond action results from the localized pressure underneath the ribs and is directly related to the shear component of the interface forces, bond performances depend on both concrete multiaxial behavior in compression (which is not very sensitive to concrete uniaxial strength in compression, f_c) and on concrete tensile strength f_{ct} (which varies less than linearly with f_c). However, f_c and f_{ct} play a major role in pull-out and splitting failures respectively. The less than linear dependence of bond action on concrete uniaxial strength in compression is shown in Figs. 1.1.5c,d. Note that, for the same bond index ($f_R = 0.1$) and embedment length ($l_d / d_b = 10$) the position of the bar during concreting is even more important than concrete strength.

As a matter of fact, bond performances are best in horizontal bars placed close to the bottom of the formwork, and in vertical bars loaded against the casting direction (in both cases the ribs push against a less porous mortar). The opposite is true for horizontal bars placed well above the bottom of the formwork (water microbubbles get stuck underneath the bar) and for vertical bars loaded in the casting direction (the ribs push against a more porous mortar).

The stress state in the concrete surrounding a bar also has a significant effect on bond action. Transverse tensile forces worsen the behavior of both splitting-prone anchorages and splices, and may even turn a pull-out failure into a splitting failure. In both cases the situation is even worse, if further tensile stresses are present, owing to temperature and shrinkage effects.

In Fig. 1.1.6a the harmful effects produced by a transverse tensile stress on a short anchorage are shown, for 3 different values of the concrete cover; note that increasing the cover does not help significantly in a splitting-prone situation. Fig. 1.1.6b refers to a series of specimens representing the outer part of a lapped splice: the failure envelope shows the mechanical decay caused by a transverse force.

Transverse compressive forces favor bond action, depending on their nature (active or passive confinement, see also Section 1.1.4). Active confinement is always favorable, particularly in a splitting-prone situation, but becomes almost irrelevant in a friction-type situation with large cover values. Passive confinement requires a certain amount of crack slip and opening (= crack dilatancy) to be activated, and is helpful after cover splitting. Finally, it should be observed that a state of tension within the concrete and parallel to the reinforcement (as in tension-stiffening problems) markedly impairs the efficiency of bond (see Section 3).

1.1.2.3 Technological aspects and environmental effects

A number of technological parameters has an influence on bond behavior. These parameters are partly related to concrete (mix and maximum aggregate size) and partly to the reinforcement (bar free interspace, number of bar layers, bar diameter and type of the material). Their role is not discussed here, since it is taken care of in other Sections and Subsections.

As for the environmental effects, the most typical are: (a) rust, (b) steel corrosion, (c) high-temperature bond decay, and (d) low-temperature bond improvement. Owing to the complexity of the environmental effects, only a few test data are recalled and commented here.

- <u>Bar rusting</u>

  Initial bar rusting owing to steel exposure to the environment as it cools down from the rolling temperature (naturally or by water quenching) or to atmospheric conditions (humidity, condensation, pollution) consists of a thin coating of iron oxide (0.3-1.5 g/dm^2, see Refs. in Morgan, 1998), which does not impair bond properties, but may even improve bond behavior with respect to newly-rolled bars (Fig. 1.1.7a).

Copyright fib, all rights reserved. This PDF copy of fib Bulletin 10 is intended for use and/or distribution only by National Member Groups of fib.

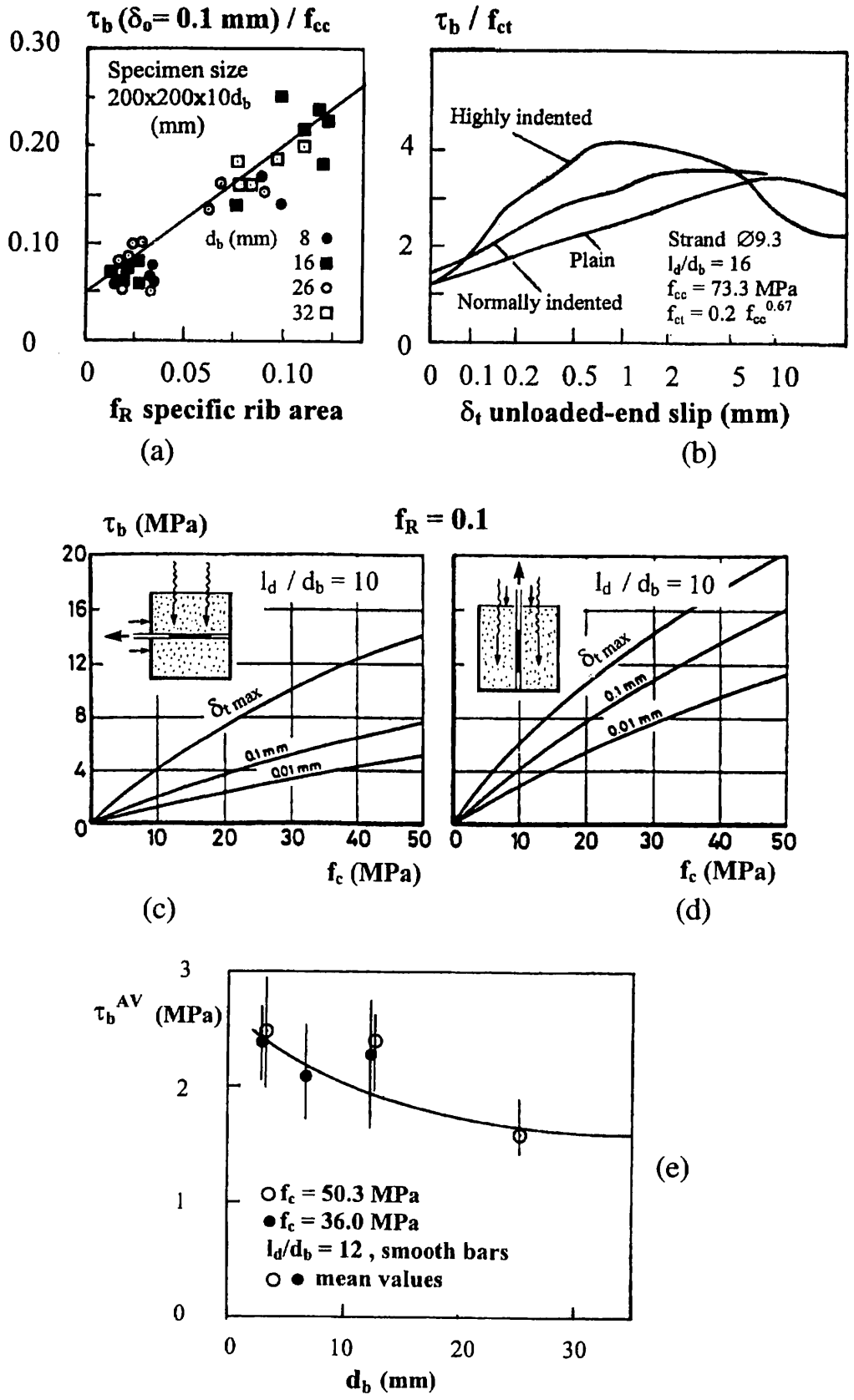

Fig. 1.1.5 - Bond response in relation to the deformations of the reinforcement surface (a,b), to concrete compressive strength (c,d), and to bar diameter (e): (a) R/C, role of the bond index or specific rib area (Rehm, 1969: the bar alignment is at right angles to the casting direction); (b) P/C, effects of surface indentation (Karlsson, 1985); (c,d) pull-out tests for different casting directions (Martin and Noakowski, 1981: bond stress versus concrete strength for different slip values at the bar unloaded end); (e) size effects in relatively-long anchorages (smooth bars, d_b=1, 1/2, 1/4 and 1/8 in., Bazant et al., 1995).

Copyright fib, all rights reserved. This PDF copy of fib Bulletin 10 is intended for use and/or distribution only by National Member Groups of fib.

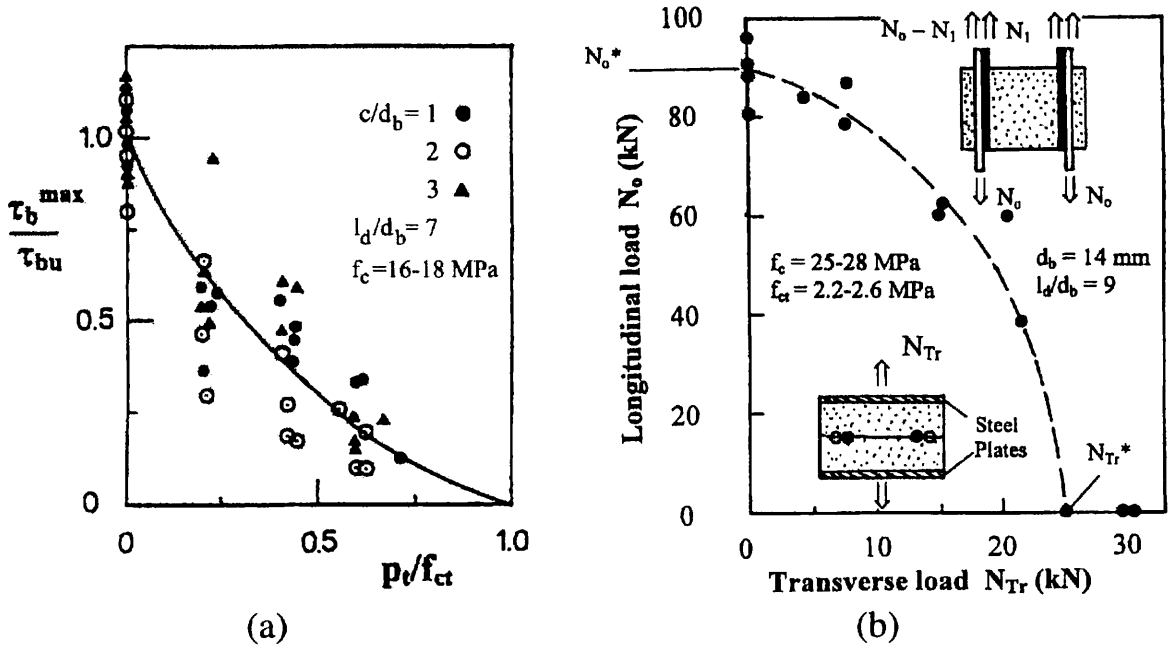

Fig. 1.1.6 - Influence of lateral tension on bond strength: (a) role of the concrete cover in a short anchorage subject to a lateral stress (p_t, Nagatomo and Kaku, 1992); and (b) failure envelope of a lapped splice subject to a lateral tensile force and exhibiting a splitting-type failure in the plane containing the bars (N_{Tr}, Reuter and Eligehausen, 1992, $N_1 = 0.38\ N_0$).

As for the reduction in bar diameter, the values often found in the literature range from 0.008 to 0.04 mm, with a section loss of up to 1% in the smaller-size bars, compared to the widely-accepted tolerance of 6-10% in most product standards.

In summary, the results show that (a) bond strength is generally helped by the presence of residual rust, possibly up to the point where the dimensions of the ribs become critical; (b) the presence of rust may inhibit further steel corrosion in good concrete; and (c) the effect of loss of section is too small to be significant, as it is well within the size tolerances.

- Bar corrosion

Chloride ions and gases (like oxygen and carbon dioxide) can penetrate porous concrete very easily, and - once the steel reinforcement is reached - these ions destabilize the film of iron oxide, which protects the bars against corrosion. As a result, an increasing loss of steel cross-sectional area and a weakening of the bar-concrete bond occur, owing to the build-up of the corrosion products at the interface, as well as to cover splitting and spalling.
The pull-out tests performed by several researchers (see for instance Carrera and Ghoddoussi, 1992), taking advantage of accelerated procedures based on electrochemical systems, show that bond strength increases with the corrosion rate up to a maximum (Fig. 1.1.7b, 5% NaCl solution), after which increasing corrosion causes a significant reduction of bond strength (the corrosion percent in Fig. 1.1.7b is the percent loss of weight compared to the original weight of the reinforcement).

The initial increase has been attributed to the expansive nature of iron oxides, whilst the subsequent decrease is related to the build-up of a soft layer of loose corrosion products at the bar-concrete interface.

In Fig. 1.1.7b the better performance reached by introducing fly ash is attributed to the increased density, resulting in a lower corrosion rate and in a better bar protection.

- High-temperature effects

Since testing at high temperature is a difficult task, most of the tests on bond properties have been performed at room temperature, after a single thermal cycle at high temperature (T = 100-800 °C,

Copyright fib, all rights reserved. This PDF copy of fib Bulletin 10 is intended for use and/or distribution only by National Member Groups of fib.

heating + rest at a prefixed temperature + cooling, quasisteady conditions). In this way the "residual" bond properties were studied, but - since the residual mechanical properties are generally worse than those at high temperature (Schneider et al., 1985) - the residual behavior is a "safe-side" indicator of that under the hot conditions. However, bond behaviors at high temperature and after cooling down to room temperature are very close, and are characterized by a marked decay beyond 400 °C (Fig. 1.1.7c).

The main features investigated were:
- mix proportions and type of aggregate;
- curing conditions and shape of specimen;
- type of reinforcement (smooth, deformed), surface conditions and bar diameter; - testing procedure.

The following conclusions can be drawn from the tests:
- plain round bars are definitely more sensitive to high temperature than deformed bars; - the diameter of the bars has little or negligible influence on the bond behavior;
- the influence of the original strength of the concrete is erratic, and the influence of the w/c ratio has not been ascertained;
- the type of aggregate is the main factor in ensuring a high bond strength, because the higher the thermal stability of the aggregate, the lesser the thermal damage in the concrete, owing to the lower differential thermal strains at high temperature;
- moist-cured specimens have a lower bond strength at high temperature or after a cycle at high temperature.

- Low-temperature effects

Information about the bond behavior at low temperature (T = -50/-150 °C) is rather limited, but is badly needed, since temperatures down to -50 °C and even less are to be expected in the arctic environment and in cryogenic conditions.

Beside temperature, the moisture content plays the most relevant role (water-satured concrete, sealed concrete, air-dry concrete).

According to van der Veen's tests (1992, pull-out tests, Fig. 1.1.8d), air-dry concrete specimens give the lowest bond resistance, while water-saturated and scaled specimens behave practically in the same way. However, the bond resistance at low temperature is always greater than at room temperature, since both the tensile and compressive strengths of the concrete increase at low temperature. As a result, the failure mode in van der Veen's pull-out tests shifted from splitting (+20 °C) to shear (-40 °C) and bar yielding (< -80°C). Unfortunately, the constitutive build behavior is overshadowed by the structural behavior of the specimens in Fig. 1.1.7d. Nevertheless, the favorable effects of low temperatures on bond are clearly shown. Note that the sudden slip increases at the lowest temperatures may be caused by bar yielding, followed by steel hardening.

1.1.2.4 Load time-history

Bond behavior, and namely the bond stress-slip relationship, is definitely influenced by load repetition (high- and low-cycle fatigue: Rehm and Eligehausen, 1979; Eligehausen et al., 1983; Balázs, 1986 and 1991), rate (Vos and Reinhardt, 1982), frequency (Adrouche and Lorrain, 1987) and long-term action (Franke, 1976), since these time-related aspects have a remarkable influence on concrete strength and deformability, which - in turn - affect bond performances. As a result, not only the bond-stress relationship, but also the failure modes (chemical adhesion, splitting and pull-out) are in some way affected by load time-history.

Since bond splitting failure is mostly related to concrete strength in tension, the fatigue effects on the former are the same observed in the latter (see the Wöhler curves in Fig. 1.1.8). As for bond pull-out failure, which is mostly related to concrete crushing underneath the ribs and to the ensuing shear failure along a sliding surface (within the concrete layer closest to the reinforcement), the fatigue effects on bond are similar to those observed in centrally-loaded plain-concrete specimens (low-cycle and high-cycle fatigue). Of course, reverse cycling is more detrimental than pulsating cycling.

The loading rate has a strong influence on bond stiffness and resistance: the higher the loading rate ($d\tau_b/dt = 0.3 \cdot 10^{-3} - 40$ MPa/ms) and the lower the concrete strength (f_c=20-60 MPa), the greater the mechanical

Copyright fib, all rights reserved. This PDF copy of fib Bulletin 10 is intended for use and/or distribution only by National Member Groups of fib.

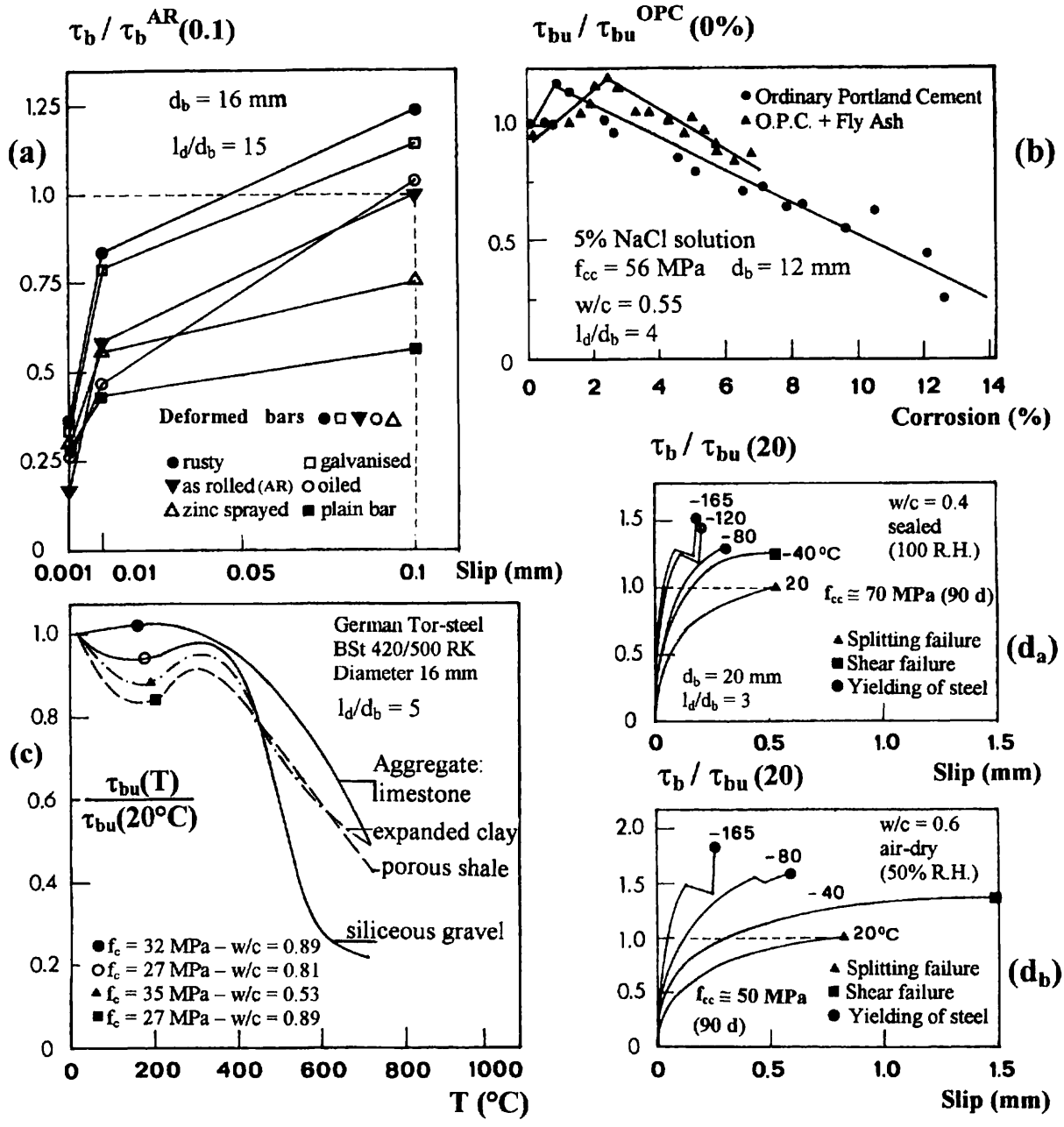

Fig 1.1.7 – Effect of various surface conditions on bond stress/slip response in a pull-out test (Morgan, 1988: $\tau_b^{AR}(0.1)$ = 10 - 11 MPa=stress value at 0.1 mm slip, as rolled); (b) effect of the loss of bar volume (corrosion) according to Cabrera and Ghoddoussi (1992: τ_{bu}^{OPC} (0%)= bond strength in Ordinary Portland Cement with no bar corrosion); (c) bond strength at high temperature (Schneider, 1985); and (d) bond stress/slip relationship for different low temperatures (van der Veen, 1992): $\tau_{bu}(20°C) \approx 0,5 f_{cc}$.

properties of bond in deformed bars (τ_{bu} up to 2.5 times bond strength in normal laboratory conditions with $d\tau_b/dt$ = 0.3 MPa/s; Vos and Reinhardt, 1982).

Finally it has been demonstrated that reverse cycling at low bond stress deteriorates bond behavior during cycling, but not at ultimate (Fig. 1.1.9a). On the contrary, reverse cycling (above 80% of bond static strength) leads to a sort of shake down (Fig. 1.1.9b).

Copyright fib, all rights reserved. This PDF copy of fib Bulletin 10 is intended for use and/or distribution only by National Member Groups of fib.

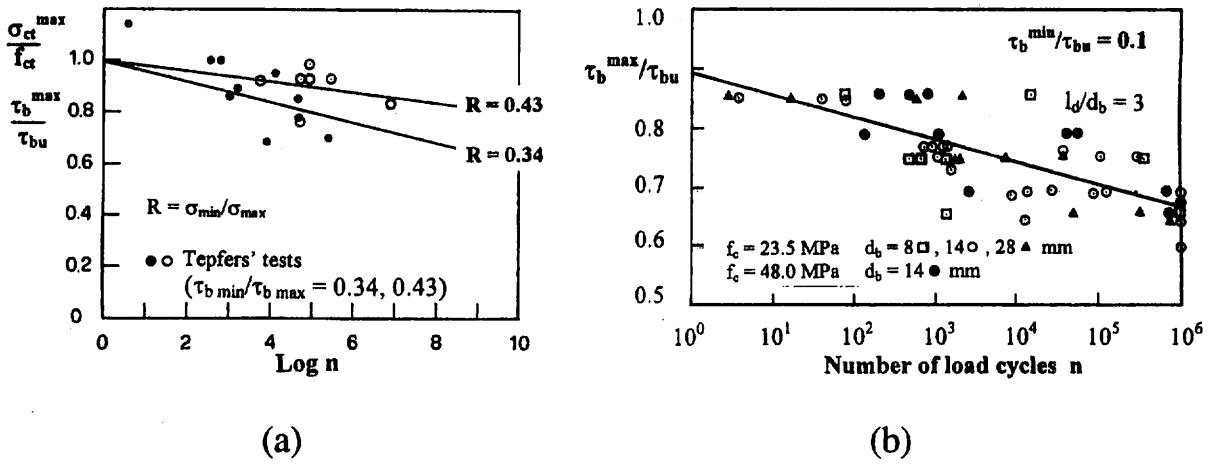

Fig. 1.1.8 - Wöhler curves: bond-strength decay (a) in splitting-prone short anchorages and comparison with concrete in tension (Tepfers, 1973), and (b) in pull-out specimens (Eligehausen, 1979, see Fig. 1.1.15d, $l_d/d_b = 3$).

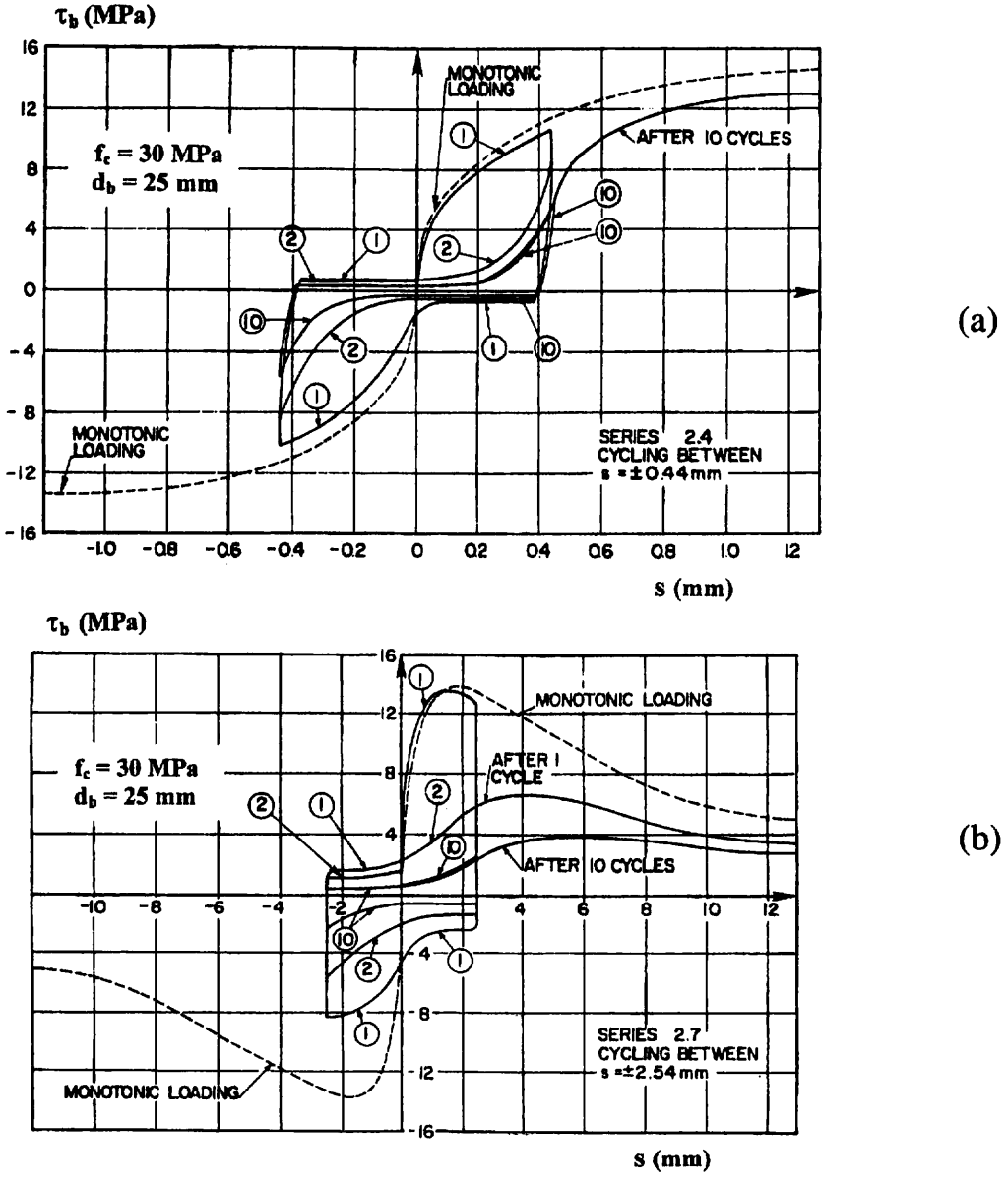

Fig. 1.1.9 - Reverse cycling under imposed displacements: (a) at low bond stress ($\tau_b < 0.8\ \tau_{bu}$, first cycle); and (b) at high bond stress ($\tau_b \approx \tau_{bu}$, first cycle), after Eligehausen et al. (1983).

Copyright fib, all rights reserved. This PDF copy of fib Bulletin 10 is intended for use and/or distribution only by National Member Groups of fib.

1.1.3 Influence of bond on structural behavior (ductility)

Bond action is necessary not only to ensure an adequate level of safety, by allowing the two materials (concrete and steel) to work together, but also to control the structural behavior, by providing an adequate level of ductility.

While safety requires bond to have good mechanical properties at the local level, ductility requires bond to withstand large steel strains along the embedded reinforcement, in order to let the strains spread between two contiguous bending cracks, and to favor the formation of densely-spaced secondary cracks in the concrete.

Paradoxically, very good bond properties may be at odds with ductility requirements. This is even more true today, because of the ongoing tendency towards the use of less ductile steels in the production of cold-worked bars. As a matter of fact, it is up to the post-yield behavior of the steel to ensure a sufficient structural ductility in bending, since ductility cannot be guaranteed only by the large plastic deformations localized near the bending cracks, while the hardening of the steel allows bar yielding to spread along the embedded length between two contiguous cracks. These large distributed strains make R/C members sufficiently ductile (Manfredi and Pecce, 1996; Eligehausen et al., 1998).

To study the influence that bar yielding and large strains have on tension stiffening (which is a structural aspect of bond), the stiffness of tension members has been investigated, and the systematic research project carried out recently in Stuttgart is recalled briefly in the following (Mayer and Eligehausen, 1998). A series of R/C elongated prisms with different reinforcement percentage, bar diameter (4 bars) and steel ductility-class (B, A and S according to CEB-FIP MC90) was tested to failure. Stirrups were spaced at a distance equal to the crack spacing calculated according to MC90. In 4 tests with hot-rolled steel (f_{st}/f_{sy} = 1.13 and $\varepsilon_{su} \approx 88\lambda$, d_b = 16 mm, Fig. 1.1.10a) up to 30 post-yield strain gages were placed in preformed grooves machined in one of the 4 longitudinal bars of each tension member, in order to obtain detailed information on the local behavior of ribbed reinforcement, in the post-yield range.

The post-yield behavior was described by employing the locally measured strains and by using the ratio ($\varepsilon_{sm}/\varepsilon_{sr}$) between the mean steel strain ε_{sm} and the steel strain ε_{sr} in the planes subjected to cracking, to evaluate the contribution of concrete between cracks. In Fig. 1.1.10a the measured steel strains are plotted as a function of the distance from a crack, for different load levels. After the strain at the crack reaches the yield threshold, a strong strain localization in the vicinity of the crack takes place up to the load level that corresponds to the onset of strain hardening (strain at the crack ε_{sr} = 0.88 to 2.30%). With further increasing load (strain at the crack ε_{sr} = 3.57 to 5.62%) the plasticized zone starts to extend and the strain gradient close to the crack decreases.These effects clearly appear if the ratio $\varepsilon_{sm}/\varepsilon_{sr}$, is plotted as a function of ε_{sr} (Fig. 1.1.10d). Two methods of evaluating $\varepsilon_{sm}/\varepsilon_{sr}$ were adopted. Firstly, the overall elongation and the measured loads (stresses) were used, as shown in Fig. 1.1.10b,c (member response). Secondly, the locally measured strains were averaged over a distance equal to crack spacing to get ε_{sm} and the local strain measured at the crack (ε_{sr}) was employed. The results of both methods turned out to be in good agreement in the whole steel strain range. Therefore, the former approach (based on the overall elongation) can be reliably used, with no need for placing strain gages.

In Figs. 1.1.10b,c the stress-strain diagrams of both a hot-rolled and a cold-worked steel are plotted: one should be aware of the meaning of the steel strain ε_s (λ), which is the <u>local strain</u> in the bare-bar response, and the <u>mean strain</u> in the member response (in this case tension stiffening is included). As a result, in Fig. 1.1.10b the yield plateau of the bare bar practically disappears in the member response, since the plastic strains in the embedded bar are limited to the regions close to the main cracks and hardly contribute to the overall elongation. The comparison between member and bare-bar responses (full and dashed curves) shows the great influence that the stress-strain behavior of the reinforcement has on tension-stiffening, in the post-yield range of steel. While the members reinforced with cold-worked steel exhibit a rather brittle behavior (Fig. 1.1.10c, $\varepsilon_{max} \approx 0.15\ \varepsilon_{su}$), the members reinforced with hot-rolled steel are much more ductile (Fig. 1.1.10b, $\varepsilon_{max} \approx 0.53\ \varepsilon_{su}$).

The general behavior of the reinforcement can be described as follows (Fig. 1.1.10d): as long as the concrete is uncracked (and mostly elastic), and bond is perfect (no slip), the ratio $\varepsilon_{sm}/\varepsilon_{sr}$ should be equal to 1, while it should decrease between first cracking and bar yielding. Such a behavior is confirmed in Fig. 1.1.10d, ($\varepsilon_{sm}/\varepsilon_{sr} \approx 0.9$ at bar yielding, $\varepsilon_{sr} = \varepsilon_{sy}$, steel ratio ρ_s = 0.8-1.5%).

Copyright fib, all rights reserved. This PDF copy of fib Bulletin 10 is intended for use and/or distribution only by National Member Groups of fib.

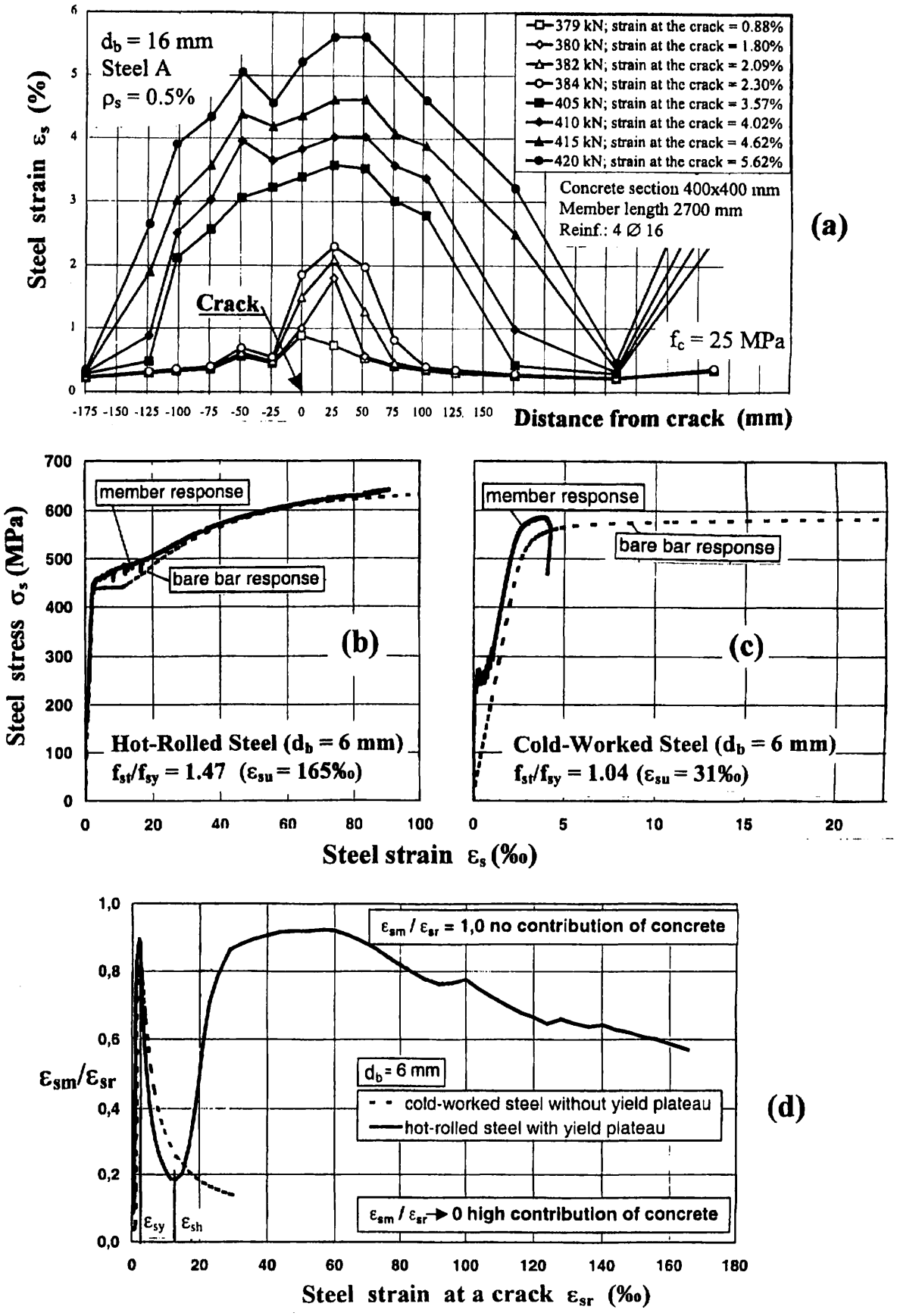

Fig. 1.1.10 (a) Steel strain as a function of the distance from a crack, for different load levels; (b,c) tension-members and bare bar responses; and (d) test results of typical tension members (Mayer and Eligehausen, 1998).

Copyright fib, all rights reserved. This PDF copy of fib Bulletin 10 is intended for use and/or distribution only by National Member Groups of fib.

Beyond ε_{sy}, and up to the end of the yield plateau (if there is any yield plateau, as in the hot rolled steel), the ratio $\varepsilon_{sm}/\varepsilon_{sr}$ significantly reduces, until hardening is activated ($\varepsilon_{sm}=\varepsilon_{sh}$, $\varepsilon_{sm}/\varepsilon_{sr} \approx 0.20$). The steep reduction is caused by the build-up of the plastic strain ε_{sr} close to the bending cracks, while the strains between the cracks are still elastic and exhibit high gradients.

After the onset of hardening, depending on the hardening ratio (f_{st}/f_{sy}), on reinforcement percentage and on possible longitudinal cracking, the ratio $\varepsilon_{sm}/\varepsilon_{sr}$ starts to increase until values close to unity are reached, since the whole bar between two contiguous cracks is either in the plastic range or in the hardening range, and the strains are almost uniformly distributed. After a maximum, the ratio $\varepsilon_{sm}/\varepsilon_{sr}$ decreases again because the stress-strain curve of the bar tends to flatten off at high strain values.

For the cold-worked steel, the very limited hardening is the culprit of the continuous reduction of $\varepsilon_{sm}/\varepsilon_{sr}$, beyond steel yielding ($\varepsilon_{sr} = \varepsilon_{sy}$) and up to steel failure ($\varepsilon_{sr} = \varepsilon_{su}$).

Summing up, only sufficiently ductile bars can guarantee an adequate ductility to structural members (Mayer and Eligehausen, 1998, see also CEB, 1998).

1.1.4 Pull-out and splitting failures

Transverse cracking and eventually splitting occur unavoidably under increasing loads, depending on a variety of physical and mechanical factors, such as confining pressure, concrete cover, transverse reinforcement and concrete toughness, the last being the basis of crack cohesion. Of course longitudinal splitting may be limited to the concrete closest to the bar (partial splitting), if one or more of the above-mentioned factors is large enough to prevent through splitting.

Depending on the type of interaction between the bar and the concrete, two types of bond failure have been traditionally acknowledged: pull-out failure and splitting failure. In the former case, bond failure is due mostly to the shearing-off of the concrete keys cast between each pair of lugs (Fig. 1.1.4a, Cairns and Abdullah, 1995), and the failure is by its very nature related to a "local mechanism" (interface collapse), even if the whole bar is involved (short anchorages and splices).

In the latter case, bond failure is due mostly to the longitudinal splitting of the concrete surrounding the bar (Figs. 1.1.4b,c, Cairns and Jones, 1995a), and bond capacity vanishes once the radial cracks get to the outer surface of the structural element. The failure is related to a sort of "structural collapse", since structural parameters other than those pertaining to bond enter the scene.

Only in the laboratory tests (representing short anchorages and splices) can the two types of failure be studied separately, since in real structures a more or less extended splitting is likely to occur. Also in pull-out tests a limited splitting, often hardly observable, may occur, but short and hairlike radial cracks (as those observed by Baranek, 1980, Fig. 1.1.1d) hardly impair bond efficiency, and bond ultimate behavior is predominantly accompanied by pull-out (mixed failure, see also Fig. 1.1.4b).

As for splitting failure, limit analysis models (see for instance Tepfers, 1979 and 1982) show that there is a critical crack extension (in the radial direction) which maximizes the ultimate bond strength (in other words, under certain circumstances splitting has favorable effects on ultimate bond strength).

Finally, actual anchorages and splices - which are usually "long" (l/ϕ > 10-20) – exhibit more complex failure modes, which can be summarized as follows:

- <u>Pull-out failure</u> with no or partial concrete splitting (not visible splitting cracks): high confinement and/or large concrete cover; shearing off of the concrete keys;
- <u>Pull-out failure</u> induced by partial or through splitting (visible splitting cracks): moderate confinement and/or limited concrete cover; shearing-off of the concrete keys accompanied by concrete slip on rib faces;
- <u>Splitting failure</u> induced by the spalling-off of the cover: no confinement and/or very limited cover; and bar slip on rib faces (see also Fig. 1.1.4c).

Copyright fib, all rights reserved. This PDF copy of fib Bulletin 10 is intended for use and/or distribution only by National Member Groups of fib.

1.1.5 Active and passive confinement

As already mentioned among the parameters affecting bond efficiency, confinement (either active or passive) plays a major role (Fig. 1.1.11a,b,c). Of course, active confinement (resulting from a direct support or from the continuity of a column in a beam-column joint) is more efficient particularly in a splitting-prone situation, since its effects do not depend on the mobilized bond stress. On the contrary, passive confinement (generally developed by the cover and the stirrups) is less efficient, since it originates from concrete dilatancy, which accompanies crack formation and is strictly related to the actual bond stress.

As for passive confinement, the major problem is how to control splitting (see for istance Fig. 1.4.22) and to evaluate the minimum transverse reinforcement, in order to prevent an abrupt loss of bond at the onset of splitting. In Giuriani et al. (1991) the minimum reinforcement is defined as the stirrup ratio, which at the same time (a) involves stirrup yielding, and (b) brings in a prefixed width of the splitting crack (as required for instance by durability), taking into account crack cohesion, which contributes to the confining effect, Fig. 1.1.11d.

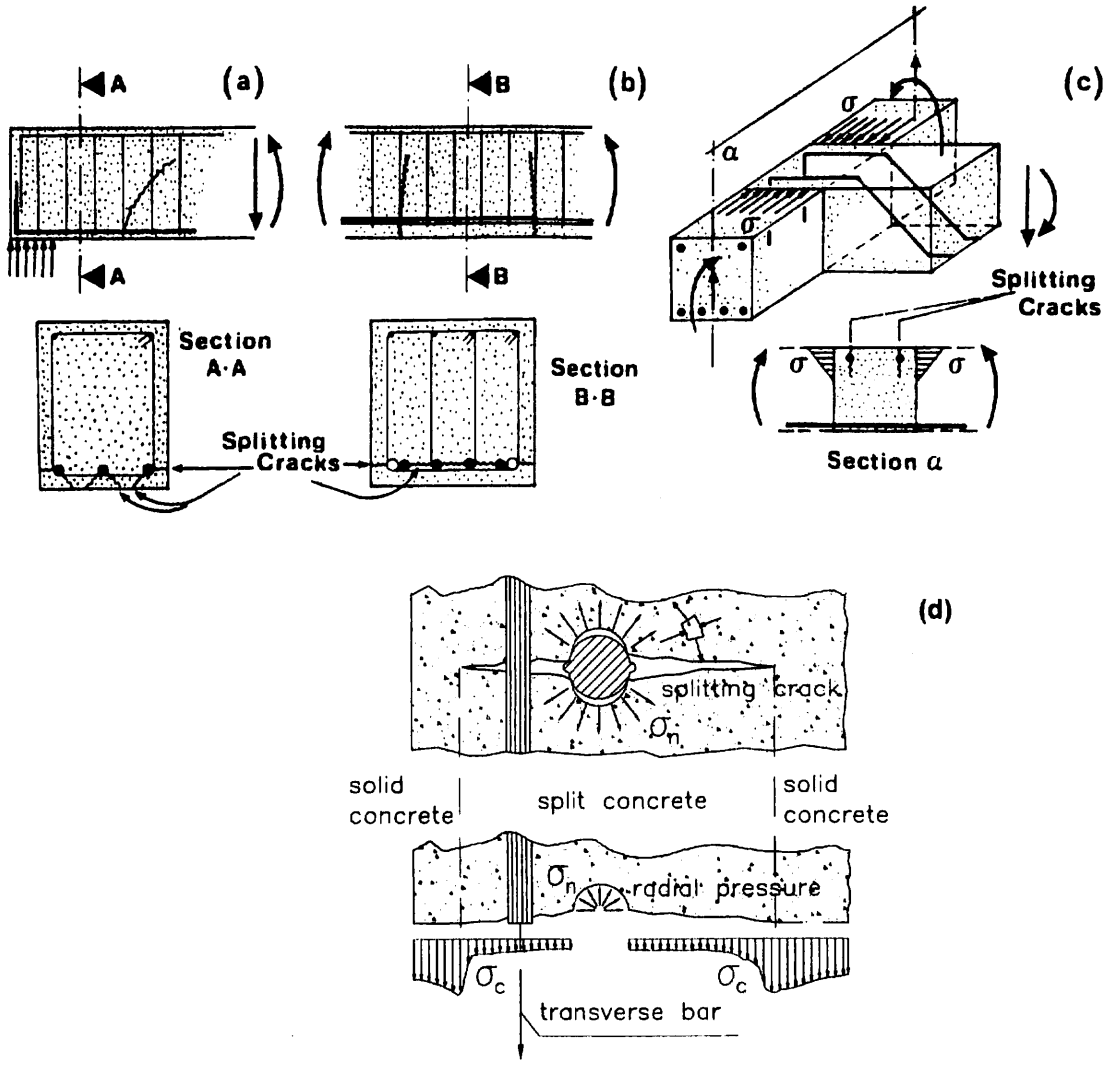

Fig. 1.1.11 – (a,b,c) Examples of bond-confinement interaction: (a) bar anchorage (partly active and partly passive confinement); (b) lapped splice (passive confinement by stirrups); (c) bar anchorage in an indirect support (active confinement); and (d) splitting crack and confining actions around a ribbed bar.

As for active confinement, the topical subject is still the hazy transition from a pull-out failure to a splitting failure, the latter being deeply affected by several structural parameters (Tepfers, 1973; Eligehausen, 1979; Nagatomo and Kaku, 1992, see Fig. 1.1.12 where a few examples are sketched). Bond strength (i.e. stress at the peak of the bond stress-slip curve) is a mostly linear function of the transverse

Copyright fib, all rights reserved. This PDF copy of fib Bulletin 10 is intended for use and/or distribution only by National Member Groups of fib.

pressure, whose beneficial effects increase with the bottom and side concrete-covers (Gambarova and Rosati, 1997, Fig. 1.1.13; Malvar, 1992, Fig. 1.1.18; Modena, 1992, Fig. 1.1.21; Gambarova et al., 1994).

Nevertheless, the cover thickness and the transverse pressure help as long as bond failure is controlled by concrete splitting (excessive covers are pointless and nullify transverse-pressure effects).

Finally, the favorable effects of transverse pressure level off beyond 0.25-0.30 f_c, as shown by many test results on either solid or presplit specimens (Nagatomo and Kaku, 1992; Malvar, 1992; Modena, 1992; Gambarova and Rosati, 1997).

1.1.6 Anchored bars and pretensioned tendons

The same anchored steel reinforcement behaves differently depending on the structural setting: an anchored bar in a R/C member does not behave like a pretensioned strand after prestressing release! Apart from a few important details (such as surface roughness and shape), in the former case the anchored bar is in a "pull-out" situation, while in the latter case the anchored strand is in a "push-in" situation (the section tends to increase transversely, owing to Poisson effect, Den Uijl, 1992). Furthermore, a pretensioned strand in the "transfer-length" region at beam ends of a simply-supported beam (Fig. 1.1.14a) is in a different setting with respect to the "flexural-bond" region (Fig. 1.1.14b), where bending prevails, and the plane-section assumption holds, with or without cracking.

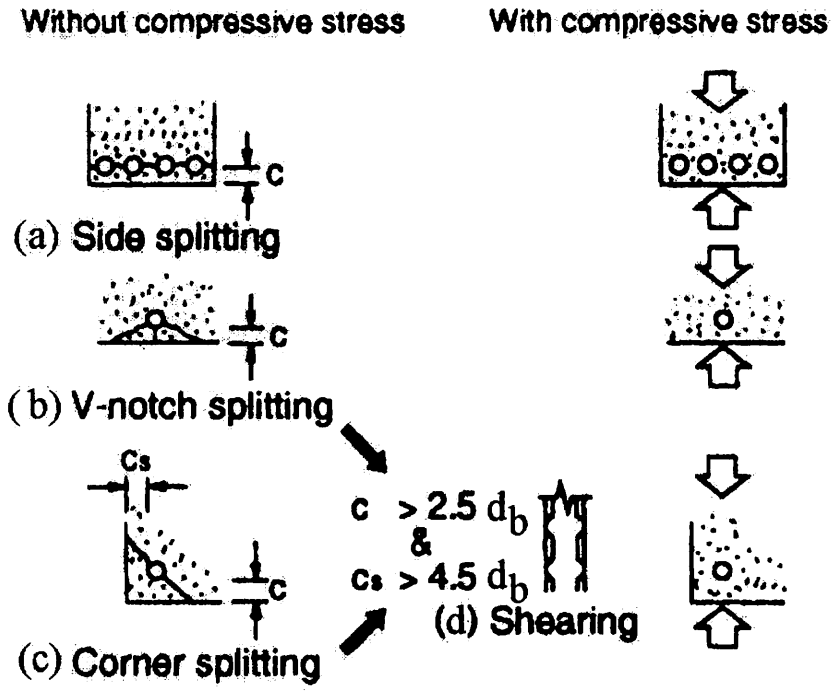

Fig. 1.1.12 – Examples of possible splitting-induced failure modes in an anchorage. Similar failure modes occur in lapped splices.

The structural effects are also typical of the tests on bond, which exhibit a wide variation of specimen types and testing methods, as will be shown later. Since these tests are supposed to provide the data for the formulation of "objective" stress-displacement relationships, the utmost care has been, and should be, taken in defining the test philosophy, in order to guarantee a sufficiently uniform bond-stress distribution along the rebar of a specimen, and to clear the results of any major structural effect.

1.1.7 Testing

Before introducing bond models, it is worth remembering the strategy, which has allowed and allows us to proceed from the perception of a problem (bond in our case) to modeling and applications. The strategy is based on 4 steps (Tepfers and Olsson, 1992):

Copyright fib, all rights reserved. This PDF copy of fib Bulletin 10 is intended for use and/or distribution only by National Member Groups of fib.

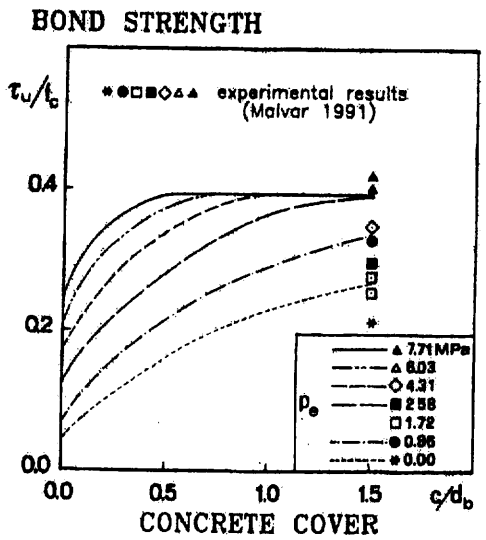

Fig. 1.1.13 - Effects of concrete cover (c) and external pressure (p_e), on bond strength (τ_u), according to the Elastic-Cracked-Cohesive Model (Gambarova and Rosati, 1997); f_c = 40-44 MPa; E_c = 28 GPa; f_c/f_{ct} = 8.5; number of the radial cracks n = 4.

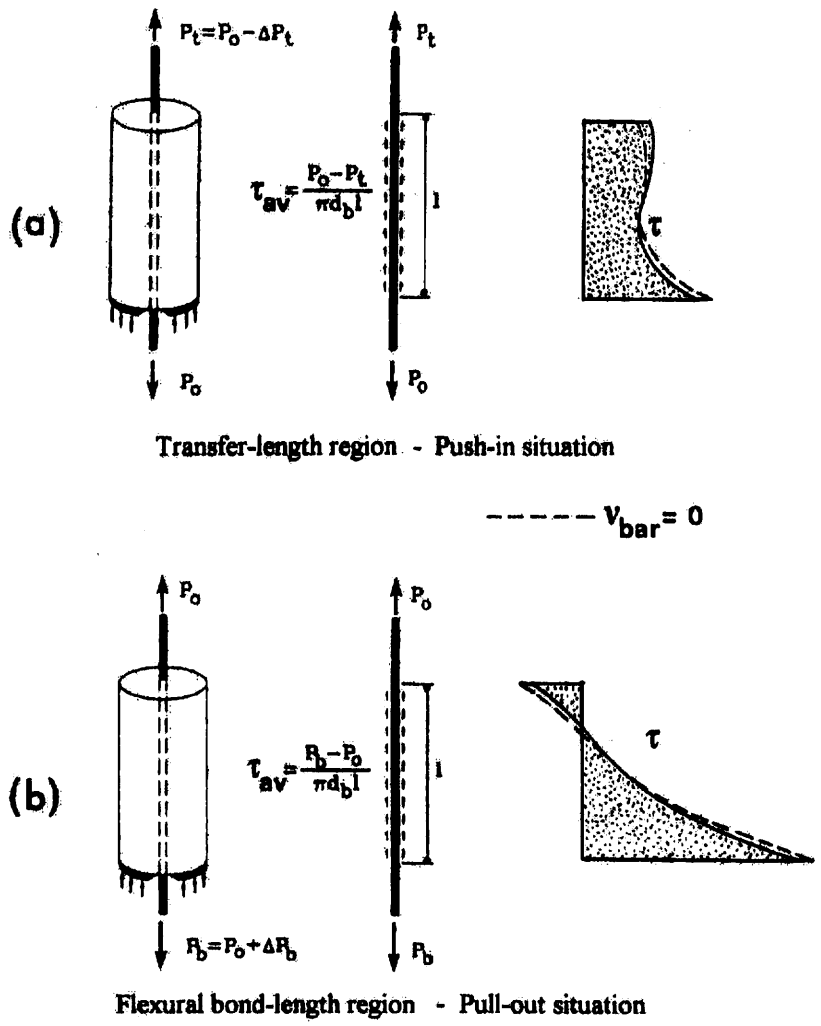

Fig. 1.1.14 - Test technique to simulate bond behavior in different regions (Abrishami and Mitchell, 1992).

Copyright fib, all rights reserved. This PDF copy of fib Bulletin 10 is intended for use and/or distribution only by National Member Groups of fib.

- Initial tests, to understand the mechanisms involved in bonding; these tests are mostly qualitative, but are instrumental in the identification of the main parameters and in the evaluation of their order of magnitude. The tests on long anchorages and splices are typical examples.

- Theoretical modeling: once the main parameters have been identified, models are conceived on the basis of a few fundamental assumptions, with the aim of describing the prevailing resistant mechanism or the local bond stress/bar slip relationship. At this stage, reference is made generally to a portion of an embedded bar, and not to the entire anchorage or splice length: a typical case is the thick-walled concrete ring subjected to an inner hydrostatic pressure simulating the wedging action of a bar (see Section 1.4.6).

- Experimental verification: the conditions assumed in the theoretical model are recreated in a laboratory test in order to validate the model and to explore its limits, by varying for instance such important parameters as concrete strength and type (HSCs and FRCs compared to NSCs), and to study the relationships between the parameters directly involved in the model and those which have not been introduced (for instance, the relationship between the bond stress and the bar-concrete pressure in split specimens).

- Numerical modeling: once the behavioral laws regarding the main parameters have been formulated by means of a suitable model, their implementation into a specifically-conceived program or into a general-purpose code allows us not only to give further insight into the structural behavior (bar + surrounding concrete), but also to extend the analysis to different structural settings and to study design problems (full anchorages and splices, with or without cover and interspace effects).

Because of the importance of testing and - more specifically - of experimental verification, the most relevant test specimens are briefly recalled in the following.

1.1.7.1 Short specimens

Most of the tests are devised to recreate a uniform distribution of the bond stress along a single bar, and to this end short anchorages are generally adopted ($l/\phi \leq 5$). In this way, stress-displacement curves (representing the local bond-slip law) are obtained.

As shown in Fig. 1.1.15, the set-up proposed in the early Sixties by Rehm was adopted (with no major variations) by other scholars, in the Seventies and Eighties.

Since the weakpoints of Rehm's test were the friction between the cubic specimen and the bearing plate, and the arch-effect in the central region (close to the bonded portion of the bar, Fig. 1.1.15a), in the RILEM/CEB/FIP standard pull-out test (Fig. 1.1.15b) the bonded length was moved away from the central region and an anti-friction rubber pad was inserted between the specimen and the bearing plate.

In Losberg's test (Fig. 1.1.15c) the arch-effect was reduced by decreasing the eccentricity of the distributed reaction force with respect to the axis of the bar (a sort of "ring" was inserted between the specimen and the bearing plate).

In the late Seventies, the original Rehm's test was extensively improved by Rehm and Eligehausen (Fig. 1.1.15d), by adopting relatively oblong cylinders, where friction and arch effects are significantly reduced.

In Tassios' test (Fig. 1.1.15e) a special load-cell makes reverse loading possible, by means of a set of push-pull members.

In all specimens, only a limited portion of the bar was bonded to the concrete, the remaining portion being "deactivated" by means of plastic tubes, rounds of tape or thin paraffin layers. In all specimens there was no transverse reinforcement and bond was supposed to fail because of pull-out (shear-type failure).

An offshoot of Rehm's main stem are the tests carried out by Giuriani (Fig. 1.1.15f) which recreate the local behavior of a single embedded rib in a cracked beam subjected to bending. The two vertical free surfaces represent as many flexural cracks, while the bottom surface is the bottom of the beam and the top restraint reproduces the continuity with the upper compressive region. In the tests, both the side and bottom covers were varied. Again the tests were devised to study pull-out failures.

Copyright fib, all rights reserved. This PDF copy of fib Bulletin 10 is intended for use and/or distribution only by National Member Groups of fib.

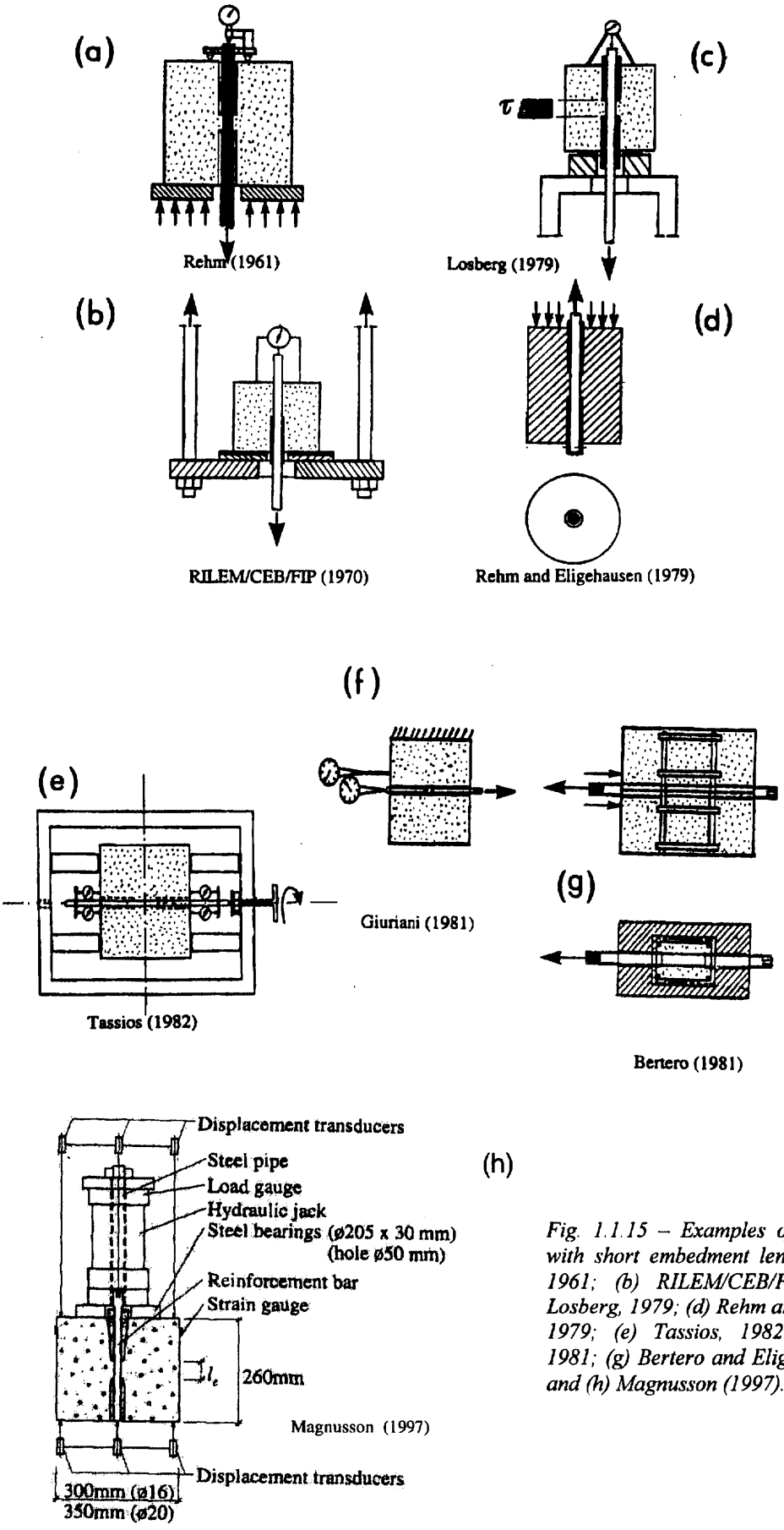

Fig. 1.1.15 – Examples of pull-out tests with short embedment length: (a) Rehm, 1961; (b) RILEM/CEB/FIP, 1970; (c) Losberg, 1979; (d) Rehm and Eligehausen, 1979; (e) Tassios, 1982; (f) Giuriani, 1981; (g) Bertero and Eligehausen, 1981; and (h) Magnusson (1997).

Copyright fib, all rights reserved. This PDF copy of fib Bulletin 10 is intended for use and/or distribution only by National Member Groups of fib.

As far as passive confinement is concerned, Bertero and Eligehausen's tests (Fig. 1.1.15g) and Noghabai's tests (Fig. 1.1.16) have to be recalled. In the former tests, the pull-out under reverse loading was at issue, and prisms provided with a single bar and a heavy transverse reinforcement (to avoid concrete splitting or to keep it under control) were tested.

In the latter tests, the confining action was provided by a steel tube: a typical test specimen and the bond-stress/slip curves are shown in Fig. 1.1.16 (Noghabai, 1995). Unfortunately, in some of the tests performed by Bertero-Eligehausen and by Noghabai, concrete splitting occurred (large diameter bars). Therefore, one should proceed with caution when referring to these results, because of the different failure modes.

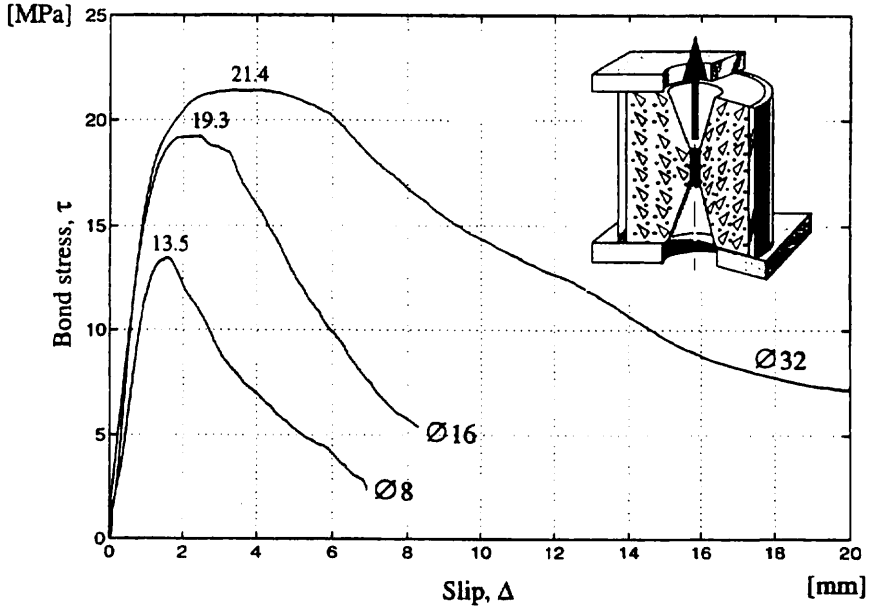

Fig. 1.1.16 - Typical bond stress-slip curves (pull-out tests, severe confinement, Noghabai, 1995); f_c = 36 MPa; bonded length/bar diameter = 2.5; steel-tube thickness = 10 mm; overall specimen diameter = 219 mm; specimen height = 184,192,196 mm.

A greater variety of test specimens has been used for studying bond-splitting interaction, as required by the greater number of geometric parameters, which come into play.

Since splitting cracks play a fundamental role in reducing bond strength and stiffness, initially unsplit (i.e. solid) specimens have been extensively adopted in the past to study the degradation of bond during the splitting process and the favorable effects of lateral confinement. On the other hand, since splitting may be caused by other occurrences than the actual loading (for instance, bar corrosion, concrete shrinkage or previous severe loading), presplit specimens have often been adopted to study bond behavior after concrete splitting.

As a matter of fact, the challenging aspect of any investigation on splitting-induced effects on bond is how to separate the two components of the bond forces, namely the "shear" component (which is the resultant of the bond stresses acting along the bar) and the "normal" component, at right angles to the bar, which is the result of the radial stresses acting on the bar (Fig. 1.1.17a). Conversely, the normal component acts as an outward pressure on the concrete and is balanced by the hoop (tensile) stresses, which are the "bugbear" of the whole business! Only by separating the two components, can the bond forces be studied (Tepfers and Olsson, 1992). With regard to this point, considerable efforts have been made lately by several researchers, and some test procedures and results are recalled below.

A very simple and efficient way to have basic data on splitting is offered by Olsson and Tepfers' "Ring Test" method (Fig. 1.1.17, Tepfers and Olsson, 1992): the shear component of the bond forces is balanced by the reaction transmitted by a circular teflon strip, which is very close to the loaded end of the bar (thus the arch-effect is minimized), while the radial component is resisted by the hoop stresses in the solid concrete, prior to splitting, and by a steel ring (or belt) afterward. The steel ring is instrumented in the circumferential direction and is an integral part of the specimen. Schematic diagrams of the applied force

Copyright fib, all rights reserved. This PDF copy of fib Bulletin 10 is intended for use and/or distribution only by National Member Groups of fib.

and the circumferential strain are plotted as a function of bar slip in Fig. 1.1.17. The Ring Test is well suited to the measurement of the splitting tendencies of different types of concrete and lug patterns in deformed bars. However, it is worth mentioning that the local splitting forces can hardly be quantified, since only average strains far from the bonded surface are measured (in the steel ring, hoop direction).

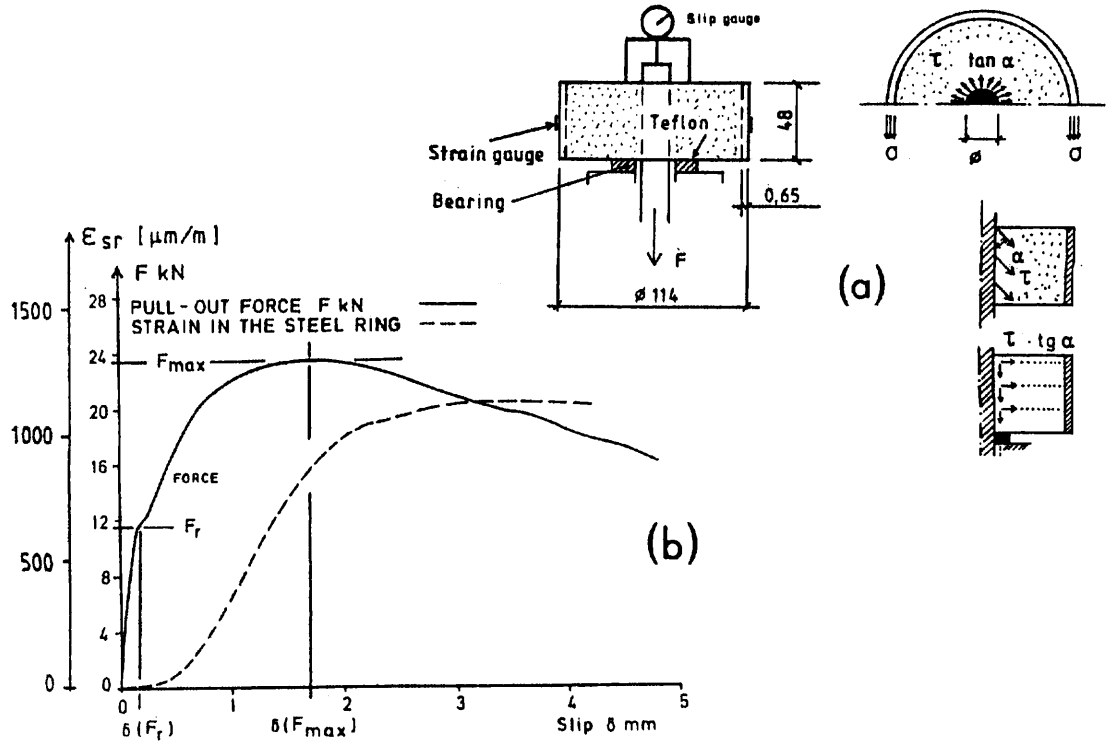

Fig. 1.1.17 - Ring Test (Tepfers and Olsson, 1992): (a) typical specimen, and (b) plots of the load and of the circumferential strain (in the ring), as a function of bar slip.

More elaborate tests, aimed at the study of the evolution of splitting, with/without passive/active confinement, have been carried out by Malvar (1992) and Noghabai (1995). In both cases concrete cylinders were involved. In the former case (Fig. 1.1.18), the specimens were loaded up to the complete loss of bond, by means of an innovative set-up consisting of a split steel-jacket, bonded to the reinforced specimen and pressed against it by a confining ring, which was tightened by a hydraulic actuator. In the latter case (Fig. 1.1.19), both "membrane" splitting tests (where a suitable pressure was applied all along a hole representing the volume of the bar) and "bar pull-out" splitting tests (with an actual bar pulled out of the concrete specimen) were carried out, with and without confinement (passive confinement provided by an embedded steel spiral). The number of the splitting cracks was 1 to 6, compared to 2 to 4 in Malvar's tests.

As shown in Fig. 1.1.19, according to Noghabai's tests a severe outer confinement (steel tube) and an embedded high-pitch spiral brings in the same peak strength and only marginal differences in the softening branch. Moreover, the relationship between the ultimate bond stress and the confinement stress seems to follow a Mohr-Coulomb criterion (a linear dependency, with a limited cohesion).

Finally, completely different approaches were adopted by Gambarova and Rosati, Modena, Plizzari et al., who tested specially-designed reinforced plates, presplit or initially unsplit, with or without transverse reinforcement.

In presplit specimens (Fig. 1.1.20a) the artifical "splitting" crack was obtained by inserting special separators in the formwork, alongside the bar, before concreting. The tests by Gambarova et al. (1989) and by Gambarova and Rosati (1996, 1997) were carried out by forcing the crack opening to remain constant throughout the whole loading process (4 different values of δ_n/d_b), while in the tests by Modena (1992) the confinement force was kept constant. All tests were displacement-controlled. In addition to the bond- and confinement-stress curves as a function of bar slip (Fig. 1.1.20b), the bond/confinement envelopes were also studied, as well as bond path-dependency, which turned out to be quite limited under severe confinement.

Copyright fib, all rights reserved. This PDF copy of fib Bulletin 10 is intended for use and/or distribution only by National Member Groups of fib.

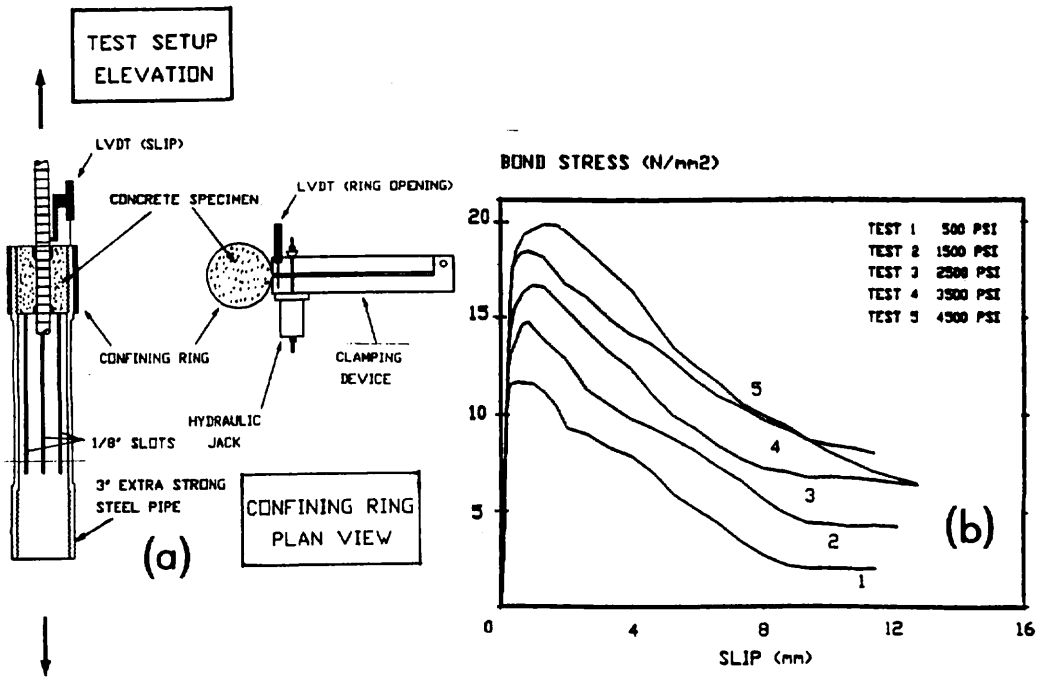

Fig. 1.1.18 - Pull-out tests with splitting failure (Malvar, 1992), at various confinement levels: (a) test set-up; and (b) bond stress-slip curves; f_c=38-40 MPa; bonded length/bar diameter = 3.5; bar diameter=19 mm; specimen diameter (concrete)= 75mm; specimen length= 100 mm.

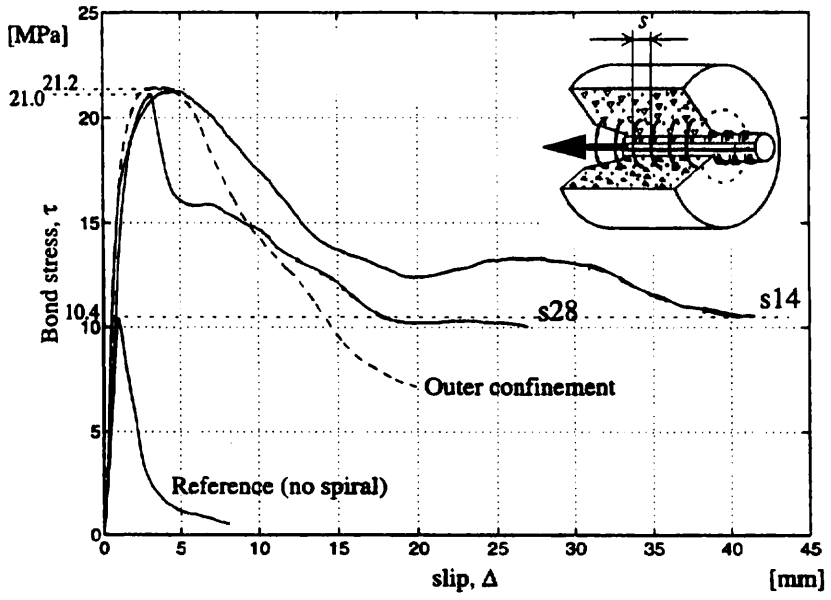

Fig. 1.1.19 - Typical bond stress-slip curves (splitting tests, severe confinement, Noghabai, 1995): f_c = 40 MPa; bonded length/bar diameter = 3.75; bar diameter = 32 mm; spiral reinf. ϕ6 mm; spiral diameter = 81 mm; spiral pitch = 14 and 28 mm; specimen diameter = 313 mm; specimen height = 175 mm. See Fig. 1.1.16 for outer confinement.

Pull-out tests are certainly one of the simplest way to test anchorages but the influence that the friction between the specimen and the reaction platens has on the confining action should not be underestimated, even more since it varies during the same test and it differs from test to test (Losberg and Olsson, 1979). In order to avoid these undesired effects, a special set-up, based on a concept previously proposed by Giuriani and Plizzari (1985), has been recently introduced by Plizzari et al. (1998). In this way, the pull-out force acting on the specimen is counteracted by two reaction blocks that allow the main splitting crack to open (see also Fig. 1.1.22a, long specimens).

Copyright fib, all rights reserved. This PDF copy of fib Bulletin 10 is intended for use and/or distribution only by National Member Groups of fib.

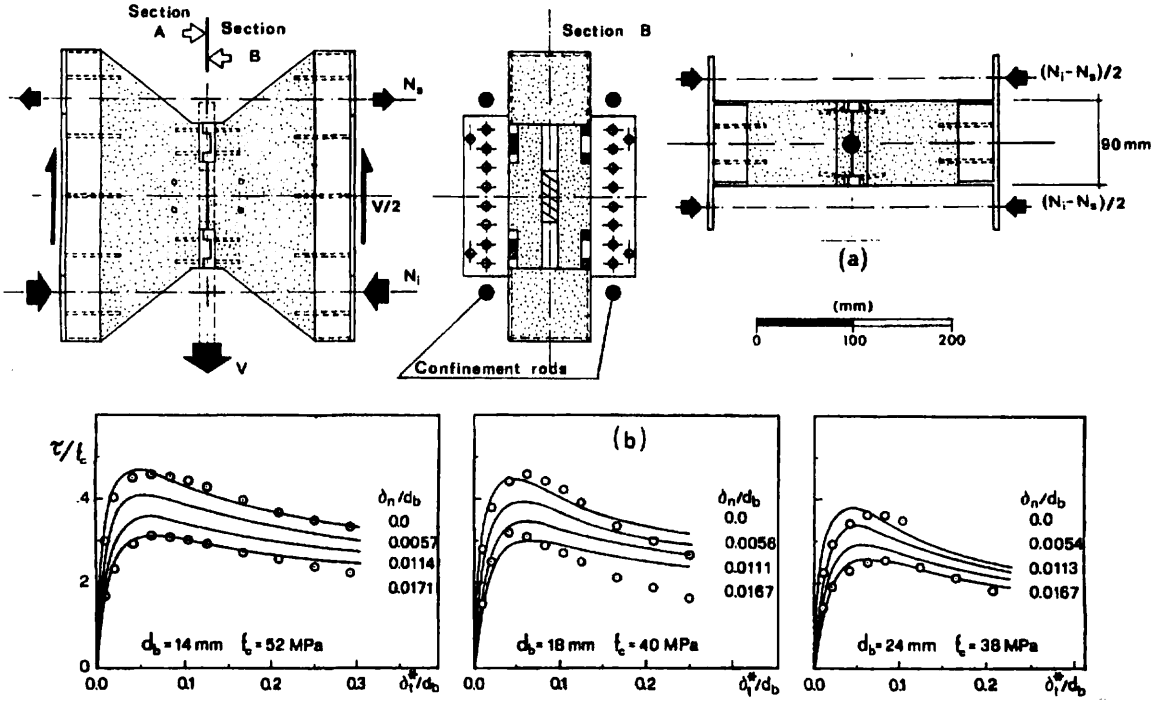

Fig. 1.1.20 - Pull-out tests in presplit specimens (Gambarova et al., 1989,96,97), for various crack widths: (a) geometry of the specimens; and (b) bond stress-bar slip curves (full line = behavioral laws; dots = test results). Bonded length/bar diameter = 3.0,2.9,2.4; bar diameter = 14,18,24 mm; specimen thickness/bar diameter = 4.3,5.0,3.8; specimen dimensions 300x300x60-90 mm

In Fig. 1.1.21 a few tests carried out at constant confinement by Modena and Gambarova-Rosati show that bond capacity (= peak stress of the stress-displacement curves) is an almost linear function of the confinement (dry-friction, see also Section 1.1.5).

A better understanding of the interaction between the tangential and normal stresses at the bar-concrete interface requires the refinement of the test methods, and the combined use of experimental and numerical techniques. Recently, Ghandehari et al. (1999) have studied the wedge effects of a short bar by using speckle interferometry, in order to monitor the crack growth and the displacements along the front face of a pull-out specimen. A special wedge-shaped bar was tested and a fracture mechanics-based numerical simulation was used to evaluate the normal stresses inside the concrete embedment, on the basis of the measured shear stress, crack pattern and displacement field.

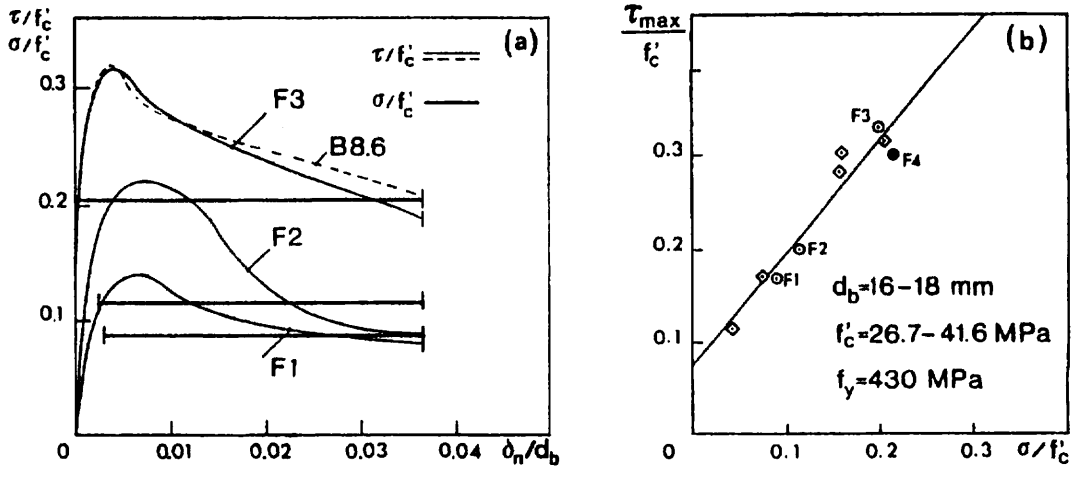

Fig. 1.1.21 - Pull-out tests in presplit specimens at constant confinement: (a) response curves; (b) bond capacity versus confinement. Tests F1-F4 by Gambarova and Rosati (1996); Test B8.6 and rhombuses by Modena (1992).

Copyright fib, all rights reserved. This PDF copy of fib Bulletin 10 is intended for use and/or distribution only by National Member Groups of fib.

1.1.7.2 Long specimens

As already mentioned, testing short anchorages is instrumental in working out the bond stress-slip relationship, and to this purpose both the bond stress and the interface displacement (slip) should be as uniformly distributed as possible (short specimens). However other approaches are possible and have been adopted successfully for many years, as in the case of long anchorages and splices, where the strain gaging of the reinforcement gives useful information on bond overall behavior (long specimens). These tests (a) provide useful information on anchorage behavior, (b) make it possible to study the bond-stress distribution along an embedded bar or splice, and (c) are a reference for FE modeling.

As an example, at the University of Durham, Scott et al. (1996) lately adopted and improved an already well-known technique for measuring reinforcement strain and bond stress distributions, which involves internally strain gaging the reinforcement with electric-resistance strain gages (up to 100 gages). This approach avoids the degradation of the bond characteristics around the surface of a bar, which occurs from the use of surface-mounted strain gages. Each strain gaged bar is manufactured by machining two solid bars to a half round and then sawing a longitudinal channel along the center of each half bar. The strain gages and wiring are then installed in the channels (typical section 4x4 mm) and the two halves glued together to give the appearance of a normal solid bar. The bar is then cast into concrete as normal reinforcement. Variations in bond stress along the length of a bar can then be analysed from differences in longitudinal strains. The technique has been used to examine behavior of straight bar laps and anchorages, hooks and bends, beam/column connections, and links. Very considerable development of this technique has been undertaken, with reference to all bar sizes from 6 to 32 mm and embedded lengths of up to 4 m.

In the study by Plizzari et al. (1996a,b and 1998) the behavior of relatively long anchorages (Fig. 1.1.22, $l_d/d_b \approx 20$) was studied by means of special specimens consisting of one or two bars, embedded along the mean transverse plane of a fairly thick concrete plate (Fig. 1.1.22a). The specimens were either unsplit or presplit in the above plane, and most were transversely reinforced (3 two-leg stirrups). The objective of the tests was threefold: to have information about the evolution of the splitting process in a relatively long anchorage subjected to passive confinement (or no confinement at all); to assess the confining action induced by crack cohesion; and to clarify the dependency of bond capacity on stirrup amount. As a matter of fact, Fig. 1.1.22b shows that beyond a certain value of the stirrup confinement-index, adding stirrups is pointless (Fig. 1.1.22b reports also the design bond values suggested by the Eurocode No. 2, 1991, and ACI-318/95, 1995, the latter including stirrup-induced confinement). It is worth noting that there are 4 main reasons for the sizeable difference between the code provisions and the test data: (a) the safety factors introduced in the codes; (b) the necessity of covering both anchorages and lapped splices; (c) the different confinement that corner bars and inner bars are subject to in real beams and structures (see Section 1.4.4); and (d) the embedment length ($l_d/d_b = 9$ in the tests; $l_d/d_b > 20$-30 in actual anchorages, where the nominal bond strength decreases considerably in case of splitting). Considering the previous aspects, EC2 agrees rather well with test results.

Finally, the well-known "beam test" (Fig. 1.1.23a) for the evaluation of the relative rib area (standardized by RILEM, 1978) and the "beam-end test" often used in the analysis of bond within a structural framework (see Section 1.5.8) should be quoted too. Unfortunately, the beam test usefulness is limited to the comparison among bars having the same nominal diameter and different deformation patterns, since the test results give mixed information on both the constitutive behavior of bond and the structural behavior of the specimen. As a matter of fact, the transverse reinforcement prevents cover splitting in the case of small bar diameters (d_b = 10-14 mm, Ω = 0.113-0.081 %), but not in the case of large bar diameters (d_b=16-32 mm, Ω = 0.196-0.098 %: only the stirrups distributed along the embedded length of the bar=10 d_b were taken into account in the evaluation of Ω.). In Fig. 1.1.23b, the hairlike splitting cracks radiating at 45° from the large-diameter bars (d_b = 24 mm) result from a local shear-type failure, that is caused by the combination of a limited cover and an insufficient confinement provided by the stirrups.

1.1.8 Modeling

The great number of test results available so far on the many aspects of bond are the basis of mathematical modeling and should always be kept in mind, if sound models capable of grasping the hidden and tricky aspects of bond are to be formulated (Shima et al., 1987b). For these reasons, it was

Copyright fib, all rights reserved. This PDF copy of fib Bulletin 10 is intended for use and/or distribution only by National Member Groups of fib.

felt necessary to recall in this introduction some previous fundamental test results, and to present some recent experimental findings, while the following chapters are entirely devoted to bond modeling.

On the other hand, only by starting from basic properties and fundamental mechanisms (microlevel) can constitutive or behavioral laws be formulated in a consistent way (mesolevel), in order to be introduced into the analysis (macrolevel). Moreover, only by knowing the role of each more or less important parameter (but who knows before testing?), can some parameters be dropped, and laws and equations simplified, to the advantage of the designer, but with no detriment to the soundness of the analysis.

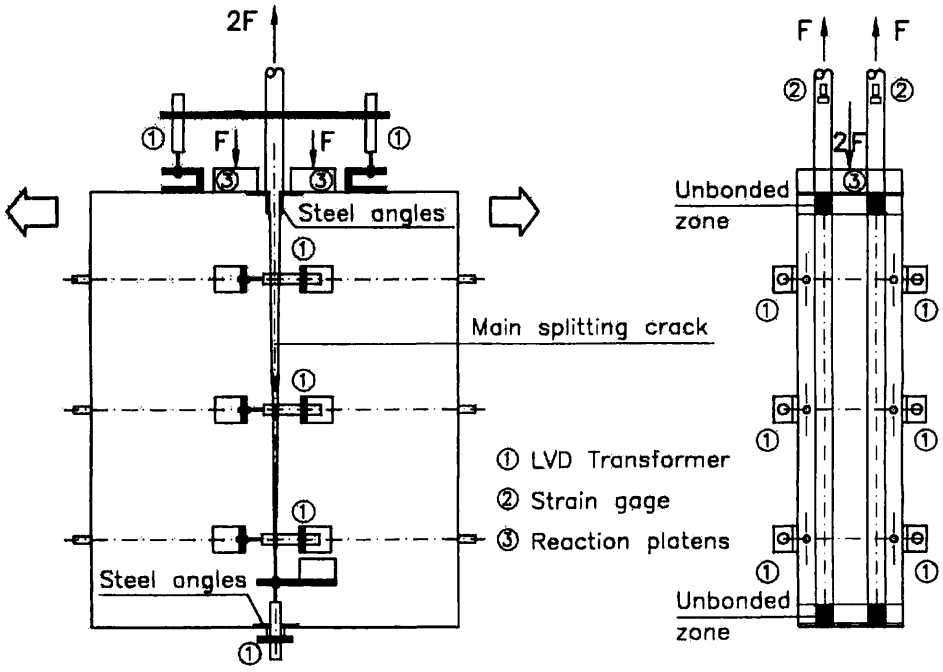

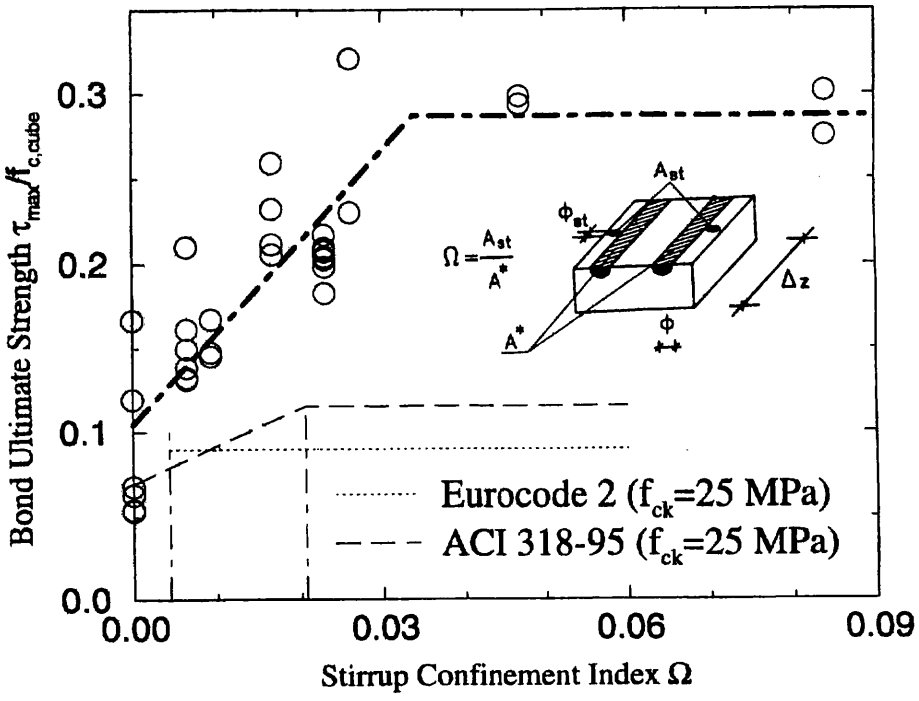

Fig. 1.1.22 - Pull-out tests of relatively long anchorages (bonded length/bar diameter = 9, Plizzari et al., 1996a and 1998): (a) plan view of a two-bar anchorage (with 6 transverse bars simulating 3 two-leg stirrups); (b) diagram of bond capacity versus stirrup confinement-index. Main reinf. 1-2 ϕ 20 bars; transverse reinf. 6 ϕ5/ϕ10 bars; specimen thickness 80-120 mm; f_c = 23-30 MPa.

Copyright fib, all rights reserved. This PDF copy of fib Bulletin 10 is intended for use and/or distribution only by National Member Groups of fib.

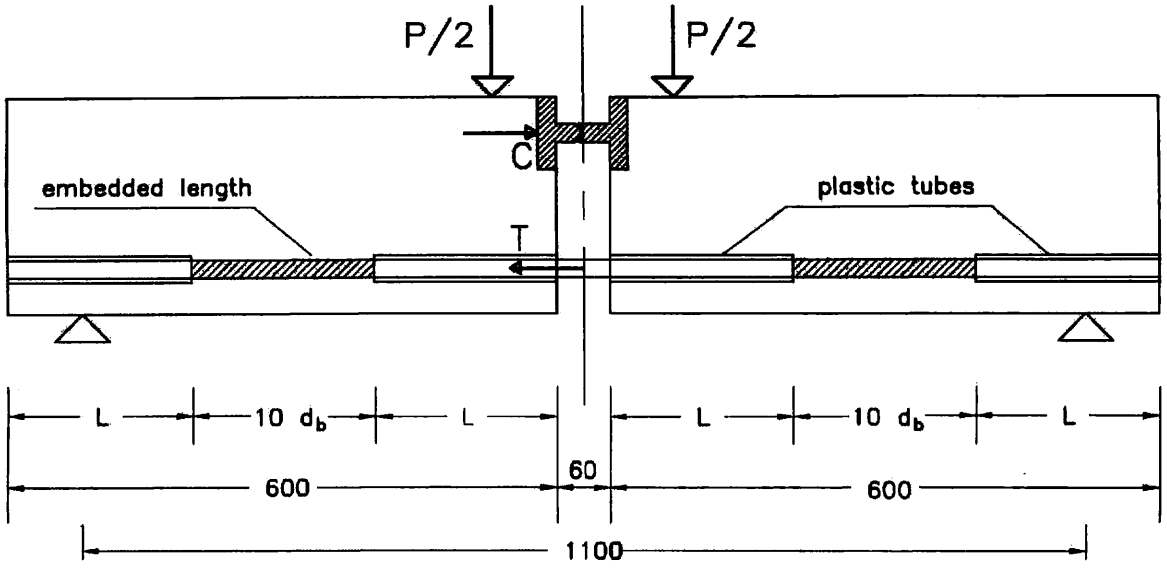

(a)

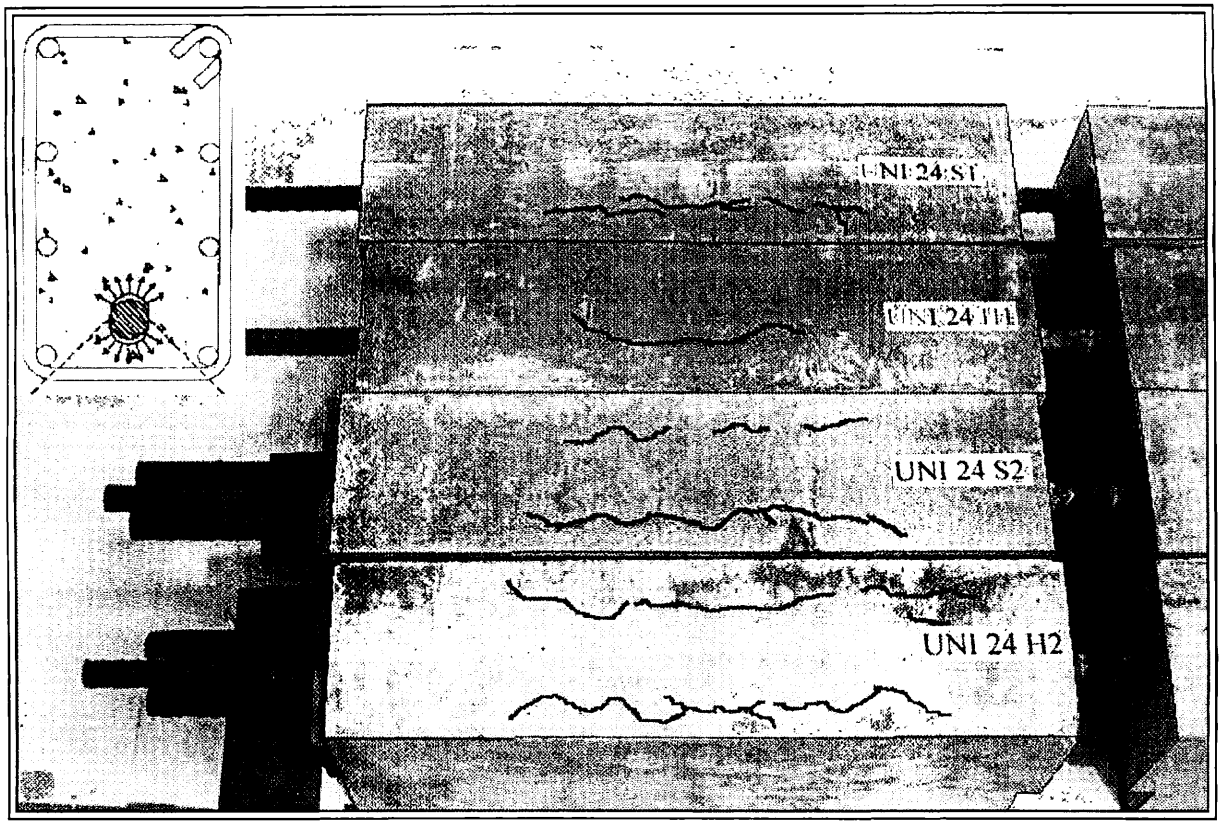

(b)

Fig. 1.1.23 – (a) Specimen geometry of the RILEM beam-test; and (b) hairlike splitting cracks along the bottom face of a beam-test specimen (d_b = 24 mm, Plizzari and Franchi, 1996).

The concise and certainly not complete presentation of the phenomenological aspects of bond makes it possible to recognize that bond models should always include in some way the following topics:

- the type of collapse (pull-out and splitting bond failure);
- the geometry of the reinforcement (relative rib area = bond index);

Copyright fib, all rights reserved. This PDF copy of fib Bulletin 10 is intended for use and/or distribution only by National Member Groups of fib.

- the type of loading (monotonic/cyclic loads; pulsating/reverse loads);
- the confining action (active/passive confinement);
- the size effects;
- the concrete type (HSC, NSC, FRC);
- the environment and its effects on bond (bar corrosion; high/low temperatures);
- the boundary restraints;
  and
- the specific requirements of PC structures.

Some of the above-mentioned aspects of bond are shown in Fig. 1.1.24.

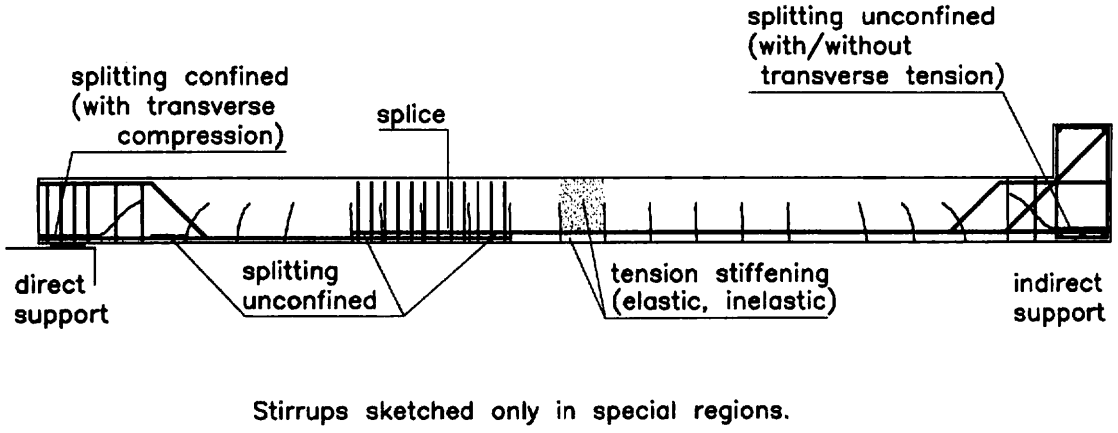

Fig. 1.1.24 - Typical bond problems in R/C beams.

In the following, bond modeling is introduced and dealt with according to a 5-step procedure: elastic materials (concrete and steel) and nonlinear interface, inelastic materials and nonlinear interface, transverse cracking effects, concrete splitting effects, and discrete modeling.

Copyright fib, all rights reserved. This PDF copy of fib Bulletin 10 is intended for use and/or distribution only by National Member Groups of fib.

1.2 Bond modeling for macroscopically uncracked concrete

The inclined compressive forces radiating from a ribbed bar are balanced by circumferential tensile stresses in the concrete surrounding the bar (Tepfers, 1979), and the failure of these rings in tension produces longitudinal cracking (splitting cracks). When concrete cover is large and/or a severe confining action is applied to the concrete surrounding the bar, splitting cracks do not reach the concrete surface, and there is no splitting failure. Consequently, the concrete appears macroscopically uncracked until the bond fails owing to bar pull-out, which is caused by the shearing-off of the concrete keys between the lugs of the bar.

Anchored bars in interior R/C beam-column joints are a typical example of severe confinement, because of the active confining action transmitted by the upper part of the column, and the passive confining action produced by the vertical reinforcement, as well as by the beams acting at right angles to the plane of the joint.

Under these circumstances, bond can be modeled by considering the concrete as a continuum and by introducing a bond stress-slip relationship at the interface.

The differential equations governing the behavior of a single bar embedded in concrete are summarized below, assuming axialsymmetry with respect to bar axis and neglecting the radial dimension.

- Reinforcing-bar equilibrium (Fig. 1.2.1):

$$A_s \frac{d\sigma_s}{dx} = -\Sigma_0 \tau(s) \tag{1.2.1}$$

where A_s = bar section; Σ_0 = reinforcing-bar circumference; σ_s = steel stress; and $\tau(s)$ bond stress as a function of relative slip s.

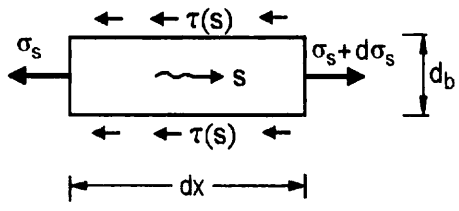

Fig. 1.2.1 - Stresses acting on a reinforcing bar (length dx).

- Strain-displacement relation (Fig. 1.2.2):

$$\varepsilon_s - \varepsilon_c = -\frac{ds}{dx} = -s' \tag{1.2.2}$$

where ε_s = steel strain; ε_c = average strain in the concrete embedment (strains caused by stretching are positive).

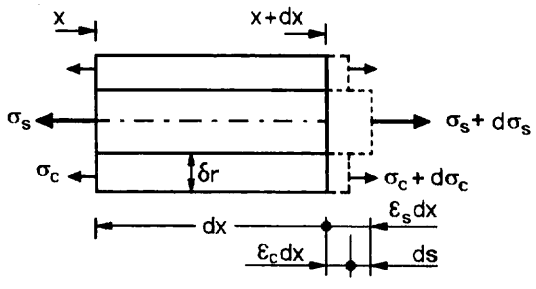

Fig. 1.2.2 - Stresses and strains in the bar and in the concrete layer (δ_r) alongside the reinforcement.

Copyright fib, all rights reserved. This PDF copy of fib Bulletin 10 is intended for use and/or distribution only by National Member Groups of fib.

- Reinforced-concrete equilibrium, or steel-to-concrete stress transfer (Fig. 1.2.3):

$$A_c \frac{d\sigma_{cm}}{dx} = -A_s \frac{d\sigma_s}{dx} \tag{1.2.3}$$

where A_c = concrete cross-section; and σ_{cm} = mean stress on concrete section A_c.

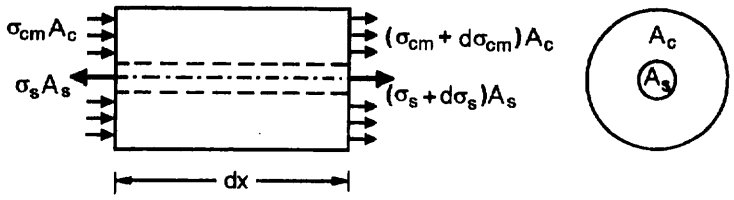

Fig. 1.2.3 - Forces acting on a reinforced-concrete element.

- Stress-strain (or constitutive) relationship for steel:

$$\sigma_s = \hat{\sigma}_s(\varepsilon_s) \tag{1.2.4}$$

- Stress-strain (or constitutive) relationship for concrete:

$$\sigma_c = \hat{\sigma}_c(\varepsilon_c) \tag{1.2.5}$$

where σ_c, ε_c = concrete stress and strain in the concrete embedment.

- Local bond stress-slip relationship:

$$\tau = \hat{\tau}[s(x)] \tag{1.2.6}$$

It should be observed that the bond stress-slip relation (Eq. 1.2.6) is strongly nonlinear for monotonic loading too. Consequently, non linear empirical expressions have been proposed by several authors (see Balázs, 1987):

1) Rehm (1961)

$$\tau = f_{c,cub} \cdot \left(\varphi \cdot s^{\alpha} \pm \psi \cdot s\right) \tag{1.2.7}$$

where $f_{c,cub}$ is the cube concrete-strength; and φ, ψ and α are theoretical or experimental constants.

2) Nilson (1968)

$$\tau = 998.4 \cdot s - 584 \cdot 10^2 \cdot s^2 + 852.2 \cdot 10^3 \cdot s^3 \tag{1.2.8}$$

3) Mirza - Houde (1979)

$$\tau = 539.8 \cdot s - 256.1 \cdot 10^2 \cdot s^2 + 592.2 \cdot 10^3 \cdot s^3 - 557.4 \cdot 10^4 \cdot s^4 \tag{1.2.9}$$

4) Martin (1973)

$$\tau = \tau_0 + c \cdot s^b \tag{1.2.10}$$

where τ_0 is the adhesion bond-stress; and c and b are experimental constants.

Copyright fib, all rights reserved. This PDF copy of fib Bulletin 10 is intended for use and/or distribution only by National Member Groups of fib.

5) Ciampi - Eligehausen - Bertero - Popov (1981, Fig. 1.2.4, monotonic loading)

$$\tau = \tau_1 \cdot \left(\frac{s}{s_1}\right)^{\alpha} \qquad 0 \le s \le s_1 \qquad (1.2.11)$$

followed by a plateau $\tau = \tau_1$ for $s_1 \le s \le s_2$, and by a linear decreasing branch starting from the point τ_2 - s_2 and leading to the value of the residual bond-resistance τ_3 at a slip value of s_3.

According to MC90 (ribbed bars, good bond conditions):

- Confined concrete: $s_1 = 1$ mm, $s_2 = 3$ mm, s_3=clear rib spacing, $\tau_1 = 2.5 f_{ck}^{1/2}$, $\tau_3 = f_{ck}^{1/2}$, $\alpha = 0.4$;
- Unconfined concrete: $s_1 = s_2 = 0.6$ mm, s_3=10 mm, $\tau_1 = 2.0 f_{ck}^{1/2}$, $\tau_3 = 0.3 f_{ck}^{1/2}$, $\alpha = 0.4$.

The above mentioned bond-stress-slip laws do not necessarily concern uncracked concrete. As a consequence, they have a more general validity than in the context assumed here. Moreover, the local bond-slip relation (Eq. 2.6) is a function of the loading history, as shown in Fig. 1.2.5 according to the model proposed by Eligehausen et al. (1983), and later improved by Filippou at al. (1983b).

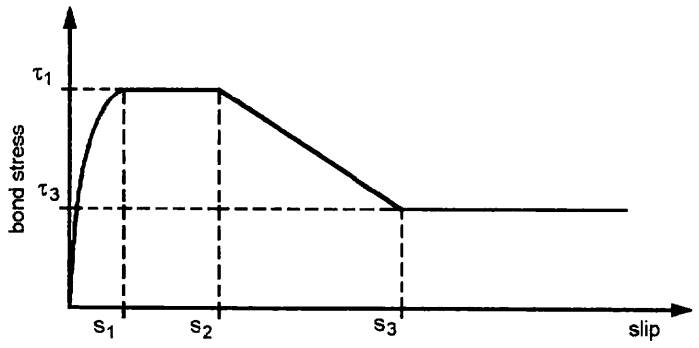

Fig. 1.2.4 - Analytical model for local bond stress-slip relationship (Ciampi et al., 1981; Eligehausen et al., 1983); monotonic loading.

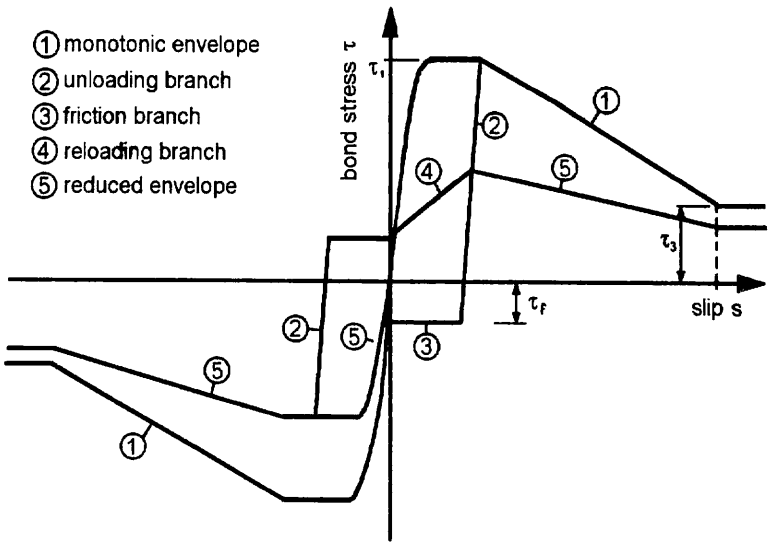

Fig. 1.2.5 - Hysteretic bond stress-slip model.

Copyright fib, all rights reserved. This PDF copy of fib Bulletin 10 is intended for use and/or distribution only by National Member Groups of fib.

6) Shima-Chou-Okamura (1987b)

$$\tau = f_c \frac{0.73\,[\ln(1+5000\,s/d_b)]^3}{1+\varepsilon_s\,10^5} \tag{1.2.12}$$

This model is a step forward since it applies also to the post-yield range, owing to the introduction of the local steel strain ε_s.

1.2.1 Elastic models with nonlinear interface

When the steel is in the elastic range, Eq. 1.2.4 becomes:

$$\sigma_s = E_s \cdot \varepsilon_s \tag{1.2.13a}$$

with E_s = Young's modulus of the reinforcing steel.

The relative bar-concrete slip consists of the elastic and the plastic deformations of the mortar under the ribs. The contribution of the elastic deformation is probably negligible (Rehm, 1961). However, since the analysis refers to the whole cylinder of area A_c (Fig. 1.2.3) whose behavior is predominantly elastic, the average stress-strain relationship for the concrete in the longitudinal direction is currently assumed to be linear and Eq. 1.2.5 has the following linear formulation:

$$\sigma_c = E_c \cdot \varepsilon_c \tag{1.2.13b}$$

where E_c is the concrete elastic modulus.

We do not know enough about the size of the loaded area A_c and about the distribution of the stresses (Rehm, 1961). However, the ratio of the mean stress σ_{cm} to the maximum concrete stress in the layer closest to the bar σ_c can be defined (Edwards and Picard, 1972) according to Eq. 1.2.14:

$$\psi = \frac{\int_{A_c} \sigma_c(r)\,dA_c}{A_c \sigma_{cm}} \tag{1.2.14}$$

where r = distance from the axis of the bar. Assuming ψ to be independent of x (Edwards and Picard, 1972; Jiang et al., 1984), Eq. 1.2.3 can be written as follows:

$$\psi \cdot A_c \frac{d\sigma_c}{dx} = -A_s \frac{d\sigma_s}{dx} \tag{1.2.15}$$

In a number of approaches (Viwathanatepa et al., 1979; Ciampi et al., 1982; Tassios and Yannopoulos, 1981; Filippou et al., 1983a, 1983b), the nonlinear equations representing equilibrium and compatibility are solved numerically taking into account the boundary conditions. Since these conditions are generally specified only at one extremity of the anchored bar, an iterative procedure (shooting technique) has been often adopted, because the unknown boundary condition at one extremity has to be guessed (Ciampi et al., 1981, 1982), in order to respect (after a few iterations) the already-known boundary condition at the other extremity. In all cases, the solution is reached by subdividing the bar in a number of linear elements and iteratively satisfying both equilibrium and compatibility at each node.

The derivation of Eq. 1.2.2, taking advantage of Eqs. 1.2.1 and 1.2.3, gives:

$$s'' - \chi \cdot \hat{\tau}[s(x)] = 0 \tag{1.2.16}$$

where $s'' = d^2s/dx^2$;

Copyright fib, all rights reserved. This PDF copy of fib Bulletin 10 is intended for use and/or distribution only by National Member Groups of fib.

$$\chi = (1+\xi)\cdot\frac{\Sigma_0}{A_s\cdot E_s} \tag{1.2.17}$$

$$\xi = \frac{n\cdot\rho}{\psi}, \qquad n = \frac{E_s}{E_c}, \qquad \rho = \frac{A_s}{A_c} \tag{1.2.18, 1.2.19, 1.2.20}$$

The differential equation of bond (Eq. 1.2.16), is very general and can be solved with any local bond stress-slip law; moreover when a local bond model consists of several branches (see Fig. 1.2.4), several solutions must be performed, each referring to a single relation representing a branch. For a linear, or constant, τ-s relation, the solution of Eq. 1.2.16 is very simple. However Eq. 1.2.11 is very appropriate for the first monotonic branch, up to maximum bond stress value. Hence, in the following Eq. 1.2.11 has been utilized, and the first integral of Eq. 1.2.16 is:

$$s' = \mp\sqrt{2(\gamma\cdot s^{1+a} + C)} \tag{1.2.21}$$

where the minus sign represents a tensile strain in the steel, C is an integration constant, and γ has the following expression:

$$\gamma = \chi\cdot\frac{\tau_1}{(1+\alpha)\cdot s_1^{\alpha}} \tag{1.2.22}$$

An early proposal (Rehm, 1961) with no concrete contribution ($\varepsilon_c = 0$) provides the solution by graphic integration of the first integral of Eq. 1.2.16, expressed here by Eq. 1.2.21. The parameter γ is a fundamental parameter of the bond problem that can be defined as "bond parameter". It takes into account both the mechanical and geometrical macro-characteristics of the materials affecting bond stress distribution along the bar (χ), and the micro-characteristics (i.e. the geometry of the surface deformations), affecting local bond behavior (τ_1, s_1,α).

The integration of Eq. 1.2.21 has been performed by a few scholars (see for instance Noakowski, 1980), with the objective of giving the slip an explicit or implicit formulation, as a function of x: $s = s(x)$ or $x = x(s)$. The implicit solution given by Russo et al. (1990) is recalled in the following:

$$x = B \mp \frac{1}{\sqrt{2\cdot C}}\cdot\sum_{k=0}^{\infty}\binom{-\frac{1}{2}}{k}\cdot\left(\frac{\gamma}{C}\right)^k\cdot\frac{s^{1+k(1+\alpha)}}{1+k(1+\alpha)} \tag{1.2.23}$$

for $-\left|\frac{C}{\gamma}\right|^{1/(1+\alpha)} < s \le \left|\frac{C}{\gamma}\right|^{1/(1+\alpha)}$

$$x = B \mp \frac{1}{\sqrt{2\cdot\gamma}}\cdot\sum_{k=0}^{\infty}\binom{-\frac{1}{2}}{k}\cdot\left(\frac{C}{\gamma}\right)^k\cdot\frac{s^{\frac{1-\alpha}{2}-k(1+\alpha)}}{\frac{1-\alpha}{2}-k(1+\alpha)} \tag{1.2.24}$$

for $\left|\frac{C}{\gamma}\right|^{1/(1+\alpha)} \le s$ or $s < -\left|\frac{C}{\gamma}\right|^{1/(1+\alpha)}$

where B is an integration constant.

It should be observed that if the integration constant C is zero, the solution of the differential equation 1.2.21 can be written in a closed form (Russo et al., 1989):

Copyright fib, all rights reserved. This PDF copy of fib Bulletin 10 is intended for use and/or distribution only by National Member Groups of fib.

$$s = \left[\mp \frac{1-\alpha}{2} \cdot \sqrt{2 \cdot \gamma} \cdot (x - B) \right]^{\frac{2}{1-\alpha}} \tag{1.2.25}$$

This case occurs when the $s(x)$ function exhibits a point with $s = 0$ and $s' = 0$.

Eq. 1.2.23 represents two convex functions $s(x)$, the former (negative sign) being a decreasing function, the latter (positive sign) an increasing function. The same holds for Eqs. 1.2.24 and 1.2.25, both representing concave functions.

By means of Eqs. 1.2.13, 1.2.18, 1.2.19 and 1.2.20, the integration of Eq. 1.2.15 provides the concrete strain:

$$\varepsilon_c = -\xi \cdot \varepsilon_s + D \tag{1.2.26}$$

where D is an integration constant.

All bond problems based on the assumption of perfect elasticity for both the reinforcement and the concrete, can be solved by means of the previous equations, and make it possible to obtain the distributions along the bar of several parameters (bar slip, concrete and steel strain and stresses). The integration constants B, C and D depend on the specific problem, which is exactly defined once the boundary conditions pertaining to both steel and concrete are specified.

Knowledge of the forces applied to steel and concrete end-sections, and that of the slip or strains or slip derivatives in some sections makes it possible to reach the solution $s(x)$ by using one or more of the six above-mentioned equations (Eqs. 1.2.23, 1.2.24 and 1.2.25).

In order to analyze a reinforced-concrete element in a typical loading condition, a qualitative prediction has to be made with regard to the possible behavior in terms of bar slip, and steel and concrete strain distributions along the element. In particular, the existence of a point or region with $s' = 0$ (R or RV, respectively, Figs. 1.2.7, 1.2.8, 1.3.4, and RS, Fig. 1.3.6) must be ascertained, since here both the steel strain and the concrete strain exhibit the same value, because of Eq. 1.2.2. Also, the existence of a point or region with no slip ($s = 0$) has to be ascertained. The occurrence of a region where $s = s' = 0$ allows the use of the closed-form solution (Eq. 1.2.25). In this way it is possible to understand what function or couple of functions (Eqs. 1.2.23, 1.2.24 and 1.2.25) are instrumental in working out the solution.

The formulation has been developed for the following typical bond problems: (a) bar pull-out, with the steel loaded at one end and the concrete in compression at the same end, (Fig. 1.2.6a); (b) bar push-in, with the steel and the concrete loaded at opposite ends, and the unloaded end of the bar flush with the concrete end (Fig. 1.2.6b). The bar is assumed to be elastic.

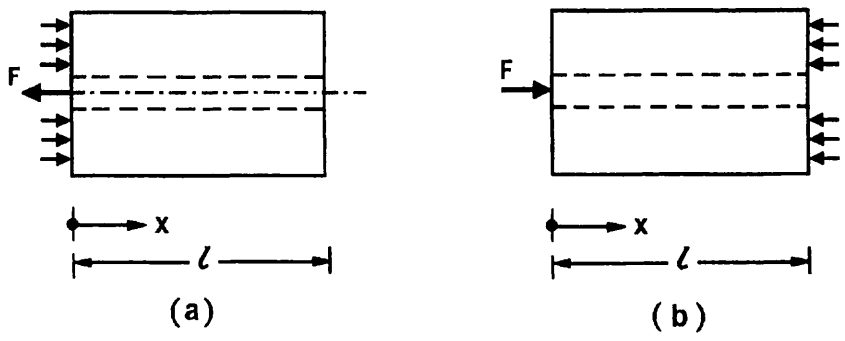

Fig. 1.2.6 - (a) Bar pull-out with concrete in compression; (b) bar push-in.

For each bond problem, two typical behaviors are possible, mostly related to the extent of the external forces and to the member length: (a) long-member behavior, or (b) short-member behavior.

Copyright fib, all rights reserved. This PDF copy of fib Bulletin 10 is intended for use and/or distribution only by National Member Groups of fib.

According to the long-member behavior, a portion of the anchorage is ineffective (Fig.1.2.7a), because of slip absence; in this case the slip distribution is provided in a closed form, by one or both of Eqs. 1.2.25.

According to the short-member behavior (Fig.1.2.7b), a finite slip occurs at any point of the reinforcing bar; in this case the solution is obtained by means of a series of functions (Eqs. 1.2.23 and 1.2.24).

For bond problem 1, the typical slip, steel and concrete strain distributions are shown in Figs. 1.2.7a and 1.2.7b, each referring to a possible behavior. It may be observed that both short-member or long-member behaviors exhibit a point R with s' = 0.

As for long-member behavior (Fig. 1.2.7a), the solution is provided by Eq. 1.2.25, while for short-member behavior the solution is provided by Eq. 1.2.24, both with a minus sign.

For bond problem 2, the typical slip, steel and concrete strain distributions are shown in Fig. 1.2.8.

For long-member behavior (Fig. 1.2.8a) the solution is provided by Eq. 1.2.25 with a minus sign in the region OR (Fig. 1.2.8a) close to the loaded end of the bar, and by Eq. 1.2.25 with a positive sign in the region VZ (Fig. 1.2.8a) close to the unloaded bar end.

As for short-member behavior, the solution is provided by Eq. 1.2.24 with a minus sign in the region OR (Fig. 1.2.8b) close to the loaded end of the bar, and by Eq. 1.2.24 with a positive sign in the remaining region (RZ in Fig. 1.2.8b).

Last but not least, it is necessary to note that, for macroscopically uncracked concrete (until bond failure), the anchorage lengths specified by most of the codes involve bar inelastic behavior before a pull-out or push-in failure.

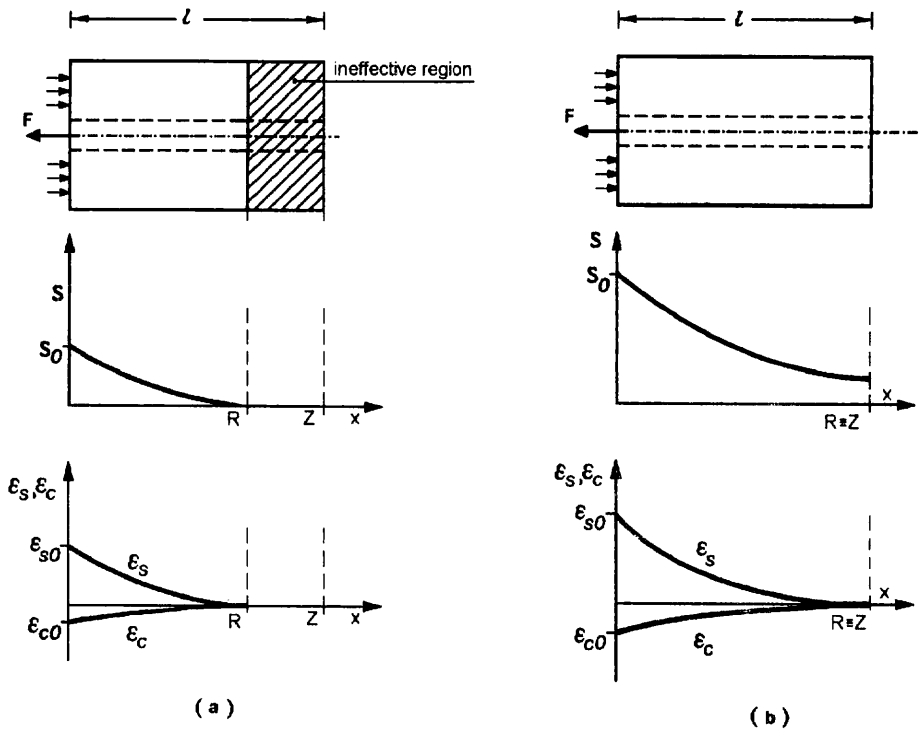

Fig. 1.2.7 - Typical slip and strain distributions for (a) long-member behavior and (b) short member behavior, in bar pull-out with concrete in compression (Russo et al., 1989a).

Copyright fib, all rights reserved. This PDF copy of fib Bulletin 10 is intended for use and/or distribution only by National Member Groups of fib.

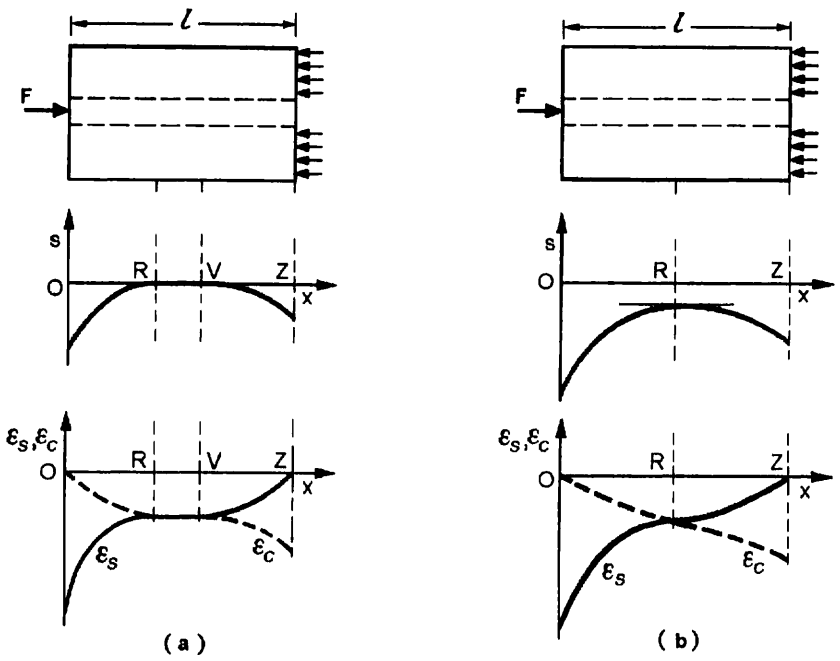

Fig. 1.2.8 - Typical slip and strain distributions for (a) long-member behavior and (b) short-member behavior, in a bar push-in (Russo and Romano, 1991).

1.2.2 Inelastic models with nonlinear interface

When the steel exceeds the yielding threshold, the slip tends to increase sharply (Eq. 1.2.2), wherever the bar is plasticized, even more since the bar section "shrinks" radially, owing to the Poisson effect, and the concrete confining action diminishes. Assuming a bilinear constitutive relationship for the reinforcement (Fig. 1.2.9), Eq. 1.2.4 becomes:

$$\sigma_s = E_s \cdot \varepsilon_s \quad \text{for } 0 \le \varepsilon_s \le \varepsilon_y \tag{1.2.27}$$

$$\sigma_s = \sigma_y + E_{sh} \cdot \left(\varepsilon_s - \varepsilon_y\right) \quad \text{for } \varepsilon_y \le \varepsilon_s \le \varepsilon_{su} \tag{1.2.28}$$

where E_{sh} = average modulus of the reinforcing steel in the inelastic domain; σ_y and ε_y = yield stress and corresponding steel strain, respectively; and ε_{su} = steel strain at stress peak ("ultimate strain").

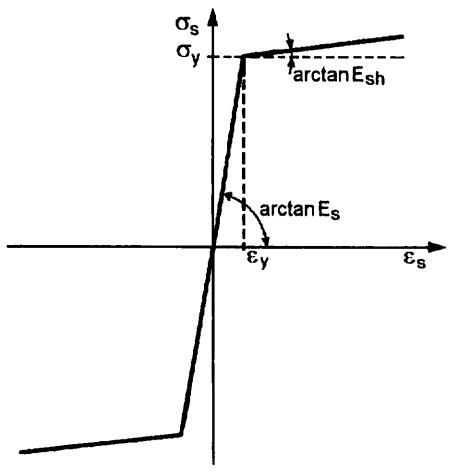

Fig. 1.2.9 - Bilinear constitutive relationship for the reinforcement.

Copyright fib, all rights reserved. This PDF copy of fib Bulletin 10 is intended for use and/or distribution only by National Member Groups of fib.

With regard to the regions where Eq. 1.2.28 applies to represent the steel behavior, Eq. 1.2.16 still holds, as do its first integral (Eq. 1.2.21) and its solution (Eqs. 1.2.23, 1.2.24 and 1.2.25), but χ and γ must be replaced with:

$$\chi_h = (1+\xi_h)\cdot\frac{\Sigma_0}{A_s\cdot E_{sh}} \tag{1.2.29}$$

$$\gamma_h = \chi_h\cdot\frac{\tau_1}{(1+\alpha)\cdot s_1^{\alpha}} \tag{1.2.30}$$

where

$$\xi_h = \frac{n_h\cdot\rho}{\psi}, \qquad n_h = \frac{E_{sh}}{E_c} \tag{1.2.31, 1.2.32}$$

The values χ and γ (see the Eqs. 1.2.17 and 1.2.22) are to be used in the region where the bar is elastic (E_s), while χ_h and γ_h (see the Eqs. 1.2.29 and 1.2.30) should be used in the region where the steel exceeds the yielding threshold, when the hardening modulus (E_{sh}) comes into play. Of course, the latter region (if any) is close to the loaded end section of the bar.

The most important bond problem where concrete appears macroscopically uncracked and steel attains the inelastic range occurs along the anchorage of beam bars inside an interior beam-column joint subjected to a seismic load. Because of the cyclic bending (Fig. 1.2.10) the beams adjoining the column may undergo through-cracking in the sections bordering the column, but the region affected by bond action turns out to be macroscopically uncracked, owing to the confinement action exerted by the column and the beams spanning in the transverse direction.

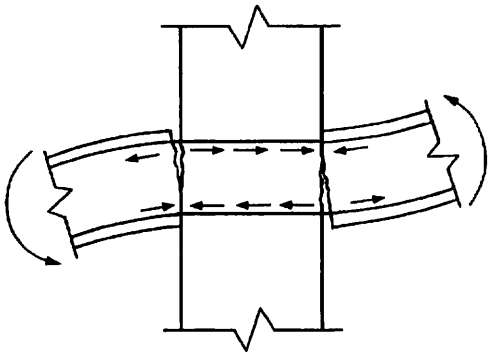

Fig. 1.2.10 - Interior beam-column joint under seismic action.

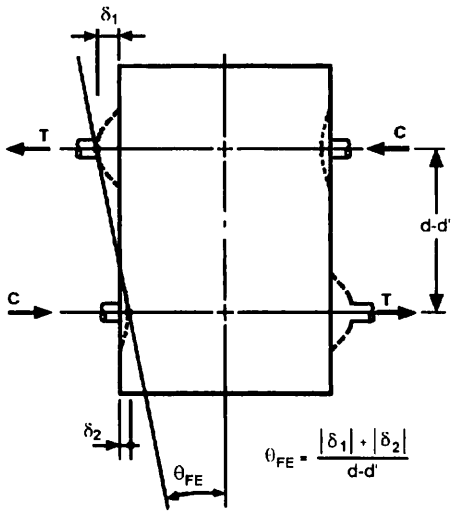

Fig. 1.2.11 - Fixed-end rotations (Viwathanatepa et al., 1979)

The cracks at the beam - column interface grow larger during exposure to severe seismic loading, because of cyclic bond deterioration, with concentrated rotations between the column and the adjoining beams ("fixed-end rotations", Filippou, 1986). These rotations are caused by the slip at the beam-column interfaces (Fig. 1.2.11) and may contribute up to 50% of overall deflections of a beam-column subassemblage (Soleimani et al., 1979).

The recommendations of the ACI - ASCE Committee 352 (1985) state that when modeling a frame structure for inelastic dynamic analysis, the slip of the reinforcing bars in interior joints should be considered. Then the bond problem of a bar running through a column, being pulled at one end and pushed at the other, arises.

Copyright fib, all rights reserved. This PDF copy of fib Bulletin 10 is intended for use and/or distribution only by National Member Groups of fib.

Since large inelastic deformations are likely to occur, the contribution of the concrete strains to the relative slip is negligible (Ciampi et al., 1981, 1982; Filippou et al., 1983a, 1983b, 1985, 1986). Thus Eq. 1.2.2 becomes:

$$\varepsilon_s = -\frac{ds}{dx} = -s'(x) \tag{1.2.33}$$

Eq. 1.2.33 is based on the assumption that concrete is a perfectly stiff material, which can transmit bond stresses with no strains ($\varepsilon_c = 0$, $E_c = \infty$).

Inside the joint, the bond conditions of the beam reinforcement vary along the embedment length, as is clearly shown in Fig. 1.2.12 (see the different stress-slip relationships, which depend on the actual confinement efficacy). Note that the concrete embedment is subject to tension in region 1, and to compression in region 2.

However, under generalized cyclic loading a bond stress-slip relationship in the unconfined concrete is still an open issue and a linear bond-stress distribution is considered adequate by several researchers (Filippou, 1986). This approximation bypasses the problem of defining a hysteretic bond stress slip-relationship for the unconfined concrete and provides excellent agreement with the finite element solutions (Filippou, 1986).

Under cyclic loading, bond deteriorates and the bond stress-slip relationship to be used depends on the accumulated damage (Eligehausen et al., 1983), i.e. on the local-slip history. At the same time, the maximum and frictional bond strengths (Fig. 1.2.5) reduce as the peak slip increases during cycling. However, for any region along the anchorage, the local law can be expressed (Fig. 1.2.5) by nonlinear (Eq. 1.2.11), linear, or constant local bond laws, the nonlinear case being the more complex.

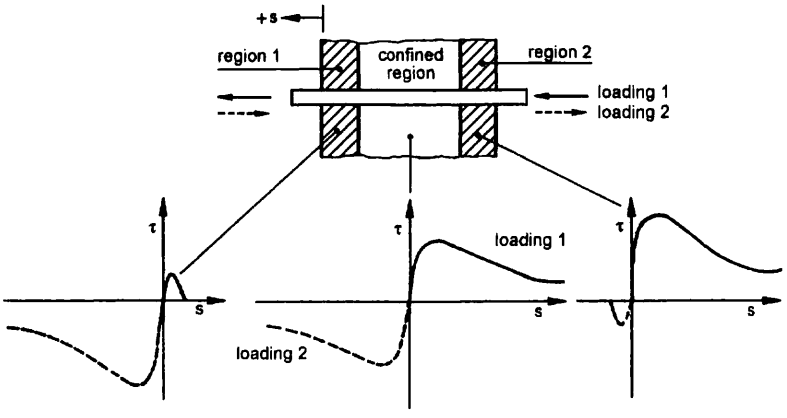

Fig. 1.2.12 - Bond stress-slip relationships under monotonic loading for different regions in a joint (Eligehausen et al., 1983).

The cyclic behavior of the reinforcing steel can be modeled (Filippou et al., 1983a) as suggested by Menegotto and Pinto (1973). The overall behavior of an anchored bar is not greatly influenced by the Baushinger effect, but depends primarily on both the yield stress and the slope of the strain-hardening branch (Ciampi et al., 1982). Therefore, a bilinear steel model can be used (Filippou et al., 1986).

The nonlinear steel and bond stress-slip laws lead to nonlinear equilibrium and compatibility differential equations (Eqs. 1.2.1, 1.2.2, 1.2.6) which can be solved by means of finite differences (Viwathanatepa et al., 1979; Ciampi et al., 1981, 1982) or finite elements (Filippou et al., 1983a, 1983b), see also Section 1.5. Other approaches utilize a piecewise linear approximation of the bond stress distribution (Filippou, 1985, 1986; Mukaddam and Kasti, 1986), or analytical solutions (Russo et al., 1990), or even a simulation technique based on discrete springs (Soroushian et al., 1991). In general, an iterative shooting technique is involved in order to satisfy the boundary conditions.

An example of the complex distributions of the main variables in the bond problem (relative slip, steel strain, steel stress and bond stress) is shown in Figs. 1.2.13 and 1.2.14, which refer to the bottom bars in a joint, subjected to several load reversals.

Copyright fib, all rights reserved. This PDF copy of fib Bulletin 10 is intended for use and/or distribution only by National Member Groups of fib.

The curves in Figs. 1.2.13 and 1.2.14 were obtained by Filippou et al. (1983a) to evaluate the effects that the reinforcing bar slip has on the response of a beam-column subassemblage subjected to a large number of load reversals, with gradually increasing deformations up to anchorage failure (point load N in Figs. 1.2.13 and 1.2.14). The theoretical response obtained by these authors agrees with the experimental results.

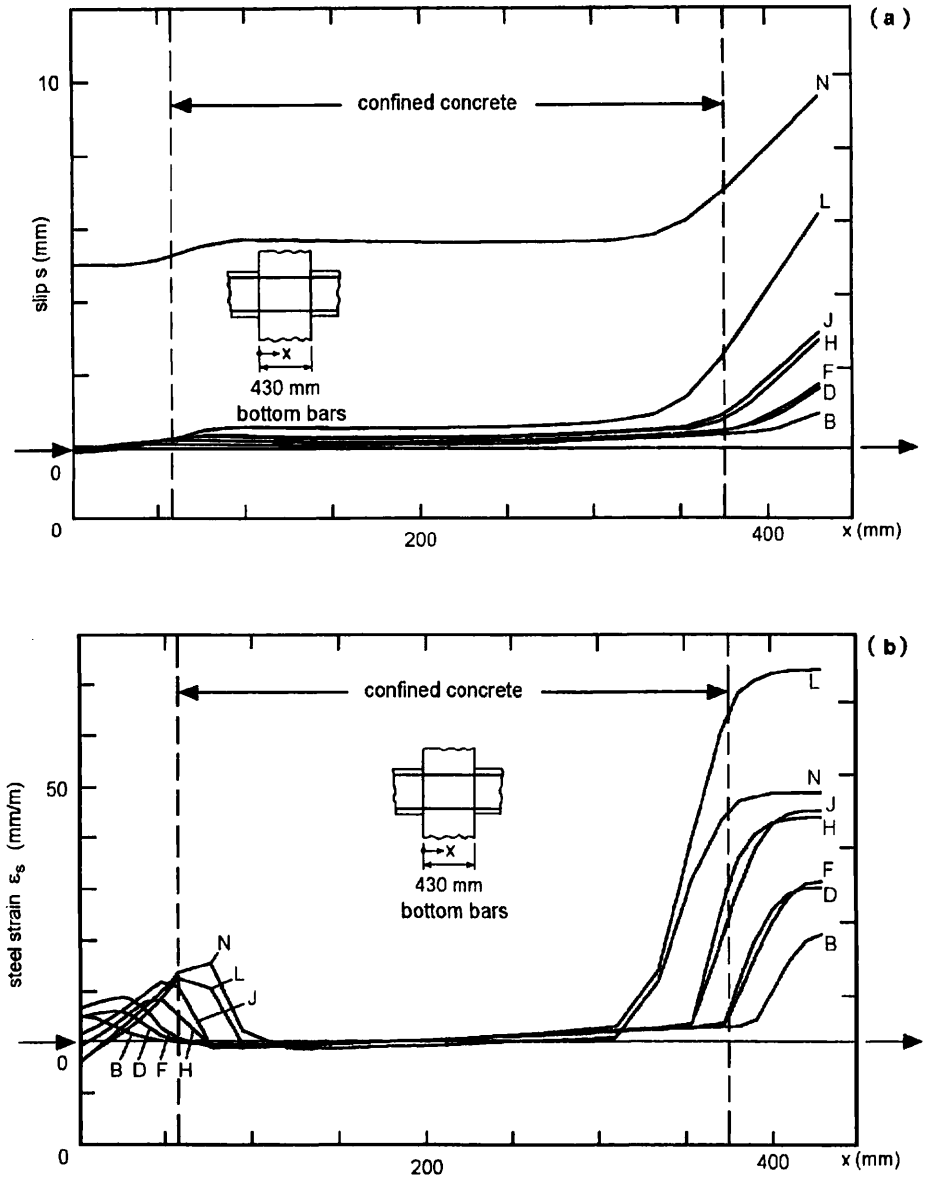

Fig. 1.2.13 - Distribution of (a) relative slip and (b) steel strain along the bottom bars of a joint, with increasing magnitude of the end slip (Filippou et al., 1983a). The bars are pulled at the right extremity and pushed at the left extremity.

The model based on the displacement method (Soroushian et al., 1991) involves (a) the preliminary discretization of the bar, the formulation of the tangent-stiffness matrix starting from the bond and steel stiffnesses of each spring-like element and (b) the use of an incremental solution algorithm with no iterations at each load step, but with many small steps.

The model based on the analytical solution obtained by Russo et al. (1990) requires the iterative shooting technique to satisfy the boundary conditions, but does not involve any preliminary discretization.

Copyright fib, all rights reserved. This PDF copy of fib Bulletin 10 is intended for use and/or distribution only by National Member Groups of fib.

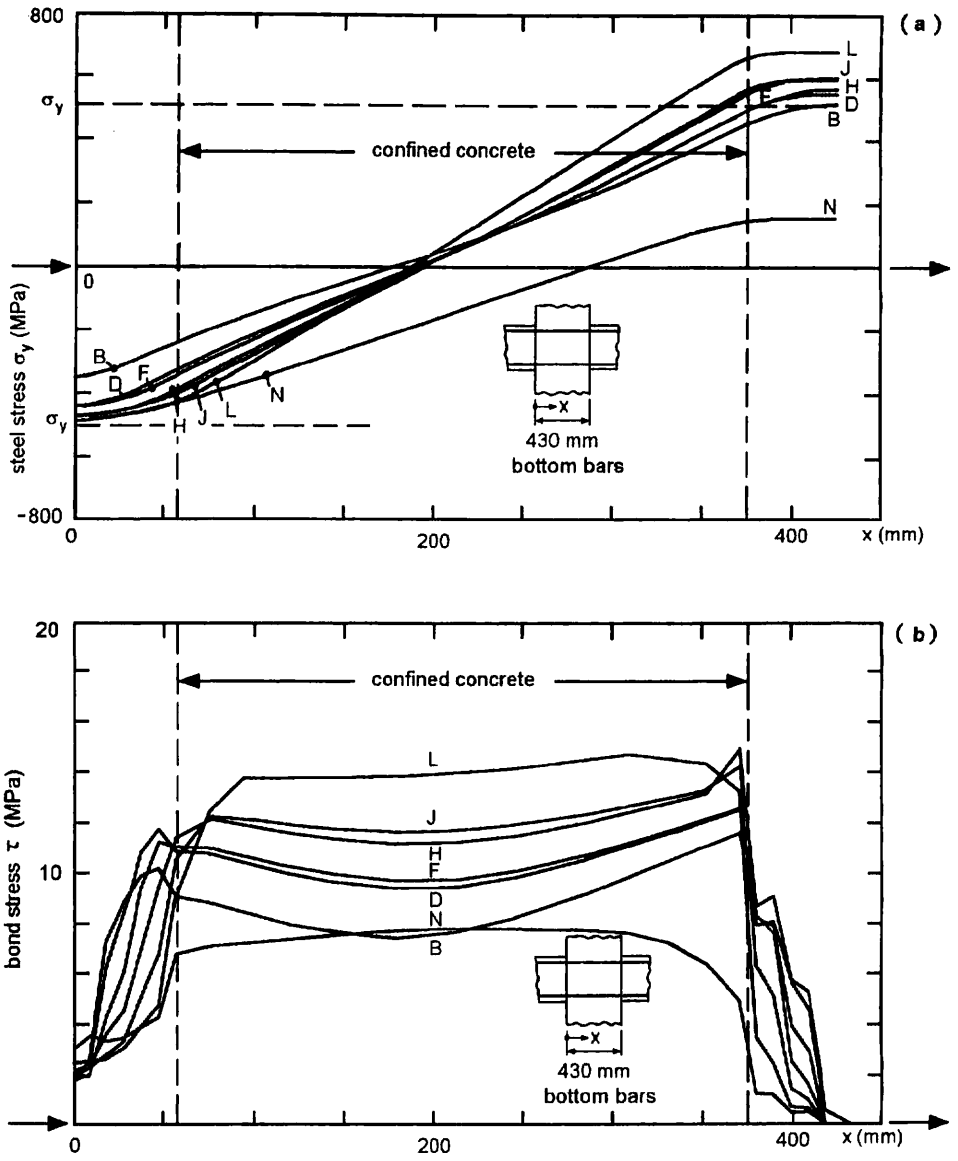

Fig. 1.2.14 - Distribution of the (a) steel stress and (b) bond stress along the bottom bars of a joint, with increasing magnitude of end slip (Filippou et al., 1983a).

Eligehausen et al. (1983) have shown that: (a) during cyclic loading bond strength and stiffness degradation depend primarily on the maximum value of peak slip in both directions reached in previous cycles; (b) applying a limited number of cycles (up to ten cycles) with bond stresses smaller than about 80 percent of the maximum bond resistance (τ_l in Fig. 1.2.5), does not significantly affect the bond stress-slip behavior at larger slip values. It follows that when the loads at bar ends are larger than those in the previous cycles, the monotonic $\tau(s)$ relationship can be used, in the portion of bar where s is lower than $s(0.8 - \tau_l)$ middle region of the joint - while some subdivision is to be made for the portion(s) of bar - near the column face(s) - where a slip $s > s(0.8\ \tau_l)$ was attained in the previous cycles.

It is worth noting that by utilizing the approximation introduced by Filippou (1986) for unconfined concrete, the analytical solution (Russo et al., 1990) does not usually involve the bar subdivision. The procedure for solving the bond problem is formulated as in an "initial-value" problem, using known values for both steel strain and slip at the loaded end (tension) and evaluating the slip values by means of an iterative process. Filippou's (1986) approximation leads to the following formulation:

Copyright fib, all rights reserved. This PDF copy of fib Bulletin 10 is intended for use and/or distribution only by National Member Groups of fib.

$$\tau(x) = \tau_C \cdot \frac{x}{x_C} \tag{1.2.34}$$

where C is the transition point between unconfined and confined concrete (Fig. 1.2.15).

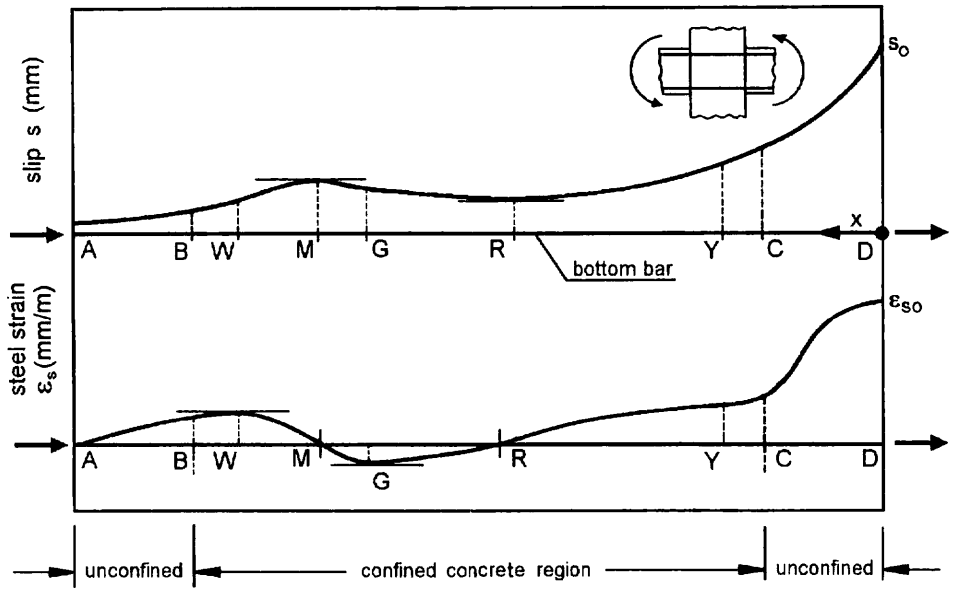

Fig. 1.2.15 - Qualitative distribution of bar-concrete slip and steel strain along a reinforcing bar inside a joint, at the end of a number of large-deformation reversals (Russo et al., 1990).

Substituting Eq. 1.2.34 into Eq. 1.2.16, their first integral provides the relation $\varepsilon_s(\tau_C, x)$ for the unconfined concrete and the following integral provides the relation $s(\tau_C, x)$ in a closed form (Russo et al., 1989b). The two integration constants are provided by the initial conditions ε_{s0} and s_0 (Fig. 1.2.15); afterwards the value of τ_C is obtained by enforcing the static admissibility in the common point between unconfined and confined concrete, i.e. by introducing Eq. 1.2.11 with $s = s_C$ in the $s(\tau_C, x)$ relation written at $s = s_C$ and $x = x_C$. The values $\varepsilon_s(x_C)$ and $s(x_C)$ are the initial-values for the confined concrete.

Eq. 1.2.24 (with a minus sign) has to be used for the portion of the anchorage where the slip decreases from the maximum value in tension at point C (Fig. 1.2.15) down to a minimum value s_R (R is the point where $s(x)$ is stationary). Wherever $\varepsilon_{sC} > \varepsilon_y$, Eq. 1.2.24 must be written both for the inelastic portion of the reinforcing bar (using χ_h) and for the elastic portion (using χ); similarly, Eq. 1.2.21 has to be written twice, with χ_h and χ.

Eq. 1.2.24 (with positive sign) has to be used for the portion of the anchorage where the slip increases from the minimum value s_R up to the point G that bounds the portion GB of the bar in the confined concrete where the yielding threshold has been exceeded in the previous half-cycle. In this portion, the steel stress and strain would have different sign and the analytical solution is linked to the cyclic behavior of the steel (Russo et al., 1990).

The integration constants appearing in the $s(x)$ relation are determined from the initial conditions and these - in turn - are obtained connecting the different displacement fields and by enforcing the kinematic admissibility in the common points ($\varepsilon_{left} = \varepsilon_{right}$, s_{left}, s_{right}).

A simplified approach has been proposed for both monotonic (Alsiwat and Saatcioglu, 1992) and cyclic loading (Saatcioglu et al., 1992). The slip of the anchorage end is computed as a result of both bar extension and interface slippage. The extension of the reinforcement is the result of the strain accumulation along the bar. A piecewise linear strain distribution is assumed along the embedded bar, with different slopes in the elastic, plastic and hardening regions. A constant bond stress along the elastic length and a constant frictional bond stress along the plastic length are assumed. For a

Copyright fib, all rights reserved. This PDF copy of fib Bulletin 10 is intended for use and/or distribution only by National Member Groups of fib.

reinforcing bar loaded at only one end, the rigid body slippage occurs when the embedment length of the bar is not sufficient to allow the strain to become zero. For a reinforcing bar loaded at both ends, the compressive force contributes to bar slippage. In both cases, the slip component is determined from the input of the bond stress value in a nonlinear relationship analogous to Eq. 1.2.11, which is a modified version of Ciampi's relationship (Ciampi et al., 1981).

Copyright fib, all rights reserved. This PDF copy of fib Bulletin 10 is intended for use and/or distribution only by National Member Groups of fib.

1.3 Bond modeling for transversely-cracked concrete

In reinforced-concrete members subjected to tensile forces, primary cracks (Fig. 1.3.1) - at roughly right angles to the element axis (transverse cracking) - can form if the concrete stress reaches the tensile strength f_{ct} in the cross section. The tensile stresses in the concrete are attributable to the load transfer from the steel to the concrete, via bond action.

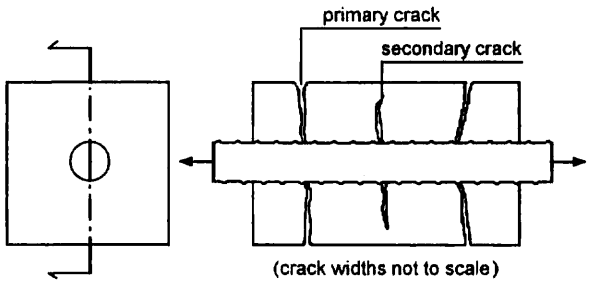

Fig. 1.3.1 - Primary and secondary cracks in a reinforced-concrete member in tension (ACI, 1986).

Since the concrete strain ε_c depends on the steel strain through bar-concrete slip (Eq. 1.2.2), it follows that the analysis of transverse cracking in concrete has to be based on bond modeling, taking advantage of the models mentioned in the previous sections (Eqs. 1.2.1 to 1.2.6 and 1.2.11 to 1.2.32) and on the control of concrete strain in tension.

As already mentioned, the local bond stress-slip relationship for R/C members with concrete subjected to tension exhibits a much lower bond strength than in the case of concrete in compression, and the same occurs for the slip value at stress-peak. However, the local bond stress-slip behavior in tension (Dörr, 1978) can be expressed by means of a nonlinear relationship with the same form as Eq. 1.2.11 (Russo and Romano, 1992), where the values τ_1 and s_1 (Fig. 1.3.2) are lower than in pull-out tests with concrete in compression.

A typical problem where the concrete is subjected to tension is represented by bar pull-out, with the steel and the concrete loaded in tension at opposite ends, and the unloaded end of the bar completely embedded in the concrete (Fig. 1.3.3). The cohesion between the concrete and the embedded end of the bar is neglected.

This bond problem is very similar to bond problem 2 (Section 1.2.1, bar push-in, Fig. 1.2.6b), since the boundary conditions (steel and concrete strains) relevant to bar ends are the same as in problem 2, while the signs are different (Russo et al., 1991). The solution changes accordingly.

The typical slip, steel and concrete strain distributions are shown in Fig. 1.3.4. The free end of the bar acts as a crack initiator across the tension zone (Park and Paulay, 1975) and, here, (point Z, Fig. 1.3.4) ε_c reaches its maximum value, whatever the behavior is. When $\varepsilon_c = \varepsilon_{ct}$, where ε_{ct} is the concrete cracking strain, a transverse crack appears but since cracking is not controlled, the fracture process spreads abruptly across the whole section.

The most typical problem where concrete appears transversely-cracked is represented by a reinforced-concrete member subjected to uniaxial tension (Fig. 1.3.5). Only a half-member is analyzed here, because of symmetry.

As already mentioned, for a R/C tension member (Fig. 1.3.5), traditionally two typical behaviors are referred to in the literature (uncracked stage): long-member behavior, and short-member behavior (Fig. 1.3.6).

Copyright fib, all rights reserved. This PDF copy of fib Bulletin 10 is intended for use and/or distribution only by National Member Groups of fib.

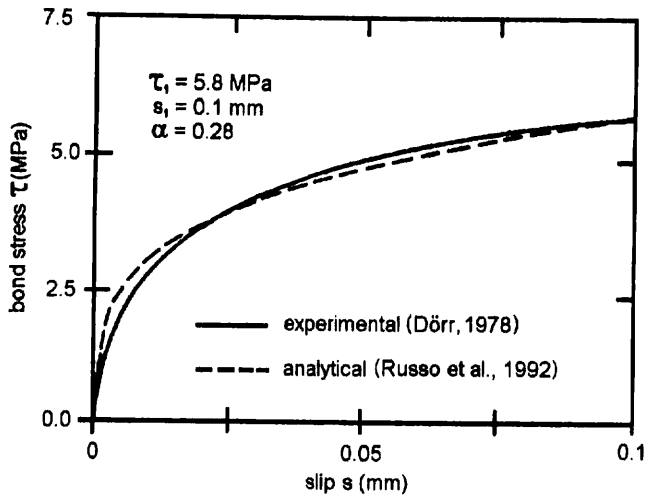

Fig. 1.3.2 - Experimental and analytical bond stress-slip relationships for tension test (Russo and Romano, 1992).

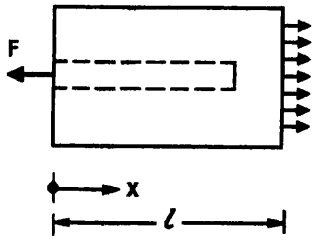

Fig. 1.3.3 - Bar pull-out with concrete in tension.

In the former case, the bond efficiency and the anchorage length favor load transmission between the bar and the concrete, with the formation of an extended region characterized by uniform and equal strains in both steel and concrete, with no bar slip (RS, Fig. 1.3.6a). On the contrary, in short members, the strains in the bar and in the concrete are never identical ($\varepsilon_s > \varepsilon_c$) and bar slip is zero only in the mid-span section, owing to symmetry.

Provided that the reference axis is chosen as in Fig. 1.3.5 and assuming, for the sake of simplicity, that the bar remains elastic, the solution for long-members is provided in a closed form by Eq. 1.2.25 with a minus sign.

The slip of the loaded end, s_0, is given by (Russo and Romano, 1992):

$$s_0 = \left(\frac{\varepsilon_{s0}^2}{2 \cdot \gamma} \right)^{\frac{1}{1+\alpha}} \tag{1.3.1}$$

where ε_{s0} is the steel strain at the loaded end.

The abscissa of the point with $s = 0$ and $s' = ds/dx = 0$ (R, Fig. 1.3.6a) is:

$$x_R = \frac{2}{1-\alpha} \cdot \left[\varepsilon_{s0} \cdot \left(\frac{1}{2 \cdot \gamma} \right)^{\frac{1}{1-\alpha}} \right]^{\frac{1-\alpha}{1+\alpha}} \tag{1.3.2}$$

Copyright fib, all rights reserved. This PDF copy of fib Bulletin 10 is intended for use and/or distribution only by National Member Groups of fib.

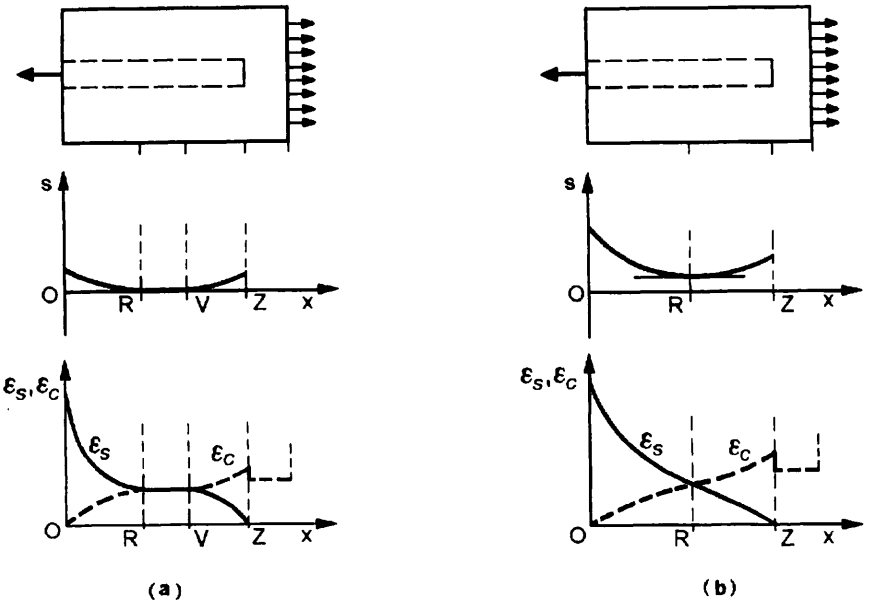

Fig. 1.3.4 - Typical slip and strain distributions for (a) long-member and (b) short-member, in bar pull-out with concrete in tension (Russo and Romano, 1991).

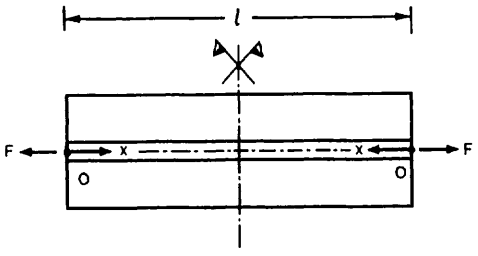

Fig. 1.3.5 - Reinforced-concrete member subjected to uniaxial tension.

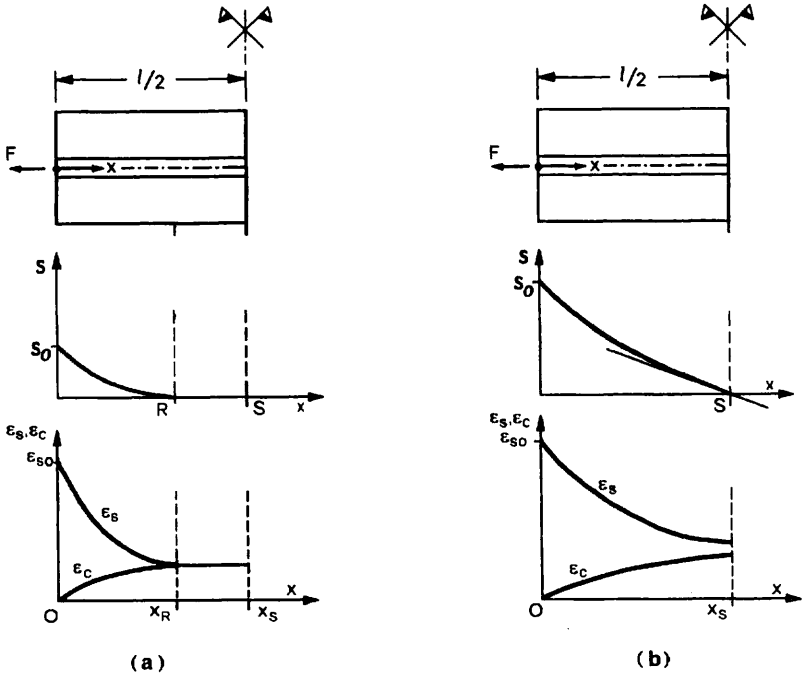

Fig. 1.3.6 - Typical slip and strain distributions in a R/C member subjected to uniaxial tension: (a) long-member behavior and (b) short-member behavior (Russo and Romano, 1992).

Copyright fib, all rights reserved. This PDF copy of fib Bulletin 10 is intended for use and/or distribution only by National Member Groups of fib.

The embedment length x_R required to satisfy the condition of equality between the strain in the steel and that in the concrete has been called "transfer length" (L_t) by Somayaji and Shah (1981). In section R (Fig. 1.3.6a) the maximum concrete strain of a long-member is:

$$\varepsilon_{c\,max,l} = \frac{\xi}{1+\xi} \cdot \varepsilon_{s0} \tag{1.3.3}$$

The load (P_{tran}) transferred from the steel to the concrete along the length x_R is:

$$P_{tran} = A_c E_c \psi \varepsilon_{c\,max,l} \tag{1.3.4}$$

P_{tran} can be expressed as a function of the load applied to the bar end, by means of Eq. 1.3.3.

In order to have a long-member behavior, the steel strain at the loaded end must fulfill the condition $\varepsilon_{s0} \leq \varepsilon_{s0l}$. For $x_R = l/2$, Eq. 1.3.2 provides the upper-limit for the steel strain value at the loaded bar end, ε_{s0l}, beyond which a "short member" behavior occurs:

$$\varepsilon_{s0l} = (2 \cdot \gamma)^{\frac{1}{1-\alpha}} \cdot \left[\frac{(1-\alpha) \cdot l}{4}\right]^{\frac{1+\alpha}{1-\alpha}} \tag{1.3.5}$$

In short members, the slip distribution is obtained by means of Eq. 1.2.23 with a minus sign (Case a) when s fulfills the following condition:

$$s < \left(\frac{C}{\gamma}\right)^{\frac{1}{1+\alpha}} \qquad \text{for } 0 \leq x \leq \frac{l}{2} \tag{1.3.6}$$

or by means of Eqs. 1.2.23 and 1.2.24 (with a minus sign, Case a), when the slip values do not satisfy the limitation in Eq. 1.3.6 along the member.

The slip s_0 has to be determinated iteratively on the basis of Eq. 1.2.23, in the Case a or of Eqs. 1.2.23 and 1.2.24 in the Case b.

The maximum concrete strain of a short-member occurs in the symmetry section S (Fig. 1.3.6b), and is a function of the slip s_0.

1.3.1 Transient cracking

The progressive cracking of a previously-uncracked member is analyzed here, on the assumption that the load is monotonically increasing.

For low values of the load and of the steel strain at the loaded end (ε_{s0}), the slip vanishes before reaching the symmetry axis (as in long members). The element will not crack, because $\varepsilon_{cR} < \varepsilon_{ct}$ where ε_{cR} is the value of ε_c at point R with $s' = 0$ and $\varepsilon_c = \varepsilon_{cmax}$ (Fig. 1.3.6 a). Any increase of the load moves the point R toward the symmetry section and ε_{cR} increases.

A further load increase may produce two different member responses:

(a) It may occur that the concrete strain attains the cracking value at a point R with $x_R \leq l/2$. In this case $x_R = x_{Rcrack}$ where x_{Rcrack} is the distance of the crack from the loaded end. The first primary cracks form, and the member is subdivided into m smaller parts (Fig. 1.3.7), with m being the first integer number not lower than l/x_{Rcrack}. It follows that the length l_p of a single part (between two contiguous cracks or between the first/last crack and the closest end-section) falls between a minimum length x_{Rcrack} and a maximum length ($l/\ x_{Rcrack}$ - m + 1) x_{Rcrack}, the average (most probable) length being l/m. This case can be defined as cracking of a long-member.

(b) On the contrary, it may occur that the point R reaches the symmetry axis ($x_R = l/2$) with the concrete strain still being smaller than ε_{ct}. In order to cause the member to crack, a greater load

Copyright fib, all rights reserved. This PDF copy of fib Bulletin 10 is intended for use and/or distribution only by National Member Groups of fib.

should be applied to the bar end to increase concrete strains. With increasing the load the maximum concrete strain ε_{cmax} which occurs at mid-span (Fig. 1.3.6b), will increase, since x_R cannot increase beyond $l/2$ because of the symmetry. Consequently the first primary crack forms, at the symmetry section, when ε_{cmax} reaches the value ε_{ct}. It follows that at cracking the member is subdivided into two parts whose length is $l/2$ (Fig. 1.3.8). This case can be defined as cracking of a short-member.

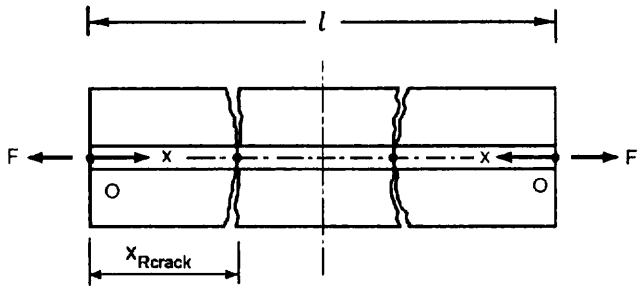

Fig. 1.3.7 - Cracking in a long-member.

In the Case (a) the steel strain at the loaded end which brings the member to the onset of cracking is:

$$\varepsilon_{s0crack} = \left(1 + \frac{1}{\xi}\right) \cdot \varepsilon_{ct} \tag{1.3.7}$$

The condition

$$\varepsilon_{s0crack} \leq \varepsilon_{s0l} \tag{1.3.8}$$

guarantees that cracking of the member will occur, when the load increases, before x_R reach $l/2$.

In this case the behavior is as a long-member up to first cracking and x_{Rcrack} is provided by

$$x_{Rcrack} = \frac{2}{1+\alpha} \cdot \left[(1+\xi) \cdot \left(\frac{1}{2 \cdot \gamma} \right)^{\frac{1}{1-\alpha}} \cdot \varepsilon_{ct} \right]^{\frac{1-\alpha}{1+\alpha}} \tag{1.3.9}$$

In the Case (b) $\varepsilon_{s0l} > \varepsilon_{s0crack}$ and the behavior is as short-member from first cracking which makes only one crack, at the symmetry section.

After the formation of the first primary crack(s), a second-generation of primary cracks occurs, for a somewhat higher load level. Before this second generation each part is in a load situation similar to the one of the original (uncracked) member but with smaller length.

A part originating from first cracking of a "long" member has a length l_p satisfying the condition

$$x_{Rcrack} \leq l_p < 2x_{Rcrack} \tag{1.3.10}$$

Since x_{Rcrack} does not depend on element length (Eq. 1.3.8), the value of x_{Rcrack} relevant to the part does not change any more even if the load is increased. Consequently, considering that the upper-limit condition in Eq. 1.3.10

$$x_{Rcrack} > \frac{l_p}{2} \tag{1.3.11}$$

it can be stated that a part originating from the previous cracking of a "long" member may crack only in its symmetry section.

Copyright fib, all rights reserved. This PDF copy of fib Bulletin 10 is intended for use and/or distribution only by National Member Groups of fib.

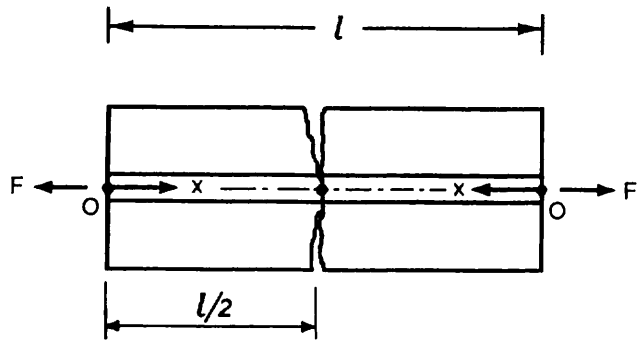

Fig. 1.3.8 - Cracking of a short-member.

Conversely, after the mid-span cracking of a "short member", the two remaining parts have obviously a "short-member" behavior, since their length l_P is lesser than the length x_{Rcrack}, which does not depend on the actual length l of the structural element (Eq. 1.3.9).

The previous considerations lead to the conclusion that under monotonically increasing loads, after the first generation of primary cracks, further cracks can occur only by cracking each single part at mid-span, provided that the spacing of the first-generation cracks is at least twice as large as the bond-transfer length. Of course this statement is valid on condition that the material is homogeneous, which is not the case for concrete, whose physical and mechanical properties have a not negligible scattering.

1.3.2 Stabilized cracking

A stabilized crack pattern is attained when the length of a single part is no longer sufficient to allow the concrete strain to reach the failure value in tension ε_{ct} at mid-span, whatever the increase of ε_{s0}.

Since the strain ε_{cmax} depends on the slip at the loaded end s_0 (which is the main unknown), the minimum distance between the cracks is determined by analyzing the progressive cracking of the member and its subdivision into smaller parts.

On the other hand, because of the stochastic variability of the tensile strength along the length of a tension member, not all cracks form at the same load level (ACI Committee 224, 1986). Clark and Spiers (1978) estimated that the first major crack forms at about 90 percent of the average concrete tensile strength and the last major crack at about 110 percent of the average tensile strength.

Furthermore, it is well known that the uniaxial tensile strength of concrete is influenced by specimen length (Kadlecek and Spetla, 1967; Komlos, 1969), and increases when the slenderness ratio decreases (Spetla and Kadlecek, 1966), owing to size effect (Walraven, 1995).

Additional primary cracks are likely to form at a later stage, before reaching the ultimate load (Broms and Lutz, 1965) until the crack spacing becomes approximately twice the cover thickness measured from the center of the reinforcing bar.

Finally it should be mentioned that other approaches for crack modeling of a tension member are available in the literature, such as those based on (a) finite elements (Bresler and Bertero, 1968; Keuser and Mehlhorn, 1987), (b) analytical expressions (Rehm, 1961; Edwards and Picard, 1972; Balázs, 1993), (c) piecewise linearizations of the local bond-slip relationship (Tassios and Yannopoulos, 1981; Lee et al., 1987; Yannopoulos and Tassios, 1991) and (d) specific functions representing the bond-stress distribution (Somayaji and Shah, 1981).

1.3.3 Tension-stiffening

In a reinforced concrete member loaded in tension the tensile force is resisted by both the reinforcing steel and the surrounding concrete because the bond stresses allow the load transfer between the bars and the embedment. Only across a crack is the load carried entirely by the reinforcement.

Copyright fib, all rights reserved. This PDF copy of fib Bulletin 10 is intended for use and/or distribution only by National Member Groups of fib.

Consequently the strains in a bar embedded in concrete are smaller than those in a naked bar, at all stress levels. The decrease in steel strain due to the concrete may be considered as a stiffness increase of the reinforcement compared to the naked bar. Therefore this bond-related phenomenon is called "tension-stiffening" (see for instance Giuriani, 1982).

The overall elongation of a naked bar is

$$\Delta l_0 = \varepsilon_{s0} \cdot l \tag{1.3.12}$$

The overall elongation of a bar embedded in a concrete member subject to uniaxial tension (Fig. 1.3.5) is:

$$l = 2\int_0^{l/2} \varepsilon_s dx \tag{1.3.13}$$

By using the above-mentioned analytical model, the elongation Δl has the following expression (Russo and Romano, 1992):

$$\Delta l = \frac{\xi \cdot \varepsilon_{s0} \cdot l + 2 \cdot s_0}{1+\xi} \tag{1.3.14}$$

The overall equivalent shortening of the bar due to concrete restraining action (Δl_c) is:

$$\Delta l_c = \Delta l_0 - \Delta l \tag{1.3.15}$$

Hence, the relative contribution of the concrete to the overall stiffness of the member can be defined (Bresler and Bertero, 1968) as follows:

$$\lambda = \frac{\Delta l_c}{\Delta l_0} \tag{1.3.16}$$

The parameter λ is an index of tension-stiffening effectiveness. The greater the value of λ, the more effective the stiffness contribution of the concrete becomes.

Eqs. 1.3.12, 1.3.14 and 1.3.15 make it possible to formulate λ on the basis of Eq. 1.3.16:

$$\lambda = \frac{1}{1+\xi} \cdot \left(1 - \frac{2s_0}{\varepsilon_{s0} \cdot l}\right) \tag{1.3.17}$$

Eq. 1.3.17 shows that tension-stiffening effectiveness is (a) a decreasing function of the width of the primary cracks ($w=2\ s_0$, where s_0 is the bar slip at the loaded end), and (b) an increasing function of both the element length and of the actual steel strain in the cracked sections.

The stiffening effect of the concrete between two contiguous cracks can also be explained by considering the relationship between the load and the average strain in both the uncracked and cracked states. A typical tensile stress-versus-strain diagram is shown in Fig. 1.3.9, where ε_{sm} is the average steel strain of the embedded reinforcement and σ_{scr} is the steel stress in a section when a primary crack forms (first cracks).

The relative slip is not taken into account in the uncracked stage (initial linear branch up to first cracking), where the tensile force is transferred partly to the reinforcement and partly to the concrete, depending on their stiffness.

Both the slip and the primary cracks are introduced indirectly (through smearing) in the subsequent nonlinear branch. Starting from point A, a relationship can be developed between the steel stress and the average strain of the embedded reinforcement ε_{sm} (that is equal to the average strain in the member ε_{cm}), as

Copyright fib, all rights reserved. This PDF copy of fib Bulletin 10 is intended for use and/or distribution only by National Member Groups of fib.

$$\sigma_s = E_{sef} \cdot \varepsilon_{sm} \tag{1.3.18}$$

where E_{sef} is the effective modulus of elasticity of the steel bar (Fig. 1.3.9).

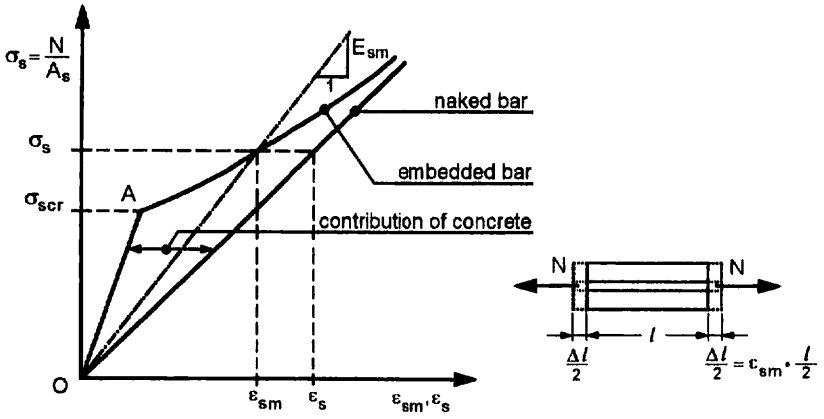

Fig. 1.3.9 - Tension stiffening: tensile stress versus (mean) tensile strain.

Several methods can be used to determine ε_{sm}. The Eurocode N.o 2 (1991) gives

$$\varepsilon_{sm} = \frac{\sigma_s}{E_s} \cdot \left[1 - \beta_1 \cdot \beta_2 \cdot \left(\frac{\sigma_{scr}}{\sigma_s} \right)^2 \right] \tag{1.3.19}$$

where β_1 and β_2 take into account the bond characteristics (β_1 = 1 for ribbed bars, = 0.5 for smooth bars) and the nature of the loads (β_2 = 1 for short-term loads, = 0.5 for long-term or repeated loads).

From Eq. 1.3.18 and 1.3.19 we have

$$E_{sef} = \frac{E_s}{1 - \beta_1 \cdot \beta_2 \cdot \left(\frac{\sigma_{scr}}{\sigma_s} \right)^2} \tag{1.3.20}$$

CEB-FIP Model Code 90 (1993) defines the following stages: uncracked concrete, crack formation, stabilized cracking (in which only crack widening occurs) and post-yielding, Fig. 1.3.10. Accordingly, a modified stress-strain (σ_s-ε_{sm}) relation of the embedded reinforcement has been proposed (Fig. 1.3.10), for modeling the tension-stiffening effect.

The transition from the pre-cracked stage (a) to the post-cracked stage (b) has been recently investigated by Fantilli et al. (1998a), who focused their attention on the descending branch after first cracking (Fig. 1.3.11), taking into account the cohesive stresses in cracked concrete. It turned out that the smaller the bar diameter, the steeper the descending branch. The authors proposed also a minimum reinforcement ratio (ρ_{min}) in order not only to avoid brittle failures, but also to limit crack width under the service loads.

Alternatively, ACI Committee 224 (1986) introduces the effective stiffness of a R/C member in terms of concrete modulus of elasticity and effective (reduced) area. This approach is similar to the "effective moment of inertia" concept adopted by ACI for the evaluation of the deflections in R/C members.

The effects that concrete splitting has on tension stiffening in R/C members were investigated also by Abrishami and Mitchell (1996). These effects were found to be significant, and a method for modeling tension stiffening, with both transverse and splitting cracks, was proposed.

Copyright fib, all rights reserved. This PDF copy of fib Bulletin 10 is intended for use and/or distribution only by National Member Groups of fib.

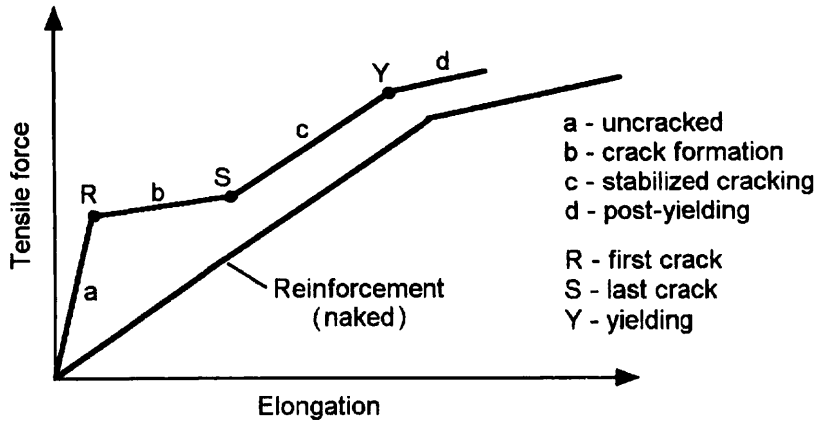

Fig. 1.3.10 - Idealized behavior of a R/C tension member (CEB-FIP Model Code 90, 1993, see also Shima et al., 1987 b).

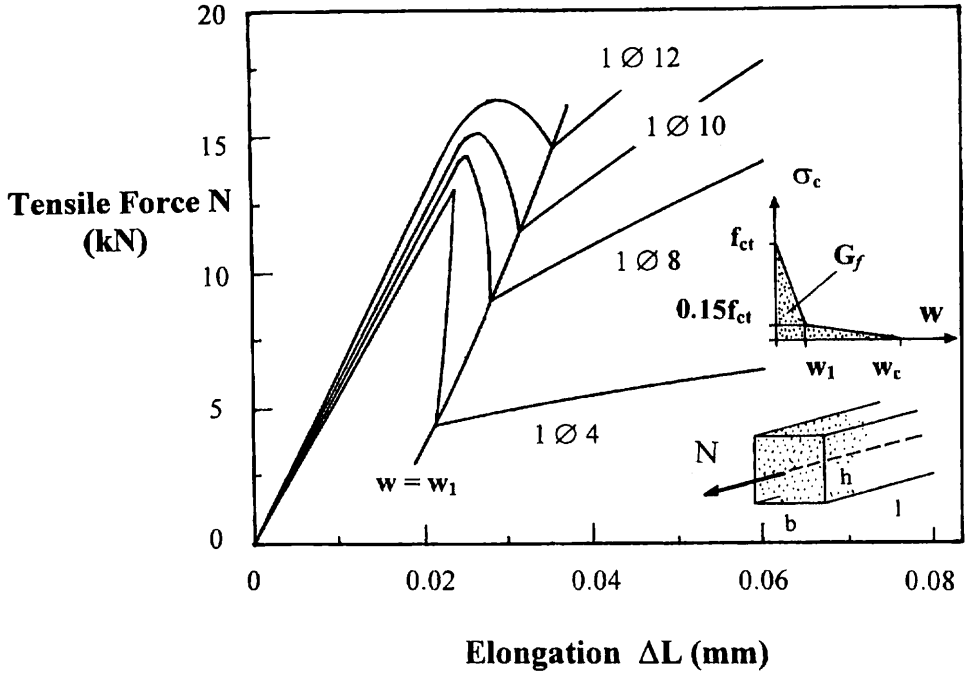

Fig. 1.3.11 – Modeling of the descending branch in lightly-reinforced tension members (Fantilli et al., 1998 a,b). f_c = 29.6 MPa; f_{ct} = 2.15 MPa; G_f = 64.1 N/m; w_1 = 0.037 mm; w_c 0.148 mm; E_c = 28000 MPa; member size : b x h x l = 50 x 50 x 300 mm; reinforcement; 1 bar ϕ 4-12 mm.

As far as bending is concerned, the results obtained by testing and modeling R/C tension members have been lately extended to flexural members by imposing strain compatibility and equilibrium in all sections of a block limited by two contiguous flexural cracks, assuming the crack tip to be located on the neutral axis. In this way, the local and average moment-curvature diagrams can be obtained, making it possible to evaluate the deformations of R/C beams (Fantilli et al., 1998b).

Finally, in a very recent paper Eligehausen et al. (1998) investigated numerically the contribution of concrete between the cracks when the reinforcement is stressed beyond the yield threshold in the cracked sections. This study shows that for relatively-low values of the steel strain in the cracked section (1-3%) the ratio between the average steel strain and that in a cracked section can be rather small, since bond remains effective even beyond bar yielding at the crack. Under these circumstances, the stiffening contribution of the concrete between the cracks limits significantly the rotation capacity of the plastic hinges, to the detriment of structural ductility. Therefore, good bond properties - albeit

Copyright fib, all rights reserved. This PDF copy of fib Bulletin 10 is intended for use and/or distribution only by National Member Groups of fib.

favorable in the service limit state (small crack width) - may be unfavorable in the ultimate limit state, after steel yielding. However, for higher values of the steel strain in the cracked sections (> 5%), because of the combined effects of steel strain-hardening and bond decay, tension stiffening is reduced, to the advantage of structural ductility (see Section 1.1.3).

Copyright fib, all rights reserved. This PDF copy of fib Bulletin 10 is intended for use and/or distribution only by National Member Groups of fib.

1.4 Concrete splitting in bond modeling

1.4.1 Overview on partial and through splitting

As already mentioned in Section 1.1.1, bond behavior depends on the many and closely-related phenomena which occur around an anchored ribbed bar. Among these phenomena, the following are particularly significant: (1) transverse microcracking that develops at a very early load phase (Goto, 1971, Figs. 1.1.1 and 1.4.1); (2) local crushing of the porous concrete-layer around the rib (Giuriani, 1981), which governs most of the slip after the failure of chemical adhesion (Figs. 1.4.1 and 1.4.2a); (3) splitting of the surrounding concrete when the radial stresses induced by the wedge action of the ribs exceed concrete tensile strength (Figs. 1.1.11 and 1.4.3).

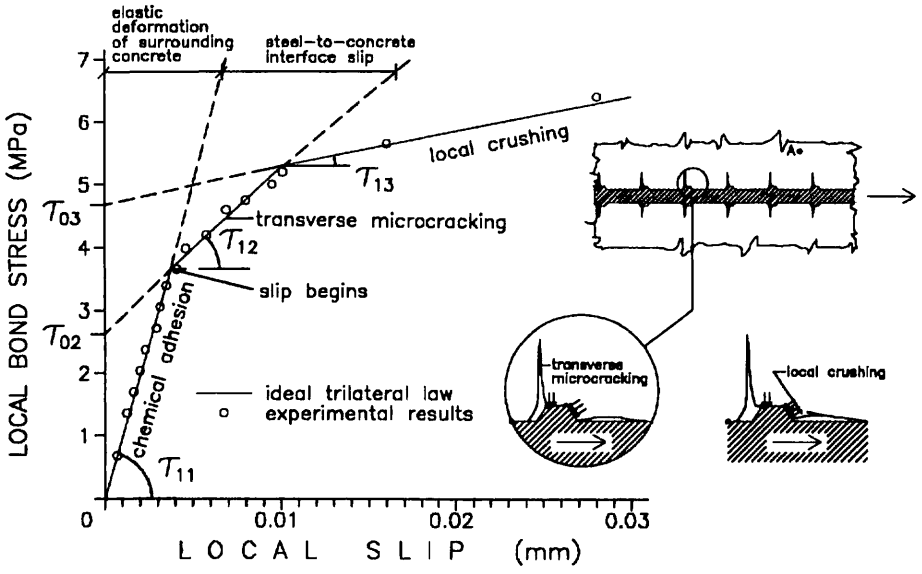

Fig. 1.4.1 - Local bond stress-slip law: role of radial microcracking and local crushing (Giuriani, 1981). In this figure, slip refers to the relative displacement between the bar and a prefixed point (A) in the concrete, undisturbed by the rebar.

The previously described phenomena may have different relevance depending mainly on the diameter of the anchored bar. In particular, for small bar diameters (ϕ<12-14 mm) and usual slip values (s < 0.2 mm), most of the slip is due to the local crushing of the porous concrete layer in front of each rib (Giuriani, 1981). Consequently, the bond stress-slip law mainly depends on the mechanical properties of the concrete and specifically on the hardness of this layer. For larger bar diameters or higher slip values, splitting cracks propagate across the concrete cover and the bond stress-slip law is significantly affected by the confinement. As for beams, splitting cracks start from flexural cracks where the bar-concrete slip reaches its maximum, and propagate along the anchored bar (Plizzari et al., 1996a; Fig.1.4.3).

The stress field in the surrounding concrete and the presence of splitting may explain the discrepancies between the experimental bond stress-slip relationships obtained by different researchers; for example, a stiffer behavior was found in the mid-span zone of tension members (Nilson, 1972; Tassios and Koroneos, 1984; Jiang et al., 1984) and at the ends of the bars in pull-out tests (Lahnert et al., 1986). If the splitting crack opening is taken into account, the local bond stress-slip law turns out to be independent of the section examined along the bar, as in the uncracked and microcracked regions (Gambarova and Giuriani, 1985).

In order to keep splitting under control and to improve bond stiffness and strength, a confining action along the anchored bar is needed to balance the radial pressure induced by the ribs. At the beginning, this confining action is provided by the tensile strength of the uncracked part of the surrounding concrete (Tepfers, 1973; Reinhardt and van der Veen, 1990; Balaguru et al., 1995), and also by the cohesive stresses between the faces of the thin splitting cracks (Plizzari et al., 1987). When the splitting cracks propagate and their width increases, further confining action should be provided by the

Copyright fib, all rights reserved. This PDF copy of fib Bulletin 10 is intended for use and/or distribution only by National Member Groups of fib.

transverse reinforcement (Tepfers, 1973; Orangun et al., 1977; Morita and Fujii, 1982; Eligehausen et al., 1983; Fig.1.1.11). Beside the two previous passive confining forces, active confining forces (as a transverse pressure), help in improving bond (Untrauer and Henry, 1965; Robins and Standish, 1984; Schmidt-Thrö et al., 1988; Modena et al., 1988; Malvar, 1991).

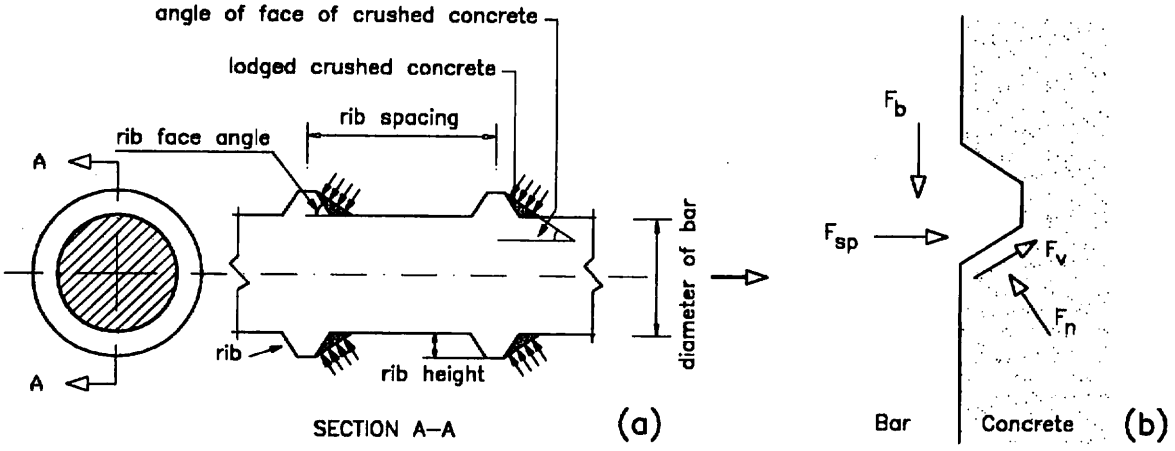

Fig. 1.4.2 - Wedge action of the ribs of a deformed bar as proposed by (a) Tepfers (1979) and (b) Cairns and Jones (1995a).

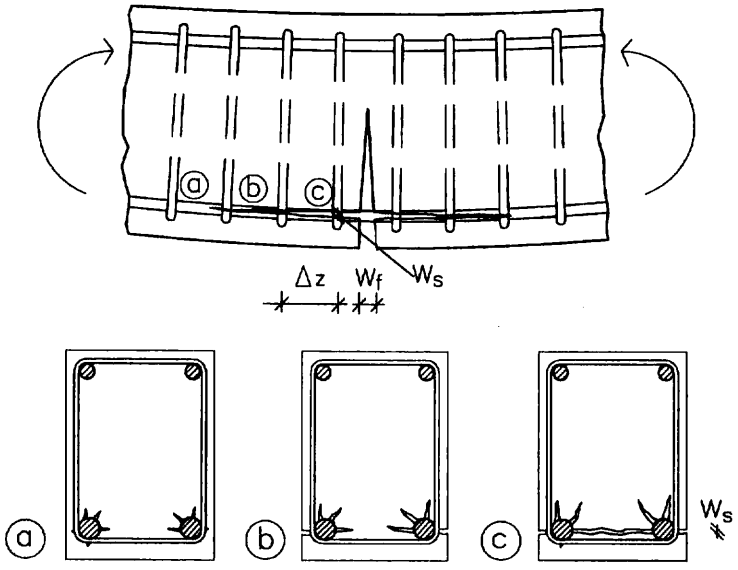

Fig. 1.4.3 - Splitting-crack propagation in an anchorage: (a) onset, (b) partial propagation, and (c) complete-propagation (Giuriani et al., 1991).

The confining action also influences the mode of bond failure. If the confining action is not adequate, splitting cracks develop abruptly along the anchored bars and through the cover, and a sudden bond collapse may occur (splitting failure: Tepfers, 1973; Ferguson, 1977; Morita and Kaku, 1979; Fig.1.1.4c). Otherwise, the bond stress increases up to the compressive failure of the concrete corbels between the ribs (pull-out failure; Figs.1.1.4a,b; see Plizzari and Schumm, 1990).

1.4.2 Local bond-stress relationships

Rehm (1961) showed that slip occurs along a reinforcing bar under loading and that the ensuing bond action is a function of the slip.

Copyright fib, all rights reserved. This PDF copy of fib Bulletin 10 is intended for use and/or distribution only by National Member Groups of fib.

The local bond behavior has often been described as a shear force between the face of the reinforcing bar and the surrounding concrete (CEB, 1982), but a thorough modeling should also consider splitting, which is related to the wedge action of the ribs.

Among the bond stress-slip relationships introduced in Section 2, it is worth recalling that the model proposed by Eligehausen, Bertero and Popov (1983, Fig. 1.2.4), as well as the closely-related model adopted in CEB-FIP MC90 (1993), distinguish the cases of unconfined (splitting failure) and confined (pull-out failure) concrete. After many pull-out tests on deformed bars (ϕ=25.4mm) with transverse reinforcement, and a concrete compressive strength $f_c \leq$30MPa, the authors found that:

- the specimens without transverse reinforcement fail because of concrete splitting in a plane containing the axis of the bar;
- bond behavior can be slightly improved by increasing the clear distance between the bars;
- for increasing values of the transverse pressure, both bond stiffness and strength increase.

These three points again underline the effects of the confining action.

Concrete is considered unconfined by MC90 when the minimum concrete cover ($c=\phi$) and the minimum total area of the stirrups (two legs) over a length equal to the anchorage length ($A_{st,min}=0.25\ n\ A_s$, where n is the number of the anchored bars enclosed by the stirrups and A_s is the area of one bar) are adopted.

Concrete is considered well confined when cover c and clear spacing a are sufficiently large ($c \geq 5\phi$, $a \geq 10\phi$), or when transverse reinforcement is closely spaced and has a sufficiently great total area ($A_{st}=nA_s$), or when a high transverse pressure is present ($p \geq 7.5MPa$). For intermediate values of both transverse reinforcement and transverse pressure, the MC90 prescribes that the values for s_1, s_3, τ_{max} ($=\tau_1$) and τ_f may be interpolated linearly between the values for unconfined and confined concrete (see Fig. 1.2.4). If both a transverse reinforcement and a transverse pressure are present, their effects may be added.

In order to account for the effects of yielding of the bar, and with reference to well-confined concrete, Engström and co-workers (see Huang et al., 1996) proposed recently a bond model similar to the MC90 model but with a decreasing softening branch (Fig.1.4.4a,I). The model can be used for Normal-Strength Concrete (NSC) as well as for High-Strength Concrete (HSC) by adopting different slip values for the break points. The fitting of the test results on both NSC and HSC was quite successful (Fig. 1.4.4b).

For good bond conditions, the authors proposed the following values for the various parameters:

- <u>Normal-Strength Concrete</u> $s_1 = 1.0$ mm, $s_2 = 3.0$ mm, s_3=clear rib spacing, $s_4 = 3\ s_3$
  $\tau_{max} = 0.45 f_{cm}$, $\tau_f = 0.4$, τ_{max}, $\alpha = 0.4$;
- <u>High-Strength Concrete</u> $s_1 = 0.5$ mm, $s_2 = 1.5$ mm, s_3=clear rib spacing, $s_4 = 3\ s_3$
  $\tau_{max} = 0.45 f_{cm}$, $\tau_f = 0.4$, τ_{max}, $\alpha = 0.3$.

A linear relationship between bond and compressive strength for HSC was found by the authors who claim that MC90 markedly underestimates bond capacity in the case of HSC.

Gambarova and co-workers (Gambarova and Karakoç, 1982; Gambarova et al., 1989, Gambarova and Rosati, 1996) determined empirical relationships between the bond stress (τ) and the bar-concrete slip (s) from pull-out specimens with a preformed splitting crack whose width was kept constant during each pull-out test (four different values, see also Section 1 and Fig.1.1.20).

As for the Poisson effect, its role tends to increase in a deformed bar after the shearing off of the concrete corbels between the ribs, because the limited roughness of the sliding plane tends to be offset by the lateral contraction of the bar. Furthermore, when the steel strain exceeds the yield strain, the effect of lateral bar contraction influences the friction mechanisms, since a decrease in the interlocking effect between the steel ribs and the concrete has to be expected. Shima et al. (1987), Engström (1992) and Bigaj (1995) found that the bond stress decreases considerably after steel yielding. When the steel strain exceeds the yield strain, the descending branch (II) sketched in Fig.1.4.4a represents Engström's proposal for normal-strength concrete, with $s_{y,f} = s_y + 2.5$ mm, $s_5 = 2\ s_3$ and $\tau_{y,f} = 0.2\ \tau_{max}$.

Copyright fib, all rights reserved. This PDF copy of fib Bulletin 10 is intended for use and/or distribution only by National Member Groups of fib.

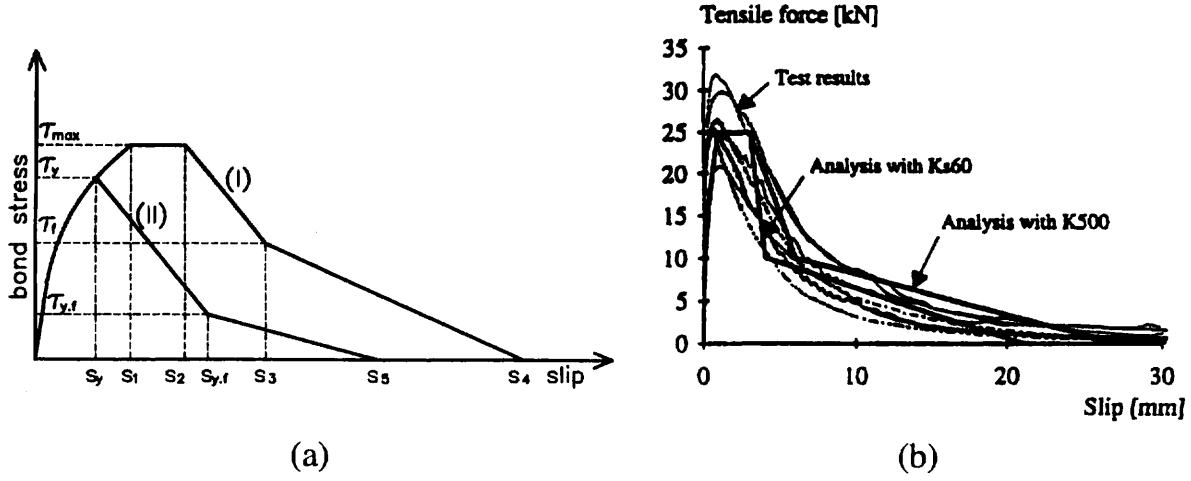

Fig. 1.4.4 - Local bond stress-slip model proposed by Huang, Engström and Magnusson (1996) for ribbed bars in well-confined concrete: (I) steel bar in the elastic stage; (II) steel bar in the plastic stage (a); fitting of the test results for NSC (b).

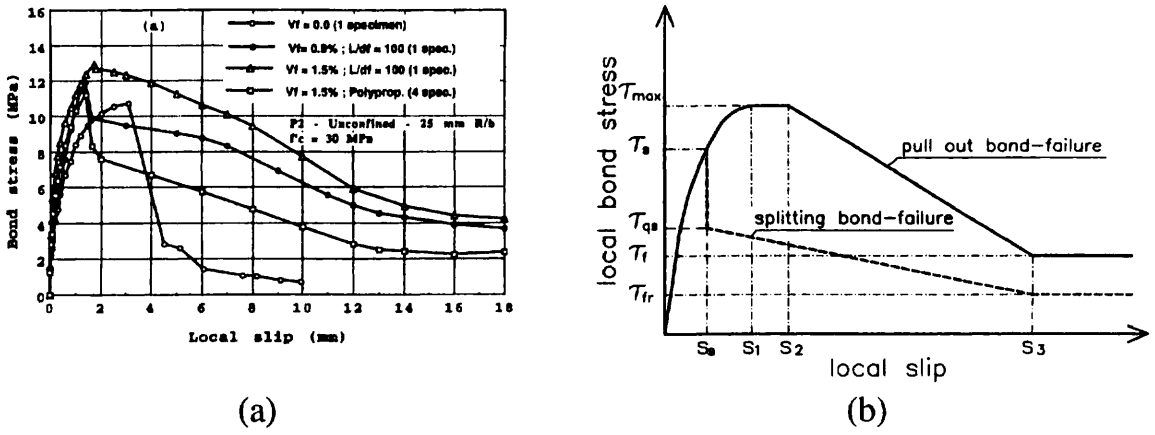

Fig. 1.4.5 –Bond stress-slip curves by Harajli et al. (1995): (a) pull-out tests on deformed bars embedded in fiber-reinforced concrete, and (b) different models proposed for pull-out and splitting failures.

Considering fiber reinforcement, an experimental study by Elzedin and Balaguru (1989) shows that fibers improve the bond strength of a deformed bar after the development of splitting cracks and lead to a much greater bond resistance under successive cyclic loads, compared to plain concrete. Harajli et al. (1995) also observed that the local bond behavior before concrete splitting is unaffected by fiber reinforcement; after concrete splitting, the bond stress decreases sharply at first, and then continues decreasing almost linearly. The last part of the local bond-slip relationship is characterized by a constant bond stress as already observed for plain concrete (Fig.1.4.5a). A simple model for the local bond stress-slip relationship was proposed, and both the pull-out and the splitting bond-failures were considered, together with the most important parameters that influence bond behavior in fiber-reinforced concrete (Fig.1.4.5b).

1.4.3 Models based on transverse reinforcement and concrete confining effects

Theoretical expressions for the bond strength of ribbed bars may be developed by equating the bursting force generated by bond action to the splitting resistance of the concrete section (together with any confining reinforcement). The majority of research efforts have been directed to the side of the equation dealing with splitting resistance; valuable work has been carried out by Ferguson and Briceno (1969), by Tepfers (1973), and by many other researchers, and there is a substantial body of test data on a variety of lapped joint and single-bar anchorages. Research findings are now assimilated into Code of Practice rules.

Copyright fib, all rights reserved. This PDF copy of fib Bulletin 10 is intended for use and/or distribution only by National Member Groups of fib.

Research into the relationship between the bond stress and the bursting force generated by bond action is less well developed. It has generally been assumed that bond generates a radial stress (σ_n or σ_r) proportional in magnitude to the bond stress itself : $\sigma_n = k\ \tau_b$. Furthermore, it is often assumed that this radial stress is uniformly distributed along the interface, as an hydraulic pressure (hydraulic pressure analogy). This assumption ignores experimental evidence that bars of differing rib geometries develop different bond strengths under otherwise identical conditions, and that geometric properties of ribs must therefore affect the relationship between bond and bursting force (Cairns and Jones, 1995b). It is also recognized that the surface condition of a bar may influence bond strength, an aspect again neglected by the "hydraulic pressure" analogy.

Clearly, both sides of the equilibrium equation should be considered in equal depth to obtain a balanced analysis of bond strength.

A rational approach to the study of the local bond behavior should also consider the splitting crack opening which is related to the confining action present along the bar (Gambarova and Giuriani, 1985).

Den Uijl and Bigaj (1996) recently proposed a local bond model based on the confining action of split concrete and within a fracture mechanics approach for both NSC and HSC. The wedge action of the steel bar is modeled by giving the bar a conical shape (Fig. 1.4.6a); consequently, the radial displacement in the concrete, at the interface with the bar, can be easily formulated as a function of the relative slip, and the relationship between the radial stress in the embedment and the radial displacement can be worked out on the basis of the theory of the thick-walled cylinder (Fig. 1.4.6b). Furthermore, this model describes both the pull-out (Fig.1.4.6c) and the splitting (Fig.1.4.6d) failure of bond and also introduces the effects of bar yielding. The contributions of the transverse reinforcement and the external pressure are not taken into account. The fitting of the test results on both NSC and HSC was quite successful (Bigaj et al., 1996), with reference also to the steel stress and to the bond stress slip relationship (Fig. 1.4.7).

The model proposed by Giuriani and Plizzari (1985), and later improved by Giuriani et al. (1991), takes into account the confining actions of both the transverse reinforcement and the concrete cover. The model applies to the region Δz pertaining to a single stirrup, when splitting runs through the whole cross-section (Fig. 1.4.3c), which is the typical situation of a beam with closely-spaced rebars (Warren, 1969). The bursting forces are introduced according to the tests by Gambarova and co-workers (Gambarova and Karakoç, 1982; Gambarova et al., 1989a, Gambarova and Rosati, 1996) who provided a relationship between the bond stress (τ) and the interface pressure (= wedge action, σ_n); this relationship was linearized by Giuriani and Plizzari (1985):

$$\tau = \left(\frac{\tau_0}{1 + K_1 \cdot w_s / \phi} \right) + \left(\frac{\tau_1}{1 + K_2 \cdot w_s / \phi} \right) \cdot \sigma_n \qquad (1.4.1)$$

where w_s is the width of the splitting crack (see also Fig.1.1.21b), and τ_0, τ_1, K_1 and K_2 are parameters that depend on the mechanical properties of the concrete and on rib geometry. Eq.1.4.1 is subjected to the limitation $\tau \leq \tau_{m,0}$, where $\tau_{m,0}$ is the maximum bond stress which can be transferred when the splitting crack is kept closed ($w_s=0$).

The confining action of stirrups was experimentally determined by Giuriani (1981, 1982) who proposed the following expression:

$$\sigma_{st} = E_s \sqrt{a_2 \left(\frac{w_s}{\alpha_s \phi_{st}} \right)^2 + a_1 \left(\frac{w_s}{\alpha_s \phi_{st}} \right) + a_0} \qquad (1.4.2)$$

where E_s is the Young's modulus of the steel, ϕ_{st} is the diameter of the stirrups; a_0, a_1 and a_2 are coefficients of the ideal trilateral local bond stress-slip law (Fig.1.4.1), and α_s is a factor characterizing the position of the splitting crack (Giuriani and Plizzari, 1985).

As for the confining action of the split concrete, the relationship proposed by Giuriani and Rosati (1986) between the cohesive stresses across the crack (σ_{rc}) and the crack width (w_s) was adopted in the model.

Copyright fib, all rights reserved. This PDF copy of fib Bulletin 10 is intended for use and/or distribution only by National Member Groups of fib.

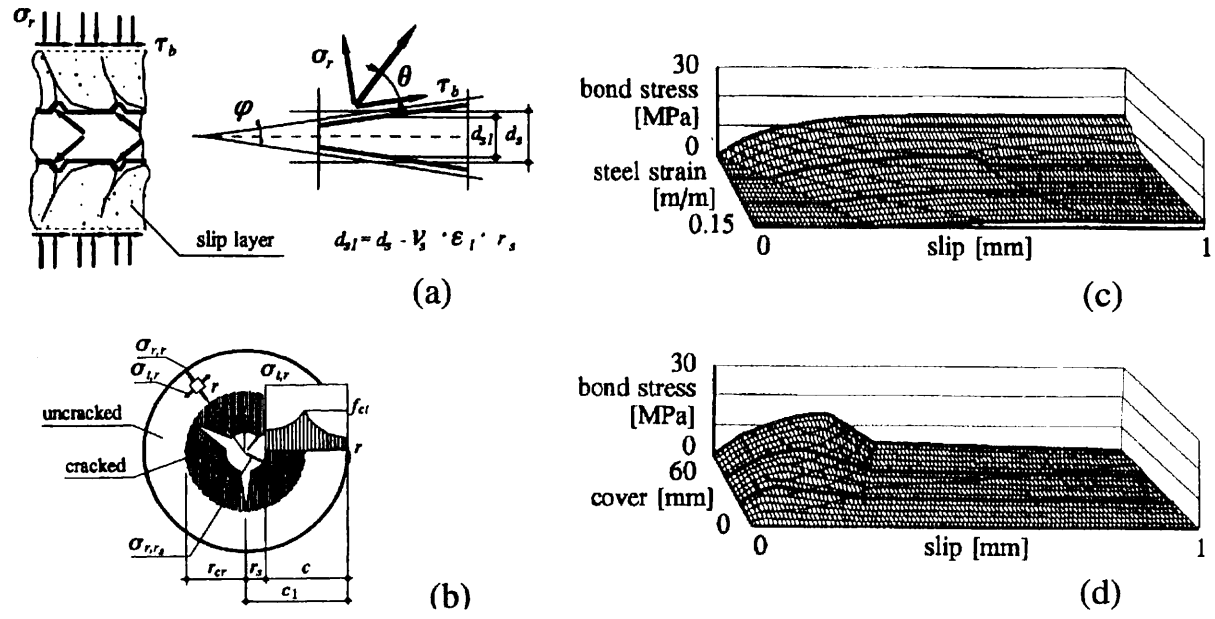

Fig. 1.4.6 – Conical bar simulating the wedge action of a deformed bar (a); partly cracked thick-walled cylinder (b); bond stress-slip relationship in a pull-out test: pull-out failure (c), and splitting failure (d) in NSC, from Den Uijl and Bigaj's (1996).

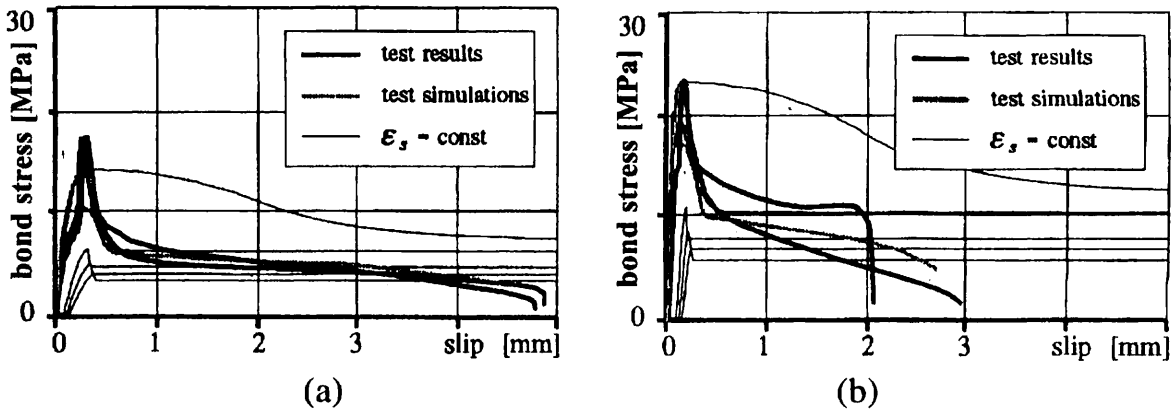

Fig. 1.4.7 – Den Uijl and Bigaj's model (1996): fitting of Bigaj's test results (1995) for a normal-strength concrete (a) and a high-strength concrete (b).

Equilibrium requires that the bursting force produced by the anchored bars in the region Δz be balanced by the global confining action produced by both the concrete cover (cohesive stresses) and the stirrups in the splitting plane (Fig.1.4.8); this yields:

$$\sigma_n = \Omega \sigma_{st} + B \sigma_{rc} \tag{1.4.3}$$

where Ω is the *Stirrup Index of Confinement*, which is defined as the ratio between the global cross-section area A_{st} of the stirrup legs and the area of the principal bar in the splitting plane A^* ($=n\,\phi\,\Delta z$), and B is the *Concrete Index of Confinement*, which is defined as the ratio between the net area of the concrete ($=(b-n\,\phi)\,\Delta z$) in the splitting plane and the area A^* (Fig.1.4.8). These two parameters govern bond behavior and are relevant to structural design; a parameter similar to Ω has been introduced in ACI 318-95 (1995) code (Plizzari et al., 1998).

Giuriani and Plizzari (1985) approximated the experimental relationship between the bond stress (τ) and the bar-concrete slip (s), with the splitting crack width kept constant during each pull-out test of Gambarova and co-workers (1982, 1989a, 1996), as follows:

Copyright fib, all rights reserved. This PDF copy of fib Bulletin 10 is intended for use and/or distribution only by National Member Groups of fib.

$$\tau = \tau_{m,0}\left(1-\gamma_1 w_s/\phi\right)\left(1-e^{-(\beta_1+\beta_2 w_s/\phi)(s/\phi-\gamma_2 w_s/\phi)}\right) \tag{1.4.4}$$

where $\tau_{m,0}$, γ_1, γ_2, β_1 and β_2 are parameters that depend on the mechanical properties of concrete and on rib geometry.

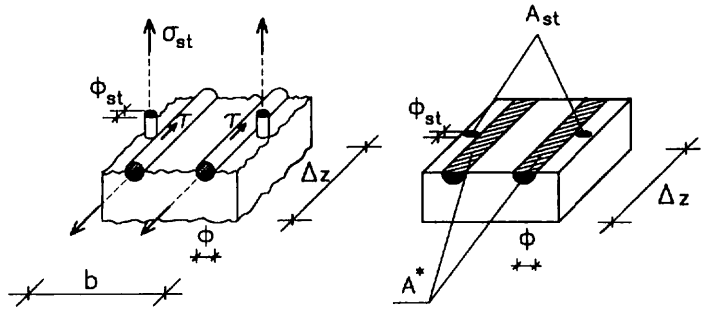

Fig. 1.4.8 – Geometrical characteristics of principal and transverse bars.

On the basis of the previous equations, the bond stress, the stirrup stress and the splitting crack opening were determined as a function of bar slip. The fitting of many tests was quite successful in terms of bond stress-bar slip response, splitting crack width, stress in the stirrups and bond capacity (Giuriani et al., 1991, Figs. 1.4.9a,b), and the best-fit values of the governing parameters were proposed by Giuriani and Plizzari (1998b).

Fig. 1.4.9c shows the theoretical predictions for the bond stress and stirrup stress (Giuriani et al, 1991); by assuming a fixed stirrup diameter, the bond strength decreases as stirrup spacing increases (and thus Ω becomes smaller). The dashed lines represent the bond behavior when the confining action of the split concrete is neglected; the comparison with the full lines highlights the sizeable contribution of this confining action, which is even more pronounced in fiber-reinforced concrete (Plizzari, 1999).

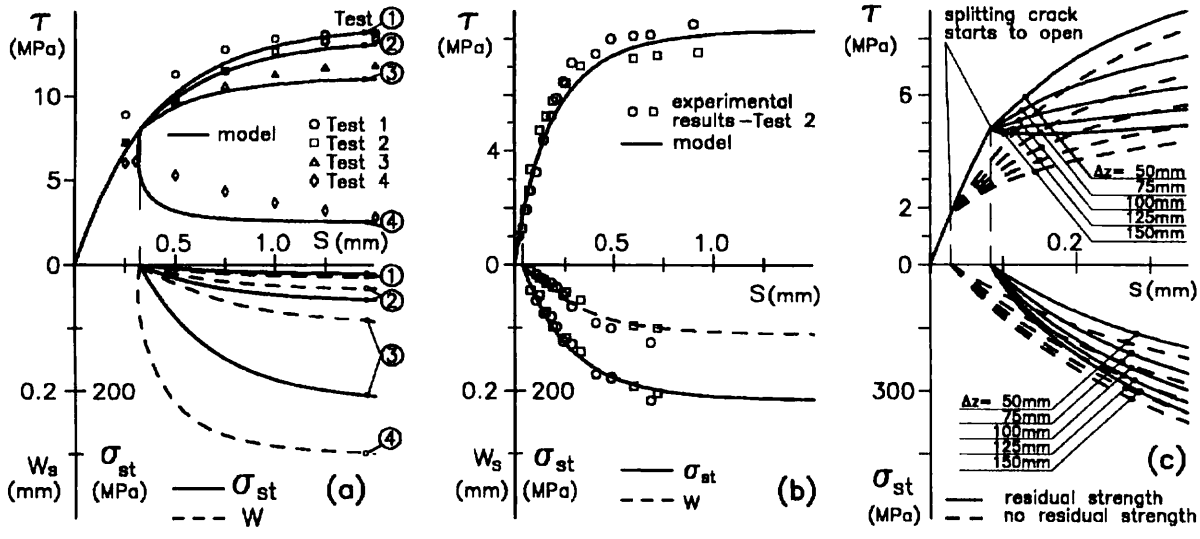

Fig. 1.4.9 – Giuriani et al. (1991) model for bond action in split, confined concrete: fitting of Giuriani and Plizzari (1985) test resuts (a), and of Eligehausen et al. (1983) test results (b); theoretical prediction for bond stress and stirrup stress in different situations (c) (Giuriani et al., 1991).

In one of the few theoretical investigations of the relationship between bond and bursting forces, Cairns (1979) analyzed forces acting on the ribs of a deformed reinforcing bar. The analysis treats bond failure as a bearing failure of the rib on the concrete. Failure is assumed to occur either by sliding on the inclined face of the rib (Fig. 1.1.4b), or by shearing off the concrete key on an inclined surface (Fig. 1.1.4a) when a limiting splitting resistance of the concrete is reached. A Mohr-Coulomb failure criteria is used to evaluate shear strength in the latter case. A similar form of criteria is also used to evaluate bar/concrete friction in the former case. The weaker of the two mechanisms is considered to control strength.

Copyright fib, all rights reserved. This PDF copy of fib Bulletin 10 is intended for use and/or distribution only by National Member Groups of fib.

Similar forms of expression are developed for both mechanisms:

$$\tau_{bu} = (\sigma_{sp} + 2 f_{coh} f_R) \cot \varphi_b \qquad (1.4.5)$$

where τ_{bu} is the bond strength, σ_{sp} is the confining stress, determined from resistance to splitting of cover with any transverse reinforcement, f_R is the relative rib area of bar, f_{coh} and φ_b are the unit cohesion and the angle of internal friction of concrete or of concrete/bar interface.

The form of Equation 1.4.5 suggests that bond strength of a ribbed bar consists of two contributions, one related to the splitting resistance provided by the section (Fig. 1.4.10a), the other to a non-splitting component dependent on the friction at the bar-concrete interface (Fig. 1.4.10b). Therefore the "hydraulic pressure" often assumed in analyses of bond strength (in which bursting stress is assumed directly proportional to bond stress, Fig. 1.4.10a), is not completely correct.

Gambarova et al (1992) presented results from tests on longitudinally cracked bond specimens to show the relationship between bond strength and confining force. Extrapolation of the relationship suggests a cohesive components of bond strength at zero confining stress equivalent to 0.08 times concrete compressive strength. Results presented by Malvar (1992) show the cohesive component to be of a similar magnitude. Cairns analysis and experimental data also gives a similar result, with the cohesive component contributing around 70% to bond strength at the fairly low confinements used in the tests. An analysis of bond strength by Vandewalle (1992) also indicates a relationship of the form of Equation 1.4.5, the non-splitting component amounting to 67% of bond strength at a cover/bar diameter ratio of 1.0.

The trends predicted by Equation 1.4.5 have been verified experimentally in splitting-type failures. They have been used to explain the increase in bond strength observed with heavy transverse reinforcement, and the increases in structural capacity associated with increases in concrete strength, confining reinforcement and transverse pressure (Cairns and Jones, 1995b) . They also explain the dependence of bond strength on the orientation of crescent shaped ribs in relation to the splitting plane. The expressions also demonstrate how the smooth surface of an epoxy coated bar reduces bond strength (Cairns and Abdullah, 1996).

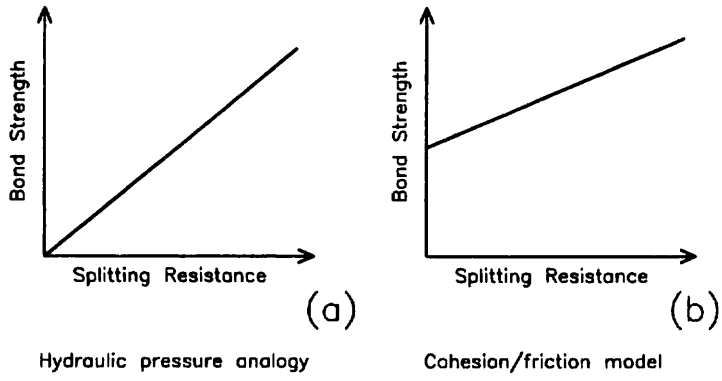

Fig. 1.4.10 – Bond strength versus splitting resistance without (a) and with (b) friction at the rib-concrete interface.

Dependence on the hydraulic pressure analogy for bond has led to difficulties in explaining the similar bond strengths developed in single bar anchorages and in laps (Reynolds and Beeby, 1982) . The hydraulic pressure analogy suggests that, as a two lapped bars will develop twice the bursting force of a single bar, then the bond strength developed by a lapped bar will be half that developed by a single bar anchorage, if the total confining force is constant. Experimental results indicate that there is little difference in strength. According to Equation 4.5, however, halving the splitting resistance will change bond strength to a lesser extent, as the cohesive component of bond strength is maintained and only the bursting component is shared (Cairns and Jones, 1995b). If, for example, the bursting component accounted for 30% of bond strength of a single bar anchorage and the balance of 70% came from the cohesive component, then in an equivalent lapped joint the bond strength would be sum of the cohesive component and half the bursting component, a total equal to 85% of the strength of the single bar anchorage. Cairns and Jones (1995a) reported a bond strength difference of 13% between lapped

Copyright fib, all rights reserved. This PDF copy of fib Bulletin 10 is intended for use and/or distribution only by National Member Groups of fib.

joints and single-bar anchorages.

1.4.4 Anchorage capacity after cover splitting

A linear increase of the anchorage capacity with the cross-section of the transverse reinforcement was observed by Morita and Fujii (1982) and by Kaku and co-workers (1988, 1989), who tested several beam specimens with No. 6 bars. These authors also found a different response for corner and inner bars without sub-ties owing to the larger splitting crack opening in the latter case. The reduced effectiveness of the stirrups in restraining the inner bars had been previously observed by Warren (1969) who tested several specimens containing from 2 to 7 bars within a single two-legged stirrup. Therefore, the importance that a correct stirrup arrangement has on anchorage capacity should always be kept in mind, in connection with concrete splitting. With regard to this point, a linear dependency of the anchorage capacity on the stirrup ratio was observed by Darwin and co-workers (1996). A bilinear dependency had been earlier found by Orangun et al. (1977), and later observed by Plizzari et al. (1996b, 1998, see the test results shown in Fig.1.1.18b), whose experiments led to the conclusion that there is no further capacity for very large values of the Stirrup Index of Confinement (Ω = 0.03-0.04).

As for the concrete confining action, Darwin and co-workers (1992) observed a linear increase of the anchorage capacity with the concrete cover and the clear spacing between the bars.

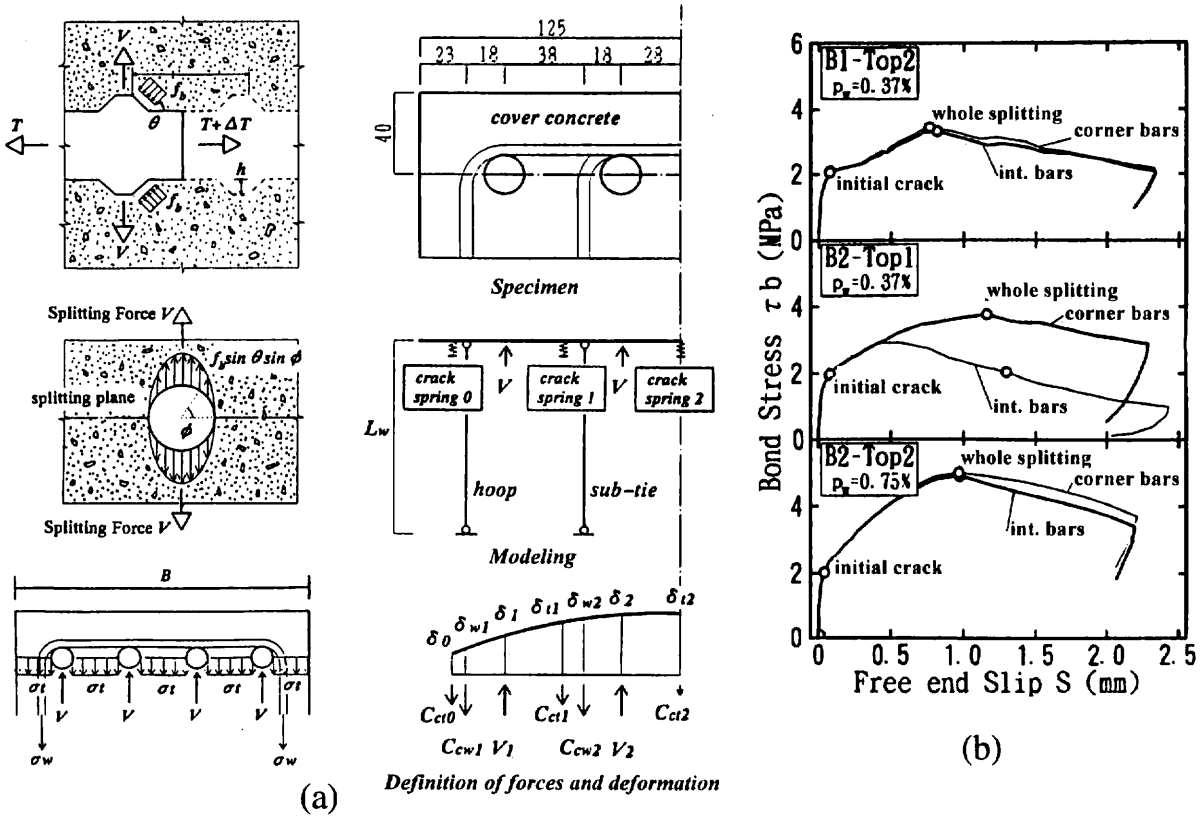

Fig. 1.4.11 – Confining actions developed by the stirrups: (a) analytical model proposed by Maeda and co-workers (1995), and (b) experimental bond stress-slip curves for a small stirrup ratio (top and middle cases: the intermediate bars are tied in the top case and untied in the middle case) and for a large stirrup ratio (bottom case: the intermediate bars are tied).

Maeda and co-workers (1995) studied the bond stress-confinement stress relationship that considers the concrete cover as a beam subjected to transverse forces (the wedge action of the ribs) and resting on nonlinear springs (the cracked concrete), with a few rigid supports (the stirrups, Figs.1.4.11a,b). A spring is assumed to be a rigid connection until its forces reaches the concrete tensile strength; then it elongates and the relationship between the elongation and the spring force is based on the tension softening model of concrete (Hillerborg et al., 1976). The model considers a non-uniform splitting crack opening across the section and describes the stiffer bond behavior of the anchored bars closest to

Copyright fib, all rights reserved. This PDF copy of fib Bulletin 10 is intended for use and/or distribution only by National Member Groups of fib.

the stirrup legs (corner bars) compared to the interior bars without sub-ties (Fig. 1.4.11c). The authors found a linear relationship between the bond strength increase due to the presence of the stirrups and the maximum stirrup stress, but the slope of this relationship for corner bars was different from that of the inner bars without sub-ties. Finally, Maeda and coworkers claimed that the NSC does not contribute to the confinement action at the ultimate state, which should have been expected, owing to the small concrete covers and clear spacings between the bars used by the authors. The same conclusions were reached by other scholars (Eligehausen et al., 1983; Plizzari et al., 1986b), who carried out pull-out tests on short anchorages with stirrups. However, small covers and bar spacings can guarantee and adequate anchorage capacity, provided that steel fibers are added to the mix, even with a limited volume fraction (0.3-0.5%, Balaguru et al., 1985, and Plizzari, 1999).

1.4.5 Splitting crack control

Since splitting develops longitudinally along anchored bars, extended parts of bar surface might be exposed to the environment and therefore are prone to corrosion. As a result, the failure caused by a loss of bond may precede the failure in bending and shear, which cannot be accepted in structural design. To assess the durability of a structure with reference to cracking, the splitting crack width should also be evaluated. Taking advantage of the analytical model presented in the preceding subchapter, Giuriani and Plizzari (1998a) worked out a relationship between the maximum splitting crack opening (w_s) and the flexural crack width (w_f), which is based on the maximum slip (s) of the anchored bar (Fig. 1.4.3). The authors also worked out a simplified expression for w_s as a function of w_f, by retaining only the terms of the series which are linearly dependent on w_s and Ω. For NSC, the following simplified equation was proposed:

$$\frac{w_s}{\phi} = \frac{\frac{1}{\alpha_f}\frac{w_f}{\phi} - 0.0022 + 0.0034 \cdot \Omega}{59.78 \cdot \Omega + 0.6703} \tag{1.4.6}$$

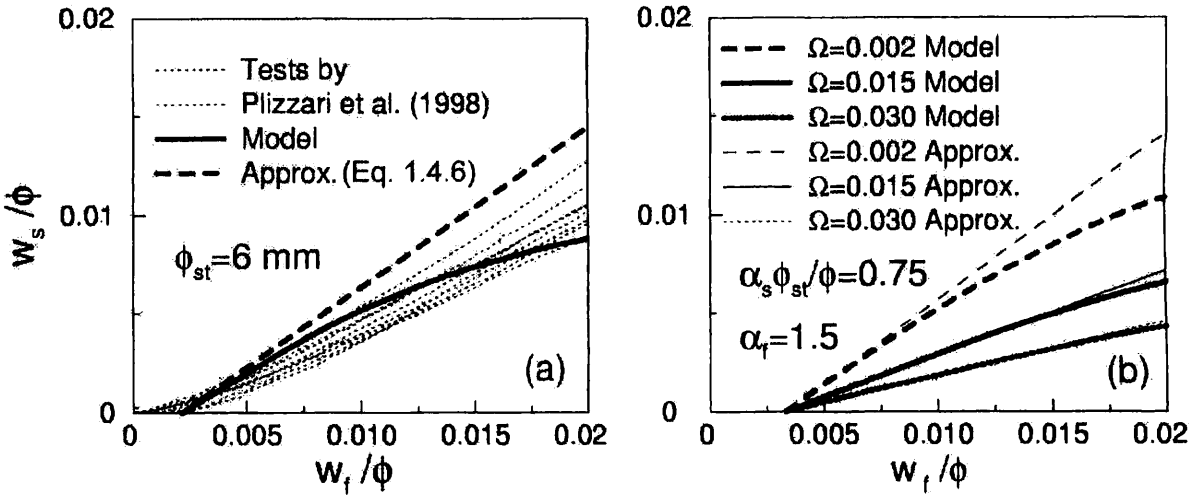

Fig. 1.4.12 – Splitting crack width (w_s) versus flexural crack width (w_f): (a) fitting of test results obtained by Plizzari et al. (1998) on a specimen with ϕ_{st}=6mm; and (b) influence of stirrup index of confinement Ω.

In this way, the splitting crack opening w_s can be easily evaluated owing to its dependence on the flexural crack opening w_f whose relationship with the loads is well-known.

Figure 1.4.12a shows the satisfactory fitting of the test results by Plizzari et al. (1998, pull-out tests of long anchorages with two bars and three two-legged stirrups, Fig.1.1.22a). The diagrams of Fig.1.4.12b are useful for practical applications. Since the width of the splitting crack is plotted versus the width of the flexural crack, for any given stirrup ratio (represented by Ω = Stirrup Index of Confinement), the designer can limit the risk of corrosion, on the basis of the width of the splitting crack. Note that, for small values of Ω, the splitting crack width is close to half the flexural crack

Copyright fib, all rights reserved. This PDF copy of fib Bulletin 10 is intended for use and/or distribution only by National Member Groups of fib.

width. Note also that Eq.1.4.6 is on the safe side, since it tends to overestimate the width of the splitting crack (thin curves in Fig. 1.4.12b).

Finally, as already observed for anchorage capacity (Section 1.4.4), even a small amount of fibers reduces the width of the splitting cracks, to the advantage of both bond efficiency and structural durability (Plizzari, 1999).

1.4.6 Hydraulic-pressure analogy

1.4.6.1 Nature of problem and previous literature

In order to predict the capacity of a short anchorage, and to describe the pattern of the splitting cracks and the hoop action in the concrete cover, the so called "hydraulic-pressure analogy" (Figs. 1.4.13 and 1.4.14) has been introduced since the mid-Seventies by Tepfers (1973 and 1979), and several researchers have lately refined Tepfers' limit-analysis model, by considering the cohesive nature of the splitting cracks.

At the same time, more or less standard Finite Element codes have been used to study the response of an anchored bar, and to model concrete crushing and cracking around a ribbed bar. Recently, both fracture-mechanics and damage-mechanics approaches have been adopted, with discrete or smeared cracking, with or without contact elements, with or without cover splitting (see Pukl et al., 1992, and Section 1.4.4), but the discrete approach is still plagued by some problems in order to describe the localization of the splitting cracks (Noghabai, 1997), which can be predicted satisfactorily by means of limit-analysis.

The limit analysis models developed by Reinhardt and van der Veen (1990), van der Veen (1990), Noghabai (1995a,b), Rosati and Schumm (1992), Gambarova et al. (1994), Bigaj et al. (1996), and Den Uijl and Bigaj (1996), see Fig. 1.4.14, are based on the elastic-cracked axial-symmetric model introduced by Tepfers (Fig. 1.4.13b), but also include the cohesion along the radial cracks (splitting cracks), which are produced by the outward pressure p (Fig. 1.4.13a) and by the associated hoop stress σ.

A recent and promising extension of the limit-analysis models (Gambarova et al., 1998) regards the concretes reinforced with high amounts of fibers. These materials (often called High-Performance Fiber Reinforced Cement Composites, HPFRCCs) are being considered for special high-ductility elements or highly-stressed regions, since fibers (a) increase concrete peak strength in tension, (b) give the concrete a pseudoplastic behavior (because of multiple cracking, Fig. 1.4.15) and (c) enhance concrete toughness (because of the greater energy-absorption capacity of the composite).

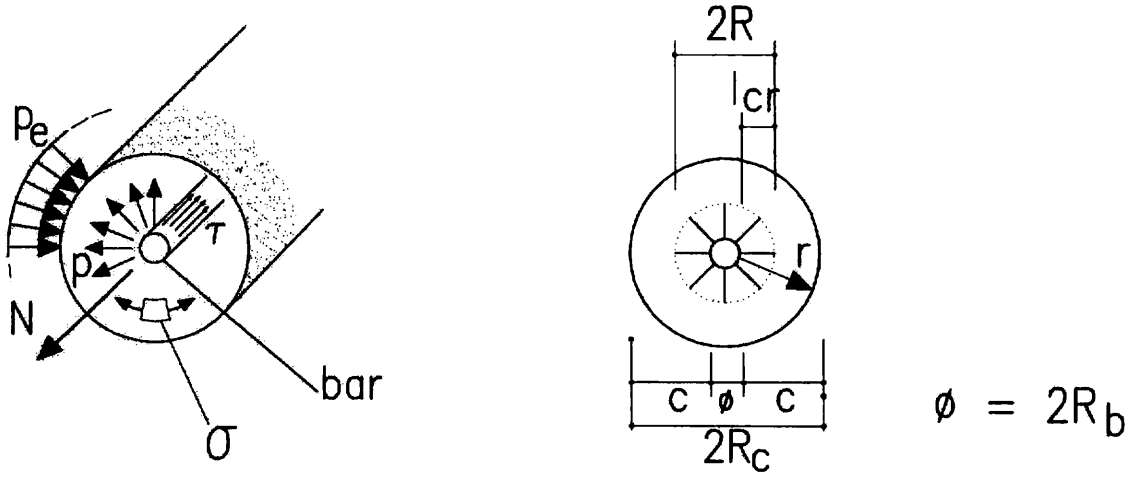

Fig. 1.4.13 - (a) Bar pull-out owing to bar wedging-action and (b) concrete splitting, with partially-cracked cover. l_{cr} = critical crack extension; c = concrete cover; ϕ = bar diameter; and r = radial coordinate.

Being limited to a 2D axisymmetric description of the 3D bond problem, the limit-analysis models based on the hydraulic pressure analogy cannot take into account the diffusion of the longitudinal stresses from the bar into the concrete, and the usually non-symmetric arrangement of the bars. However, in spite of their limits, these models are quite valuable for the understanding of basic bond mechanisms.

Copyright fib, all rights reserved. This PDF copy of fib Bulletin 10 is intended for use and/or distribution only by National Member Groups of fib.

Both the 3D effects and those related to bar arrangement may be lumped into the bond strength/radial pressure relationship, $\tau_u = f\ (p_{max}, ...)$, whose introduction is needed in order to evaluate the ultimate capacity of bond (τ_u or τ_{bu} in the other sections, Fig. 1.4.13a). Last but not least, the function f should also include the friction coefficient and the initial cohesion, both related to the the surface conditions and shape of the bars.

1.4.6.2 Elastic-cracked model

The elastic-cracked model for the evaluation of the ultimate capacity of a short anchorage embedded in a radially-split concrete mass was introduced by Tepfers in the Seventies (Figs. 1.4.13b and 1.4.14b).

Bond is assumed to be governed exclusively by mechanical interaction, and is accompanied by a wedging action, with the ribs of the bar pushing against the surrounding concrete. Only the outward, radially-oriented component of the interface pressure is considered (p, Fig. 1.4.13a), and the relationship between the bond stress and the confining pressure is formulated in terms of simple friction ($\tau = kp$). The concrete cover behaves like a two-phase thick-walled cylinder, with an inner cracked core (smooth and smeared cracking), and an outer solid sleeve (perfectly elastic according to Tepfers).

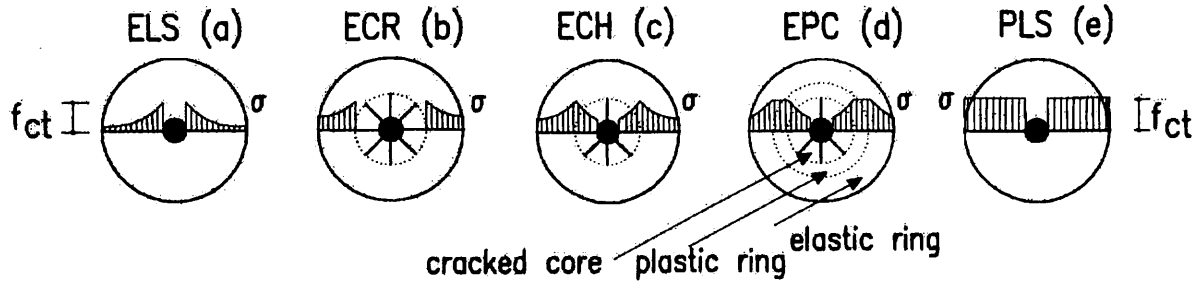

Fig. 1.4.14 - 2-D Limit Analysis Models for short anchorages subjected to cover splitting: ELS = ELaStic; ECR = Elastic-CRacked; ECH = Elastic-CoHesive; EPC = Elastic-Plastic-Cohesive; and PLS = PLaStic.

Tepfers found that splitting is not detrimental to bond capacity as long as crack extension l_{cr} is smaller than or equal to a critical value, which maximizes the bar-concrete pressure and the related bond stress. As a matter of fact, the concrete keys between the splitting cracks allow the radial pressure to decrease:

$$p'(r) = p\frac{R_b}{r} < p$$

where $R_b = \phi/2$ (Fig. 1.4.13b).

Consequently, the maximum statically-admissible value of p ($\sigma \leq f_{ct}$) does not belong to the situation with an uncracked cover (no splitting), but to a situation with partial splitting, the outer solid sleeve being capable of resisting the pressure p' by means of hoop stresses (σ, Fig. 1.4.13a).

The model proposed by Tepfers makes it possible to evaluate the bond capacity ($\tau_u = k\ p_{max}$) prior to the unstable extension of the splitting cracks to the whole cover (end of phase III, Fig. 1.1.1). An upper and a lower limit to the value of bond capacity are provided by the fully-plastic model (Fig. 1.4.14e) and by the fully-elastic model (Fig. 1.4.14a, with $l_{cr} = 0$). For k = 1:

- fully-plastic model : $\sigma = f_{ct} = constant,\ \tau_u / f_{ct} = 2\frac{c}{\phi}$ (1.4.7)

- fully-elastic model : $\sigma_{max} = \sigma(R_b) = f_{ct},\ \tau_u / f_{ct} = 2\frac{c}{\phi}\frac{1 + c/\phi}{1 + 2(c/\phi) + 2(c/\phi)^2}$ (1.4.8)

Tepfers' solution is:

$$l_{cr} = 0.486\ R_c\ ,\ \tau_u / f_{ct} = p_{max} / f_{ct} = 0.3\frac{R_c}{R_b} = 0.3\left(1 + \frac{2c}{\phi}\right) \quad (1.4.9)$$

Copyright fib, all rights reserved. This PDF copy of fib Bulletin 10 is intended for use and/or distribution only by National Member Groups of fib.

since $R_c = R_b + c = \phi/2 + c$.

The bond ultimate capacities provided by the elastic model (ELS) and by the elastic-cracked model (ECR) are plotted in Fig. 1.4.18, as a function of the concrete-cover ratio (c/ϕ).

The elastic-cracked model has recently been the object of two papers (Vandewalle, 1992, and Cappellini, 1996). In the former, Vandewalle introduced a linear relationship between the ultimate bond stress and the maximum interface pressure (Coulomb's failure criterion):

$$\frac{\tau_u}{f_{ct}} = \frac{1}{2\sqrt{K}}\left[1 + (1-K)\frac{p_{\max}}{f_{ct}}\right] \quad with \quad K = \frac{f_{ct}}{f_c} \tag{1.4.10}$$

The previous equation is plotted in Fig. 1.4.18 (ECR*), with $K = 0.1$ and

$$p_{\max} / f_{ct} = 0.3\left(1 + \frac{2c}{\phi}\right) \tag{1.4.11}$$

In the latter paper Cappellini developed an energy-based approach, which leads to the same results obtained by Tepfers, but brings in new information about the limit-equilibrium corresponding to the maximum of the interface pressure $dp/dl_{cr} = 0$, $p = p_{max}$: the equilibrium is stable. This conclusion cannot be drawn on the basis of a purely static approach.

Finally, one should remember that beyond $c/\phi = 2.5$-4.5 (Fig. 1.1.12, see C/D and C_s/D) bond failure is no longer governed by cover splitting, but by the shearing-off of the concrete keys between the lugs of the bar and by local concrete crushing; consequently, bond capacity should flatten-off (see also Fig. 1.4.20).

1.4.6.3 Elastic-cohesive model

Tepfers' model, though simple and based on clear and sound assumptions, does not grasp a few important aspects of the splitting failure, such as (a) crack cohesion (which is related to concrete softening in tension), (b) crack number, (c) the bidimensional nature of the state of stress in the transition region between the cracked core and the solid "ring" (tension+compression), and (d) the favorable effects of external pressure (Fig. 1.4.15, as occurs in proximity to a direct support).

Several models have been developed lately to introduce crack cohesion, which in turn requires the introduction of crack kinematics and number, since the crack width is the ruling parameter of any cohesive law. As a result, a statically-admissible approach (as in Tepfers' model) is no longer sufficient, since a suitable assumption on crack kinematics must be introduced.
All models developed from 1990 (Reinhardt, van der Veen, Noghabai and Rosati-Schumm) are based on the assumption of partial cracking in the cover and perfect elasticity in both the outer ring and the concrete keys between the splitting cracks.

Different stress displacement laws were adopted for crack cohesion (exponential; non linear polynomial; linear; hyperbolic or linear).

As for crack kinematics, different assumptions have been introduced for the circumferential elongation in the cracked core, leading to as many relationships between the elongation of any circumferential fiber ($R_b \le r < R$) and the elongation at the interface between the cracked core and the outer ring ($r = R$):

- constant circumferential elongation, with the fibers at the onset of cracking between the splitting cracks (the equilibrium in the hoop direction is not satisfied inside each concrete key, Reinhardt and van der Veen, 1990);

- constant circumferential elongation, with each fiber subjected to the same stress which develops along the splitting cohesive cracks (the equilibrium in the hoop direction is satisfied, Gambarova, Rosati and Schumm, 1994; Noghabai, 1995);

- variable circumferential elongation, according to the hoop-strain distribution of an "equivalent" elastic case, or to a hyperbolic distribution (Cappellini, 1996).

Copyright fib, all rights reserved. This PDF copy of fib Bulletin 10 is intended for use and/or distribution only by National Member Groups of fib.

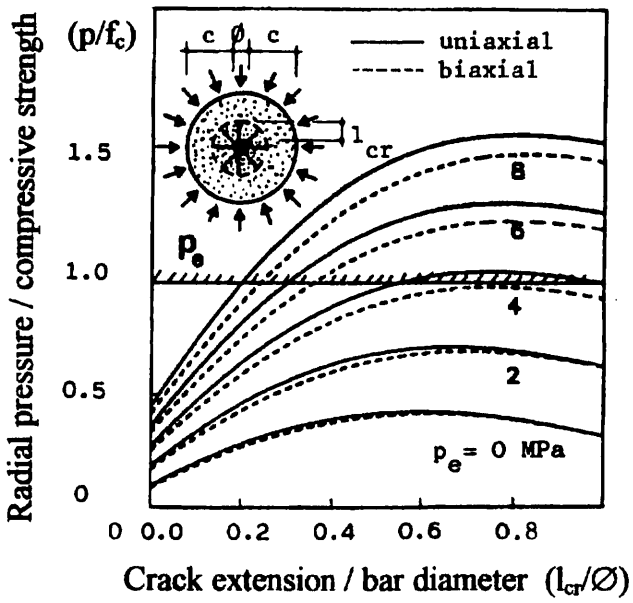

Fig. 1.4.15 - Plots of the bar-concrete pressure (radial pressure p) as a function of crack extension (Gambarova et al., 1994), for different values of the external pressure (p_e): the full and dashed curves refer to a uniaxial and biaxial failure criterion respectively. ϕ = 12 mm; R_c = 42 mm; c/ϕ = 3; d_a = 16 mm; f_{ct}/f_c = 0.1; f_c = 45 MPa; E_c = 30 GPa; G_f = 100 J/m^2; w_c (critical crack width) = 0.2 mm; n (crack number) = 3.

Depending on the kinematic assumption made, different crack-width distributions are obtained: for instance, the first formulation (constant circumferential elongation) implies a linear distribution of the splitting-crack width, with the maximum width at the bar-concrete interface.

By writing the equilibrium along any radial, partially-split section, the bar-concrete pressure can be formulated as follows:

$$p(R_c, R_b, l_{cr}, f_{ct}, E_c, n, w_c \text{ or } G_f) \tag{1.4.12}$$

By maximizing the pressure with respect to crack extension (dp/dl_{rc}=0) and by giving the crack-number n a prefixed value, bond capacity (always related to p_{max}) is found (Reinhardt, van der Veen and Noghabai, 1990, 95).

According to Gambarova, Rosati, Schumm and Cappellini (1992, 94, 96) the crack number is not given a-priori, but is one of the unknowns of the problem. By definition, it is the number that at the same time corresponds to the smallest value of the pressure maximums, and satisfies both static and kinematic admissibility:

$$0 \le \sigma(r, l_{cr}, n) \le f_{ct}, \; w(r, l_{cr}, n) \ge 0 \tag{1.4.13}$$

It is worth noting that the effects of the external pressure have also been introduced (Fig. 1.4.16): bond capacity increases, but not beyond an upper limit, which is related to the compressive strength of the concrete in the radial direction; the crack number, critical extension and maximum width decrease because of the external pressure.

Finally, in Fig. 1.4.16 several models are compared, for n = 2, which is the crack number obtained with the elastic-cracked-cohesive model developed by Cappellini (1996), in the wake of Rosati and Schumm's earlier papers. Note that in spite of the different assumptions, the maximums (p_{max}, i.e. maximum bond esploitation and ultimate bond capacity) are pretty close ($p_{max}/f_{ct} \approx$ 3.4-3.8) for the models based on exponential, linear or hyperbolic cohesive laws; on the other hand, the plastic model (PLS) and the elastic-cracked model (ECR, Tepfers) provide an upper and lower bond respectively. It should be observed that the highest values are the closest to the "true" solution of the problem, since all models are based on the static approach of limit analysis.

Copyright fib, all rights reserved. This PDF copy of fib Bulletin 10 is intended for use and/or distribution only by National Member Groups of fib.

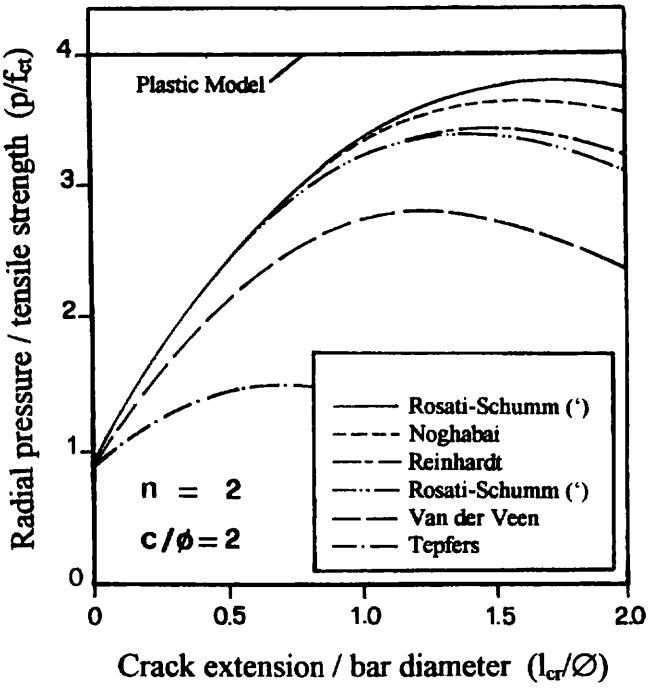

Fig. 1.4.16 - Plots of the bar-concrete pressure (radial pressure p) as a function of crack extension (l_{cr}) (according to Cappellini, 1996). ϕ = 19 mm; R_c = 47.5 mm; c/ϕ = 2; d_a= 16 mm; f_{cr}/f_c = 0.1; f_c = 32 MPa; E_c = 30 GPa; G_f = 100 J/m^2; n (crack number) = 2.(') Same hyperbolic cohesive law, different kinematic conditions in the cracked core.

1.4.6.4 Elastic-plastic-cohesive model

The fundamental aspects of the elastic-plastic-cohesive model (Fig. 1.4.14d) are as follows:

1. The concrete mass surrounding the bar consists of a three-phase material, with an inner radially-cracked and cohesive core, an intermediate plastic ring and an outer elastic ring; the intermediate ring is a late development, since the hoop action was developed only by the elastic ring and by the cohesion of the radial cracks in the original model (Fig.1.4.14c).

2. The hoop action in the elastic and plastic rings (with the contribution of the external pressure p_e, if any, Fig. 1.4.13a) prevents the pull-out of the bar as long as the penetration of the radial cracks l_{cr} (Fig. 1.4.13b) is less than or equal to a "critical" value which maximizes bar-concrete pressure p and consequently pull-out strength T. Beyond this critical value, the equilibrium of the bar is no longer possible, since the radial cracks become unstable and spread across the whole cover.

3. The solid parts of the radially-cracked core behave elastically and are subject to uniaxial compression in the radial direction (ν=0). Furthermore, the strains in the hoop and radial directions are assumed to be equal (homothetic displacements) on a global level, i.e. accounting for crack contribution.

4. The radial cracks have some residual strength in tension (crack cohesion) and can transfer tensile stresses, as shown by the softening branch of the stress-strain/stress-displacement curve (Fig. 1.4.17, curve 1). The law adopted here for concrete softening (Giuriani and Rosati, 1986) contains a few parameters related to concrete fracture, such as concrete tensile strength f_{ct} and critical crack opening w_c:

$$\sigma / f_{ct} = (1 - w/w_c) / (1 + k\, w/d_a) \qquad (1.4.14)$$

where σ is the cohesive tensile stress, w is the crack opening, d_a is the maximum aggregate size and k is a parameter related to fracture energy G_f. In the case of fiber-reinforced concrete, both f_{ct} and w_c depend on fiber content.

Copyright fib, all rights reserved. This PDF copy of fib Bulletin 10 is intended for use and/or distribution only by National Member Groups of fib.

5. The radial cracks stabilize if and when the hoop stress at their tip is equal to concrete strength in uniaxial tension (uniaxial criterion) or in tension-compression (biaxial criterion): tension-compression interaction is detrimental to both tensile and compressive strength.

6. Crack width in the concrete core and bar-concrete pressure can be formulated in terms of a few geometric and mechanical parameters by writing (a) the equilibrium condition along any radially-cracked section, and (b) the kinematic condition in the cracked core; this condition (which can be formulated in different ways, see Section 1.4.3.3) governs the shape of the radial cracks, i.e. the dependence of the width on the radial coordinate (r). In the paper by Gambarova et al. (1998) the kinematic condition was based on the assumption that the circumferential elongation is constant and equal to that at the inner boundary of the plastic ring:

$$2\pi R\, \varepsilon_{cr} = n\, w(r) + 2\pi r\, \varepsilon_h^{sc} \qquad (1.4.15)$$

where $\varepsilon_{cr} = f_{ct}/E_c$, n = crack number, $w(r)$ = crack width, r = radial coordinate, $\varepsilon^{sc} = \sigma^{sc}(r)/E_c$ = hoop strain in the solid concrete between two contiguous cracks. In the above-mentioned paper, $\sigma^{sc}(r)$ was assumed to be equal to the cohesive stress at the crack interface: $\sigma^{sc}(r) = \sigma(w(r))$. The crack width $w(r)$ is quite a complex function of r, and <u>not</u> a linear function, as assumed by Reinhardt and van der Veen (1990): $w(r)$ also depends on the adopted cohesive law.

7. In the uncracked region the hoop strains are assumed to have an elastic-type distribution according to an elastic constitutive law, energetically equivalent to the actual elastic-plastic law. However, the hoop stresses are introduced according to the actual elastic-plastic behavior of the concrete, and as such they appear in the equilibrium equation.

8. The critical crack extension representing the maximum exploitation of bond, is obtained by maximizing bar-concrete pressure p (Fig. 1.4.13a) with respect to crack extension, for any given crack number.

9. The crack number is defined as the number corresponding to the smallest value of the pressure maximums, in fulfillment of both static and kinematic admissibility (see also Section 1.4.6.3). Smaller or greater crack numbers, albeit statically and kinematically admissible, prevent the maximum exploitation of bond in the former case, or may cause unstable situations, in the latter case.

1.4.6.5 Applications

A first example concerns the case of a bar embedded in plain concrete (Fig. 1.4.17, curve 1), or in high-volume fiber-reinforced concrete (Fig. 1.4.17, curves 2 and 3). In Fig. 1.4.17, the stress-strain/stress-displacement curves do not refer to any specific normal or fiber-reinforced concrete, but are three possible and realistic, albeit arbitrary, constitutive laws (concrete 1: G_f = 150 J/m^2; w_c = 0,8 mm; E_c = 32 Gpa; d_a = 16 mm). The three curves have the same initial slope (fiber content does not significantly alter the elastic behavior), slightly different strengths (fibers add some strength in tension), different plateaus (HPFRCCs have a remarkable pseudo-plastic behavior, depending on fiber content) and slightly different softening branches, representing crack localization. The extension of the plastic plateau $\Delta\varepsilon$ is 0, 7 ε_l, 15 ε_l respectively (ε_l = peak strain in plain concrete = f_{ct}/E_c). Fig. 1.4.18 shows how rapidly bond behavior tends to approximate to fully plastic behavior, because of the contribution of the fibers (fiber content should be in excess of 4-5% by volume). Figs. 1.4.19 and 1.4.20 show the evolution of crack number and width (at the bar-concrete interface) for increasing concrete covers. Finally, in Fig. 1.4.21 the critical crack penetration or extension, l_{cr}, (see Fig. 1.4.13b) is plotted versus the concrete cover.

Summing up, high fiber-contents (which turn concrete behavior in tension from elastic-brittle to elastic-plastic) guarantee much better bond characteristics for the same concrete cover, as well as thinner and less extended splitting cracks, and in the end greater strength and durability.

A second example concerns the passive confining action that a steel sleeve (or pipe) can exert on a concrete cylinder reinforced with a single bar (Figs. 1.4.22a,b), for a given extension of the split concrete around the bar. Depending on the thickness (t) of the sleeve (t = 0-18 mm, d_b = 16 mm, c/d_b = 4) and on crack extension (r), the pressure at the concrete-bar interface (p) reaches different values. As should be expected, the thicker the sleeve, the greater the pressure, which may-or may not- exhibit a relative maximum (p_{max}).

Copyright fib, all rights reserved. This PDF copy of fib Bulletin 10 is intended for use and/or distribution only by National Member Groups of fib.

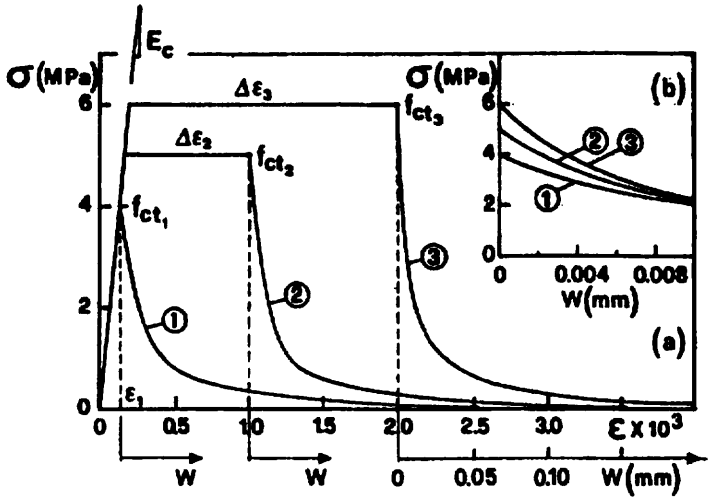

Fig. 1.4.17 - Typical stress-strain and stress-displacement relations: (1) plain concrete; (2) and (3) high-volume fiber-reinforced concretes (HPFRCCs).

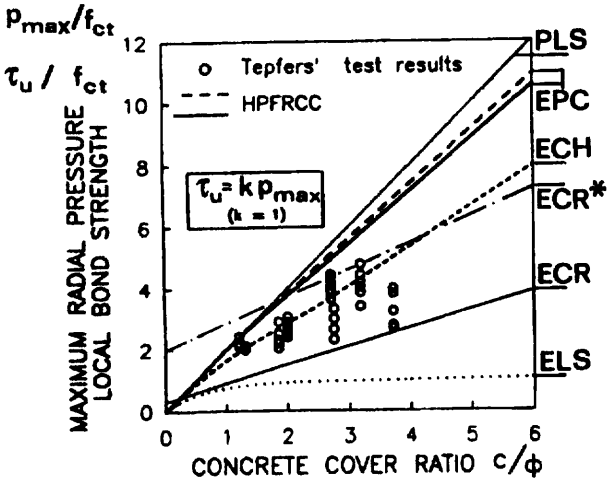

Fig. 1.4.18 – Plots of bar-concrete pressure and bond strength versus concrete cover, according to different models, and fitting of test results. Bar diameter ϕ = 16 mm. k (friction coefficient) =1.

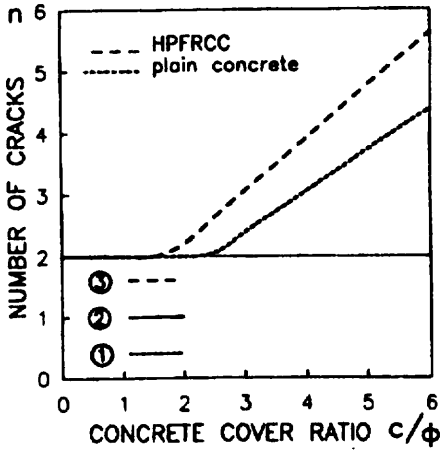

Fig. 1.4.19 – Plots of crack number versus concrete cover for plain and high-volume fiber-reinforced concretes. Fractional numbers should be rounded to the nearest whole number.

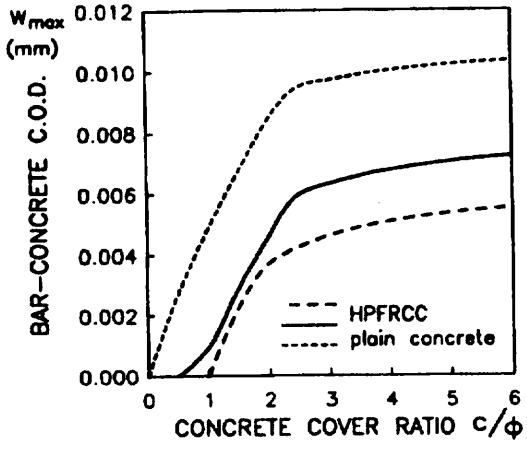

Fig. 1.4.20 – Plots of maximum crack-width versus crack cover.

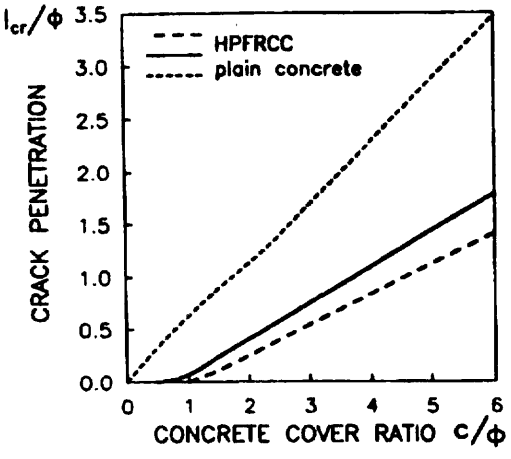

Fig. 1.4.21 – Plots of crack penetration versus concrete cover.

Copyright fib, all rights reserved. This PDF copy of fib Bulletin 10 is intended for use and/or distribution only by National Member Groups of fib.

In Fig. 1.4.22c the reference value $p_{max}/f_c = 0.45$ corresponds to the often quoted bond capacity $\tau_{bu} = 0.45\ f_c$, according to the relationship $\tau_{bu} = k\ p_{max}$, with k=1 (see also Eq. 2.3 in Chapter 2). For t = 18 mm, the ultimate capacity 0.45 f_c can be developed in partial-splitting conditions (crack extension r ≈ 4.5 times the bar radius), while for t ≈ 7 mm the same pressure is developed in through-splitting conditions (r = 9 R_b: the cover is fully split). Since the pressure 0.45 f_c represents bond ultimate capacity in a highly-confined segment of the anchorage ($p_{max} = \tau_{bu}/k$, Fig. 1.4.22b, k = 1), for t < 7 mm bond is never fully exploited ($p_{max} < 0.45\ f_c$). The plots of Fig. 1.4.22c were obtained by Coronelli (1999), on the basis of Tepfers' cohesionless elastic-cracked model, by enforcing the compatibility between the outer solid ring of the partially-split concrete cylinder, and the steel sleeve. The results of this study clearly show how passive confinement can control splitting radial extension.

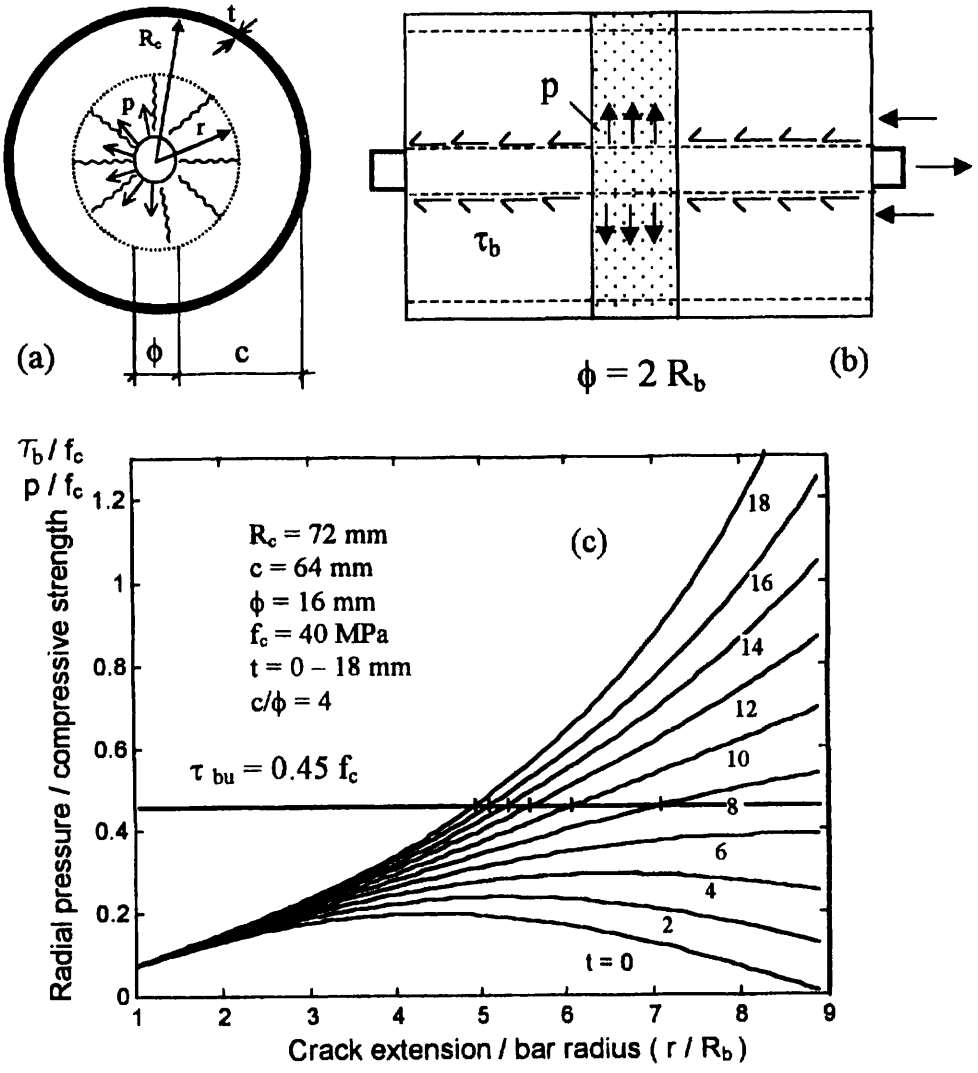

Fig. 1.4.22 – Plots of the radial pressure at the bar-concrete interface, as a function of the extension of the splitting cracks, for different levels of passive confinement. The confinement is exerted by a steel sleeve (thickness t = 0-18 mm; concrete cover c = 4 ϕ, Coronelli, 1999).

Copyright fib, all rights reserved. This PDF copy of fib Bulletin 10 is intended for use and/or distribution only by National Member Groups of fib.

1.4.6.6 Concluding remarks

The elastic-plastic-cohesive models proposed for bar-concrete bond belong to the mainstream of the recently-developed models which describe bond behavior in terms of concrete fracture or damage, localization included. With regard to this, the proposed models are a useful tool for a better understanding of the transition from solid to radially-cracked concrete in anchorage pull-out, as well as from splitting failures to true pull-out failures.

Moreover, these models allow a reliable estimate of the effects of the many factors influencing bond, such as concrete strength and stiffness, fracture energy, fiber content, concrete cover and aggregate size, bar diameter, transverse pressure and environmental effects (Diederichs and Schneider, 1981; Morley and Royles, 1983; Shih et al., 1988a,b).

Because of their open structure, the models based on the hydraulic-pressure analogy (mostly limit-analysis models) can be easily modified and extended to the "special" materials now coming onto the scene (high-strength concretes with or without fibers, epoxy-coated bars, non-metallic bars) and may be instrumental in modifying the equations, that are included in the actual codes for ordinary concretes and rebars. The favorable effects that the passive confinement (spiral or stirrups) has on bond, may be easily included too, by enforcing the compatibility in the hoop direction between the solid (or cracked) concrete and the confining reinforcement.

Since these models allow bar-concrete pressure p_{max} to be evaluated, as well as some properties of the radial cracks (such as crack number n, and maximum width w_{max}) at impending collapse, the evaluation of the corresponding ultimate bond stress τ_u requires the introduction of a suitable relationship among the above-mentioned parameters:

$$\tau_u = F\,(p_{max}, w_{max}, n, k, \tau_0 \ldots) \qquad (1.4.16)$$

as already shown in Section 1.4.3 (see for instance Eq. 1.4.1). In Eq. 1.4.16, k and τ_0 are the friction coefficient and the cohesive stress at the bar-concrete interface: these parameters take into account the surface conditions and the shape of the reinforcement.

As an example, and for the sake of simplicity, in Fig. 1.4.18 simple linearity was assumed for Eq. 1.4.16 $\tau_u = k\,p_{max}$, with $k = 1$.

Copyright fib, all rights reserved. This PDF copy of fib Bulletin 10 is intended for use and/or distribution only by National Member Groups of fib.

1.5 Discrete models in bond analysis

The needs of bond modeling as a 3-D or axialsymmetric problem have been and are still dealt with by means of FE discretization, with three main objectives: (1) to investigate bond behavior at the local level (microlevel) in order to take care of the various resistant mechanisms, which are activated at that scale (friction, bearing action, interface slip); (2) to relate the sectional behavior to the structural parameters (bottom and side concrete cover, bar diameter and free interspace, pull-out and push-off situations), in order to check and possibly improve the relatively simple equations required by structural design; and (3) to assess the soundness and numerical efficiency of the various bond stress-bar slip laws that have been proposed so far.

As a matter of fact, bond has so many structural aspects that it cannot be considered -strictly speaking- as an intrinsical physical property of reinforced concrete. Even if reinforced concrete is assumed to be a 3-phase material, consisting of steel (or reinforcement) and concrete plus an interlayer (where all the properties contributing to bond behavior are lumped together), the 3rd phase -the interlayer- is so sensitive to bar and stirrup arrangement, and section size (not to speak of the external pressure, if any) that true constitutive laws can hardly be introduced. Such a situation has been clear since the first studies on the subject (see for instance Lutz and Gergely, 1967).

While FEs make it possible to model the complex context of bond, a fundamental question still hangs overhead: is FE modeling a "model"? The answer may be "yes" if modeling is intended as a system of mathematical and physical laws, rules, assumptions and numerical procedures aimed at the description of a phenomenon, but the answer may be "no" if modeling is intended as a self-contained set of rational relations aimed at giving a closed-form response on the basis of a set of input data.

Since there is no univocal answer to the above question, bond modeling by FEs and FE models will be considered as synonyms in the following, with the 2nd expression being slightly preferred for its obvious simplicity.

Although the first FE models for bond-slip of reinforcing bars were proposed by Ngo and Scordelis (1967), Bresler and Bertero (1968) and Nilson (1968), with the introduction of linear and nonlinear springs for bond response, and suitable "boundary layers", most FE modeling of bond-related problems has been performed from the mid-Eighties onwards. However, these studies took advantage of the astonishing amount of research activity in the domain of R/C structures, that was carried out in the Seventies and was presented in the well-known State-of-the-Art Report by ASCE (1982). In this report, Chapter 3 is devoted entirely to both reinforcement modeling and bond representation, via three different approaches (distributed, embedded and discrete reinforcement), and such tricky problems as cyclic loading, tension stiffening, primary and secondary cracking are treated, with reference mostly to tension specimens.

Several valuable contributions should be mentioned, concerning a variety of topics, such as nonlinear fracture mechanics (Ingraffea et al., 1984; Rots, 1990), 2-D and 3-D nonlinear modeling of concrete embedment (Reinhardt et al., 1984; Cox and Herrmann, 1992; Ozbolt and Eligehausen, 1992), dedicated FEs (De Groot et al., 1981; Filippou et al., 1983; Yankelewsky, 1985; Keuser and Mehlhorn, 1987; Hemmaty et al., 1991; Mainz, 1993; Kwak, 1997; Monti et al., 1997), concrete damage mechanics (Pijaudier-Cabot et al., 1991), discrete-crack FEs (Yao and Murray, 1995), special models for steel-concrete interface (van Mier and Vervuurt, 1995), not to speak of the attempt to model bond by means of a boundary-element approach (Davì et al., 1994) or by combining boundary and finite elements (La Mendola, 1997).

1.5.1 Layer models

Since bond-induced effects occur mostly in the concrete layers closest to the bar, the FE axisymmetric discretization of the concrete embedment was subdivided by Bresler and Bertero (1968) into two regions (Fig. 1.5.1): an inner "boundary layer" (to take into account the inelastic deformations and fracture in the concrete closest to the bar) and an outer annular cylinder of undamaged concrete. Both regions were assumed to have a linearly-elastic isotropic behavior, but the elastic constants of the boundary layer were suitably "tuned" ($E_{BL} = 0.06\ E_c$, $\nu_{BL} = 2.5\ \nu_c$). The thickness of the boundary layer was assumed to be ≈ 0.4 times the bar diameter (11 and 28 mm respectively). It is worth noting that the displacement field of the boundary layer represents the local slip at the bar-concrete interface. Of course the boundary layer is a "homogeneized" representation of the complex and highly "disturbed"

Copyright fib, all rights reserved. This PDF copy of fib Bulletin 10 is intended for use and/or distribution only by National Member Groups of fib.

local behavior of bond, and the stresses in the embedment are greatly reduced owing to the relatively "soft" boundary layer.

A "slip layer" was also used by Reinhardt et al. (1984), for modeling the bond-related nonlinear phenomena (Fig. 1.5.2), this layer being divided into torus-like elements, whose thickness is equal to the bar diameter. Both the steel and the outer portion of the concrete were considered as elastic. The torus-like elements exactly match the shape of the ribs, and their nonlinear behavior is described by means of an elastic-plastic law in compression, and by an elastic-softening law in tension (linear softening). A Mohr-Coulomb failure surface with tension cut-off is adopted for multiaxial loading. The mortar in contact with the bar can slip (hence friction is taken care of), but not along the inclined sides of the lugs. Once these slip-layer elements have been calibrated, their introduction into any FE code with axialsymmetric elements may in principle allow any bond problem to be modeled. Also the effects of a radial pressure and those of a high-rate displacement applied to a bar can be modeled.

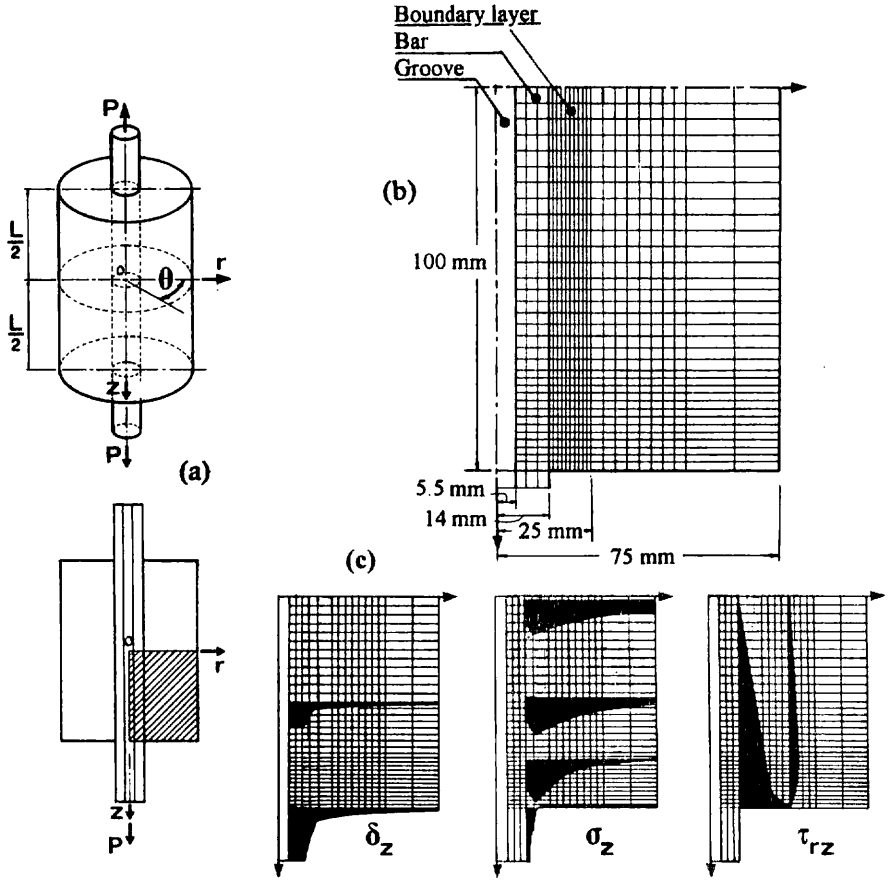

Fig. 1.5.1 - Finite Element idealization according to Bresler and Bertero (1968): (a) coordinate system; (b) finite element idealization; and (c) diagrams of the longitudinal displacement and normal stress, and of shear stress. The bar was cut longitudinally, and a groove was milled in each half to place a set of electrical strain gages; then the two halves were tack-welded together.

A 2-D plasticity model for bond was developed by Cox and Herrmann (1992 and 1994), on the basis of several test results that provide some information on the confinement stress developed by the concrete during a pull-out test. The model relates the local slip and radial dilation (in the zone closest to the bar) to both the bond stress and the radial confinement stress in a finite-thickness region around the bar ("process zone" according to the authors), its thickness being close to the height of a rib. The form of the yield surface, the evolution laws for the internal variables and the flow rule reflect qualitatively the micromechanics of bond (crushing, fracture and friction). The model was implemented in a research-oriented FE code. Most of Eligehausen (Fig. 1.5.3), Gambarova, Malvar, Rehm and Shima's test results were successfully fitted.

Finally, a quite peculiar approach to concrete modeling in the layers closest to the bar was introduced by

Copyright fib, all rights reserved. This PDF copy of fib Bulletin 10 is intended for use and/or distribution only by National Member Groups of fib.

van Mier and Vervuurt (1995), who took advantage of a recently-developed "lattice" model for concrete, which is basically a micromechanics-based model (see also Section 1.5.6). According to this model the embedment hetereogeneity is taken care of by replacing the concrete with a regular or randomly-generated lattice of microbeams in tension /compression /bending (Fig. 1.5.4). Fracture is simulated by removing - at each load step - the microbeam with the highest stress over strength ratio. Three examples are shown: local cracking in the bond zone (owing to rib-induced disturbances); a tension test and an anchor pull-out test. The beam behavior is assumed to be elastic, hence the analysis at each load step is purely elastic, but with a step-by-step reduced lattice. The delicate aspect is how to determine the length, section and mechanical properties of the microbeams, since the lattice is supposed to represent the microstructure, while the previously-cited parameters can be calibrated only on the basis of macrotests. In Fig. 1.5.5 the mesh used in the simulation of a pull-out test is shown, together with some details of the real specimen. Note that the lattice model is used only to describe the concrete layer closest to the bar, while normal 4-node plane-stress elements are used in the outer region (where cracking is unlikely to occur) and the metal tube is modeled by means of a set of elastic springs. The bond problem is solved as a 2-D problem, and the bar-concrete slip results from the extensive microcracking in the layer closest to the bar. The model seems to be very promising for its simplicity, but to what extent a microlattice can represent the microstructure of a concrete or mortar is debatable.

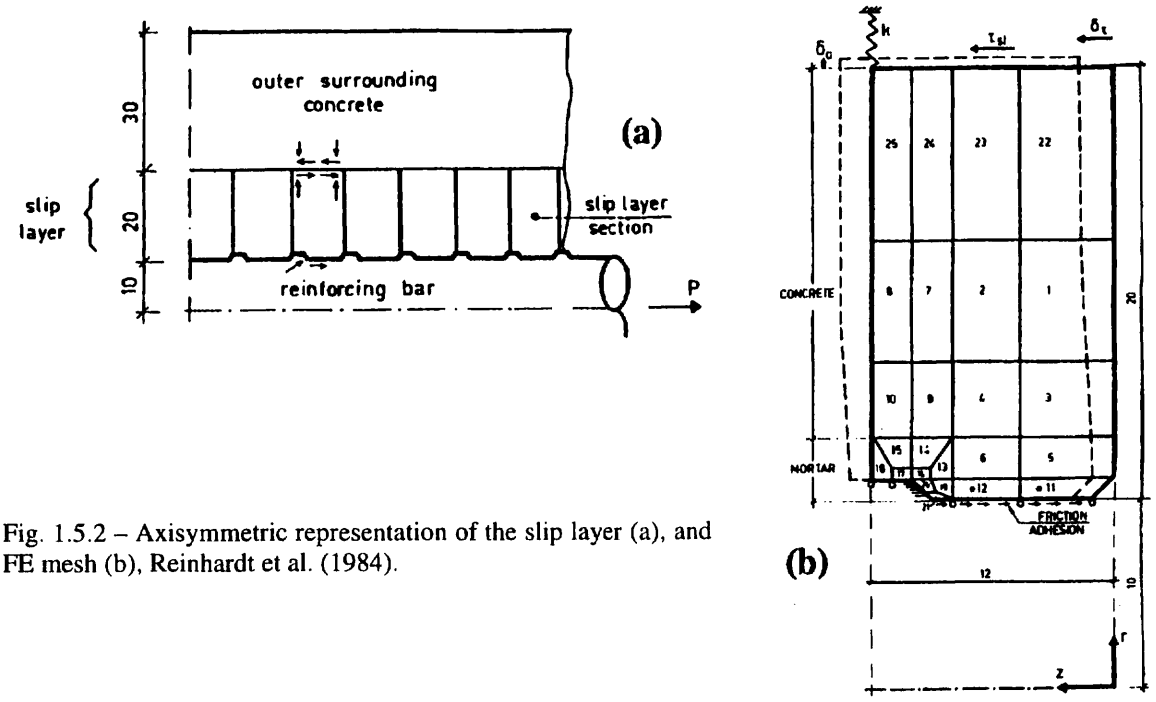

Fig. 1.5.2 – Axisymmetric representation of the slip layer (a), and FE mesh (b), Reinhardt et al. (1984).

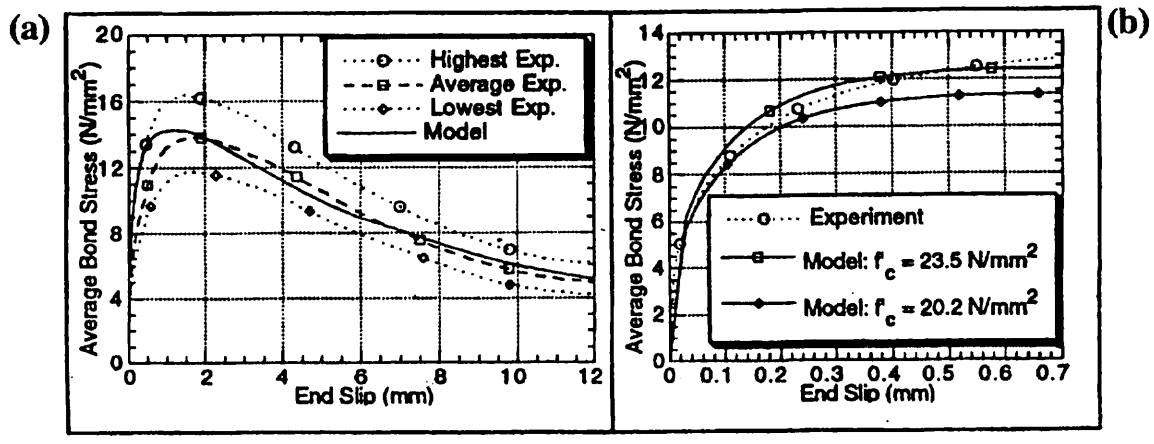

Fig. 1.5.3 - Comparison of the model proposed by Cox and Herrmann (1992) to monotonic results of (a) Eligehausen et al. (1983), and (b) Rehm and Eligehausen (1979).

Copyright fib, all rights reserved. This PDF copy of fib Bulletin 10 is intended for use and/or distribution only by National Member Groups of fib.

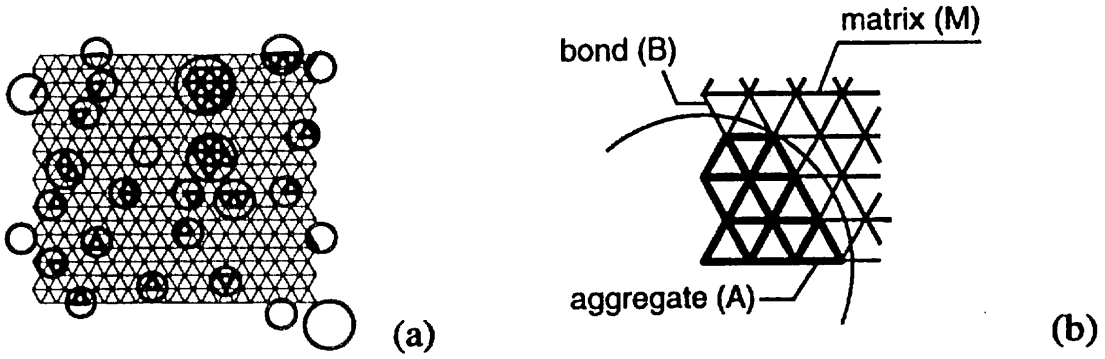

Fig. 1.5.4 - (a) Particle overlay, and (b) different properties assigned to beam elements belonging to either of the three phases (bar + interface or bond + concrete), according to van Mier and Vervuurt (1995).

1.5.2 Fracture mechanics models

While in slip-layer models the tensile cracking in the concrete closest to the bar is dealt with by means of a smeared-crack approach, Ingraffea et al. (1984) modeled cracking discretely, through the use of a "crack nucleation and propagation code" and a nonlinear fracture-mechanics scheme. Through the use of interface elements and the computation of the stress-intensity factors at increasing loads, and by updating the mesh ("remeshing"), crack formation, propagation and direction was described. Modeling of secondary cracks (radially slanting from the bar, Fig. 1.5.6) by means of the relationships between the normal and shear stresses across a crack, and the crack displacements (opening and slip) forms the basis of the nonlinear model. Longitudinal splitting and local crushing of the concrete underneath the lugs were not studied, while the introduction of special "tension-softening" elements at each intersection of a bar with a primary crack (flexural crack) was envisaged.

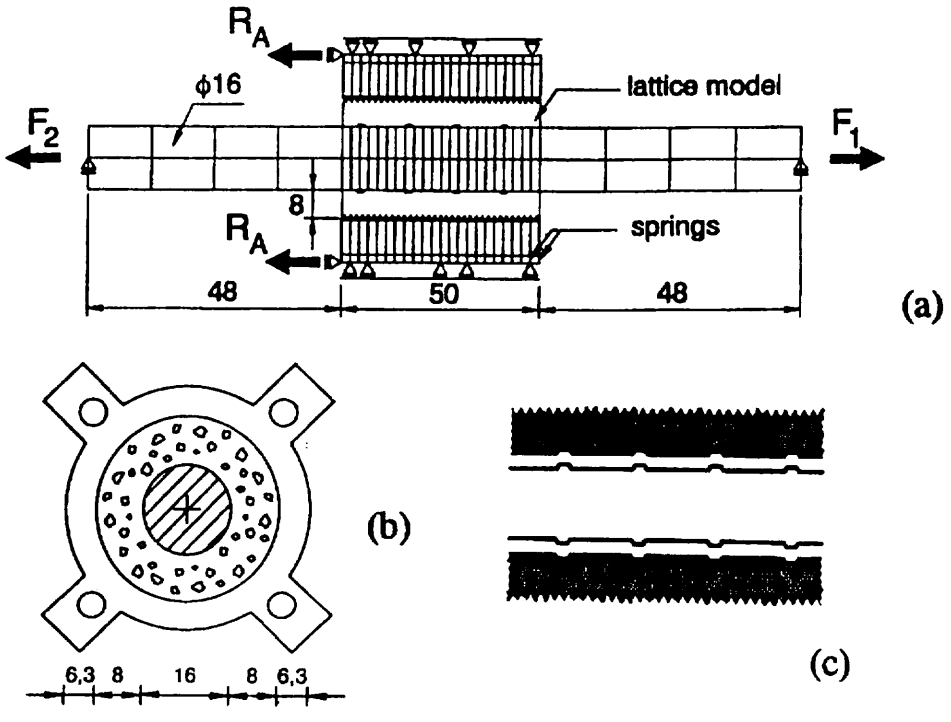

Fig. 1.5.5 - (a) FE mesh, (b) cross-section of the real specimen (Dragosavic et al., 1987), and (c) lattice model (van Mier and Vervuurt, 1995).

Copyright fib, all rights reserved. This PDF copy of fib Bulletin 10 is intended for use and/or distribution only by National Member Groups of fib.

Two applications of "softening fracture mechanics" to bond and anchorage problems are presented in the study by Rots (1990), where smeared and discrete crack models (including tensile softening) are used to simulate the fracture behavior in a tension pull-out specimen and in an anchorage. Both problems involve axisymmetry. Both secondary and primary cracks (i.e. partial and throughout transverse cracking) were allowed to rotate, and their formation and propagation were governed by axisymmetry (Fig. 1.5.7a), while the crack pattern of longitudinal splitting (i.e. crack number and location) had to be introduced among the input data. The numerical examples support the verification and validation of the traction-slip rules available in literature, and the results correctly reveal that the elastic energy stored in the structure is released for creating fracture surfaces, which are accompanied by a brittle load-displacement behavior (Fig. 1.5.7b).

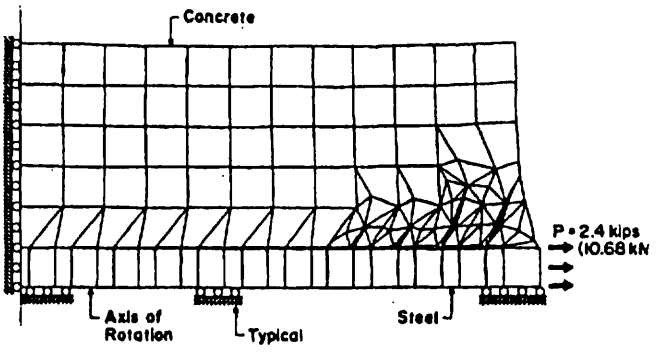

Fig. 1.5.6 - Deformed mesh of portion of tension pull-out specimen, with 4 secondary cracks (Ingraffea et al., 1984).

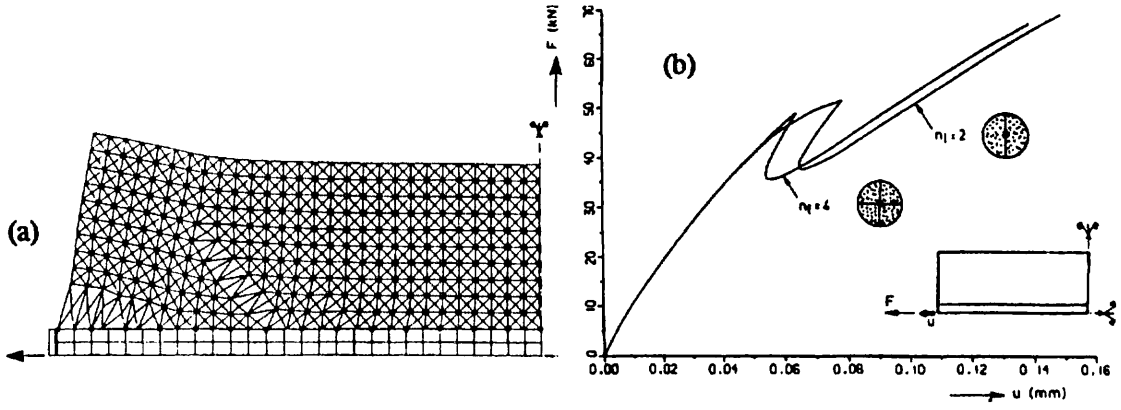

Fig. 1.5.7 - (a) Secondary-crack formation in a tension pull-out specimen, and (b) bond-displacement curves for 2 and 4 splitting cracks (Rots, 1990).

1.5.3 Dedicated finite elements

A "weighted" residual formulation of the differential equations of equilibrium and compatibility of a single bar embedded in concrete was presented by Filippou et al. (1983). The bar was subdivided into a number of linear elements and a secant stiffness formulation was adopted to linearize both the bond stress and the steel stress. Independent shape functions were introduced to discretize the displacement and steel-stress fields in the bar (mixed FE formulation). A nonlinear matrix relation between the incremental state vectors at the two ends of the bar (displacements and stresses) was derived and then applied successfully to obtain the fixed-end rotations of beam-column subassemblages.

Yankelevsky (1985) formulated a one-dimensional finite element model for bond-slip analysis, by piece-wise linearizing the bond stress-slip curve and by solving the differential equilibrium equation for each of the linear branches. After the global stiffness matrix of a bar element (divided into 1-D FEs) has been built-up, the solution is reached iteratively, when the compatibility at the extremities of each element is respected. Typical results are shown in Fig. 1.5.8, where the hollow circles ensue from the test data on bar slip.

Copyright fib, all rights reserved. This PDF copy of fib Bulletin 10 is intended for use and/or distribution only by National Member Groups of fib.

Since bond may be reduced to a "contact problem" (assuming for the layer closest to the bar a negligible thickness compared to bar and cover size), special "contact" elements (= elements connecting two nodes with identical coordinates) were introduced in the past, and a concise but useful review is presented by Keuser and Mehlhorn (1987). The contact element may give a discontinuous or continuous connection between two adjacent elements (linear or higher-order displacement fields, Fig. 1.5.9). Also the normal stress between the concrete and the reinforcement have been taken into account. The contact element with a linear displacement function seems to be the best in terms of good fitting of test results and computational efficiency. Of course, besides the displacement function, the formulation of an adequate bond stress-bar slip relationship is of paramount importance, in order to construct the element stiffness matrix. Four bond stress-bar laws are considered by Keuser and Mehlhorn, and a thorough study on a tensile specimen is presented.

A critical examination of bond-slip modeling was carried out by Hemmaty et al. (1991), within the framework of the FE code ANSYS. At first Tassios' bond-slip curve (Fig. 1.1.1), is recalled, together with a few simplified relations (rigid-plastic and elastic-plastic, the latter adopted in the FE code DIANA), and Vandewalle's relation, which takes into account the initial cohesive behavior of bond. Then both "material models" and "periferic models" for modeling the concrete closest to the bar and the interface are discussed, but the former (based on artificially-reduced concrete properties to take into account local microcracking and crushing, see for instance Dragosavic, 1987) are discarded on the grounds of the arbitrary definition of the reduced properties. The periferic models are in turn divided into "bond-zone models" (like the layer models introduced in Section 1.5.1, thickness $\phi/2$ in the FE code DIANA), and "spring models" or "bond-link models" (Fig. 1.5.10). Hemmaty et al. described the contact between the bar and the concrete with unidirectional spring elements (Fig. 1.5.10, ANSYS element 39) characterized by a nonlinear generalized force-deflection capability.

Contact elements similar to those shown in Fig. 1.5.10b were used also by Ichinose and Hayashi (1998), who studied RC lap splices, considering concrete splitting, bar-concrete friction, local cracking in front of rib faces and stirrup-cover interaction. Different failure modes for bond behavior between two contiguous ribs (Mohr-Coulomb, and friction with and without dilatancy) were included.

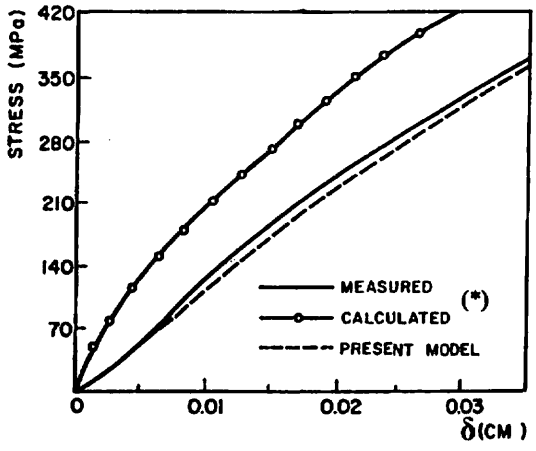

Fig. 1.5.8 - Pull-out test: stress (in the bar) versus slip (at the loaded end) according to Yankelevski's model (1985). (*) Tests by Viwathanatepa, Popov and Bertero (1979).

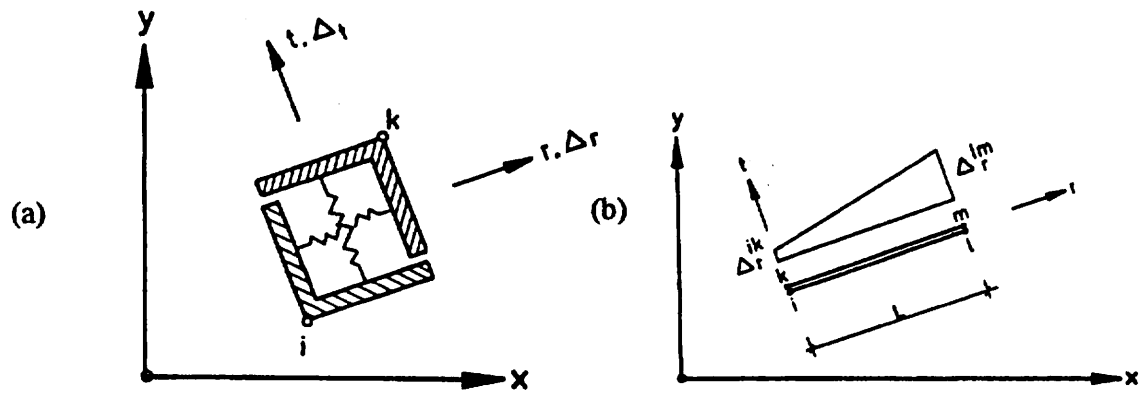

Fig. 1.5.9 - (a) Bond-link element and (b) contact element (Keuser and Mehlhorn, 1988).

Copyright fib, all rights reserved. This PDF copy of fib Bulletin 10 is intended for use and/or distribution only by National Member Groups of fib.

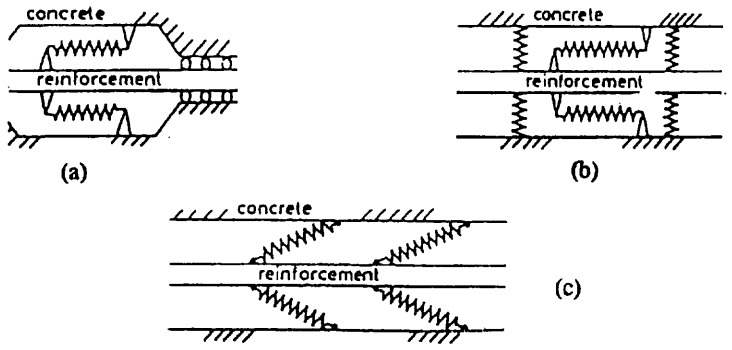

Fig. 1.5.10 - Various possible spring models (Hemmaty et al., 1991).

Tension bars and beam-column joints were successfully modeled, including concrete cracking, since concrete was modeled with special solid elements taking into account both nonlinearity and cracking. Kwak (1997) developed an "equivalent reinforcing steel" model, which describes the bond-slip effect without introducing the double nodes, by condensing the steel nodes internally. Both analytical and experimental results were fitted successfully (various pull-out and push-pull cases, cyclic loading).

Finally, the numerical advantages to approximate the smooth distributions of the bond and steel stresses - rather than the steep slip gradients- led Filippou and his co-workers (see Monti et al., 1997) to adopt a force-based element formulation for modeling a reinforcing bar. Since modeling a bar implies four unknown fields (Fig. 1.5.11: bond stress, bar strain, bar stress and relative slip), which are related by the governing equations of the stress-transfer problem, the proposed rebar model can be viewed as a simple system made up of two components in parallel: the bar and the interface with the surrounding concrete. In the end, the element stiffness matrix is determined by inverting the element flexibility matrix. Several pull-out and push-pull tests were performed numerically, taking advantage of a few bond-slip relationships, and the fitting of the test results was very good. Also several anchorages subjected to cyclic loading were studied numerically and the hysteretic cycles were very close to the real ones.

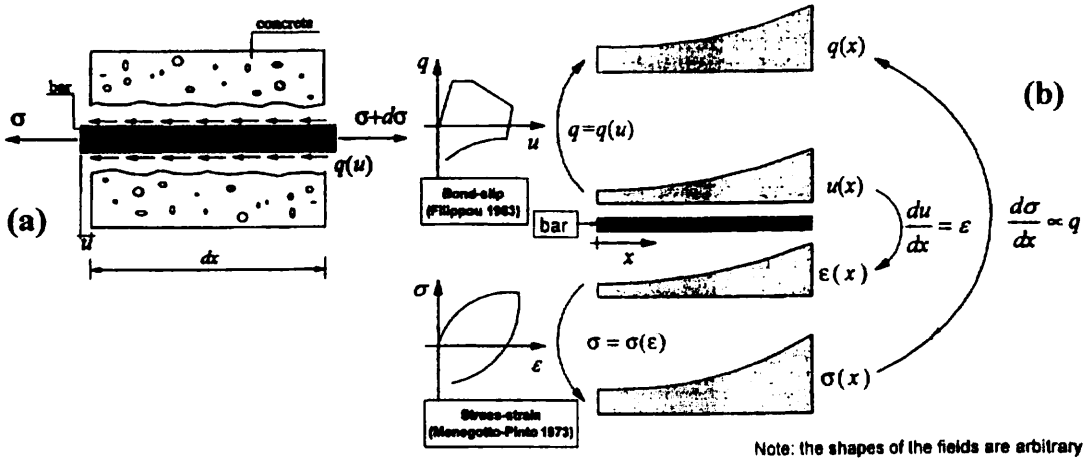

Fig. 1.5.11 - (a) Infinitesimal segment of an anchored reinforcing bar, and (b) relation among the four fields of bond problem (Monti et al., 1997).

1.5.4 Damage mechanics models

Instead of introducing contact or interface elements whose properties need to be defined and are easily given arbitrary values, it is possible to tackle efficiently bond problems by modeling adequately concrete nonlinearity (microcracking included) through Damage Mechanics. Mazars, Pijaudier-Cabot et al. (1990, 1991) did this by developing a scalar damage model for concretelike materials. This model was

Copyright fib, all rights reserved. This PDF copy of fib Bulletin 10 is intended for use and/or distribution only by National Member Groups of fib.

formulated in both the local and nonlocal versions. It is worth recalling that the "damage" represents the density of microcracks in a medium, and that damage should be a vectorial state variable (since microcracking develops in specific planes). However, scalar (isotropic) damage is sufficient to describe many problems, such as notched plates and laboratory-type fracture specimens. The stress-strain relationship is:

$$\sigma_{ij} = (1-\Omega)\, C_{ijkl}\, \varepsilon_{kl} \tag{1.5.1}$$

where σ_{ij} and ε_{kl} are the components of the stress and strain tensors respectively (i,j,k,l = 1-3), C_{ijkl} is the initial stiffness matrix and Ω is the damage function ($0 \leq \Omega \leq 1$).

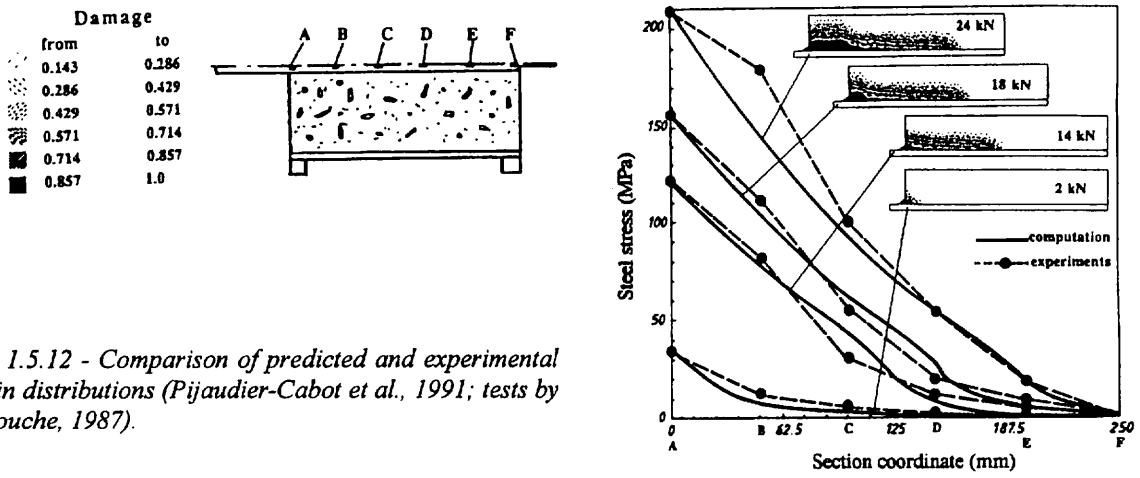

Fig. 1.5.12 - Comparison of predicted and experimental strain distributions (Pijaudier-Cabot et al., 1991; tests by Adrouche, 1987).

In order to avoid spurious crack-localization modes (owing to strain softening) Ω is governed by a nonlocal variable, this variable being based on an "equivalent strain" which is related to the positive strains. By implementing the constitutive equations for damage in a FE code (code CESAR, axisymmetric mesh), several pull-out tests were numerically reproduced (Fig. 1.5.12), and the test results were successfully fitted. Also the strong size effect in pull-out tests was numerically confirmed (see also Bazant and Desmorat, 1994).

1.5.5 Distributed/discrete crack FE models

On the grounds of the paramount importance that both transverse and longitudinal cracking have on bond behavior and bar slip, Yao and Murray (1995) adopted triangular-toroidal elements to model the axisymmetric concrete mass surrounding a bar (Fig. 1.5.13).

The regular triangular elements (with two 45° and one 90° angles) exactly match the shape of the lugs (Fig. 1.5.13) and make it possible to reproduce 8 different crack orientations to simulate concrete cracking.As soon as the principal tensile stress equals concrete tensile strength within the concrete mass, the nodes are split and a crack forms. However, at the contact with the bar cracking develops only after an "adhesive strength" has been exceeded. The split nodes are linked by "link elements" to simulate crack softening (i.e. crack cohesion). While transverse cracking is localized along certain planes (and transverse cracks can even close), splitting in longitudinal planes is simulated by resorting to a smeared crack approach, in order to respect axisymmetry. When the circumferential (hoop) stress reaches concrete tensile strength in the concrete embedment at any radial distance from the axis, the hoop stiffness along the corresponding circumference is set to zero. Several tests (by Goto, Nilson and Tanner) were successfully simulated.

The novelty of Yao and Murray's approach is that the whole crack system can be described (interface cracking with the concrete lifting up from bar surface, transverse cracking and longitudinal splitting in the concrete), with of course some limitations concerning the orientation of the transverse cracks and the lack of localization of the splitting cracks, the latter aspect being rather important, since the opening of the splitting cracks is directly related to their number (see Section 1.4.3).

Copyright fib, all rights reserved. This PDF copy of fib Bulletin 10 is intended for use and/or distribution only by National Member Groups of fib.

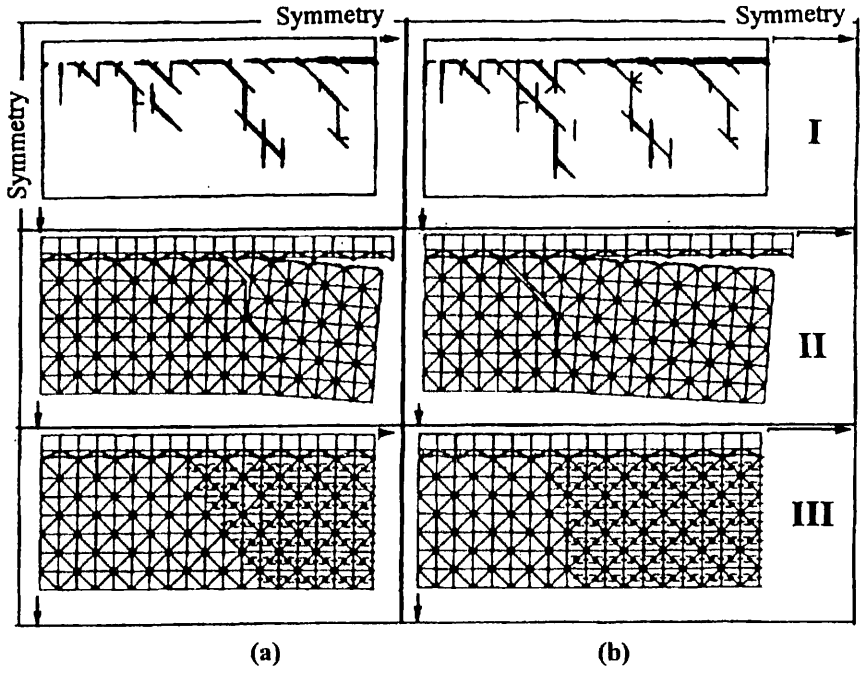

Fig. 1.5.13 - Solution for Goto's Case 1: steel stress σ_s = 185.3 MPa (a), and σ_s = 211.9 MPa (b), according to Yao and Murray's model (1995). I = crack distribution; II = deflection; III = longitudinal splitting.

1.5.6 Micromechanics-based FE models

Among the few models so far developed and based on a more or less simplified micromechanical representation of concrete (such is the case - for instance - of van Mier's lattice model, see Section 1.5.1), a particularly successful example is the microplane model, which was developed in the Eighties by Bazant and Associates, to describe concrete nonlinear behavior. The concrete is considered as a system of randomly-oriented planes (representing such local discontinuities as interaggregate contacts, microcracks, interfaces and thin mortar layers between the coarse aggregate particles), whose mechanical response is represented only by two shear stresses and strains, and one normal stress and strain (Fig. 1.5.14). By calibrating, once and for all, the 2 constitutive laws of a single "microplane", any load history and stress state can be modeled (1D, 2D and 3D, monotonic and cyclic loading), since the local response of the concrete is the resultant of the stresses and strains pertaining to each microplane. The local failure of the material occurs when the stresses and strains concerning most of the microplanes enter into the softening phase (in tension, compression or shear) or are deactivated (after reaching a limit strain), and the material (as a whole) loses its strength and stiffness. As a result, cracking can be described by means of "cracked regions" (or bands), and the underlying philosophy is close to the smeared-crack approach.

Taking advantage of the microplane model and of a 3-D code, Ozbolt and Eligehausen (1992) modeled the pull-out of a bar by means of axisymmetric 4-node finite elements with 4 integration points. Both the yielding of the bar and the splitting of the cover were prevented by properly designing the concrete embedment, which was confined by a steel sleeve. The shape of the deformed bar was exactly modeled in order to recreate a realistic situation.

Since bond cycling causes strength and stiffness degradation both in the direction of loading and in the opposite direction, the shear stiffness of the microplane was modified by introducing a "damage" function d (adopted also by Kwak, 1997), which is related to the shear energy E dissipated by each microplane:

$$\frac{d\tau}{d\gamma} \approx 1 - d = e^{-1.2(E/E_0)^{1.1}} \qquad (1.5.2)$$

The results compare favorably with previous experimental observations, in terms of hysteretic loops, stiffness degradation and stress peaks, but the slip at peak load is much smaller than that obtained in the tests. The numerical analysis was also very sensitive to lateral confinement (see also Section 3.6).

Copyright fib, all rights reserved. This PDF copy of fib Bulletin 10 is intended for use and/or distribution only by National Member Groups of fib.

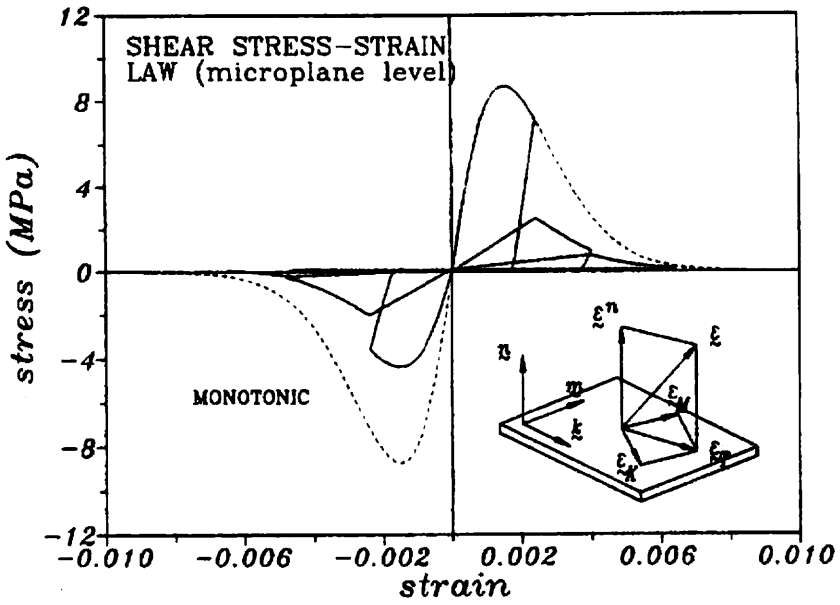

Fig. 1.5.14 - Shear stress-strain law of each microplane; f_c = 28 MPa; f_{ct} = 1.9 MPa; E_c = 25000 MPa; ν_c = 0.18.

1.5.7 Element-embedded crack model - Inner Softening Band

Among the most advanced continuum-based FE approaches for fracturing materials, a recent contribution is based on the concept of the so-called "Inner Softening Band". In this approach, a strong displacement discontinuity (associated with concrete fracture) is inherent in the constitutive formulation of each element, without an apriori definition of the location and orientation of the discontinuity. The further extension of previously formed cracks depends on the current state of stresses, and not on the previously formed cracks.

Concrete type		*NSC*	*HSC$_I$*	*HSC$_{II}$*	*HSC$_{III}$*
Compressive strength, f_c	*MPa*	*57,0*	*105,0*	*157,4*	*114*
Tensile strength, f_{ct}	*MPa*	*3,8*	*5,0*	*8,0*	*5,1*
Modulus of elasticity, E_c	*GPa*	*33*	*39,4*	*41,2*	*40*
Fracture energy, G_f	*N/m*	*105*	*145*	*172*	*217*

Experiment

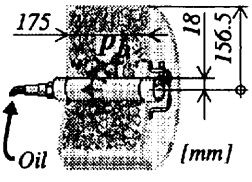

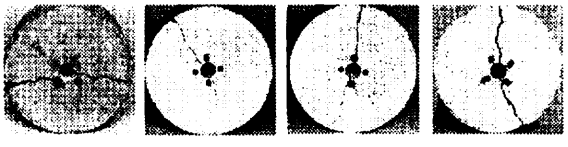

$p_{b,max}$=20,2 MPa 26,7 28,1 30,9

Computational (ISB)

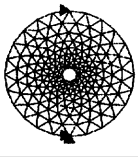

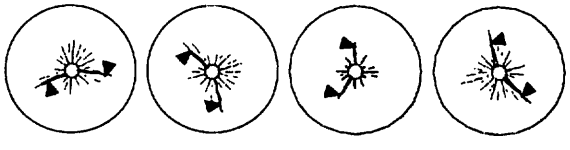

$p_{b,max}$=19,2 MPa 24,7 28,3 28,4

Fig. 1.5.15 - Comparison between the ultimate pressure capacity, $p_{b,max}$, obtained from the splitting tests on thick-walled concrete rings and the ISB model. A linear softening relation was assumed in all cases. For the ISB model, the markers indicate active cracks, while the other cracks tend to close because of unloading (Noghabai, 1997).

Copyright fib, all rights reserved. This PDF copy of fib Bulletin 10 is intended for use and/or distribution only by National Member Groups of fib.

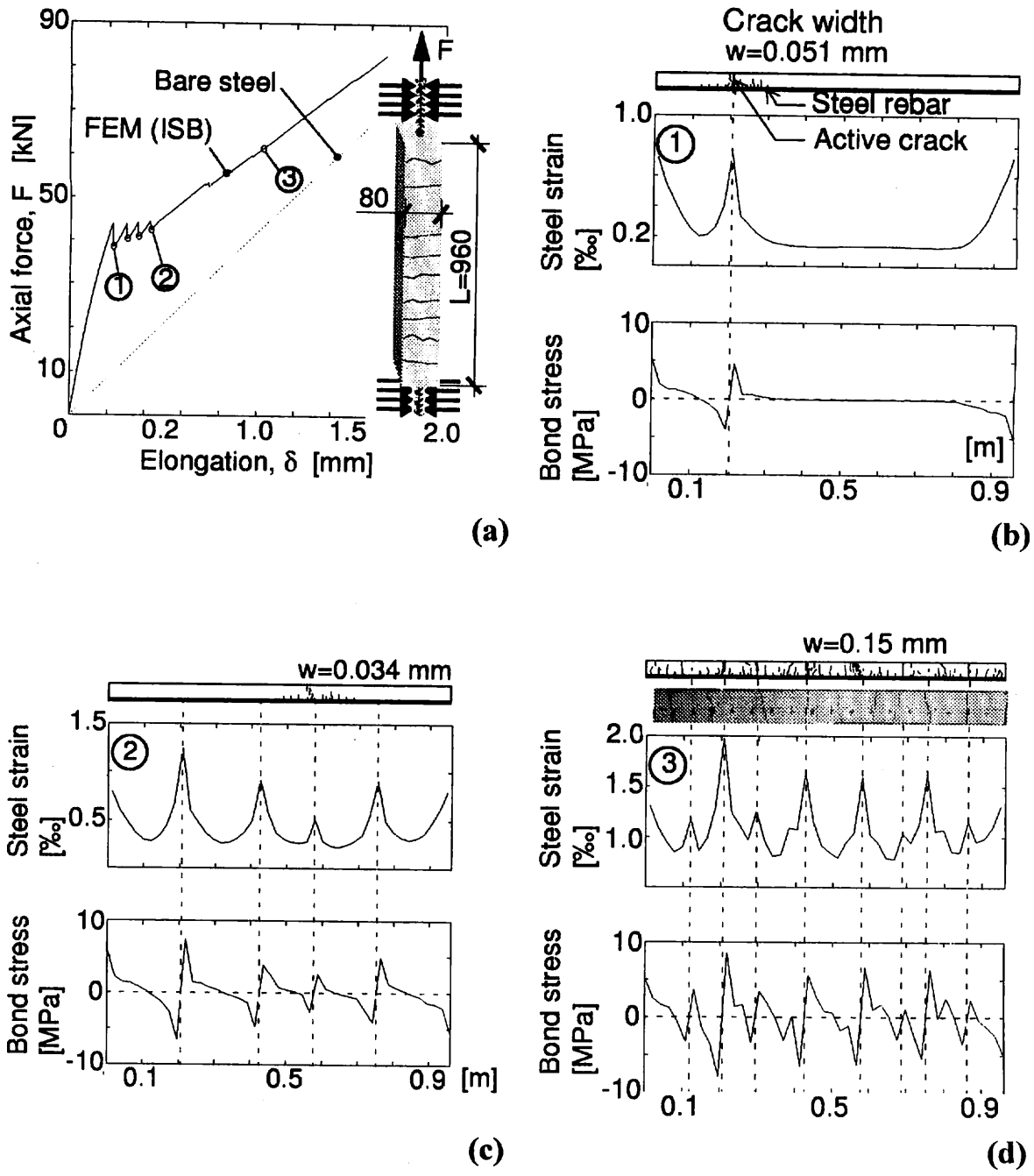

Fig. 1.5.16 - (a) Simulation of a pull-tension test of a rebar embedded in a concrete prism with square cross-section. (b) Bond stress and steel strain at load level 1. (c) and (d) Bond stress and steel strain at load levels 2 and 3. A discrete model is used for the concrete-bar interface, whereas the concrete is modeled by ISB-elements. The crack pattern obtained by means of the ISB model is in very good agreement with the test results (Noghabai, 1997).

The inner softening band (ISB) approach, introduced by Klisinski et al. (1991), was codified in the package MATLAB (Ohlsson and Olofsson, 1997). The constitutive formulation is based on the incremental theory of plasticity and on the decomposition of the nodal displacement rates into two parts, the first related to the continuum and the second to the softening band. The initiation and orientation of a softening band/crack is governed by a criterion based on the current stress state in the *stress space*. After initiation, the crack evolution abides by a constitutive law expressed in the *crack traction space*. The material softening rule is close to the fictitious crack concept used in the discrete crack model. The main advantage of the model lies in providing credible crack patterns and plausible explanations to fracturing phenomena in concrete. The code was used to model two 2-D problems, both presented in Noghabai (1997) and shown in Figs. 1.5.15 and 1.5.16.

In Fig. 1.5.16, a bond stress-slip relation according to CEB-FIP Model Code 90 (1993) - and its extension

Copyright fib, all rights reserved. This PDF copy of fib Bulletin 10 is intended for use and/or distribution only by National Member Groups of fib.

to high-strength concrete - was used as a constitutive law for the rebar-to-concrete interface, albeit the slip in this relation incorporates also the deformation due to concrete cracking. The case in Fig. 1.5.16 should only be viewed in the context of replicating a phenomenon (shape of the response curve and the crack distribution on the specimen). As shown by the examples, the model needs only a few material parameters which are experimentally attainable and no calibration or intrinsic length parameters are needed.

1.5.8 Structural models

Since bond strength and - more generally - bond behavior is a structural rather than a material property, controlled by both the geometry of the structure and the properties of the steel and the concrete, much effort has been devoted lately to model full-size R/C specimens, in order to determine the effects that rib shape, concrete cover, embedment length, transverse reinforcement, concrete tensile strength and fracture energy have on bond stiffness and strength. To achieve this goal, Darwin and McCabe (see Darwin et al., 1994) modeled a beam-end specimen (Fig. 1.5.17), by means of a somewhat simplified 3-D discretization of the real problem (note the square-section bar, Fig. 1.5.17b). Symmetry was assumed with respect to the vertical plane passing through the bar axis, and the plane of symmetry was assumed to be a potential fracture surface (splitting could not form in any other plane).

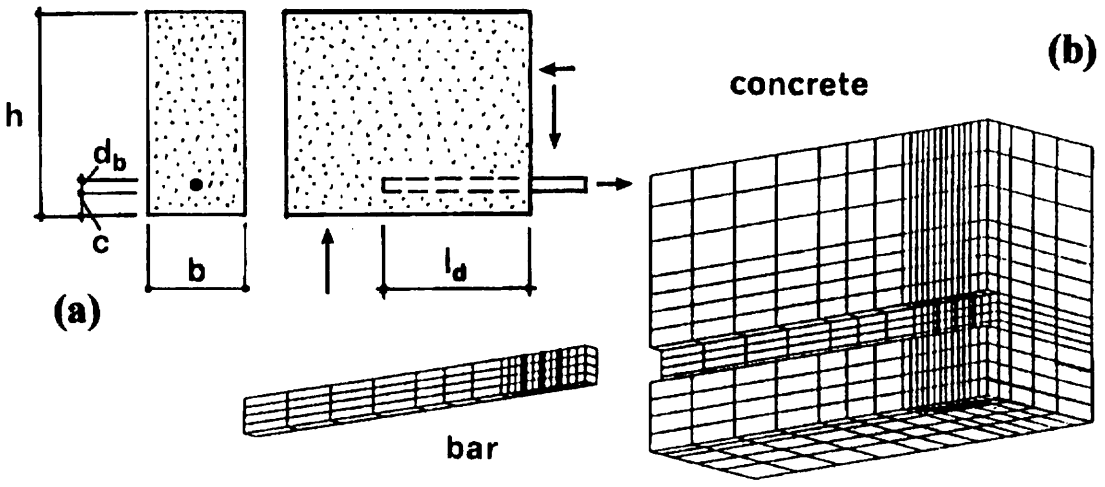

Fig. 1.5.17 - (a) Beam-end test specimen; and (b) concrete and steel substructures (rib number n_R = 3); b = 229 mm; l_d = 305 mm; h = 178-279 mm; d_b = 25 mm; c = 25-76 mm; rib spacing s_R = 16 mm; n_R = 1,2,3,6,12; E_c = 27.6 GPa; E_S = 200 GPa; ν_c = 0.2; f_{ct} = 1.37-5.50 MPa; G_f = 50-200 N/m.

The 3-D isoparametric "brick" elements used for concrete are connected to the nodes belonging to the plane of symmetry, by means of rod elements, whose stress-displacement properties are linked to concrete fracture properties, within a "fictitious crack model" approach.

The steel-concrete interface is represented using a three-dimensional interface link element. Interfacial strength follows a Mohr-Coulomb surface, and the elements on the interface will be in a contact/stick, a contact/slip, or a separation state. In the contact/slip condition, residual stresses are used to correct the stresses at the interface back to the Mohr-Coulomb surface. The properties of the interface are controlled by the cohesion, c = 1.7 MPa and the coefficient of friction, μ = 0.3 or 0.6. The ribs were generally modeled by means of prisms with a triangular cross-section: the front and back faces had an angle of 45°, and the rib height was 1.5 or 2.3 mm.

The analysis is accomplished using an incremental, iterative Newton-Raphson procedure. Loads are applied by imposing small displacements on the front end of the reinforcing steel substructure. Material properties are updated after each iteration, and unbalanced forces are reapplied to the structure following each iteration.

Some results are shown in Fig. 1.5.18. Note that under conditions of low confinement (Fig. 1.5.18a), the initial stiffness but not the peak load depend on rib height. The same conclusion is confirmed by the response for different values of the cover (Fig. 1.5.18b), where the effects of rib height are practically nil,

Copyright fib, all rights reserved. This PDF copy of fib Bulletin 10 is intended for use and/or distribution only by National Member Groups of fib.

as previously observed experimentally.

Fig. 1.5.18c compares bond ultimate capacity with the product of the embedment length, l_d, and the cover to the center of the bar, $c^*=c+1/2\ d_b$. The analysis confirm the empirical expressions found in the literature, about the monotonic but less than linear increasing of bond capacity with c^*. Of course, for $c^*=0$ also τ_{bu} should be zero.

As for splitting, the analysis shows that rib height becomes a major factor in favoring cover splitting only after the peak of the bond stress-slip curve, but further studies are needed (in other terms, rib height has little or no effect on crack opening before the peak is reached).

In spite of their relative simplicity, the structural models are promising, since they provide a strong basis for establishing rational design criteria for anchorages and splices in R/C structures.

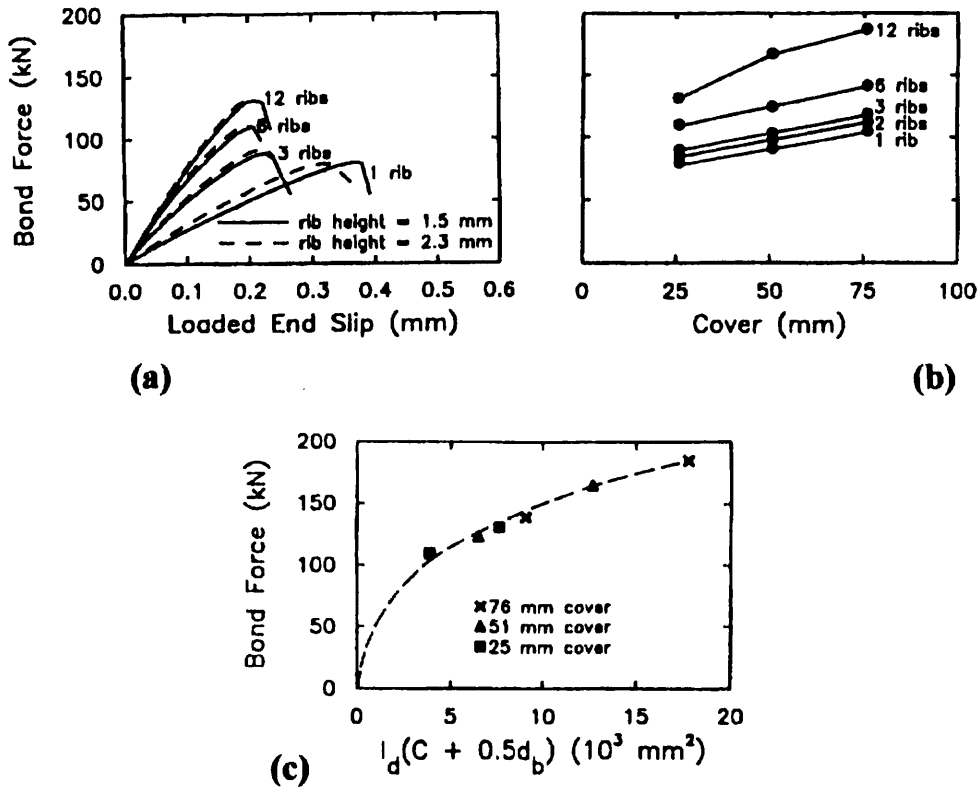

Fig. 1.5.18 - (a) Bond force-slip (loaded end) curves for c = 25 mm; (b) bond force versus cover (h = 1.5-2.3 mm); and (c) bond force versus the embedment length-cover product, for n_R = 6 and 12.

Copyright fib, all rights reserved. This PDF copy of fib Bulletin 10 is intended for use and/or distribution only by National Member Groups of fib.

1.6 Concluding remarks

The extensive database available today to both Designers and Researchers gives them the opportunity to think of the bond problems in terms of rational and comprehensive modeling-something that has never been systematically attempted in the past, because of the many structural aspects of bond, which seem to make any bond problem a case apart.

Rational and comprehensive modeling has always been -and still is- a strategic objective, but is the fulfilment of such an objective close to hand, or is it mere wishful thinking? If the answer to the former question is "yes", another question hangs overhead: to what avail, since comprehensive formulations would certainly be burdensome and too complex for most cases, and still not sufficiently reliable in other cases?

To be honest, the answer to the above uncertainties of opinion seems to be that we need several models to capture the different mechanisms which characterize bond in the different limit states, even more since bond behavior is not uniform along a given anchorage or lapped splice. Concerning this last point, can the different models be combined together in the case of a long anchorage or splice, or is it necessary to study each single system as a whole, by discretizing the problem?

For sure, discrete modeling by means of FEs is in principle always capable of giving an answer, but only by combining discrete and closed-form models can true advances in improving bond-related design equations be achieved. For instance, FEs are instrumental in solving different classes of problems (anchorages and splices, with different geometrical ratios, bar arrangements and active/passive confinement), in order to identify in each class the prevailing resistant mechanism. Then, the most convenient simplified model (elastic, elastic-fracturing, elastic-plastic-fracturing) should be adopted for each class of problem, and this model may be the basis of rational, yet simple design-oriented expressions.

The combination of discrete and simplified modeling might also be helpful in formulating the design expressions which are required by the "new" materials now entering the scene or by extreme environmental conditions:

- high-performance concrete, where the presence of silica fume makes the bar-concrete transition zone denser, with better local bond properties, but with a less uniform stress distribution over the embedment length and a greater proneness to cover splitting, because of the reduced tensile-to-compressive strength ratio in HPCs; with regard to splitting, even a relatively low fiber content helps;

- epoxy-coated reinforcement, where the lack of chemical adhesion increases bar slippage and requires a larger confinement action in the surrounding concrete (with a greater danger of splitting), while the extent of coating damage and the ensuing rusting of the reinforcement can make the problem worse, owing to the expansion of the corrosion products;

- non-metallic reinforcement, where the lack of chemical adhesion, the low Poisson ratio and the relative weakness of the lugs make bond much more dependent on the confinement;

- environmental effects:

  - bar rusting: depending on the attack penetration, bond performances may even improve, but generally they don't, because of the softer corrosion products and of their larger volume, which make concrete cover more splitting-prone;

  - high temperature: at temperatures higher than 400°C bond strength decreases sharply, both at high temperature and after cooling down to room temperature ("residual" bond properties). This is much more so in mild-steel plain round bars, than in cold-drawn deformed bars, and more so in siliceous than in calcareous concretes;

  - freezing cycles: under both monotonic and reversed cyclic loading bond strength decreases as the number of previous freezing cycles increases. As a matter of fact, freezing cycles produce a diffused damage in the material skeleton, as the moisture entrapped in the pore system undergoes a phase transformation under constraint and in transient conditions;

  - low temperature: low temperatures markedly increase the compressive strength of both normal- and high-strength concretes, with lesser effects on the tensile and bond strengths, on Young's modulus

Copyright fib, all rights reserved. This PDF copy of fib Bulletin 10 is intended for use and/or distribution only by National Member Groups of fib.

and Poisson's ratio. Furthermore, the rate of increase of the mechanical properties is less marked in HSC than in NSC. However, for both NSC and HSC the bond strength at -50°C is 45-120% greater than at room temperature (monotonic, pulsating and reversed cyclic loading).

- size effects: as is always the case in softening behaviors, the bar-concrete interface exhibits a softening-induced damage, which consists of a localization of the debonding (a sort of interface fracture running along the bar). Size effects have been shown to be substantial in smooth bars, but absent in well-confined deformed bars and barely noticeable in splitting-prone anchorages of deformed bars. However, experimental evidence is still scant in the last case, and both numerical modeling and testing are badly needed.

Summing up, bond modeling is going to keep its key role, since bond is one of the top players in the complex realm of Reinforced Concrete. It is the governing phenomenon of most RC performances, from cracking and deformability to strength and durability, not to speak of the visual impact of RC structures, which are more acceptable when reinforcement-controlled fracturing brings in thinner and more uniform cracks, owing to better bond efficiency.

Copyright fib, all rights reserved. This PDF copy of fib Bulletin 10 is intended for use and/or distribution only by National Member Groups of fib.

References

1954 Ferguson P.M., Turpin R.D., Thompson J.N.: Minimum bar spacing as a function of bond and shear strength, ACI Journal 50(10), 869-888.

1955 Chinn J., Ferguson P.M., Thompson J.M.: Lapped splices in reinforced concrete beams, ACI Journal 52(15), 201-213.

1961 Rehm G.: On the fundamentals of steel-concrete bond (in German), Deutscher Ausschuss für Stahlbeton (138), 1-59.

1965 Broms B.B., Lutz L.A.: Effects of arrangement of reinforcement on crack width and spacing of reinforced concrete members, ACI Journal 62(11), 1395-1410.

Untrauer R.E., Henry R.L.: Influence of normal pressure on bond strength. ACI Journal 62(5), 577-586.

1966 Ferguson P.M.: Bond stress: the state of art, Report by ACI Committee 408, ACI Journal 63(11), 408.1-408.22.

Spetla Z., Kadlecek V.: Effect of the slenderness of the direct tensile strength of concrete cylinders and prisms, RILEM Bulletin 33, Paris, 403-412.

1967 Kadlecek V., Spetla Z.: Effect of size and shape of test specimens on the direct tensile strength of concrete, RILEM Bulletin 36, Paris, 175-184.

Lutz L.A., Gergely P.: Mechanics of Bond and Slip of Deformed Bars in Concrete, ACI Journal 76(1), 19-46.

Ngo D., Scordelis A.C.: Finite element analysis of reinforced concrete beams, ACI Journal 64(3), 152-163.

1968 Bresler B., Bertero V.V.: Behavior of reinforced concrete under repeated load, ASCE, J. Struct. Div. 94(6), 1567-1590.

Nilson A.H.: Nonlinear analysis of reinforced concrete by the finite element method, ACI Journal 65(9), 757-766.

1969 Ferguson P.M., Briceno E.A.: Tensile lap splices - Part 1: Retaining wall type, varying moment zone, Research Report 113-2, Center for Highway Research, University of Texas at Austin, 31 pp.

Komlos K.: Factors affecting the stress-strain relation of concrete in uniaxial tension, ACI Journal 66(2), 111-114.

Rehm G.: Evaluation criteria for high-bond rebars (in German), Festschrift Rüsch.

Warren G.E.: Anchorage strength of tensile steel in reinforced-concrete beams, PhD Thesis, Iowa State University, Ames (IA, USA).

1971 Goto Y.: Crack formed in concrete around deformed tension bars, ACI Journal 68(4), 244-251.

1972 Edwards A., Picard A.: Theory of cracking in concrete members, ASCE, J. Struct. Div. 98(12), 2687-2700.

Nilson A.H.: Internal Measurement of Bond Slip, ACI Journal, 69(7), 439-441.

1973 Martin H.: On the interrelation among surface roughness, bond and bar stiffness in the reinforcement subject to short-term loading (in German), Deutscher Ausschuss Stahlbeton (228), 1-50.

Menegotto M., Pinto P.: Method of analysis for cyclically-loaded R/C plane frames including changes in geometry and nonelastic behavior of elements under combined normal force and bending, IABSE Symposium on Resistance and Ultimate Deformability of Structures Acted - on by Well-Defined Repeated Loads, Final Report, Lisbon.

Tepfers R.: A theory of bond applied to overlapped tensile reinforcement splices for deformed bars, Chalmers University of Technology, Goteborg, Publ. 73/2, 328 pp.

1975 Park R., Paulay T.: Reinforced concrete structures, John Wiley and Sons, New York (N.Y., USA).

1976 Franke L.: Influence of long-term loads on steel-concrete bond (in German), Deutscher Ausschuss für Stahlbeton (268).

Hillerborg A., Modéer M., Petersson P.E.: Analysis of crack formation and crack growth in concrete by means of fracture mechanics and finite elements, Cement and Concrete Research (6), 773-782.

1977 Ferguson P.M.: Small bar spacing or cover - A bond problem for the designer, ACI Journal 74(39), 435-439.

Orangun C.O., Jirsa J.O., Breen J.E.: Re-evaluation of test data on development length and splices, ACI Journal 74(3), 114-122.

1978 Clark L.A., Spiers D.M.: Tension stiffening in reinforced concrete beams and slabs under short-term load, Technical Report No. 42.521, Cement and Concrete Association, Wexham Springs, 19 pp.

Dörr K.: Bond-behaviour of ribbed reinforcement under transversal pressure, Proceedings of IASS Symposium on Nonlinear Behaviour of Reinforced Concrete Spatial Structures, Darmstadt, 1, Edited by G. Mehlhorn, H. Rühle and W. Zerna, Werner-Verlag, Düsseldorf (Germany), 13-24.

Copyright fib, all rights reserved. This PDF copy of fib Bulletin 10 is intended for use and/or distribution only by National Member Groups of fib.

Edwards A.D., Yannopoulos P.J.: Local bond stress-slip relationship under repeated loading, Magazine of Concrete Research 30(103), 62-72.

1979 Cairns J.: Analysis of the ultimate strength of lapped joints of compression reinforcement, Magazine of Concrete Research 31(106), 19-27.

Eligehausen R.: Lapped splices of ribbed bars with straight ends (in German), Deutscher Ausschuss für Stahlbeton (301).

Kemp E.L., Wilhelm W.J.: Investigation of the parameters influencing bond cracking, ACI Journal 76(1), 47-71.

Losberg A., Olsson P.A.: Bond failure of deformed reinforcing bars based on the longitudinal splitting effect of the bars, ACI Journal 76(1), 5-18.

Mirza S.M., Houde J.: Study of bond stress-slip relationships in reinforced concrete, ACI Journal 76(1), 19-46.

Morita S., Kaku T.: Splitting bond failures of large deformed reinforcing bars, ACI Journal 76(1), 93-110.

Rehm G., Eligehausen R.: Bond of ribbed bars under high-cycle repeated loads, ACI Journal 76(2), 297-309.

Rilem/CEB/FIP recommendation: Bond test for reinforcing steel - 1. Beam test (RC5) - 2.Pull-out test (RC6).

Skorogobatov S.M., Edwards A.D.: The influence of the geometry of deformed steel bars on their bond strength in concrete, Proc. Instn Civil Engrs. Part 2 (67), 327-339.

Soleimani P., Popov E.P., Bertero V.V.: Hysteretic behavior of reinforced-concrete beam-column subassemblages, ACI Journal 76(11), 1179-1195.

Tassios T.P.: Properties of bond between concrete and steel under load cycles idealizing seismic actions, Proc. AICAP-CEB Symposium, Rome, CEB Bulletin No. 131, 67-122.

Tepfers R.: Cracking of concrete cover along anchored deformed reinforcing bars, Magazine of Concrete Research 31(106), 3-12.

Viwathanatepa S., Popov E.P., Bertero V.V.: Effects of generalized loadings on bond of reinforcing bars embedded in confined concrete blocks, Report No. UCB/EERC 79-22, Univ. of California, Berkeley (Ca, USA).

1980 Baranek W.J., IBBC-TNO, Afd. Experimentele Mechanica, Delft.

Noakowski P.: Correct procedure for the analysis (of bond) at the extremities of prestressed elements (in German), Beton-und Stahlbetonbau (4).

1981 Ciampi V., Eligehausen R., Bertero V.V., Popov E.P.: Analytical model for deformed-bar bond under generalized excitations, Trans. IABSE Colloquium on Advanced Mechanics of Reinforced Concrete, Delft, Netherlands.

de Groot A.K., Kusters G.M.A., Monnier T.: Numerical modeling of bond-slip behavior, HERON, Concrete Mechanics, 26(1B), 90 pp.

Diederichs U., Schneider U.: Bond strength at high temperature, Magazine of Concrete Research 33(115), 75-84.

Giuriani E.: Experimental investigation on the bond-slip law of deformed bars in concrete, IABSE Colloquium on Advanced Mechanics of Reinforced Concrete, Final Report, Delft, The Netherlands, 121-142.

Martin H., Noakowski P.: Bond behavior in reinforced concrete (in German), Research Report IV, München Technical University.

Somayaji S., Shah S.P.: Bond-stress versus slip relationship and cracking response of tension members, ACI Journal 78(3), 217-225.

Tassios T.P., Yannopoulos P.J.: Analytical studies on reinforced concrete members under cyclic loading based on bond stress-slip relationships, ACI Journal 78(3), 206-216.

1982 ASCE – State-of-the-Art Report on "Finite Element Analysis of Reinforced Concrete", Chapter 3 "Modeling of Reinforcement and Representation of Bond", Task Committee "FE Analysis of R/C Structures", Chairman Arthur H. Nilson, 149-203.

Bartos P. (Editor): Bond in Concrete, Proc. Int. Conf. on "Bond in Concrete", Paisley (Scotland, U.K.), Publ. by Applied Science (London, U.K.).

Comité Euro-International du Béton: Bond action and bond behaviour of reinforcement - State of the Art Report, C.E.B., Bulletin d'Information No. 151.

Ciampi V., Eligehausen R., Bertero V.V., Popov E.P.: Analytical model for concrete anchorages of reinforcing bars under generalized excitations, Report No. UCB/EERC 82-83, Univ. of California, Berkeley (Ca, USA).

Copyright fib, all rights reserved. This PDF copy of fib Bulletin 10 is intended for use and/or distribution only by National Member Groups of fib.

Gambarova P.G., Karakoç C.: Shear-confinement interaction at the bar-to-concrete interface, in "Bond in Concrete", Edited by P. Bartos (Applied Science, London), 82-96.

Giuriani E.: On the effective axial stiffness of a bar in cracked concrete, in "Bond in Concrete", Edited by P. Bartos (Applied Science, London), 107-126.

Morita S., Fujii S.: Bond capacity of deformed bars due to splitting of surrounding concrete, in "Bond in Concrete", Edited by P. Bartos, Applied Science Publishers, London, 331-341.

Reynolds G.C., Beeby A.W.: Bond strength of deformed bars, "Bond in Concrete", Edited by P. Bartos, Applied Science Publishers, London, 434-445.

Tepfers R.: Lapped tensile reinforcement splices, ASCE, J. Struct. Div. 108 (1), 283-301.

Vos E., Reinhardt H.W.: Influence of loading rate on bond behaviour of reinforcing steel and prestressing strands, Materials and Structures, RILEM 15(85), 3-10.

1983 Eligehausen R., Popov E.P., Bertero V.V.: Local bond stress-slip relationships of deformed bars under generalized excitations, Report No. UCB/EERC 83-23, Univ. of California, Berkeley (Ca, USA).

Filippou F.C., Popov E.P., Bertero V.V. (a): Effect of bond deterioration on hysteretic behavior of reinforced concrete joints, Report No. UCB/EERC 83-19, Univ. of California, Berkeley (Ca, USA).

Filippou F.C., Popov E.P., Bertero V.V. (b): Modeling of reinforced concrete joints under cyclic excitations, ASCE, J. Struct. Engrg. 109(11), 2666-2684.

Morley P.D., Royles R.: Response of the bond in reinforced concrete to high temperatures, Magazine of Concrete Research 35(123), 67-74.

1984 Ingraffea A.R., Gerstle W.H., Gergely, P., Saouma V.: Fracture Mechanics of Bond in Reinforced Concrete, ASCE, J. Struct. Engrg. 110(4), 871-890.

Jiang D.H., Shah S.P., Andonian A.T.: Study of the transfer of tensile forces by bond, ACI Journal 81(4), 251-259.

Reinhardt H.W., Blaauwendraad J., Vos E.: Prediction of bond between steel and concrete by numerical analysis, RILEM Materials and Structures 17(100), 311-320.

Robins P.J., Standish I.G.: The influence of lateral pressure upon anchorage bond, Magazine of Concrete Research 36(129), 195-202.

Tassios T.P., Koroneos E.G.: Local bond-slip by means of the moiré method, ACI Journal 81(4), 27-34.

1985 ACI 352 R-85: Recommendations for design of beam-column joints in monolithic reinforced-concrete structures, ACI Journal 82(3), 266-283.

Filippou F.C.: A simple model for reinforcing bar anchorages under cyclic excitations, Report No UCB/EERC 85-05, Univ. of California, Berkeley (Ca, USA).

Gambarova G.P., Giuriani E.: Discussion of "Study of transfer of tensile forces by bond", by D.H. Jiang, S.P. Shah, A.T. Andonian, ACI Journal 82(3), 381-383.

Giuriani E., Plizzari G.A.: Local bond-slip law after splitting of concrete, Studi e Ricerche, School for the Design of R/C Structures, Milan University of Technology, 7, Milan (Italy), 57-118 (in Italian).

Karlsson, D.: Bond between strands and concrete in hollow-core slabs, Nordic Seminar: Bond and Anchorage of Reinforcement in Concrete, Chalmers University, 1985.

Schneider U. (Editor): Properties of materials at high temperatures - Concrete, RILEM Committee 44-PHT, Gesamthochschule - Kassel Universität, Kassel (Germany), 131 pp.

Yankelevsky D.Z.: New finite element for bond-slip analysis, ASCE J. Struct. Engrg. 111(7), 1533-1542.

1986 ACI Committee 224: Cracking of concrete members in direct tension, ACI Journal 78(1), 3-19.

Balázs, G.: Bond behaviour under repeated loads, Studi e Ricerche, School for the Design of R/C Structures, Milan University of Technology, 8, Milan (Italy), 395-430.

Filippou F.C.: A simple model for reinforcing-bar anchorages under cyclic excitations, ASCE, J. Struct. Engrg. 112(7), 1639-1659.

Giuriani E., Rosati G.P.: Behaviour of concrete elements under tension after cracking, Studi e Ricerche, School for the Design of R/C Structures, Milan University of Technology, 8, Milan (Italy), 65-82.

Lahnert B.J., Houde J., Gerstle K.H.: Direct measurement of slip between steel and concrete, ACI Journal 83(2), 974-982.

Mukaddam M., Kasti M.B.: Reinforced-concrete joints under cyclic loading, ASCE, J. Struct. Engrg. 112(4), 937-954.

1987 Adrouche K., Lorrain M.: Influence des paramètres constitutifs de l'association acier-béton sur la résistance de l'adhérence aux chargements cycliques lents (Influence of the constitutive parameters for steel-concrete association on bond strength under slow cyclic loading), Materials and Structures, RILEM, 20, 315-320.

Balázs G.: Bond model with non-linear bond-slip law, Studi e Ricerche, School for the Design of R/C Structures, Milan University of Technology, 9, 157-180.

Copyright fib, all rights reserved. This PDF copy of fib Bulletin 10 is intended for use and/or distribution only by National Member Groups of fib.

Dragosavic M.: Modeling of bond, IABSE Colloquium Delft 1987 on Computational Mechanics of Concrete Structures - Advances and Applications, Delft, 131-138.

Keuser M., Mehlhorn G.: Finite element models for bond problems, ASCE, J. Struct. Engrg. 113(10), 2160-2173.

Lee S.L., Mansur M.A., Tan K.H., Kasiraju K.: Cracking behavior of concrete tension members reinforced with welded wire fabric, ACI Struct. J. 84(6), 481-491.

Plizzari G.A., Schumm C.E., Giuriani E.: The effect of residual tensile strength of cracked concrete on the local bond-slip law after splitting, Studi e Ricerche, School for the Design of R/C. Structures, Milan University of Techonology, 9, Milan (Italy), 129-155.

Shima H., Chou L.L., Okamura H. (a): Bond characteristics in post-yield range of deformed bars, Concrete Library of JSCE, 10, 113-124.

Shima H., Chou L.L., Okamura H. (b): Micro and macro models for bond in reinforced concrete, J. of the Faculty of Engrg., University of Tokio, 39(2), 133-194.

1988 Bazant Z.P., Sener S.: Size effects in pull-out tests, ACI Materials J., 85(4), 347-351.

Kaku T., Yamada M., Shibata M., Takahashi H.: Bond splitting strength of simply-supported reinforced concrete beams, Transactions of the Japan Concrete Institute.

Modena C., Coltro T., Rossaro G.P.: A study of steel-to-concrete bond after concrete splitting: experimental results at constant confinement (in Italian), Studi e Ricerche, School for the Design of R/C Structures, Milan University of Techonology, 10, Milan (Italy) 179-218.

Schmidt-Thrö G., Stöckl S., Kupfer H.: Influence of uniaxial lateral pressure and anchorage length on the bond behavior of deformed bars in concrete (in German), Deutscher Ausschuß für Stahlbeton (D.A.f.St) 389, 99-174.

Shih T.S., Lee G.C., Chang K.C. (a): Effect of freezing cycles on bond strength of concrete, ASCE, J. Struct. Engrg. 114(3), 717-726.

Shih T.S., Lee G.C., Chang K.C. (b): High strength concrete-steel bond behavior at low temperature, ASCE, J. Cold Regions Engrg. 2(4), 157-168.

1989 Elzedin E., Balaguru P.N.: Bond behavior of normal- and high-strength fiber-reinforced concrete, ACI Materials J. 86(5), 515-524.

Gambarova P.G., Rosati G.P., Zasso B.: Steel-concrete bond after concrete splitting: (I) test results; (II) constitutive laws and interface deterioration, Materials and Structures, RILEM, 22, 35-47 and 347-356.

Kaku T., Yamada M., Gouraku M.: Effect of transverse reinforcement on bond splitting strength of reinforced concrete beams, Transactions of the Japan Concrete Institute.

Russo G., Zingone G., Romano F.: Solution of the bond problem on the basis of a nonlinear local bond stress-slip relationship, taking into account concrete strains (in Italian), Studi e Ricerche, 10, Milan Univ. of Technology, Milan (Italy), 157-177.

1990 Mazars J., Pijaudier-Cabot J., Clement J.L.: Analysis of steel-concrete bond with damage mechanics: non-linear behaviour and size effect, Applications of Fracture Mechanics to Reinforced Concrete, Ed. by A.Carpinteri, Elsevier Applied Science, 307-311.

Plizzari G.A., Schumm C.E.: On bond collapse due to bar pull-out and concrete splitting, Studi e Ricerche, School for the Design of R/C. Structures, Milan University of Techonology, 12, Milan (Italy), 81-116.

Reinhardt H.W., van der Veen C.: Splitting failure of a strain-softening material due to bond stresses, Applications of Fracture Mechanics to Reinforced Concrete, Ed. by A. Carpinteri, Elsevier Applied Science, 333-346.

Rots, J.G.: Simulation of bond and anchorage: usefulness of softening fracture mechanics, Applications of Fracture Mechanics to Reinforced Concrete, Ed. by A. Carpinteri, Elsevier Applied Science, 285-306.

Russo G., Zingone G., Romano F.: Analytical solution for bond-slip of reinforcing bars in R.C. joints, ASCE, J. Struct. Engrg. 116(2), 336-355.

van der Veen C.: Cryogenic bond stress-slip relationship, Ph.D.Thesis, Delft University of Technology, 111 pp.

1991 Balázs G.: Fatigue of bond, ACI Materials Journal 88(6), 620-629.

ENV 1992-1-1: Eurocode 2 – Design of concrete structures – Part 1-1: General rules and rules for buildings, European Prestandard, December 1991.

Giuriani E., Plizzari G.A., Schumm C.: Role of stirrups and residual tensile strength of cracked concrete on bond, ASCE, J. Struct. Engrg. 117(1), 1-18.

Hemmaty Y., De Roeck G., Vandewalle L.: Finite Element modeling of reinforced concrete taking into consideration bond-slip, 5th ANSYS Int. Conf. (Pittsburgh, Penn, USA).

Klisinski M., Runesson K., and Sture S.: Finite element with inner softening band, ASCE J. Engrg. Mech. 117(2), 575-587.

Copyright fib, all rights reserved. This PDF copy of fib Bulletin 10 is intended for use and/or distribution only by National Member Groups of fib.

Malvar R.J.: Bond of reinforcement under controlled confinement, Technical Report N-1833, Naval Civil Engineering Laboratory, Port Hueneme (Ca, USA).

Pijaudier-Cabot G., Mazars J., Pulikowski J.: Steel-concrete bond analysis with nonlocal continuous damage, ASCE J. Struct. Engrg. 117(3), 862-882.

Russo G., Romano F.: Bond response in a push-in/pull-out test when the rebar and the concrete are loaded at opposite ends, Studi e Ricerche, 12, Milan University of Technology, Milan (Italy), 19-44.

Soroushian P., Obaseki K., Marikunte S.: Analytical modeling of bonded bars under cyclic loads, ASCE, J. Struct. Engrg. 117(1), 48-60.

Yannopoulos P.J., Tassios T.P.: Reinforced concrete axial elements analyzed under monotonic and cyclic actions, ACI Structural J. 88(1), 3-11.

1992 Abrishami H.H., Mitchell D.: A new approach for studying bond characteristics, Proc. Int. Conf. "Bond in Concrete: from Research to Practice", CEB-RTU (Riga Technical University), Riga (Latvia), 1.28-1.37.

Alsiwat J.M., Saatcioglu M.: Reinforcement anchorage-slip under monotonic loading, ASCE, J. Struct. Engrg. 118(9), 2421-2438.

Andreasen B.S.: Anchorage of ribbed reinforcing bars, Proc. Int. Conf. "Bond in Concrete: from Research to Practice", CEB-RTU (Riga Technical University), Riga (Latvia), 1.18-1.27.

Cabrera J.G., Ghoddoussi P.: The effect of reinforcement corrosion on the strength of steel/concrete bond, Proc. Int. Conf. "Bond in Concrete: from Research to Practice", CEB-RTU (Riga Technical University), Riga (Latvia), 10.11-10.24.

Cairns J.: Design of concrete structures using fusion bonded epoxy coated reinforcement, Proc. Inst. of Civil Engineers: Structures & Buildings 94(1), 93-102.

CEB-RTU (Riga Technical University), "Bond in Concrete: from Research to Practice", Proc. Int. Conf., Riga (Latvia).

Cox J.V., Herrmann L.R.: Confinement-stress dependent bond behavior, Part II: a two-degrees of freedom plasticity model, Proc. Int. Conf. "Bond in Concrete: from Research to Practice", CEB-RTU (Riga Technical University), Riga (Latvia), 11.11-11.20.

Darwin D., McCabe S.L., Idun E.K., Schoenekase S.P.: Development length criteria: bars not confined by transverse reinforcement, ACI Structural J. 89(6), 709-720.

Den Uijl J.A.: Bond and splitting action of prestressing strand, Proc. Int. Conf. "Bond in Concrete: from Research to Practice", CEB-RTU (Riga Technical University), Riga (Latvia), 2.79-2.88.

Engström B.: Ductility of tie connections in precast structures, PhD Thesis, Chalmers University of Technology, Goteborg (Sweden).

Gambarova P.G., Rosati G.P., Sharif O.S.: Bond and splitting in reinforced concrete, Proc. Int Conf. "Bond in Concrete: from Research to Practice", CEB-RTU (Riga Technical University), Riga (Latvia), pp. 1.48-1.57.

Malvar L.J.: Bond of reinforcement under controlled confinement, ACI Materials Journal 89(6), 593-601.

Modena C.: Bond behaviour with longitudinal cracks of normal and epoxy-coated deformed bars, Proc. Int. Conf. "Bond in Concrete: from Research to Practice", CEB-RTU (Riga Technical University), Riga (Latvia), 5.31-5.40.

Nagatomo K., Kaku T.: Bond behavior of deformed bars under lateral compressive and tensile stress, Proc. Int. Conf. "Bond in Concrete: from Research to practice", CEB-RTU (Riga Technical University), Riga (Latvia), 1.69-1.78.

Ozbolt J., Eligehausen R.: Simulation of cycling bond-slip behavior, Proc. 1st Int. Conf. on Fracture Mechanics of Concrete Structures, Ed. by Z.P. Bazant, Elsevier Applied Science, Breckenridge (Co, USA), 912-917.

Pukl R., Schlottke B., Ozbolt J., Eligehausen R.: Computer simulation: splitting tests of concrete thick-walled rings, Proc. 1st Int. Conf. on Fracture Mechanics of Concrete Structures, Ed. by Z.P. Bazant, Elsevier Applied Science, Breckenridge (Co, USA), 367-372.

Reuter M., Eligehausen R.: On the influence that the load introduction by means of fastening devices has on the load-bearing capacity of R/C members (in German), Bauingenieur (67), 461-474.

Rosati G.P., Schumm C.E.: Modelling of local bar-to-concrete bond in R.C. beams, Proc. Int. Conf. "Bond in Concrete: from Research to Practice", CEB-RTU (Riga Technical University), Riga (Latvia), 12.34 12.43.

Russo G., Romano F.: Cracking response of RC members subjected to uniaxial tension, ASCE, J. Struct. Engrg. 118(5), 1172-1190.

Saatcioglu M., Alsiwat J.M., Ozcebe G.: Hysteretic behavior of anchorage slip in R/C members, ASCE, J. Struct. Engrg. 118(9), 2439-2458.

Copyright fib, all rights reserved. This PDF copy of fib Bulletin 10 is intended for use and/or distribution only by National Member Groups of fib.

Tepfers R., Olsson P.A.: Ring test for evaluation of bond properties of reinforcing bars, Proc. Int. Conf. "Bond in Concrete: from Research to Practice", CEB-RTU (Riga Technical University), Riga (Latvia), 1.89-1.99.

Van der Veen C.: Cryogenic bond behavior and tension stiffening, Proc. Int. Conf. "Bond in Concrete: from Research to Practice", CEB-RTU (Riga Technical University), Riga (Latvia), 10.1-10.10.

Vandewalle, L.: Theoretical prediction of the ultimate bond strength between a reinforcement bar and concrete, Proc. Int. Conf. "Bond in Concrete: from Research to Practice", CEB-RTU (Riga Technical University), Riga (Latvia), 1.1-1.8.

1993 Balázs G.: Cracking analysis based on slip and bond stresses, ACI Materials Journal 90(4), 340-348.

CEB-FIP Model Code 90, Bulletin d'Information No. 213-214.

Darwin D., Graham E.K.: Effect of deformation height and spacing on bond strength of reinforcing bars, ACI Structural Journal 90(6), 646-657.

Mainz J.: Modeling of bond behavior of deformed bars in RC (Modellierung des Verbundtragverhaltens von Betonrippenstahl), PhD Thesis, 3/93, Technische Universität München (Germany), 157 pp.

1994 Bazant Z.P., Desmorat R.: Size effect in fiber or bar pull-out with interface fracture and softening slip, ASCE J. Engrg. Mech. 120(9), 1945-1962.

Darwin D., McCabe S.L., Brown C.J.: Fracture analysis of steel-concrete bond, Proc. Europe-US Workshop on Fracture and Damage in Quasibrittle Structures, Ed. by Z.Bazant, Z.Bittnar, M.Jirasek and J.Mazars, Prague (Czech Republic), 549-556.

Davì G., La Mendola L., Papia M.: Boundary element model for bond problems in reinforced concrete members, Computers and Structures, 52(1), 49-59.

Gambarova, P.G., Rosati, G.P., Schumm, C.E.: An elasto-cohesive model for steel-concrete bond, Proc. Europe-US Workshop on Fracture and Damage in Quasibrittle Structures, Ed. by Z.Bazant, Z.Bittnar, M.Jirasek and J.Mazars, Prague (Czech Republic), 557-566.

Herrmann L.R., Cox J.V.: Development of a plasticity bond model for reinforced concrete – Preliminary calibration and cyclic applications, Contract Report 94.001-SHR, Naval Facilities Engrg. Service Center, Port Hueneme (CA, USA), 113 pp.

Morita S., Fujii S., Kondo G.: Experimental study on size effect in concrete structures, Size effect in concrete structures, Ed. by H. Mihashi, H. Okamura and Z.P. Bazant, E&FN Spon, London, 27-46.

1995 ACI-Committee 318: Building Code Requirements for Reinforced Concrete (ACI 318-95), ACI Institute.

Balaguru P., Gambarova P.G., Rosati G.P., Schumm C.E.: Bond of reinforcing bars and prestressing tendons in HPFRCC matrices, Second International Workshop on High-Performance Fiber-Reinforced Cement Composites, Ed. by A. Naaman and H.W. Reinhardt, Ann Arbor (Mi, USA).

Bazant Z.P., Li Z., Thoma M.:Identification of stress-slip law for bar or fiber pull-out by size effect test, ASCE J. Engrg. Mech. 121(5), 620-625.

Bigaj A.J.: Bond behaviour of deformed bars in NSC and HSC: experimental study, Delft University of Technology, Dept. of Civil Engineering, N. 25.5-95-II, September.

Cairns J., Abdullah R.: An evaluation of bond pullout tests and their relevance to structural performance, The Structural Engineer 73(1), 179-185.

Cairns J., Jones K. (a): The splitting forces generated by bond, Magazine of Concrete Research 47, 153-165.

Cairns J., Jones K. (b): Influence of rib geometry on strength of lapped joints: an experimental and analytical study, Magazine of Concrete Research 47(172), 253-262.

CEB (Comité Euro-International du Béton): High performance concrete, recommended extensions to the Model Code 90, Research needs, Bulletin d'Information No 228, Stuttgart, 33+12.

Harajli M.H., Hout M., Jalkh W.: Local bond stress-slip behaviour of reinforcing bars embedded in plain and fiber concrete, ACI Materials Journal 92(4), 343-354.

Maeda M., Otani S., Aoyama H.: Effect of confinement on bond splitting behavior in reinforced concrete beams. IABSE Structural Engineering International 5(3), 166-171.

Noghabai K. (a): Splitting of concrete in the anchoring zone of deformed bars: a fracture-mechanics approach to bond, PhD Thesis, Div. Struct. Engrg., Luleå Univ. of Technology, Luleå (Sweden), 131 pp.

Noghabai, K. (b): Splitting of concrete covers - A fracture mechanics approach, Proc. 2nd Int. Conf. on Fracture Mechanics of Concrete Struct., Ed. by F.H. Wittmann, Aedificatio Publ., Zurich (CH), 1575-1584.

van Mier J.G.M., Vervuurt A.: Lattice model for analysing steel-concrete interface behaviour, Mechanics of Geomaterial Interfaces, A.P.S. Salvadurai and M.J. Boulon (Editors), Elsevier Science B.V., 201-225.

Walraven J.C.: Size effects: their nature and their recognition in building codes, Studi e Ricerche, School for the Design of R/C Structures, Milan University of Technology, 16, Milan (Italy), 113-134.

Copyright fib, all rights reserved. This PDF copy of fib Bulletin 10 is intended for use and/or distribution only by National Member Groups of fib.

Yao B., Murray W.: Study of concrete cracking and bond using a distributed discrete crack finite element model, ACI Materials J., 92(1), 93-104.

1996 Abrishami H.H., Mitchell D.: Influence of splitting cracks on tension stiffening, ACI Structural J., 93(6), 703-710.

Bigaj A.J., Den Uijl J.A., Walraven J.C.: A bond model for ribbed bars in HSC and NSC: an experimental study, 4th Int. Symposium on the Utilization of High-Strength/High-Performance Concrete - BHP 96, Paris, 1125-1134.

Cairns J., Abdullah R.: Bond strength of black and epoxy coated reinforcement - A theoretical approach, ACI Materials J., 93(4), 362-369.

Cappellini, L.: On the ultimate capacity of short anchorages embedded in elastic-cohesive cement composites (in Italian), MS Thesis, Dept. of Structural Engineering, Milan University of Technology, Milan (Italy), 171 pp.

Darwin D., Zuo Z., Tholen M.L., Idun E.K.: Development length criteria for conventional and high relative rib-area reinforcing bars, ACI Structural Journal 93(3), 347-359.

Den Uijl J.A., Bigaj A.J.: A bond model for ribbed bars based on concrete confinement, HERON 41(3), 201-226.

Gambarova P.G., Rosati G.P.: Bond and splitting in reinforced concrete: test results on bar pull-out, Materials and Structures, RILEM 29, 267-276.

Huang Z., Engström B., Magnusson J.: Experimental and analytical studies of the bond behaviour of deformed bars in high strength concrete, 4th International Symposium on Utilization of High Strength/High Performance Concrete-BHP 96, Paris, 1115-1124.

Manfredi G., Pecce M.: Behaviour of bond between concrete and steel in a large post-yielding field, Materials and Structures, RILEM, 29, 506-513.

Plizzari G.A., Franchi A.: Bond testing according to various European National Codes (in Italian), Technical Report 5-4/96, Department of Civil Engineering, University of Brescia.

Plizzari G.A., Marchina E., Giuriani E. (a): Experimental study of splitting and flexural cracks in a R/C beam with overlapped splices, Materials and Structures, RILEM, 29, 19-27.

Plizzari G.A., Deldossi A.M., Massimo S. (b): Experimental study on anchored bars in R/C elements with transverse reinforcement, Materials and Structures, RILEM, 29, 534-542.

Scott R.H.: Intrinsic mechanisms in reinforced concrete beam-column connection behaviour, ACI Structural Journal 93(3), 336-346.

1997 Gambarova P.G., Rosati G.P.: Bond and splitting in bar pull-out: behavioral laws and concrete-cover role, Magazine of Concrete Research 49(179), 99-110.

Kwak H.G.: Improved numerical approach for the bond-slip behavior under cyclic loads, Struct. Engrg. and Mechanics 5(5), 663-677.

La Mendola L.: Cracking analysis of RC members by using coupled BE-FE modeling, ASCE J. Engrg. Mechanics 123(7), 758-761.

Magnusson J.: Bond and anchorage of deformed bars in high-strength concrete, Chalmers University of Technology, Division of concrete structures, Goteborg, Publ. 97/1, 234 pp.

Monti G., Filippou F.C., Spacone E.: Finite element for anchored bars under cyclic load reversals, ASCE J. Struct. Engrg., 123(5), 614-623.

Ohlsson U. and Olofsson T.: Mixed-mode fracture and anchor bolts in concrete analysis with inner softening bands, ASCE J. Engrg. Mechanics, 123(10), 1027-1033.

Noghabai K.: Environmental effects on bond between deformed bars and concrete - A fracture mechanics approach, in CANMET/ACI International Conference on Durability of Concrete (ed V.M. Malhotra), Sydney, III, 189-203.

1998 Comité Euro-International du Béton: Ductility of reinforced-concrete structures, C.E.B. Bulletin d'Information No. 242.

Eligehausen R., Ozbolt J., Mayer U.: Contribution of concrete between cracks at inelastic steel strains and conclusions for the optimization of bond, ACI-International SP-180 "Bond and Development of Reinforcement: a tribute to Dr. Peter Gergely", Ed. by R. Leon, 45-80.

Fantilli A.P., Ferretti D., Iori I., Vallini P. (a): Behaviour of R/C elements in bending and tension: the problem of minimum reinforcement ratio, Special Technical Publication, ESIS Technical Committee 9 on "Minimum Reinforcement in Concrete Members", ELSEVIER.

Fantilli A.P., Ferretti D., Iori I., Vallini P. (b): Flexural deformability of reinforced-concrete beams, ASCE J. Struct. Engrg., 124 (9), 1041-1049.

Copyright fib, all rights reserved. This PDF copy of fib Bulletin 10 is intended for use and/or distribution only by National Member Groups of fib.

Gambarova P.G., Rosati G.P., Schumm C.E.: Bond and splitting in R/C: a vexing question, ACI-International SP-180 "Bond and Development of Reinforcement: a tribute to Dr. Peter Gergely", Ed. by R. Leon, 23-43.

Giuriani E., Plizzari G.A. (a): Interrelation of splitting and flexural cracks in R.C. beams, ASCE J. Struct. Engrg. 124(9), 1032-1040.

Giuriani, E., Plizzari, G.A. (b): Confinement role in anchorage capacity, ACI-International SP-180 "Bond and Development of Reinforcement: a tribute to Dr. Peter Gergely", Ed. by R. Leon, 171-193.

Ichinose T., Hayashi T.: Fundamental analysis of RC Lap splices, ACI-International SP-180 "Bond and Development of Reinforcement: a tribute to Dr. Peter Gergely", Ed. by R. Leon, 431-457.

Mayer U., Eligehausen R.: Bond behaviour of ribbed bars at inelastic steel strains, Proc. 2nd Int. PhD Symposium in Civil Engineering, Ed. by G.L. Balázs, Technical Univ. of Budapest (Hungary), 39-46.

McCabe, S.L., Pantazopoulu, S.J.: Evaluation of bond performance in R/C structures, ACI-International SP-180 "Bond and Development of Reinforcement: a tribute to Dr. Peter Gergely", Ed. by R. Leon, 1-21.

Morgan E.: The effect of rust on reinforcement, Concrete (1), 25-27.

Plizzari G.A., Deldossi M.A., Massimo S.: Transverse reinforcement effects on anchored deformed bars, Magazine of Concrete Research, 50(2) 161-177.

Tholen M.L., Darwin D.:Effect of reinforcing bar deformation pattern on Flexural ductility, ACI Structural J. 95(1), 37-42.

1999 Coronelli D., Private Communication to P.G. Gambarova, Dept. of Structural Engrg., Milan Univ. of Technology, Milan (Italy).

Ghandehari M., Krishnaswamy S., Shah S.: Tecnique for evaluating kinematics between rebar and concrete, ASCE J. Struct. Engrg., 125(2), 234-241.

Plizzari G.: Bond and splitting crack development in normal and high-strength fiber-reinforced concrete, 13th Engrg. Mechanics Division Conference – EMD99, Baltimore (MD, USA), on CD ROM support.

Copyright fib, all rights reserved. This PDF copy of fib Bulletin 10 is intended for use and/or distribution only by National Member Groups of fib.

Notation

A_R	projection of a rib on bar cross-section
A_s, A_{st}	nominal section of a bar and of a stirrup
c	thickness of the concrete cover
d	damage function
d_b	nominal bar diameter
E	shear energy dissipated by each microplane (microplane model)
E_c	concrete Young's modulus
f_c, f_c', f_{cm}; f_{ck}	mean value of concrete compressive strength measured on cylinders; characteristic value
f_{cc}	concrete compressive strength measured on cubes
f_{coh}	cohesive strength at the bar-concrete interface
f_{ct}	concrete strength in tension
f_R	bond index (or relative rib area)
f_{st}	steel stress at the onset of bar failure in tension
F_b, F_n, F_{sp}, F_v	forces transmitted by a ribbed bar to the surrounding concrete
G_f	concrete fracture energy (mode I)
l	length of a tension member, or embedded length in a pull-out specimen
l_{cr}	extension of a splitting crack around a bar
l_d	embedded length in a pull-out specimen
l_p	distance between two primary cracks in a tension member, or distance between the first/last crack and the nearest end-section in a tension member
n	number of the splitting cracks around a bar
N	number of the load cycles
N,P,T	longitudinal force applied to a bar
OPC	Ordinary Portland Cement
p^*, p^{**}	bar-concrete pressure underneath the rib faces
p_e, p_t	lateral pressure applied to an anchorage (compression, tension = active confinement)
r	radial coordinate; crack tip coordinate in the split concrete around a bar
R	radius of the cracked core in the concrete around a bar
R_b	nominal bar radius
R_c	radius of the concrete mass surrounding a bar in a pull-out axisymmetric specimen
s	bar slip
s'	pitch of the steel spiral in a confined anchorage, or first derivative of bar slip with respect to the longitudinal coordinate x

Copyright fib, all rights reserved. This PDF copy of fib Bulletin 10 is intended for use and/or distribution only by National Member Groups of fib.

s_R	rib spacing in a deformed bar
w	crack width in a concrete specimen subject to tension
w_f	width of a flexural crack
w_s	width of a splitting crack
w/c	water/cement ratio
x	coordinate (along bar axis)
α	angle of the inclined forces exerted by a bar on the surrounding concrete (α is measured with reference to bar axis), or exponent of the bond stress-slip law
δ, Δ, δ_t	bar slip
ε_c, ε_s	normal strain in the concrete, in the reinforcement
ε_{sh}, ε_{sm}, ε_{sr}, ε_{sy}	tensile strain in a bar at the onset of steel hardening, mean strain, strain in a cracked section, strain at yielding
ϕ, ϕ_{st}	nominal diameter of a longitudinal bar, of a stirrup
φ_b	angle of internal friction in the concrete at the bar interface
ν_c	concrete Poisson modulus
μ	coefficient of friction at the bar interface
σ_c, σ_{ct}	normal stress in the concrete (compression, tension)
σ_s, σ_y	normal stress in the steel, stress at yielding
τ , τ_b; τ_u ,τ_{bu}	local or mean bond stress; ultimate bond stress
Ω	stirrup confinement index, or damage function

Copyright fib, all rights reserved. This PDF copy of fib Bulletin 10 is intended for use and/or distribution only by National Member Groups of fib.

2 Anchorage and bond in high strength concrete

Working Party 2:

Björn Engström[①] (Convener, Chalmers University of Technology, Göteborg, Sweden), **Atorod Azizinamini** (University of Nebraska, Lincoln, USA), **Agniezka Bigaj-van Vliet** (University of Stuttgart, Germany), **Joop den Uijl** (Delft University of Technology, The Netherlands), **Rolf Eligehausen** (University of Stuttgart, Germany), **Pietro Gambarova** (Milan University of Technology, Italy), **Jonas Magnusson** (Chalmers University of Technology, Göteborg, Sweden), **Keivan Noghabai** (Luleå University of Technology, Sweden), **Giovanni Plizzari** (University of Brescia, Italy)

[①] principal author

2.1 General considerations **100**
2.1.1 Typical properties of high-strength concrete 100
2.1.2 Expected influence on bond and anchorage 103
2.1.3 Recent research on bond and anchorage in high-strength concrete 105

2.2 Local bond behaviour **105**
2.2.1 Local bond behaviour in well confined concrete 105
2.2.2 Local bond behaviour in lightly confined concrete 114
2.2.2.1 Introduction 114
2.2.2.2 Local splitting behaviour and modelling 115
2.2.3 Other factors influencing the local bond behaviour in high-strength concrete 118
2.2.3.1 Factors influencing the local bond behaviour 118
2.2.3.2 Influence of bar position 118
2.2.3.3 Influence of silica fume 119
2.2.3.4 Influence of fibres 120
2.2.4 Local bond behaviour in the service state 121

2.3 Behaviour and design of anchorage regions **122**
2.3.1 Anchorage of single bars 122
2.3.1.1 Anchorage in well confined concrete 122
2.3.1.2 Anchorage in lightly confined concrete 125
2.3.2 Anchorage behaviour and anchorage capacity in anchorage regions 131
2.3.3 Behaviour and capacity of lap splices in structural members 139
2.3.4 Design of anchorage regions and lap splices 143
2.3.4.1 Design philosophy 143
2.3.4.2 Design approaches 144

2.4 Reinforced concrete ties **147**

2.5 References **150**

Notations **155**

Copyright fib, all rights reserved. This PDF copy of fib Bulletin 10 is intended for use and/or distribution only by National Member Groups of fib.

2.1 General considerations

This chapter deals with bond between reinforcing steel and high-strength concrete, and anchorage of reinforcing steel in high-strength concrete. The high-strength concrete considered here has a mean compressive strength in the range of 60 - 120 MPa according to standard tests on concrete cylinders. This chapter will focus on the most pronounced aspects of bond and anchorage in high-strength concrete relative to those in normal-strength concrete. The principal aspects concerning bond in normal-strength concrete are reported in chapter 1.

2.1.1 Typical properties of high-strength concrete

The specific properties of high-strength concrete are thoroughly presented and explained in FIP/CEB (1990), CEB (1994), Nischer (1994), and Walraven (1995). Here only some of the most important characteristics will be presented. It will especially be discussed how these properties influence the bond behaviour and the anchorage capacity.

In comparison with normal-strength concrete, high-strength concrete in uniaxial loading is characterised by an increased initial stiffness, an increased maximum stress, an increased strain at maximum stress, a reduced ultimate strain, and a more brittle post-peak behaviour. Furthermore, the portion of the ascending branch with an almost linear elastic behaviour is larger in high-strength concrete than in normal-strength concrete. A comparison between typical stress-strain relationships of high-strength and normal-strength concrete in uniaxial compression is shown in Fig. 2.1-1 [CEB (1995)].

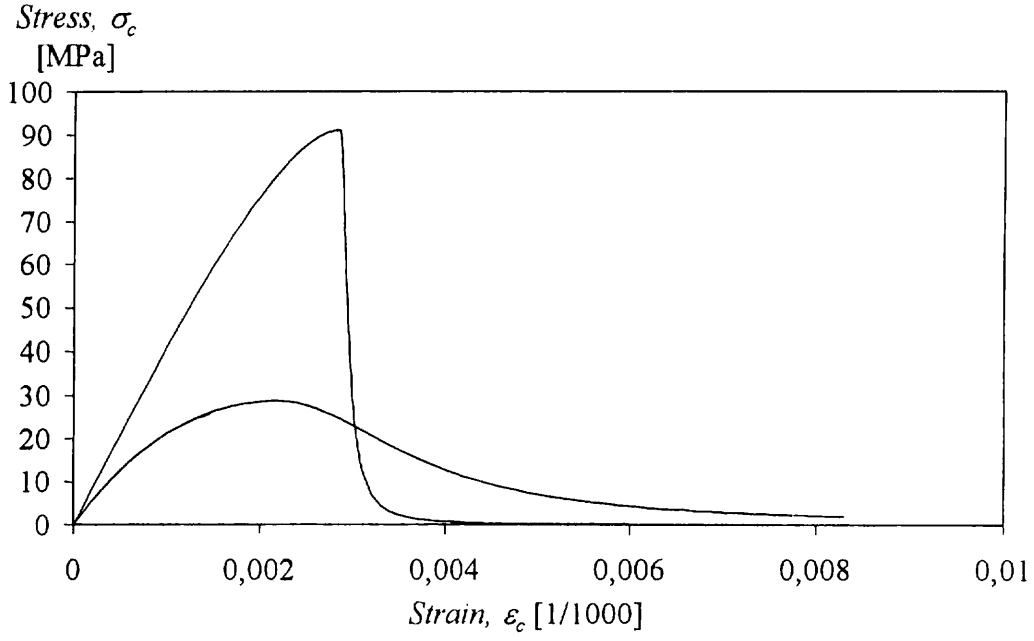

Fig. 2.1-1: Typical stress-strain relationships of high-strength and normal-strength concrete in uniaxial compression [CEB (1995)]

The typical properties of high-strength concrete in relation to that of normal-strength concrete can be explained to some extent by an improved bond between the cement paste and the aggregates and a more uniform rigidity within the concrete. As the cement paste is less porous and denser in high-strength concrete, the difference in rigidity between the cement paste and the aggregates is not so accentuated in high-strength concrete as in normal-strength concrete. When normal-strength concrete is loaded in compression, this non-uniform rigidity results in the formation and successive development of microcracks in the cement paste around the aggregates and along the interfaces between the cement

Copyright fib, all rights reserved. This PDF copy of fib Bulletin 10 is intended for use and/or distribution only by National Member Groups of fib.

paste and the aggregates. The typical non-linear ascending branch of the stress-strain diagram can be explained by this microcracking. To obtain similar softening due to microcracking in high-strength concrete, much higher compressive stresses are needed. This means that the stress level, in relative terms, where the non-linearity becomes apparent is considerably higher in high-strength concrete than in normal-strength concrete. The extent of microcracking at the maximum stress can also be assumed to be reduced in high-strength concrete in comparison to normal-strength concrete.

The tensile strength is considerably higher in high-strength concrete than in normal-strength concrete. However, the tensile strength increases less than linearly with the compressive strength. The following relationship between the mean tensile strength and the mean compressive strength according to CEB Bulletin d'Information 228 [CEB (1995)] is valid for both normal-strength and high-strength concrete:

$$f_{ctm} = f_{ctk0,m}\left(\frac{f_{cm}}{f_{cm0}}\right)^{0.6} \tag{2.1-1}$$

where $f_{ctk0,m}$ = 1,80 MPa

f_{cm0} = 18,0 MPa

This relationship is presented graphically in Fig. 2.1-2.

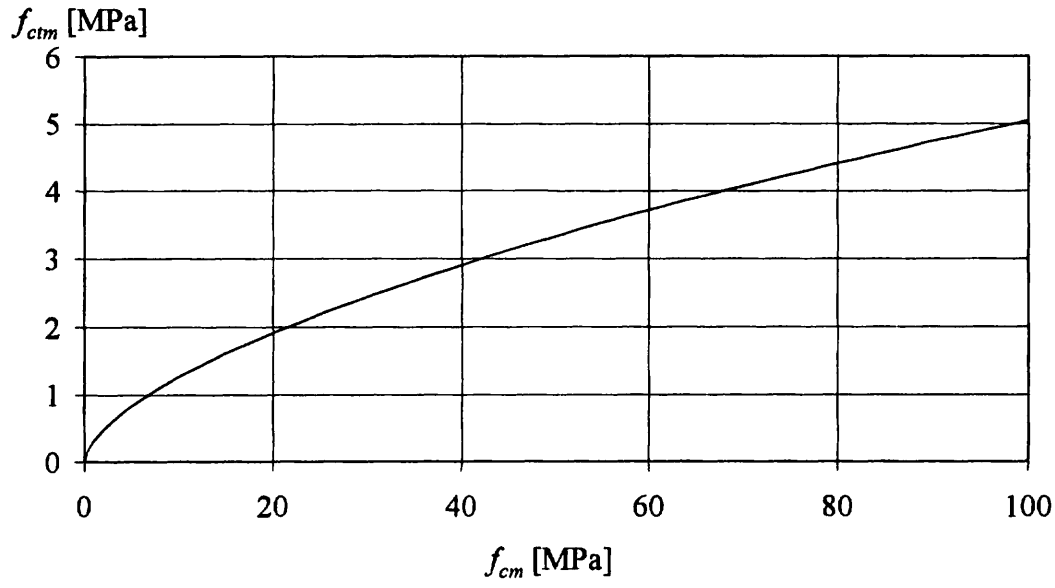

Fig. 2.1-2: Relationship between the mean tensile strength and the mean compressive strength according to CEB Bulletin d'Information 228[CEB (1995)]for both normal-strength and high-strength concrete.

According to Gerard et al. (1996), the tensile strain at maximum stress is approximately the same for high-strength and normal-strength concrete. For high-strength concrete the stress-strain relationship is more linear up to the maximum stress. After the maximum stress is reached, a fracture localises in the concrete and the post-peak deformations are concentrated to the opening w of the main crack. Uniaxial test for monitoring the softening behaviour of concrete in tension (σ_{ct}-w) is generally considered as too sophisticated and has not yet been accepted as a standard test method. However, the test method gives the relevant tensile properties of concrete, albeit one must be aware of various effects of the testing procedure on the results, see van Mier (1997) and Noghabai (1998). The method is particularly useful

Copyright fib, all rights reserved. This PDF copy of fib Bulletin 10 is intended for use and/or distribution only by National Member Groups of fib.

when fibres are added to the concrete matrix, because many indirect methods either will not be valid or they will not give necessary information on e.g. the shape of the softening σ_{ct}-w relationship.

In Fig. 2.1-3 some typical σ_{ct}-w relationships for normal-strength as well as plain and fibre-reinforced high-strength concrete are presented, [Noghabai (1998)].

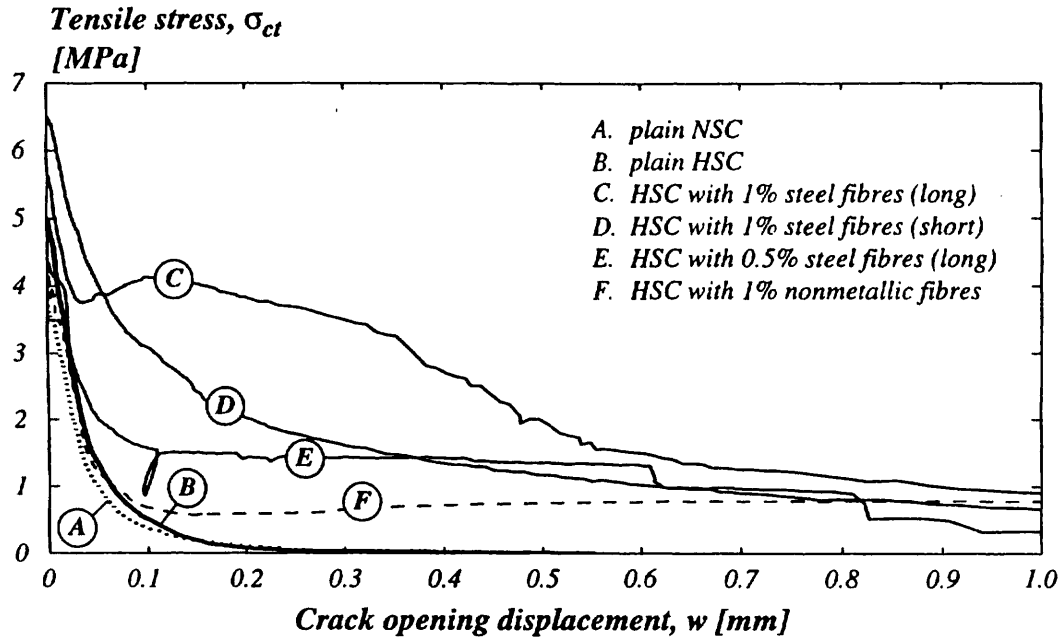

Fig. 2.1-3: Typical tension softening behaviours of plain and fibre-reinforced high-strength concrete in comparison with that of plain normal-strength concrete. The elastic unloading of the concrete outside the fracture zone is subtracted. Modified from Noghabai (1998).

In order to describe the crack development and the fracture process in concrete, the fracture energy is an important parameter. It is generally assumed that the fracture energy increases with the compressive strength. The following empirical relation between the fracture energy and the mean compressive strength is proposed in CEB-FIP Model Code 90 [CEB-FIP (1993)], which generally applies to concrete with a characteristic compressive strength not exceeding f_{ck} = 80 MPa.

$$G_F = G_{F0}\left(\frac{f_{cm}}{f_{cm0}}\right)^{0,7} \tag{2.1-2}$$

where G_{F0} = 25 N/m for d_{max} = 8 mm
30 N/m for d_{max} = 16 mm
58 N/m for d_{max} = 24 mm
f_{cm0} = 10 MPa

This expression is displayed in Fig. 2.1-4 where it is compared to some experimental results, according to Magnusson (1997). These results indicate that eq. (2.1-2) can be reasonably applied also to high-strength concrete with a mean compressive strength in the range of 80 - 120 MPa.

Copyright fib, all rights reserved. This PDF copy of fib Bulletin 10 is intended for use and/or distribution only by National Member Groups of fib.

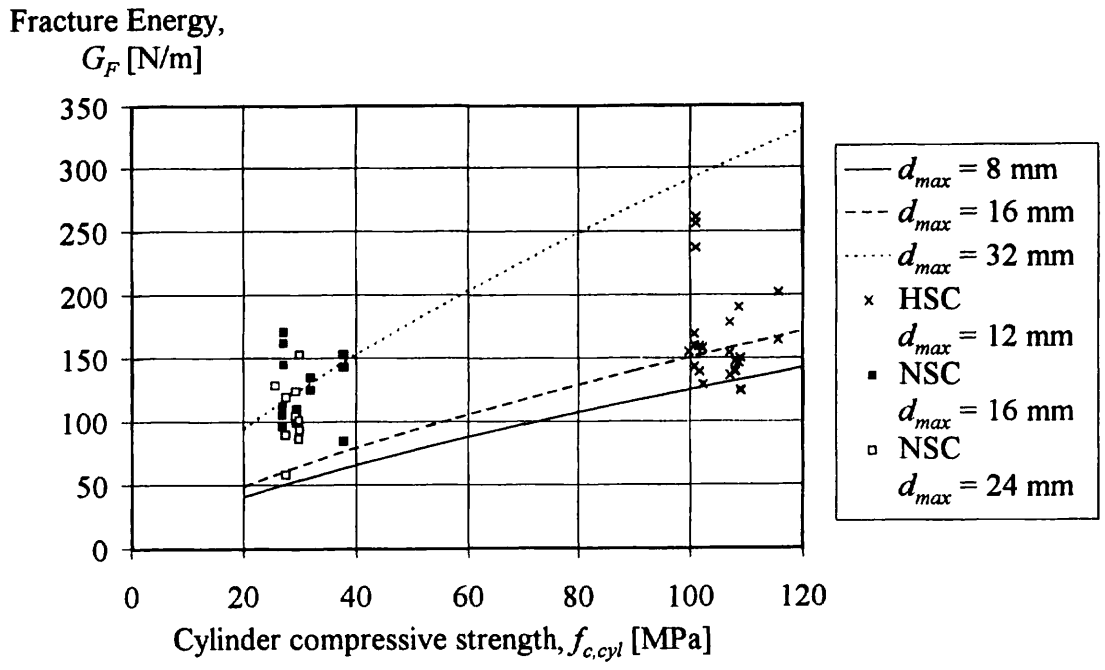

Fig. 2.1-4: Relationships between the fracture energy and the mean compressive strength for concrete with aggregates of various size according to CEB-FIP Model Code 90 [CEB-FIP (1993)] in comparison with test data by Magnusson (1997). The relationships are valid for concrete with a characteristic strength not in excess of f_{ck} = 80 MPa.

2.1.2 Expected influence on bond and anchorage

The specific properties of high-strength concrete in relation to those of normal-strength concrete can be expected to influence bond to reinforcing steel and anchorage behaviour. When this influence is to be discussed, it is appropriate to distinguish the local behaviour in a section across an anchored bar, and the global behaviour of an anchorage region.

The local behaviour describes the sectional interaction between the reinforcement bar and the surrounding concrete and is characterised by the bond stress at the interface and the local slip. The maximum bond stress (peak value) that can be resisted in a section is referred to as the bond strength. When the bond stress has reached the peak value and decreases for increasing slip, this could be considered as a local bond failure.

The global behaviour summarises the local behaviours along one or more anchored bars within a region. The global behaviour is characterised by the total anchored force, in one bar or in a group of bars, and the end slip at the loaded end of the anchorage region. The maximum force that can be resisted in the anchorage region is referred to as the anchorage capacity. It should be noted that even if the bond stress has reached the maximum stress in a section and decreases for increasing slip, the anchored force in the anchorage region could still be increasing. Some examples of anchorage regions in flexural members are shown in Fig. 2.1-5.

In ordinary tensile and flexural reinforced concrete members, the local bond behaviour and the global anchorage behaviour are influenced to a high extent by the formation of internal radial cracks and longitudinal splitting cracks along the anchored bars.

One may assume that the higher tensile strength of high-strength concrete would result in a stiffer local bond behaviour and also in an increased local bond strength. As well known, in normal-strength concrete bond behaviour and strength are considerably influenced by the actual confinement of the

Copyright fib, all rights reserved. This PDF copy of fib Bulletin 10 is intended for use and/or distribution only by National Member Groups of fib.

concrete surrounding the bar, [Tepfers (1973)], [Eligehausen et al. (1983)], [Gambarova and Giuriani (1985)], [Giuriani et al. (1991)]. The bond resistance increases with an increasing confinement until a certain limit, beyond which a further increase of the confinement gives no additional effect, [Orangun et al. (1977)], [Plizzari et al. (1996,1998a)]. The confinement depends on the concrete cover and possible external transverse pressure on the anchorage region. A confining action can also be developed by a sufficient amount of transverse reinforcement or stirrups in the anchorage region, especially when cracks begin to develop, see also Chapter 1, section 1.1.5.

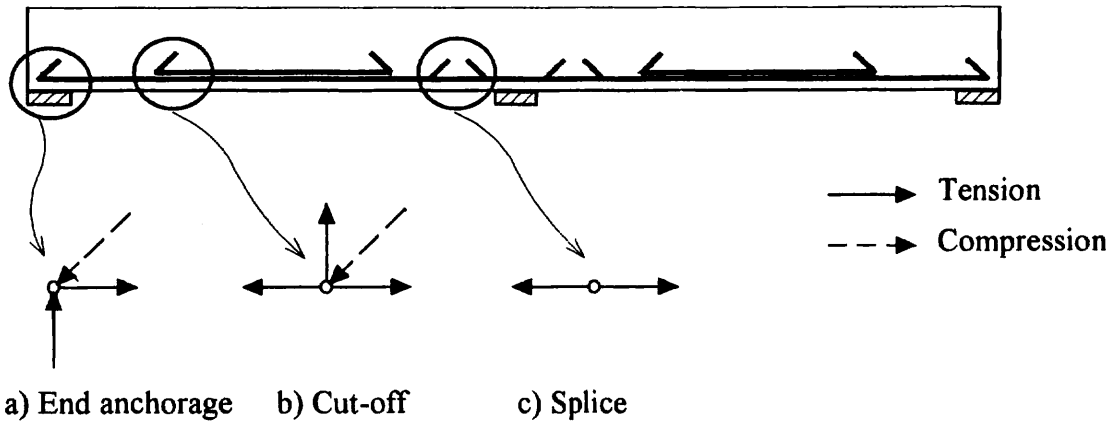

Fig. 2.1-5: Examples of special anchorage regions in flexural members; (a) end anchorage; (b) anchorage at point of cut-off; and (c) anchorage at lapped splice; from Magnusson (1997).

Since high-strength concrete has a stiffer response than normal-strength concrete in both compression and tension and cracking is delayed, the confinement effect developed by a given concrete cover should be more effective in high-strength concrete. It could also be expected that the maximum concrete cover that gives an improvement of the bond resistance is different in high-strength and normal-strength concrete.

In traditional approaches for the design of anchorage regions, it is commonly assumed that the bond stresses are uniformly distributed along the anchorage length at failure. This assumption is reasonable from the practical point of view, as it simplifies the calculations and makes the design model more easy to understand. However, in ordinary applications with normal (moderate) confinement this simplifying assumption has also some relevance with regard to the real anchorage behaviour. When the anchored force increases, radial and longitudinal cracks form and develop successively around the anchored bars. This results in a softening of the surrounding concrete and a redistribution of the stresses in the anchorage region. As a result the bond stresses will be more and more uniformly distributed before anchorage failure.

Because of the higher tensile strength in high-strength concrete and the smaller extent of microcracking, less softening can be expected in otherwise comparable anchorage regions. In addition, the fracture process is expected to be more brittle in high-strength concrete. Consequently, it could be anticipated that in high-strength concrete the peak stress in a non-uniform bond stress distribution could, like a trigger, induce a premature brittle anchorage failure.

Hence, the effect of high-strength concrete on the anchorage capacity is not obvious. On one hand, the improved material properties seem to give a favourable effect on the local bond resistance. On the other hand, since the redistribution of the stresses is prevented by the more brittle behaviour, the bond stress will be less uniformly distributed in high-strength concrete. This is an unfavourable effect on the global resistance of anchorages. Furthermore, the brittle material behaviour could also result in very brittle anchorage failures. Therefore, since predicting bond behaviour and anchorage capacity in high-strength concrete is not easy, specific tests and studies have been carried out lately to address this problem.

Copyright fib, all rights reserved. This PDF copy of fib Bulletin 10 is intended for use and/or distribution only by National Member Groups of fib.

2.1.3 Recent research on bond and anchorage in high-strength concrete

The increasing interest for utilising high-strength concrete in structures during the last years has resulted in considerable research efforts. This is obvious not least from all papers that have been prepared for symposia and conferences concerning the application and properties of high-strength concrete. The bond behaviour of reinforcing bars embedded in concrete is fundamental for the structural behaviour and the specific bond and anchorage behaviours in high-strength concrete have been studied in a number of recent research projects. For instance, the proceedings of the Berkley Symposium 1990 [ACI (1990)] include one paper dealing with bond, the proceedings of the Lillehammer Symposium [High-Strength Concrete (1993)] have 2 papers on bond, the proceedings of the Paris Symposium [Utilization of High Strength/High Performance Concrete (1996)] have 10 papers on bond, and the proceedings of the Sandefjord Symposium [Utilization of High Strength/High Performance Concrete (1999)] have 5 papers related to bond. An international conference on high-performance concrete was arranged in Singapore 1994 by ACI and the proceedings [ACI (1994)] include 2 papers on bond and anchorage in high-strength concrete. In connection with the "Second Multilateral Meeting on Structural performance on High-Strength Concrete in Seismic Regions", selected papers were published in a Special Publication of ACI [ACI (1998a)] and several papers on bond and anchorage problems in high-strength concrete were included.

During the last years there have also been two international conferences directed towards bond between reinforcing steel and concrete. In 1992 a conference on "Bond in Concrete" was held in Riga [CEB-RTU (1992)] and in 1997 a conference on "Bond and Development of Reinforcement" was organised by ACI as a tribute to Dr. Peter Gergely [ACI (1998b)]. The proceedings from these conferences had several papers concerning applications in high-strength concrete. Valuable overviews of recent research results and identification of research needs have been prepared by Taerwe (1996), McCabe (1998), Azizinamini (1998c) and Fujii et al. (1998).

The following sections give the present state of knowledge, with regard to the local bond behaviour (Section 2.2), the global behaviour and resistance of anchorage regions (Section 2.3), and the cracking behaviour of reinforced concrete ties (Section 2.4). Some recommendations for the design of anchorage regions in high-strength concrete are presented. However, the behaviour of anchorage regions in ordinary structural members is very complex and it is still difficult to model and to understand its many aspects. For this reason, the present recommendations will give, as a rule, a conservative design approach. However, the results from the research carried out so far are very promising, as high-strength concrete is very effective in anchoring reinforcing bars. With deeper knowledge of the behaviour of anchorage regions, it would be possible in the future to benefit more from the improved properties of high-strength concrete also in the design. It would be possible not always to apply general design rules developed for the "worst case", but to reduce the anchorage lengths in certain typical applications like anchorages in support regions.

2.2 Local bond behaviour

2.2.1 Local bond behaviour in well-confined concrete

The local bond behaviour is characterised by the relationship between the bond stress at the interface and the local slip. In the past, various types of pull-out tests with a "short" embedment length have been carried out in order to evaluate this local relationship for various types of reinforcement and concrete strengths, on the assumption that if the embedment length is reasonably short in relation to rib spacing, the bond stress distribution is almost uniform. Typical in these tests is that the yield capacity of the reinforcement bar is far in excess of the total bond resistance that can be obtained within this very short embedment length. Normally, the concrete cover in the test specimen was sufficiently thick to prevent

Copyright fib, all rights reserved. This PDF copy of fib Bulletin 10 is intended for use and/or distribution only by National Member Groups of fib.

splitting cracks through the test specimen. In these cases the bond conditions can be assumed to correspond to that of well-confined concrete. However, this has not always been the case, especially when the same specimen dimensions have been adopted in the pull-out tests of large diameter bars.

The meaning of this type of test has been questioned, since the bond conditions varies considerably from those in ordinary applications. However, the bond-slip relationship obtained in the tests represents an upper limit for the interfacial behaviour (well-confined concrete). Short embedment, well-confined applications also exist in practice, such as in the case of anchor bars used for fastenings, tie bars used in prefabricated concrete structures, and other reinforcement bars anchored with large concrete covers. Furthermore, the bond-slip relationship for anchorage in well-confined concrete can be regarded as a "virgin curve", which can be used as a basis in modelling lightly confined regions.

In order to compare the bond-slip behaviours in well-confined high-strength and normal-strength concrete, a series of pull-out tests was carried out by Magnusson (1997). Great care was taken in order to obtain a sufficiently good confinement, in order to prevent splitting effects, and to detail the test specimen in such a way that the small embedment length was kept constant during the test. A cylindrical test specimen was used with a diameter that varied depending on the bar dimension (16 or 20 mm) and a constant height (Fig. 2.2-1). The embedment length was 2,5 times the bar diameter, i.e. 40 mm and 50 mm respectively. The mean concrete compressive strength was about 25 MPa for the normal-strength concrete and about 100 MPa for the high-strength concrete. The bond stress was evaluated from the tests as the tensile force divided by the interfacial area along the short embedment length and was related to the end slip at the unloaded end.

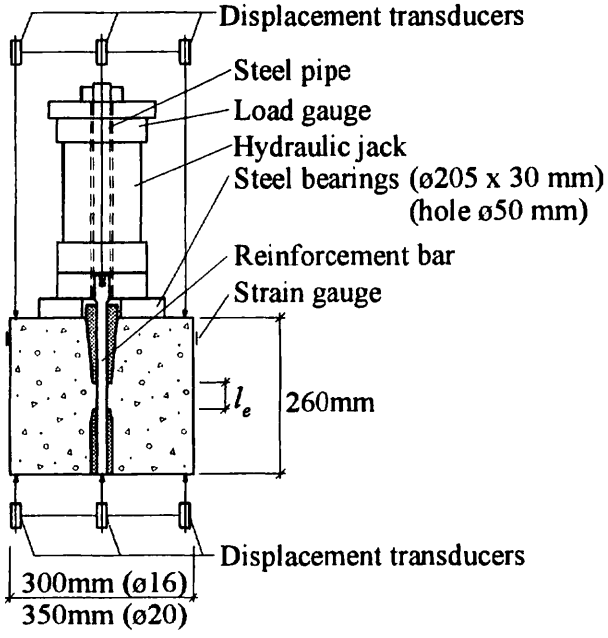

Fig. 2.2-1: Pull-out test with a short embedment length, according to Magnusson (1997).

The influence of high-strength concrete on the bond-slip relationship is exemplified in Fig. 2.2-2 for 16 mm ribbed bars type K500 (f_{yk} = 500 MPa). The curves represent the average behaviour of 4 similar specimens in high-strength concrete and 5 similar specimens in normal-strength concrete. It is evident that the bond resistance increases considerably in high-strength concrete compared to normal-strength concrete. However, the general behaviour is fairly the same for both types of concrete.

Copyright fib, all rights reserved. This PDF copy of fib Bulletin 10 is intended for use and/or distribution only by National Member Groups of fib.

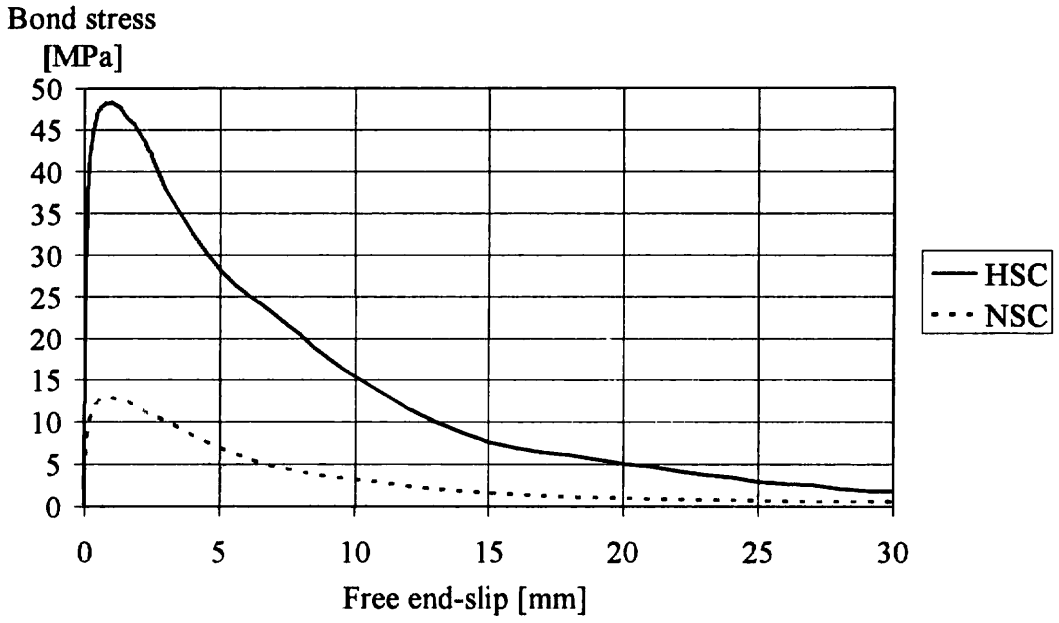

Fig. 2.2-2: Influence of the concrete type on the average bond stress-slip relationship as obtained in pull-out tests with short embedment-length and 16 mm ribbed bars of type K500, according to Magnusson (1997). The free end-slip is measured at the passive end of the bar.

It was found from the evaluation of the tests that the bond strength (maximum bond stress) increases in proportion to the mean compressive strength. This appears from Fig. 2.2-3, which shows the relationship between the bond strength (maximum bond stress, $\tau_{b,max}$) and the mean compressive strength (f_{cm}) in various pull-out tests (high-strength and normal-strength concrete). Based on the experiences from these pull-out tests, Huang, Engström, Magnusson (1996b) proposed to relate the bond strength to the mean compressive strength as

$$\tau_{b,max} = 0{,}45 f_{cm} \tag{2.2-1}$$

This expression was found to be valid also for other tests using similar testing techniques and types of reinforcement [Lestander (1993); Hansen and Thorenfeldt (1996)] (Fig. 2.2-4).

This result contradicts earlier experiences from normal-strength concrete. In fact, it has often been assumed that the bond strength increases in proportion to the concrete tensile strength, proportional to the square root (or 2/3 power) of the compressive strength. For instance, the following expression was proposed by Eligehausen et al. (1983), for normal-strength concrete.

$$\tau_{b,max} = 13{,}5\left(\frac{f_{cm}}{30}\right)^{\beta} \tag{2.2-2}$$

where β varies between 1/2 and 2/3

Eq. (2.2-2) with $\beta = 1/2$ has been adopted in CEB-FIP Model Code 1990 [CEB-FIP (1993)] for the maximum bond strength in case of "good" bond conditions. In case of "other" bond conditions the same expression is used, but the bond strength is reduced by 50%.

Copyright fib, all rights reserved. This PDF copy of fib Bulletin 10 is intended for use and/or distribution only by National Member Groups of fib.

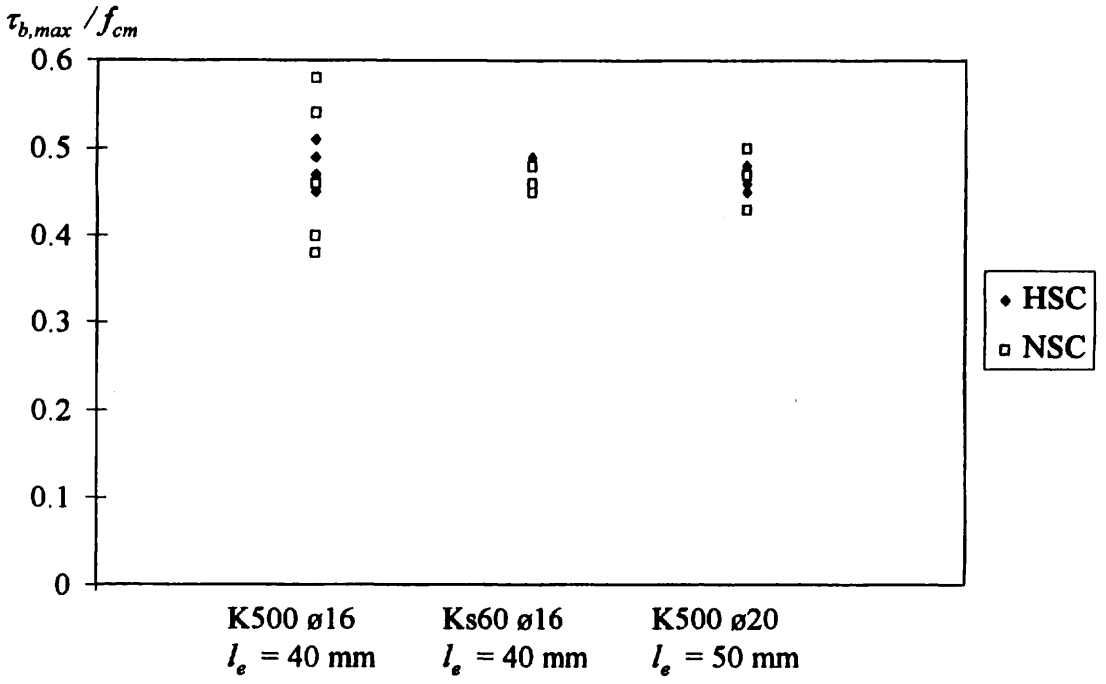

Fig. 2.2-3: Relative bond strength $\tau_{b,max}/f_{cm}$ versus type of reinforcement bar in pull-out tests with short embedment-length in high-strength and normal-strength concrete, according to Magnusson (1997).

A comparison between the proposed relationship, eq. (2.2-1), valid for both normal and high-strength well confined concrete, the relationship (2.2-2) based on experiences from normal-strength concrete, and experimental results for various concrete strengths is presented in Fig. 2.2-4. It can be noticed that the test results from pull-out tests in normal-strength concrete are in fairly good agreement with both expressions (2.2-1) and (2.2-2), and the expression (2.2-1) seems to be reasonably valid for both normal and high-strength concrete.

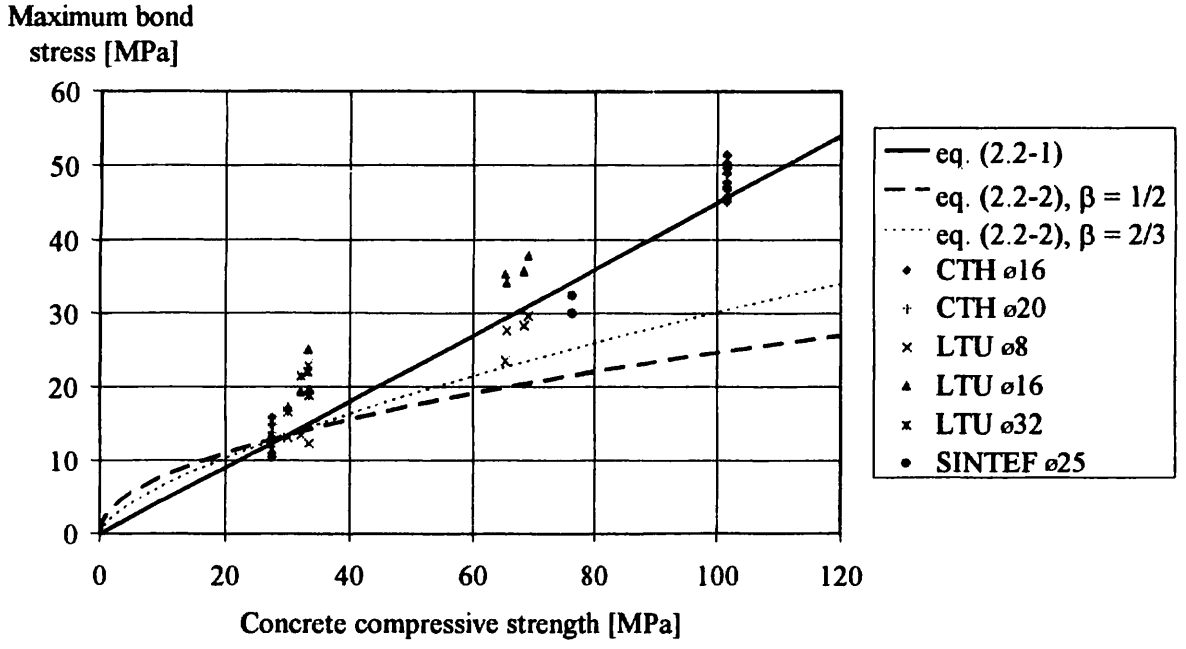

Fig. 2.2-4: Comparison between some test results and eqs. (2.2-1) and (2.2-2) with $\beta = 1/2$ or $\beta = 2/3$. Test results: CTH [Magnusson (1997)]; LTU [Lestander (1993)]; SINTEF [(Hansen and Thorenfeldt (1996)]

Copyright fib, all rights reserved. This PDF copy of fib Bulletin 10 is intended for use and/or distribution only by National Member Groups of fib.

Further to the conclusion that the bond strength is proportional to the concrete compressive strength, it is interesting to examine the dependency of the relative bond stress τ_b / f_{cm} on bar slip. Fig. 2.2-5 shows the same average bond-slip behaviours as in Fig. 2.2-2, but here on the basis of the relative bond slip. It appears that the relative bond stress-slip relationships are almost the same for high-strength and normal-strength concrete. Similar results were obtained from other pull-out tests by Magnusson (1997). However, to some extent this impression depends on the scale of the figure, which is limited to a slip of 30 mm. In Fig. 2.2-6 only the first parts of the same relative bond-slip relations are shown. This figure reveals somewhat stiffer bond behaviour in high-strength concrete. It is assumed that this difference depends on the smaller amount of microcracking in high-strength concrete. This rather small difference in stiffness may be quite significant for the bond behaviour in both service and the ultimate states.

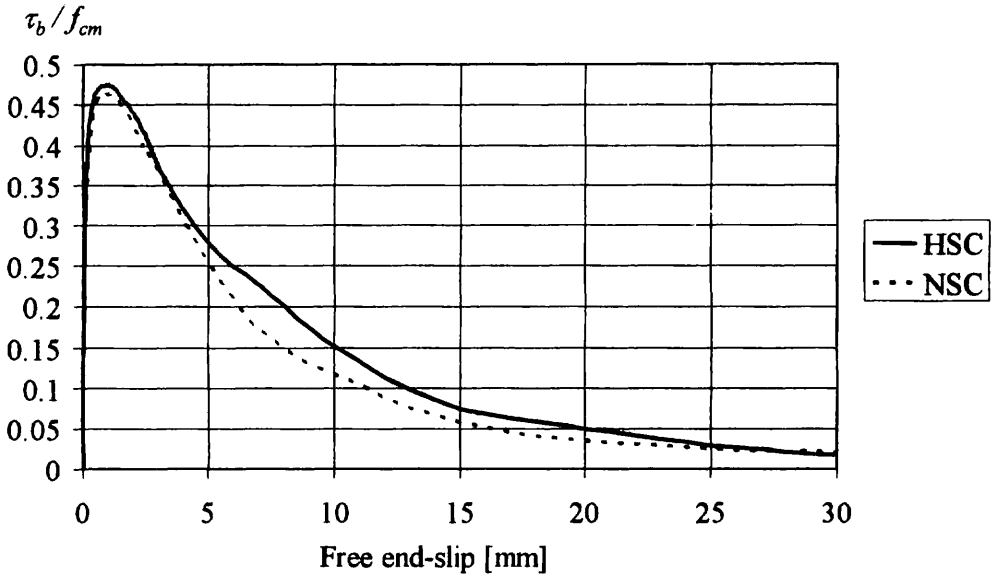

Fig. 2.2-5: Influence of the concrete type on the relative bond stress-slip relationship, as obtained in pull-out tests with short embedment-length and 16 mm ribbed bars of type K500 (the same tests as in Fig. 2.2-2) [Magnusson (1997)]

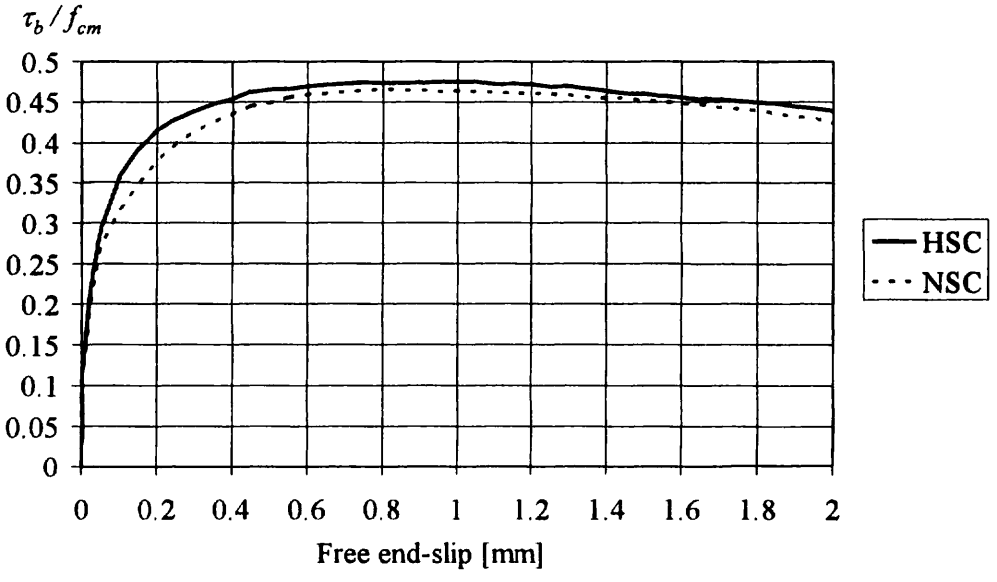

Fig. 2.2-6: Influence of the concrete type on the ascending branch of the relative bond stress-slip relationship, as obtained in pull-out tests with a short embedment-length and 16 mm ribbed bars of type K500 (the same tests as in Fig 2.2-2) [Magnusson (1997)]

Copyright fib, all rights reserved. This PDF copy of fib Bulletin 10 is intended for use and/or distribution only by National Member Groups of fib.

Similar types of pull-out test with short embedment-length, as the one shown in Fig. 2.2-1, have been used by Lestander (1993) and Hansen and Thorenfeldt (1996) to examine the local bond-stress slip behaviour in well-confined concrete, see results in Fig. 2.2-4. However, in order to obtain confined conditions and prevent splitting cracks, the concrete specimens were encased by a steel tube. Hansen and Thorenfeldt (1996) examined the bond behaviour in high-strength concrete with both normal and lightweight aggregates. The bar had a diameter of 16, 25 or 32 mm, and the embedment length ranged between 3ϕ and 7ϕ. They found that the bond stress-slip relations were influenced by the bar diameter and that the bond model in CEB-FIP Model Code 90 [CEB-FIP (1993)] gives conservative predictions of bond strength.

In order to examine the local bond behaviour of a new type of deep-ribbed reinforcement bars, a series of pull-out tests was carried out by Tue and Krumbach (1998). The surface characteristics of the reinforcing bars were modified to reduce the splitting effects, especially for applications in high-strength concrete. The bar diameters were 10, 14 and 16 mm and the embedment-lengths were 1,5ϕ, 2ϕ, 3ϕ and 4ϕ. The concrete specimens had a square cross-section of 120×120 mm. Pull-out failures were obtained in all cases. The test results confirmed that a more ductile bond behaviour was obtained with the new type of reinforcing steel.

In the pull-out test with a short embedment length the bond-slip relationship is governed by the softening behaviour of the concrete around the bar. As mentioned above, the force applied to the bar is normally rather small compared to its capacity. However, the bond-slip relationship may change considerably when the reinforcement bar yields. In order to reach the yield load in the bars and monitor the bond behaviour until steel rupture, considerably longer embedment lengths are normally required. Then a uniform bond stress distribution can not be assumed.

One possibility is to make pull-out tests with various long embedment lengths and measure the global response, represented by the relationship between the applied tensile force and the end-slip at the loaded end. By various assumptions concerning the effect of yielding on the bond-slip relationship, it is possible (by trial calculations) to find a local bond-slip relationship that satisfies the measured global response and the observed yield penetration and strain distribution for various loads. This technique was used by Huang, Engström, and Magnusson (1996b) who proposed a simplified bond-slip relationship, valid for anchorage of ribbed bars in well-confined concrete (normal-strength and high-strength concrete), where the bar may yield or not before a pull-out failure is obtained. The proposed relationship is shown in Fig. 2.2-7 and the governing parameters are presented in Table 2.2-1.

The proposed concept is basically the same as in CEB-FIP Model Code 1990 [CEB-FIP (1993)], but the recent tests concerning high-strength concrete and bond deterioration due to yielding were instrumental in modifying the original model. As long as the reinforcement bar is in the elastic range, the relationship (I) in Fig. 2.2-7 should be applied. As a whole, this relationship is the same as in CEB-FIP Model Code 1990 [CEB-FIP (1993)] for normal-strength concrete, but with two differences. Firstly, the maximum bond stress is determined according to eq. (2.2-1) in case of "good" bond conditions, but half as much should be used when "other" bond conditions apply. Secondly, the fourth branch representing the final frictional phase is a decreasing function, instead of being constant as in the Model Code. This was explained by the gradual degradation of the interface in the final frictional phase.

In the Model Code the ascending branch is defined by the following relationship

$$\tau_b = \tau_{b,max}\left(\frac{s}{s_1}\right)^{\alpha} \qquad \text{for } s \le s_1 \qquad (2.2\text{-}3)$$

Copyright fib, all rights reserved. This PDF copy of fib Bulletin 10 is intended for use and/or distribution only by National Member Groups of fib.

The same expression applies in the proposed model, but owing to the stiffer bond behaviour in high-strength concrete, a different choice of parameters for the ascending branch was required, see Table 2.2-1.

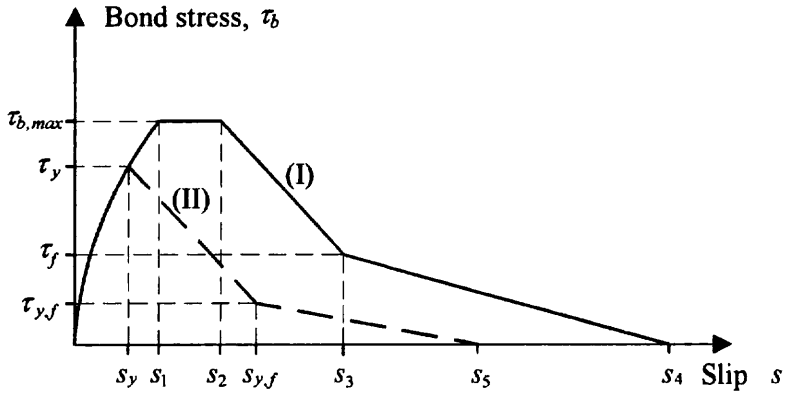

Fig. 2.2-7: Proposed simplified bond-slip relationship for ribbed bars in well-confined concrete, according to Huang, Engström, and Magnusson (1996b); (I) steel bar in the elastic range; (II) steel bar in the plastic range.

Parameters	Bond conditions			
	Normal-strength concrete		High-strength concrete	
	Good	All other cases	Good	All other cases
s_1	1,0 mm	1,0 mm	0,5 mm	0,5 mm
s_2	3,0 mm	3,0 mm	1,5 mm	1,5 mm
s_3	Clear rib spacing	Clear rib spacing	Clear rib spacing	Clear rib spacing
s_4	3(rib spacing)	3(rib spacing)	3(rib spacing)	3(rib spacing)
α	0,4	0,4	0,3	0,3
$\tau_{b,max}$	$0{,}45f_{cm}$	$0{,}225f_{cm}$	$0{,}45f_{cm}$	$0{,}225f_{cm}$
τ_f	$0{,}40\tau_{b,max}$	$0{,}40\tau_{b,max}$	$0{,}40\tau_{b,max}$	$0{,}40\tau_{b,max}$
$s_{y,f}$	s_y+2,5 mm	s_y+2,5 mm	s_y+0,25 mm	s_y+0,25 mm
s_5	2(rib spacing)	2(rib spacing)	2(rib spacing)	2(rib spacing)
$\tau_{y,f}$	$0{,}20\tau_{b,max}$	$0{,}20\tau_{b,max}$	$0{,}20\tau_{b,max}$	$0{,}20\tau_{b,max}$

Table 2.2-1: Parameters governing the simplified bond-slip relationship given in Fig. 2.2-7, according to Huang, Engström and Magnusson (1996b).

The relationship (II) (in Fig. 2.2-7) should be applied in the areas where the bar is beyond the yield threshold. One should note that the values of the initial point (τ_y, s_y) of branch (II) depends on the global response of the anchorage region and should be determined for each section along the bar with regard to equilibrium and compatibility. When the activated transmission length (with bond stresses) is equal to the embedment length, also the unloaded end of the bar will slip. In this case, the values of the initial point (τ_y, s_y) will be different for various sections along the bar, which means that all sections in the plastic region will have different bond-slip relations.

Fig. 2.2-8 shows a comparison between the proposed simplified relationship and the relations obtained in pull-out tests with short embedment length in well-confined high-strength concrete with 16 mm ribbed bars of type K500, as in Fig. 2.2-1. (In this case the bar remained in the elastic range and only relationship (I) applies). The validity of the schematic relationship (II) after bar yielding is discussed in Section 2.3.1.1.

Copyright fib, all rights reserved. This PDF copy of fib Bulletin 10 is intended for use and/or distribution only by National Member Groups of fib.

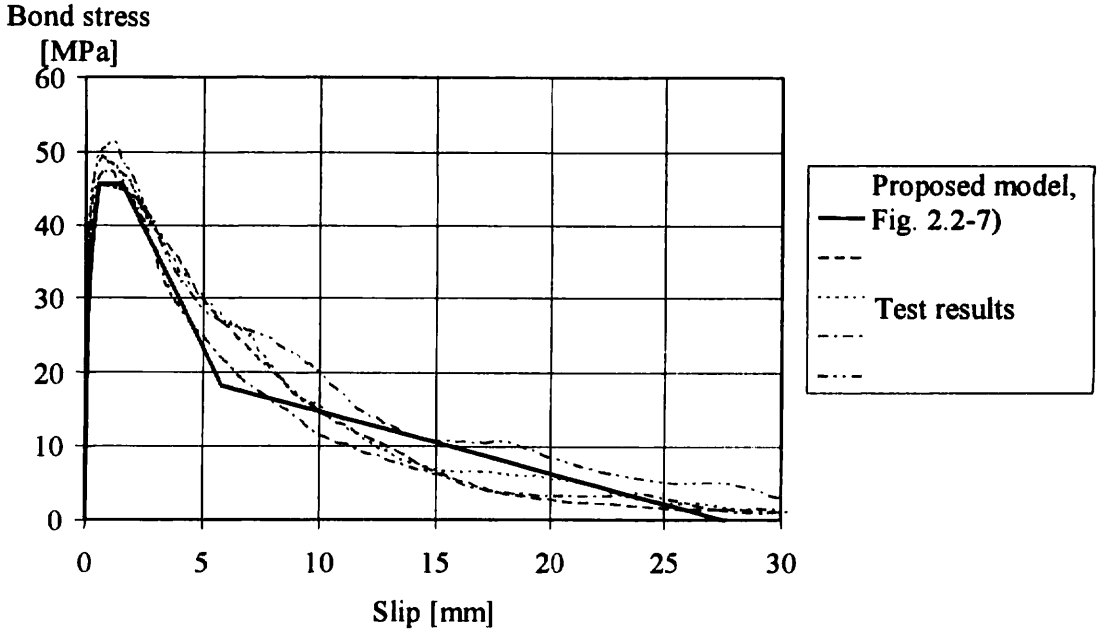

Fig. 2.2-8: Comparison of the proposed simplified bond-slip relationship and test results from pull-out tests with short embedment-length (16 mm ribbed bar of type K500 in well-confined high-strength concrete). Test results according to Magnusson (1997).

Another approach to study the influence of bar yielding on bond behaviour was used by Bigaj et al. (1996a, 1998), who measured the strain distribution along a well confined bar in pull-out tests with long embedment lengths and bar dimension 16 or 20 mm. With the help of the stress-strain relationship of the bar (yield stress $f_y \approx 530$ MPa), the steel stress distribution was found, from which the bond stress distribution was deduced. The longitudinal displacement of each point along the bar was obtained by integrating the steel strains. By neglecting the concrete strains, these displacements were assumed as local slips. Therefore, for each test a relationship between the bond stress and the slip was derived. Fig. 2.2-9 summarises the bond stress-slip curves obtained for normal-strength and high-strength concrete ($f_c = 28$ and 95 MPa, respectively).

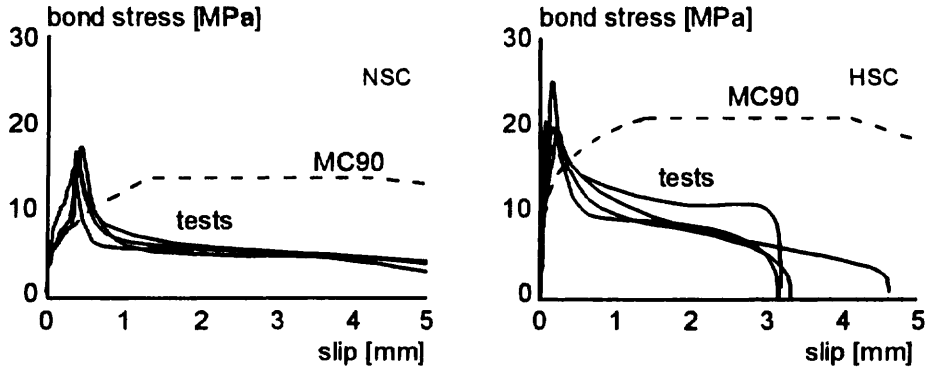

Fig. 2.2-9: Bond stress-slip relationship derived from pull-out tests on 20 mm diameter bars with long embedment length; (left) f_{cm} = 28 MPa; (right) f_{cm} = 95 MPa; [Bigaj et al. (1996a), (1998)]

The bond stiffness observed in high-strength concrete was higher than in normal-strength concrete. Also bond strength was higher in the former case. When the bond strength was normalised to $f_c^{1/2}$, about 25% lower values of the relative strength were found for high-strength concrete compared with normal-strength concrete. The results presented in Fig. 2.2-9 have been obtained after smoothing of the measurements, which means that the 'local' bond stress represents the average behaviour over a certain length.

Copyright fib, all rights reserved. This PDF copy of fib Bulletin 10 is intended for use and/or distribution only by National Member Groups of fib.

The shape of the ascending branch of the MC90 bond stress-slip curve is similar to the experimental results and the agreement is better for normal-strength concrete than for high-strength concrete. Nevertheless, for both concrete types, the MC90 expression underestimates the bond stiffness in this range. Starting with a sudden drop of the bond stress after having reached the peak value, the bond stress-slip diagram shows a further reduction of the bond stress with increasing slip. In this respect it is important to realise that steel strain implies different slip values at subsequent ribs, especially when the bar yields. The MC90 bond model does not reflect the experimentally observed change in the bond resistance due to yielding of the steel. Moreover, the descending branch and the residual bond stress values proposed in MC90 fall far above the experimental values. This disagreement is likely to be the result of deriving the empirical MC90 bond model from the results of pull-out tests with short embedment length, where the steel strain is far below the yield strain.

As will be discussed in the next paragraph, the bond stress-slip relation is more susceptible to a change in steel strain after having reached the bond strength than before. Pull-out failure is coupled with the occurrence of a cylindrical sliding plane along the crests of the ribs and a transition of the bond mechanism from rib bearing into friction. Compared to the ribbed bar, the new sliding surface is much smoother. Hence, the wedge action of this surface is more influenced by a radial displacement due to the Poisson effect than the wedge action of a ribbed bar. Wear of the sliding surface with increasing slip will further reduce the wedge action, and thus the bond stress. In fact, the bond stress-slip relationship observed in pull-out tests is the intersecting line of a test dependent load path with a three-dimensional surface that describes the bond stress as a function of slip and steel strain. This three-dimensional surface can be described with a model that considers the bond stress as a frictional mechanism and the normal stress in the steel-to-concrete interface as being generated by the concrete confinement that is activated when the bar slips (Den Uijl & Bigaj, 1996). A concise description of this model has already been given in Section 1.4.3. By conceiving the bar as a cone, the radial displacement of the steel-to-concrete interface is directly linked to the slip, the cone angle being coupled with the wedge action of the bar. To evaluate the normal stress acting at the interface, a thick-walled cylinder model is used, with which the normal stress is described as a function of the radial displacement of the interface, taking into account the softening behaviour of concrete loaded in tension (Fig. 1.4-6). Of course, the transition from rib bearing into friction is coupled with a reduction of the cone angle.

In Fig. 2.2-10 the resulting surface is shown for good confinement, that is to say enough confinement is available to prevent splitting of the entire cover and, hence, the bond failure mode is pull-out. In Fig. 1.4-7 this surface has been displayed in a two-dimensional way by a number of bond stress-slip curves, each for a different steel strain value. In the test and corresponding simulations, as already mentioned, the steel strain is not a constant.

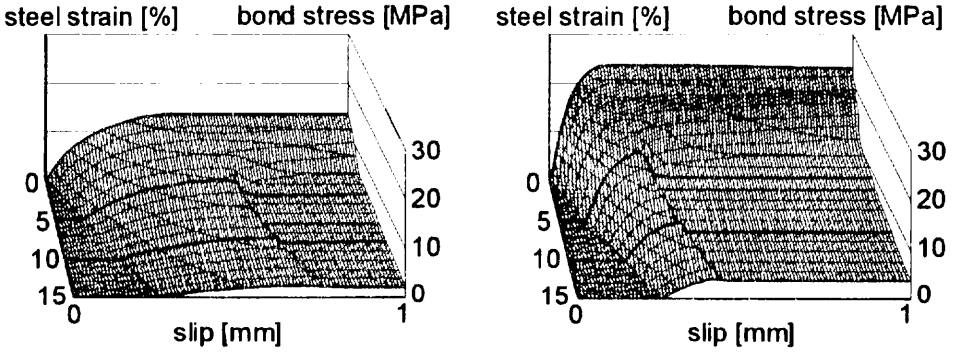

Fig. 2.2-10: Bond stress as a function of slip and steel strain in case of pull-out failure from confinement based bond mode; (left) normal-strength concrete; (right) high-strength concrete; [Den Uijl & Bigaj (1996)]

Copyright fib, all rights reserved. This PDF copy of fib Bulletin 10 is intended for use and/or distribution only by National Member Groups of fib.

2.2.2 Local bond behaviour in lightly confined concrete

2.2.2.1 Introduction

In well confined concrete the bond resistance will be governed by a pull-out failure where the concrete keys between the ribs are sheared off and the reinforcement bar slips in a frictional mode of behaviour. However, when the bar is embedded in concrete with low confinement, splitting through the entire concrete cover occurs. As pointed out in Section 1.4.3, stirrups play an important role in limiting the width of the splitting cracks and thus contribute to the bond resistance after splitting occurs, [Morita and Fujii (1982)], [Eligehausen et al. (1983)], [Giuriani et al. (1991)]. It may even be the case that the confinement from stirrups is sufficient to enable a pull-out failure mode in the already split concrete; in such a case, the pull-out resistance is reduced in relation to the pull-out resistance in well-confined concrete.

In the absence of a transverse pressure by external loads or support reactions, or without sufficient transverse reinforcement, a cover of about three times the bar diameter seems to be necessary to assure pull-out failure, similar for normal-strength and high-strength concrete. The bond stress at which through splitting occurs strongly depends on the confining capacity of the surrounding concrete and, hence, on its tensile properties. However, the spacing and arrangement of bars in a concrete section also influence the splitting tendency. After the occurrence of a through splitting crack, the local bond stress quickly drops due to loss of confinement. Splitting cracks can be limited around the anchored bar or can develop along the whole anchorage. Splitting failure may occur when the reinforcing bar is large in relation to the dimensions of the concrete specimen or is placed with a small concrete cover so that splitting cracks develop along the whole embedded length.

Various types of pull-out tests with a short embedment length have been made where the concrete specimens eventually split before the bar was pulled out in a frictional mode. However, the splitting failure observed in such tests is not always a local phenomenon related to the bond action but could be a global failure caused by the stress field created in the specimen by the load arrangements. Pull-out tests in high-strength concrete specimens have been reported for instance by Zhiming and Zhiman (1992), Shin and Choi (1996), Esfahani and Rangan (1998a). However, the results from this type of tests may be difficult to interpret and to transfer into design rules as the results might depend on the actual structural effects governed by the test specimen geometry and the load arrangement.

Zhiming and Zhiman (1992) made pull-out tests with the reinforcing bar placed in the centre of the specimen. The bar diameter varied between 12, 16, 18, and 20 mm. The concrete specimens had a cross-section of 100×100 mm and in some of them a spiral reinforcement was provided. In all specimens splitting cracks formed through the concrete cover, but in the specimens with spiral reinforcement, a pull-out failure occurred in the split specimen, since the spiral reinforcement provided a certain restraint. The authors found that the average bond stress at maximum load was proportional to the tensile strength of the concrete used. The concrete compressive strength varied from 60 to 100 MPa.

Shin and Choi (1996) carried out 32 pull-out tests using bars with a diameter of 13 or 22 mm, placed eccentrically in small specimens to study the effect of the cover. The embedment length was 5 times the bar diameter. Both splitting and pull-out failures occurred.

Esfahani and Rangan (1998a) made 45 pull-out tests on short length specimens (splices). The bar diameter was 19,3 or 23,3 mm and the bar was placed eccentrically in the specimen to study the effect of the cover. The concrete compressive strength ranged from 26 to 75 MPa. All specimens failed because of splitting of the concrete cover.

Copyright fib, all rights reserved. This PDF copy of fib Bulletin 10 is intended for use and/or distribution only by National Member Groups of fib.

2.2.2.2 Local splitting behaviour and modelling

Splitting failure is more brittle in high-strength concrete than in normal-strength concrete (Fig. 2.2-11). This has been previously explained by the uneven bond stresses along the bar and by the relative inability of high-strength concrete to redistribute stresses along the bar. An interesting point is to quantify the degree of confinement to be able to predict the stresses that give cover splitting. Noghabai (1995, 1998) studied the influence of the actual test set-up on the bond test results in terms of observed number of splitting cracks and its influence on the maximum load. As already mentioned, test results cannot be conclusive until the boundary conditions and the other influential factors in the experiments are clearly identified and quantified. In order to understand the problem better, the global response must be broken down to essential components that are analysed independently.

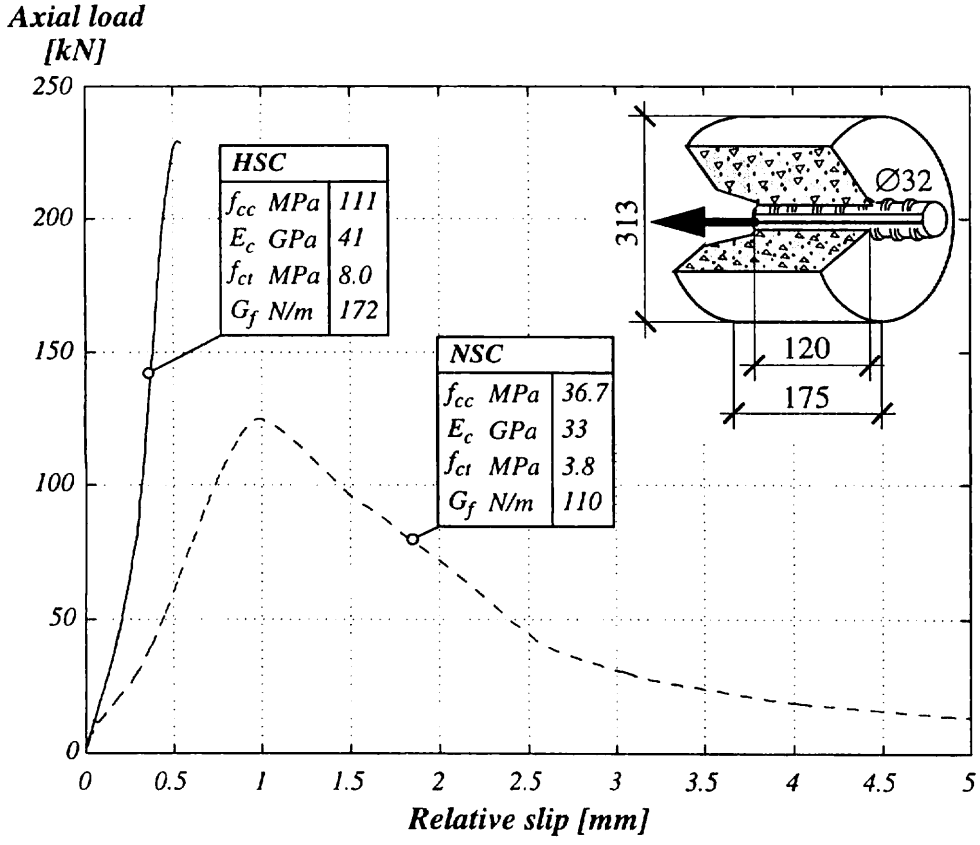

Fig. 2.2-11: Pull-out behaviour of rebars in unconfined rings. From Noghabai (1995).

The bursting (splitting) action is often simulated by the well-known model of a thick-walled concrete ring subjected to an internal pressure, introduced by Tepfers (1973). Based on the above arguments, it is necessary to understand how the ring model works under well-defined and controlled loading and boundary conditions before using it in more complex bond models.

Noghabai (1995, 1998) performed so-called "membrane" splitting tests on thick-walled concrete rings of both normal and high-strength concrete, with and without spiral reinforcement, as well as on rings of fibre-reinforced high-strength concrete. The rings were subjected to an inner pressure by a pressurising device (sleeve or membrane) until concrete splitting occurred, see Fig. 2.2-12. In all cases without spiral reinforcement, two radial cracks were observed at the ultimate pressure $p_{i,max}$. This splitting behaviour agrees with other similar tests on both plain concrete and rock, see Clifton et al. (1976), Neuner et al. (1978), Bilcík and Priechodsky (1991) and Plizzari et al. (1998b).

Copyright fib, all rights reserved. This PDF copy of fib Bulletin 10 is intended for use and/or distribution only by National Member Groups of fib.

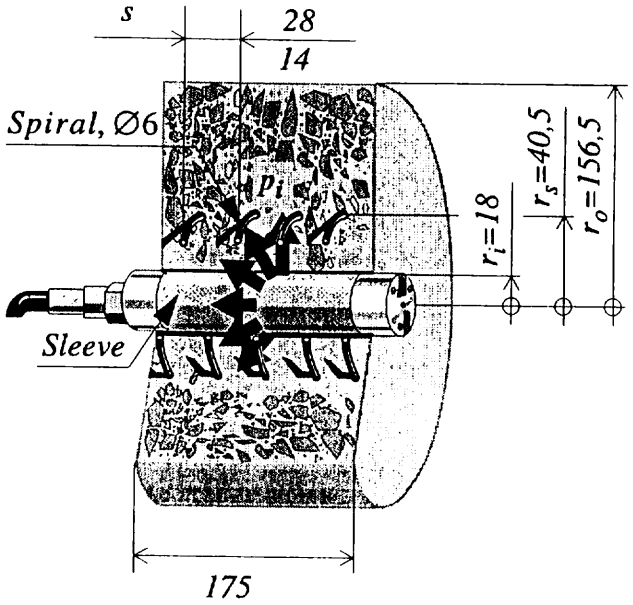

Fig. 2.2-12: Experimental set-up and specimen for "membrane" splitting test, according to Noghabai (1995, 1998).

The experiments were also analysed by different finite element methods, see Noghabai (1995, 1998; 1999), and Plizzari et al. (1998b), which showed how the cracks initiate, propagate and finally localise into two fracture zones in rings at ultimate pressure (see also Fig. 1.5-15 in Chapter 1). The important conclusion drawn from Noghabai (1995) is that the splitting capacity ($p_{i,max}$) of concrete covers is not governed by the individual values of the modulus of elasticity, the tensile strength or the fracture energy, but rather by a combination of all of them. This combined material property may be expressed by the physically validated *characteristic length*, $l_{ch} = E_c \cdot G_F / f_{ct}^2$, introduced by Hilleborg et al. (1976). High-strength concrete is generally considered as "brittle". However, brittleness makes sense only when material is viewed in the context of a structure under defined loading conditions. The brittleness may be quantified by a number B expressed as the ratio between a structural parameter and the characteristic length l_{ch}, see Bache (1995).

In Fig. 2.2-13, the maximum inner pressure ($p_{i,max}$), as obtained from analytical models (see Section 1.4.6.) and from experimental results, is plotted versus the brittleness number (B), defined as the ratio between the structural parameter (r_0) and the characteristic length. A ring of high-strength concrete with a small number B may be more ductile and have a larger pressure capacity than a ring of normal-strength concrete despite having a considerably higher compressive strength. Thus, with respect to spalling of concrete covers, it is not justified to categorically label high-strength concrete as "more brittle". Another important conclusion from Fig. 2.2-13 is the intensity of strength-based models to not only a variation in material but also to different cover thicknesses. However, for many covers of normal thickness a plastic model may suffice.

The brittleness of rings may be changed either by adding fibres to the concrete (hence by changing the characteristic length l_{ch}) or by applying reinforcement. The results of Noghabai (1998) for rings of fibre-reinforced high-strength concrete (containing a volume fraction of 1% or 2% steel fibres) are also included in Fig. 2.2-13. An analytical ring model used by Noghabai (1995) assumes the presence of two radial cracks (based on the experimental observations), along which the tensile stresses vary according to a linear σ_{ct} -w relationship. The linear softening assumption is too crude for fibrous concrete, hence the agreement for these cases are not as good. Afterwards, Noghabai (1998) generalised the previous model by using a multilinear softening relation in good agreement with the experimental results of uniaxial tension tests, e.g. according to Fig. 2.1-3. By using this model, the predictions for rings of fibrous high-strength concrete remarkably improved.

Copyright fib, all rights reserved. This PDF copy of fib Bulletin 10 is intended for use and/or distribution only by National Member Groups of fib.

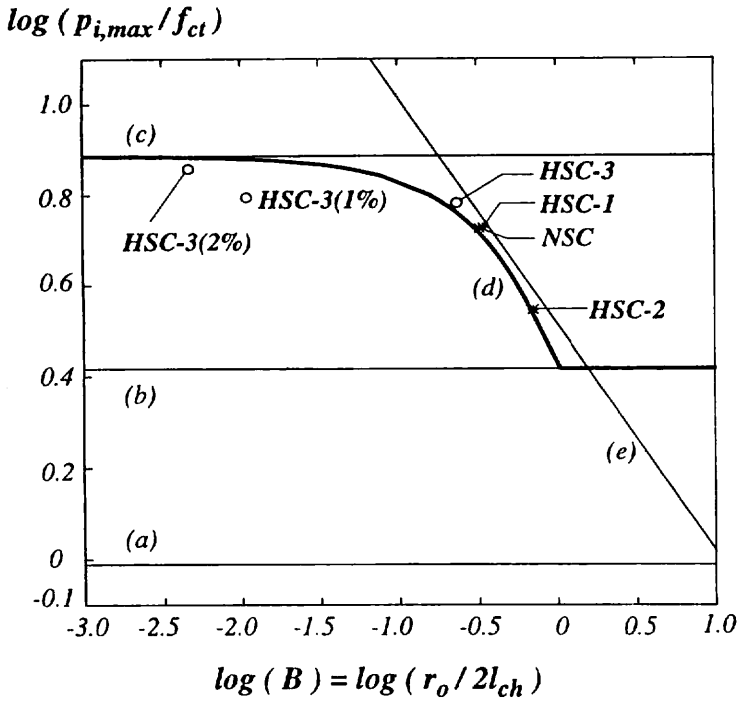

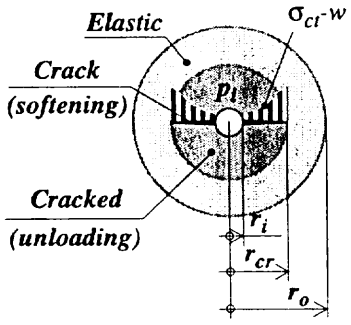

	f_{cc}^{cube} [MPa]	l_{ch} [m]
NSC	57.0	0.240
HSC-1	105.0	0.229
HSC-2	157.4	0.111
HSC-3	114.2	0.334
HSC-3(1%)	113.0	7.163
HSC-3(2%)	119.6	19.688

Fig. 2.2-13: The analytical models as function of the brittleness number B. The ring models are: (a) perfectly-elastic; (b) partly-cracked-elastic; (c) perfectly-plastic; (d) non-linear fracture mechanics assuming a linear softening (the bold, full line according to Noghabai (1995); (e) linear elastic fracture mechanics. Modified from Noghabai (1998).

Noghabai (1995) tried to change the degree of confinement by using spirals with different pitches. On all specimens with spiral reinforcement, 4 to 6 splitting cracks could be observed. Spirals or stirrups will not have any influence on the ultimate splitting capacity if located outside the critical crack front (r_{cr} in Fig. 2.2-13) where the splitting cracks are not present. They might enhance the post-failure ductility, by keeping the pieces together. The important aspect is how cracking in concrete covers is affected by the restraint provided by stirrups, surrounding structures, interaction of multiple bars, etc. Thus, single-bar models have to be modified to represent the real cases for which the degree of surrounding confinement needs to be quantified.

The bursting component has traditionally been coupled to bond forces along the rebar with recourse to plasticity type of models (see Chapter 1). In limit analysis models the correlation has been based on a single fixed "wedge angle". Such a value has very limited generality, due to variations in different parameters (e.g. bar-to-cover ratio, transverse reinforcement, external pressure, etc) as well as the possible influence of the test set-up, see Noghabai (1995). Plasticity models with more sophisticated hardening rules and internal variables require computational aid but they may give better phenomenological explanation to test results. Consequently, they form the basis for local bond models that are sufficiently reliable for engineering and design of reinforced concrete structures. For instance, the plasticity model of Lundgren and Gylltoft (1998) was also able to capture the modes of failure in the experiments of Noghabai (1995), albeit on normal-strength concrete. In this context, the model of Den Uijl and Bigaj (1996) should also be mentioned. These authors assume that, after concrete splitting, the bond mechanism is not changed and, hence, the cone angle needs not to be modified as in the case of pull-out failure, as assumed in Section 2.2.1. With respect to the loss of confinement due to splitting, the influence of the Poisson effect on the confinement can be neglected. Therefore, steel strain of the main bars needs not to be taken into account when modelling splitting failure.

The proposed model has been validated using results of experiments with well-defined confinement conditions (Den Uijl & Bigaj, 1996). Fig. 2.2-14 shows the outcomes obtained with this model for

Copyright fib, all rights reserved. This PDF copy of fib Bulletin 10 is intended for use and/or distribution only by National Member Groups of fib.

normal and high-strength concrete in the case of splitting failure for different concrete covers. It is clearly seen that the local bond strength increases with the cover, that the bond stiffness is much higher in high-strength concrete than in normal-strength concrete, and that after the peak, the bond stress drops faster in high-strength concrete than in normal-strength concrete. Note that for equal concrete covers, the slip at which bond is totally lost is significantly smaller in high-strength concrete than in normal-strength concrete.

These previous results are in agreement with the findings of Azizinamini (1998d), who investigated the capacity of tension splices embedded in high-strength concrete with small concrete covers and without stirrup reinforcement. The fact that the capacity did not increase proportional to the lap length was explained by the higher bond stiffness, which does not allow for a uniform bond stress to be developed along the lap splice. Instead, a zipping effect occurs and the only way to increase the splice capacity is by increasing the confinement, preferably by means of stirrup reinforcement.

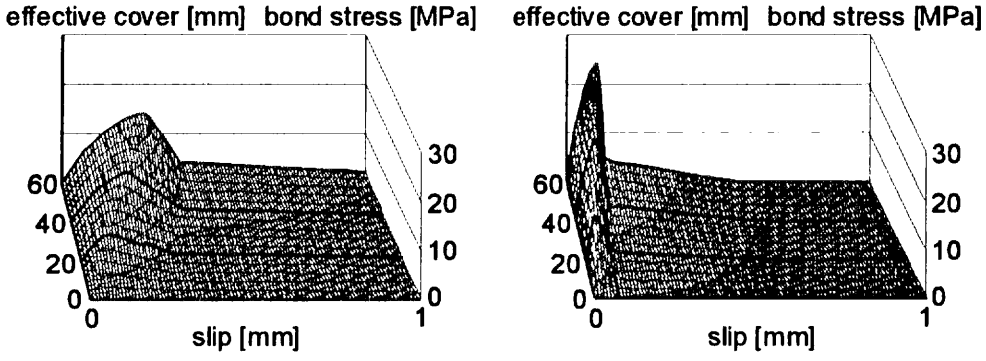

Fig. 2.2-14: Bond stress as a function of slip and steel strain in case of bond splitting failure from confinement based bond mode; (left) normal-strength concrete; (right) high-strength concrete; [Den Uijl & Bigaj (1996)]

2.2.3 Other factors influencing the local bond behaviour in high-strength concrete

2.2.3.1 Factors influencing the local bond behaviour

Many factors influence the bond and anchorage behaviour of reinforcement bars in concrete (see also Section 1.1.2). In the CEB/FIP Model Code 1990 [CEB-FIP (1993)], distinction is made between factors related to the local bond behaviour, and factors related to the regional response. The local bond behaviour is controlled by the basic bond conditions and is influenced for instance by the casting position and the loading direction relative to the casting direction. The regional bond and anchorage behaviours are influenced by various factors related to the confinement of the anchorage regions, like the sectional arrangement of the anchored bars, arrangement of transverse steel, and presence of transverse pressure. In this section some factors that seem to be significant for the local bond behaviour in high-strength concrete are discussed.

2.2.3.2 Influence of bar position

For bars anchored in normal-strength concrete, it has been observed that bottom cast bars have better bond performance than top cast bars. It is generally assumed that this effect depends on an increased tendency of bleeding of the concrete around top bars. In high-strength concrete several researchers have found that top cast bars have a better bond performance than bottom cast bars.

Copyright fib, all rights reserved. This PDF copy of fib Bulletin 10 is intended for use and/or distribution only by National Member Groups of fib.

Azizinamini et al. (1993b) carried out a series of tests on lap splices in beams. The beams were grouped in pairs with identical detailing and similar strength but different position of the spliced bars (top cast or bottom cast bars). Hence, each lap splice with bottom cast bars could be compared to a companion lap splice with top cast bars. The concrete compressive strength evaluated from cylindrical specimens was about 35 - 40 MPa for the normal-strength concrete and ranged from 75 to 100 MPa for high-strength concrete specimens. The high-strength concrete used had water to cemetitious materials ratios in the range from 0,21 to 0,27. The slump of the high-strength concrete varied between 190 to 270 mm. The diameter of the anchored bars was 35 mm. The top concrete cover was equal to one bar diameter and the bottom concrete cover was either 337 or 387 mm. It was assumed that other parameters, such as slump, vibration, cover and method of finishing the concrete, could influence the bond behaviour of top cast bars. However, these parameters were not investigated in this study.

In all cases a brittle splitting failure occurred. The average bond stress at maximum load was normalised to $\sqrt{f_{cm}}$ and similar beams with either top cast or bottom cast bars were compared. In one pair of tests in normal-strength concrete, the specimen with top cast bars showed a lower bond stress (about 8 %) than the test with bottom cast bars. However, in three pairs of tests in high-strength concrete, the beams with top cast bars showed a slightly higher splice capacity than the companion test specimen with bottom cast bars. The improvement was in the range of 1 - 8 %. Based on the observed behaviour in high-strength concrete specimens, the authors assumed that the bond stress distributions along the splices at failure were less uniform in high-strength concrete than in normal-strength concrete. This could be explained by higher bearing capacity under the lugs in high-strength concrete and by the fact that the splitting resistance, which is related to the concrete tensile strength, is not increasing in proportion to compressive strength. Hence, possible bleeding of concrete around top cast bars, which has an unfavourable effect in normal-strength concrete, could have a favourable effect in high-strength concrete. In fact, since the bearing capacity of the lugs is reduced, a more uniform bond stress distribution is obtained at failure. Since more lugs are active, a higher splice capacity would result.

Similar results on top cast bars have been reported by Gjørv et al. (1990) and Kaku et al. (1992).

2.2.3.3 Influence of silica fume

To obtain a dense, high performance, and high-strength concrete, silica fume is normally added to the concrete mix. The effect of silica fume on the bond behaviour is twofold. On one hand the concrete strength is improved, which results in stiffer bond behaviour and higher bond strength (see the previous sections). On the other hand, the silica fume seems to have a negative influence on the bond resistance in case of local splitting failure.

Gjørv et al. (1990) studied the effect of condensed silica fume on the bond resistance by means of pull-out tests and by scanning electron microscopy and X-ray diffraction analysis to determine the properties of the transition zone between steel and concrete. Concrete with various amount of silica fume, ranging from 0 to 16 % of the cement weight, but with a similar compressive strength was compared. The pull-out tests were made according to ASTM Standard. Both deformed and plain bars of dimension 19 mm were used. In case of deformed bars, the concrete specimens failed due to splitting. The conclusions were that the pull-out resistance increased with increasing additions of condensed silica fume and that the porosity and thickness of the transition zone were reduced.

The effect of silica fume was also studied experimentally by Hwang et al. (1994). Eight beams in four pairs were tested to compare the capacity of lap splices in regions with constant negative bending moment. In each pair one beam was made from concrete with Portland cement only and the other beam was made from concrete where 10 % of the cement was replaced by an equal weight of silica fume. The main bars (f_{ym} = 478 MPa) had a diameter of 29 mm and the splice length was 300 mm. The concrete covers (side and top covers) of the main bars were equal to one bar diameter and the clear spacing

Copyright fib, all rights reserved. This PDF copy of fib Bulletin 10 is intended for use and/or distribution only by National Member Groups of fib.

between splices was 2 bar diameters. Specimens both with and without stirrups over the slice length were used. The concrete compressive strength, evaluated from tests on ϕ150×300 mm cylinders, varied between 60 and 80 MPa and the ratio between water and cementitious materials was either 0,28 or 0,33. In each pair of beams the concrete compressive strength as well as the concrete tensile strength were always higher in the concrete with silica fume. Nevertheless, in each pair the average bond stress at maximum load was always smaller in the concrete with silica fume. The capacity of the lap splices was always determined by a face-and-side splitting failure before yielding was reached in the bars. The failures were preceded by longitudinal splitting cracks along the spliced bars through the top concrete cover. Hwang et al. (1994) compared their results with other reported similar tests and came to the conclusion that the bond degradation was attributed to the loss of adhesion between concrete and steel due to the presence of silica fume. The comparison showed that the average bond stress at maximum load, normalised with respect to the square root of the concrete compressive strength, could be decreased by 15 % due to the presence of silica fume. They argued that a decrease of frictional resistance along the inclined lug interface results in a decreased bond stress and in an increased splitting effect which in turn results in a decreased bond resistance in case of local splitting failure. After testing, the concrete cover was removed and the bars were inspected. In case of Portland cement, concrete particles were found firmly attached to the bar between the ribs, in contrast to the specimens with silica fume. The improved adhesion also results in improved friction.

A similar test series was performed by Hamad and Itani (1998a, 1998b) with the aim to study the effect of silica fume on the bond characteristics in high performance concrete. The test series included sixteen beams with lap splices in regions with constant positive bending moment. Two 25 mm bars of Grade 60 (f_{ym} = 426 MPa) were spliced with a splice length of 305 mm. No transverse reinforcement was provided to allow for random formation of cracks. The variables were percentage of replacement (by weight) of cement by silica fume (0, 5, 10, 15 and 20 percent), casting position (top or bottom), and superplasticizer dosage (2 or 4 l/100 kg cementitious materials). The concrete side and top covers were 38 mm corresponding to 1,5 times the bar diameter. The clear spacing between splices was 3 bar diameters. The concrete compressive strength varied in general between 65 and 85 MPa. The water to cemetitious materials ratio ranged from 0,33 to 0,37. The splices failed due to splitting of the concrete cover before yielding of the bars. The test results indicated that a replacement of 5 to 20 percent of the cement by an equal weight of silica fume resulted in average in a 10 percent reduction of the average bond stress at maximum load, regardless of casting position or superplasticizer dosage. This is in accordance with the results by Hwang et al. (1994). Furthermore, for beams with no silica fume, top cast bar splices had a greater splice capacity than companion bottom cast bars. This trend was valid for both the superplasticizer dosages used. Increasing the superplasticizer dosage from 2 to 4 l per 100 kg of cement had a negative effect on bottom cast bars and a positive effect on top cast bars.

De Almeida (1996) examined the influence on the bond properties of chemical and mineral admixtures in high-strength concrete. Pull-out tests with short embedment length (5ϕ) were used. The bar dimension was 20 mm and all specimens failed due to splitting. It was shown that the bond resistance was strongly influenced by the type of cementing material. However, the concrete strength varied considerably between various concrete mixes.

2.2.3.4 Influence of fibres

The concrete confining action strongly depends on the presence of fibres in matrix [Harajli et al. (1995)]. The use of fibres can be even more effective in high-strength concrete, which exhibits a particularly brittle post-peak behaviour due to its more homogeneous microstructure and the intragranular nature of the cracking phenomenon [Balaguru and Shah (1992)].

Plizzari (1999) performed pull-out tests on short anchorages (embedded length/bar diameter ≈ 8), simulating the influence zone Δz of one two-legged stirrup (see in Fig. 1.1-22 a specimen with three

Copyright fib, all rights reserved. This PDF copy of fib Bulletin 10 is intended for use and/or distribution only by National Member Groups of fib.

stirrups). Tests were performed on specimens made with normal as well as high-strength concrete (with silica fume), with and without steel fibres (hooked steel fibres with a volume fraction of 0.38%). Furthermore, the influence of the transverse reinforcement area was investigated by testing specimens with different stirrup diameters.

Fig. 2.2-15a exhibits the bond stress as a function of the loaded end slip, as obtained from tests on specimens without stirrups. The remarkable increment of stiffness and bond strength in specimens with fibres can be noticed. These specimens are usually characterised by a very brittle behaviour [Plizzari et al. (1998a)]; however, when fibres are adopted, a more ductile behaviour is obtained. In fact, the ultimate loaded end slip of fibre-reinforced concrete is three times the value observed from concrete without fibres. This underlines the importance of the confining action of the cohesive stresses transmitted across the split concrete, and the remarkable influence of fibres on anchorage behaviour.

Figure 2.2-15b shows the average maximum bond stress τ_{max} versus the stirrup index of confinement (Ω, see Section 1.4.3), as obtained from all specimens tested. In specimens without transverse reinforcement (Ω=0), the confining action is due only to the contribution of the concrete surrounding the bars. The results from specimens (of the same material) having the same concrete index of confinement (B, see Section 1.4.3) are connected by a continuous line. The larger the stirrup index of confinement, the higher the bond capacity becomes. As mentioned above, a low volume fraction of fibres remarkably increases bond strength; steel fibres have a better efficiency in a high-strength matrix.

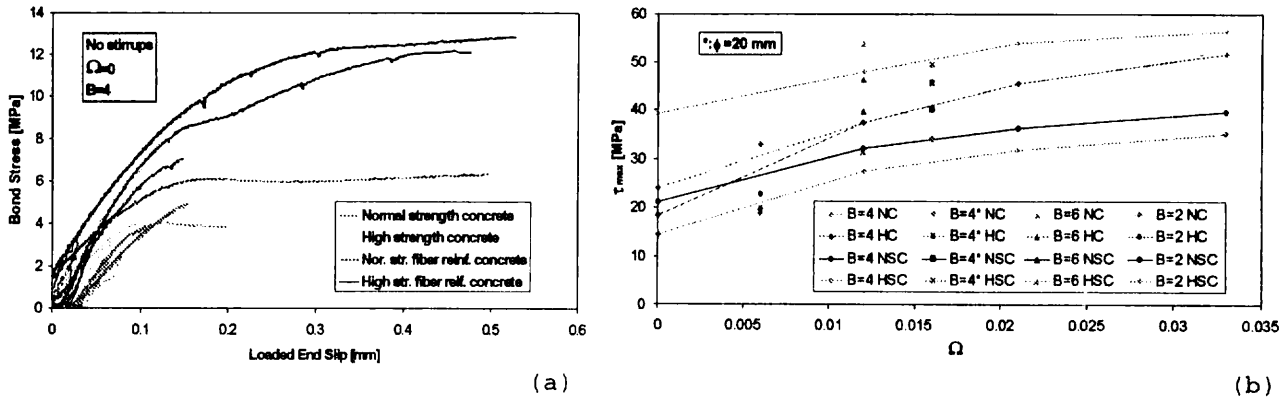

Fig. 2.2-15: (a) bond stress versus loaded end slip as obtained from specimens without stirrups; (b) bond strength versus Stirrup Index of Confinement; according to Plizzari et al. (1998a).

2.2.4 Local bond behaviour in the service state

In 1995 the joint CEB/FIP Working Group on HSC/HPC gave some guidelines for the bond stress-slip relationship to be used in the serviceability limit state [CEB (1995)]. The Working Group concluded that, in general, the local bond stress-slip model given in CEB-FIP Model Code 90 [CEB-FIP (1993)] is applicable also to high-strength concrete, but the numerical values defining the model should be improved. For analysis of the cracking behaviour in the serviceability limit state, only the first ascending branch of the bond stress-slip relation is assumed to be relevant. In general the ascending branch can be described by the following expression.

$$\tau_b(s) = \tau_{b,max}\left(\frac{s}{s_1}\right)^{\alpha} \qquad (2.2\text{-}4)$$

For analysis of cracking in the serviceability limit state, the Working Group, [CEB (1995)], gave the following numerical values for confined concrete and mean bond conditions in high-strength concrete:

Copyright fib, all rights reserved. This PDF copy of fib Bulletin 10 is intended for use and/or distribution only by National Member Groups of fib.

$\tau_{b,max} = 0{,}22 f_{cm}$ (maximum bond stress)

$f_{cm} = f_{ck} + \Delta f$

$\Delta f = 8$ MPa

$s_1 = 1{,}0$ mm (slip at maximum bond stress)

$\alpha = 0{,}21$

Then the bond stress-slip relationship can be expressed as

$$\tau_b(s) = 0{,}22 f_{cm} \cdot s^{0{,}21} \tag{2.2-5}$$

The local bond stress-slip model is valid only if no longitudinal cracks occur. According to CEB (1995), this condition may be assumed to be satisfied provided that

$$\sigma_s \leq f_{yk}$$

According to CEB (1997), it was found that the maximum bond stress for cracking problems is proportional to $f_{cm}^{1,0}$ rather than to $f_{cm}^{0,5}$. Even if the bond stress-slip models given in CEB-FIP Model Code 90 are relevant for normal-strength concrete, it is assumed that the modified expression, given above, yields better predictions for both normal-strength and high-strength concrete, for monotonic loading and for high bond rebars.

Based on an extensive experimental program on reinforced concrete tension members [Farra (1995)], referred to in Section 2.4.1, the following bond stress-slip relationship was proposed by Farra (1995) to be used for short term monotonic loading and usual concrete covers:

$$\tau_b(s) = 0{,}4 f_{cm}^{0{,}95} s^{0{,}3} \tag{2.2-6}$$

2.3 Behaviour and design of anchorage regions

2.3.1 Anchorage of single bars

2.3.1.1 Anchorage in well confined concrete

The typical behaviour of a single bar anchorage in well confined concrete and the influence of anchorage length and concrete strength appear from a series of pull-out tests reported by Huang et al. (1996a), Magnusson (1997) and Engström et al. (1998). In total, 14 tests were made with two types of concrete, high-strength concrete with a compressive strength about 105 MPa (cylinder strength according to ISO-Standard), and ordinary concrete with a strength of about 30 MPa. In all the tests, the anchored bar was a 16 mm ribbed bar of type K500 (f_{yk} = 500 MPa). The actual yield strength was 569 MPa and the tensile strength (at steel rupture) was 642 MPa. The specimen was cubical, with dimensions of 400×400×400 mm and with the anchored bar placed along a centroidal axis, Fig. 2.3-1.

The concrete cover was 192 mm or 12 times the bar diameter. No stirrups were provided. The anchorage length varied between 90, 130, 170, 210 and 250 mm in specimens of high-strength concrete, and between 150, 220, 290, 360 and 500 mm in specimens of normal-strength concrete. In the test with the longest anchorage length, the depth of the specimen was increased to 500 mm. Some of the tests were repeated. The test procedure was displacement controlled.

Copyright fib, all rights reserved. This PDF copy of fib Bulletin 10 is intended for use and/or distribution only by National Member Groups of fib.

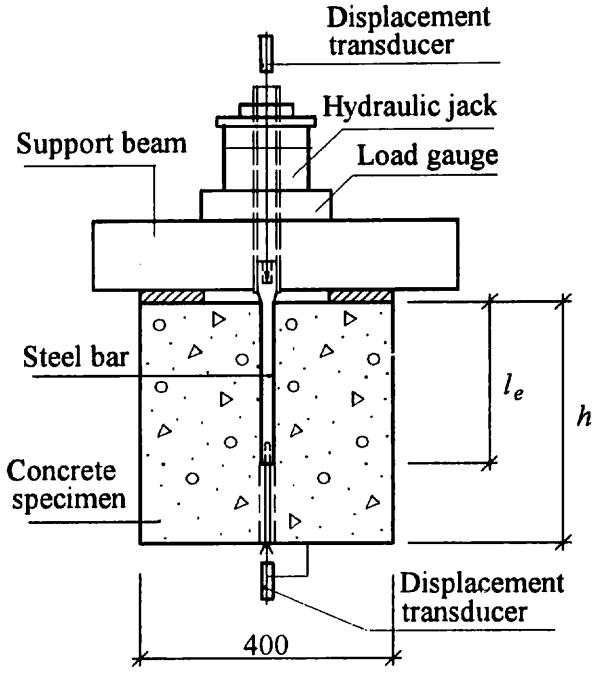

Fig. 2.3-1: Test specimen (type I) with the reinforcing bar anchored along the centroidal axis under well-confined conditions, according to Huang et al. (1996a).

Three types of failures were observed. For the tests with short anchorage lengths, smaller than 150 mm in high-strength concrete and 250 mm in normal-strength concrete, a pull-out failure occurred when the steel bar was still in the elastic range. When the anchorage length was more than 200 mm in high-strength concrete and 300 mm in normal-strength concrete, the anchorage capacity exceeded the capacity of the reinforcement bar and the steel bar finally ruptured. For the intermediate anchorage lengths, 170 mm in high-strength concrete and 290 mm in normal-strength concrete, the anchorage could resist the yield capacity of the bar, but during strain hardening of the steel, a pull-out failure occurred after considerable plastic deformations and a simultaneous yield penetration at the end of the embedded bar. In case of pull-out failure, either before or after yielding of the steel, the bar seemed to be sliding along a cylindrical crack plane along the tips of the ribs. Concrete was still left in between the ribs, when the bar was pulled out from the specimen. During the tests no visible splitting cracks were observed on the exterior faces of the test specimen. However, a local failure cone was formed in the concrete around the active end of the bar. This concrete cone remained bonded to the bar, also in the final state, and moved with the bar (Fig. 2.3-2).

The depth of the failure cone was measured after the test. Of a total of seven pull-out tests in normal-strength concrete, the depth of this failure cone varied between 18 and 35 mm with an average value of 26,4 mm, which corresponds to 1,65 times the bar dimension. For seven tests in high-strength concrete specimens, the depth of the failure cone varied between 16 and 30 mm with an average value of 27,0 mm or 1,68 times the bar diameter. Hence, the failure cone seemed to develop in the same way in high-strength and normal-strength concrete.

It was found that the anchorage capacity in the pull-out type of failure increased almost linearly with an increased anchorage length. For the same embedded length the anchorage capacity was about twice as large in high-strength concrete as in normal-strength concrete. The tensile force development in the anchored bars was evaluated from steel strain measurements. Typical distributions of the tensile force along the bar at maximum load are presented in Fig. 2.3-3.

Copyright fib, all rights reserved. This PDF copy of fib Bulletin 10 is intended for use and/or distribution only by National Member Groups of fib.

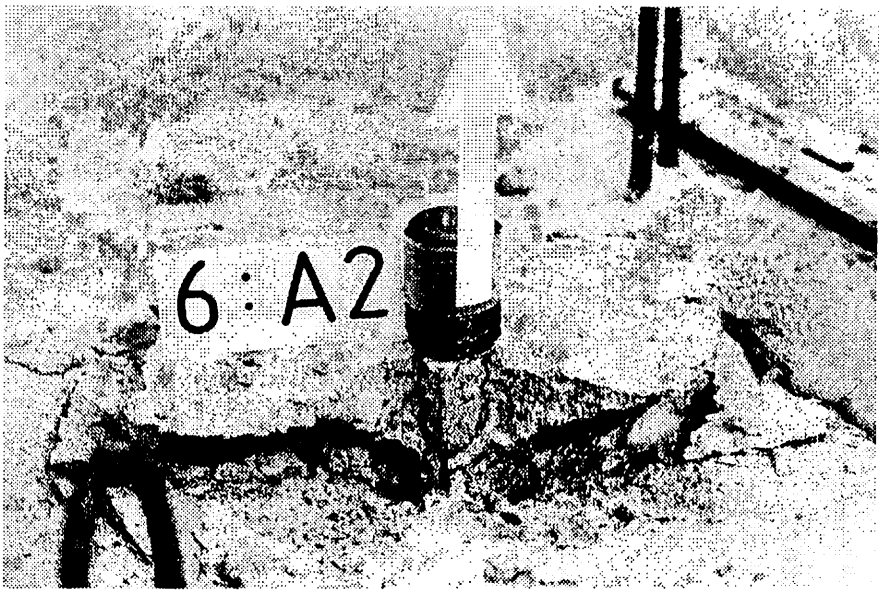

Fig. 2.3-2: Local conic failure at the active (loaded) end of the bar, according to Engström et al. (1998).

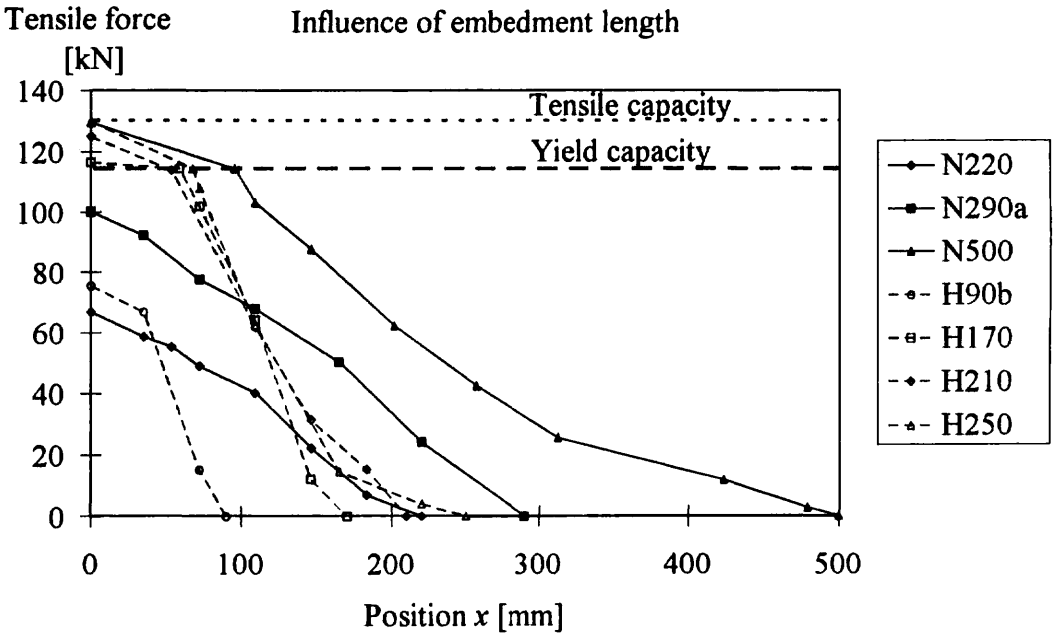

Fig. 2.3-3: Typical examples of the tensile force distribution along the anchored bar at maximum load. Pull-out tests in well-confined concrete (type I) (Fig. 2.3-1), according to Engström et al. (1998). Legend: N = normal-strength concrete; H = high-strength concrete; number = embedment length in [mm]

It appears that the tensile force varied almost linearly along the elastic part of the bar, except for the tests with the longest anchorage lengths. Here the steel to concrete interface at the passive end of the bar was not fully strained at maximum load. It is also possible to recognise a certain boundary effect near the loaded end of the bar, indicating that the bond was not fully effective near the free end face of the specimen. In the region where the yield stress was exceeded, the tensile force varied with a much smaller rate than in the region that was still in the elastic range. Hence, it is obvious that the yielding of the steel results in a drastic decrease of the bond stress (see Section 2.2.1).

Copyright fib, all rights reserved. This PDF copy of fib Bulletin 10 is intended for use and/or distribution only by National Member Groups of fib.

Due to the local conic failure, the effective transfer length decreased during the test. For the tests with pull-out failures, the average bond stress at the maximum load along the final reduced transfer length is presented in Table 2.3-1 and related to the concrete compressive strength.

Test specimen	Concrete strength f_{cm} [MPa]	Final transfer length $l_{e,red}$ [mm]	Maximum load N_{max} [kN]	Average bond stress $\tau_{m,max}$ [MPa]	$\frac{\tau_{m,max}}{\sqrt{f_{cm}}}$	$\frac{\tau_{m,max}}{f_{cm}}$
N150a	26,8	125	47,5	7,55	1,46	0,282
N150b	29,6	125	35,9	5,71	1,05	0,193
N220	26,8	185	66,7	7,17	1,39	0,268
N290a	26,8	260	102,8	7,87	1,52	0,294
N290b	30,6	260	126,7	9,69	1,75	0,317
average					1,43	0,271
H90a	101,5	70	75,8	21,5	2,13	0,212
H90b	103,3	60	75,6	25,1	2,47	0,243
H130a	101,5	100	94,2	18,7	1,86	0,184
H130b	103,3	105	78,5	14,9	1,47	0,144
H170	101,5	145	116,4	16,0	1,59	0,158
average					1,90	0,188

Table 2.3-1: Maximum bond stress in the pull-out test (type I) (Fig. 2.3-1), average value along the final transfer length related to the concrete compressive strength, according to Engström et al. (1998).

It appears that the average bond stress at failure is proportional to the concrete compressive strength for the smaller anchorage lengths and proportional to the square root of the compressive strength for the larger embedment lengths. This is a result of the length effect.

The model presented in Fig. 2.2-7 for the local bond stress-slip behaviour was used to predict numerically the global behaviour of the tests, i.e. the relationship between the tensile force and the end-slip at the loaded end of the bar [Huang et al. (1996b)]. Predictions were made for two alternative bond conditions, either good bond conditions or other bond conditions. For good bond conditions the maximum bond stress was assumed to be $\tau_{max} = 0{,}45 f_{cm}$, and for other bond conditions half this value.

It was found generally a good agreement between the numerical predictions and the experimental results, both for the failure mode and for the end-slip response. The scatter in the experimental results was normally well in between the estimates for "good" and "other" bond conditions but the results were normally closer to the predicted one for the case "other bond conditions". Hence, the proposed local bond stress-slip relationship (Fig. 2.2-7) seemed to be valid for predictions of the global response in well-confined concrete. The evaluation of the pull-out tests showed that the rate of the bond deterioration due to yielding was higher in high-strength concrete than in normal-strength concrete. Bigaj (1995) drew the same conclusion.

Lorrain and Hamouine (1996) tested the pull-out capacity of both smooth and deformed bars in high-strength concrete at various ages. The bar diameter (ϕ 10-32 mm) and the anchorage length varied. However, the anchorage length was always rather small ranging from 50 to 150 mm. A negative influence of increasing bar diameters was observed for both smooth and deformed bars.

2.3.1.2 Anchorage in lightly confined concrete

A series of 36 pull-out tests with long anchorage lengths was reported by Al-Jahida et al. (1994). The reinforcing bar was placed concentric in slender concrete specimens subjected to tension. The concrete

Copyright fib, all rights reserved. This PDF copy of fib Bulletin 10 is intended for use and/or distribution only by National Member Groups of fib.

cross section was 180×180 mm. The concrete compressive strength varied from 42 to 78 MPa and the bar diameters were 14, 16, 18 and 20 mm. The anchorage length varied between 5ϕ and 20ϕ. In most of the tests, a splitting failure was obtained, but often after yielding in some parts of the anchored bar. The test results indicated that the average bond stress at failure increases with the concrete strength and decreases with the anchorage length.

Similar types of pull-out tests were performed by Yerlici et al. (1996). However, they used two types of specimens with concentric or eccentric placement of the reinforcement bar. Aarup and Jensen (1998) reported various types of pull-out tests of reinforcing bars in high-strength fibre reinforced concrete.

The influence of confinement on the anchorage behaviour of single bars was studied by Engström et al. (1998) who performed pull-out tests with a rather long anchorage length. In this study, a more realistic anchorage situation was simulated, but in an idealised way with well-defined conditions. The pull-out specimens were similar to the ones described in Section 2.3.1.1 (Fig. 2.3-1), here referred to as specimen type I, but the anchored bars were now placed with less confinement. The main parameters were the confinement and the concrete type (high-strength or normal-strength concrete). The high-strength concrete had a compressive strength of about 105 MPa (cylinder strength according to ISO-Standard), while the compressive strength of the ordinary concrete was about 30 MPa.

The anchored bar was placed either in a middle position of an edge region (specimen type II), or in a corner region (specimen type III), see Fig. 2.3-4. The type and dimension of the reinforcement bar were kept constant through all the test series. It was a 16 mm ribbed hot-rolled bar of type K500. The anchorage length was constant, but the concrete cover and the number of stirrups enclosing the anchored bar varied. The cross-section of the test specimen was 400×400 mm. The specimen had a nose-like extended part, which was used to support the specimen in the testing machine (Fig. 2.3-4). Thereby, the eccentricity of the applied tensile force could be balanced and the force transferred from the bar to the concrete could be linked off in a natural way in the specimen. The state of stresses was then similar to that present in an anchorage region of a reinforced beam.

In most of the specimens, 2 or 4 stirrups of ribbed bars ϕ6 K500 were distributed along the embedment length, enclosing the main bar which had a concrete cover equal to the bar diameter. However, in some of the type II tests, the main bar was anchored in plain concrete with a concrete cover of one or two times the bar diameter. The embedment length was chosen to be just sufficient to anchor the yield capacity of the anchored bar in case of well-confined conditions, but insufficient to anchor the tensile capacity at steel rupture. Hence, an embedment length of 170 mm was used for specimens of high-strength concrete and an embedment length of 290 mm was used for normal-strength concrete. The test procedure was displacement controlled.

For the tests in type II specimens, with one bar placed in a middle position at an edge, a longitudinal splitting crack always appeared along the bar through the rather small concrete cover. The splitting crack developed successively, and in a controlled way, when the load increased. Also transverse cracks appeared successively during the test. They were inclined and developed in direction towards the loaded end. The cracking behaviour was approximately the same in high-strength concrete as in normal-strength concrete. In the specimens with stirrups, it was observed that the location and the development of the transverse crack were influenced by the stirrups. Typical crack patterns are shown in Fig. 2.3-5.

Copyright fib, all rights reserved. This PDF copy of fib Bulletin 10 is intended for use and/or distribution only by National Member Groups of fib.

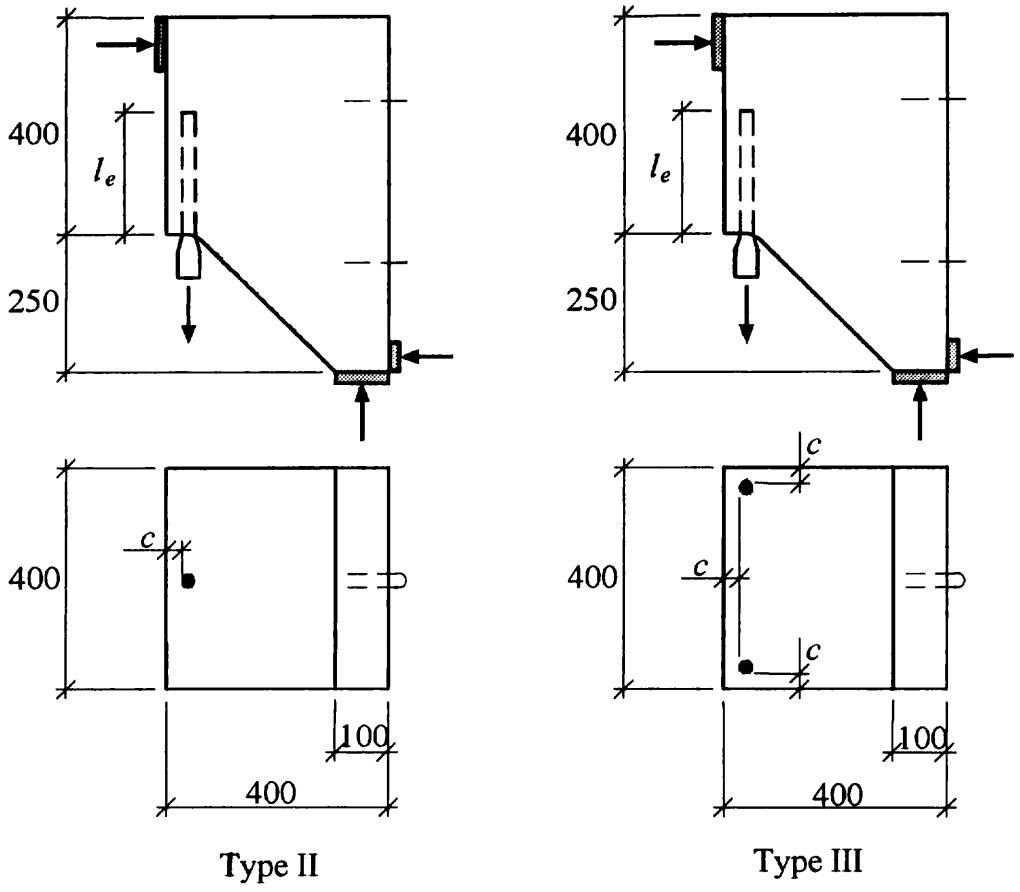

Fig. 2.3-4: (left) test specimens of type II with the bar anchored in a middle position near a free edge; (right) test specimen of type III with bars anchored in corner regions; according to Engström et al. (1998).

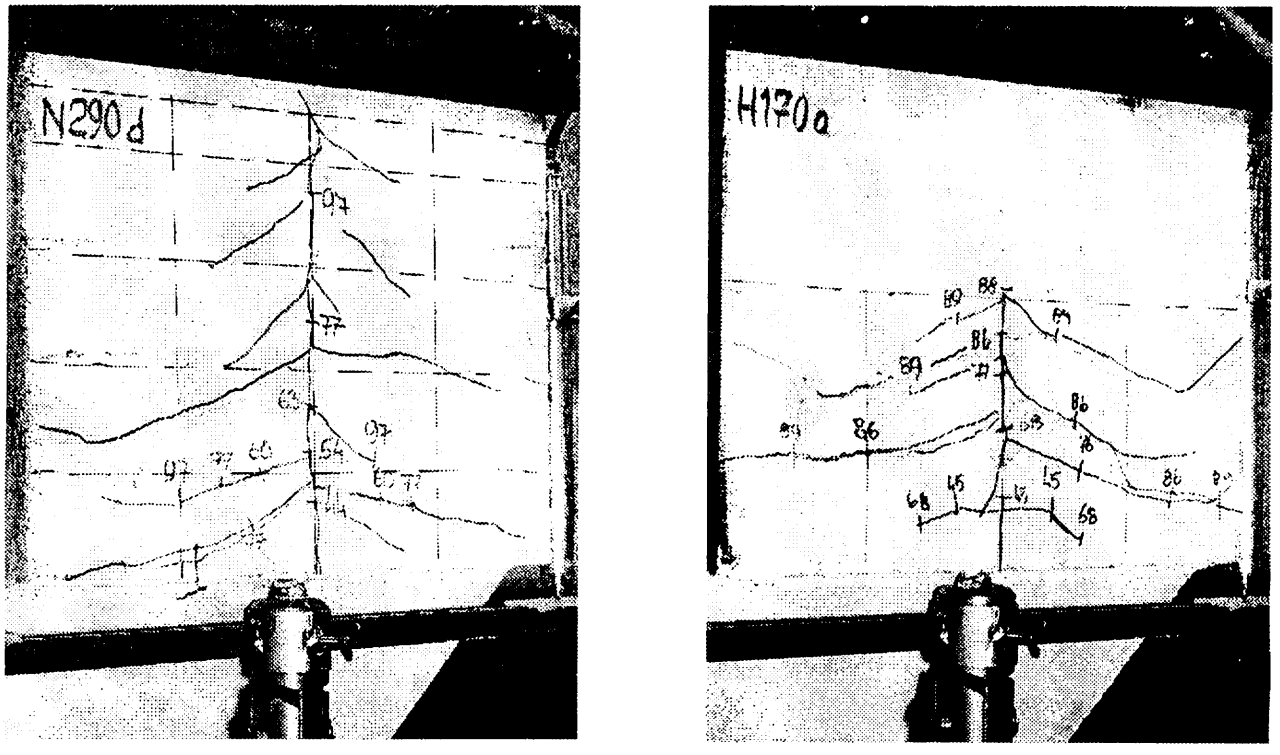

Fig. 2.3-5: Typical crack pattern in test specimens of type II (Fig. 2.3-4); (left) normal-strength concrete; (right) normal-strength concrete; according to Engström et al. (1998).

Copyright fib, all rights reserved. This PDF copy of fib Bulletin 10 is intended for use and/or distribution only by National Member Groups of fib.

In spite of the rather small concrete cover and the longitudinal splitting cracks that developed along the bar, the anchorage capacity in the type II specimens was almost the same as in the corresponding tests in well-confined concrete (type I), see Fig. 2.3-1. However, at the maximum load, an abrupt anchorage failure occurred resulting in a sudden drop of the tensile force. For this reason, the post-peak behaviour was quite different compared to the corresponding specimens with the bar in the centre. The test with a small concrete cover had a more brittle behaviour and a very small residual capacity in the post-peak stage, while the specimens with the bar in the centre had a rather ductile behaviour during the pull-out frictional mode, with a residual capacity that decreased gradually. The different behaviours appear from the relationships between tensile force and end-slip presented in Fig. 2.3-6 a - b.

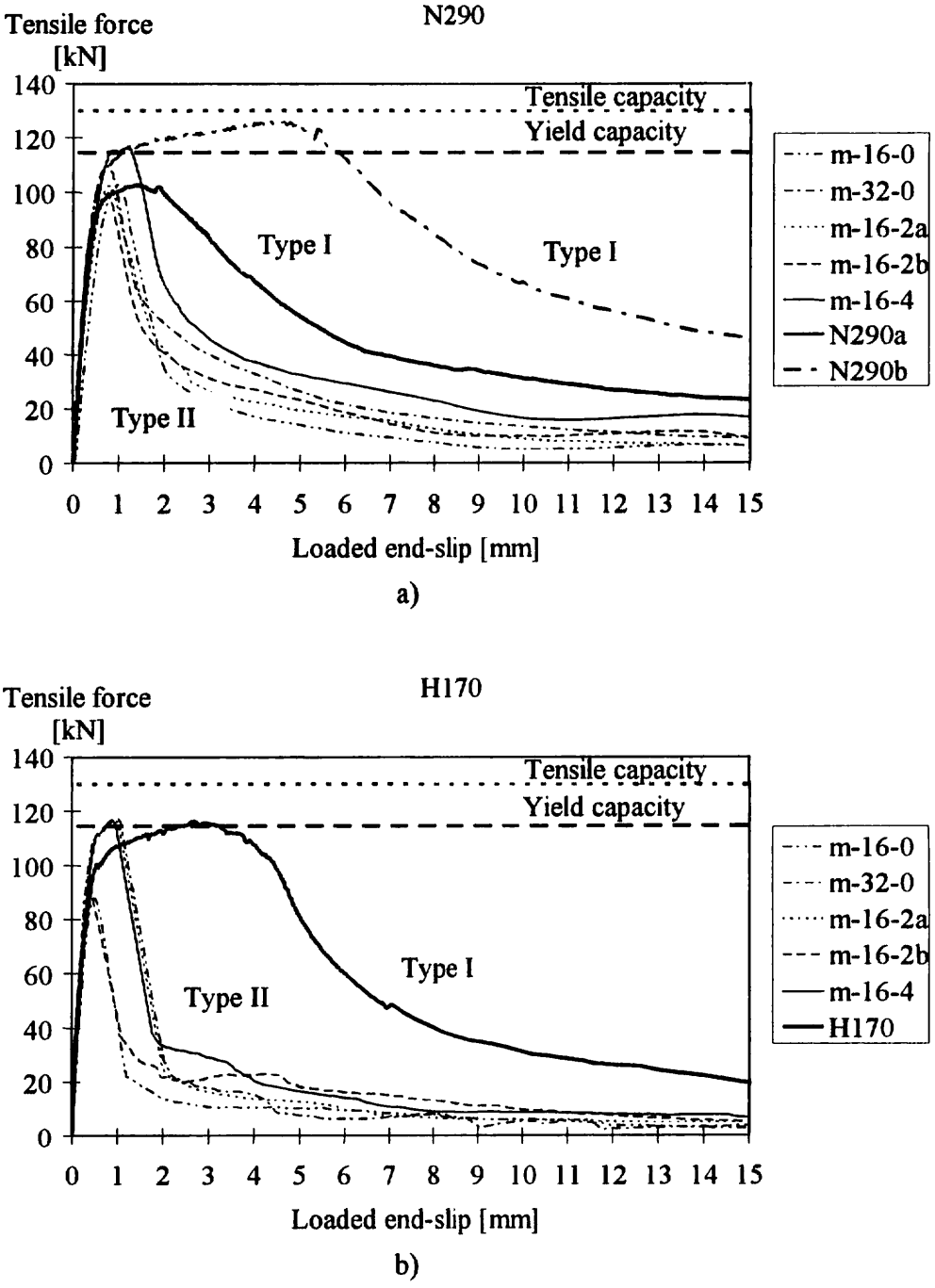

Fig. 2.3-6: Relationships between tensile force and end-slip from test specimens of type II (Fig.2.3-4) in comparison with that in well-confined concrete (type I) (Fig. 2.3-1); (a) normal-strength concrete; (b) high-strength concrete; according to Engström et al. (1998). Legend: m = mid position at edge; first number = cover in [mm]; second number = number of stirrups

Copyright fib, all rights reserved. This PDF copy of fib Bulletin 10 is intended for use and/or distribution only by National Member Groups of fib.

The tests showed that the reduced confinement had no essential influence on the anchorage capacity in the specimens of normal-strength concrete. When the concrete cover on one side of the bar was only 16 mm (one bar diameter) without stirrups or with two stirrups (ϕ6 mm) along the anchorage length, the anchorage capacity was reduced by about 10% compared to the average capacity in well confined concrete. When four stirrups (ϕ6 mm) were placed in a 16-mm concrete cover, or when the concrete cover was twice as large but without stirrups, the anchorage capacity was about the same as in well confined concrete.

The high-strength concrete specimens seemed to be more sensitive to a reduction of the confinement. Here a reduction of the concrete cover to 16 mm resulted in a reduction of the maximum load of about 25 - 30%. When two stirrups were provided, there was no increased capacity in one test, but a considerable increase in a twin test. However, four stirrups (ϕ6 mm) along the transfer length, or an increased concrete cover to 32 mm without stirrups, resulted in about the same anchorage capacity as in the reference test. Hence, compared to the case with smallest confinement, the effect of either an increased concrete cover or an increased amount of transverse reinforcement seemed to be similar in high-strength and in normal-strength concrete.

In the type III specimens, with two main bars placed in the corner regions (Fig. 2.3-4), the crack development was similar to that of the type II specimens. Longitudinal splitting cracks developed along the anchored bars as well as transverse cracks. The latter were inclined towards the loaded end of the bar, but in this case on both sides of the loaded corner region. In a late state, the transverse cracks from the two adjacent corner regions joined each other to a combined system of cracks (Fig. 2.3-7). The crack pattern was similar in specimens of high-strength and normal-strength concrete.

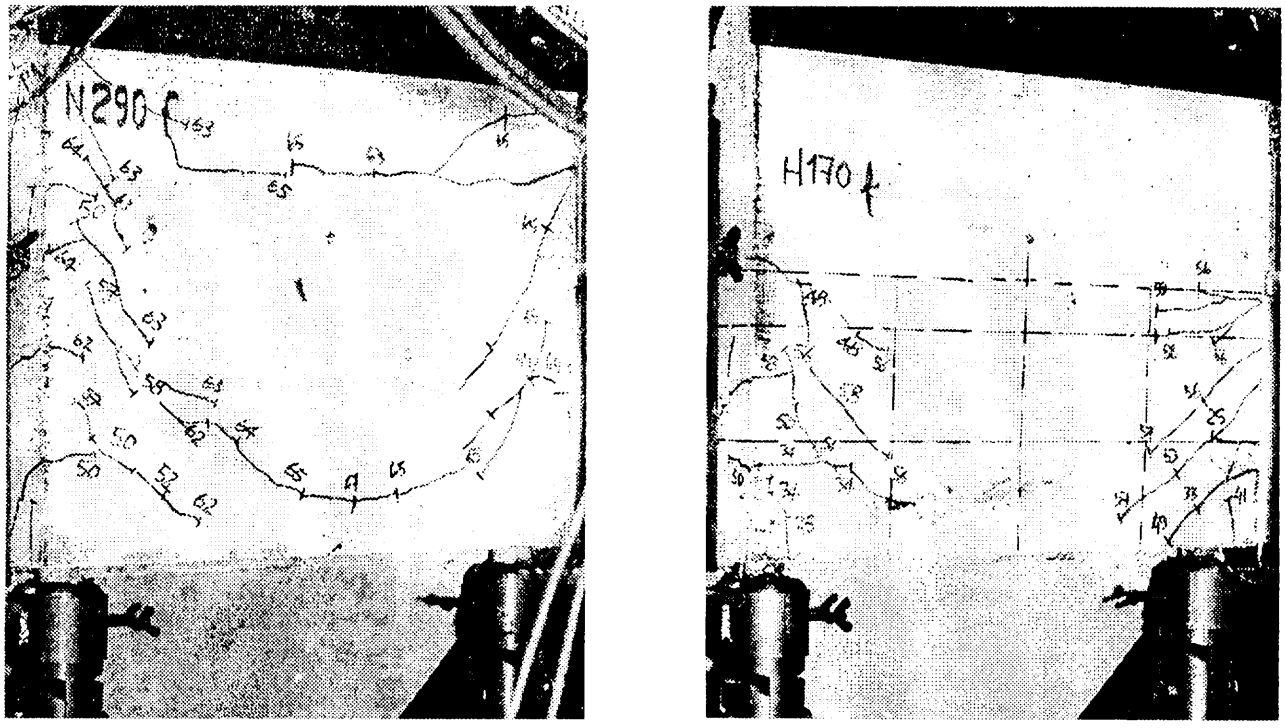

Fig. 2.3-7: Typical crack pattern in test specimens of type III (Fig. 2.3-4); (left) normal-strength concrete; (right) high-strength concrete; according to Engström et al. (1998).

The anchorage capacity was substantially reduced when the bar was anchored in a corner region compared with anchorage in well-confined concrete, as well as in a mid position with small concrete cover (type II). At maximum load there was an abrupt anchorage failure, normally associated with a sudden drop of the tensile force, and the corner regions fell apart successively when the bars were forced

Copyright fib, all rights reserved. This PDF copy of fib Bulletin 10 is intended for use and/or distribution only by National Member Groups of fib.

to slip further. However, in specimens with stirrups the residual capacity in the post-peak stage was much higher than in the comparable tests of type II. This was especially true in case of the higher amount of transverse reinforcement. The different behaviours in the post-peak stage appear from the relationships between tensile force and end-slip presented in Fig. 2.3-8 a-b.

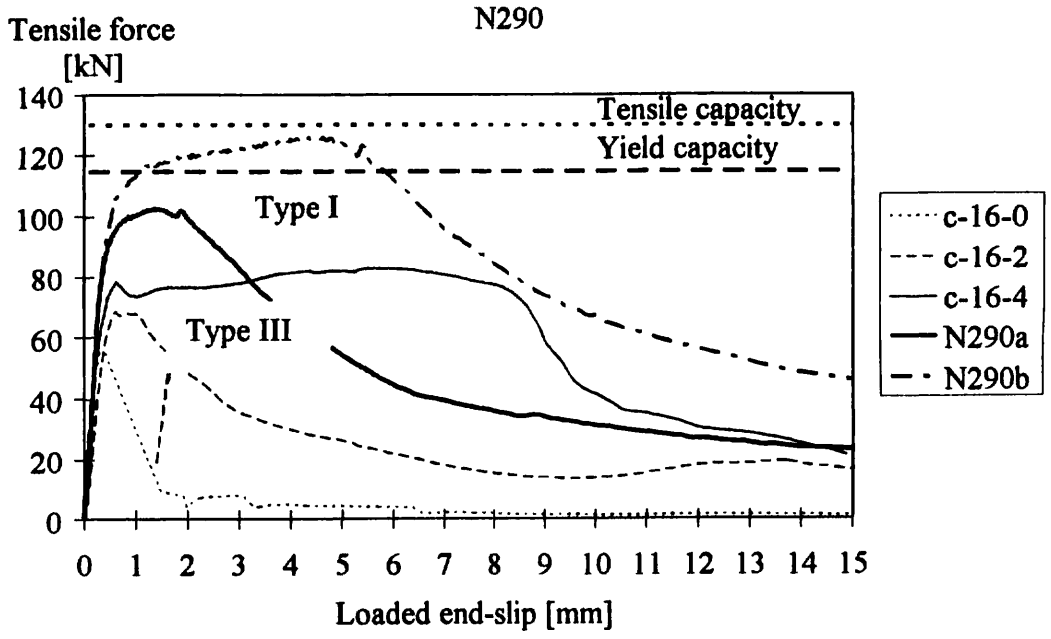

a)

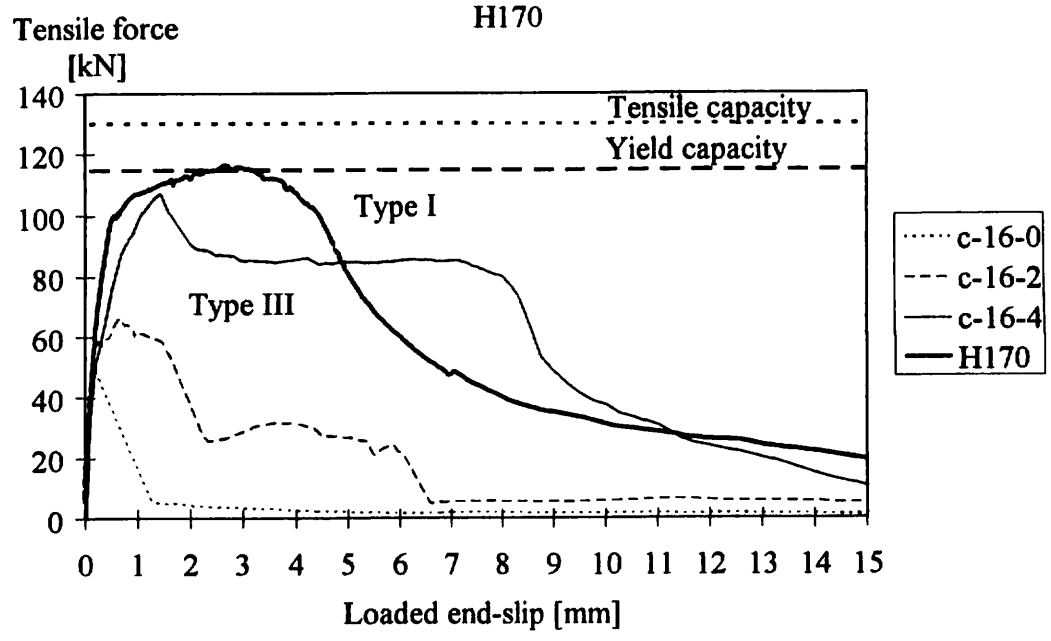

b)

Fig. 2.3-8: Relationships between tensile force and end-slip from anchorage in corner regions (type III) (Fig. 2.3-4) in comparison with that in well-confined concrete (type I) (Fig. 2.3-1); (a) normal-strength concrete; (b) high-strength concrete; according to Engström et al. (1998). Legend: c = corner position; first number = cover in [mm]; second number = number of stirrups.

Copyright fib, all rights reserved. This PDF copy of fib Bulletin 10 is intended for use and/or distribution only by National Member Groups of fib.

Hence, the transverse reinforcement seemed to have a more positive influence on the anchorage in a corner region than in a middle position. One explanation could be the better confinement from stirrups in the corner where two stirrup legs meet and the different splitting crack development around anchored bars close to the corners (see also Fig. 1.1-12). However, the results showed that the anchorage capacity was considerably reduced when the bar was anchored in a corner region compared to anchorage in confined concrete. For specimens without transverse reinforcement, the reduction was about 55% in normal-strength concrete and even larger in high-strength concrete (about 60 - 75%).

In each specimen it was possible to determine the anchorage capacity of each corner bar individually. It is noticeable that the difference between the two anchorage capacities in the plain concrete specimens was small in normal-strength concrete, but fairly large in high-strength concrete specimens. This indicates that the possibility for force redistribution is smaller in high-strength concrete. This has also been observed by Ghassemi (1997). When 2 or 4 stirrups were provided, the two anchorage capacities in one specimen were always close to each other in normal-strength concrete as well as in high-strength concrete. This underlines the very strong influence of confinement on bond behaviour in split concrete.

The stirrups had a positive influence on the anchorage capacity, which increased with an increased amount of transverse reinforcement. However, the effect was moderate in normal-strength concrete specimens. With 4 transverse bars (ϕ6 mm), the anchorage capacity in normal-strength concrete was about 35 - 40 % smaller than in the reference test in well confined concrete. In high-strength concrete, the same amount of transverse reinforcement resulted in an anchorage capacity that was about 10 – 15 % smaller than in the reference test. However, it should be mentioned in the high-strength concrete specimens the anchorage length was smaller and hence, the 4 stirrups were more closely spaced. This indicates that not only the number of transverse bars is of importance, but especially the stirrup percentage that can be defined by the stirrup index of confinement (see Section 1.4.3).

It was found that the bond model in CEB-FIP Model Code 90 [CEB-FIP (1993)] was in reasonable good agreement with the observations from specimens of type II and III, when unconfined concrete was presumed. The model seemed to be applicable also to high-strength concrete, which means that the maximum bond strength was calculated as $\tau_{b,max} = 2.5(f_{ck})^{1/2}$, in contradiction to the results found for anchorage in well confined concrete, see Section 2.2.1.

2.3.2 Anchorage behaviour and anchorage capacity in anchorage regions

In flexural members the following types of main anchorage regions are found:

- Region at an end support with support pressure
- Region at a suspended end (no support pressure)
- Region where the bars are cut off in the span (top or bottom bars)

In practical design, the anchorage region at end supports is very often a problem. Due to the successive development of inclined cracks in the shear span (at the ultimate state), a considerable tensile force must be resisted in the sections very close to the support (Fig. 2.3-9). With the successive cracking in the shear span, the critical section moves towards the edge of the support when the load increases. For this reason, the design rules for reinforced concrete members prescribe that inclined cracks must be assumed to reach the edge of the support and that the anchorage region should be designed accordingly. Very often special solutions with a complicated detailing are required to secure the anchorage capacity within the limited area above and behind the support length. In the regions with cut-off points in the span, the situation is less critical, since it is easier to solve the anchorage problem by extending the cut reinforcement bars.

Copyright fib, all rights reserved. This PDF copy of fib Bulletin 10 is intended for use and/or distribution only by National Member Groups of fib.

Because of the experimental difficulties, the anchorages at end supports have not been studied very much in the past. On the other hand, the behaviour and capacity of lap splices have been subjected to extensive research. The splices have often been placed in heavily loaded regions like sections of maximum moments.

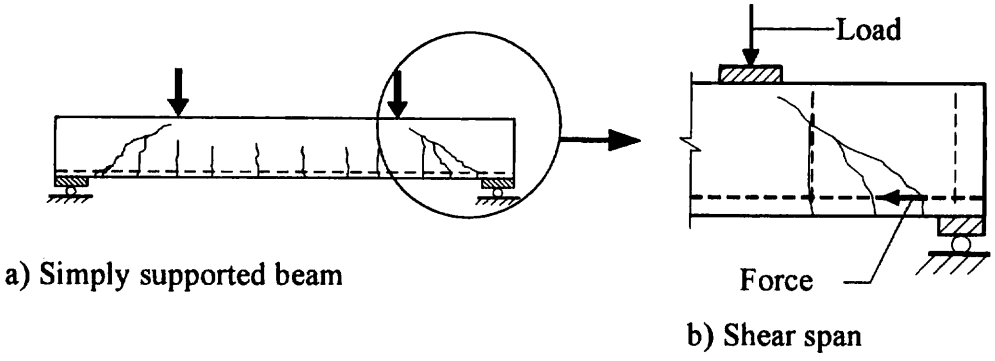

Fig. 2.3-9: The anchorage at an end support depends on the development of shear cracks in the shear span; from Magnusson (1997).

In order to simulate the design situation indicated in Fig. 2.3-9 and study the anchorage behaviour in this type of anchorage regions, several tests have been carried out recently, [Trebeschi (1996)], [Ghassemi (1997)], [Magnusson (1997)], [Durán (1998)]. The aim of these tests was first to study the anchorage behaviour and capacity in high-strength concrete. However, for each specimen in high-strength concrete, a similar companion specimen in normal-strength concrete was also tested as a reference. The compressive strength was about 30 MPa for the normal-strength and about 100 MPa for the high-strength concrete specimens. Two types of specimens were adopted. In the first type, two or three ribbed bars K500 (f_{yk} = 500 MPa) or Ks60 (f_{yk} = 620 MPa) with a diameter of 16 mm were anchored in a specially-designed concrete specimen that simulated the end region of a beam after the formation of a critical shear crack (Fig. 2.3-10). The concrete cover was 1,0ϕ or 1,5ϕ. This "beam-end" was connected to a steel structural member in such a way that the anchorage force could be produced by transverse loading. In this specimen the anchorage zone was well defined by the geometry of the test specimen. Both directly supported and indirectly supported (suspended) anchorage regions were tested.

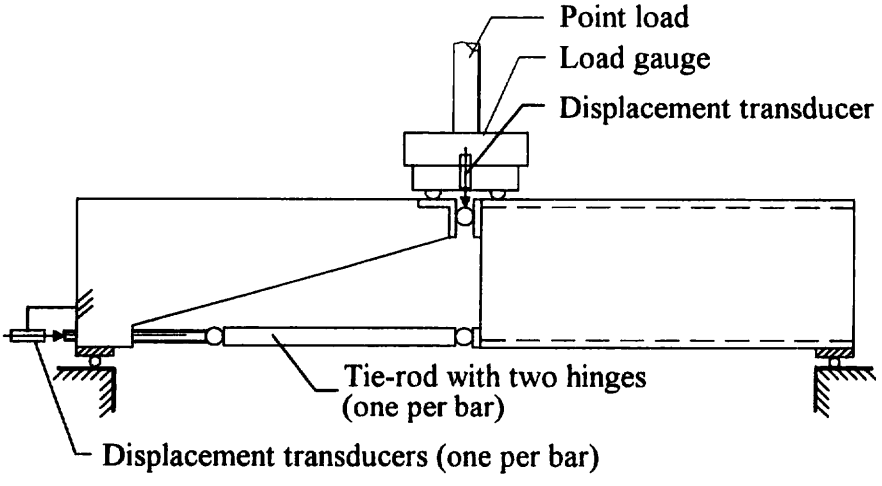

Fig. 2.3-10: Test arrangement of anchorage tests in idealised beam-ends, according to Ghassemi (1997) and Magnusson (1997).

In the second type of tests the anchorages were inside simply supported beams loaded by two concentrated forces that were arranged symmetrically, with a shear span of two times the effective depth (Fig. 2.3-11). In this case the anchorage behaviour and the anchorage capacity depend on the crack

Copyright fib, all rights reserved. This PDF copy of fib Bulletin 10 is intended for use and/or distribution only by National Member Groups of fib.

development in each specific beam. In this way the tests were more realistic, but the analysis of the results was definitely more difficult. The width of the section was 200 mm and the depth was 240 or 340 mm. The main reinforcement consisted of three or four ϕ20 mm ribbed bars of type K500 (f_{yk} = 500 MPa). The detailing (stirrups in the shear span, stirrups in the support regions, support length, concrete cover and the arrangement of the main bars) varied. The concrete cover was 1,0ϕ or 1,5ϕ. In most of the beam tests all main bars were retained to the support, but in some tests two of four bars were cut off in the shear span.

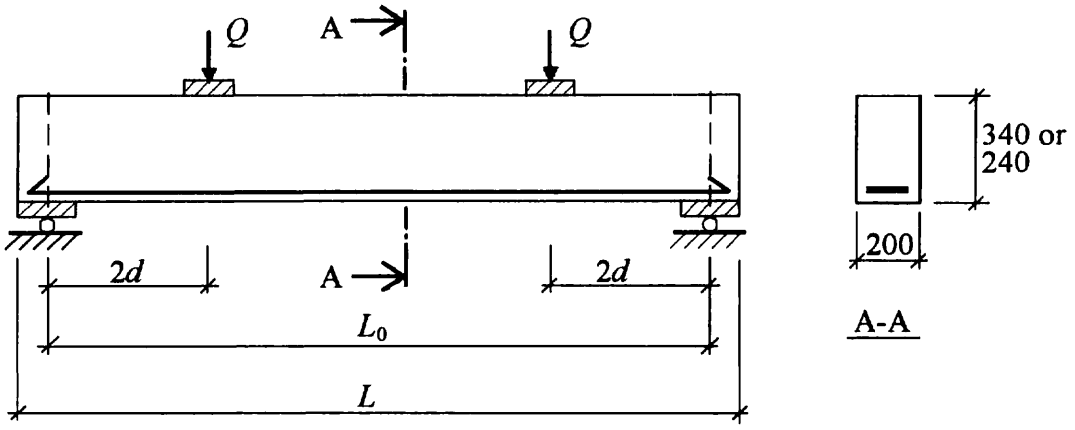

Fig. 2.3-11: Test arrangement in beam tests with the anchorages at the end supports, according to Trebeschi (1996), Magnusson (1997), and Durán (1998).

In the beam tests, a pronounced inclined shear crack near the edge of the support was identified as the final critical crack with regard to the anchorage capacity. It was assumed that even if the tensile force in the main steel was partly anchored in the span outside this crack, an anchorage failure occurred in the support region when the tensile force in the critical crack reached a critical value. Strain gauges along the embedded bars made it possible to estimate the tensile force in the longitudinal bars during the test.

The anchorage capacity was evaluated as the maximum value of the total tensile force in the steel bars where they were crossed by the critical crack. In general the anchorage capacity in both normal-strength and high-strength concrete beams was much larger than predicted by the usual design models (with no safety coefficients). For this reason, no anchorage failures were obtained in the first series of the high-strength concrete beams, but the beam resistance was determined by flexural failure. In order to induce anchorage failure in the high-strength concrete beams with 3 or 4 bars (ϕ20 mm) anchored over the support, it was in general necessary to reduce (a) the support length to about 75 mm, (b) the concrete cover to about one time the bar diameter, and (c) the number of the stirrups in the support region to one ϕ6 mm stirrup. With these changes, most of the beams in high-strength concrete failed owing to anchorage collapse at the end support.

The tensile force in the longitudinal bars near the support region was evaluated continuously during the test, together with the end-slip of the bars at the free (passive) end of the anchorage region. It was found that the tensile force increased drastically at the onset of diagonal cracking in the shear span. Before this event, the anchorage at the end support was hardly strained at all. After shear cracking, the tensile force was smaller in the beams with a greater number of stirrups in the shear span. The development of the flexural and shear cracks in the shear span and the general behaviour of the beam were quite similar in both high-strength and normal-strength concrete beams. However, the crack occurrence was considerably delayed in high-strength concrete.

Most of the anchorage failures, both in high-strength and normal-strength concrete beams, started with the development of radial and longitudinal cracks around the main bars in the anchorage region. Often, more than one longitudinal crack radiated from the bar and became visible at the end face of the beam.

Copyright fib, all rights reserved. This PDF copy of fib Bulletin 10 is intended for use and/or distribution only by National Member Groups of fib.

Some typical crack patterns at the end face after anchorage failure are shown in Fig. 2.3-12. However, in spite of these cracks, the anchorage zone was still confined by the pressure from the support and by the stirrups in the support region, and it was possible to obtain a rather ductile pull-out failure, with a substantial residual capacity remaining after the peak load. Nevertheless, the pull-out resistance was reduced by the occurrence of the longitudinal splitting cracks. The failure mode, here referred to as a "splitting-induced pull-out failure", was quite similar in high-strength and normal-strength concrete beams. The anchorage failure was always preceded by a notable end-slip development at the unloaded end of the anchorage.

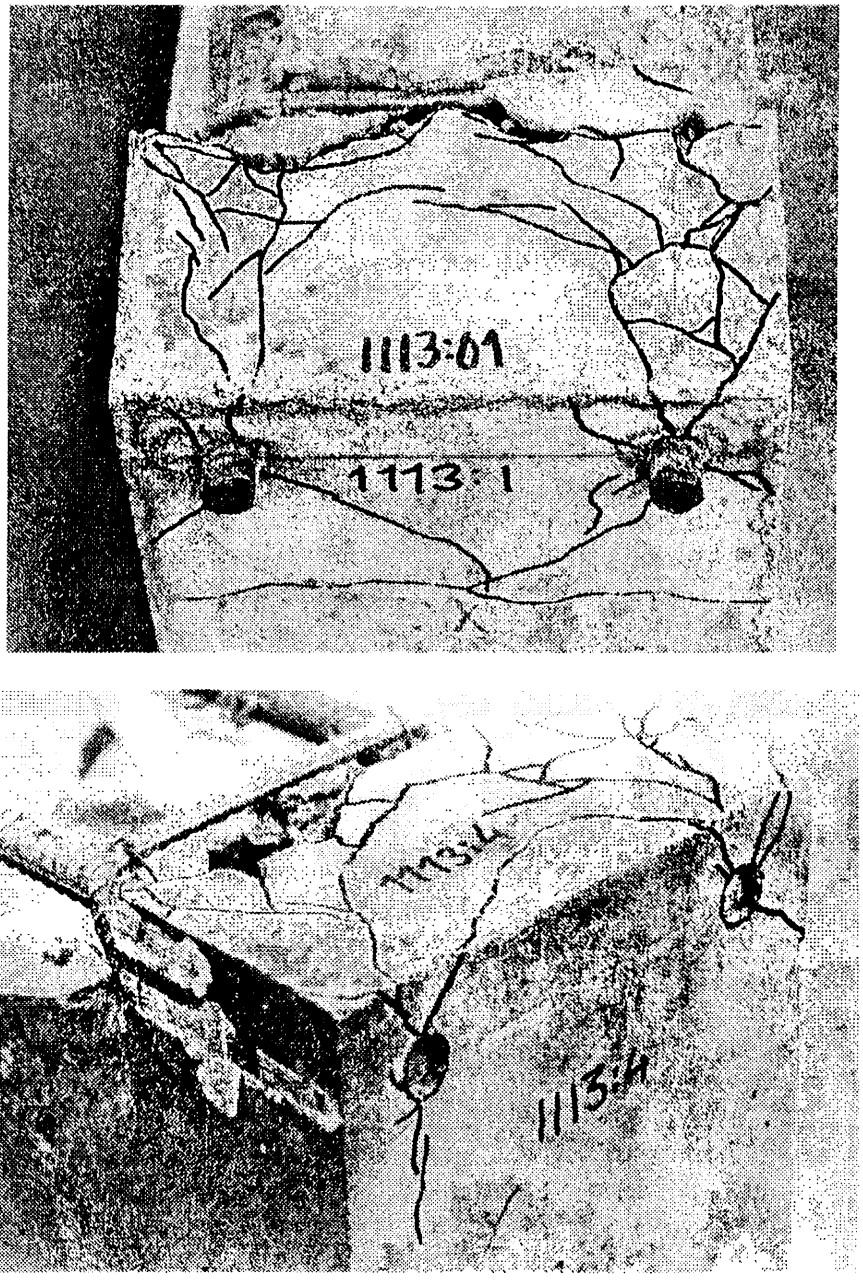

Fig. 2.3-12: Beam-end specimens (Fig. 2.3-10) at failure: typical crack patterns at the end face of tested beams in case of splitting-induced pull-out failure; (top) normal-strength concrete beam; (bottom) high-strength concrete beam; according to Magnusson (1997).

At anchorage failure, when the maximum tensile force was reached, the unloaded end-slip was close to 0,3 - 0,6 mm, with the smaller values in high-strength concrete. Typical load-end-slip relationships (splitting-induced pull-out failures) are presented in Fig. 2.3-13. The figure shows that the tensile force

Copyright fib, all rights reserved. This PDF copy of fib Bulletin 10 is intended for use and/or distribution only by National Member Groups of fib.

decreased more rapidly after the peak value in high-strength concrete beams. This was also found when comparing other similar tests on high-strength and normal-strength concrete specimens. However, for both types of concrete, the residual capacity was still considerable.

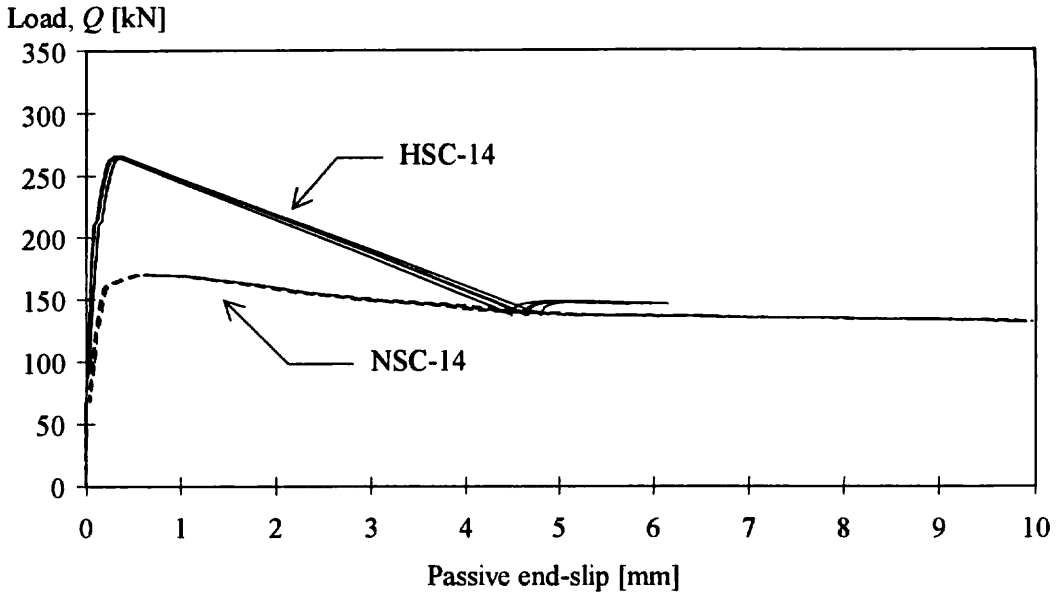

Fig. 2.3-13: Typical load-slip relationships at the unloaded end of the anchorage region in case of splitting-induced pull-out failures in high-strength and normal-strength concrete beams (same detailing); beam test (Fig. 2.3-1); [Magnusson (1997)]

Some of the high-strength concrete beams exhibited a very brittle anchorage failure, where the concrete cover in the anchorage region split away abruptly and no residual capacity remained. All these beams had a very small amount of stirrups in the anchorage region or no stirrups at all. Such a brittle failure mode is exemplified in Fig. 2.3-14, which shows an anchorage region after failure for a beam with only one stirrup $\phi 6$ mm in the anchorage region. The companion beam in normal-strength concrete, also shown in the figure, obtained a ductile anchorage failure (splitting induced pull-out failure) in spite of the small amount of stirrups in the anchorage region. The corresponding load-end slip relationships for the two beams are shown in Fig. 2.3-15. It was also found that this type of brittle failure sometimes occurred after some yielding of the main longitudinal bars. Therefore, in order to avoid brittle failures, it is not sufficient to resist just the yield capacity of the bars, but the anchorage regions must be designed and detailed to resist both yield penetration and steel stresses above the yield strength. Then a proper combination of anchorage length and confining stirrups is needed. Similar observations were made also by Azizinamini et al. (1993a, 1995) in a series of tests on lapped tensile splices (see Section 2.3.3).

The authors found that, for the actual dimension of the main bars ($\phi 20$ mm), even a very small amount of transverse reinforcement in the support regions together with the support pressure could prevent brittle failure of the anchorage and make the more ductile "splitting-induced pull-out failure" possible. In several cases, but not always, even as little as one stirrup $\phi 6$ mm was sufficient for an anchorage length of only 75 mm.

The effect of the support pressure was examined in some of the tests of the first type, with the idealised beam-ends [Ghassemi (1996), [Magnusson (1997)], see Fig. 2.3-10. Anchorage regions with 2 or 3 main bars, $\phi 20$ K500 (f_{yk} = 500 MPa), were either supported directly on a 100 mm wide bearing or indirectly by suspension at the ends by vertical stirrups. The concrete cover to the main bars was equal to the main bar diameter and the anchorage length was the same as the support length.

Copyright fib, all rights reserved. This PDF copy of fib Bulletin 10 is intended for use and/or distribution only by National Member Groups of fib.

In the case of indirect support, the beam end was hinged to the loading frame in the upper part of the end region. Then the beam end was provided with a transverse, circular recess in the top. A steel cylinder was placed through this recess to connect the beam to the loading frame. The anchorage zone, of the longitudinal bars, was encased by vertical stirrups designed to suspend the expected reaction force to the hinged connection in the top. For the specimen of normal-strength concrete, 2 stirrups (ϕ6 mm K500) were used as suspension ties, while the high-strength concrete specimen had 2 stirrups ϕ8 K500. The companion beams with direct support were provided with the same amount of stirrups in the anchorage region, which means that the only difference between comparable beams was the pressure from the support underneath.

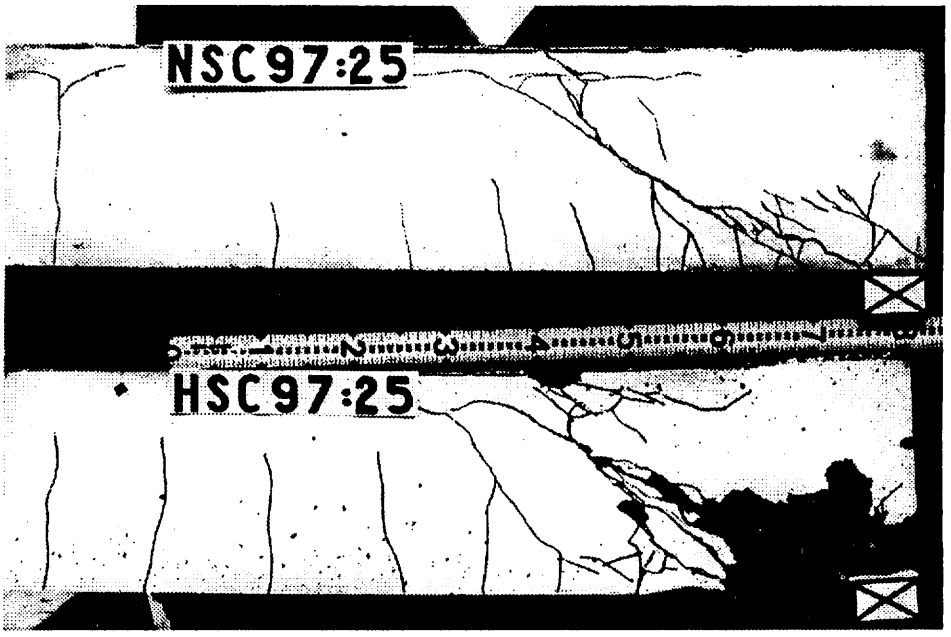

Fig. 2.3-14: (bottom) typical example of a brittle splitting failure in a high-strength concrete beam (Fig. 2.3-11) with only one stirrup ϕ 6 mm in the anchorage region; (top) the companion beam in normal-strength concrete obtained a ductile type of anchorage failure (splitting induced pull-out failure); [Magnusson (1997)]

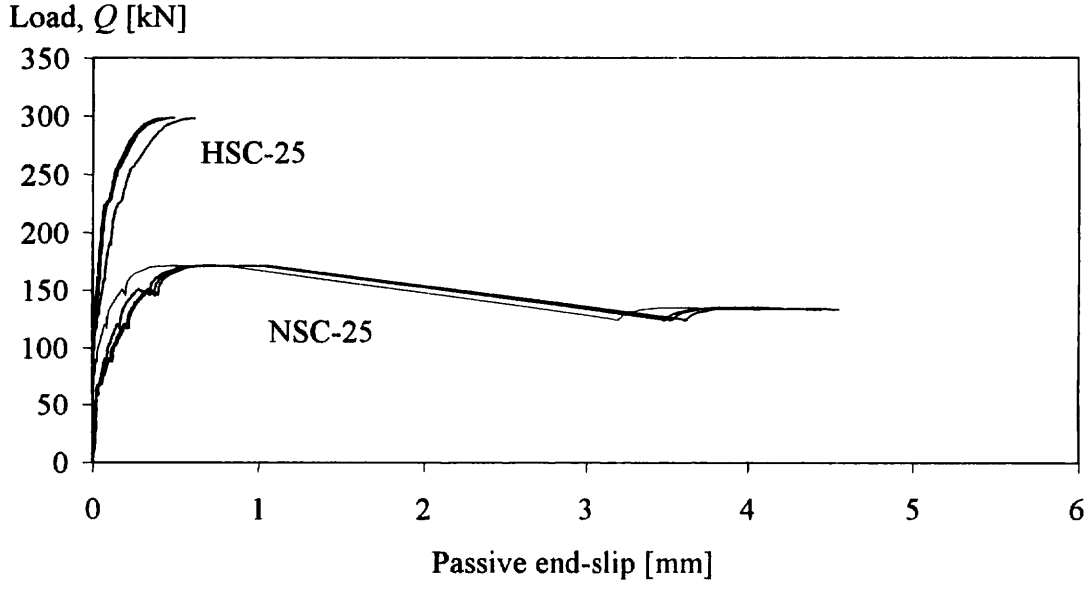

Fig. 2.3-15: Load-slip relationships at the unloaded end of the anchorage region for the companion beams shown in Fig. 2.3-14. Only one stirrup ϕ6 mm was provided in the anchorage region) [Magnusson (1997)]

Copyright fib, all rights reserved. This PDF copy of fib Bulletin 10 is intended for use and/or distribution only by National Member Groups of fib.

Apart from the various support arrangements, the specimens had the same detailing. As expected, the anchorage capacity increased when the anchorage region was directly supported, and the increase was higher than predicted by the method given in CEB-FIP Model Code 90 [CEB-FIP (1993)]. The anchorage capacity was always higher in the high-strength concrete specimens, but the failure modes were the same. It was interesting to observe that the effect of the direct support was proportionally the same in high-strength concrete as in normal-strength concrete (see Table 2.3-2).

NSC $f_{cm} \approx 30$ MPa	N_{max} [kN]	$N_{max,n}$ [kN]	$\frac{N_{max,n(DS)}}{N_{max,n(IS)}}$	HSC $f_{cm} \approx 100$ MPa	N_{max} [kN]	$N_{max,n}$ [kN]	$\frac{N_{max,n(DS)}}{N_{max,n(IS)}}$
2 bars, DS	97,3	97,3	—	2 bars, DS	187,0	187,0	—
2 bars, IS	69,0	68,8	1,41	2 bars, IS	120,5	122,6	1,53
3 bars, DS	152,3	152,3	—	3 bars, DS	291,6	294,9	—
3 bars, IS	79,2	78,4	1,94	3 bars, IS	159,3	160,9	1,83

1) DS = direct support
IS = indirect support (suspended)
$N_{max,n(DS)}$ = The normalised anchorage capacities from the test with direct supports.
$N_{max,n(IS)}$ = The normalised anchorage capacities from the test with indirect supports.

Table 2.3-2: Influence of transverse pressure at the end supports: results from tests on beam-ends (Fig. 2.3-10) with direct or indirect support [Ghassemi (1996), Magnusson (1997)]

In the design of anchorage regions it is generally assumed that the anchorage capacities of the individual bars can be added. From Table 2.3-2 it appears that when the number of bars increased from two to three and the anchorage zone was directly supported, the anchorage capacity increased proportionally in both normal-strength and high-strength concrete. However, when the anchorage region was indirectly supported, there was an unfavourable interaction between the adjacent bars, and the anchorage capacity did not increase in proportion to the number of bars, in spite of the fact that the concrete covers were the same for all bars in the group. This means that a certain confinement is needed in order to avoid large splitting cracks and increase the anchorage capacity of all bars. In this respect, there was no significant difference between anchorage in high-strength and normal-strength concrete.

The tested beams with curtailed reinforcement showed a very advanced crack pattern and a complex anchorage behaviour. In general, it was not possible to obtain anchorage failure in the nodes with cut reinforcement, but anchorage failures occurred at the end supports or, alternatively, the failure was of flexural type. At first sight this may seem surprising, since the anchorage lengths were approximately the same in the two nodes, and the favourable effect of direct support was absent in the node with cut bars. However, due to compatibility conditions, the cut bars can not slip, relatively to the surrounding concrete, independently of the retained bars. This means that the force distribution between the cut and retained bars is statically indeterminate and, depending on the crack development, there will be a successive redistribution of forces. In this respect, there was no significant difference between beams in high-strength and normal-strength concrete. A typical crack pattern in the shear span of a high-strength concrete beam with curtailed reinforcement is shown in Fig. 2.3-16 together with that of the companion beam in normal-strength concrete. In this beam, two interior bars, in a total of four main bars in one layer, were cut off in the shear span.

The results from the tests on idealised beam-ends and simply supported beams showed that the anchorage capacity increased in high-strength concrete compared with normal-strength concrete. However, the crack development and the failure modes were generally the same. Hence, one may conclude that the anchorage behaviours in high-strength and normal-strength concrete are governed by

Copyright fib, all rights reserved. This PDF copy of fib Bulletin 10 is intended for use and/or distribution only by National Member Groups of fib.

the same basic parameters. In some cases, where the confinement provided by the stirrups was limited, brittle anchorage failures occurred in high-strength concrete. This unfavourable failure mode should be prevented by providing sufficient confinement.

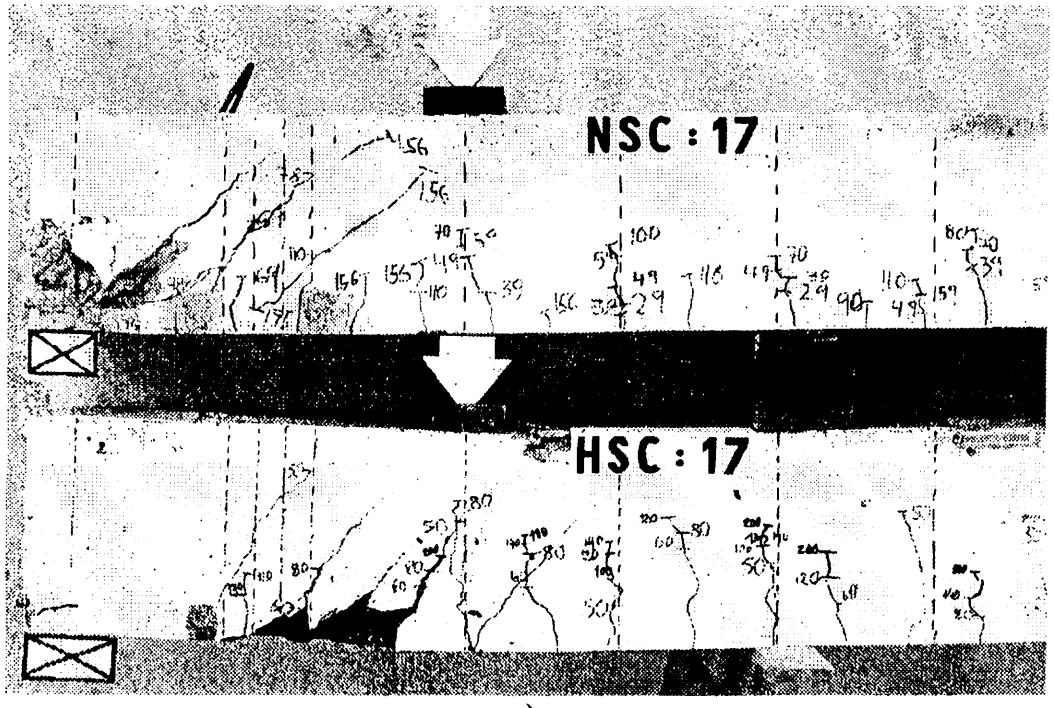

a)

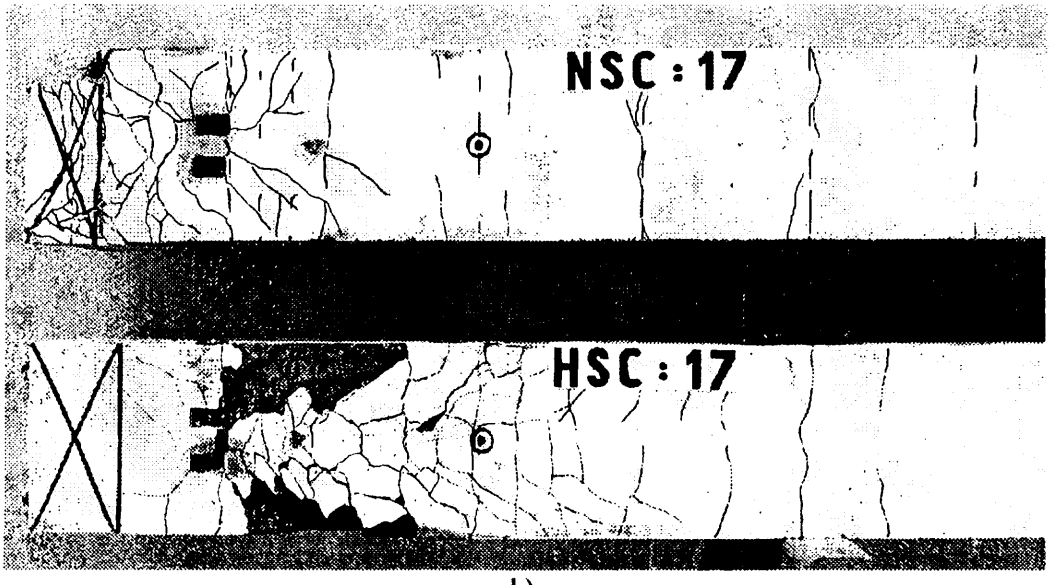

b)

Fig. 2.3-16: Typical crack patterns in the shear span of corresponding beams (Fig. 2.3-11) with curtailed reinforcement in normal-strength and high-strength concrete, according to Magnusson (1997); beam in normal-strength concrete (NSC:17) with anchorage failure at the support and beam in high-strength concrete (HSC:17) with flexural failure after substantial cracking in the cut-off region; (a) side view; (b) bottom view.

Another general observation concerns the distribution of forces between the bars anchored in one group. In normal-strength concrete specimens, the total force in the anchored group was more uniformly distributed between the bars at the anchorage failure than in the high-strength concrete specimens. In the latter case, the difference between the individual forces could be quite considerable. It was assumed that the softer behaviour of normal-strength concrete, with more extensive microcracking, made a

Copyright fib, all rights reserved. This PDF copy of fib Bulletin 10 is intended for use and/or distribution only by National Member Groups of fib.

redistribution of the forces easier within the group of the anchored bars. On the other hand, it seems that, in the case of high-strength concrete, an anchorage failure can be initiated by a highly stressed area before the full resistance in all bars was reached. This is an unfavourable effect of high-strength concrete and should be considered in the design of anchorage regions. Also in this respect, confining reinforcement would be beneficial.

2.3.3 Behaviour and capacity of lap splices in structural members

The ACI Building Codes 318-89 and 318-95 [ACI Committee 318 (1989) and (1995)] stipulate an upper limit to the concrete compressive strength that may be utilised in the design of lap splices and anchorage regions (development lengths). This limit is prescribed to 69 MPa. The reason for this limit is the lack of relevant test results from high-strength concrete applications. Therefore the code writers have preferred a conservative approach. Still the basic design rules for lap splices and anchorage regions are mainly based on tests results obtained from tests with normal-strength concrete. Then the concrete compressive strength was typically less than about 35 MPa. In recent years several research projects have been initiated with the aim of studying the behaviour of lap splices in high-strength concrete beams.

A major study, including not less than 50 beam tests, has been reported by Azizinamini et al. (1998a). As a result of this study, an extension of the ACI Building Codes was finally proposed [Azizinamini (1998b)] and is briefly presented in Section 2.3.4. The investigation was divided in two phases. The aim of the first phase was to study and compare the behaviours of lap splices in normal-strength and high-strength concrete members [Azizinamini et al. (1993b)]. The second phase focused more on measures to obtain a ductile behaviour of lap splices in high-strength concrete beams, especially to find the appropriate combinations of lap splice lengths and amounts of transverse reinforcement (stirrups) over the splice length [Azizinamini et al. (1998a)]. Intermediate tests results and indicative recommendations for the design have been published continuously during the project [Azizinamini (1992); Azizinamini et al. (1993a) and (1995); Hatfield et al. (1996); Azizinamini (1998d)].

In the first phase two test series of totally 19 beam tests with lap splices in concrete of different strengths were carried out [Azizinamini et al. (1993b)]. The concrete compressive strength, evaluated from cylinder specimens, was about 35 - 40 MPa for the normal-strength concrete and about 75 - 100 MPa for the high-strength concrete specimens. The high-strength concrete used had water to cemetitious materials ratios ranging from 0,21 to 0,27. Two or three main bars were spliced in regions of constant negative bending moment. The aim was to study the anchorage behaviour under severe anchorage conditions. Since it was assumed that the bond resistance decreases with increased bar dimension and decreased concrete cover, it was decided to use large diameter bars (ϕ = 35 mm) of Grade 60, and place them with small concrete covers. Consequently, the side and top covers provided were only one times the bar diameter. The clear space between spliced bars was 92 mm (2,6ϕ). The splice length normally ranged between 610 and 1143 mm, corresponding to 17ϕ - 33ϕ. However, tests with splice lengths of 330 mm (9ϕ) or 2032 mm (58ϕ) were also included for comparison. None of the tests in this first phase were provided with transverse reinforcement over the splice length.

In all the specimens, the maximum load was determined by splitting failures. Inspection of the surface conditions of the reinforcement bars after failure showed signs of concrete crushing at the lugs in normal-strength concrete specimens, while the bar surfaces were clean without signs of concrete crushing in high-strength concrete.

It was found that the average bond stress at maximum load, normalised with respect to $\sqrt{f_{cm}}$, decreased with increasing compressive strength and this rate of decrease increased as the splice length increased. Furthermore, the normalised average bond stress at maximum load decreased with increased splice length. Two specimens in high-strength concrete were designed according to ACI Building Code 318-83

Copyright fib, all rights reserved. This PDF copy of fib Bulletin 10 is intended for use and/or distribution only by National Member Groups of fib.

[ACI Committee 318 (1983)] and ACI Code 318-89 [ACI Committee 318 (1989)] respectively, but without limitation of the concrete strength and using the nominal yield strength of the reinforcement steel. However, both beams exhibited very brittle failures of splitting type before yielding was reached. The steel stress at failure exceeded the nominal yield stress with approximately 15 %, but the actual yield strength was about 23% greater than the nominal value. In all the tests, the average bond stress at failure exceeded the value calculated according to ACI 318-89 with no limit for the concrete strength. However, the behaviour of the specimens at the ultimate stage was not desirable. The authors drew the conclusion that a removal of the current strength limitation could lead to a design of tension splices predestined to have a brittle failure. This would be in contradiction to ACI's general design philosophy of preventing brittle failure modes. They suggested that compensatory requirements should be added to secure a ductile type of failure.

Based on the observed behaviour in the high-strength concrete specimens, Azizinamini et al. (1993b) assumed that the bond stress distributions along the splices at failure were less uniform in high-strength concrete than in normal-strength concrete. This could be explained by higher bearing capacity by the lugs in high-strength concrete and by the fact that the splitting resistance, which is related to the concrete tensile strength, is not increasing in proportion to compressive strength. Hence, in high-strength concrete a splitting failure could be triggered more easily by highly loaded lugs, before a uniform bond stress distribution is obtained. The conclusion was that, especially for small concrete covers and little or no transverse reinforcement, increasing the splice length is not an appropriate measure to increase the capacity of the splice and may even be totally ineffective. Even if the yield stress of the spliced bars could be resisted by the lap splice, this is not sufficient as a brittle splitting failure might occur before sufficient ductility has been developed in the structural member. Azizinamini et al. (1993a) proposed that some minimum amount of transverse reinforcement should be provided over the spliced region to secure the participation of all lugs along the splice length before failure.

In the second phase of the research program [Azizinamini et al. (1998a)], the aim was to evaluate the bond performance of reinforcing bars in high-strength concrete and develop provisions for removal of the concrete strength limit in the ACI 318-89 Building Code. The research was directed towards the design of lap splices in high-strength concrete members to obtain a ductile structural behaviour, preventing premature brittle failures in the splice region. It was then of special interest to search for ideal combinations of splice length and transverse reinforcement over the splice region. Totally 70 beam specimens (including the 19 tests discussed previously [Azizinamini et al. (1993b)]) with tension lap splices were tested. Each specimen had two or three reinforcing bars, Grade 60, spliced in a region with constant negative bending moment. The parameters studied were: bar size (25,4 or 35 mm), splice length, rib pattern and geometry, concrete side and top covers (one or two times the bar diameter), amount of ϕ10 mm stirrups over the splice length, casting position, and concrete compressive strength. The clear spacing between reinforcing bars in the splice region was approximately two times the side cover. The transverse reinforcement consisted of stirrups (ϕ10 mm), with spacing ranging from 75 to 380 mm. For specimens with ϕ25,4 mm bars, the splice lengths were in the range of 254 - 1041 mm, corresponding to 10ϕ - 41ϕ. For specimens with ϕ35 mm bars, the splice lengths varied between 330 - 2032 mm, corresponding to 9ϕ - 58ϕ. The high-strength concrete had a compressive strength ranging from 74,7 to 113 MPa. For the high-strength concrete used, the water to cementitious materials ratio ranged from 0,21 to 0,27.

The splice lengths used in the tests were basically determined by the prescribed method in ACI 318-95 [ACI Committee 318 (1995)], but without applying the limitation of the concrete compressive strength. In order to improve splice behaviour two approaches were used. Either the splice length was increased with no transverse reinforcement, or the calculated splice length was kept or even reduced, but with various amount of transverse reinforcement over the splice length. For the specimens with stirrups, displacement control was used for testing. A displacement ductility index was used as an index to evaluate the test results.

Copyright fib, all rights reserved. This PDF copy of fib Bulletin 10 is intended for use and/or distribution only by National Member Groups of fib.

Even if the average bond stress at failure exceeded the average bond stress assumed in the building code, brittle types of splitting failures were observed before yielding was reached. The failure mode for specimens, which did not include any stirrups over the splice region, was very brittle and violent, even in the case of longer splice lengths. However, the presence of a minimum amount of transverse reinforcement resulted in a significant increase in ductility. For specimens with stirrups over the splice region, it was found that the strains in the stirrups were quite non-uniform along the splice length, especially near failure. This was especially true for specimens with long splice lengths, in which the outermost stirrups were strained much more than the interior ones.

The observed effect of transverse reinforcement over the splice region on the splice behaviour was similar for specimens with ϕ25,4 or ϕ35 mm bars and with concrete cover thickness of one or two times the bar diameter. The amount of stirrups that in the tests ensured a ductile behaviour is presented in Table 2.3-3 for various bar dimensions, concrete covers and splice lengths [Azizinamini et al. (1998a)].

Number of spliced bars	Bar dimension [mm]	Concrete cover	Splice length [mm]	Sufficient stirrup amount	Insufficient stirrup amount
3	35	1ϕ	1020	ϕ10 *s*127	no information
			1140	ϕ10 *s*203	ϕ10 *s*305
			1460	ϕ10 *s*305	ϕ6 *s*254
2	35	2ϕ	508	ϕ10 *s*64	ϕ10 *s*114
			610	ϕ10 *s*64	ϕ10 *s*127
			710	ϕ10 *s*305	no information
2	25	1ϕ	635	ϕ10 *s*203	no information
			812	ϕ10 *s*381	no information
2	25	2ϕ	381	ϕ10 *s*76	ϕ10 *s*114
			483	ϕ10 *s*165	no information

Table 2.3-3: Amount of stirrups that assured an adequate level of ductility in tests on lap splices in high-strength concrete members reported by Azizinamini et al. (1998a).

For the specimens with splices of the smaller bar dimension (ϕ25 mm) and no transverse reinforcement, the behaviour was improved by increasing the splice length. Nevertheless, even when an adequate level of ductility was demonstrated, the specimens eventually failed violently by splitting of the concrete cover over the splice region. The behaviour also demonstrated larger variation compared to specimens with stirrups.

On basis of the test results, Azizinamini et al. (1998a) drew the following conclusions: for lap splices in high-strength concrete a mechanism that could delay splitting of the concrete cover would be more effective in increasing the splice capacity. This mechanism could be provided by requiring some minimum amount of stirrups over the splice length. This is especially true in case of small concrete covers, for which an increase of the splice length is not an efficient measure. In order to obtain a ductile member response, a minimum amount of stirrups over the splice length seems to be required. Even in the case of larger concrete cover (two times the bar dimension) some minimum amount of stirrups over the splice length is needed. It was also concluded that the use of stirrups should be combined with some minimum splice length.

In addition, it was found that the specimens with 35 mm bars and concrete cover of one bar diameter provided the lowest ductility. However, with a proper combination of splice length and transverse reinforcement, these specimens were able to attain a displacement ductility of 2,7 at failure without splitting the concrete. This ductility factor was selected as target ductility, when evaluating proper

Copyright fib, all rights reserved. This PDF copy of fib Bulletin 10 is intended for use and/or distribution only by National Member Groups of fib.

combinations of splice length and transverse reinforcement for other tests. However, for each cross-section used, the actual target ductility was modified with regard to the actual reinforcement ratio of that section. The required quantity of transverse reinforcement was evaluated from the test results and expressed in relation to the total area nA_s of the spliced bars. It was found that the needed amount varied between $0{,}16nA_s$ and $0{,}80nA_s$ depending on the bar dimension, the concrete cover, and the splice length. For beams with a splice length determined according to ACI 318-95 Building Code for beams without transverse reinforcement and no limitation of the concrete strength utilised, the required quantity of transverse reinforcement varied between $0{,}20nA_s$ and $0{,}48nA_s$. On the basis of the experiences from the test series, a modification to ACI Code 318-95 was proposed [Azizinamini et al. (1998b)] (see Section 2.3.4.2). To be conservative, the value $0{,}5nA_s$ was proposed for the required amount of transverse reinforcement.

Hwang et al. (1994) presented a series of static tests on 8 beams with lap splices with or without stirrups over the splice length. The diameter of the spliced bars was 28,7 mm and the splice length was 300 mm (10ϕ). When present, the stirrups (ϕ10 mm) were spaced 100 mm. The side and top concrete covers to the main bars were one time the bar diameter, and the clear space between the spliced bars was two times the bar diameter. The concrete compressive strength was about 60 - 80 MPa. The tests focused on the effect of silica fume in concrete mixes with similar strengths (see Section 2.2.3.3). The average bond stress at maximum load was compared to predictions according to the empirical design equation in ACI 318-89. Among others, they found that the current strength limit in the codes appears to be unnecessary.

Another series of 10 beam tests with lap splices was reported by Hwang et al. (1996). The spliced bars had a diameter of 28,7 mm in all tests, but the splice length varied between 150, 200 and 300 mm. The side and top concrete covers to the main bars were 50 mm (1,7ϕ) and the clear space between the spliced bars was 85 mm (3ϕ). In most of the tests the splice was provided with stirrups (ϕ10 mm) with spacing of about 60 - 70 mm. The concrete compressive strength was about 50 - 70 MPa. Splitting failures were obtained in all tests. The average bond stress at maximum load was compared with various design equations. The tests showed that the confinement effect of concrete cover and transverse reinforcement was more effective than expected for the concrete strength used.

Sixteen beam specimens with lap splices were tested by Hamad and Itani (1998a) with the aim of studying the effect of silica fume, casting position, and superplasticizer dosage, but also to study the validity of the upper strength limit in the ACI Building Code 318-95. The spliced bars had a dimension of 25 mm and a splice length of 305 mm. No transverse reinforcement was provided over the splice region. The concrete side and bottom covers were 38 mm (1,5ϕ) and the clear spacing between spliced bars was 76 mm (3ϕ). The concrete compressive strength varied between 50 and 85 MPa. Among others the authors concluded that the concrete stress limit in the code is unnecessary, but its removal should be connected with some ductility requirement.

Esfahani and Rangan (1998b) presented the results from a series of 22 beam tests with lap splices in high-strength concrete. The concrete strength varied between 65 and 100 MPa. Two bar diameters were used 19,3 mm and 23,3 mm. The splice length varied between 200 and 550 mm. The test series concerned in first hand the influence of the bar arrangement in the section; i.e. various covers and clear spacing between spliced bars were used. No transverse reinforcement was provided over the splice length. The authors presented an analytical equation to determine the average bond stress at maximum load. The equation that considers the bond stress distribution is valid for both normal-strength concrete and high-strength concrete and is in good agreement with the test results.

Other tests on lap splices in high-strength concrete have been reported by Olsen (1990a) and (1990b), Hansen (1993), Hansen and Thorenfeldt (1996) and Christensen (1995). Olsen (1990b) concluded that the splice strength was strongly influenced by the fracture energy of concrete. Hansen and Thorenfeldt

Copyright fib, all rights reserved. This PDF copy of fib Bulletin 10 is intended for use and/or distribution only by National Member Groups of fib.

(1996) made detail tests on splices in both ordinary high-strength concrete and in high-strength lightweight-aggregate concrete.

Darwin et al. (1996) and (1998) made a statistical analysis of results from tests on anchorage regions and lap splices. The tests included 133 specimens without transverse reinforcement and 166 tests with confining transverse reinforcement over the anchorage/splice region. The results were used to formulate empirical design criteria that covers concrete strengths between 17 and 110 MPa.

2.3.4 Design of anchorage regions and lap splices

2.3.4.1 Design philosophy

The experience from anchorage in high-strength concrete members is still rather limited. For instance, the influence of direct support and transverse reinforcement, and the behaviour in the regions with cut bars have not been sufficiently investigated. Furthermore, anchorage in slabs and other members without stirrups has not been studied thoroughly. For the time being it seems necessary to adopt a rather conservative approach in the design of anchorage regions and lap splices in high-strength concrete members, and to take advantage of the available experience in normal-strength concrete.

It is evident from the last experiences of anchorage regions at end supports [Magnusson (1997)] and lap splices [Azizinamini et al. (1998a)] that very brittle and unpredictable splitting failures can occur when the confinement is insufficient. However, with a certain amount of confinement from stirrups and/or from a transverse pressure, it is possible to obtain a well controlled and ductile anchorage behaviour, where the anchorage resistance depends on the frictional resistance along the anchorage length in already split concrete. This failure mode has been described in Section 2.3.2 and is referred to as a "splitting induced pull-out failure".

In most applications, the anchored bars are placed with relatively small concrete covers and the design of the anchorage region must be based on the assumption that splitting cracks develop in the concrete covers. A certain confinement must be provided that prevents the splitting effects from provoking a global and brittle type of splitting failure. Basically the design of an anchorage region must include the following items:

a) selection of a confinement, by stirrups and/or transverse pressure, needed to prevent brittle splitting failures and allow the formation of a ductile type of "splitting induced pull-out failure".
b) selection of a bond resistance that represents the average bond stress possible to obtain in split concrete. This bond strength depends on the confinement provided.
c) selection of an adequate anchorage length that is needed to build up the required tensile capacity of the reinforcing bars.

It should be noted that even if the yield stress of the bars can be resisted, a brittle failure may occur before an adequate level of ductility is obtained in the structural member. Closely spaced stirrups over the anchorage regions have been an effective measure to obtain a well-controlled and ductile behaviour, not only for the anchorage regions but also for the structural member [Azizinamini et al. (1998a) and (1998b)]. It is obvious that this design concept allows certain flexibility. As long as a desired behaviour is controlled by a minimum amount of confinement, various combinations of splice length, confinement and bond strength are possible. This was shown by Azizinamini et al. (1998b), see Section 2.3.3. To some extent, it means that a short splice length can be compensated by an increased confinement and the opposite. However, it is most important to use appropriate combinations of bond strength and confinement and to adapt the anchorage length accordingly. In this respect, full information about possible combinations is not yet available.

Copyright fib, all rights reserved. This PDF copy of fib Bulletin 10 is intended for use and/or distribution only by National Member Groups of fib.

For the detailing rules of anchorage and lap regions in high-strength concrete, very little information is available. At present, it seems justified to have a conservative approach and provide transverse reinforcement that is able to balance the transverse splitting forces along the anchorage region. More research is needed to find the required transverse reinforcement in relation to the length of the anchorage region.

In the ultimate state, it must be expected that the reinforcement bars yield in critical cracks at the front of anchorage regions or splices. However, ductile member behaviour in the ultimate state means that plastic regions must form and develop. The extension of plastic regions is associated with yield penetration along the reinforcing bars from the critical crack into the anchorage zones. The yield penetration is caused by an increase of the steel stress above the yield strength in the critical crack. Consequently, to obtain ductile member behaviour, the anchorage regions should resist not only the yield stress of the reinforcing bars but an increased stress above yielding. However, as discussed in Section 2.2.1, the bond stress is strongly reduced when the steel yields. A possible design concept to obtain ductile member behaviour was proposed by Engström (1992). According to this concept, the required anchorage length is divided in an elastic and a plastic zone. In the elastic zone the reinforcing bar remains in the elastic stage, while in the plastic zone the steel stresses are above the yield strength. The first zone should be designed to resist the yield stress and ordinary methods can be used. The plastic zone should resist the stress increase above the yield stress and, for this zone, a reduced bond strength is applied.

Design with regard to bond and anchorage in high-strength concrete in seismic regions was discussed at the "Second Multilateral Meeting on Structural Performance of High-Strength Concrete in Seismic Regions" and was summarised by Azizinamini (1998c). The discussion covered design issues and research needs.

2.3.4.2 Design approaches

With regard to the risk of brittle splitting failures of anchorage regions in high-strength concrete members, a minimum amount of transverse reinforcement seems to be necessary. A conservative approach would be to assume that splitting cracks develop through the concrete cover in the anchorage region and design the transverse reinforcement to resist the total radial pressure from the bond action of the anchored bars. The radial pressure should be resisted in both the horizontal and the vertical direction. Assuming that the ratio between the internal radial pressure and the bond stress is equal to 1,0, the required transverse reinforcement is found as:

$$A_{st} = 0{,}5 \cdot nA_s \tag{2.3-1}$$

where n = number of anchored/spliced bars
A_s = cross-sectional area of one anchored bar

This assumption corresponds to the case when the bond forces act under an angle of 45° to the bar axis.

In the following some recent proposals for the design of anchorage regions and lap splices in high-strength concrete structural members are presented.

Modifications to ACI 318-95 [ACI Committee 318 (1995)] concerning tension development and lap splice provisions for high-strength concrete have been proposed by Azizinamini et al. (1998b). They claim that adequate ductility and bond resistance can be achieved by (a) using a minimum splice length, as defined by ACI 318-95 for beams without transverse reinforcement and no limitation of the concrete strength utilised, plus (b) a minimum quantity of transverse reinforcement over the tension

Copyright fib, all rights reserved. This PDF copy of fib Bulletin 10 is intended for use and/or distribution only by National Member Groups of fib.

development/lap splice length. This transverse reinforcement should cross the potential plane of splitting through the reinforcement being developed and have a total cross-sectional area A_{st} determined as

$$A_{st} = 0{,}5 \cdot nA_s \cdot \frac{f_c}{103} \tag{2.3-2}$$

where f_c = concrete compressive strength [MPa]

The stirrups should have a minimum dimension of 10 mm and a maximum spacing of 305 mm. A minimum of three stirrups should be provided and stirrups designed primarily with regard to shear and torsion may be utilised. The minimum dimension of stirrups was recommended, since fracture of stirrups was observed in tests with smaller stirrup dimension [Azizinamini et al. (1998a)].

The design approach in CEB-FIP Model Code 90 for anchorage regions is based on the assumption that the anchorage capacity is determined by pull-out failure in concrete with longitudinal splitting cracks, and that more dangerous failure modes are prevented by detailing rules [Eligehausen, Balázs (1993)]. With regard to the most recent experience, this design approach seems suitable also in the case of high-strength concrete.

The applicability of the design methods proposed in the Model Code 90 for both anchorage regions and lap splices was checked by using recent experimental results from both normal-strength and high-strength concrete [Magnusson (1997)]. For anchorage regions, the anchorage capacity was evaluated as the total force in the anchored group of bars in the section where the reinforcement was crossed by a critical crack near the support (Fig. 2.3-9). The predicted capacities of anchorage regions and lap splices were determined by the existing code expressions, but without safety coefficients, and by introducing the mean strength values, with no consideration of the minimum requirements (Figs. 2.3-17 and 2.3-18).

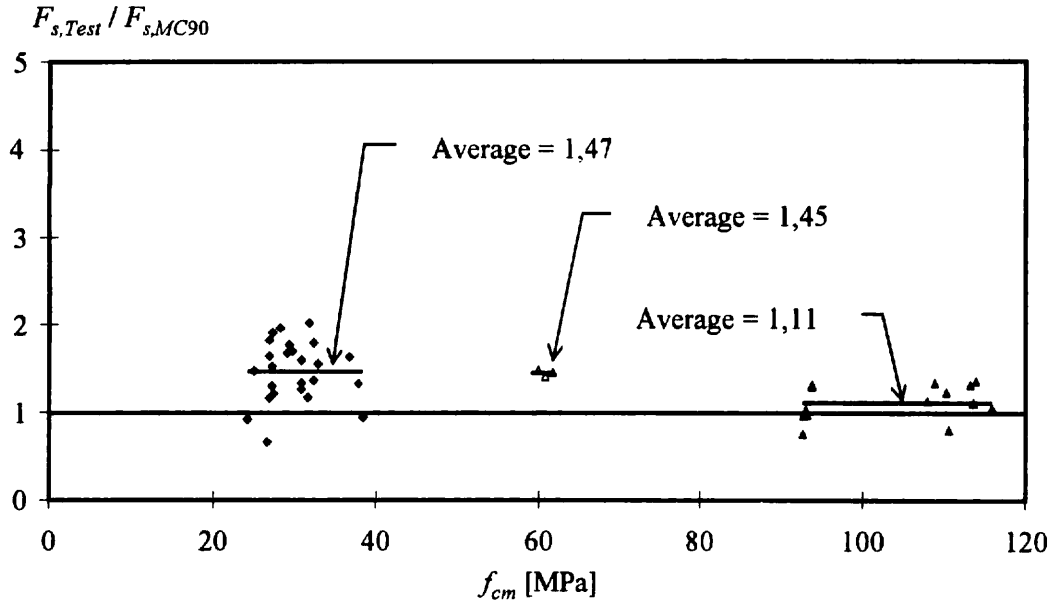

Fig. 2.3-17: Ratios between actual and predicted anchorage capacities of anchorage regions at end supports, as a function of the mean concrete compressive strength (from beam tests); predictions according to CEB-FIP Model Code 90 [CEB-FIP (1993)], according to Magnussson (1997).

The capacities of anchorage regions at end supports (Fig. 2.3-17) were evaluated from the beam tests presented in Section 2.3.2, [Magnusson (1997; Trebeschi (1998)]. The capacities of lap splices (Fig. 2.3-18) were evaluated from the tests by Tepfers (1973), Azizinamini et al. (1992, 1993a, 1993b, 1995,

Copyright fib, all rights reserved. This PDF copy of fib Bulletin 10 is intended for use and/or distribution only by National Member Groups of fib.

1996), Christensen (1995), Esfahani et al. (1996), Hwang et al, (1994, 1996) and Olsen (1990b). Only tests with anchorage failures were considered.

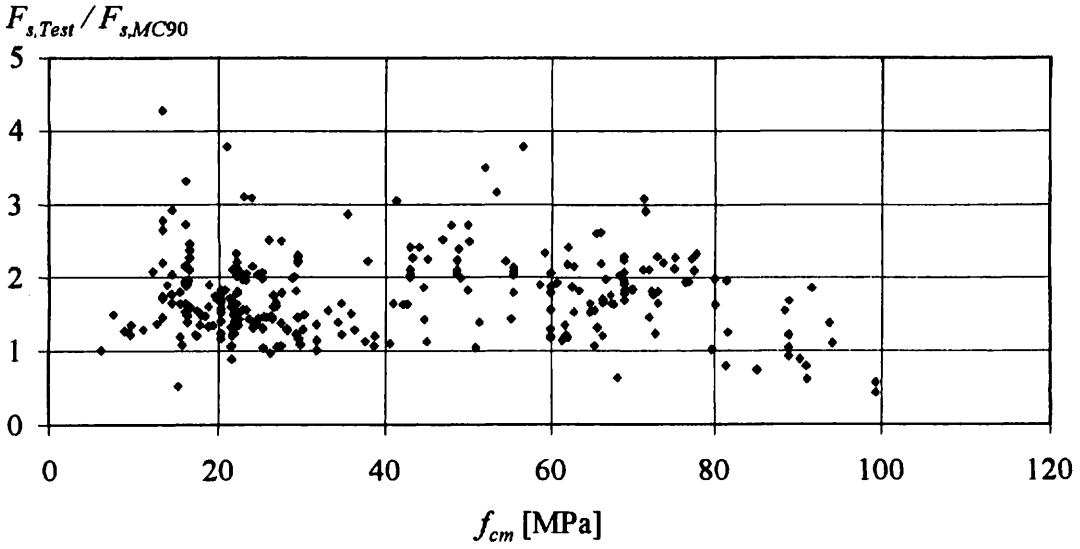

Fig. 2.3-18: Ratios between actual and predicted capacities of lap splices, as a function of the mean concrete compressive strength; predictions according to CEB-FIP Model Code 90 [CEB-FIP (1993)], according to Magnussson (1997).

If the safety coefficients and the minimum requirements are disregarded, the results of the code equations are generally on the safe side with regard to the test results. However, there was a tendency for the safety to decrease with increasing concrete strength, owing probably to the relatively smaller anchorage and splice capacities in high-strength concrete due to the limited stress redistribution compared to normal-strength concrete. This can be observed both in long anchorages and lap splices, as well as between bars anchored in the same region. This conclusion is also supported by the results from beam-end tests (Fig. 2.3-10) with either direct or indirect support (Table 2.3-4).

NSC	Normal-strength concrete			HSC	High-strength concrete		
$f_{cm} \approx 30$ MPa	$F_{s,test}$	$F_{s,MC90}$	Ratio	$f_{cm} \approx 100$ MPa	$F_{s,test}$	$F_{s,MC90}$	Ratio
Specimen	[kN]	[kN]		Specimen	[kN]	[kN]	
2 bars, DS	97,3	63,6	1,53	2 bars, DS	187,0	169,6	1,10
2 bars, IS	69,6	55,0	1,27	2 bars, IS	120,5	119,3	1,01
3 bars, DS	152,3	105,8	1,44	3 bars, DS	291,6	251,0	1,16
3 bars, IS	79,2	82,3	0,96	3 bars, IS	159,3	179,7	0,89

Table 2.3-4: Influence of different support conditions on the anchorage capacity in beam-end tests (Fig. 2.3-10), comparison between the test results, according to Ghassemi (1997) and CEB-FIP Model Code 90 [CEB-FIP (1993)]

In order to have roughly the same reliability for anchorage and lap splices in high-strength concrete as in normal-strength concrete, when the design methods of Model Code 90 are applied, it seems necessary to increase the required net anchorage and splice length by about 20% compared to the one determined by the expressions in the Code, but using the strength of the high-strength concrete. Furthermore, brittle anchorage failures, which have been observed in high-strength concrete members with low confinement, must be prevented by a sufficient amount of transverse reinforcement in the anchorage region.

On basis of the evaluation made by Magnusson (1997), recommendations for the design of anchorage regions and lap splices were introduced in a Swedish handbook for design of high performance concrete

Copyright fib, all rights reserved. This PDF copy of fib Bulletin 10 is intended for use and/or distribution only by National Member Groups of fib.

structures [Apleberger et al. (1998)]. In general the recommendations follow the methods and detailing rules given in CEB-FIP Model Code 90 [CEB-FIP (1993)], but in case of high-strength concrete the bond strength determined according to the code expressions is reduced by 20% and a minimum amount of transverse reinforcement is always required. The latter is not always the case for normal-strength concrete structures according to the existing Swedish Code [BBK 94 (1994)].

An overview of the New Zealand Code Provisions for bond and anchorage in concrete, including high-strength concrete is given by Bull (1998).

2.4 Reinforced concrete ties

The serviceability of reinforced concrete members subjected to tensile or flexural loading is strongly influenced by the cracking behaviour, since this is fundamental for both global deformations and crack widths. The cracking behaviour, namely the successive crack formation, crack spacing and crack widths, depends on the interaction between the reinforcing steel and the surrounding concrete in the tensile zone and thereby on the bond characteristics. Cracking behaviour has often been experimentally studied using reinforced concrete tension members (ties) subjected to external tensile loading or restrained to imposed deformations. This type of tests has also been used to study the cracking behaviour in reinforced high-strength concrete members.

An extensive research program on the cracking behaviour of reinforced concrete tension members has been carried out at EPFL, [Farra and Jaccoud (1992); Jaccoud et al. (1993); Farra (1995); Jaccoud et al. (1996)]. Totally, 135 tests were made on concrete tension elements with a length of 1,10 m, a square cross section 100×100 mm and with one reinforcing bar in the centre [Farra (1995)]. The diameter of the reinforcing bar of type S500 was 10, 14 or 20 mm, corresponding to reinforcement ratios of 0,79 %, 1,54 % and 3,14 %. Fifteen different concrete compositions were used and the concrete strength ranged from 30 MPa to 90 MPa. At an age of 28 days, the specimens were subjected to a short-term imposed deformation. Three samples of the same specimen type were tested.

For the behaviour of tensile members in the crack formation phase and in the phase of stabilised cracking, the bond behaviour is important for tension stiffening and, consequently, for the overall structural behaviour. It has been found that the bond performance seems to increase faster than the concrete tensile strength, when the concrete grade is increasing.

In case of imposed loads, it was found that crack widths were reduced (about 30 %) in high-strength concrete specimens compared to normal-strength concrete specimens, due to the stiffer bond behaviour. However, in case of imposed strain of reasonable magnitude with regard to practical applications, high-strength concrete did not significantly improve the cracking behaviour. The reason was that for a certain imposed strain, the steel stress increases in high-strength concrete with respect to normal-strength concrete, which is an unfavourable effect, but this is almost balanced by the improved bond behaviour. There was no indication that the formula for crack spacing used for normal-strength concrete members should be changed in case of high-strength concrete. The reason is that the ratio between average bond stress and tensile strength seems to remain almost constant with increasing concrete compressive strength. It was also found that numerical results were sensitive to the assumed bond stress-slip relation.

The following economical consequences of using high-strength concrete were pointed out [Jaccoud et al. (1993) and (1996)]: it is possible to allow higher steel stresses under service load (for a given allowable crack width), and the required minimum reinforcement is only slightly increased or may even be considered as constant, as long as the reinforcement is designed to limit the crack widths. However, when minimum reinforcement is designed to prevent yielding in case of cracking, the amount increases proportionally to the tensile strength of concrete.

Copyright fib, all rights reserved. This PDF copy of fib Bulletin 10 is intended for use and/or distribution only by National Member Groups of fib.

With the aim of studying the influence of concrete strength on tension stiffening, Abrishami and Mitchell (1996) performed a series of tension tests. It was of special interest to study the influence of splitting cracks on tension stiffening. The specimens had a length of 1500 mm, rectangular cross-section of various size and shape, and one bar in the centre with specified yield strength of 400 MPa. The bar dimension varied between 11,3 and 30 mm, but due to the various cross-sections, the reinforcement ratio was the same in all the tests and equal to 1,23 %. The minimum concrete covers of the rectangular sections were always 40 mm (top and bottom covers); consequently, the ratio between cover and bar diameter varied with the bar diameter. The concrete strength was either 30 MPa or 90 MPa
The high-strength concrete members exhibited larger tension stiffening than the companion normal-strength concrete members. However, with increasing deformation in the post-cracking state, the response of the high-strength concrete members approached the one of the normal-strength concrete specimens. The stiffer response of high-strength concrete specimens was more pronounced in specimens with larger concrete cover/bar diameter ratios.

Tension stiffening was considerably reduced by longitudinal splitting cracks. The ratio between concrete cover and bar diameter was found to be a useful indicator for determining the extent of longitudinal splitting cracks. Splitting cracks were found to be significant when this ratio was less than about 2,5, for both normal-strength and high-strength concrete specimens. However, more splitting cracks were found in the high-strength concrete specimens. For smaller ratios between cover and bar diameter, the splitting cracks started at lower steel stresses than for larger ratios, and there were more splitting cracks and less transverse cracks. This may be significant for service load levels. Splitting cracks may even appear before any transverse cracks, which means that members without any transverse cracks may already have a non-linear response.

Cracking behaviour of normal-strength and high-strength concrete tension ties under short term imposed load was investigated experimentally by Lorrain et al. (1998). Twenty-five reinforced concrete ties were subjected to short-term imposed load. The specimens had a length of 2000 mm and square cross-section 100×100 mm. Five different concrete mixes were used and the compressive strength ranged from 40 to 100 MPa. The bar diameter varied between 10, 12, 16, and 20 mm, and the corresponding reinforcement ratios were 0,78 %, 1,13 %, 2,0 %, and 3,14 %. The reinforcing bars had a yield strength of about 600 MPa (mean value). However, to study the influence of an increased yield strength, some tests were provided with 16 mm high-strength bars (f_{ym} = 830 MPa). It was found that with high-strength concrete, tension stiffening was significantly improved in the crack formation phase, but decreased during the phase of stabilised cracking due to bond damage. With high-strength concrete specimens, stabilised cracking was reached at a higher steel stress compared to normal-strength concrete. Crack spacing mainly depended on the reinforcement ratio and was not influenced significantly by an increased concrete strength.

Other similar test series were reported by Creazza et al. (1996) and Bernardi et al. (1999). Their test results were generally in agreement with the investigations referred above.

An extensive study of the cracking behaviour of hardening concrete was reported by König and Bergner (1996). In this case, early restraint cracking due to temperature variations and early shrinkage was of main concern. Various concrete compositions with normal-strength and high-strength concrete were included, [Bergner (1994) and (1995)].

The influence of the concrete compressive strength on the cracking behaviour is discussed in Chapter 4 of CEB Bulletin 235 [CEB (1997)]. The following concluding remarks are given:

The bond properties are considerably improved when the compressive strength of concrete is increasing. Provided that the reinforcing bars doesn't yield, it is theoretically established and experimentally verified that:

Copyright fib, all rights reserved. This PDF copy of fib Bulletin 10 is intended for use and/or distribution only by National Member Groups of fib.

- crack widths in high-strength concrete are significantly smaller, if cracking is due to loads;
- crack widths increase very little and therefore may be considered as practically constant if cracking is due to imposed deformations.

Consequently, the required minimum reinforcement quantities are practically independent from concrete strength. This is evidently in contradiction with most present design codes, which require a minimum amount of reinforcement proportional to the tensile strength of concrete. In the future it will be necessary to modify some design rules in these codes, i.e. as proposed in CEB Bulletin No. 228, [CEB (1995)]. However, the present rules in MC90 for crack control can be considered to be still valid up to C100.

In the stabilised cracking phase, crack widths may be largely reduced by using higher concrete grades, which have a favourable effect on the transmission length due to improved bond properties.

Tests on reinforced concrete tensile members using fibrous concrete were also performed by Abrishami and Mitchell (1997) and Noghabai (1998). Procedure for performing tests on tensile element of both normal-strength and high-strength concrete has been proposed by a RILEM Committee [RILEM TC147-FMB (1996)] for Round Robin Analysis and Tests on Bond. The tests of Noghabai (1998) comply with the recommendations of the RILEM Committee. Based on the experimental observations (Fig. 2.3-19), Noghabai (1998) describes the behaviour of a reinforced concrete tensile member by a composite model using two parallel springs representing the reinforcement bar and concrete respectively.

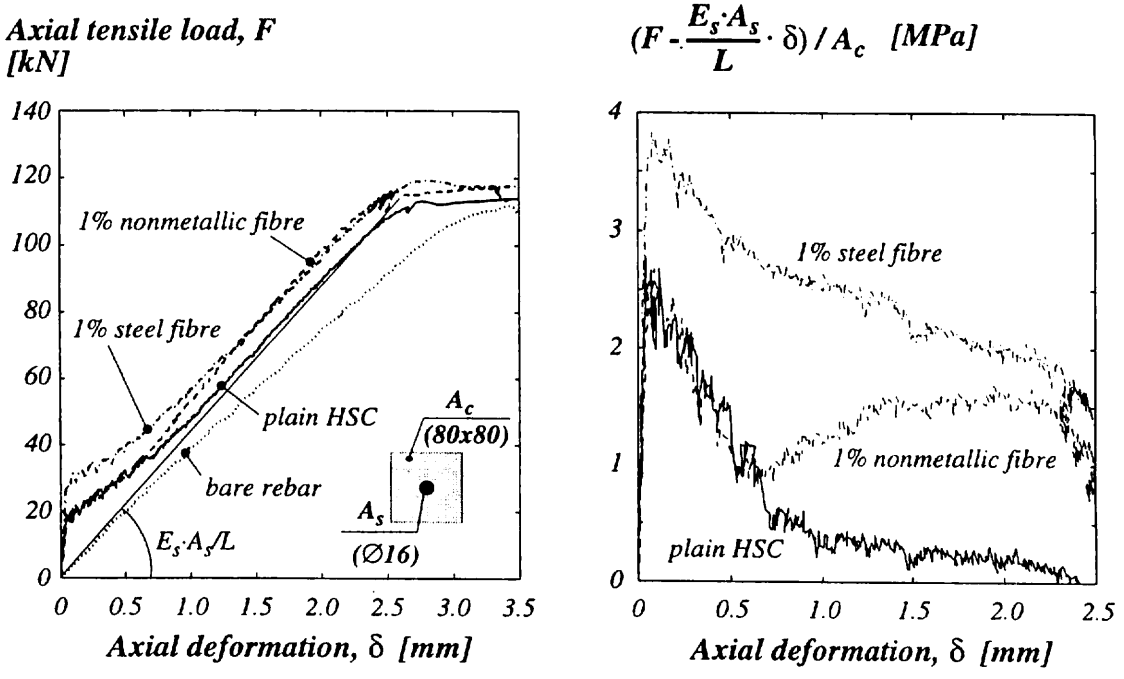

Fig. 2.3-19: Effect of tension stiffening of the bare rebar that is tested under the same conditions as the reinforced concrete tensile members of plain an fibrous high-strength concrete (left). Contribution of the concrete tensile capacity when the steel contribution is subtracted from the axial load (right). Modified from Noghabai (1998).

The material law for the rebar depends on the confinement of the surrounding concrete so that the rebar stiffness approaches the modulus of elasticity of the steel for larger covers. The σ_{ct} - w relationship defines the material behaviour for concrete at localised cracks. The model of Noghabai is in good agreement with results from plain as well as fibre-reinforced high-strength concrete and thus seems to

Copyright fib, all rights reserved. This PDF copy of fib Bulletin 10 is intended for use and/or distribution only by National Member Groups of fib.

have general validity with respect to the concrete grade (i.e. no empirical constants are needed). However, some model parameters, such as crack spacing or degree of stiffening of the rebar when encased, are based on direct experimental observations and have not yet been explicitly formulated, although theoretically identified

2.5 References

1973 Tepfers R. (1973): *A Theory of Bond Applied to Overlapped Tensile Reinforcement Splices for Deformed Bar*. Chalmers University of Technology, Division of Concrete Structures, Publication 73:2, Göteborg 1973, 328 pp.

1976 Clifton R. J., Simonson E. R., Jones A. H. and Green S. J. (1976): *Determination of the critical-stress-intensity factor KIC from internally pressurized thick-walled vessels*. Journal of Experimental Mechanics, June 1976, pp. 233-238.

- Hillerborg A., Modeer M. and Petersson P.-E. (1976): *Analysis of crack formation and crack growth in concrete by means of fracture mechanics and finite elements*. Cement and Concrete Research, Vol. 6, pp. 773-782.

1977 Orangun C. O., Jirsa J. O., Breen J. E. (1977): *Re-evaluation of test data on development length and splices*. ACI Journal, Vol. 74, No. 3, pp. 114-122.

1978 Neuner J., Stöckle S. and Grasser E. (1978): *Versuche an Dickwandigen, Unbewehrten Betonringen mit Innendruckbeanspruchung*. (Tests on thick-walled plain concrete cylinders with internal pressure. In German). Deutscher Ausschuss für Stahlbeton, Heft 299, Technical University of München, 1978.

1982 Morita S., Fujii S. (1982): *Bond capacity of deformed bars due to splitting of surrounding concrete*, in "Bond in concrete", Edited by P. Bartos, Applied Science Publishers, London, pp. 331-341.

1983 ACI Committee 318 (1983): *Building Code Requirements for Reinforced Concrete (ACI 318-83)*. American Concrete Institute, Detroit, 1983.

- Eligehausen R., Popov E. P., Bertero V. V. (1983): *Local bond stress-slip relationships of deformed bars under generalized excitations*. Report No. UCB/EERC 83-23, Univ. of California, Berkely (Ca, USA).

1985 Gambarova G. P., Giuriani E. (1985): *Discussion of "Study of transfer of tensile forces by bond"*, by D. H. Jiang, S. P. Shah, A. T. Andonian. ACI Journal, Vol. 82, No. 3, pp. 381-383.

1989 ACI Committee 318 (1989): *Building Code Requirements for Reinforced Concrete and Commentary (ACI 318-89/ACI 318R-89)*. American Concrete Institute, Detroit, 1989, 353 pp.

1990 ACI (1990): *High-Strength Concrete. Second International Symposium*. W.T. Hester (Editor). ACI Special Publication, SP-121, 1990.

- FIP/CEB (1990): *High Strength Concrete, State of the Art Report*. CEB Bulletin d'Information No. 197, August 1990, 61 pp.
- Gjørv O. E., Monteiro P. J. M., Mehta P. K. (1990): *Effect of condensed Silica fume on the Steel-Concrete Bond*. ACI Materials Journal, November-December 1990, pp. 573-580.
- Olsen N. H. (1990a): *Strength of Lapped Splices in High-Strength Concrete*. Second International Symposium on High-Strength Concrete. ACI, SP-121, Detroit, 1990, pp. 179-193.
- Olsen N. H. (1990b): *The Strength of Overlapped Deformed Tensile Reinforcement Splices in High Strength Concrete*. Technical University of Denmark, Department of Structural Engineering, R-234, 1990.

1991 Bilcík J. and Priechodsky V. (1991): *Stresses and strains in a model ring under internal radial pressure*. IABSE Colloquium, Stuttgart, Germany, 1991, pp. 755-760.

- Giuriani E., Plizzari G. A., Schumm C. (1991): *Role of stirrups and residual tensile strength of cracked concrete on bond*. ASCE, Journal of Structural Engineering, Vol. 117, No. 1, pp. 1-18.

1992 Azizinamini A. (1992): *Parametric Study of Variables Affecting Tension Development Length in High Strength Concrete*. International Conference: Bond in Concrete from Research to Practice, Proceedings, Riga Technical University, October 1992, pp. 4-27 - 4-36.

- Balaguru P. N. and Shah S. P. (1992): *Fiber Reinforced Cement Composites*. McGraw Hill, New York 1992.
- CEB-RTU (1992): Bond in Concrete *International Conference Bond in Concrete - From Research to Practice. Proceedings*. CEB and Riga Technical University, Riga, Latvia, October 1992.
- Engström B. (1992): *Ductility of tie connections in precast structures*. Chalmers University of Technology, Division of Concrete Structures, Publication 92:1, Göteborg 1992, 368+88 pp.

Copyright fib, all rights reserved. This PDF copy of fib Bulletin 10 is intended for use and/or distribution only by National Member Groups of fib.

- Farra B., Jaccoud J.-P. (1992): *Bond Behaviour, Tension Stiffening and Crack Prediction of High Strength Concrete.* International Conference: Bond in Concrete from Research to Practice, Proceedings, Riga Technical University, October 1992, pp. 9-1 - 9-10.
- Kaku T., Iizuka S., Yamada M., Zhang J. (1992): *A Proposal of Bond Strength Equation for R. C. Members Including High Strength Concrete Levels.* International Conference: Bond in Concrete from Research to Practice, Proceedings, Riga Technical University, October 1992, pp. 4-1 - 4-10.
- Zhiming T., Zhiman Y. (1992): *Bond Behaviour of Deformed bars in High Strength Concrete.* International Conference: Bond in Concrete from Research to Practice, Proceedings, Riga Technical University, October 1992, pp. 4-11 - 4-18.

1993 Azizinamini A., Russel H. G. (1993a): *Design Criteria for Tension Splices in High-Strength Concrete.* High Strength Concrete 1993. Proceedings, Volume 1, 1993, pp. 99-106.
- Azizinamini A., Stark M., Roller J. J., Ghosh S. K. (1993b): *Bond Performance of Reinforcing Bars Embedded in High-Strength Concrete.* ACI Structural Journal, September-October 1993, pp. 554-561.
- CEB-FIP (1993): *CEB-FIP Model Code 1990.* CEB Bulletin d'Information 213/214, Thomas Telford Ltd 1993, ISBN 0-7277-1696-4; 462 pp.
- Eligehausen R. and Balázs G. L. (1993): *Bond and Detailing.* CEB Bulletin d'Information No. 217, Lausanne 1993, pp. 173 – 226.
- Hansen E. (1993): *Tension Lap Splices and Crack Widths.* HSC Phase 3. Report 3.1. SINTEF Report STF70 A95019, SINTEF, 1993.
- High-Strength Concrete (1993): *High-Strength Concrete 1993.* I. Holand, E. Sellevold (Editors). Proceedings, Norwegian Concrete Association, Lillehammer, Norway, 1993.
- Jaccoud J.-P., Charif H., Farra B. (1993): *Cracking Behaviour of HSC Structures and Practical Consequences for Design.* High Strength Concrete 1993, Proceedings, Volume 1, Norwegian Concrete Association, 1993, pp. 225-232.
- Lestander U. (1993): *Bond Properties of High Performance Concrete, Pull-Out Tests with Monotonicly Increasing Loads.* Luleå University of Technology, Master's Thesis 1993:176E, 1993.

1994 ACI (1994): *High-Performance Concrete. Proceedings ACI International Conference Singapore 1994.* V.M. Malhotra (Editor). ACI Special Publication, SP-149, 1994.
- Al-Jahadi F.A., Wafa F.F Shiata: *Development Length for Straight Deformed Bars in High-Strength Concrete.* ACI SP-149, pp 507-521.
- BBK 94 (1994): *Boverkets handbok om betongkonstruktioner, Band 1 Konstruktion.* (Handbook on concrete structures, Volume I Design. In Swedish). National Board of Housing, Building and Planning (Boverket), Karlskrona, 1998, 166 pp.
- Bergner H. (1994): *Minimum Reinforcement of High-Strength concrete Members under Centrical Restraint.* Darmstadt Concrete, Annual Journal of Concrete and Concrete Structures, Vol. 9, 1994, pp. 41-48.
- CEB (1994): *Application of High Performance Concrete.* CEB Bulletin d'Information No. 222, Lausanne, November 1994, 66 pp.
- Hwang S.-J., Lee Y.-Y., Lee C.-S. (1994): *Effect of Silica Fume on the Splice Strength of Deformed Bars of High-Performance Concrete.* ACI Structural Journal, May-June 1994, pp. 294-302.
- Nischer P. (1994): *High Performance Concrete - Workability, Strength, E-Modulus, Resistance against Dissolution Attack.* Concrete Precasting Plant and Technology, Issue 3/194, pp. 68-77.

1995 ACI Committee 318 (1995): *Building Code Requirements for Structural Concrete (ACI 318-95) and Commentary (ACI 318R-95).* American Concrete Institute, Farmington Hills, 1995, 369 pp.
- Azizinamini A., Chisala M., Ghosh S. K. (1995): *Tension Development Length of Reinforcing Bars Embedded in High-Strength Concrete.* Engineering Structures, Vol. 17, No. 7, 1995, pp. 512-522.
- Bache H. H. (1995): *Concrete and concrete technology in a broad perspective.* Proceedings, Nordic Symposium on Modern Design of Concrete Structures, Aalborg University, Denmark, pp. 1-45.
- Bergner H. (1995): *Rissbreitenbeschränkung zwangbeanspruchter Bauteile aus hochfestem Normalbeton.* (Crack width limitations in high strength concrete structures under restraint loading. In German), Dissertation, TH Darmstadt 1995.
- Bigaj A.J. (1995): *Bond Behaviour of Deformed Bars in NSC and HSC.* Stevin Report 25.5-95-II, TU Delft, 1995.
- CEB (1995): *High Performance Concrete. Recommended Extensions to the Model Code 90, Research Needs.* CEB Bulletin d'Information 228, Lausanne, July 1995.
- Christensen L. (1995): *Forankring af armeringsjern. Stødforsøg med bjælker i højstyrkebeton.* (Anchorage of reinforcing bars. Lap tests of beams in high strength concrete. In Danish), Technical University of Denmark, Department of Structural Engineering. Laboratory Report, June, 1995.

Copyright fib, all rights reserved. This PDF copy of fib Bulletin 10 is intended for use and/or distribution only by National Member Groups of fib.

- Farra B. (1995): *Influence de la résistance du béton et de son adhérence avec l'armature sur la fissuration.* (Influence of concrete strength and bond to reinforcement on cracking. In French), Ecole Polytechnique Fédérale de Lausanne, Ph.D. Thesis No. 1359, 1995.
- Harajli M.H., Hout M., Jalkh W. (1995): *Local bond stress-slip behaviour of reinforcing bars embedded in plain and fibre concrete*, ACI Materials Journal, Vol. 92, No. 4, pp. 343-354.
- Noghabai K. (1995): *Splitting of Concrete in the Anchoring Zone of Deformed Bars - A Fracture Mechanics Approach to Bond.* Luleå University of Technology, Division of Structural Engineering, Licentiate Thesis 1995:26 L, 131+46 pp.
- Walraven J. C. (1995): *High Strength Concrete for Precast Concrete Members.* Concrete Precasting Plant and Technology, Issue 4/1995, pp.50-54.

1996 Abrishami H. H., Mitchell D. (1996): *Influence of Splitting Cracks on Tension Stiffening.* ACI Structural Journal, November-December 1996, pp. 703-710.
- Azizinamini A., Hatfield E., Pavel R. (1996): *Minimum Stirrups Requirements for Tension Splices in High Strength Concrete.* Fourth International Symposium on Utilization of High-Strength/High Performance Concrete. Proceedings. Vol. 3, Laboratorie Central des Ponts et Chaussées, Paris, 1996, pp. 1145-1154.
- Bigaj A. J., den Uijl J. A., Walraven J. C. (1996a): *A Bond Model for Ribbed Bars in HSC and NSC - An Experimental Study.* Fourth International Symposium on the Utilization of High Strength/High Performance Concrete. Proceedings, Vol. 3, Laboratorie Central des Ponts et Chaussées, Paris 1996, pp. 1125 - 1134.
- Bigaj A. J., Walraven J. C. (1996b): *Modelling of Size Effect on Rotation Capacity of Plastic Hinges in Reinforced Concrete Members.* Proceedings of AIO-Congress 1996 "From Materials to Building Structures".'
- Creazza G., di Marco R., Russo S., Siviero E. (1996): *Tension Stiffening in High Strength Concrete.* Fourth International Symposium on the Utilization of High Strength/High Performance Concrete. Proceedings, Vol. 3, Laboratorie Central des Ponts et Chassées, Paris 1996, pp. 1135 - 1143.
- Darvin D., Zuo J., Tholen M. L., Idun E. K. (1996): *Development Length Criteria for Conventional and High Relative Rib Area Reinforcing Bars.* ACI Structural Journal, May-June 1996, pp. 347-359.
- De Almeida I. R. (1996): *Bond between Reinforcing Steel and High Strength Concrete.* Fourth International Symposium on the Utilization of High Strength/High Performance Concrete. Proceedings, Vol. 3, Laboratorie Central des Ponts et Chaussées, Paris 1996, pp. 1097 - 1104.
- Den Uijl J. A., Bigaj A. J. (1996): *A Bond Model for Ribbed Bars Based on Concrete Confinement.* HERON, Vol. 41, No. 3, pp. 206-226.
- Esfahani M. R., Rangan B. V. (1996): *Studies on Bond between Concrete and Reinforcing Bars.* Curtin University of Technology, School of Civil Engineering, Research Report No. 1/96, Perth, March 1996, 315 pp.
- Gerard B., Marchand J., Breysse D., Ammouche A. (1996): *Constitutive Law of HPC under Tensile Strain.* Forth International Symposium on Utilization of High-Strength/High Performance Concrete, Proceedings Vol. 2, Laboratorie Central des Ponts et Chaussées, Paris, May 1996, pp. 675-685.
- Hansen E. A., Thorenfeldt E. (1996): *Bond Properties of Deformed Reinforcement Bars in High Strength Concrete.* Fourth International Symposium on the Utilization of High Strength/High Performance Concrete. Proceedings, Vol. 3, Laboratories des Ponts et Chaussées, Paris 1996, pp. 1105 - 1149.
- Hatfield E., Azizinamini A., Pavel R. (1996): *Minimum Stirrups Requirements for Tension Splices in High Strength Concrete.* Fourth International Symposium on the Utilization of High Strength/High Performance Concrete. Proceedings, Vol. 3, Laboratories des Ponts et Chaussées, Paris 1996, pp. 1145 - 1104.
- Huang Z., Engström B., Magnusson J. (1996a): *Experimental Investigation of the Bond and Anchorage Behaviour of Deformed Bars in High Strength Concrete.* Chalmers University of Technology, Division of Concrete Structures, Report 95:4, Göteborg 1996, 32 pp.
- Huang Z., Engström B., Magnusson J. (1996b): *Experimental and Analytical Studies of the Bond Behaviour of Deformed Bars in High Strength Concrete.* Fourth International Symposium on the Utilization of High Strength/High Performance Concrete. Proceedings, Vol. 3, Laboratories des Ponts et Chaussées, Paris, 1996, pp. 1115 - 1124.
- Hwang S.-J., Leu Y.-R., Hwang H.-L. (1996): *Tensile Bond Strengths of Deformed Bars of High-Strength Concrete.* ACI Structural Journal, January-February 1996, pp. 11-20.

Copyright fib, all rights reserved. This PDF copy of fib Bulletin 10 is intended for use and/or distribution only by National Member Groups of fib.

- Jaccoud J.-P., Farra, B., Leclercq A. (1996): *Improvement of Existing Codes for Their Application to Crack Control of HSC/HPC Structures.* Fourth International Symposium on the Utilization of High Strength/High Performance Concrete. Proceedings, Vol. 3, Laboratories des Ponts et Chaussées, Paris 1996, pp. 1155 - 1161.
- König G., Bergner H. (1996): *Minimum Reinforcement of High-Strength Concrete Members under Centrical Restraint.* Fourth International Symposium on the Utilization of High Strength/High Performance Concrete. Proceedings, Vol. 3, Laboratories des Ponts et Chaussées, Paris 1996, pp. 1225 - 1231.
- Lorrain M., Hamouine A. (1996): *Bond Performance of High-Strength Concrete.* Fourth International Symposium on the Utilization of High Strength/High Performance Concrete. Proceedings, Vol. 3, Laboratories des Ponts et Chaussées, Paris 1996, pp. 1195 - 1200.
- RILEM TC147-FMB (1996): *Round Robin analysis and Tests on Bond.* Materials and Structures, RILEM, Paris, Vol. 29, August-September 1996, pp. 453-454.
- Shin S. W., Choi J. S. (1996): *Bond Characteristics of Reinforcing Bars Embedded in High Strength Concrete.* Fourth International Symposium on the Utilization of High Strength/High Performance Concrete. Proceedings, Vol. 3, Laboratories des Ponts et Chaussées, Paris 1996, pp. 1185 - 1193.
- Taerwe L. (1996): *Structural Behaviour of HS/HPC, Part II: Bond and Related Phenomena.* Fourth International Symposium on Utilzation of High-Strength/High Performance Concrete, Proceedings, Vol. 1, Laboratories des Ponts et Chaussées, Paris 1996, pp 57-66.
- Trebeschi C. (1996): *Anchorage of Ribbed Bars in Normal and High Strength Concrete Beams.* Chalmers University of Technology, Division of Concrete Structures, Master's Thesis 96:2, September 1996, 167 pp.
- Utilization of High Strength/High Performance Concrete (1996): *Fourth International Symposium on the Utilization of High Strength/High Performance Concrete.* F. de Larrard, R. Lacroix (Editors). Laboratorie Central des Ponts et Chaussées, Paris, 1996.
- Yerlici V., Ersoy U., Özturan T., Türk M., Özden S. (1996): *An Investigation on Bond Performance oh High Strength Concrete.* Fourth International Symposium on the Utilization of High Strength/High Performance Concrete. Proceedings, Vol. 3, Laboratories des Ponts et Chaussées, Paris 1996, pp. 1201 - 1207.

1997 Abrishami H., Mitchell D. (1997): *Influence of Steel Fibres on Tension Stiffening.* ACI Structural Journal, Vol. 94, No. 6, November-December 1997, pp. 769-776.
- CEB (1997): *Serviceability Models. Behaviour and modelling in serviceability limit states including repeated and sustained loads, Progress report.* (Jaccoud J.-P.: *Cracking under long term loads or imposed deformations.* pp 143-155), CEB Bulletin 235, Lausanne , April 1997.
- Ghassemi N. (1997): *Inverkan av upplagstryck på kamstängers förankring i höghållfast betong* (Influence of Support Pressure on the Anchorage of Ribbed Bars in High-Strength Concrete. In Swedish). Chalmers University of Technology, Division of Concrete Structures, Master's Thesis 96:3, Göteborg, January 1997, 132 pp.
- Magnusson J. (1997): *Bond and Anchorage of Deformed Bars in High-Strength Concrete.* Chalmers University of Technology, Division of Concrete Structures, Licentiate Thesis, Publication 97:1, Göteborg, November 1997, 234 pp.
- van Mier J. G. M. (1997): *Fracture Processes of Concrete - Assessment of Material Parameters for Fracture Models.* CRC Press, 448 pp.

1998 ACI (1998a): *High-Strength Concrete in Seismic Regions.* C.W. French, M. E. Kreger (Editors). ACI Special Publication, SP-176, 1998.
- ACI (1998b): *Bond and Development of Reinforcement. A Tribute to Dr. Peter Gergely.* R. Leon (Editor). ACI Special Publication, SP-180, 1998.
- Aarup B., Jensen B. C. (1998): *Bond Properties of High-Strength Fibre Reinforced Concrete.* Bond and Development of Reinforcement - A Tribute to Dr. Peter Gergely, ACI SP-180, 1998, pp.459-472.
- Apleberger L., Cederwall K., Elfgren L., Grauers M., Nylinder K. (Editors) (1998): *High Performance Concrete Structures. Design Handbook. Draft Version.* Luleå University of Technology, Division of Structural Engineering, Luleå, 1998, 110 pp.
- Azizinamini A., Pavel R., Hatfield E., Ghosh S. K. (1998a): *Behaviour of Lap-Spliced Reinforcing Bars Embedded in High-Strength Concrete.* Paper submitted for publication in ACI Structural Journal. Final draft 7/7/98.
- Azizinamini A., Darwin D., Eligehausen R., Pavel R., Ghosh S. K. (1998b): *Proposed Modification to ACI 318-95, Tension Development and Lap Splice Provisions for High-Strength Concrete.* Paper submitted for publication in ACI Structural Journal. Final draft 7/31/98.

Copyright fib, all rights reserved. This PDF copy of fib Bulletin 10 is intended for use and/or distribution only by National Member Groups of fib.

- Azizinamini A. (1998c): *Bond and Anchorage of Reinforcement in HSC: Discussion Summary*. High-Strength Concrete in Seismic Regions. ACI, SP-176, Farmington Hill, 1998, pp. 445-447.
- Azizinamini A. (1998d): *Preventing Brittle Failure of Tension Splices in High-Strength Concrete*. Bond and Development of Reinforcement - A Tribute to Dr. Peter Gergely, ACI SP-180. Farmington Hills, 1998, pp.243-259.
- Bigaj A. J., den Uijl J. A., Walraven J. C. (1998): *Bond of Ribbed Bars Modelled through Concrete Confinement*. Bond and Development of Reinforcement - A Tribute to Dr. Peter Gergely, ACI SP-180, Farmington Hill 1998, pp. 195-213.
- Bull D. (1998): *Bond and Anchorage of Reinforcement in Concrete - New Zealand Code Provisions*. High-Strength Concrete in Seismic Regions, ACI, SP-176, Farmington Hill, 1998, pp. 45-56.
- Darwin D., Zuo J. Tholen M. L. (1998): *Overview of Research to Improve the Development Characteristics of Reinforcing Bars*. Bond and Development of Reinforcement - A Tribute to Dr. Peter Gergely, ACI SP-180. Farmington Hills, 1998, pp.299-318.
- Durán G. B. (1998): *Influence of Shear Span Detailing on the Anchorage of Ribbed Bars in Normal and High Strength Concrete*. Chalmers University of Technology, Division of Concrete Structures, Master's Thesis 98:5, Göteborg April 1998, 151 pp.
- Engström B., Magnusson J., Huang Z. (1998): *Pull-Out Bond Behaviour of Ribbed Bars in Normal and High-Strength Concrete with Various Confinements*. Bond and Development of Reinforcement - A Tribute to Dr. Peter Gergely, ACI SP-180, February 1998, pp.215-242.
- Esfahani M. R., Rangan B. V. (1998a): *Local Bond Strength of Reinforcing Bars in Normal Strength and High-Strength Concrete (HSC)*. ACI Structural Journal, March-April 1998, pp 96-106.
- Esfahani M. R., Rangan B. V. (1998b): *Bond between Normal Strength and High-Strength Concrete (HSC) and Reinforcing Bars in Splices in Beams*. ACI Structural Journal, May-June 1998, pp. 272-280.
- Fuji S., Noguchi H., Morita S. (1998): *Bond and Anchorage of Reinforcement in High-Strength Concrete. High-Strength Concrete in Seismic Regions*, ACI, SP-176, Farmington Hill 1998, pp. 23-43.
- Hamad B. S., Itani M. S. (1998a): *Bond Strength of Reinforcement in High-Performance Concrete: The Role of Silica Fume, Casting Position, and Superplasticizer Dosage*. ACI Materials Journal, September-October 1998.
- Hamad B. S., Itani M. S. (1998b): *Bond Studies of Reinforcing Bars in Silica Fume Concrete*. Bond and Development of Reinforcement - A Tribute to Dr. Peter Gergely, ACI SP-180.Farmington Hills, 1998, pp.473-491.
- Lorrain M. Maurel O. Seffo M. (1998): *Cracking Behaviour of Reinforced High-Strength Concrete Tension Ties*. ACI Structural Journal, September-October 1998, pp. 626-635.
- Lundgren K. and Gylltoft K. (1998): *Modelling splitting and fatigue effects of bond*. Third International Conference on Fracture Mechanics of Concrete Structures FRaMCoS3. H. Mihashi and K. Rokugo (Editors). Gifu, Japan, AEDIFICATiO, pp. 675-684, ISBN 3 931681 22 X.
- McCabe S. L. (1998): *Bond and Development of Steel Reinforcement in High-Strength Concrete - An Overview. High-Strength Concrete in Seismic Regions*. ACI SP-176, Farmington Hills 1998, pp. 1-13.
- Noghabai K. (1998): *Effect of Tension Softening on the Performance of Concrete Structures - Experimental, Analytical and Computational Studies*. Luleå University of Technology, Division of Structural Engineering, Doctoral Thesis 1998:21, Luleå, Sweden, 1998, pp. 135+10.
- Plizzari G. A., Deldossi M. A., Massimo S. (1998a): *Transverse reinforcement effects on anchored deformed bars*, Magazine of Concrete Research, Vol. 50, No. 2, pp. 161-177.
- Plizzari G. A., Klink T. and Slowik V. (1998b): *Investigations into the failure of concrete rings under inner pressure*. Third International Conference on Fracture Mechanics of Concrete Structures FRaMCoS3. H. Mihashi and K. Rokugo (Editors). Gifu, Japan AEDIFICATO, pp. 1311-1320, ISBN 3 931681 23 8.
- Tue N. V., Krumbach R. (1998): *Bond Behaviour between the Newly Developed Reinforcing Steel and HPC*. Leipzig Annual Civil Engineering Report, No. 3 1998, University of Leipzig 1998, pp. 73-85.

1999 Bernardi S., Mesureur B., Rivillon Ph. (1999): *Cracking of Reinforced High-Strength Concrete Structures*. Fifth International Symposium on Utilization of High Strength/High Performance Concrete, Proceedings, Volume 1, Norwegian Concrete Association, 1999, pp. 147-153.

- Noghabai K. (1999): *Discrete versus smeared versus element-embedded crack models on ring problem*. Journal of Engineering Mechanics, ASCE, Vol. 125, No. 3, pp. 307-315.
- Plizzari G. (1999): *Bond and splitting crack development in normal and high-strength fibre-reinforced concrete*, 13th Engrg. Mechanics Division Conference – EMD99, Baltimore (MD, USA) on CD ROM support.

Copyright fib, all rights reserved. This PDF copy of fib Bulletin 10 is intended for use and/or distribution only by National Member Groups of fib.

- Utilization of High Strength/High Performance Concrete (1999): *Fifth International Symposium on the Utilization of High Strength/High Performance Concrete*. I. Holand, E. Sellevold (Editors). Norwegian Concrete Association, Sandefjord, Norway, 1999.

Notations

A_c	cross-sectional area of concrete
A_s	cross-sectional area of reinforcement bar
A_{st}	total cross-sectional area of transverse reinforcement
B	brittleness
B	concrete index of confinement
c	concrete cover
d	effective depth
d_{max}	maximum aggregate size
E_c	modulus of elasticity of concrete
E_s	modulus of elasticity of steel
F	axial tensile force
F_s	anchorage capacity (anchored force)
f_c, f_{cc}	concrete compressive strength
f_{ck}	concrete compressive strength, characteristic value
f_{cm}	mean concrete compressive strength (cylinder strength)
f_{cm0}	mean concrete compressive strength, reference value
$f_{ctk0,m}$	concrete tensile strength, reference value
f_{ct}	concrete tensile strength
f_{ctm}	mean concrete tensile strength
f_y	yield strength of reinforcing steel
f_{yk}	characteristic yield strength of reinforcing steel
f_{ym}	mean yield strength of reinforcing steel
G_F, G_f	fracture energy (mode I)
G_{F0}	fracture energy, reference value
h	height
L	length
L_0	span
l_{ch}	characteristic length
l_e	embedment length (bond length)
$l_{e,red}$	effective embedment length after local conic failure
N_{max}	tensile force, peak value
$N_{max,n}$	tensile force, peak value, normalised
n	number of bars
p_i	internal pressure
$p_{i,max}$	internal pressure, peak value
Q	load
r_0	radius of thick-walled cylinder
r_{cr}	radius of cracked region in thick-walled cylinder
r_i	radius of opening in thick-walled cylinder
r_s	radius of spiral reinforcement
s	slip
s	spacing
s_1	slip when peak value of bond stress is obtained
s_y	slip obtained in section where steel starts to yield
w	crack width
x	co-ordinate (along bar axis)

Copyright fib, all rights reserved. This PDF copy of fib Bulletin 10 is intended for use and/or distribution only by National Member Groups of fib.

α	exponential factor
β	exponential factor
δ	axial deformation
ε_c	concrete compressive strain
ϕ	diameter
σ_c	concrete compressive stress
σ_{ct}	concrete tensile stress
σ_s	steel stress
τ_b	bond stress
$\tau_{b,max}$, τ_{max}	bond stress, peak value
$\tau_{m,max}$	average bond stress at maximum load
τ_y	bond stress obtained in section where steel starts to yield
Ω	stirrup index of confinement

Copyright fib, all rights reserved. This PDF copy of fib Bulletin 10 is intended for use and/or distribution only by National Member Groups of fib.

3 Bond under repeated loading

Working Party 3:

György L. Balázs (Convener, Technical University of Budapest, Hungary), **Atorod Azizinamini** (University of Nebraska, Lincoln, USA), **Rolf Eligehausen** (University of Stuttgart, Germany), **Roberto Leon** (Geogia Institute of Technology, Atlanta, USA), **Elisabeth Vintzileou** (National Technical University of Athens, Greece), **Josko Ozbolt** (corresponding member, University of Stuttgart, Germany)

3.1 Introduction **158**

3.2 General **158**

3.3 Cyclic bond behaviour **160**
3.3.1 Constant amplitude repeated loading 160
3.3.1.1 Slip versus number of load cycles relationship 160
3.3.1.2 S-N (Wöhler) diagram 164
3.3.1.3 Influence of the loading amplitude 165
3.3.2 Variable amplitude repeated loading 165
3.3.2.1 Program loading 165
3.3.2.2 Random loading 167

3.4 Reversed cyclic bond behaviour **167**
3.4.1 Description of the behaviour 167
3.4.2 Analytical models 169

3.5 Concrete under repeated loading **172**

3.6 Numerical analysis of bond under repeated loading **175**
3.6.1 Finite element analysis 176
3.6.1.1 Phenomenological (macroscopic) modeling 176
3.6.2 Detailed analysis 177
3.6.3 Numerical example 179

3.7 Conclusions **180**

3.8 Literature **183**

Copyright fib, all rights reserved. This PDF copy of fib Bulletin 10 is intended for use and/or distribution only by National Member Groups of fib.

3 Bond under repeated loading

In this chapter bond behaviour under repeated loading is discussed including repeated and reversed cyclic loading and considering loading parameters like maximum and minimum levels of repeated load, type of amplitudes (constant or variable), sequence of amplitudes, type of load control (force or slip control) and number of load cycles, etc., respectively. In addition to, various proposals for modelling are discussed and evaluated.

3.1 Introduction

Repeated or cyclic loading produces a progressive deterioration of bond that may lead to failure at cyclic bond stress levels lower than the ultimate stress under monotonic loading. Accumulation of bond damage is supposed to be caused by the *propagation of micro-cracks* (Broms 1965, Goto and Otsuka, 1971) *and progressive crushing* (Gambarova and Giuriani, 1985) of concrete in front of the lugs. Their effect is observed as slip increase.

A distinction is generally made between low cycle high amplitude fatigue (*low cycle fatigue*) and high cycle low amplitude fatigue (*high cycle fatigue*). The former involves a small number of load or slip cycles of high stress or slip levels at lower rate of loading (e.g. earthquakes and storms) indicating ultimate conditions, while the latter is characterized by a large number of load cycles of low stress level at a higher rate of loading (e.g. traffic loading, vibrating machinery, wave and wind loads) indicating service conditions. There is no clear limit between these two loading types, therefore, distinction is not made herein but on the type of applied stress: *repeated loading* will imply that the bar stress does not change sense and *reversed cyclic loading* will indicate that the bar is subjected alternatively to tension and compression.

Most of the results considered here were obtained over *a short length* (1 to 5 bar diameters) giving the basic characteristics of the behaviour which should be extended by the redistribution of forces for studies on longer lengths (like Ciampi, Eligehausen, Bertero and Popov, 1982). References will be given to the cyclic behaviour of concrete as well, owing to the correlation in the cyclic behaviour of bond and that of concrete, respectively.

Following observations concern bond in normal strength concrete made of normal weight aggregate. Rather little is known on cyclic bond behaviour in high strength concrete, in light weight aggregate concrete, in fiber reinforced concrete and with epoxy coated bars. These will not be addressed here.

Previous State of Art reports on bond under repeated loading (e.g. Tassios 1979, CEB 1982, CEB 1983, CEB 1991, ACI 1992) made very valuable efforts in summarizing the phenomenon, the influencing factors and the consequences of repeated loading on steel concrete interfaces, however, they even left a large number of open questions. This chapter intends to cope with some of these questions.

3.2 General

Progressive deterioration of bond under repeated loading is observed in increasing slip (Bresler and Bertero, 1968; Edwards and Yannopoulos, 1978; Rehm and Eligehausen, 1979). Slip is significantly influenced by the load history. *Important loading parameters* are: maximum and minimum levels of the repeated load, type of amplitude (constant or variable), frequency and sequence of amplitudes, type of load control (force or slip control) and number of load cycles.

Deterioration of bond under repeated loading primarily depends on the peak slip (and not the peak stress) reached in the last cycle (Eligehausen, Popov and Bertero, 1983; Balázs, 1991).

Bond deterioration does not only take place due to the repeated loading but partly due to the long term effect (ACI, 1992) if the minimum value of cyclic load level differs from zero and has the same sign as the maximum level (see recent results in Ch. 3.3.1.3).

In case of steel reinforcing bars, fatigue bond failure takes place by failure of the concrete either by shearing off the concrete between the lugs or by longitudinal splitting of the concrete cover. Bond resistance before failure is basically provided by bearing of the lugs, therefore,

Copyright fib, all rights reserved. This PDF copy of fib Bulletin 10 is intended for use and/or distribution only by National Member Groups of fib.

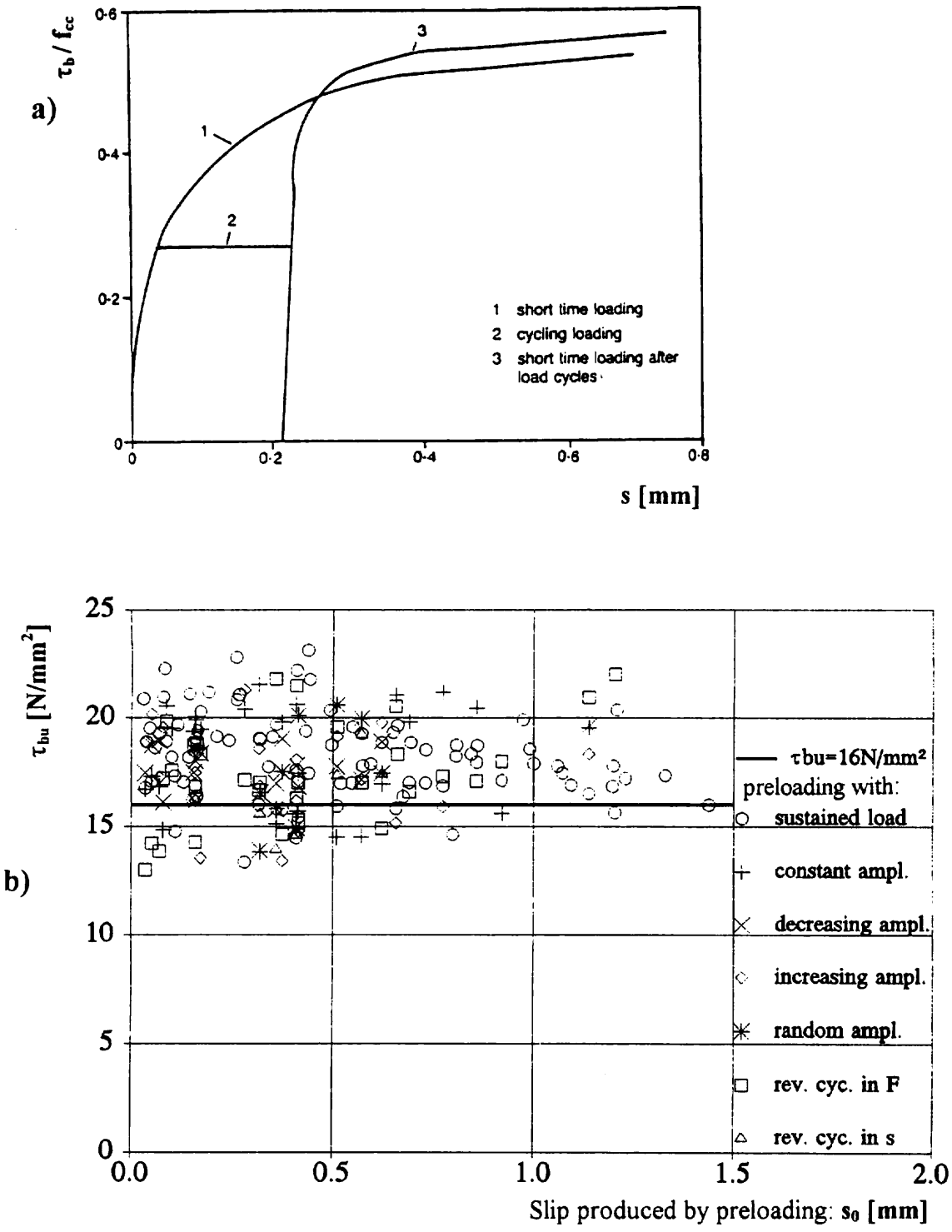

Fig.3.1 Effect of preloading on the bond strength (residual bond strength)
a) preloading: constant amplitude repeated loading;
Rehm and Eligehausen (1977, 1979)
b) preloading: constant or variable amplitude repeated loads, force or slip controlled reversed cyclic loads or long term loads (ℓ_b=5∅, ∅16, f_y=500 N/mm², f_{ccm}=30 N/mm²);
Balázs and Koch (1996)

Copyright fib, all rights reserved. This PDF copy of fib Bulletin 10 is intended for use and/or distribution only by National Member Groups of fib.

concrete compressive strength is generally considered to be the key parameter and not the tensile strength (ACI, 1992). Adequate confinement is very important against early splitting mainly under reversed cyclic loading.

A general question is the *residual bond strength* after repeated (or long term loading). Rehm and Eligehausen (1977, 1979) shown (**Fig.3.1.a**) that if fatigue failure does not take place in constant amplitude cycling, *then the previous repeated load does not negatively influence the bond stress versus slip behaviour near ultimate load compared with the monotonic loading behaviour*. It indicates that the monotonic envelop can be reached even after a high number of repetitions. 202 recent pull-out tests by Balázs and Koch (1996) on specimens loaded initially constant or variable amplitude cyclic loads, force or slip controlled reversed cyclic loads or long term loads supported the observations by Rehm and Eligehausen (1977, 1979). The residual bond strength was on average 12 % higher than the monotonic bond strength for specimens loaded cyclically up to a slip value less than the slip related to the monotonic bond strength (**Fig.3.1.b**). The small increase in bond strength may be partly explained by the increase in concrete strength during the relatively long tests (Koch and Balázs, 1992).

3.3 Cyclic bond behaviour

Test results with constant or variable amplitude repeated loads are dealt with separately.

3.3.1 Constant amplitude repeated loading

In this Chapter various presentations of cyclic pull-out test results with constant amplitude loading are discussed including description of slip development, fatigue bond failure and influence of loading amplitude.

3.3.1.1 Slip versus number of load cycles relationship

One of the most typical representation of cyclic bond test results is the slip versus number of load cycles diagram indicating the development of slip (s) as a function of the load cycles (n).

According to the pull-out test results by Rehm and Eligehausen (1977, 1979) with constant amplitude repeated loading, the slip versus number of load cycles relationship was found to be *approximately linear in double logarithmic scale* if the fatigue failure of bond has not been reached (**Fig.3.2.a**). This approach was adopted in MC 90 (1993) for the prediction of cycle dependent slip (s_n) as a function of the initial slip before cyclic loading (s_0) and the number of load cycles (n):

$$s_n = s_0 \cdot (1 + k_n)$$

where

$$k_n = (1+n)^b - 1 \qquad \text{and} \qquad b = 0.107$$

Another series of test results by Balázs, Koch and Harre (1994) with constant amplitude cyclic loading in double logarithmic scale is indicated in **Fig.3.2.b**. None of the tests ended with pull-out failure up to the load levels ≤ 50% of the pull-out strength within 2 million load cycles. By fitting the 40 test results of **Fig.3.2.b** in the form of the MC 90 approach, *power b was found to be practically constant up to the* $\tau_{b,max}$ τ_{bu}*=0.5 load level being b=0.119 which is slightly higher than b=0.107, and, it increased for higher load levels* (Balázs and Koch, 1996).

When considering the whole bond fatigue process under constant amplitude repeated loading in linear scale Balázs (1991) observed that *the slip rate tends to decrease initially, then remains constant, and increases rapidly before pull-out failure* (**Fig.3.3.a-c**). The third failure phase starts by reaching $s(\tau_{bu})$ - the slip at the monotonic bond strength. If $s(\tau_{bu})$ has not been reached, the failure phase is avoided. This behaviour was found to be independent of the load level or number of cycles to failure, however, the slip rate during all the three phases is a function of the load level. Further test results (Koch and Balázs 1993; Daerga 1993, Balázs 1994) seem to support this hypothesis (e.g. **Fig.3.3.d-e**).

Copyright fib, all rights reserved. This PDF copy of fib Bulletin 10 is intended for use and/or distribution only by National Member Groups of fib.

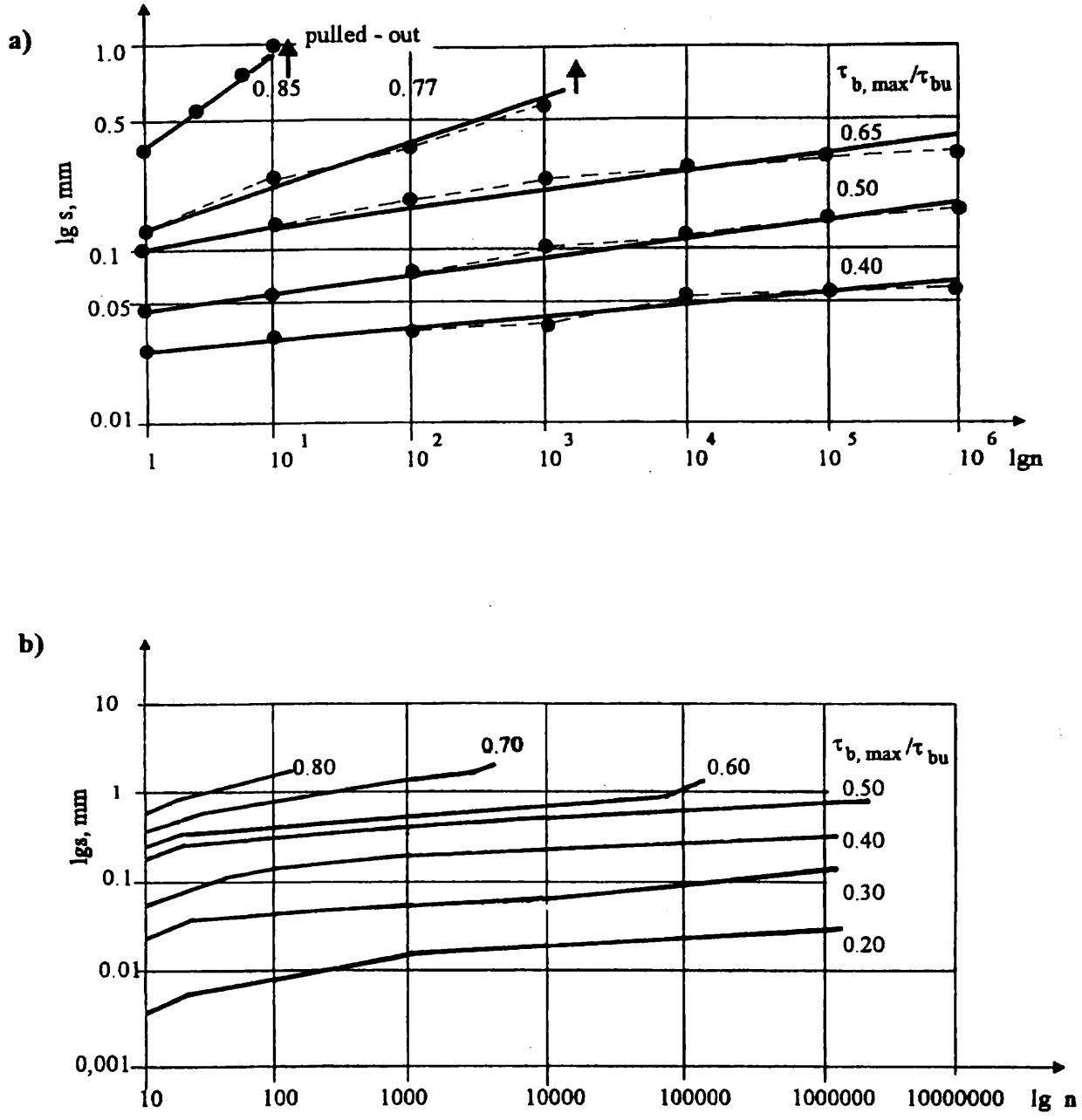

Fig.3.2 Unloaded-end slip vs. number of load cycles diagrams under constant amplitude repeated loading in double logarithmic scale
a) Ø14, $\ell_b=3Ø$, $f_y=500$ N/mm², $f_{ccm}=23$ N/mm², $\tau_{b,min}=0.1\tau_{b,max}$
Rehm and Eligehausen (1979)
b) Ø16, $\ell_b=5Ø$, $f_y=500$ N/mm², $f_{ccm}=30$ N/mm², $\tau_{b,min}=0.1\tau_{b,max}$, (every curve is an average of 5 measurements)
Balázs, Koch, Harre (1994)

Copyright fib, all rights reserved. This PDF copy of fib Bulletin 10 is intended for use and/or distribution only by National Member Groups of fib.

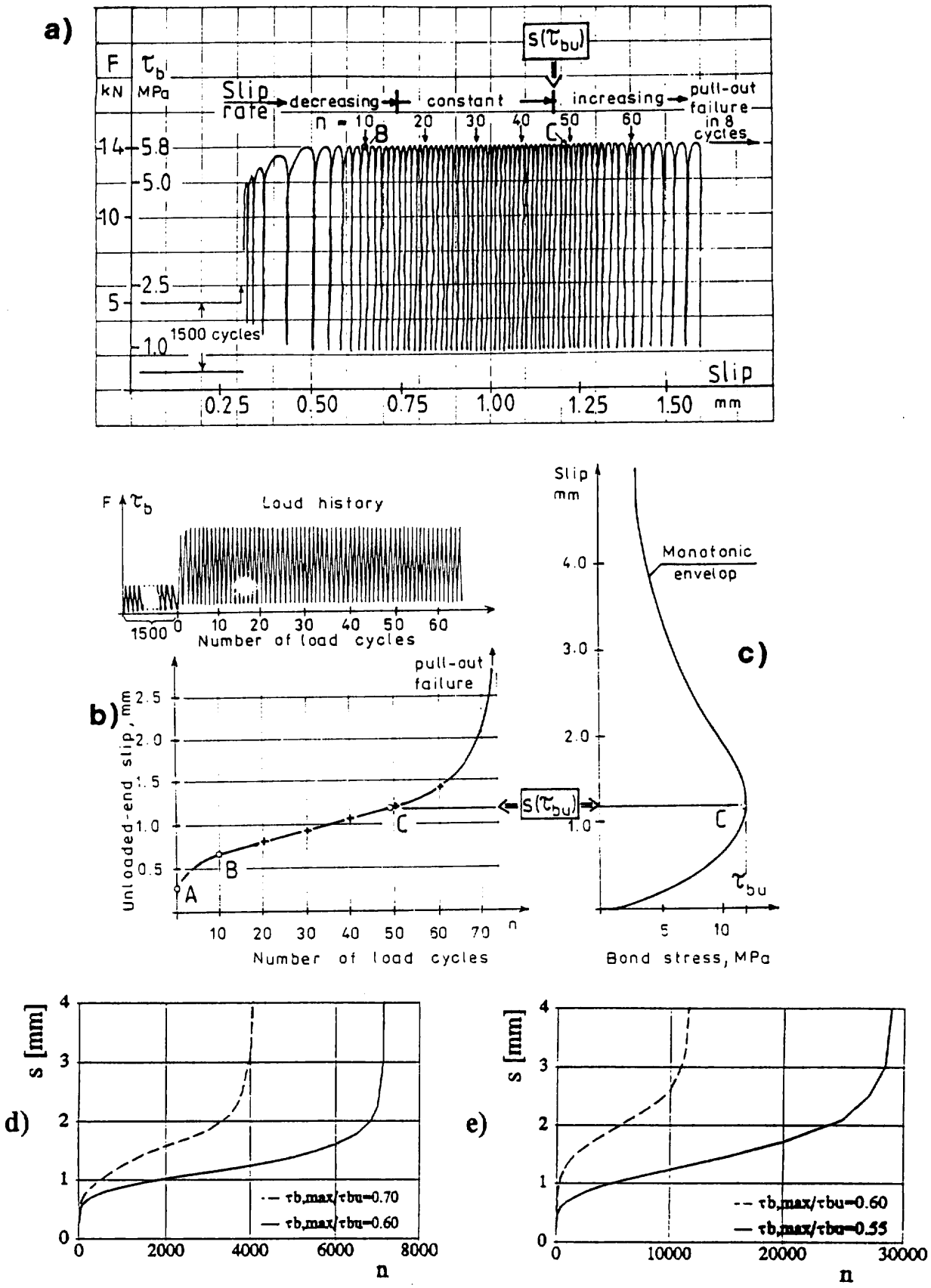

Fig.3.3 Bond fatigue process under constant amplitude repeated loading
a) cyclic τ_b-s b) s-n c) monotonic τ_b-s (Balázs, 1991)
Ø8, ℓ_b=12Ø, f_y=400 N/mm², f_{ccm}=20 N/mm², $\tau_{b,min}$=0.15$\tau_{b,max}$
d) s-n e) s-n (Koch and Balázs, 1993)
Ø16, ℓ_b=5Ø, f_y=500 N/mm², f_{ccm}=30 N/mm², $\tau_{b,min}$=0.1$\tau_{b,max}$

Copyright fib, all rights reserved. This PDF copy of fib Bulletin 10 is intended for use and/or distribution only by National Member Groups of fib.

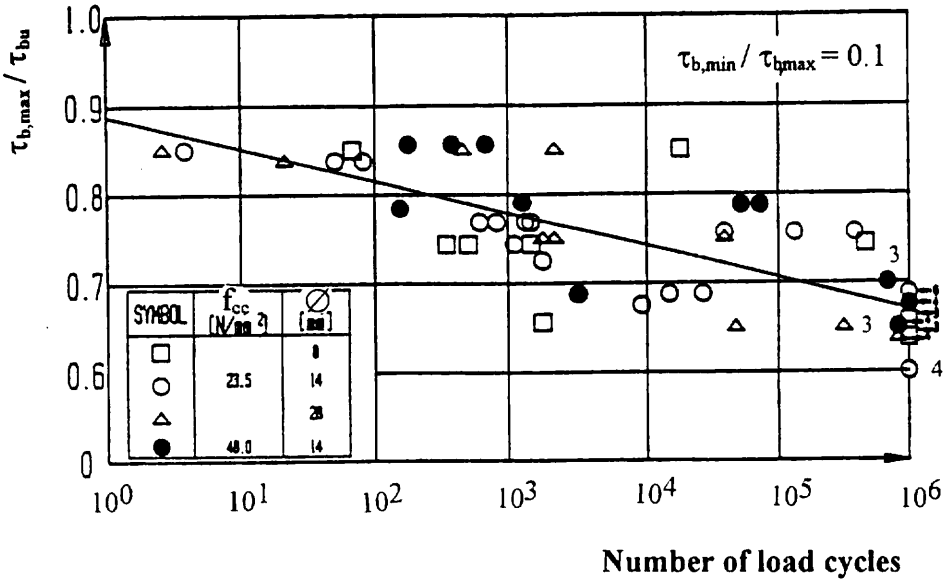

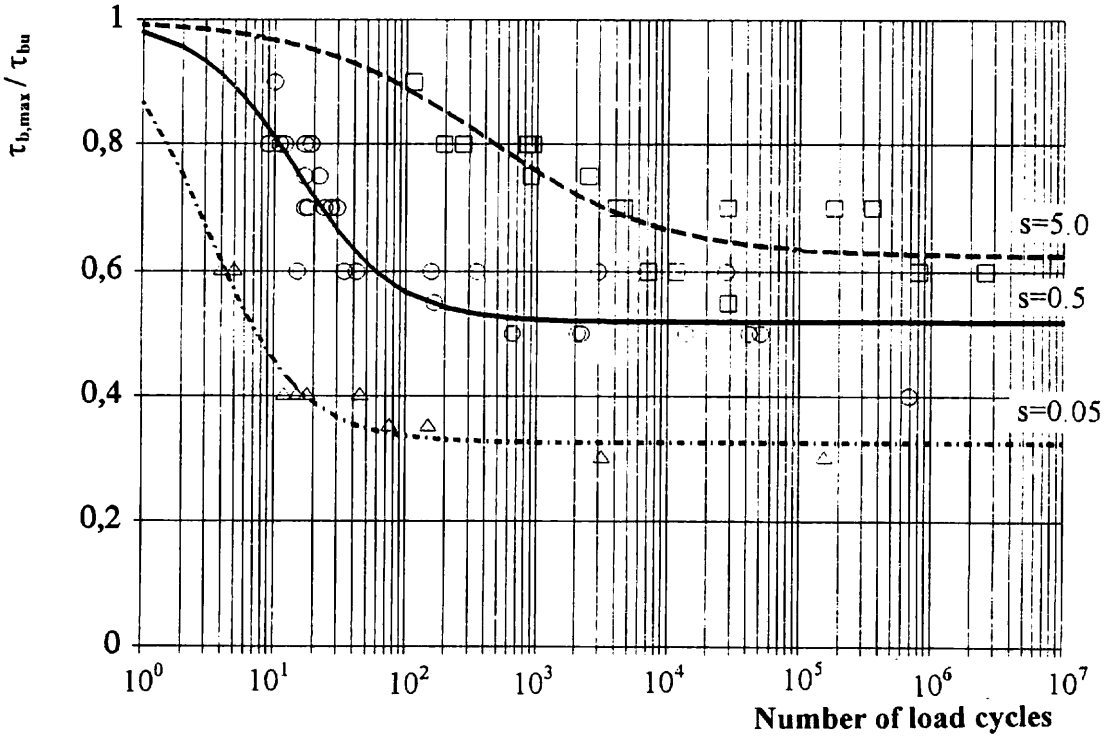

Fig.3.4 Wöhler diagrams to fatigue of bond
a) An arrow means no bond failure. Numbers beside the arrows give the number of similar tests. (Rehm and Eligehausen, 1979)
b) *Ø16, ℓ_b=5Ø, f_y=500 N/mm², f_{ccm}=30 N/mm², $\tau_{b,min}$=0.1 $\tau_{b,max}$ (Balázs and Koch 1996)*

Copyright fib, all rights reserved. This PDF copy of fib Bulletin 10 is intended for use and/or distribution only by National Member Groups of fib.

3.3.1.2 S-N (Wöhler) diagram

Above mentioned test results can be presented in so called S-N or Wöhler diagrams indicating the relationship between the cyclic stress level (here the maximum value of cyclic load related to the bond strength: $\tau_{b,max}/\tau_{bu}$) versus the number of load cycles at failure. **Fig.3.4.a** indicates the results by Rehm and Eligehausen (1979) at pull-out failure. The observed fatigue bond strength by $n=10^6$ load cycles was appr. 0.65. An influence of concrete strength (23.5 N/mm^2 and 48.0 N/mm^2) and bar diameter (8 to 28 mm) was not observed on the fatigue bond strength within the investigated range.

In case of the bond fatigue process not only the ultimate but also the serviceability behaviour of bond may control the design process (e.g. crack control). Therefore, *Wöhler diagrams may be required as a function of the slip in addition to the number of load cycles*. Above test results by Balázs and Koch (1996) are presented in **Fig.3.4.b** for s=0.05 mm, s=0.5 mm and s=5 mm (i.e. pull-out failure) indicating a four-parameter (k_0, k_1, k_2, k_3) non-linear approach proposed by Stüssi (1965):

$$\frac{\tau_{b,\max}}{\tau_{bu}} = \frac{k_0 + k_1 n^{k_2}}{1 + k_3 n^{k_2}}$$

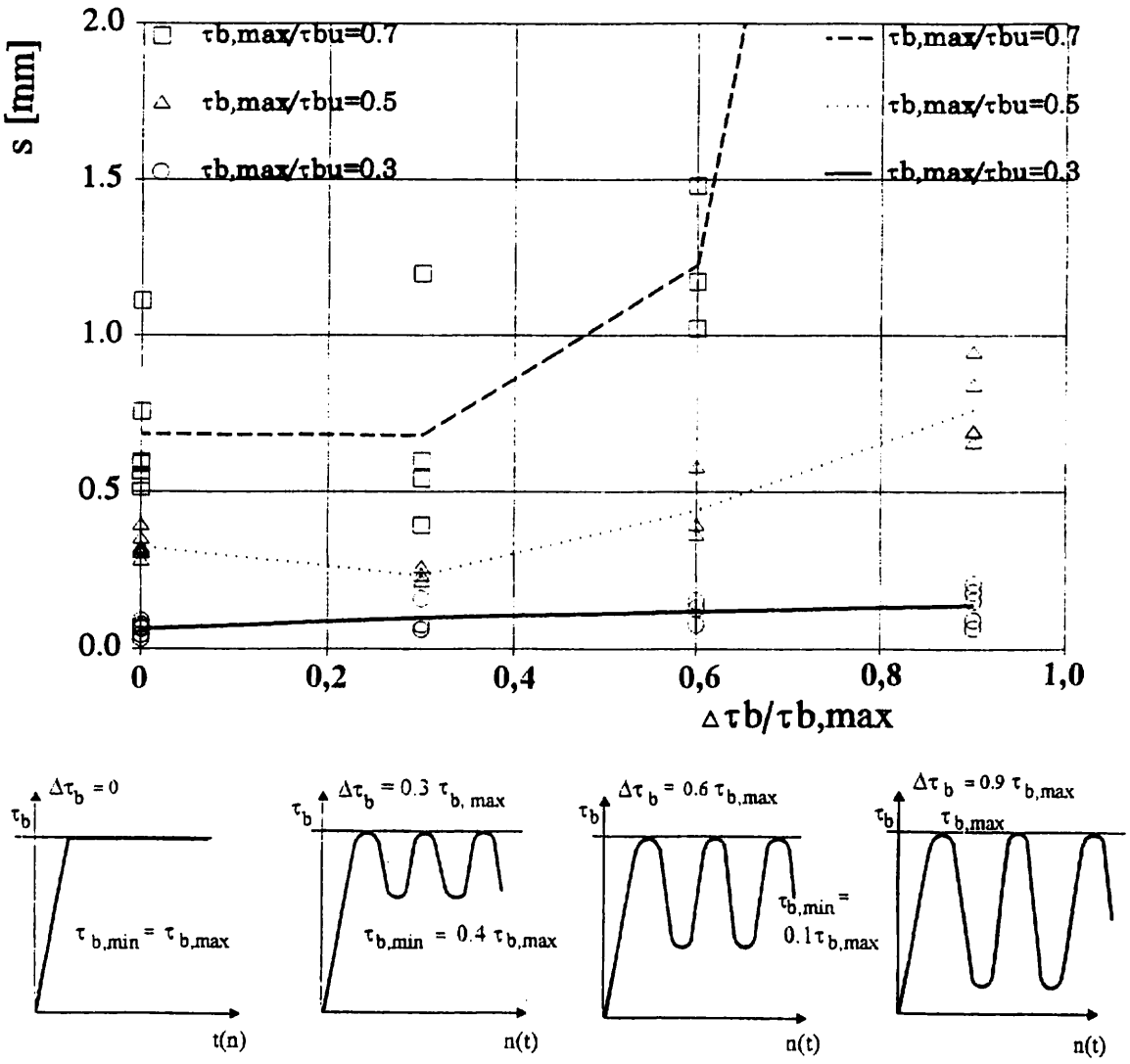

Fig.3.5 Slip increase as a function of the amplitude of the cyclic load (Balázs and Koch, 1996)

Copyright fib, all rights reserved. This PDF copy of fib Bulletin 10 is intended for use and/or distribution only by National Member Groups of fib.

A comparison of Wöhler diagrams for cyclic bond test results indicated that a presentation of the related bond stress amplitude ($(\tau_{b,max}-\tau_{b,min})/\tau_{bu}$) on the ordinate instead of the related maximum value of cyclic load ($\tau_{b,max}/\tau_{bu}$) is more reasonable. In this way all cyclic and reversed cyclic bond test results can be analysed in the same diagram even those with asymmetric amplitudes (Balázs and Koch, 1995).

3.3.1.3 Influence of the loading amplitude

Fig. 3.5 gives a comparison of cyclic pull-out test results with different amplitudes (Balázs and Koch, 1996). There are three series of results on load levels related to the monotonic bond strength: $\tau_{b,max}/\tau_{bu}$=0.3, 0.5 and 0.7 considering amplitudes related to the cyclic load level: $\Delta\tau_b/\tau_{b,max}$=0, 0.3, 0.6 and 0.9 where ($\Delta\tau_b=\tau_{b,max}-\tau_{b,min}$). The ordinate of **Fig.3.5** presents the slip after 2 million load cycles and the abscissa presents the related amplitude. Zero amplitude ($\Delta\tau_b/\tau_{b,max}$=0) means long term tests over the same testing time.

Fig.3.5 indicates that the higher the amplitude the higher the slip increase to the same cyclic load level. The slip increase is a non-linear function of the amplitude. Between $\Delta\tau_b/\tau_{b,max}$=0 to 0.3 amplitudes the influence of the amplitude is, however, almost neglectable.

3.3.2 Variable amplitude repeated loading

Distinction is made between cyclic load histories where the maximum load level is given by a formula (program loading) and those in which the amplitude is obtained by a random value generator (random loading).

3.3.2.1 Program loading

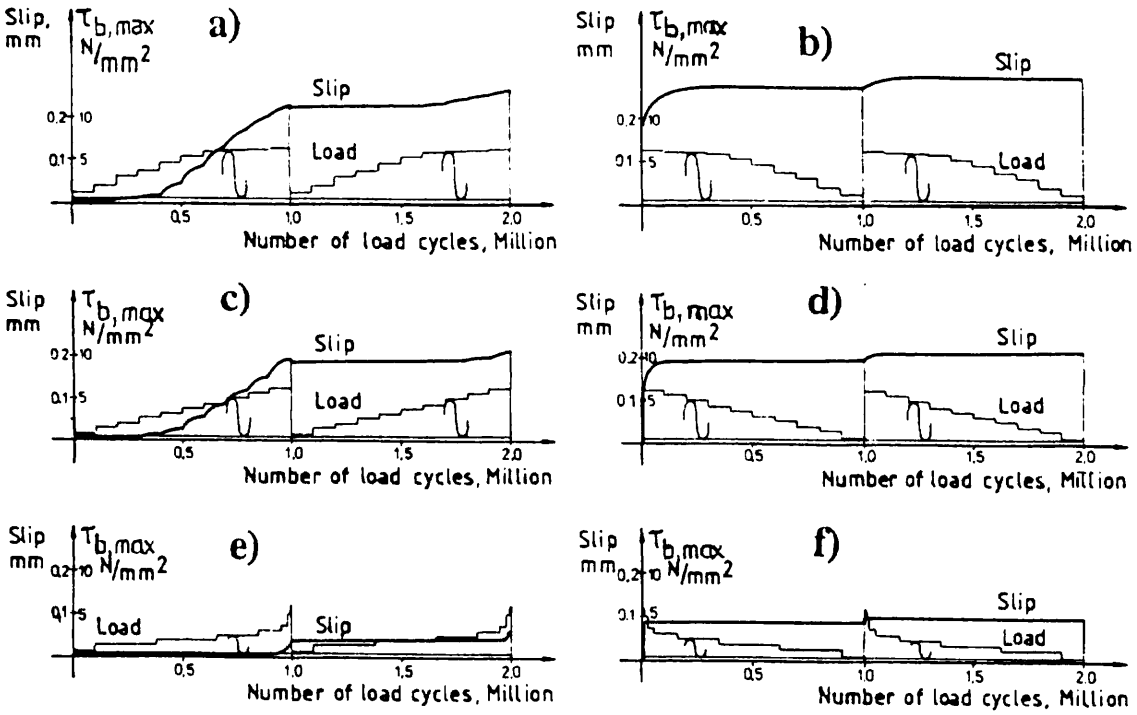

Fig.3.6 Slip increase as a function of the load history; load level: $\tau_{b,MAX}/\tau_{bu}$=0.4
a)-b) parabolically- c)-d) linearly- e)-f) logarithmically variable amplitudes
(Balázs and Koch, 1992)

In an experimental study by Balázs and Koch (1992) variable amplitude cyclic loading was applied on pull-out specimens based on load spectrum analyses of bridges and cranes. The

Copyright fib, all rights reserved. This PDF copy of fib Bulletin 10 is intended for use and/or distribution only by National Member Groups of fib.

maximum value of cyclic load had a *linearly, parabolically or logarithmically increasing or decreasing tendency*. The load histories and the observed slip versus number of load cycles relationships are indicated in **Fig.3.6**.

The length of one block in these tests was 1 million cycles. One block consisted of 10 subblocks of constant amplitude cycles.

With increasing sequence of amplitudes (**Fig.3.6.a,c and e**), the first block of loading produced a pronounced slip increase with increasing slip rate. Cycling at lower load levels in the next block, however, did not contribute to the slip increase.

With decreasing sequence of amplitudes (**Fig.3.6.b,d and f**) a significant slip increase was produced only by the highest cyclic load levels both in the first and the later blocks. Lower levels have no influence on the slip increase. The same slip development trends were observed when further blocks of loading were applied.

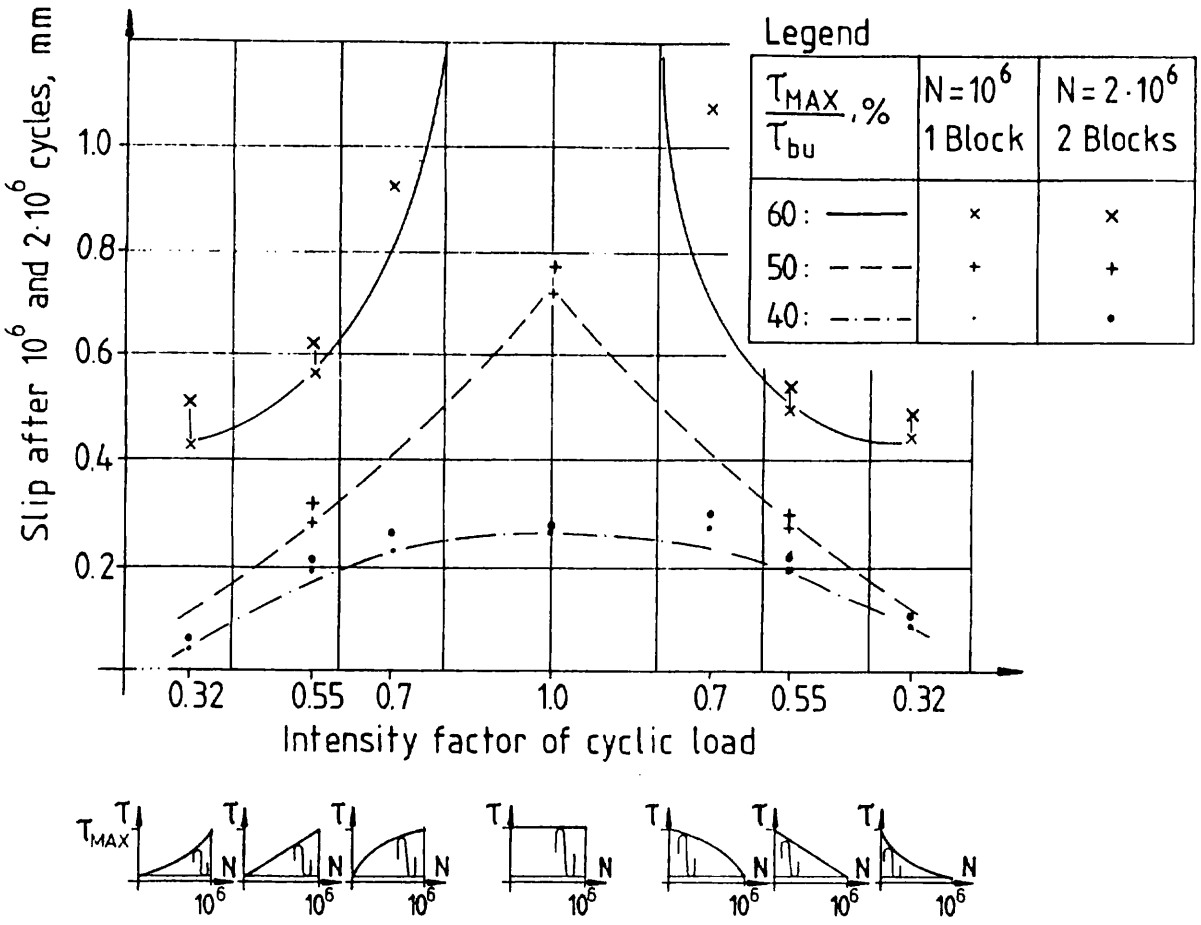

Fig.3.7 Slip increments due to 10^6 and $2\cdot10^6$ load cycles as a function of the cyclic load history and that if the cyclic load level: $\tau_{b,MAX}/\tau_{bu}$=0.4, 0.5 and 0.6 (Balázs and Koch, 1992)

Fig.3.7 compares slip increments reached during 10^6 and $2\cdot10^6$ load cycles as a function of the cyclic load history. The load histories are numerically defined as the integral of the bounding curves of $\tau_{b,max}$ related to the integral of constant amplitude loading.

They essentially describe the intensity of the cyclic load. Therefore, the obtained value may be termed as cyclic load intensity factor. **Fig.3.7** indicates that the higher the cyclic load intensity factor, the higher the slip increment.

Copyright fib, all rights reserved. This PDF copy of fib Bulletin 10 is intended for use and/or distribution only by National Member Groups of fib.

3.3.2.2 Random loading

Test results in **Fig. 3.8** are obtained by applying a series of random cyclic load levels on pull-out specimens (Balázs and Koch, 1994). One block of the load history indicates 10000 load cycles with the same amplitude, i.e. 200 blocks to 2 million load cycles. Random values were generated between 0 and 1, where 1 meant the highest value of cyclic load ($\tau_{b,MAX}$) for one specific test taken as 60, 70 and 80% of the monotonic pull-out strength (τ_{bu}). Random values smaller than 1 meant cyclic load levels $\tau_{b,max} < \tau_{b,MAX}$. **Fig. 3.8** gives a comparison to three test results on high ($\tau_{b,max}/\tau_{bu}$=0.6, 0.7 and 0.8) load levels. *The comparison clearly indicates that only load levels approaching or exceeding the previous highest level induce considerable slip increase. The contribution of low load levels is almost negligible.*

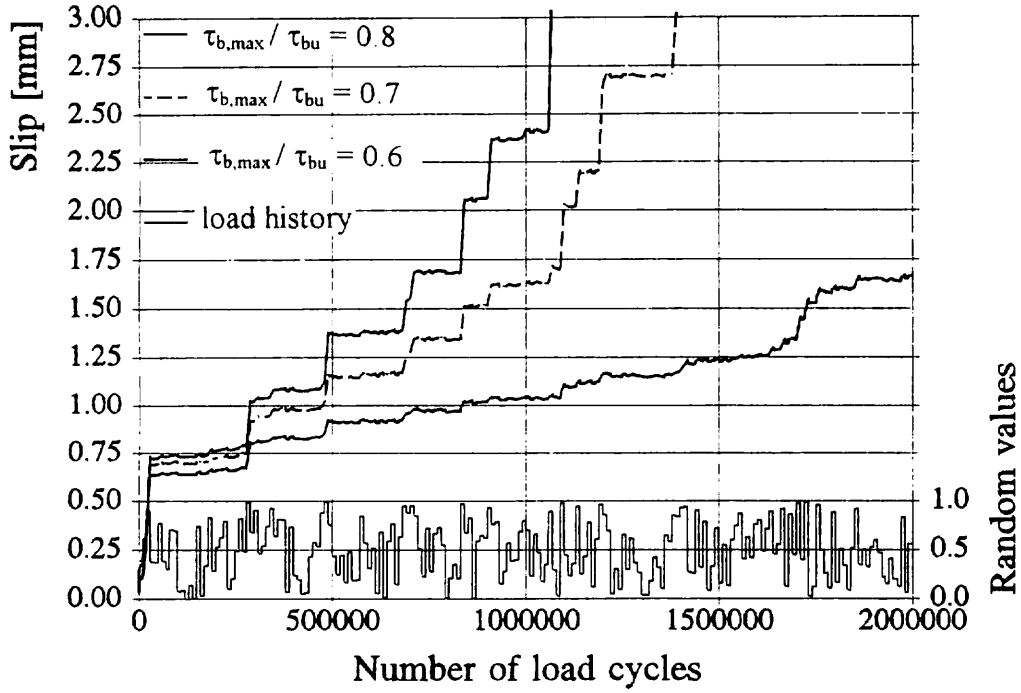

Fig.3.8 Slip increase under random cyclic loading (Balázs and Koch, 1994) parameters: Ø16, ℓ_b=5Ø, α_{sb}=0.065, f_y=500 N/mm^2, f_{ccm}=30 N/mm^2, load levels: $\tau_{b,MAX}/\tau_{bu}$=0.6, 0.7 and 0.8; $\tau_{b,min}$=0.1 $\tau_{b,MAX}$

Based on the analysis of a high number of constant and variable amplitude bond tests, Sippel (1999) developed the description of bond behaviour compared to those given in Ch. 3.3.1.1.

3.4 Reversed cyclic bond behaviour

3.4.1 Description of the behaviour

Cycles with reversed loading produce degradation of bond strength and bond stiffness that is more severe than for the same number of load cycles with unidirectional repeated loading. Degradation primarily depends on the peak slip in either direction reached previously. Other significant parameters are rib pattern, concrete strength, confining effects, number of load cycles and peak value of slip between which the bar is cyclically loaded. Under otherwise constant conditions, the largest deterioration will occur for full reversals of slip. The accumulation of bond damage is supposed to be caused by the progressive growth of microcracks and concrete microcrushing in front of the protruding lugs.

Copyright fib, all rights reserved. This PDF copy of fib Bulletin 10 is intended for use and/or distribution only by National Member Groups of fib.

The interactional behaviour under reversed cyclic loading (including also monotonic loading) may be understood through the following reasoning by Eligehausen, Popov and Bertero (1983). *When loading for the first time*, the assumed bond stress-slip relationship follows the monotonic envelop, which is valid for monotonically increasing slip (path 0ABCD in **Fig.3.9.a**). The initial slope, all other variables being equal, depends mainly on the related rib area. At low bond stresses (point A), inclined cracks begin to propagate from the top of the ribs; their growth and size is contained by the confining pressure provided by e.g. transverse reinforcement. Transfer of forces will be mostly by bearing, with a shallow angle of inclination ($\alpha \approx 30°$). Increasing the load, local crushing of the concrete in front of the lugs produces reduction of the tangent of the bond stress-slip curve (point B). When the maximum bond stress is attained the concrete key is sheared off, forming a cone with a length of about four times the lug height. At this point the line of action of the force is at an angle of about 45°. With increasing slip the bond stress will begin to drop slowly. As the bond cracks reach the bottom of the adjacent lug (point D) the bond stress begins to drop, and by the time the slip has reached the lug spacing only the frictional component remains (point E).

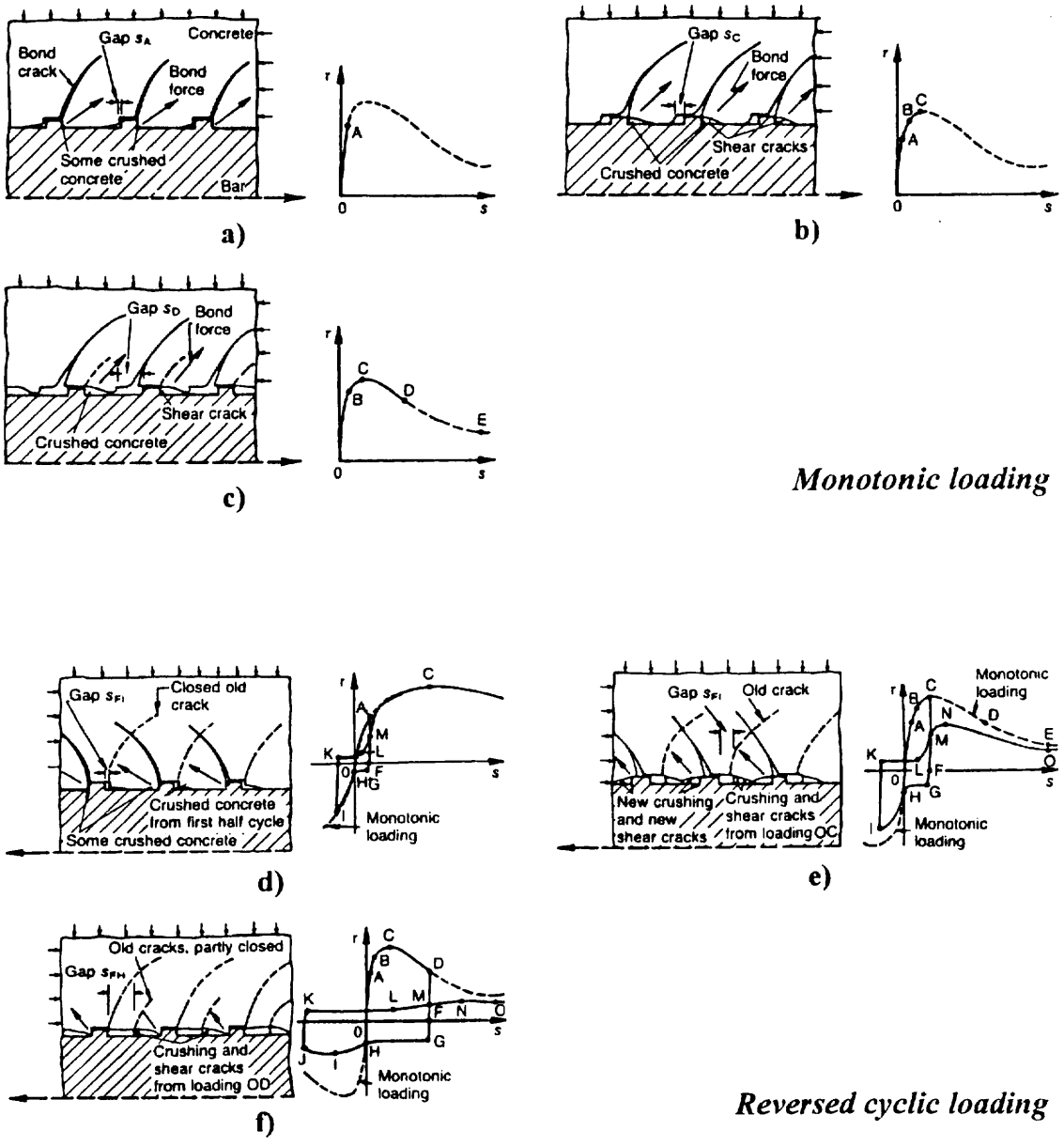

Fig.3.9 *Qualitative explanation of bond mechanism: Eligehausen, Popov, Bertero (1983), CEB (1991)*

Copyright fib, all rights reserved. This PDF copy of fib Bulletin 10 is intended for use and/or distribution only by National Member Groups of fib.

Under load reversals (**Fig.3.9.d, e, f**), the initial loading follows the monotonic curve, but the cyclic load behaviour is sensitive to the level of slip at which the reversal occurs. Three possible qualitative models have been proposed, depending on whether or not inclined cracks have formed. In the first case (**Fig.3.9.e**) imposing a slip reversal at an arbitrary slip value below the level where inclined cracking occurs, results in a stiff unloading branch (path AF) because only a small part of the slip is caused by inelastic concrete deformations. As soon as slip in the opposite direction is imposed, the friction branch is reached (path FH). The slope of this portion of the curve is small because the surface of the concrete surrounding the bar is smooth. As soon as the cracks close, the stiffness differs little from that of the monotonic envelop (point I).

Unloading from point I, where the slip in the two directions is about equal, the curve (path IKL) is very similar to that from the initial unloading curve (path AFH). The major difference is that due to previous cracking and crushing of the concrete in front of the ribs, the point where the bond stresses begin to pick up again (point L) will be shifted to the right of the origin. The lug will not be bearing fully until point M is reached. Further loading follows the bond-slip curve up to the monotonic envelop.

If unloading occurs after the inclined cracks have formed (**Fig.3.9.f**), and therefore near the slip at which ultimate bond stress has been attained, the unloading path is similar to that of the first case up to the point F. Since there is more damage to the concrete, a higher frictional resistance is mobilized (point G). When the loading is reversed the lug presses against a key whose resistance has been lowered by inclined cracks over a part of its length that were induced by the first half-cycle. The splitting cracks created in the first half-cycle close at a higher load than those of the first case (point H), and lead to an earlier formation of splitting cracks in the opposite direction. Splitting cracks, combined with the existing inclined cracks along the bar, result in a reduced envelop (path HI) and a reduction of bond capacity in the second direction (point I). Unloading from this peak (path IKLMN) and reversing the load results in a reduced stiffness and strength because only the remaining uncrushed concrete between the lugs must be sheared off. The bond strength (point N) is substantially lower than that of point C, and lower than that of point I.

In unloading occurs after the slip has reached a value much larger than the slip at maximum strength (point C), the behaviour will be very poor (**Fig.3.9.g**). Since more damage has occured, the frictional resistance (point G) will be larger than for either of the previous cases. However, since the concrete between the lugs is completely sheared very little force can be transmitted by bond when direction of loading is reversed (path HIJ). Unloading and reloading in the opposite direction (path JKLMN) results in very little additional bond capacity beyond that provided by friction since most of the mechanical anchorage has been lost.

Degradation of the bond-slip relationship under slip controlled load reversals for small slip values (±0.44 mm), for slip values in the range of the bond strength (±1.65 mm) and for high slip values (±4.57 mm) are shown in **Fig.3.10** based on test results by Eligehausen, Popov and Bertero (1983). These indicate that the degradation primariliy depends on the peak slip reached previously in either directions.

Whenever the load cycles are limited to produce slip in one direction only, there is not very significant degradation of the bond strength (Hawkins et al., 1982).

Load reversals between increasing slip values (**Fig.3.11**) indicated that there is a reduction both in the bond strength and in the corresponding slip under reversed cyclic loading compared to monotonic loading (Balázs, 1991).

3.4.2 Analytical models

A relatively short overview of the analytical models for reversed cyclic bond behaviour is given herein, because almost all nowadays available models were summarized in the state-of-the-art report by CEB (1991, 1996).

The first analytical model for reversed cyclic bond behaviour was proposed by *Morita and Kaku (1973)*. After cycling between arbitrary slip values, it is assumed that the monotonic

Copyright fib, all rights reserved. This PDF copy of fib Bulletin 10 is intended for use and/or distribution only by National Member Groups of fib.

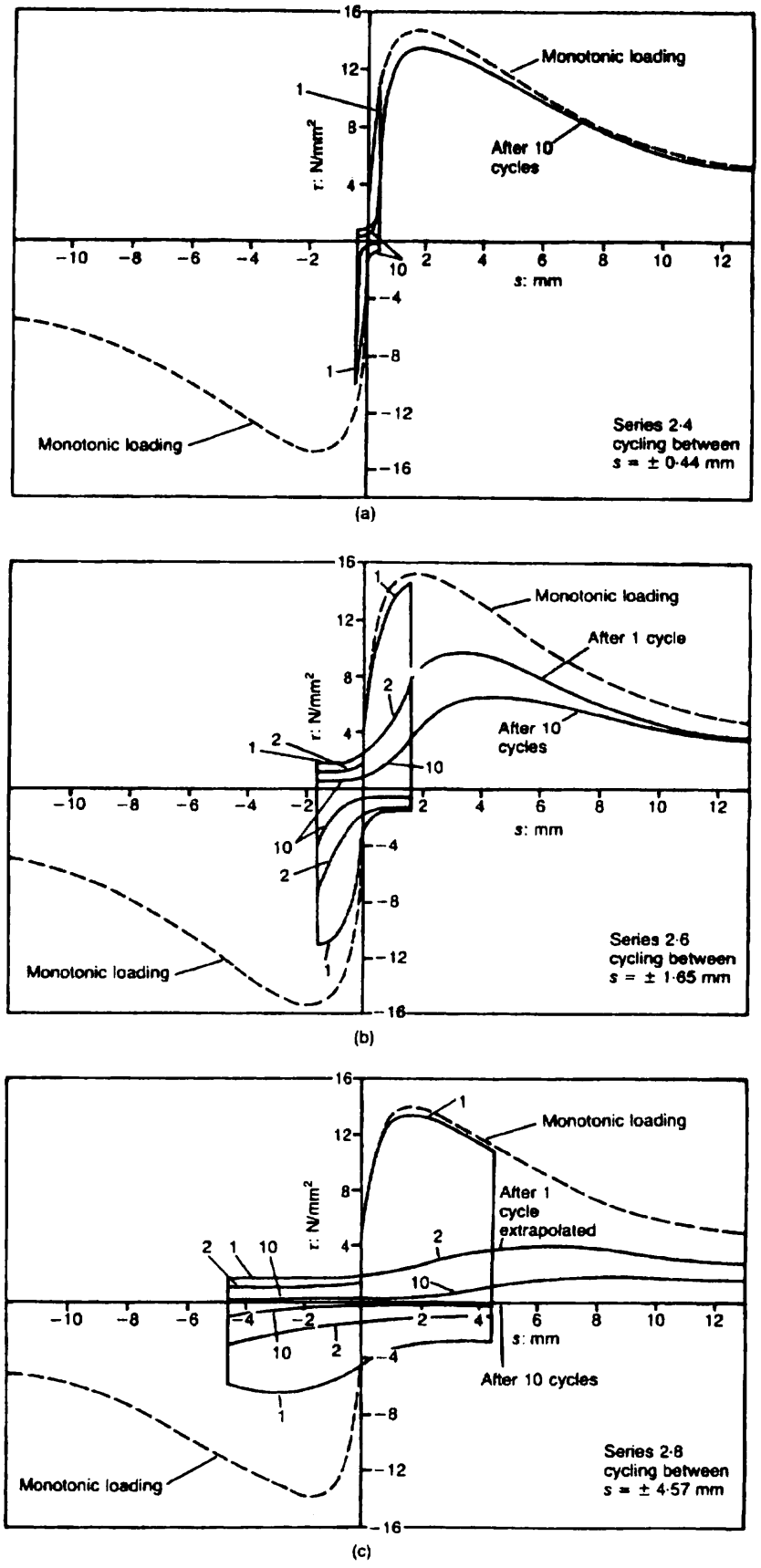

Fig. 3.10 Experimental bond stress-slip relationships for various slip controlled load reversals; Eligehausen, Popov and Bertero (1983)

Copyright fib, all rights reserved. This PDF copy of fib Bulletin 10 is intended for use and/or distribution only by National Member Groups of fib.

envelop is reached at slip values larger than the peak value in the previous cycle and followed thereafter. The model is sufficiently accurate for small number of cycles between relatively small slip values, however, it is inaccurate for several load cycles, and it is not valid for larger slip values.

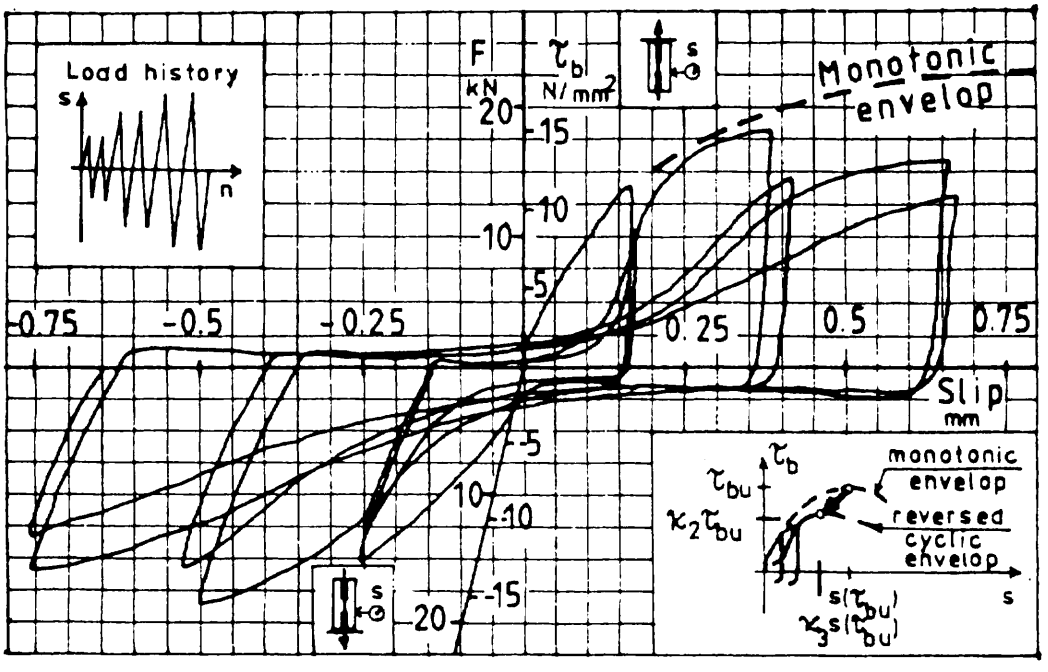

Fig.3.11 Deterioration of the envelop curve under reversed load cycles; Balázs (1991)

Tassios' model (1979) was an improvement so far as the descending branch of the local bond stress-slip relationship is given and the influence of load cycles on bond deterioration for slip values smaller than or equal to the peak slip value of the previous cycle is taken into account (**Fig.3.12**). Bond stresses in the reversed direction are reduced by one-third compared to the monotonic envelop.

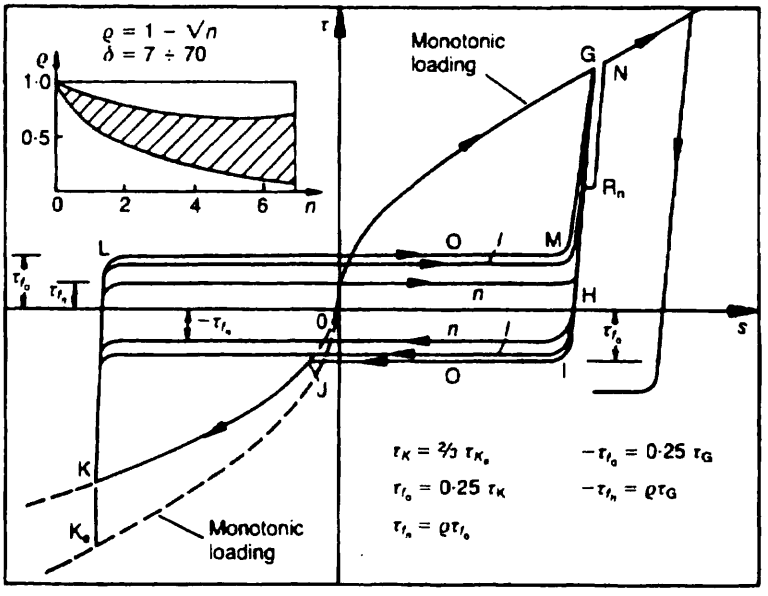

Fig.3.12 Model for reversed cyclic bond behaviour proposed by Tassios (1979)

Copyright fib, all rights reserved. This PDF copy of fib Bulletin 10 is intended for use and/or distribution only by National Member Groups of fib.

Model by Viwathanatepa et al. (1979) was a major improvement, however, in spite of being rather complicated, it is not general enough. Some 20 parameters that are needed have no physical meaning and must be evaluated from test results.

Model by Hawkins et al. (1982) uses a monotonic envelop that is idealized by a trilinear bond stress-slip relationship. The characteristic values of slip, bond stresses and tangents are obtained by statistical evaluation of test data yielding to three linear equations. The model is applicable for low as well as for high slip values. The ascending branch of the trilinear approach for the cyclic envelop give reasonable values for slip values higher than in the previous cycle but relatively rough approach for lower ones owing to the low loading modulus. Frictional bond stress formulated as the previously reached maximum bond stress does not satisfactorily follow force-controlled reversed cycles.

Model by Ciampi et al. (1982) intends to take into account the significant parameters that appear to control the behaviour observed in tests. Reduced cyclic envelops are obtained from the monotonic envelop by decreasing the characteristic bond stress τ_1 and τ_3 **(Fig.3.13)** through reduction factors which are formulated as a function of the so called damage parameter, d. For no damage, d=0, i.e. the reloading branch reaches the monotonic envelop. For full damage, d=1, bond is completely destroyed. It was assumed that the damage parameter is a function of the total dissipated energy only. However, it has also been taken into account that only a fraction of the energy dissipated during subsequent cycles between fixed peak slip values appears to cause damage, while the other part appears to be used to overcome the frictional resistance and is transformed into heat.

In the model by Pochanart and Harmon (1989) the deterioration of the bond strength is obtained by the maximum total excursion and a strength model. Their model appears to be able to predict a wide range of bond-slip behaviours, including the results of both slip controlled and force controlled tests from 100 to 40 000 cycles (the limits were given by the authors). The behaviour under cyclic loading can be predicted reasonably well by repeated applications of a simple damage law applied to the reduced envelop. The shifting of the ordinate axis of the bond-slip co-ordinate system is a visual interpretation of the slip increase without an increase of bond stress during the frictional bond behaviour, however, the value of shifting and the shape of the ascending branch may need more specific studies.

Model by Balázs (1991) summarizes the characteristics observed in bond behaviour under slip controlled or force controlled load reversals. A reversed cyclic envelop is defined considering reductions of both the bond strength and that of the related slip. The reductions depend on the actual load history, the number of load reversals and the maximum previous slip. The deterioration of bond during a slip controlled test is represented by the decrease of the maximum bond stress itself. During a force controlled test the deterioration is indicated by a remarkable slip increase. Following slip controlled load reversals, the maximum bond stress decreases asymptotically. The frictional bond stress increase force controlled load reversals and decreases during slip controlled reversals, consequently the frictional bond stress is a function of the actual slip and the number of previous load cycles. Its maximum value is approximately 70 % of the residual bond stress obtained after the concrete between bar lugs is sheared off.

3.5 Concrete under repeated loading

Failure of bond in concrete using steel reinforcing bars takes place in the concrete layer surrounding the bar giving a possibility for comparisons in fatigue behaviour of bond and concrete, respectively.

Fatigue of concrete is a process of progressive internal structural changes which may be observed as increase in strains **(Fig.3.14.a)**. Observations on the fatigue of concrete structures is summarized in CEB (1988).

Both the *strain versus number of load cycles diagrams under constant amplitude repeated loading* obtained on compressed concrete cylinders by Holmen (1979, 1982) and prisms by Sparks (1982) as well as on tensioned cylinders by Cornelissen (1984) indicate three different

Copyright fib, all rights reserved. This PDF copy of fib Bulletin 10 is intended for use and/or distribution only by National Member Groups of fib.

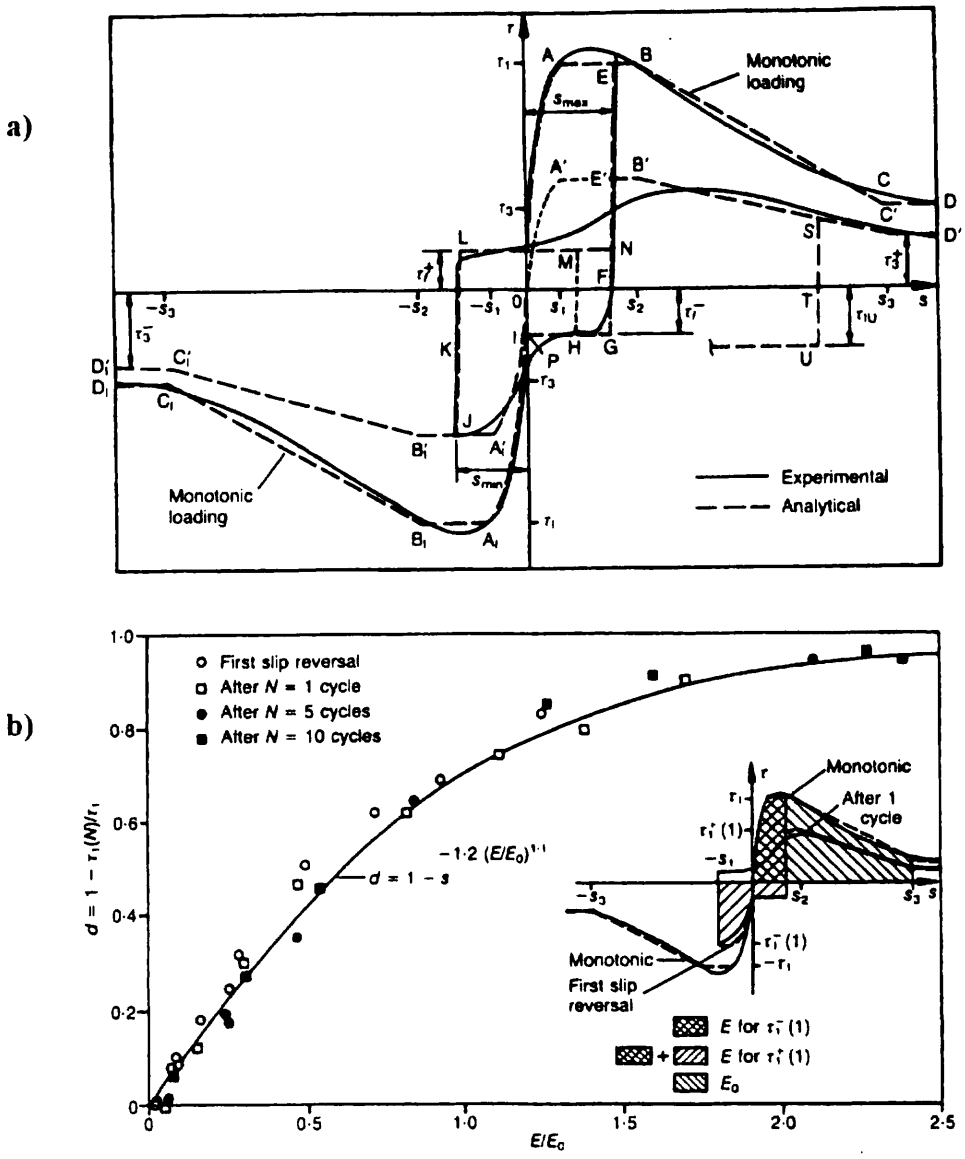

Fig.3.13 Analytical model by Ciampi et al (1982)
a) Bond stress-slip relationship
b) Damage parameter, d, as a function of the dimensionless energy dissipation

phases (**Fig.3.14.b and c**). The only difference produced by the compressive or tensile repeated load is that the ascending branch before failure is relatively short in the case of repeated tensile loading. Holmen (1979, 1982) distinguished the three phases for cyclic compression in the following way: first rapid increase of the strain from 0 to about 10 % of the failure strain, which is followed by a uniform increase from 10 to 80 % and then a rapid increase until failure. The variation of the total strain seemed to be independent of the number of load cycles to failure (provided that the duration of the test was less then a few ours - in tests of longer duration the total strain increased faster.)

The above three phases of the stress vs. strain diagram were distinguished in the fracture mechanics approach by Mihashi and Izumi (1984). Hordijk (1991) contributed to the fracture mechanics modelling of concrete in fatigue.

Considering the waveform of repeated load, Tepfers, Görlin and Samuelsson (1973) concluded their tests that a cyclic load with a rectangular waveform causes considerably larger deformations in the concrete after the same number of load cycles than sinusoidal or triangular waveforms and causes also failure after the least number of load cycles.

Copyright fib, all rights reserved. This PDF copy of fib Bulletin 10 is intended for use and/or distribution only by National Member Groups of fib.

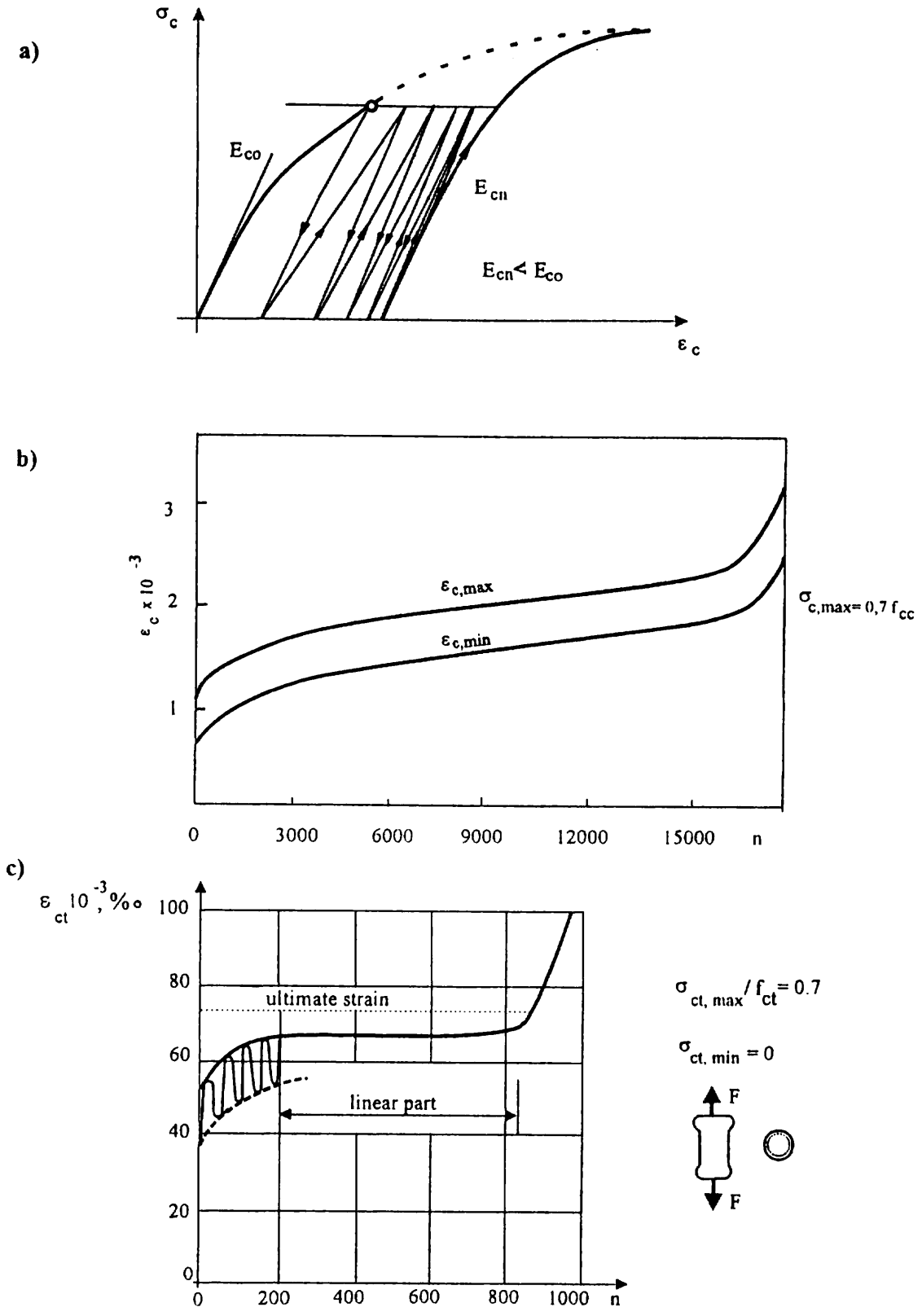

Fig.3.14 Fatigue of plain concrete
a) stress vs strain diagram
b) concrete compressive strain (under max. and min. levels of the cyclic load) vs. number of load cycles diagram obtained on concrete prism (Sparks, 1982)
c) concrete tensile strain vs. number of load cycles diagram obtained on concrete cylinders (Cornelissen, 1984)

Copyright fib, all rights reserved. This PDF copy of fib Bulletin 10 is intended for use and/or distribution only by National Member Groups of fib.

The total *maximum strain* by failure both for tension and compression seemed to be independent of the sequence effect and the load history (Cornelissen 1984, Holmen, 1982). The absorbed energy to failure was found to be the same for static and for fatigue load with different intensities (Tepfers, Hedberg and Szczekocki, 1984).

The secant modulus of elasticity reduces during the fatigue life. The lower the stress level the larger the decrease, but at failure it seemed to approach a common limit equal to about 60 % of its initial value (Holmen, 1982).

Several attempts were made to approve or disapprove the linear cumulative damage hypothesis by Palmgren (1924) and Miner (1945). Siemens (1982) found the *Palmgren-Miner hypothesis* in variable amplitude loading remarkably good. However, Holmen (1979, 1982) found that variable amplitude loading seems to be more damaging than predicted by the Plamgren-Miner hypothesis. Holmen obtained Palmgren-Miner sums ranging from 0.3 to 1.68. Holmen explained it with the sequence effect which is not taken into account by the hypothesis.

In tests by Oh (1991) the Palmgren-Miner sum was found to be greater than 1 when the magnitude of fatigue loading is gradually increased and less than 1 when the magnitude of loading is gradually decreased. Oh (1991) proposed a non-linear cumulative damage theory which intends to take into account the influence of the magnitude and the sequence of the variable amplitude fatigue loads.

In contrary to steel *no fatigue limit of concrete* was found meaning that no stress level is known where the fatigue life will be infinite (Holmen 1979, 1992, Cornelissen 1982).

Fatigue tests on ***high strength concrete*** (C65...C95) was studied by Petković (1991, Petković et al. 1990) indicated no reason for distinguishing between the fatigue properties of normal strength and high strength concretes in design rules, when the load levels are expressed relatively to the static strength of the concretes.

From test results with ***reversed cyclic loading*** Tepfers (1982) concluded that the stress reversals may not negatively influence the fatigue strength of concrete. The explanation may be that the tension and compression acting in the same direction mainly form micro-cracks transverse to the tensile stresses and consequently parallel to the compressive stresses. The two transverse crack populations thus formed may not have an additive effect on degrading the concrete.

3.6 Numerical analysis of bond under repeated loading

To transfer tensile forces from reinforcement into concrete one has to rely on the bond resistance. The behavior of reinforced concrete elements under monotonic or repeated actions can be highly dependent on the interaction between reinforcement steel and concrete. This is especially true for structures or parts of the structural members which have to transfer large tensile forces from reinforcement into concrete (beam-column connections, splices, fastening elements etc.). In such cases the bond resistance (strength) should be high enough and it has to assure a ductile structural response.

In the past a number of experimental investigations have been carried out in order to clarify and understand behavior of deformed bars pulled out from a concrete block under monotonic and cycling loading. The results, which are in the literature well documented (CEB 230, 1996), show that reversed cycling loading causes a degradation of bond resistance and significant pinching effect. Based on the experimental results, some explanations for this behavior has been offered. However, the reason for the bond degradation and development of cracks in concrete during reversed cycling loading have not been fully understood. Based only on the experimental results it is difficult to filter out the influences of different material and geometrical parameters such: (a) concrete and steel properties, (b) rib size, shape and their distance and (c) the influence of boundary conditions. In order to do this one has to use the numerical analysis.

Copyright fib, all rights reserved. This PDF copy of fib Bulletin 10 is intended for use and/or distribution only by National Member Groups of fib.

3.6.1 Finite element analysis

Numerical modeling of cyclic bond behaviour by the use of the finite elements is principally possible from two different modeling levels: *(1) Phenomenological modeling* based on the bar-concrete interface type of formulations and *(2) detailed analysis* based on the macroscopic or microscopic material models where the geometry of the bar-concrete connection (ribs) are discretized.

3.6.1.1 Phenomenological (macroscopic) modeling

In the phenomenological models concrete and reinforced concrete members as well as steel bars are modeled by two- or three-dimensional finite elements. The link between the steel bar and concrete can be realized either by a continuous or discontinuous connection. These models are generally not able to automatically predict the bond resistance for general geometrical conditions. For instance, it is not possible to model the influence of the rib geometry as well as the influence of their spacing on the bond resistance, i.e. these properties should be in advance stored in the bond model.

The bond model can be formulated based on the continuous or discontinuous approach. In the continuous (smeared) approach the macroscopic cyclic stress-strain constitutive relationship has to be employed. In the second, discontinuous approach, the bond relationships are defined by discrete elements (springs) whose behaviour is controlled by the stress-slip (displacement) relation. If we use realistic constitutive relations, not only for bond but also for surrounding concrete, both models are able to predict the cyclic bond resistance for different geometrical configurations of concrete structure, i.e. for different boundary conditions.

(1) Continuous connection – smeared approach

In case of the continuous connection perfect bond between steel bar and concrete is assumed. The steel bar is represented by simple linear (truss) finite elements that are connected with two- or three-dimensional concrete finite elements. The bond around the steel bar (truss element) is modeled by surrounding two- or three-dimensional concrete finite elements. The constitutive law of these elements is defined by usual macroscopic constitutive stress-strain relationship of concrete. The constitutive law has to be able to realistically predict the concrete behavior for two- or three dimensional cyclic loading. The type of the analysis may be *local* or *nonlocal*.

The local type of the analysis has to be based on the so called crack band approach (Bazant and Oh, 1983). Namely, in order to prevent strong influence of the mesh size on the bond resistance one has to assure that the total energy dissipation due to bond-slip, as observed in experiments, is localized into a shear band h. Furthermore, h should be chosen such that the used stress-strain constitutive law for concrete assures a realistic peak resistance and displacement (slip). The size of the concrete finite elements around the bar-(truss finite element) should be equal to the width of the shear band. According to present experience with this type of models, if the usual macroscopic properties for concrete are used, the realistic width of the shear damage zone is approximately $h = 30 - 60$ mm (Ozbolt et al., 1997).

The resulting shear-slip (τ_b-s) relationship is controlled by the local constitutive law for concrete and the size of the concrete finite elements around the steel (truss) element. The bond stress for each truss element is calculated as $\tau_e = F_e / (\phi \pi l_e)$ with F_e = the force in the truss element, ϕ = the bar diameter, l_e = the length of the truss element. The corresponding slip is obtained as $s_e = \gamma_e h$ with γ_e = shear deformation of surrounding concrete finite elements.

The other possibility to avoid mesh sensitivity in a continuous (smeared) fracture type of the analysis is the use of the so called higher order methods (Cosserat continuum, nonlocal integral or gradient approach; Bazant, 1991;). In these methods damage localizes into a volume of the material whose size is independent of the mesh size (Mazars and Pijaudier-Cabot, 1990). The size of the damage localization zone, shear damage zone for the bond analysis, is controlled by the so called localization limiter known as the characteristic length. Physically the size of the characteristic length is related to the maximum aggregate size d_a (Bazant, 1991). The size of the damage zone h depends on the characteristic length l and on the local constitutive law.

Copyright fib, all rights reserved. This PDF copy of fib Bulletin 10 is intended for use and/or distribution only by National Member Groups of fib.

According to the experience with the nonlocal integral methods, the bond behavior can be well simulated using usual macroscopic constitutive laws for concrete with the characteristic length $l = d_a$ (Ozbolt et al., 1996). This leads to the size of the damage shear zone of approximately $h = 3d_a$. If the maximum aggregate size is assumed to be 12 to 20 mm than the size of the shear damage zone yields to approximately $h = 3d_a = 36$ to 60 mm. This agrees well with the experience made so far by the local (crack band) type of modeling ($h = 30$ to 60 mm). The resulting shear-slip (τ_b-s) relationship in the nonlocal methods is calculated in the same way as described for the local approach.

(2) Discrete approach – bond interface models

In contrary to the smeared type of modeling, in discrete models the reinforced bar (truss element) is not directly connected with the surrounding elements i.e. the connection is realized over interface elements. At each connection node the interface element must be defined by a component normal and tangential to the bar direction. The component normal to the bar direction is controlled by the stress-crack opening law and the tangential (bond) component by an shear-slip relationship. To be able to correctly model the influence of the boundaries for general concrete geometries, the bond resistance (tangential component) should depend on the normal component i.e. on the confinement. These relations are for the general cyclic loading rather complex (CEB, 1996). Therefore, from this point of view are models based on the smeared approach the more general since once the constitutive law for concrete is formulated the cyclic bond-slip relationship comes out from the finite element analysis automatically.

A new interface model has been recently developed by Lundgren and Gylltoft (1998). The model uses the *concept of damaged/undamaged deformation zones* indicating that after applying a reversed slip only an almost constant, low bond stress exists until the previous bond-slip curve is reached. A hardening parameter is also established that will be almost equivalent to the axial slip. Concrete was modelled with a constitutive model based on non-linear fracture mechanics with a combined Drucker-Prager and Rankine elasto-plastic model. The FE models were axisymmetric; the localization of the deformations due to cracking of the concrete was then smeared over the concrete elements assuming that there were four radial cracks in a cylinder. Yielding was modelled using associated flow and isotropic hardening. Comparisons to test results including monotonic and reversed cyclic loadings are indicated in **Fig.3.15**.

3.6.2 Detailed analysis

This analysis makes possible to get a better insight into the physical mechanism of bond behavior under cyclic loading. Furthermore, it makes possible to study the influence of the reinforced bar size as well as the influence of the rib geometry and their spacing on the bond resistance. The steel bar and the shape of the ribs are exactly modeled. The surrounding concrete can be represented by an macroscopic continuous or discontinuous material model for concrete. The detailed analysis can principally be able to correctly predict the concrete behavior under general 3D cyclic loading conditions.

An continuous material model should not be used in the same sense as in the phenomenological type of the bond analysis. Namely, the size of the finite elements in the bond zone are approximately of the same order of magnitude as the rib size i.e. the elements are much smaller than the concrete aggregate size (Darwin et al., 1994; Ozbolt and Eligehausen, 1992). Furthermore, due to the very limited size of the loading (contact) zone under the ribs, the concrete is loaded very locally. Consequently, in that zone one should not use standard macroscopic concrete properties. The analysis results show that with the use of the macroscopic concrete properties one can realistically model the resistance however, the deformability (slip) is underestimated by factor of 10 (**Fig.3.16**) (Ozbolt and Eligehausen, 1992). In contrast to this, the experimental evidence indicate at about the same resistance (bond strength) much larger slip i.e. the locally loaded material generally exhibit softer behavior. The reason for this is partly due to the contact problem between the rib and the concrete and partly it is a consequence of the fact that the concrete is loaded in zones between larger aggregate pieces (mortar), which is porous and possibly with a number of microcracks and therefore softer. Note, that when the loading zone is small, the volume of the pores is relative to the volume of the loading zone large, what means lower stiffness of that zone. (Further details on these investigations are given in Chapter 1.5.)

Copyright fib, all rights reserved. This PDF copy of fib Bulletin 10 is intended for use and/or distribution only by National Member Groups of fib.

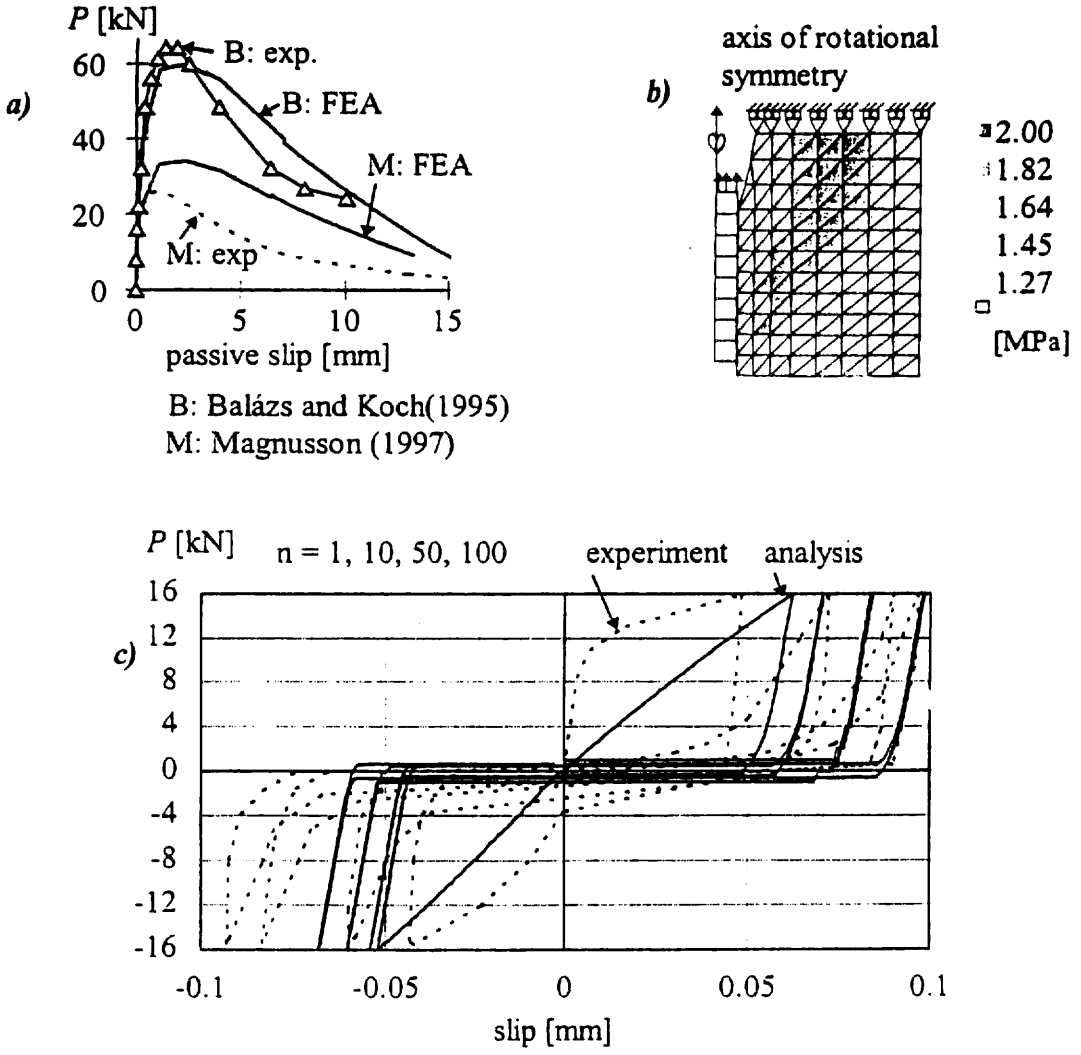

Fig.3.15 Load vs. slip diagrams for pull-out tests. Lundgren and Gylltoft (1998)
a) monotonic pull-out tests
b) finite elements and tangential stresses
c) reversed cyclic loading

The detailed type of the analysis may also be performed by employing an discrete (micromechanical) type of model for concrete such as random particle or Lattice models (Roelfstra et al., 1985; Bazant et al., 1990; van Mier and Vervuurt, 1995). In these models one needs to specify the uniaxial cyclic rules for each particle (truss element) and the macroscopic material response comes automatically out. Due to the large computational demand the experience with these models is so far limited only on two-dimensional problems. Similar as the continuous models the properties of these models in the bond zone are not the same as those used for the macroscopical concrete analysis i.e. they have to be adopted in order to be able realistically *predict the local behavior of concrete in small volume under the ribs.*

According to the numerical experience with the continuous models and the comparison with the experimental evidence, the initial stiffness of the local material zone should be reduced approximately by a factor of three to five compared to the macroscopical initial properties of concrete (Ozbolt et al., 1998). Furthermore, the peak resistance should be set approximately the same as for the macroscopic properties. The strains at peak stress should also be three to five

Copyright fib, all rights reserved. This PDF copy of fib Bulletin 10 is intended for use and/or distribution only by National Member Groups of fib.

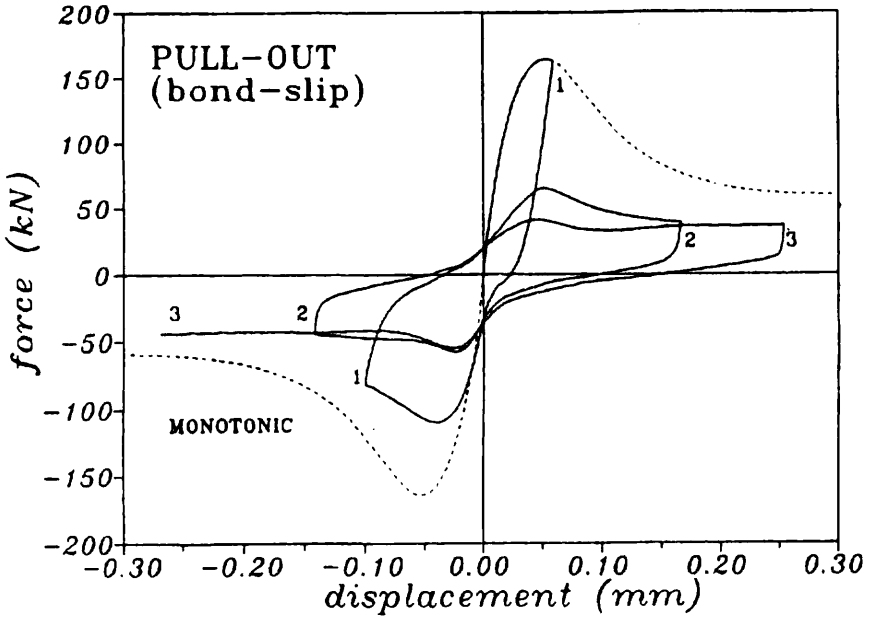

Fig.3.16 Reversed cyclic bond-slip relationship obtained by finite element analysis. Ozbolt and Eligehausen, 1992

times larger than in the case of macroscopic concrete properties. It is normally assumed that the shear resistance as well as resistance under uniaxial tensile (concrete fracture energy) and compressive stresses are the same as observed for macroscopic concrete properties. The size of the material zone with the local concrete properties should approximately be proportional to the bar diameter.

When the continuous model is employed the analysis must be of the local type since in such a relatively small volume the nonlocal type of the analysis has no sense. However, to assure the objectivity of the analysis with respect to the energy consumption capacity as a consequence of damage one has to adopt the constitutive relationship to the size of the finite element i.e. the crack band approach should be used. Due to the fact that the finite elements are relatively small (approximately 1 to 3 mm), the stress-strain curve for uniaxial tension is relatively ductile i.e. almost elasto-plastic.

3.6.3 Numerical example

In order to illustrate the application and importance of the bond resistance on the structural cyclic response an example of the three-dimensional cyclic analysis of beam-column connection (**Fig.3.17**) made of normal concrete is shown (Ozbolt et al., 1998). It is well known that the resistance of the beam column connections rely on the bond resistance since the reinforcing bars have to transfer the tensile force from the beam into concrete by bond stresses. The connection must assure enough structural resistance and at the same time it should provide sufficient ductility which is important for energy dissipation during cyclic (seismic) loading.

In the numerical analysis the material and geometrical properties are taken the same as in the experiment (Ehsani and Wight, 1986). The bond was modeled by using a phenomenological continuous type constitutive law (cyclic microplane model for concrete; Ozbolt et al., 1996). **Fig.3.18** shows calculated and in experiment obtained load-displacement curve. The load and displacement were monitored at the beam cantilever end. As may be seen from **Fig.3.18** the agreement between experimental and numerical data is good. Both results show a decrease of the structural resistance when the number of loading cycles increases. Furthermore, from both results

Copyright fib, all rights reserved. This PDF copy of fib Bulletin 10 is intended for use and/or distribution only by National Member Groups of fib.

the pinching effect which is typical for shear i.e. bond type of behavior. **Fig.3.19** shows typical "X" formed damage zones obtained in the numerical analysis and plotted in terms of the principal strains. Not going into the detailed analysis of the numerical results, it is obvious that the present type of cyclic bond modeling realistically predicts the structural response.

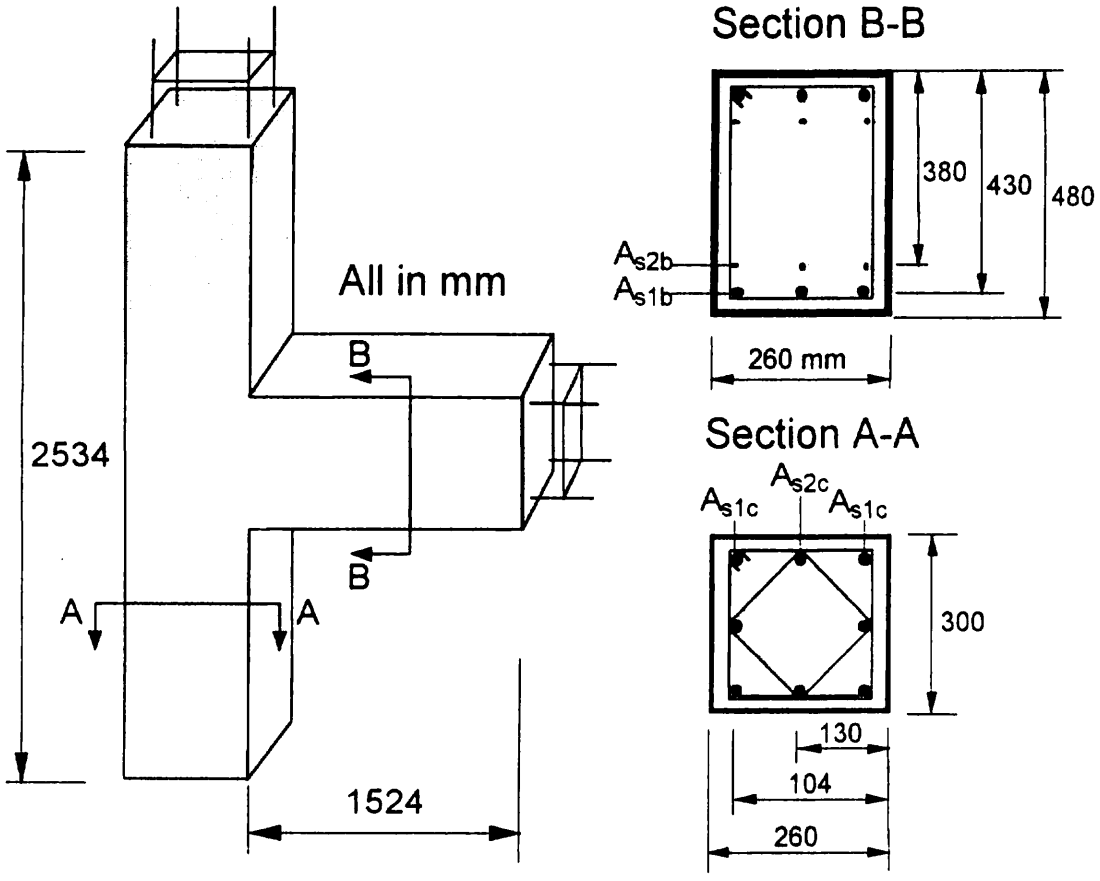

Fig.3.17 Geometry of the beam-column connection (Ozbolt, Li and Eligehausen, 1998)

3.7 Conclusions

Repeated loading

Repeated loading produces increase in slip between reinforcing bar and concrete. The rate of slip increase is governed by the load level, frequency of load, shape of load function, strength of concrete, confining effects, etc. Fatigue bond failure may occur either by pull-out of the bar or by splitting of the concrete cover.

Tests with constant amplitude and with variable amplitude repeated loading indicated that the upper bound of test results (concerning slip development) is reached by the constant amplitude loading. The higher the integral of the load history, the higher the slip increment using the same upper value of the repeated load. In case of variable amplitude loading the contribution of low load levels is almost negligable. Amplitudes smaller than 30 % of the maximum valaue of the repeated load did not indicate differences. The slip increase above 30 % amplitude is a non-linear function of the amplitude.

If bond fatigue failure does not take place during cycling then it does not negatively influence the bond stress versus slip behaviour near ultimate load compared to the monotonic loading behaviour.

Copyright fib, all rights reserved. This PDF copy of fib Bulletin 10 is intended for use and/or distribution only by National Member Groups of fib.

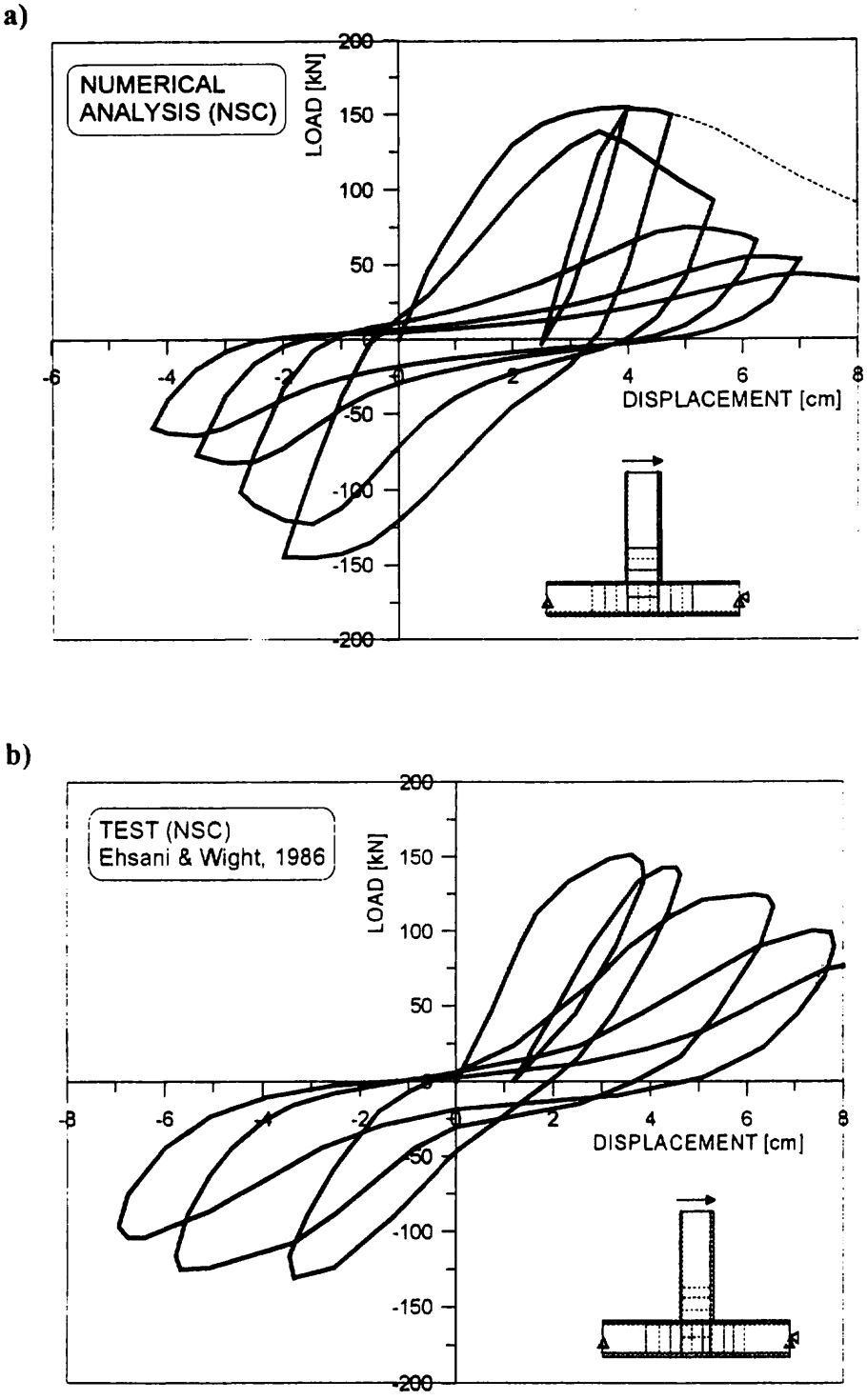

Fig.3.18 Calculated (a) and in experiment measured (b) load-displacement curves at the end of the beam cantilever (Ozbolt, Li and Eligehausen, 1998)

Copyright fib, all rights reserved. This PDF copy of fib Bulletin 10 is intended for use and/or distribution only by National Member Groups of fib.

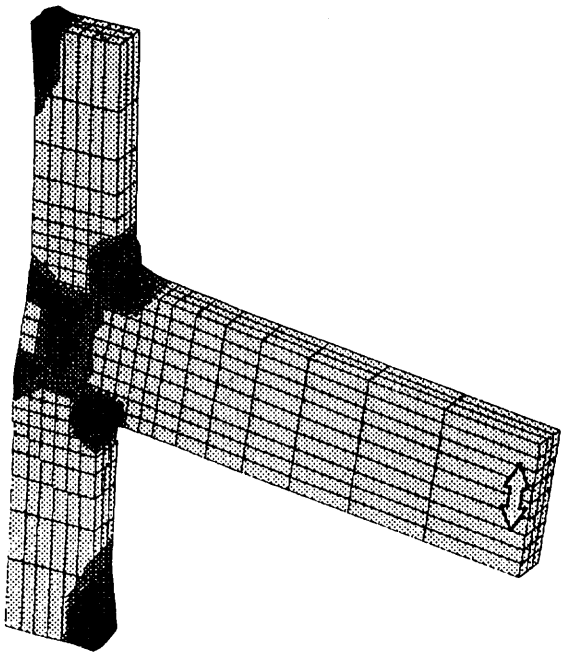

Fig.3.19 Typical X-shaped damage pattern in the beam-column connection observed in the finite element analysis (Ozbolt, Li and Eligehausen, 1998)

Reversed cyclic loading

Cycles with reversed loading produce degradation of bond strength and bond stiffness that is more severe than for the same number of load cycles with unidirectional repeated loading. Degradation primarily depends on the peak slip in either direction reached previously. Other significant parameters are rib pattern, concrete strength, confining effects, number of load cycles and peak value of slip between which the bar is cyclically loaded. Under otherwise constant conditions, the largest deterioration will occur for full reversals of slip. The accumulation of bond damage is supposed to be caused by the progressive growth of microcracks and concrete microcrushing in front of the protruding lugs.

Modeling

Although the models simplify the real behaviour, they intend to take into account parameters which appear to control the behaviour observed in the experiments, these being: deterioration of bond strength, deterioration of related slip, increase of slip under load controlled reversals, decrease of bond stress under slip controlled reversals, deterioration of frictional bond stress and deterioration of residual bond strength. Using the described rather sophisticated bond models, the behaviour of bars embedded in concrete under cyclic excitations can be predicted with sufficient accuracy for practical purposes.

Two different principal approaches for numerical modeling of bond under cyclic loading are possible – phenomenological and detailed. In the *phenomenological* type of the analysis bond constitutive relations are stored in the interface element which may be of a discrete or continuous type. The interface elements should be calibrated for different bar sizes, rib spacings, shapes and sizes. They may realistically predict the bond response for different concrete geometries, however, basic physical bond phenomena must be in advance stored in the interface elements.

In contrary to the phenomenological models, the *detailed models* should principally be able to predict physical phenomena related to the cyclic bond response automatically. However, the

Copyright fib, all rights reserved. This PDF copy of fib Bulletin 10 is intended for use and/or distribution only by National Member Groups of fib.

success of their prediction depends on the assumptions and the constitutive relations used in the local zones close to the steel bar.

3.8 LITERATURE

1924 Palmgren, A. (1924), Die Lebensdauer von Kugellagern, Zeitschrift des Vereines deutscher Ingenieure, April, 339-341.

1945 Miner, M.A. (1945), Cumulative Damage in Fatigue, Journal of the Applied Mechanics, Sept., 159-164.

1965 a Broms, B.B. (1965a), Technique for Investigation of Internal Cracks in Reinforced Concrete Members, ACI Journal, Vol.62, No.1, Jan., 35-43.
b Broms,B.B. (1965b), Crack Width and Crack Spacing in Reinforced Cocrete Members, ACI Journal, Proceedings V.62, No.10, Oct., 1237-1256.
Stüssi, F. (1965) Die Ermüdung vom Eisen und Stahl und anderen Metallen, Schaffhausen: Nachrichten aus der "Eisen-Bibliothek" der G Fischer AG., Nr.31, 1965

1968 Bresler, B., Bertero, V. (1968) Behaviour of Reinfoced Concrete Under Repeated Load, ASCE Journal of Structural Division, Vol.94, ST6 June, 1968, 1567-1590

1971 Goto, Y., Otsuka, K. (1971), Studies on Internal Cracks Formed in Concrete Around Deformed Tension Bars, ACI Journal, Vol.68, No.4, April 1971, 244-251

1973 Morita, S., Kaku, T. (1973), Local Bond Stress-Slip Relationship Under Repeated Loading, Proceedings, IABSE Symposium: Resistance and Ultimate Deformability of Structures Acted on by Well Defined Repeated Loads, Lisboa, 1973, 221-227
Tepfres, R., Görlin, J. and Samuelsson, T. (1973), Concrete subjected to pulsating load and pulsating deformation of different pulse waveforms, Nordic Concrete Journal, 1973/4, 27-36.

1977 Rehm, G., Eligehausen,R. (1977), Einfluss einer nicht ruhenden Belastung auf das Verbundverhalten von Rippenstäben, Betonwerk-Fertigteil-Technik, Heft 6, 1977

1978 Edwards, A.D., Yannopoulos, P.J. (1978) Local bond stress-slip relationship under repeated loading, Magazine of Concrete Research, Vol.30, No.103, June 1978, 62-72

1979 Holmen, J.O. (1979), Fatigue of Concrete by Constant and Variable Amplitude Loading, Report of the University of Trondheim Division of Concrete Structures, No. 79-1, Nov., 218 p.
Rehm, G., Eligehausen, R. (1979), Bond of Ribbed Bars Under High-Cycle Repeated Loads; ACI Journal, Vol.76, No.2, Feb. 1979, 297-309
Tassios, T.P. (1979), Properties of Bond Between Concrete and Steel Under Load Cycles Idealising Seismic Actions, AICAP-CEB Symposium: Structural Concrete Under Seismic Action, Rome, CEB Bulletin d' Information No.131, Vol.1, 1979
Viwathanatepa, S., Popov, E.P., Bertero,V.V. (1979), Effects of Generalized Loadings on Bond of Reinforcing Bars Embedded in Confined Concrete Blocks", Earthquake Engineering Research Center, Report UCB/EERC-79/22, August 1979

1982 CEB (1982), Bond Action and Bond Behaviour of Reinforcement, Chapter 7.4.2: Sustained and repeated loadings and Chapter 11: Loading history effects, CEB Bull.No.151, April 1982
Ciampi, V., Eligehausen, R., Bertero, V.V., Popov, E.P. (1982), Analytical Model for Concrete Anchorages of Reinforcing Bars Under Generalized Excitations", Report No.

Copyright fib, all rights reserved. This PDF copy of fib Bulletin 10 is intended for use and/or distribution only by National Member Groups of fib.

EERC82-83, Earthquake Engineering Research Center, University of Califonia, Berkeley, California, Dec.1982, 111 p.
Hawkins, N.M., Lin,I.J., Jeang,F.L. (1982), Local bond strength of conrete for cyclic reversed actions, Proceedings, Bond in Conrete, Applied Science Publishers London, 1982, 151-161
Holmen, J.O. (1982), Fatigue of Concrete by Constant and Variable Amplitude Loading, Fatigue of Concrete Structures (ed. S.P.Shah), ACI SP-75, 71-110
Siemens, A.J.M. (1982), Miner's Rule with Respect to Plain Concrete, Fatigue of Concrete Structures (ed. S.P.Shah), ACI SP-75, 343-372.
Sparks, P.R. (1982), The Influence of Rate of Loading and Material Variability on the Fatigue Characteristics of Concrete, Fatigue of Concrete Structures (ed. S.P.Shah), ACI SP-75, 331-341.
Tepfers, R. (1982), Fatigue of Plain Concrete Subjected to Stress Reversals, ACI SP 75-9, 195-215.

1983 Eligehausen, R., Popov, E.P., Bertero, V.V. (1983), Local Bond Stress-Slip Relationships of Deformed Bars Under Generalized Excitations, Report No UCB/EERC 82-23, Earthquake Engineering Research Center, University of California, Berkeley, California, Oct., 1983.
Bazant, Z.P., and Oh. (1983). Crack band theory for fracture of concrete. Materials and Structures, RILEM, 93(16), 1983, 155-177.

1984 Cornelissen, H.A.W. (1984), Fatigue of concrete in tension, HERON Publications Delft University of Technology, No.4, 1984, 1-67.
Mihashi, H., Izumi, M. (1984), Damage mechanism and mechanical behaviour of concrete under cyclic loads, contribution of the transaction of the Architectural Institute of Japan, April, 1-7
Tepfers, R. Hedberg, B. and Szczekocki, G., (1984), Absorption of energy in fatigue of plain concrete, Materials and Structures, Vol. 17, No. 97, 59-64.

1985 Gambarova, P. and Giuriani, E. (1985), Fracture Mechanics of Bond in Reinforced Concrete, Discussion, Journal of Structural Engineering ASCE, Vol.111, No.5, May, 1161-1164.
Roelfstra, P.E., Sadouki, H. and Wittmann, F.H. (1985). Le beton numerique. Materials and Structures, RILEM, 18(107).

1986 Ehsani, M.R. and Wight, J.K. (1986). Exterior reinforced concrete beam-olumn connections subjected to earthquake type loading. Journal of ACI, Vol.82, No. 43, pp. 492-499.

1988 CEB (1988), Fatigue of Concrete Structures, CEB Bulletin d' Information No.188, June 1988, 300 p.

1989 Pochanart, S., Harmon, T. (1989), Bond-Slip Model for Generalized Excitation Including Fatigue, ACI Materials Journal, Sept-Oct. 1989, 465-476

1990 Petković, G., Lenschow, R., Stemland, H., Rosseland, S. (1990),"Fatigue of High-Strength Concrete", ACI SP-121 "High Strength Concrete", 1990, pp.505-525.
Bazant, Z.P., Tabbara, M.R., Kazemi, M.T. and Pijaudier-Cabot, G. (1990). Random particle model for fracture of aggregate or fiber composits. Journal of Eng. Mechanics (ASCE), 116, 1686-1705.
Mazars, J., Pijaudier-Cabot, J. and Clement, J.L. (1990). 'Analysis of steel-concrete bond with damage mechanics: nonlinear behavior and size effect.' Application of Fracture Mechanics to Reinforced Concrete, Ed. By A. Carpinteri, Elsevier Applied Science, 307-311.

Copyright fib, all rights reserved. This PDF copy of fib Bulletin 10 is intended for use and/or distribution only by National Member Groups of fib.

1991 Balázs G.L. (1991), Fatigue of Bond, ACI Materials Journal, Vol.88, No.6, Nov-Dec. 1991, 620-629.
CEB (1991), Behaviour and Analysis of Reinforced Concrete Structures Under Alternate Actions Including Inelastic Response, Chapter 4: Bond between Concrete and Steel, CEB Bull.No.210, July 1991 (Published also by Thomas Telford, London 1996)
Oh, B.H. (1991), Cumulative Damage Theory of Concrete under Variable Fatigue Loadings, ACI Materials Journal, Jan-Feb., 41-48.
Petković, G. (1991), Properties of Concrete related to fatigue damage with emphasis on high strength concrete",Ph.D. thesis, NTH Trondheim, Rapport 1991:2, 1991, 217 p.
Bazant, Z.P. (1991). Why continuum damage is nonlocal: micromechanics arguments, Journal of Engineering Mechanics (ASCE), 117(5), 1070-1087.

1992 ACI 408.2.R-92 (1992), State-of-the-Art Report on Bond Under Cyclic Loads, ACI Com. 408, Nov.1992
Balázs G.L., Koch, R. (1992), Influence of Load History on Bond Behaviour, Proceedings of the "Bond in Concrete" Conference Riga 1992, 7-1.-7-10
Koch, R., Balázs G.L. (1992), Influence of Cyclic Loading on Bond Strength and Related Slip, Proceedings of the "Bond in Concrete" Conference Riga 1992, 7-11.-7-20
Koch, R., Balázs G.L. (1993), Slip Increase Under Cyclic And Long Term Loads, Otto Graf-Journal, Vol.4, 1993, 160-191
Ozbolt, J, Eligehausen, R. (1992), Numerical simulation of cycling bond-slip behaviour, Proceedings of the "Bond in Concrete" Conference Riga, 12-27 to 12-33.
Ozbolt, J. and Eligehausen, R. (199_). 'Simulation of cyclic bond-slip behavior,' Proc. of 1st Int. Conf. On Fracture Mechanics of Concrete Structures, Ed. By Z.P. Bazant, Elsevier Applied Science, Breckenridge, USA, 912-917.

1993 CEB (1983), Response of R.C. Critical Regions Under Large Amplitude Reversed Actions, CEB Bulletin d' Information No.161, 1983, 48-60
CEB (1993): CEB-FIP Model Code 1990 - Design Code, Comité Euro -International du Béton, Thomas Telford, London, 1993
Daerga, P,A. (1993), A Fatigue Failure Criterion for Concrete Based on Deformation, Nordic Concrete Research No.13, 2/1993, 6-20

1994 Balázs G.L. (1994), Deformation Based Fatigue Failure Criterion, Proceedings of the Conference on Locale Damage III, Udine 1994, Computational Mechanics Publications Southampton, 631-638
Balázs, G.L., Koch, R. (1994), Bond Behaviour under Random Cyclic Loading, Otto-Graf-Journal, Vol.5, 1994, 52-67
Balázs, G.L., Koch, R., Harre, W. (1994), Verbund von Stahl in Beton unter Betriebsbeanspruchung, Deutscher Ausschuss für Stahlbeton - 30. Forschungs-kolloquium, 04-05. Nov. 1994. Stuttgart, 167-176
Darwin, D., Mccabe, S.L., Brown, C.J. and Tholen, M.L. (1994). 'Fracture analysis of steel-concrete bond,' Fracture and Damage of Quasibrittle Structures, Ed. By Bazant, Bittnar, Jirasek and Mazars, 549-556.

1995 Balázs G.L., Koch, R. (1995), Bond charactersitics under reversed cyclic loading, Otto Graf-Journal, Vol.6, 1995, 47-62.
Noghabai, K. (1995), Splitting of Concrete in the Anchoring Zone of Deformed Bars: A Fracture Mechanics Approach to Bond, Licentiate Thesis, Div. of Structural Engineering, Lulea University of Technology, Publication 1995:26L
Van Mier, J.G.M. and Vervuurt, A. (1995). 'Lattice model for analysing steel-concrete interface behavior,' Mechanics of Geometrical Interfaces, Ed. By A.P.S. Salvadurai and M.J. Boulon, Elsevier Applied Science B.V., 201-225.

Copyright fib, all rights reserved. This PDF copy of fib Bulletin 10 is intended for use and/or distribution only by National Member Groups of fib.

1996 CEB (1996). 'RC elements under cyclic loading,' CEB Bulletin d' Information No. 230, State of the art report, Ed. By T. Telford, Thomas telford Service Ltd, London.

1997 Magnusson, J. (1997), Bond and Anchorage of Deformed Bars in High-Strength Concrete, Licentiate Thesis, Div. of Concrete Structures, Chalmers University of Technology, Publication 97:1
Ozbolt, J., Y.-J. Li and Kozar, I. (1997). Microplane-Model for Quasibrittle Materials. Stuttgart University, Institut fuer Werkstoffe im Bauwesen, Bericht Nr. 96-1a,b AF.

1998 Lundgren, K., Gylltoft, K. (1998), Modelling Splitting and Fatigue Effects of Bond, Proceedings, Fracture Mechanics of Concrete Structures (FRAMCOS-) 3 Conf., Sept. 1998, AEDIFICATIO Publishers
Ozbolt, J., Y.-J. Li and Eligehausen, R. (1998). '3D-Analyse von Balken-Stützen Verbindungen aus Normal- und Hochfestem Beton unter Zyklischer Beanspruchung,' Beton und Stahlbetonbau 93, (4), 91-97.
Ozbolt, J., Mayer, U. and Eligehausen, R. (1998). Bond failure mechanism- 3D finite element analysis. To be published at EURO-C conference in Austria, Ed. by de Borst, Bicanic and Mang

1999 Sippel, T. (1999), Verbundmodell für langdauernde und nicht ruhende Belastung, Proceedings for the 75. birthday of Prof. Rehm, 261-272.

Copyright fib, all rights reserved. This PDF copy of fib Bulletin 10 is intended for use and/or distribution only by National Member Groups of fib.

4 Bond of corroded reinforcement

Working Party 4:

John Cairns (Convener, Heriot Watt University, Edinburgh, UK), **Voula Pantazopoulou** (Demokritos University of Thrace, Prokat, Greece), **Keivan Noghabai** (Luleå University of Technology, Luleå, Sweden), **Jesus Rodriguez** (Geocisa Dragados Group, Madrid, Spain)

4.1 Introduction **188**

4.2 Corrosion of reinforcement **188**
4.2.1 Corrosion and its effect on structural capacity 188
4.2.2 Effects of corrosion on bond 189
4.2.3 Existing guidance for assessment of corrosion damaged structures 190

4.3 Review of test data on bond of corroded reinforcement **190**
4.3.1 Specimen conditioning 190
4.3.2 Corrosion induced cracking 191
4.3.3 Results from anchorage bond tests 194
4.3.4 Results from tests on RC elements 197

4.4 Analytical modeling of effects of corrosion **200**
4.4.1 General deterioration models 200
4.4.2 Onset of cracking 203
4.4.3 Local bond stress-slip relationship 204
4.4.4 Bond strength 205
4.4.4.1 Cracking of concrete cover 205
4.4.4.2 Changes in physical characteristics of bar/concrete interface 206
4.4.4.3 Loss of rib area and disengagement of ribs 207
4.4.5 Effects of bond loss on structural capacity 209

4.5 Conclusions **211**

4.6 References **212**

Copyright fib, all rights reserved. This PDF copy of fib Bulletin 10 is intended for use and/or distribution only by National Member Groups of fib.

4.1 Introduction

The degree to which performance of reinforced concrete is impaired as a result of reinforcement corrosion is a matter of great concern to those responsible for assessment and maintenance of affected structures. While much research effort has been devoted to researching the causes and mechanisms of reinforcement corrosion and to questions of durability of repair materials, relatively little attention has been devoted to the problem of assessing the residual strength of the corroded structure. Many authoritative reports on deterioration and its detection, such as that by Parrott [1987], ignore questions of residual strength despite a comprehensive coverage of other aspects of deterioration and its detection. The absence of detailed guidance on assessment of residual strength of corrosion damaged structures has been pointed out by a number of practitioners [e.g. DoT 1989]. Information on the effect of corrosion on structural integrity is essential for the development of effective tools for the prediction of residual service life and for the development of cost effective repair strategies. With the continuing development of a diverse range of repair techniques such as desalination, realkalisation and cathodic protection, it becomes of increasing importance to understand and quantify the effect of reinforcement corrosion on structural behaviour. The purpose of this report is thus to review available information on the changes in bond characteristics of reinforcement induced by corrosion and the consequences of that reduction on residual structural capacity of reinforced concrete elements. Advantage is also taken of the opportunity to assess the usefulness of existing bond models in a novel situation.

This report is concerned solely with corrosion which occurs after concrete is cast. The effect of pre-existing corrosion on bond is insignificant unless there is appreciable loss of bar section. Murphy [1977] and Maslehuddin et al [1990] provide test data on bond performance of bars in a corroded condition when cast into concrete.

4.2 Corrosion of Reinforcement

4.2.1 Corrosion and its Effect on Structural Capacity

In fresh and uncontaminated concrete, the alkaline environment surrounding reinforcement results in the formation of a passivating layer on the surface of the bar. It is only when the passivating layer is broken by carbonation of cover concrete, by penetration of chlorides through the cover, or by other less common mechanisms such as sulphide ion attack or stray dc electrical currents that active corrosion may develop. Minor differences in materials properties or environment, for example in chemical composition or in chloride or oxygen concentration, will then lead to formation of an electrochemical cell with anodic and cathodic areas on the bar surface.

Corrosion of reinforcement may be classified as general or as local. General corrosion may occur due to either chloride contamination or due to carbonation. It is invariably associated with formation of 'brown rust' iron oxides. The oxides occupy a greater volume than the parent metal, and the expansion of the diameter of the bar as it corrodes generally leads to cracking and eventually spalling of concrete cover before an appreciable proportion of the cross sectional area is lost. Local or pitting corrosion is invariably associated with chloride contamination and not with carbonation. These compounds do not exhibit the same degree of volumetric expansion as brown rust. Consequently, the tendency of a corroding bar to split the concrete cover is less with local corrosion, and extreme loss of bar section may occur without signs of deterioration on the surface of the member. The electrochemistry of corrosion is a complex subject, and discussion here is largely confined to its physical effects. A thorough review of mechanisms of corrosion and its influencing factors may be found in other CEB publications [CEB 1989, 1992] and elsewhere [Schiessel 1988].

Fig. 4-1 illustrates the potential consequences of reinforcement corrosion on residual strength. Residual strength of concrete structures may be affected by local or general loss of reinforcement cross section, through changes in the concrete cross section as a result of cracking or spalling, or through loss of bond. Loss of strength and ductility of reinforcement are of greatest concern when assessing structures affected by local corrosion, and are not considered further here. In the case of general corrosion, bond is more likely to affect structural capacity than is loss of tensile strength of reinforcement. This review is concerned principally with the effect of general corrosion on bond strength and on residual structural capacity. Other consequences of deterioration are considered here

Copyright fib, all rights reserved. This PDF copy of fib Bulletin 10 is intended for use and/or distribution only by National Member Groups of fib.

only insofar as required to allow the loss of capacity associated with bond to be compared to that caused by other factors.

Corrosion effects are considered only at the ultimate limit states. It is evident that longitudinal cover cracking as a consequence of corrosion will have a far more serious effect on serviceability than will the relatively small changes in flexural/tension crack widths, in tension stiffening and in deflections that may be induced through reductions in bond stiffness. Checks on these aspects of structural performance are therefore deemed irrelevant.

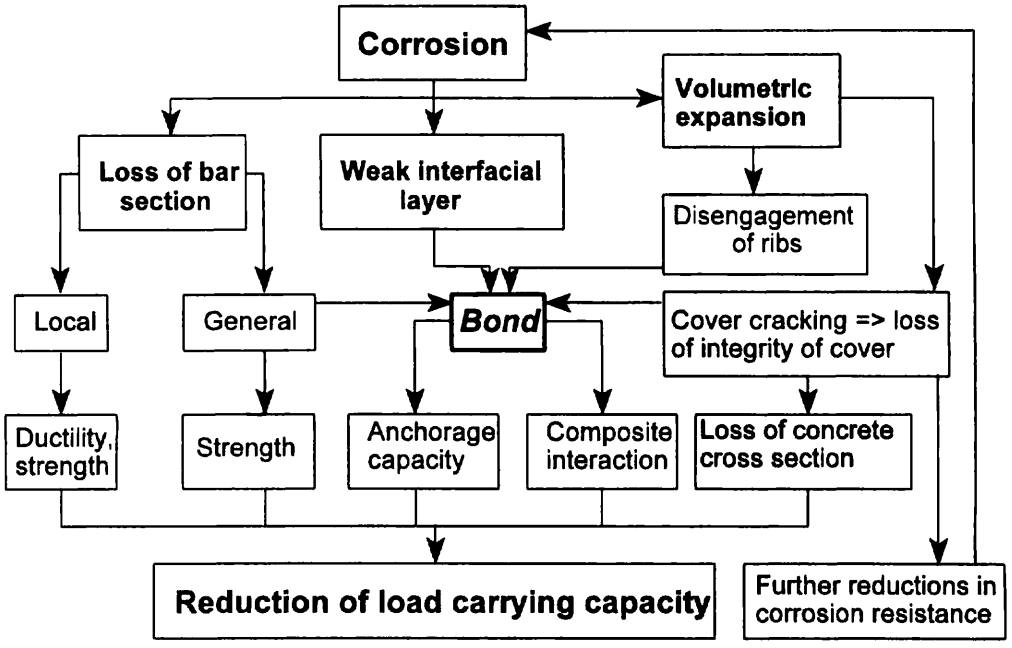

Figure 4-1 Effects of corrosion on residual strength

4.2.2 Effects of Corrosion on Bond

Bond between reinforcement and concrete is necessary to ensure composite interaction of the two materials. Bond stress may conveniently be regarded as a shear stress over the surface of a bar, although this represents a considerable simplification of the real behaviour. Bond strength initially comes from weak chemical bonds between steel and hardened cement, but this resistance is broken at a very low stress. Once slip occurs, friction contributes to bond. In plain round bars, this is the major component of strength. With ribbed bars, under increasing slip bond comes to depend principally on the bearing, or mechanical interlock, between ribs rolled on the surface of the bar and the surrounding concrete. In this stage, the reinforcing bar generates bursting forces which tend to split the surrounding concrete. The failure load may be limited by the resistance provided to these bursting forces by concrete cover and confining reinforcement.

Corrosion could be expected to affect bond strength in several ways, Fig. 4-1;

- Increases in the diameter of a corroding bar at first increases radial stresses between bar and concrete and hence increases the frictional component of bond. However, further corrosion will lead to development of longitudinal cracking and a reduction in the resistance to the bursting forces generated by bond action.
- Corrosion products at the bar/concrete interface will affect friction at the interface. Some

Copyright fib, all rights reserved. This PDF copy of fib Bulletin 10 is intended for use and/or distribution only by National Member Groups of fib.

suggest that a firmly adherent layer of rust may contribute to an enhancement in bond strength at early stages of corrosion [Al-Sulaimani et al 1990]. At more advanced stages of corrosion, weak and friable material between bar and concrete will certainly be at least partially responsible for reductions in bond strength [Cabrera & Ghodussi 1992].

- Corrosion may reduce the height of the ribs of a deformed bar above the bar core. This is unlikely to be significant except at advanced stages of corrosion, however.
- Disengagement of ribs and concrete. The layer of corrosion products formed by oxidation of the steel may force the concrete away from the bar and reduce the effective bearing area of the ribs, Fig. 4-2.

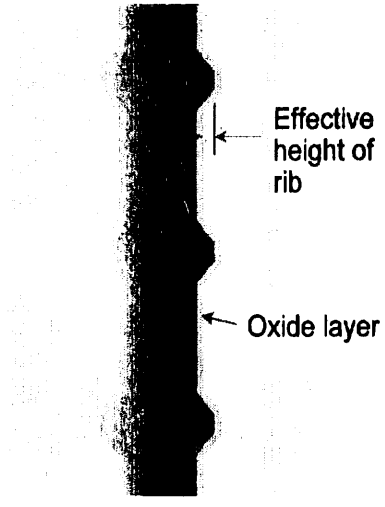

Figure 4-2 Disengagement of ribs

4.2.3 Existing guidance for assessment of corrosion damaged structures

Design Codes and Standards are intended primarily for new construction, and may not contain the information required for an assessment of a deteriorated structure. Many publications specifically intended for appraisal of existing structures provide no specific guidance on effects of reinforcement corrosion, other than pointing out that bar section loss is to be taken into account [Institution of Structural Engineers 1996]. One guide on strength evaluation of bridges states that bond loss should be considered insignificant unless it affects the anchorage near ends of individual bars [Imbsen et al 1987]. No guidance is offered on anchorage strength reduction, however. The UK Highways Agency have produced a guidance note [Highways Agency 1995] for the assessment of highway structures damaged by reinforcement corrosion. The document makes a distinction between general corrosion, which will become visible on the surface of the structure before loss of bar section becomes significant, and pitting corrosion, in which localised loss of bar section can be significant. The guide states that the major strength loss for general corrosion arises from the loss of bond and from spalling. For local corrosion, loss of bar section is significant. It is also emphasised that the two types of corrosion may occur together, and that the presence of general corrosion should not be taken to indicate an absence of local corrosion. The Note gives guidance on quantifying loss of structural strength from corrosion, but recognises that many of the assumptions made may be conservative.

4.3 Review of Test Data on Bond of Corroded Reinforcement

4.3.1 Specimen conditioning

In the majority of bond tests on corroded bars, the corrosion process has been activated by chloride salts and accelerated by electrical polarisation of reinforcement. In this technique, a positive electrical potential is applied to the bars to make the reinforcement anodic and encourage dissolution of Fe^{2+} ions. (The process may be considered the opposite of cathodic protection, where a negative potential is applied to reinforcement to make it cathodic and thus attract/retain Fe^{2+} ions). Conditioning has been carried out with test specimens wholly or partially submerged in some instances, and with ponding of salt solution or by spraying in others. Submersion will tend to restrict the availability of oxygen to the

Copyright fib, all rights reserved. This PDF copy of fib Bulletin 10 is intended for use and/or distribution only by National Member Groups of fib.

post-dissolution reactions, and corrosion products and the expansive forces generated may thus differ from those found in field exposures where structures are subjected to wetting and drying cycles. Results of accelerated tests must therefore be treated with caution, as they may be unrepresentative of field conditions.

Clark & Saifullah [1994] have demonstrated that the current density applied to accelerate corrosion exerts a significant influence on bond strength. The amount of corrosion (expressed as percentage weight loss) to cause cracking over bars with a cover/bar diameter ratio of 1.0 ranged from 0.2% for high rates of corrosion (current density of 4mA/cm^2 and a few hours to cracking) to 1.2% at low rates (current density of 0.04mA/cm^2 and 8-12 days to cracking). Even the lowest of these corrosion rates is appreciably higher than the highest rates of corrosion recorded in service, which typically are of the order of 10-25μA/cm^2 in chloride contaminated concrete according to field measurements reported by Rodriguez et al [1994c]. Rates tend to be appreciably lower in structures affected by carbonation. Bond strengths at cracking, expressed as a proportion of the non-corroded specimen strength, ranged between 0.5 and 1.2 for 'high' and 'low' corrosion rates respectively. At high rates of corrosion, there was a large initial drop in bond strength at time of cracking and a gradual subsequent strength reduction with further corrosion. However, at low rates of corrosion, the opposite occurred. The differences were attributed to the effects of differences in the chemistry of corrosion products, to their ability to disperse into the cement matrix, and to creep of concrete. Cabrera has also criticised use of high corrosion currents for conditioning [Cabrera & Ghodussi, 1991].

Work carried out at the Institute Torroja and at Geocisa has examined current densities within the range of values between 1-3 to 100 μA/cm^2, which are more representative of values found in practice, ranging from values found in corroding structures up to 5-10 times these values. The influence of current density on cracking initiation and on crack width is reported to be negligible when compared to other parameters such as cover/bar diameter ratio and concrete strength [Rodriguez et al. 1996b, Alonso et al. 1998]. Coronelli [1997] has suggested that current densities should be limited to a maximum of 0.05mA/cm^2 to avoid mechanical damage when conditioning corrosion bond specimens.

The most widely adopted measure of corrosion is the weight of metal lost after completion of strength tests. Some investigators quantify corrosion simply as Section Loss, i.e. weight loss divided by original weight, expressed as a percentage. This is clearly an appropriate parameter to adopt where residual tensile strength of the bars is of principal concern. However, there is evidence that average corrosion penetration, i.e. the thickness of steel lost through corrosion, assessed as an average over the original bar surface, offers a better measure of corrosion for assessment of residual bond strength, Fig. 4-3 and Rodriguez et al [1994b]. Weight loss per unit area of bar surface provides an equivalent measure.

Fig. 4-3, derived from results presented by Al-Sulaimani et al [1990] compares the amount of corrosion to cracking required by bars of different diameter (but with constant cover). The results are quantified by weight loss on the left y-axis and by radius of steel lost to corrosion (corrosion penetration) on the right y-axis. Corrosion to cracking is almost constant when assessed by corrosion penetration, but increases markedly with reducing bar diameter when assessed by section loss, suggesting that the former may be a more useful measure. Yet others have suggested that it is the proportion of the bar surface affected by corrosion which offers the best measure[1]. An understanding of the mechanisms affecting bond strength of corroding bars and the establishment of an appropriate measure of damage is clearly a priority in reconciling conflicting test data and development of assessment guidelines.

4.3.2 Corrosion Induced Cracking

The volumetric expansion of a corroding bar generates hoop strains in the surrounding concrete. Longitudinal cracks develop once the tensile strain capacity of the concrete is exhausted. Continued corrosion will eventually lead to spalling of the cover. The reduction in confinement on cracking of the cover will lead to a progressive reduction in bond strength. The problem has been investigated experimentally by Andrade and co-workers [1993] amongst others. They drew attention to the

[1]Personal communication, M Webster

Copyright fib, all rights reserved. This PDF copy of fib Bulletin 10 is intended for use and/or distribution only by National Member Groups of fib.

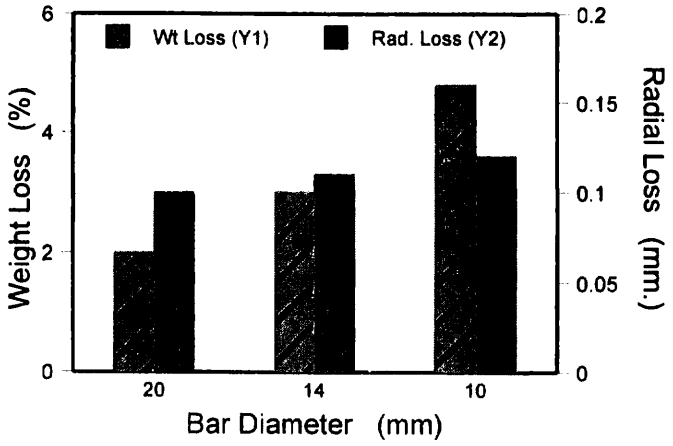

Figure 4-3 Alternative measures for corrosion damage, derived from Al-Sulaimani et al [1990].

conservatism in assuming the end of service life to occur at the onset of corrosion, and pointed to the need to distinguish between Ultimate and Serviceability Limit States when assessing remaining service life of a corroding structure.

Rodriguez et al [1994a] conducted accelerated corrosion tests on chloride contaminated reinforced concrete specimens in the laboratory. They report that cracking first developed at corrosion penetrations (i.e. reductions in bar radius) of between 0.015mm and 0.040mm. This represents a reduction of less than 2% of cross sectional area for a small diameter bar, and less for larger bars. (For comparison, UK production tolerances on reinforcement are ±6.5% for 8mm and 12mm diameter reinforcement and ±4.5% for sizes 12 and above [BSI 1988]). Clearly, cracking developed well before loss of bar section became significant for the test conditions pertaining in the study) It was also reported that cover cracking is delayed by increased cover, concrete tensile strength, and where bars are cast near the top of the pour. Andrade et al [1993] reported similar corrosion to first cracking, but found cover/bar diameter ratio to have a negligible effect. Al-Sulaimani et al[1990] reported initiation of cracking when loss of cross section lay between 2% and 4.5% for covers between 3.5 and 7.5 bar diameters, equivalent to an average corrosion penetration of around 0.1mm for the diameters used. The latter specimens were corroded at a significantly higher rate, which may help account for the different results [Cabrera & Ghodussi 1991]. Clark & Saifullah [1993] report section losses of 0.3% to 1.5% on crack formation for intermediate corrosion rates and lower cover ratios. Al-Qadi et al [1993] review three studies which reported metal loss to cracking of between 0.003mm and 0.7mm. In carbonated concrete, Tuutti [1982] reported that longitudinal cracking developed when corrosion penetration reached 0.1mm, but Browne [1985] reported lesser values. It is also known that severe pitting corrosion can develop in service without any signs of cracking on the surface, and the absence of surface cracking cannot be presumed to indicate an absence of significant corrosion.

Table 4-1 compares section loss and corrosion penetration to the onset of cracking reported in various studies of bond. It is evident that the relationship between section loss and formation of longitudinal splitting cracks is dependant on a number of factors including the method employed to condition test specimens. A relationship that can be relied upon for practical purposes of assessment has yet to be developed. The results do suggest a tendency for a greater corrosion loss to be required to crack thicker covers and at higher corrosion rates. However, at least where general corrosion is concerned, it can safely be concluded that longitudinal cracking will precede significant loss of bar section. {Note that beneficial effects of cover on time to cracking reported in these studies concern only the propagation phase of the deterioration process, and exclude the beneficial effect on the initiation phase, see Section 4.4.1}.

Rodriguez [1994a] also derived relationships between crack width and corrosion penetration as corrosion progressed, Fig. 4-4, which shows a mean surface crack width of 1mm to be associated with an attack penetration of around 0.2mm. A uniform metal loss of 0.2mm around the circumference of 10mm and 25mm diameter bars represents cross sectional area losses of 7.8% and 3.2% respectively. Cover to bar diameter varied between 2 and 4 in these tests. It may also be inferred from the paper that

Copyright fib, all rights reserved. This PDF copy of fib Bulletin 10 is intended for use and/or distribution only by National Member Groups of fib.

Investigation	Bar dia. mm	Cover Ratio	Impressed Current mA/cm²	Section Loss %	Corrosion Penetration mm
Al-Sulaimani et al	20	3.75	2	2	0.10
[1990]	14	5.36	2	3	0.11
	10	7.50	2	5	0.13
Cabrera & Ghodussi [1992]	12	V. Large	3 Volts	1-2	0.03-0.06
Clark & Saifullah	8	0.5	0.5	0.4	0.008
[1993]	8	1.0	0.5	0.6	0.012
	8	2.0	0.5	1.3	0.026
Andrade et al	16	1.25-1.88	0.1	0.4-0.5	0.015-0.02
[1993]		1.25	0.01	0.45	0.018
Clark & Saifullah	8	1.0	2	0.3	0.006
[1994]	8	1.0	0.5	0.55	0.011
Rodriguez et al. [1994]	16	2.0 - 4.0	0.003-0.10	0.4 - 1.0	0.015 - 0.04
Almusallam et al [1996]	12	5.0	10	4.0	0.12

Table 4-1 Corrosion to cause cracking of concrete cover.

concrete cover did not spall even where cracks reached 2mm in width. Cabrera & Ghodussi [1993] independently developed expressions for the relationship between crack width and corrosion, based on different parameters. Predictions of the two sets of expressions are broadly consistent despite significant differences in conditioning. Others report crack widths in excess of 0.6mm without spalling. Given the importance of confinement from cover and links to bond, it is clear that bond will be severely depleted prior to spalling.

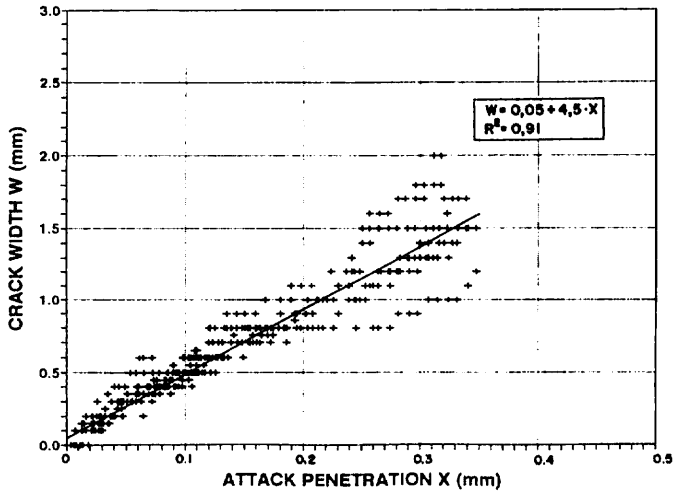

Figure 4-4. Relationship between surface crack width and corrosion. [Rodriguez et al, 1994a]

Copyright fib, all rights reserved. This PDF copy of fib Bulletin 10 is intended for use and/or distribution only by National Member Groups of fib.

4.3.3 Results from anchorage bond tests

A number of studies into the variation in bond strength as corrosion progresses have been undertaken using a variety of dedicated bond test specimens and conditioning procedures. Dedicated bond tests are here taken to encompass axial pullout, eccentric pullout and beam end specimens. All studies have reported the same general pattern of changes to bond strength as corrosion develops, Fig. 4-5. The same pattern is observed in tests on plain and ribbed surface bars. Initially, bond strength is increased by small amounts of corrosion, but with further increases, bond starts to reduce. It appears, however, that bond strength does not reduce below the 'as new' value prior to development of externally visible longitudinal cover cracks. For purposes of assessment of residual strength of concrete structures suffering from general corrosion, it thus appears that bond can be assumed to be sound in the absence of visible corrosion induced cracking.

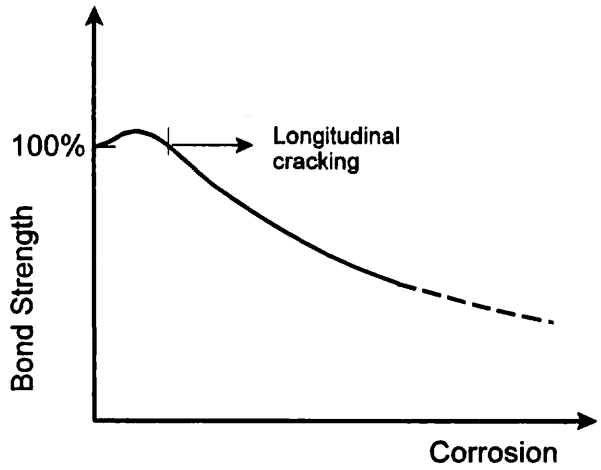

Figure 4-5 Variation in bond strength with corrosion (Schematic)

Once cracking develops, appreciable loss of bond strength may develop, particularly if no confining reinforcement is present. Residual strength decreases with increasing corrosion, and reductions of over 50% are reported. Table 4-2 provides a rough comparison of bond strength loss measured by various investigators at fairly advanced levels of corrosion. The comparison has been estimated for a nominal corrosion penetration (thickness of material lost averaged over the bar surface, and equivalent to the reduction in bar radius) of 0.25mm and represent conditions well beyond the corrosion levels required to crack the concrete cover. In Fig. 4-4, for example, a corrosion penetration of 0.25mm corresponds to a surface crack width of 0.8mm-1.5mm. Some values given in Table 4-2 have been obtained by interpolation between original results in order to obtain a more consistent basis for comparison.

Residual bond strengths quoted by the various investigators could hardly vary more widely, with values from 0% (complete loss of bond strength) to 110% (a modest gain in strength) reported. The majority of results were obtained using specimens without confining reinforcement. Al-Sulaimani et al [1990] report strength losses exceeding 70%, as does Rodriguez et al [1994b]. Cabrera & Ghodussi [1992] report a reduction of only 35%, not dissimilar to that reported by Clark & Saifullah [1993], although these Authors have also pointed out that results are markedly influenced by corrosion rate [Clark & Saifullah 1994].

Lesser reductions are reported in specimens provided with links. Rodriguez et al [1994b], for example, found strength losses to be reduced by half to a third where links were provided.

Berra et al [1997] alone report a continuing increase in bond strength with increasing corrosion to 8% section loss, equivalent to 0.3mm penetration, despite extensive longitudinal cracking. This is probably because stirrups, being at some distance outside the anchored bar, were particularly well arranged to maintain confinement in these specimens.

There appear to be inconsistencies between reductions reported in these studies, and apart from the presence of confining reinforcement, no clear pattern of influencing parameters emerges. However,

Copyright fib, all rights reserved. This PDF copy of fib Bulletin 10 is intended for use and/or distribution only by National Member Groups of fib.

Investigators	Cover Ratio	Corrosion rate mA/cm^2	Links?	Crack Width mm	Section Loss %	Residual Bond Strength %
Al-Sulaimani et al [1990]	3.75	2	N	-	5	35
	5.36	2	N	-	7	15
	7.50	2	N	-	10	0
Cabrera & Ghodussi [1992]	Large	3 Volts	N	-	8	65
	Large	3 Volts	Y	-	8	95
	Large	3 Volts	Y	-	8	110
Clark & Saifullah [1993]	0.5 - 2	0.5	N	-	12.5	75
Clark & Saifullah [1994]	1.0	0.04	N	-	12.5	60
	1.0	0.25	N	-	12.5	105
	1.0	4.0	N	-	12.5	50
Rodriguez et al. [1994]	1.5	0.1	N	1.6-2.2	5.4 - 9.1	20
	1.5-2.5	0.1	Y	1.0-2.0	5.4 - 9.1	65
	1.5	0.1	Y	1.1-1.4	14	75
Almusallam et al [1996]	5.0	10	N	0.4	8.0	15
Coronelli [1997]	2.5	0.05	Y	-		110
Stanish [1997]	2.0	0.21	N	-	10	60

Table 4-2 Summary of tests on bond strength of corroded reinforcement

in the majority of cases the reduction in bond attributable to corrosion clearly exceeds the corresponding reduction in tensile strength of the bar.

That the presence of longitudinal cracking may not of itself cause a major reduction in bond strength has been demonstrated in several sets of tests using non-corroded bars. Tests by Cairns & Jones [1995] on lapped joints confined by light links showed an insignificant reduction in bond strength in spite of longitudinal cracking over the entire length of the joint. In this case the longitudinal cracking was induced by load and not by corrosion. Jiang et al [1992] conducted bond transfer tests using two types of specimen, one with a single bar concentrically embedded in a concrete prism and the other with a pair of instrumented split bars on opposite faces of the specimen. The latter could be considered equivalent to the concentrically embedded bar but with the concrete cover completely cracked. Neither type of specimen contained links. The difference in measured bond stress between the two types of specimen is only 10%. Clark has reported similar results from tests at the University of Birmingham in which a longitudinal saw cut was made in the cover[2].

[2]Personal Communication, L A Clark

Copyright fib, all rights reserved. This PDF copy of fib Bulletin 10 is intended for use and/or distribution only by National Member Groups of fib.

In what is probably the most extensive study undertaken to date, Rodriguez, Ortega, Casal and Diez developed empirical expressions for residual bond strength of corroded bars [1994a, 1994b, 1996a]. The experimental work was mainly based on tests carried out with cubic specimens reinforced with four bars, one in each corner, reproducing part of a beam subjected to constant shear force. These tests allowed bond strength values representative of the splitting failure modes considered in design Codes of Practice to be developed. They will, however, underestimate failure strengths where bars are well confined by high cover or large amounts of transverse reinforcement. Tests were conducted with and without stirrups, and used 16mm and 10mm diameter bars. Neither the concrete quality nor the cover size/bar diameter ratio influenced residual bond strength when cover was cracked by reinforcement corrosion.

A statistical analysis was carried out with these results and expressions obtained to predict the characteristic value of residual bond strength. If the ratio ρ_{tr} of the transverse reinforcement area at anchorage length (considering the reduction due to corrosion) versus the area of the main bars is higher than 0.25 (minimum value established in EC2), the bond strength f_b (in MPa) can be predicted by eq. (4-1).

$$f_b = 4.75 - 4.64\,x \qquad (4\text{-}1)$$

where x is the attack penetration (bar radius reduction) in mm. On the contrary, if ρ_{tr} is lower than 0.25, f_b can be estimated by eq. (4-2).

$$f_b = 10.04 + (-6.62 + 1.98\,(\rho_{tr}/0.25))\,(1.14 + x) \qquad (4\text{-}2)$$

Eqs. (4-1), (4-2) and (4-3) are applicable once longitudinal cover cracks develop, and are not applicable to small amounts of corrosion. Although the experimental values of the attack penetration x ranged from 0.04 to 0.5 mm, the Authors believe extrapolation up to x = 1.0 mm is reasonable (although bond strengths in eq.(4-2) actually become negative at corrosion penetrations greater than 0.4mm if no links are present). This proposal gives bond strength values for each attack penetration, taking account of the actual residual stirrup section at the anchorage length. The expressions can be used to demonstrate a more rapid reduction in bond strength where links are not provided, Fig. 4-6. An attack penetration of 0.2mm corresponds to a mean surface crack width of around 1.0mm, Fig. 4-4.

According to the Investigators, these expressions can also be applied to the evaluation of composite interaction at intermediate parts of the bar. In these cases, the estimation of the ρ_{tr} value has to be made by replacing the number of stirrups within the anchorage length by 200/s, where s is the stirrup spacing in mm.

It is well known that external pressure, as occurs at support regions, for example, enhances the

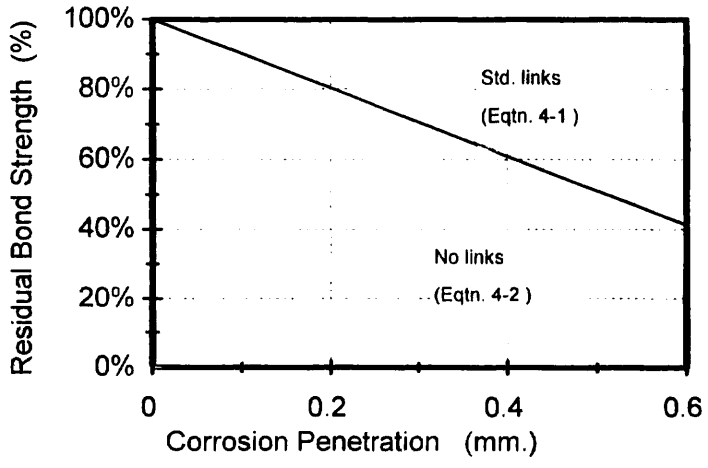

Figure 4-6 Effect of links on residual bond strength. Derived from Rodriguez et al

Copyright fib, all rights reserved. This PDF copy of fib Bulletin 10 is intended for use and/or distribution only by National Member Groups of fib.

confinement of the bars. Consequently it improves bond strength, and its positive effect is considered in EC2 when calculating ultimate bond stresses in sound ribbed bars. In order to explore this bond enhancement in corroded bars, tests were carried out on beams designed to fail at anchorage of main tension bars. A similar expression to that of EC2 was obtained from the experimental results to predict the characteristic value of the residual bond strength f_b, eq. (4-3) :

$$f_b = (4.75 - 4.64\ x) / (1-0.08\ p) \qquad (4\text{-}3)$$

where p is the external pressure at the anchorage length in MPa. This expression can be used in the assessment of the bar anchorage at the support zone, independently of the amount of stirrups and their level of corrosion. This fact was verified in beam tests where bars anchored at support zones did not slip although heavy deterioration had been produced with significant stirrup corrosion and concrete cracking.

4.3.4 Results from tests on RC elements

A reduction in bond may affect element strength in two ways, Fig. 4-1 :

1) the stress that can be developed in reinforcement may be limited by a reduction in anchorage capacity at laps and points of bar curtailment (including end anchorages). This could influence flexural and shear strength of beams and slabs as well as axial strength of columns and walls.
2) partial or complete loss of composite interaction between reinforcement and concrete over the affected length and beyond may occur due to marked reductions in bond stiffness. The plane strain assumptions normally made in section analysis/design would then no longer hold, and the pattern of strains in a member would be altered. Structural behaviour of a beam will tend to move away from purely flexural action towards a tied arch form of action (provided that end anchorage is maintained).

Researchers have addressed the effect of corrosion on element strength in various ways :

- physical tests on simulated damage where specimens were cast without concrete cover to the bar to simulate delamination of concrete cover. This approach ignores the effect of a layer of corrosion products at the bar/concrete interface, however. The absence of cover may also affect any residual contribution from confining links.
- laboratory tests and analyses of behaviour of beams in which bond was eliminated over a portion of the span although ends of bars remained anchored. These tests, although generally aimed at effects of repair, represent an extreme loss of bond. Analytical aspects of these studies are discussed in later sections on modelling.
- tests on elements corroded in the laboratory at an accelerated rate.
- full scale tests on deteriorated concrete structures in the field.

Results of a number of investigations are summarised in Table 4-3.

Pritchard & Chubb [1987] described tests on members weakened by simulated delamination of concrete cover. Specimens were cast without cover concrete to main reinforcement, and reinforcement was not corroded. A significant loss in strength was reported, and was attributed to a reduction in the stress developed in curtailed reinforcement i.e. to a reduction in anchorage capacity.

Minkarah and Ringo [1982] carried out a series of tests on beam specimens in which loss of cover to and full debonding of tension reinforcement due to corrosion damage was simulated. A single beam section and span were tested with a varying length of bar exposed. The section contained 0.95% reinforcement. All beams were tested under a single point load offset from midspan. Load was always applied at a section where reinforcement remained bonded to concrete. They reported that beam strength was not adversely affected by the absence of cover. However, a marked difference in the pattern of crack formation was noted in specimens with bars disbonded. Structural action was described as changing from flexural to tied arch behaviour with secondary effects. The results indicate little loss of load carrying capacity when reinforcement was exposed over up to 20% of the span of the beam, and a strength loss of around 20% when reinforcement was exposed over 60% of the span.

Cairns [1993,1995] Eyre and Nokhasteh [1992] and Raoof and Lin [1996] have all conducted tests which demonstrate that beams may possess considerable strength despite bond being entirely eliminated over part of the span, provided ends of bars remain adequately anchored. For example, in one test

Copyright fib, all rights reserved. This PDF copy of fib Bulletin 10 is intended for use and/or distribution only by National Member Groups of fib.

conducted by Cairns & Zhao [1993] the disbonding of all main reinforcement over 93% of the span produced a negligible loss of strength, although a more heavily reinforced beam section showed a 50% reduction in strength with bars exposed over the same proportion of the span. Tests by Cairns [1995] on beams designed for a shear mode of failure even produced a substantial increase in strength. The work is reviewed in more detail in the 'Modelling' sections of this Chapter.

The difference between the trends observed by Pritchard and Chubb and the others is because loss of cover affected the anchorage zone in the former case, whereas in the latter studies the simulated damage lay within the span and the anchorage zone was unaffected.

Investigators	Cross Sect. Lost %	Thick-ness Lost mm.	Long. Crack Width mm.	Links	Details of End Anchorage.	Local Bond Stress N/mm^2	Residual Strength %
Okada et al[1988]	-	-	0.02-0.15	Y	End hook	1.7	≥ 91%
Tachibana et al [1990]	up to 5%	up to 0.2	up to 0.75	N	15 d_b straight	1.8	≥ 87%
Al Sulaimani et al [1990]	up to 4%	up to 0.12	up to 1.3	Y	12 d_b straight	5.3	≥90%
Cabrera [1992] Series 1	up to 9.2%	up to 0.28	up to 0.6	Y	None	4.3	≥80%
Series 2	up to 7.8%	up to 0.24	up to 0.6	Y	None	7.2	100%
Rodriguez et al [1995], [1996]	10%-25%	0.30 - 0.53	-	Y	12.5/15 d_b straight	1.6 - 1.9	75% - 50%
Kawamura et al[1995]	-	-	up to 1.0	Y	End hook	2.1	Av. 99%
	-	-	up to 1.0	N	End hook	2.1	Av. 94%
	-	-	0.08-0.20	Y	Lapped joint	N/A	80% - 60%
	-	-	0.04	N	Lapped joint	N/A	25%
Daly [1995]	up to 17%	up to 0.5	-	Y	12 d_b straight	1.3-4.1	≥70%
Almusallam et al [1996]	up to 75%	up to 1.5	-	N	8.5 d_b straight	5.7	100%-15%

Table 4-3 Summary of tests on strength of beams and slabs with corroded reinforcement.

Several laboratory studies have been conducted into strength of simply supported beams corroded under accelerated conditions by application of anodic polarisation. A study by Okada et al [1988] indicated that ultimate strength of reinforced concrete beams was barely affected by longitudinal cracks up to 0.15mm wide. Test specimens had span/depth ratios of 8 or less, and contained 0.9% reinforcement. Local bond stresses, i.e. the bond stresses resulting from the variation of bending moment along the length of the member, were relatively low in these specimens, and member behaviour may therefore be expected to be insensitive to changes in bond characteristics. The presence of links in the specimens would also have slowed bond loss. In any case, no loss of strength would be

Copyright fib, all rights reserved. This PDF copy of fib Bulletin 10 is intended for use and/or distribution only by National Member Groups of fib.

expected as a result of bond loss even if reinforcement were fully disbonded over the entire span (always provided end anchorage at supports is adequate) according to the numerical model developed by Cairns [1993].

Tachibana et al [1990], Kawamura et al [1995] and Al Sulaimani et al [1990] also report small reductions in the strength of simply supported beams containing continuous reinforcement after corrosion had led to a loss of section of 4%-5% and 0.1mm-0.2mm loss of steel around the bar circumference. Only in the latter study did specimens contain links. Tachibana et al report a 12% reduction in strength and a shift towards from a flexural towards a bond-shear failure mode of a simply supported beam reinforced with a pair of 16mm diameter bars when longitudinal cracks were 0.5-0.75mm wide. Al Sulaimani et al report reductions in beam load capacity of up to 11% at 4% section loss on a single 12mm diameter bar. Kawamura et al report capacity reductions of around 10% when longitudinal cracks are 1.0mm wide. The studies encompassed a range of local bond stresses.

Almusallam et al [1996] report larger reductions in their tests on deteriorated slabs which did not contain links. A high current density of around 3mA/cm^2 was used to corrode reinforcement. Residual slab strength is reported as around 25% and 50% respectively of 'as new' strength at 5% and 15% section loss. It is also reported that failures become increasingly brittle as corrosion increases. Uomoto and Misra [1988] also report greater reductions in strength loss, and quote load capacity reductions of 4%, 8% and 17% respectively for section losses of 1%, 1.2% and 2.4%.

Rodriguez et al [1996a] tested around 40 beams in total, and reported that conventional plane section analyses could be used to estimate strength of deteriorated sections provided allowance was made for loss of reinforcement section and the reduced dimensions of the concrete section (i.e. making allowance for spalling of concrete cover). Local bond stresses at ultimate were again low in the specimens tested. They also concluded that residual bond strength values remained high enough to justify assumptions of "almost purely flexural action" when shear and compression reinforcement were present. However, in one series a partial recovery in shear capacity was reported as the degree of corrosion increased. It is difficult to see what could have been responsible for such an increase if tied arch action, a consequence of significant loss of bond within the span, had not started to develop.

Daly [1994, 1995] reports tests on simply supported beams corroded under accelerated conditions, some designed to fail in flexure and others to fail in shear. He reported no evidence of bond failure in beams with 3% loss of bar section designed for a flexural mode of failure, but longitudinal cracking on beams with 12% corrosion suggested a local bond failure. In two of the 12% corrosion specimens, collapse was attributed to bond failure. For shear, the capacity of beams with plain bars was enhanced by corrosion, even where the corrosion was heavy, which is consistent with Cairns [1995] observations on beams in which bond was eliminated by exposure of main bars. No shear strength enhancement occurred in beams with deformed bars, presumably because ribbed bars were better able to maintain bond, and bars with lower covers were more susceptible to loss of bond.

Kawamura et al [1995] also tested simply supported beams containing lapped bars. Measurements of section loss were not reported, but corrosion was clearly sufficient to develop longitudinal cracking. In the one specimen tested with lapped bars unconfined by links, residual strength was around 75% of the 'as new' strength and the mode of failure was somewhat brittle. Links were provided to the laps in the remaining tests. In four cases, the loss of strength as a result of corrosion was minimal, and might well have been attributable to loss of bar section. Ductile failures ensued. The remaining three specimens showed varying degrees of strength loss of up to 40%. It is unclear from the paper whether there were significant differences between these specimens.

Findings thus tend to show that loss of anchorage capacity is more likely to be significant than loss of local bond. There is little evidence to suggest that conventional calculation procedures for flexural and shear strength are unsafe, provided allowance is made for reductions in cross sectional area. Nonetheless, there is also evidence that loss of local bond may influence behaviour of corrosion damaged structures, particularly where plain round bars are used for main flexural reinforcement or in the absence of confining reinforcement to maintain residual bond strength, and tied arch action may come into play in such circumstances. Obviously tied arch action can only develop where ends of bars are adequately anchored.

The difficulties inherent in analysis of results of physical tests on deteriorated specimens should be

Copyright fib, all rights reserved. This PDF copy of fib Bulletin 10 is intended for use and/or distribution only by National Member Groups of fib.

noted, as the effect of a change in bond characteristics on member behaviour cannot be entirely separated from the effects of section loss of reinforcement and of spalling of concrete.

No information is available on the effect of corrosion on anchorage capacity of hooks or bends.

Rodriguez et al [1996c] also conducted tests on axially loaded concrete columns where reinforcement was corroded under an impressed current, and should also be mentioned here for the sake of completeness. However, as test specimens were axially loaded and reinforcement was not lapped, column strength was not influenced by loss of bond. As in their beam tests, it was concluded that a lower bound to ultimate strength could be obtained by use of conventional strength models, taking into account of a reduced bar cross section and delaminated concrete cover along with an increased load eccentricity. It was also noted that premature buckling of longitudinal reinforcement may occur if links suffer severe loss of section.

Rostam et al [1987] report on tests conducted on beams, columns and slabs of a concrete framed building in the Arabian Gulf region. Parts of the frame had suffered extensive cracking as a result of corrosion of reinforcement in the aggressive Gulf environment. One of the two beams selected for test appeared structurally sound whereas the other exhibited extensive longitudinal cracking along the bottom layer of reinforcement and delamination at the top layer. Load capacity of the beams was found to exceed Code design values by 162% and 184% respectively. The excess load capacity was attributed to the interaction of the test beams with the remainder of the structure, and was to be expected in view of actions such as tension membrane behaviour which are ignored in Code design procedures. The two tests together suggested that any strength reduction attributable to deterioration would have been small. In contrast, the measured difference between sound and deteriorated test slabs was around 20%. The deteriorated slab showed significant loss of cover and of bar section, some bars having entirely corroded. It is reported that membrane action did not develop in the slabs. The strength reduction and brittle failure mode of the deteriorated slab was attributed to loss of reinforcement section and to loss of composite interaction between reinforcement and concrete.

Prior to test, the two columns investigated exhibited longitudinal cracks 10-12mm wide. Measured strengths were 45% and 67% of theoretical values. The strength reduction was attributed to the ineffectiveness of concrete cover outwith the core of the section due to longitudinal cracking.

In general, strength loss measured on structural elements is less than might be feared given the relatively large bond strength reductions measured in bond tests at similar levels of deterioration in similarly reinforced specimens. The loss of element strength reported is often only slightly greater than the average loss of cross section, which might be attributable to uneven corrosion along the bars or to a reduction in average yield strength[3]. However, it is also apparent that many of the beam specimens tested would have been insensitive to loss of bond within the span, and end anchorage would have been enhanced by lateral pressure at simple supports. Many contained links which would have helped to maintain splitting resistance of cover concrete after longitudinal cracks developed, and structural elements without links might have shown greater susceptibility to bond loss.

4.4 Analytical Modelling of Effects of Corrosion

4.4.1 General deterioration models

The model presented by Tuutti [1982] is frequently cited as representing the deterioration process, Fig. 4-7. The model comprises two phases, an initiation period and a propagation period. The initiation phase represents the time t_0 for either chlorides or carbonation (or both) to permeate the concrete cover until the threshold level for initiation of corrosion is reached. Active corrosion conditions occur during the propagation phase, which terminates when the end of service life is reached at some (undefined) damage limit. Tuutti's model was intended purely as a conceptual device, and has a number of shortcomings for practical assessment of corroding structures. The assumption of a linear growth in deterioration once corrosion initiates, for example, is highly simplistic. Axes are unscaled, and the

[3] L A Clark, University of Birmingham, UK. Private communication.

Copyright fib, all rights reserved. This PDF copy of fib Bulletin 10 is intended for use and/or distribution only by National Member Groups of fib.

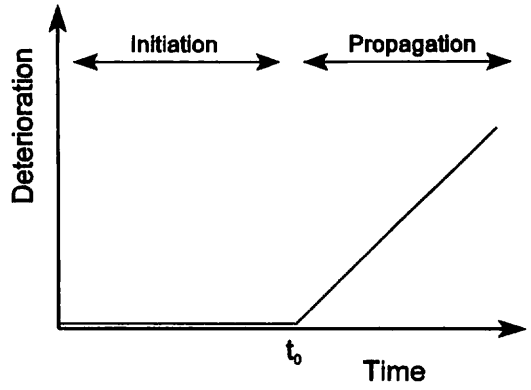

Figure 4-7. Tuutti's deterioration model

measure of deterioration on the vertical axis is not specified. However, as deterioration is zero prior to initiation of corrosion, it must implicitly be measured by a parameter related to loss of bar section. Finally, the model gives no guidance on the criteria to adopt for the 'end of service life' condition.

Other models have been proposed which provide a more refined representation of the deterioration process. The four-phase model shown in Fig. 4-8 has been obtained through combination of models presented by Bamforth [1997] and Berra et al [1997]. The model represents both the deterioration process and effect of deterioration on residual strength. The first phase, up to time t_0, is the same as the initiation phase described by Tuutti, and terminates when conditions for corrosion develop at the reinforcing bar. However, corrosion does not reach an appreciable rate until time t_1. Residual strength may increase up to t_1 as a result of the increase in concrete strength with continued cement hydration. Time t_2 marks the development of longitudinal cracking. Corrosion rate may be expected to increase once longitudinal cracks develop, although there is little information on this [Andrade et al 1993]. Accelerated corrosion bond tests suggest that residual bond strength will not differ significantly from 'as new' strength at this stage. The period up to time t_3 represents the time for significant structural distress to be caused and most of the physical testing described in the preceding section is concerned with the evaluation of the residual structural capacity during this phase. Little durability related research has been carried out in this phase. Beyond t_3, a structure could only remain in service through imposition of load limits or provision of additional support.

The limiting damage criteria for service life are not well defined, and may indeed have to be derived individually for each assessment [BCA 1996]. Some researchers have taken development of longitudinal cover cracks as the limiting damage criterion. However, earlier sections of this review

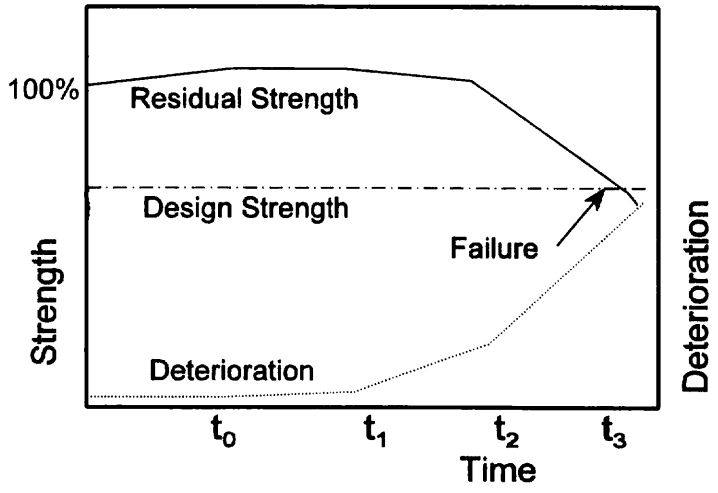

Figure 4-8. Improved deterioration/residual strength model

Copyright fib, all rights reserved. This PDF copy of fib Bulletin 10 is intended for use and/or distribution only by National Member Groups of fib.

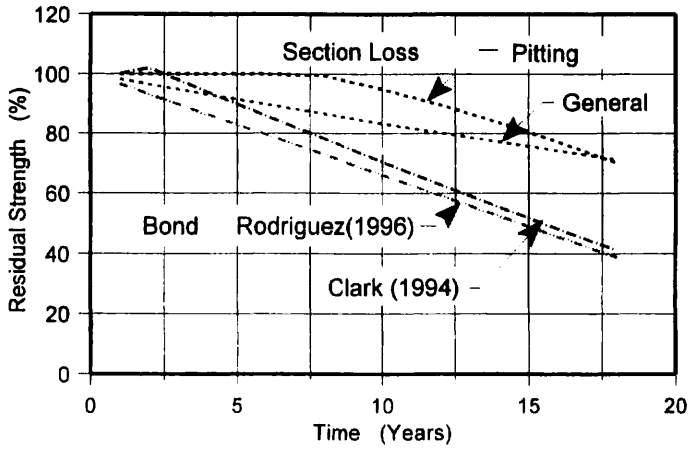

Figure 4-9 Influence of corrosion on residual bond strength

have shown that residual structural capacity may still be a high proportion of 'as new' capacity despite appreciable longitudinal cracking. Initiation of longitudinal cover cracks may therefore not be a particularly appropriate indicator of unsatisfactory residual structural capacity. Indeed, some practitioners appear to regard the limit as 10% loss of bar section to corrosion. Bond strength may have decreased to a negligible value before such a large section loss occurs. Andrade et al[1993] suggest that a limiting crack width of 0.3mm-0.4mm marks the end of service life. This limit was obtained from Code limitations on width of flexural cracks for aesthetic reasons, not from strength considerations. Neither appear to have considered the harmful effects of longitudinal cracking on bond strength.

Cairns has compared the effect of corrosion on bond strength with that from pitting and from general corrosion [Cairns 1998], Fig. 4-9. Clark & Saifullah give empirical coefficients for residual bond strength of 8mm bars corresponding to various degrees of current density i_{corr}; those used in Fig. 4-9 are for i_{corr}=0.25mA/cm^2. Expressions developed by Rodriguez et al and presented earlier as eq. (4-1) are also shown. Although the two residual bond strength plots show similar reductions, it would be unwise to assume that they are consistent, for reasons mentioned earlier. It is evident from Fig. 4-9 that the reduction in bond strength presents a greater threat to the integrity of concrete structures than loss of reinforcement section for bars of 8mm diameter; the difference would be greater for larger diameter bars. The comparison assumes that bond and bar strength were originally designed to the same margin of safety. The factor that will control load carrying capacity of any given structure will, of course, depend on the individual design.

It can be deduced from eq. (4-1) that the depth of corrosion required for a 10% reduction in bond strength is of the order of 0.1mm, roughly 5 times that required to crack the cover. (Loss of bar section is unlikely to be critical and may be ignored in this comparison). Now, if rate of corrosion were constant throughout the active corrosion phases, an assumption which may be reasonable under some conditions [Andrade et al 1993], and if a 10% reduction in bond strength were defined as a limiting condition, a presumption which need not represent a major risk to safety, then it would follow that the time interval between the development of longitudinal cracking at t_2 and an unacceptable state of structural deterioration being reached at t_3 would be five times greater than the time between initiation of corrosion at t_0 and the development of longitudinal cracking at t_2. While no great faith can be placed in the accuracy of such a simple comparison, the outcome suggests that definition of the onset of longitudinal cracking as the 'end of service condition' may significantly underestimate residual service life. The comparison also suggests that continued research into the effect of corrosion on bond strength and of the effect of longitudinal cracking on corrosion rate may offer significant benefits by enabling deteriorating structures to remain in service for longer periods of time.

As an aside, it is worth mentioning the work currently underway on electrochemical NDT methods for assessment of corrosion rates of embedded reinforcement. These techniques could assist in the evaluation of the gradient of the deterioration function of Fig. 4-8. The reader is referred to other publications on this subject for more information. [Feliu et al 1990, Gannon & Cady 1992, Rodriguez et al 1994c].

Copyright fib, all rights reserved. This PDF copy of fib Bulletin 10 is intended for use and/or distribution only by National Member Groups of fib.

4.4.2 Onset of cracking

Clark and Saifullah [1993], amongst others, have presented empirical 'best fit' relationships to their own results. These empirical observations were covered in Section 4.3.2 and are not considered further here.

Bazant [1979] developed analytical expressions for time to cracking which take account of bar diameter, spacing and cover, tensile strength of concrete as well as corrosion parameters including rate of corrosion and density of corrosion products.

Noghabai [1996] uses a model for the splitting capacity of a thick-walled concrete ring subjected to an inner pressure, based on nonlinear fracture mechanics. Thick-walled concrete ring models are frequently used in bond models. The model assesses the pressure from a single bar required to initiate a surface crack. It adopts the assumptions of Molina et al [1993] regarding the correlation of circumferential deformations in the concrete around the hole (due to the expansive action of corrosion) to a corrosion rate of the rebar. Bond stresses along the rebar are related to radial splitting pressure by a Mohr-Coulomb type of relationship. Noghabai assumes that prior to occurrence of splitting crack, the action of corrosion and the bursting action of the lugs may be superimposed. However, the inclination of the wedge angle in the bond model becomes steeper due to corrosion.

Computational analyses, conducted mainly by the finite element method (FEM), have focussed on damage process to the concrete cover through 2-dimensional plane-strain analyses of sections perpendicular to the bar. All the models consider the volumetric strains associated with corrosion of reinforcement to be applied in the absence of bursting stresses associated with bond action. Dagher and Kulendran [1992] used a smeared crack analysis simulating the action of corrosion by a uniform expansion of the nodes of the hole that defines the location of the reinforcement. It was found that an expansion as little as 0.008 mm was enough to cause a delamination in concrete bridge deck. Molina et al. [1993] also used a smeared crack model for the FE-analysis. In contrast to all other models mentioned here, Molina defined the loading through modelling of the corrosion process of the rebar and not by a displacement of the nodes of a hole. The accumulated load was equivalent to an corrosion attack penetration of $x = 0.060$ mm, applied in three consecutive steps. The analysis were based on the experiments of Andrade et al. [1993], where the location of the bar vis-a-vis the free surfaces was altered, using covers 1.25 and 1.9 times bar diameter for 16 mm bars. In the experiments a corrosion penetration of 0.020 mm was enough to initiate a surface crack on the specimens. Both the experimental evidence and the FE-analysis indicated that the actual cover-to-bar diameter ratio had no influence on corrosion to occurrence of a surface crack, in contrast to conclusions reported elsewhere. Siewiec et al. [1994] investigated the mechanical action of a conical wedge pushed into a hole in a flat specimen and analogized it to the expansive action of corrosion. The specimens were made of both fibrous and plain mortars as well as concretes. The experiments served as reference for a FE-analysis, based on the smeared crack concept. The model revealed that some surface cracks are caused by a bending action.

The assumptions of Molina et al. [1993] and Andrade et al. [1994] with respect to the corrosion rate was adopted in the FE-analysis of Noghabai [1997b]. With these assumptions, the evolution of the surface cracks as a function of time was roughly modelled, Fig. 4-10. The FEM used in the analysis of Noghabai is based on a relatively new approach called the inner softening band (ISB), whose accuracy was proved in analysis of thick-walled concrete rings subjected to inner pressure. Contrary to the smeared crack models, the ISB model gives explicit values for the crack opening. The variables in the analysis of Noghabai were the concrete cover, the material (plain and fibrous high-strength concrete) and stirrups. Some important findings were that for small covers an inclusion of fibres (up to 2% per volume of concrete) may not make a difference on the initiation of surface cracks. This confirms the thick-walled concrete ring models. However, the fibres facilitate an extensive stress redistribution in the cross-section which delays spalling. Further, the stirrups may give rise to unexpected surface cracking due to bending actions.

All the authors agree that the models are based on simplifications. All consider the volumetric strains associated with corrosion of reinforcement to be applied in the absence of bursting stresses associated with bond action. The analyses assume that the onset, rate and geometry of corrosion are known; these are major assumptions, and NDT techniques for measurement of corrosion are not yet sufficiently developed to enable these parameters to be determined with any degree of accuracy or

Copyright fib, all rights reserved. This PDF copy of fib Bulletin 10 is intended for use and/or distribution only by National Member Groups of fib.

Concrete type	NSC	HSC_I	HSC_{II}	HSC_{III}
Compressive strength, f_{cc} MPa	57,0	105,0	157,4	114
Tensile strength, f_{ct} MPa	3,8	5,0	8,0	5,1
Modulus of elasticity, E_c GPa	33	39,4	41,2	40
Fracture energy, G_f N/m	105	145	172	217

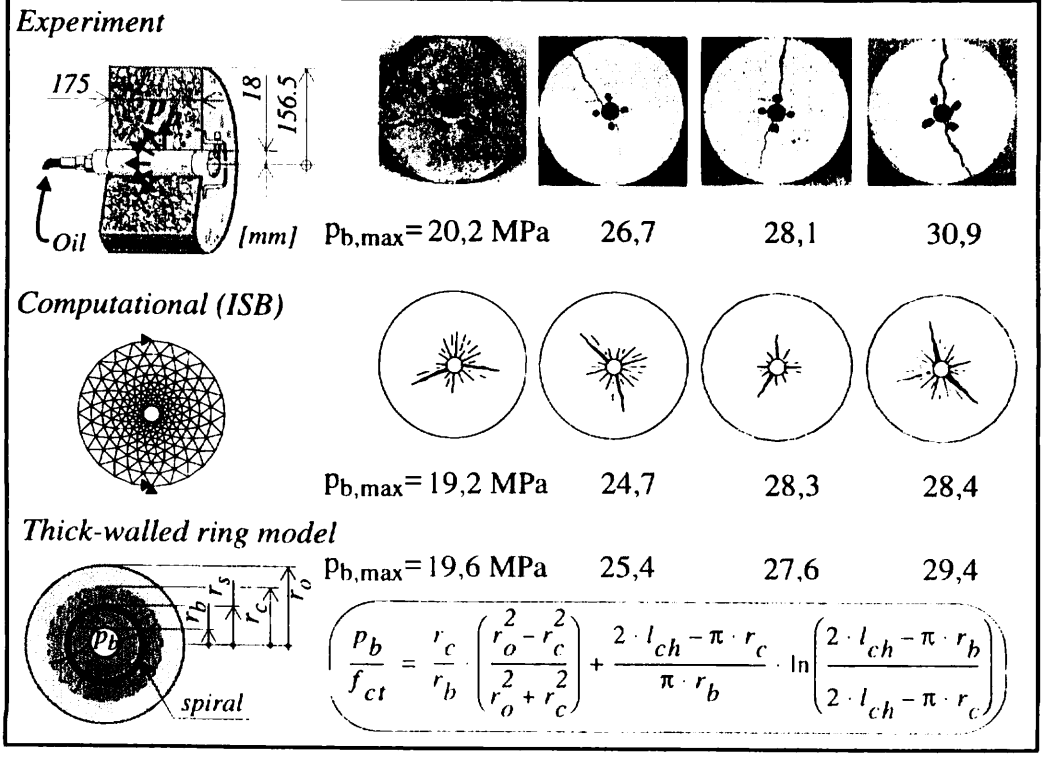

Figure 4-10 Modelling assumptions. Noghabai(1996)

reliability in practice. Noghabai pointed out that in practice degradation is a long term effect, whereas experimental studies of corrosion are generally carried out under accelerated conditions, and that due account needs to be taken of time dependent effects including creep and shrinkage. While these effects can be incorporated into FE-analyses, data on the effects of creep and shrinkage on tensile behaviour is very scarce. Modelling of such effects has been carried out by Dahlblom [1987] and Zhou [1992]. It was further pointed out by Noghabai that alterations to the constitutive law for crack unloading may alter the course of fracture in the concrete cover. This implies that crack mechanisms - as of course any nonlinear phenomena - are dependent on the previous state of deformations and loading history. This may be decisive for the performance of structures in general. The effects of corrosion may thus alter the mode of failure in a structure depending on the time of initiation of the corrosion process and its rate of progress. It is worth pointing out, however, that the significance of initiation of longitudinal cracking as a limit state criterion remains a matter of debate.

4.4.3 Local bond stress-slip relationship

The CEB-FIP Model Code 90 [1992] provides an average 'local bond' vs. 'local slip' model for

Copyright fib, all rights reserved. This PDF copy of fib Bulletin 10 is intended for use and/or distribution only by National Member Groups of fib.

black ribbed reinforcing bars and for smooth bars, Fig. 4-11. (Fig. 3.1.1 from MC 90). The relationship is divided into 4 phases, defined by (Eqs. 3.1-1 to 3.1-4). Two states of confinement are considered. Bond failure occurs by shearing across the tops of the ribs where concrete is 'confined', and by splitting where concrete is 'unconfined'. For both confinement states, the form of the rising branch of the relationship is given by MC90 eq.3.1-1, reproduced here as eq. (4-4).

$$\tau = \tau_{max}(s/s_1)^{\alpha} \text{ for } 0 \le s \le s_1 \qquad (4\text{-}4)$$

Several investigators present bond-slip data from a diverse range of pullout tests. Most show only the rising part of the curve, and therefore coefficients can only be estimated for the ascending part of the relationship, $s \le s_1$. Results invariably do not conform precisely to the shape of the CEB expression, and therefore it is not possible to obtain reliable values for coefficients. However, the qualitative effect of corrosion on the various parameters represented in eq. (3.1-1) is summarised in Table 4-3. The value of the coefficient α has been obtained by curve fitting through points on the relationship corresponding to τ_{max} and $\tau_{max}/2$. Differing trends are reported by the various studies. For example, a substantial decrease in s_1, slip at maximum load, is recorded in some cases and an increase recorded in others. Within the limits of the accuracy of the method of calculation, the value of α does not appear to be as greatly affected, although Almusallam et al [1996a] provide an exception. Clearly a far greater understanding of the many factors affecting bond of corroded reinforcement is required before a reliable model for the influence of corrosion on bond slip behaviour is developed.

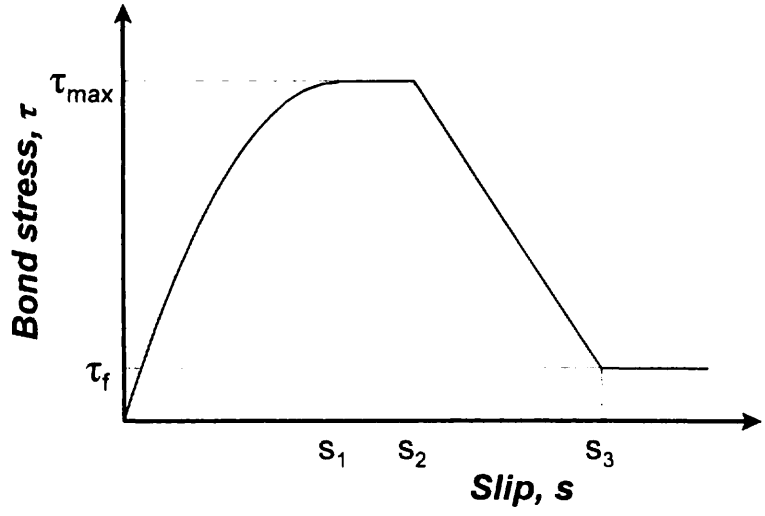

Figure 4-11 Local bond stress-slip model of CEB-FIP MC90 [CEB-FIP 1992]

4.4.4 Bond strength

Fig. 4-1 illustrated four mechanisms through which bond strength could be affected by corrosion. Models that might be used to predict the reduction in bond strength attributable to each of these mechanisms are now reviewed. Empirical expressions for bond strength of corroding bars presented by Rodriguez and co-workers [1994, 1996b] have already been described in the review of experimental work, and will not be discussed further here.

4.4.4.1 Cracking of concrete cover.

Dagher and Kulendran[1992] make reference to the danger of a reduction in bond capacity due to cracking of the concrete cover in their FEM analyses of corrosion induced cracking, but do not attempt to draw or infer any conclusion regarding the magnitude of the effects. Capuzzoca [1995] presented a model for the effect of corrosion on bond strength of ribbed reinforcement. He postulated that both bond and corrosion generate bursting stresses that tend to split the surrounding concrete, and that the effect of these bursting stresses may be superimposed. He therefore surmised that bursting stresses generated by corrosion would decrease the splitting resistance available to the bursting stresses generated by bond action, and hence that bond strength would start to reduce once corrosion initiates.

Copyright fib, all rights reserved. This PDF copy of fib Bulletin 10 is intended for use and/or distribution only by National Member Groups of fib.

	Section Loss %	α	s_1 mm	τ_{max} N/mm^2
Al-Sulaimani et al. [1990]	0	0.35	0.16	15.7
	7.8	0.4	0.27	4.0
	Change	+15%	+70%	-75%
Tachibana et al [1990]	0	0.35	0.27	12
	6 day	0.3	0.08	9
	Change	-15%	-70%	-25%
Cabrera & Ghodussi [1992]	0	0.25	0.43	20
	6.9	0.35	0.52	15
	Change	+40%	+20%	-25%
Almusallam et al. [1996]	0	0.10	0.7	16
	5.1%	0.01	0.1	13.5
	Change	-90%	-85%	-15%

Table 4-4. Comparison of coefficients for new and corroded bars in CEB-FIP Bond Model, derived from various studies.

Expressions which showed a reduction in bond strength in splitting failure modes with propagation of corrosion prior to development of longitudinal cracking were presented. The expressions predict zero bond resistance if cover is cracked by corrosion. As demonstrated in the earlier review of test data, bond strength actually tends to increase in the earlier stages of corrosion, and does not reduce below the 'as new' strength prior to the development of longitudinal corrosion cracking. It must therefore be concluded that the model is in error.

Concrete does not loose all tensile strength immediately on cracking, and some ability to transmit tensile and shear stresses across fine cracks is retained. Phillips and Zhang [1993], for example, show a rapid decrease in tensile stress after peak load followed by a slower strain softening phase until tensile strength is exhausted at a crack width of 0.10mm - 0.15mm. A number of other studies show similar trends [Noghabai 1995]. This suggests that confinement from concrete cover would be insignificant once longitudinal cracks exceeded 0.15mm in width. It is commonly assumed that bond strength is directly proportional to splitting resistance, from which it follows that bond strength should be negligible once longitudinal cracks reach 0.15mm. However, expressions for residual bond strength and crack widths derived from statistical analysis of test results by Rodriguez et al (Eqs 4-1, 4-2 and Fig. 4-4) suggest a negligible loss of bond strength at cracks of this size, even if no confining reinforcement is present. Thus even bond models based on a sophisticated representation of strain softening of concrete fail to correctly represent observed behaviour.

These observations, together with others reviewed in Section 4.3.3, raise questions over the contribution of tensile strength of concrete cover to bond strength, and suggests a need to rethink some of the fundamental assumptions which underpin many existing bond theories.

4.4.4.2 Changes in physical characteristics of bar/concrete interface.

It has been recognised for a number of years that bond behaviour of ribbed bars is dependent on the surface properties of the ribs. For example, Lutz & Gergeley [1967] reported a reduction in the slope of the bond/slip relationship where friction properties of the rib face were reduced by grease. A

Copyright fib, all rights reserved. This PDF copy of fib Bulletin 10 is intended for use and/or distribution only by National Member Groups of fib.

reduction was found for rib face angles greater than 45°, but greater reductions were found with ribs with lower rib face angles. The smooth surface of epoxy coated bars also results in a reduction in bond strength. Cairns and Jones [1995] and Darwin & Idun [1995] have independently developed models to take account of the difference in surface characteristics of ordinary mill scale and epoxy coated bars.

Friction between bar and concrete will be reduced by a weak layer of oxides at the interface between the two, and might therefore affect bond strength. Both Cairns and Jones and Darwin & Idun models require data on frictional properties of the bar/concrete interface, but unfortunately no such data for corroded bars appears to be available at the time of writing, and the models thus cannot be tested in a rigorous way. It may be noted, however, that both models suggest that the frictional characteristics of the rib face will have little influence if rib face angle exceeds a value of 40°-45°. The majority of European bars have rib face angles around or above this threshold. Some North American bars do have less steep face angles, and their bond strength will be susceptible to a reduction in bar/concrete friction.

4.4.4.3 Loss of rib area and disengagement of ribs.

It has been established through tests on a range of different bar patterns that bond strength of ribbed bars increases with increases in relative rib area, at least where bars are confined by links or higher cover [Cairns & Jones 1995, Darwin & Graham 1993]. The area of bar ribs bearing on concrete might be reduced by corrosion in two ways:

1) as the products of corrosion of steel occupy a greater volume than that of the material oxidised, the corrosion products will tend to prise apart bar and concrete. This is, of course, this same expansive action which also leads to cracking of the concrete cover. The interlock between bar rib and concrete will be reduced by an amount equal to the thickness of the corrosion layer, Fig. 4-12 (the layer of oxides on top of the rib will be mechanically weak and may be ignored). The reduction in rib bearing height will also be roughly equal to half the width of the longitudinal crack generated by corrosion. The effect of disengagement is likely to become significant as soon as longitudinal cracking develops.
2) ribs of deformed bars will eventually be lost due to corrosion. This effect is likely to be significant only where there is an appreciable loss of section, and is not considered further here.

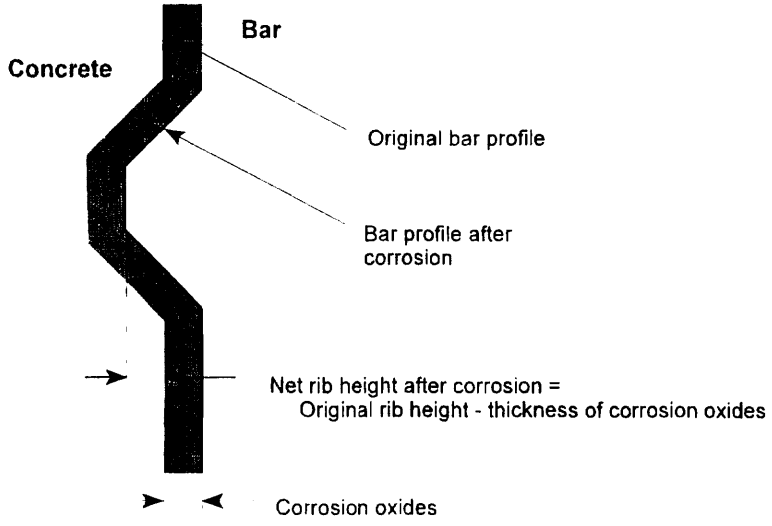

Figure 4-12 Reduction in rib/concrete interlock as a result of corrosion

Analyses of the influence of rib geometry, based on statistical analysis of bond strength of a variety of bars in similar test specimens, have been conducted by Cairns & Jones [1995] amongst others. Cairns' empirical expression was derived from tests on a particular lapped joint test specimen, and the predicted bond strengths are therefore not of general applicability. The expression has, however, been supported by theoretical models in which bond failure is considered as a bearing failure of the ribs

Copyright fib, all rights reserved. This PDF copy of fib Bulletin 10 is intended for use and/or distribution only by National Member Groups of fib.

[Cairns & Jones 1995, Cairns & Abdullah 1996] . The expression is used here to explore the nature of the change in bond strength that might be expected as a result of disengagement of ribs.

Cairns' empirical expression is given by eq. (4-5). It has been assumed that only relative rib area is affected by corrosion, and all other parameters including the confining force developed by concrete cover and the characteristics of the bar/concrete interface are unchanged. The original ribs have been assumed annular with a height of 0.0625 times bar diameter at a spacing of 0.8 times diameter, giving a relative rib area of 0.078 (the values are representative of normal production bars). Rib face angle and rib inclination have been taken as 45° and 60° respectively, values representative of normal production. It has been assumed that corrosion products occupy a volume twice that of the original metal, in line with commonly accepted values. Corrosion is assumed to reduce rib height by an amount equal to the thickness of the oxide layer.

$$f_b = 15.5\, f_r + 0.039\, \beta + 0.007\, \alpha \qquad (4\text{-}5)$$

where f_b - ultimate bond strength
f_r - relative rib area
β - rib face angle
α - rib inclination

Fig. 4-13 provides a comparison between residual bond strength predicted in this way and that measured by Rodriguez et al [1994] in accelerated corrosion tests on beam end specimens. Depth of corrosion attack has been related to surface crack width using Rodriguez' empirical expression, Fig. 4-4. The comparison must be treated extremely cautiously, as different test specimens were cast using different concrete grades in the two investigations and different bond strengths were measured. It is apparent, however, that the above analysis and Rodriguez' measurements show similar trends, and that predictions from this deterioration mechanism bear a closer relationship to loss of bond strength than do predictions based on loss of confinement from longitudinal cracking of concrete cover. Were this factor to control residual bond strength, however, it would be expected that smaller diameter bars would suffer greater loss of bond than larger diameter bars, at a given attack penetration, but no evidence in support of this has been found in the relatively limited experimental data available.

The models reviewed above all concentrate on a single deterioration factor, and may thus ignore important interactions between different failure mechanisms. Further work is required to understand the mechanisms which control residual bond strength of corrosion affected bars and to identify the controlling factors. For the time being practical models for residual bond strength are limited to empirical correlations based on interpretations by individual research groups of their own results.

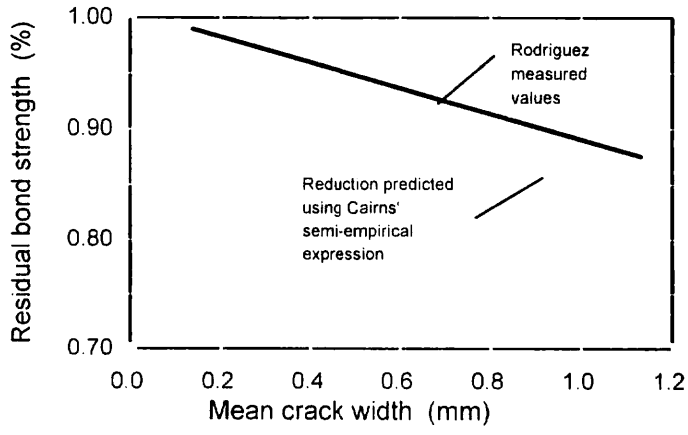

Figure 4-13 Predictions for residual bond strength of corroded bars based on reduction in rib interlock.

Copyright fib, all rights reserved. This PDF copy of fib Bulletin 10 is intended for use and/or distribution only by National Member Groups of fib.

4.4.5 Effects of bond loss on structural capacity

Codes of Practice for Design are not intended to cover conditions where bond is substantially reduced by corrosion or eliminated by breaking out of concrete around bars. When reinforcement is disbonded from concrete, the two materials can no longer act compositely. Normal assumptions of plane section behaviour do not hold true, and the pattern of strains in a beam under load is altered. This has led practising engineers to conservatively ignore bars where substantial longitudinal cracks have developed. Such procedures would suggest that members would have greatly reduced strength, but studies by Cairns [1993, 1995] and by Eyre and Nokhasteh [1992] on simply supported beams have demonstrated that considerable reserves may exist if ends of bars remain adequately anchored. A change from flexural to tied arch action was observed within the portion of the span over which reinforcement was exposed. The check on 'local bond' contained in some Codes may originally have been intended to ensure plane section action was maintained.

Cairns & Zhao [1993] reported a numerical model to take account of complete bond loss between tension reinforcement and the remainder of the concrete section. Their model used the normal stress-strain relationships given by design Codes, but employed a member based compatibility criterion in place of the normal section based criterion. They described the transformation of member behaviour from the purely flexural response of a beam with fully bonded bars to that of a tied arch where bond is eliminated. The change in behaviour is shown in the stress contour plots of Fig. 4-14, derived from numerical analyses of similar specimens, one with bars fully bonded and the other with bond eliminated throughout the span. The neutral surface (shown chain-dashed on the plots) remains horizontal throughout the span of the beam with fully bonded bars, apart from a small kink marking the point at which flexural cracking develops. By contrast, the plot for the beam with reduced bond shows higher compressive strains at the top face near midspan and a neutral surface which increases in depth towards the support. The increase in compressive strains explains the reduction in ductility and flexural strength observed when bond is eliminated; the variation in neutral surface depth shows that the compressive part of the moment couple is inclined, and not horizontal as in a beam with bonded reinforcement. Loads perpendicular to the axis of the member are resisted by the vertical component of the inclined compressive strut and not by shear stresses. Elimination of bond thus precludes a shear failure. Good agreement was obtained with results of physical tests. Fig. 4-15 illustrates typical results for simply supported beams as the length over which bond is lost is increased. Each line on the graph represents a different reinforcement percentage. No appreciable loss of strength occurs if bond is lost within the constant moment zone where shear force (and hence overall bond stresses) are zero. Once the length over which bond is lost extends outwith the constant moment zone, more heavily reinforced sections are affected first and to a greater degree. The principal factors found to affect behaviour are :

- length of bar disbonded.
- position of disbonded length.
- percentage area of reinforcement in beam section.
- strength of concrete, reinforcement and bond between the two.
- form of loading.
- concrete cross section shape.
- presence of compression reinforcement

The work demonstrated that lightly reinforced sections might be able to develop their full strength,

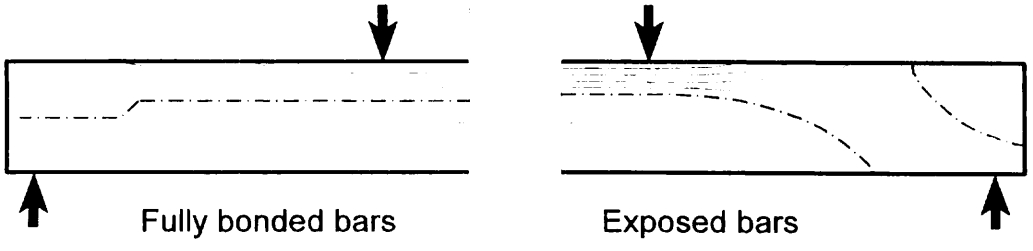

Figure 4-14 Stress contour plot for beams with fully bonded and exposed bars.

Copyright fib, all rights reserved. This PDF copy of fib Bulletin 10 is intended for use and/or distribution only by National Member Groups of fib.

as calculated using plane strain assumptions, despite bond being entirely lost over 90% of the span, (always provided ends of bars were adequately anchored). More heavily reinforced sections with reduced ductility were more vulnerable to strength loss.

In tests by Raoof & Lin [1996], sections without compression bars were also found to be susceptible to strength loss. Fig. 4-14 shows that tensile strains may develop on the top (compression) face of the beam where bond is lost. The effect is more marked if concrete is removed from the tension face of the beam, as would be the case while repairs are undertaken. 'Compression' bars are then required to act in tension, and beam strength is naturally impaired if none are present.

Cairns' and Eyre's analyses can be used to show that the specimens tested by Minkarah and Ringo [1982], and on which the recommendations of the NCHRP Report 292 mentioned in Section 4.2.3 [Imbsen 1987] are based, would not be particularly sensitive to bond loss.

Further work by Cairns & Watson [1993] and by Cairns [1995] showed that shear capacity may increase when bond is lost. Shear strength of reinforced concrete beams is conventionally regarded as the sum of contributions from four sources [Kong & Evans 1987], namely :

a) concrete in the compression zone
b) aggregate interlock in the tension zone
c) dowel action of flexural reinforcement
d) transverse reinforcement in the form of links or bent up bars

On the basis of this concept, it is to be expected that loss of bond between concrete and tension reinforcement would lead to a reduction in shear strength. In addition to the obvious loss of dowel capacity due to splitting of concrete cover, the reduction in bond will lead to wider crack widths, which in turn reduces aggregate interlock. Where the corner of a link is exposed, the contribution of the exposed leg of the link to shear strength may also be reduced. A qualitative analysis based on the conventional view of shear behaviour therefore suggests that shear capacity will be reduced on exposure of reinforcement. However, the change in structural action from flexural to tied arch behaviour means that loads applied perpendicular to the axis of the member may be resisted not by shear but by an inclined compression strut [Swamy et al 1970]. In a series of physical tests, disbondment of bars was found to increase strength of beams designed to fail in shear, in some cases by a substantial margin. Daly [1995] has observed a similar enhancement when bond of plain round bars is impaired by corrosion. Such an enhancement is, of course, dependent on adequate end anchorage of flexural reinforcement. A method of estimating the enhanced shear strength of reinforced concrete beams with exposed bars was proposed, based on semi-empirical rules for shear strength in the UK design Code BS8110. Note, however, that Clark and Thorogood [1985] reported the opposite effect, and attributed a reduction in shear capacity in the hogging region of beams to the reduced bond capacity of bars cast near the top of a pour.

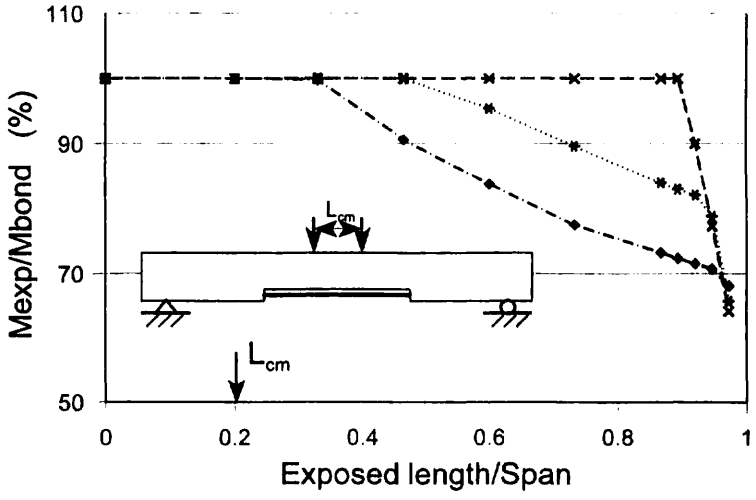

Figure 4-15 Effect of bond loss on beam strength. Cairns & Zhao [1993]

Copyright fib, all rights reserved. This PDF copy of fib Bulletin 10 is intended for use and/or distribution only by National Member Groups of fib.

Tachibana et al [1990] report a brief series of finite element analyses on a reinforced concrete beam. Bond was modelled by special joint elements using different parameters. Results from the FE model were compared with results of physical tests on corroded beam specimens. Bond parameters obtained from pullout tests were found not to be a reliable indicator of beam performance; their constitutive model, being based on pullout tests, used maximum bond stresses far higher than the average bond stresses in the beam. The model also appears to have assumed bond to continue at its maximum value above a slip of around 0.1mm, i.e. the bond-slip relationship did not have a falling branch. No bond slip information from the FE analysis is presented. Better results are claimed by the Authors for models which include the effects of longitudinal cracking. However, the formulation of the parameters used in the analyses is not clearly explained.

4.5 Conclusions

1 Bond strength may be reduced as a result of corrosion. Contributory factors may be some or all of:
   a) the loss of confinement resulting from cracking of concrete cover and from loss of link reinforcement cross section.
   b) the formation of a weak layer of corrosion products at the bar/concrete interface.
   c) the reduction of the effective bearing area of the ribs of deformed bars through loss of steel or through disengagement of bar and concrete.

   It is not clear at present which of these mechanisms exert the greatest influence on residual strength.

2 Initially bond strength increases with corrosion. There is no evidence that bond strength is reduced by corrosion prior to the formation of longitudinal cover cracks over the bar.

3 Loss of bond strength is potentially more severe than loss of bar cross section. Tests demonstrate that under general corrosion bond strength can be reduced by 50% when loss of bar cross section is only 10-12%.

4 The problem of assessing the influence of bond loss from corrosion on the load carrying capacity of structural elements can be separated into two parts, one concerned with end anchorage, the other with composite interaction.

5 Tests conducted to date on simply supported beams and slabs to date indicate that reductions in anchorage capacity are more likely to be responsible for loss of strength than reductions in composite interaction. However, it is suspected that some specimens may have been insensitive to reductions in local bond strength/stiffness. Most investigators report that failure becomes increasingly brittle with increasing corrosion.

6 Links provide a valuable role in maintaining residual bond strength of corroded beams. They are, however, more vulnerable to corrosion than main bars due both to a lesser cover and a greater surface/cross-sectional area ratio.

7 The majority of tests to date have been conducted under accelerated conditions using an impressed current. It is doubtful whether quantitative conclusions from these studies can be reliably applied to structures in the field.

8 There are considerable variations in the amount of corrosion required to initiate cracking and in the influence of cover/bar diameter ratio on time to cracking reported in various studies. An understanding of the mechanisms affecting bond strength of corroding bars and the establishment of an appropriate measure of damage is clearly a priority in reconciling conflicting test data and development of assessment guidelines.

9 There are also considerable variations in the loss of bond as a result of a given amount of corrosion reported by the various investigators. The cause of the variations is not entirely clear, but may be related (amongst several possibilities) to the method of specimen conditioning, bar diameter, cover, confining reinforcement, specimen configuration, concrete quality.

10 Theoretical models have been developed to predict the onset of longitudinal cracking. Such models are as yet unable to predict loss of bond strength as a result of corrosion.

Copyright fib, all rights reserved. This PDF copy of fib Bulletin 10 is intended for use and/or distribution only by National Member Groups of fib.

11 A better understanding of the mechanism through which corrosion affects bond is necessary to enable the controlling factors to be better understood, to reconcile apparent inconsistencies between different studies, and to enable effective models to be developed.

12 Most test data is for ribbed bars. There is a need for data relating to older types of bars also.

4.6 References

1967 Lutz, L.A. & Gergely, P. (1967) Mechanics of bond and slip of deformed bars in concrete. Proceedings of the American Concrete Institute, Vol. 64, No. 11, Nov. pp711-721

1970 Swamy, R. N., Andriopoulos, A, and Adepegba D. Arch action and bond in concrete shear failures. Proceedings American Society of Engineers, Journal of Structural Division, Vol 96, No. ST6. June 1970. pp1069-1091.

1973 Tepfers, R. A theory of bond applied to overlapped tensile reinforcement splices for deformed bars. Chalmers University of Technology, Publication No. 73:2, Gothenburg 1973. pp 328.

1977 Murphy F G. (1977) The effect of initial rusting on the bond performance of reinforcement. CIRIA Report 71. London

1979 Bazant Z P. (1979) Physical model for steel corrosion in concrete sea structures - theory and application. Journal Structural Division, Proceedings American Society of Civil Engineers. Vol 105, No. ST6.

1982 Jiang D H, Andonian A T, & Shah S P. (1982) A new type of bond test specimen. Bond in Concrete, Ed. Bartos, P. ASP London. pp 127-139.

- Minkarah, I., & Ringo, B.C. (1982) Behaviour and repair of deteriorated reinforced concrete beams. Transportation Research Record. No. 821.

- Tuutti K. Corrosion of steel in concrete. Swedish Cement & Concrete Institute. Report Fo4. 1982. 468pp.

1985 Browne, R (1985) Practical consideration in producing durable concrete. Proc ICE Seminar on Improving concrete Durability, London. pp 97-130.

- Clark, L.A. & Thorogood P. (1985) Shear strength of concrete beams in hogging regions. Proc. Inst. of Civil Engineers, Vol 79 Pt. 2. pp315-326.

1987 Dahlblom O (1987), "Constitutive Modelling and Finite Element Analysis of Concrete Structures with Regard to Environmental Influence", Dissertation, Report TVSM-1004, Lund Institute of Technology, Lund, Sweden, 1987, 154 pp.

- Imbsen R A. Liu W D. Schamber R A & Nutt R V. (1987) Strength evaluation of existing reinforced concrete bridges. NCHRP Report No. 292. Transportation Research Board. Washington D.C. 133 pp.

- Kong F.K. & Evans R.H. Reinforced and Prestressed Concrete (3rd Edition). Van Nostrand Reinhold. London. 1987.

- Parrott L J. (1987) A review of carbonation in reinforced concrete. Building Research Establishment. 42 pp.

- Pritchard,B. & Chubb,M. (1987) Concrete bridge integrity assessment. Structural Assessment; the use of full and large scale testing. Ed Garas, F K, Clarke J L, & Armer, G S T. Butterworths, London.

- Rostam S, Sorensen K A & Bergholt K. (1987) Full scale load tests of damaged concrete structures. Deterioration & repair of reinforced concrete in the Arabian Gulf. Bahrain Society of Engineers. Bahrain. pp 333-347.

1988 BSI (1988) BS4449 :1988 Carbon steel bars for the reinforcement of concrete. British Standards Institution. London. 13 pp.

- Okada K. Kobayashi K & Miyagawa T. (1988) Influence of longitudinal cracking due to reinforcement corrosion on characteristics on reinforced concrete members. ACI Structural Journal. Vol 85, No.2. March-April. pp134-140.

- Schiessel P. (Ed) (1988) Corrosion of steel in concrete. RILEM Report of Technical Committee 60-CSC. 96pp.

- Uomoto T & Misra S. (1988) Behaviour of concrete beams and columns in marine environment when

Copyright fib, all rights reserved. This PDF copy of fib Bulletin 10 is intended for use and/or distribution only by National Member Groups of fib.

corrosion of reinforcing bars takes place. ACI SP 109. American Concrete Institute, Detroit. pp 127-146.

1989 CEB (1989) Diagnosis and Assessment of Concrete Structures. CEB Bulletin 192. Lausanne. 130 pp.

- Department of Transport. (1989) Repairs and maintenance of the Midlands Links viaducts; working party report. Birmingham, UK.

1990 Al-Sulaimani, G J, Kaleemullah M, Basunbul I A, & Rasheeduzzafar. (1990) Influence of corrosion and cracking on bond behaviour and strength of reinforced concrete members. Proceedings American Concrete Institute, Vol 87, No. 2, Mar-Apr. pp220-231.

- Maslehuddin M, Allam I M, Al-Sulaimani G J, Al-Mana A L & Abduijauwad S N. (1990) Effect of rusting of reinforcing steel on its mechanical properties and bond with concrete. ACI Materials Journal, Sept-Oct. pp 496-502.

- Tachibana Y, Maeda K-I, Kajikawa Y, & Kawamura M. (1990) Mechanical behaviour of RC beams damaged by corrosion of reinforcement. Corrosion of reinforcement in Concrete. Ed Page, Treadaway and Bamforth. Elsevier. London.

1991 Cabrera G J & Ghodussi P. (1991) Discussion of Al-Sulaimani et al (1990). ACI Structural Journal. Jan-Feb. pp 125-126.

1992 Cabrera J G, and Ghodussi, P. (1992) Effect of reinforcement corrosion on the strength of steel concrete bond. Proc Int. Conf. On Bond in Concrete- from research to practice. Riga, Latvia. pp 10.11-10.24.

- CEB (1992) Design Guide Durable Concrete Structures. CEB Bulletin 183. Thomas Telford, London.

- CEB-FIP (1992) CEB-FIP Model Code 90. Telford. London.

- Dagher H J & Kulendran S. (1992) Finite element modelling of corrosion damage in concrete structures. ACI Structural Journal, Vol. 89, No. 6. pp 699-708.

- Eyre, J.R., & Nokhasteh, M.-A. (1992) Strength assessment of corrosion damaged reinforced concrete slabs and beams. Proceedings Institution of Civil Engineers, Structures & Buildings. Vol 94. pp 197-203.

- Feliu S, Gonzalez J A, Feliu S Jr., & Andrade M C. (1992) Confinement of the electrical signal for in-situ measurement of polarisation resistance in reinforced concrete. ACI Materials Journal, Vol 87, No. 5. Sept-Oct 1990. pp 457-460.

- Zhou F P (1992), "Time-Dependent Crack Growth and Fracture in Concrete", Dissertation, Report TVBM-1011, Lund Institute of Technology, Division of Building Materials, Lund, Sweden, 1992, 132 pp.

- Gannon, E J & Cady P D. (1992). Condition evaluation of concrete bridges relative to reinforcement corrosion, Volume 1: State of the art of existing methods. Strategic Highway Research Program Report SHRP-S-323. National Research Council, Washington DC.

1993 Andrade C, Alonso C, and Molina F J (1993), "Cover Cracking as a Function of Rebar Corrosion: Part 1 - Experimental Test", Materials and Structures, RILEM, Paris, vol 26, 1993, pp 453-464.

- Cabrera J G, and Ghodussi, P. (1993) The effect of corrosion level on the crack characteristics of reinforced concrete. Deterioration and Repair of Reinforced Concrete in the Arabian Gulf, Ed. Macmillan G L. Vol 2 pp 797-814.

- Cairns, J. & Watson, D. (1993) Structural aspects of concrete repairs : behaviour of beams with exposed reinforcement. Proceedings 4th International Conference on Deterioration & Repair of Reinforced Concrete in the Arabian Gulf. Bahrain.

- Cairns, J., & Zhao, Z. (1993) Structural behaviour of concrete beams with reinforcement exposed. Proceedings Institution of Civil Engineers : Structures & Buildings. Vol 99. pp141-154.

- Clark L A & Saifullah, M. (1993) Effect of corrosion on reinforcement bond strength. Proceedings Conference on Structural Faults & Repair. Ed Forde M. Engineering Technics Press. Edinburgh. Vol 3 pp 113-119.

- Darwin D & Graham E K. (1993) Effect of deformation height and spacing on bond strength of reinforcing bars. ACI Structural Journal, Vol 90, No. 6. Nov/Dec. pp 646-657.

- Molina F J, Alonso C and Andrade C (1993), "Cover Cracking as a Function of Rebar Corrosion: Part 2 - Numerical Model", Materials and Structures, RILEM, Paris, vol 26, 1993, pp 532-548.

- Phillips D V and Zhang (1993) Direct tension tests on notched and un-notched plain concrete specimens. Magazine of Concrete Research, Vol 45, No. 162. pp 25-35.

Copyright fib, all rights reserved. This PDF copy of fib Bulletin 10 is intended for use and/or distribution only by National Member Groups of fib.

1994 Andrade C., Alonso C., Somerville G., Pettersson K. and Tuutti K. (1994) The practical assessment of damage due to corrosion, in International Conference on Concrete Across Borders, 22-25 June, 1994, Odense, Denmark.

- Clark L A & Saifullah, M. (1994) Effect of corrosion rate on the bond strength of corroded reinforcement. Corrosion and Corrosion Protection of Steel in Concrete. Ed. Swamy, R N. Sheffield Academic Press. Sheffield, 1994. pp 591- 602.
- Daly A F (1994) Effects of accelerated corrosion on the flexural strength of small scale beams. TRL Research Report PR/CE/15/94. Unpublished. Transport Research Laboratory. Crowthorne UK.
- Rodriguez J, Ortega L M, & Garcia A M. (1994a) Assessment of structural elements with corroded reinforcement. Corrosion and Corrosion Protection of Steel in Concrete. Ed. Swamy, R N. Sheffield Academic Press. Sheffield. pp 171-185.
- Rodriguez J., Ortega L.M and Casal J. (1994b) Corrosion of reinforcing bars and service life of reinforced concrete structures: Corrosion and bond deterioration. Int. Conf. on Concrete across Borders, Odense, Denmark, Vol. II, pp 315-326.
- Rodriguez J., Ortega L.M, Garcia A M., Johansson L. & Petterson K. (1994c) On site corrosion rate measurements in concrete structures using a device developed under the Eureka project EU-401.Int. Conf. on Concrete across Borders, Odense, Denmark.
- Siwiec P., Moczko A. T. and Stroeven P. (1994) Study of steel bar corrosion by experimental and analytical simulation, DIANA Computational Mechanics `94 (eds G.M.A. Kusters and M.A.N. Hendriks), Kluwer Academic Publishers, the Netherlands, 383-394.

1995 Al-Qadi I L, Petersen J E, Weyers, R E. (1995) A time to cracking model for critically contaminated reinforced concrete structures. Proceedings Conference on Structural Faults & Repair. Ed Forde M. Engineering Technics Press. Edinburgh. Vol 3 pp 91-99.

- Cairns, J. (1995) Strength in shear of concrete beams with exposed reinforcement. Proceedings of the Institution of Civil Engineers, Structures & Buildings. Vol 110, No. 2. pp176-185.
- Cairns, J., & Jones, K. (1995) Influence of rib geometry on strength of lapped joints : an experimental and analytical study. Magazine of Concrete Research. Vol 47, No. 172, Sept.
- Cairns J. & Jones K. (1995) The splitting forces generated by bond. Magazine of Concrete Research, Vol. 47, No. 171. pp 153-165.
- Capozucca, R (1995) Damage to reinforced-concrete due to reinforcement corrosion. Construction and Building Materials. Vol 9, No. 5 pp 295-303
- Daly A F (1995) Effects of accelerated corrosion on the shear behaviour of small scale beams. TRL Research Report PR/CE/97/95. Unpublished. Transport Research Laboratory. Crowthorne UK.
- Darwin D & Idun E K. (1995) Discussion of " Influence of rib geometry on strength of epoxy coated reinforcement splices". American Concrete Institute Structural Journal. Vol 92, No. 6. Nov. Dec.1995. pp 782-784.
- Highways Agency. (1995) Design Manual for Roads and Bridges, Vol 3 Section 4, Part 13. BA51/95 The assessment of concrete structures affected by steel corrosion. HMSO, London. Feb.
- Kawamura A, Maruyama K, Yoshida S, & Masuda T. (1995) Residual capacity of concrete beams damaged by salt attack. Concrete under severe conditions, environment & loading. Vol. 2. Ed Sakai K, Banthia N, & Gjorv o E. Spon. London. pp 1449-1457.
- Noghabai K (1995) Splitting of concrete in the anchoring zone of deformed bars. Licentiate Thesis, Lulea University of Technology. 131 pp.
- Rodriguez J, Ortega L M , Casal J. (1995) Load carrying capacity of concrete structures with corroded reinforcement. Structural Faults & Repair.

1996 Almusallam A A, Al-Gahtani A S, Aziz A R, & Rasheeduzzafar (1996a) Effect of reinforcement corrosion on bond strength. Construction and Building Materials. Vol 10, No. 2. pp 123-129.

- Almusallam A A, Al-Gahtani A S, Aziz A R, Dakhil F H & Rasheeduzzafar (1996b) Effect of reinforcement corrosion on flexural behaviour of concrete slabs. Journal of Materials in Civil Engineering. Vol 8, No. 3. pp 123-127.
- BCA (1996) The residual service life of reinforced concrete structures. Final Technical Report on BRITE Project 4062. Confidential Report.

Copyright fib, all rights reserved. This PDF copy of fib Bulletin 10 is intended for use and/or distribution only by National Member Groups of fib.

- Cabrera, J G (1996) Deterioration of concrete due to reinforcement steel corrosion. Cement & Concrete Composites, Vol 18, No. 1. pp 47-59
- Cairns, J., & Abdullah, R. (1996) Bond strength of black and epoxy coated reinforcement - a theoretical approach. American Concrete Institute Materials Journal, Vol. 93, No. 4. July-Aug 1996. pp 362-369.
- Institution of Structural Engineers (1996) Appraisal of existing structures. London. 106 pp.
- Noghabai K (1996), "Environmental Effects on Bond in Reinforced Concrete Structures", Durability of Building Materials & Components 7 (ed C Sjöström). vol 1, E&F N Spon, London, 1996, pp 605-614.
- Raoof M, and Lin Z. (1996) Structural characteristics of RC beams with exposed main steel. Proceedings Institution of Civil Engineers, Structures & Buildings. Vol 122. pp 35-51.
- Rodriguez J, Ortega L M , Casal J and Diez J M. (1996a) Assessing structural conditions of concrete structures with corroded reinforcement. 4th Int .Congress on Concrete in Service Mankind, Dundee, UK.
- Rodriguez J, Ortega L M , Casal J and Diez J M. (1996b) Corrosion of reinforcement and service life of concrete structures. 7th Int. Conf. on Durability of Building Materials and Components, Stockholm.
- Rodriguez J, Ortega L M , Casal J (1996c) Load bearing capacity of concrete columns with corroded reinforcement. Proceedings 4th Int. Conf. on Corrosion of Reinforcement in Concrete Structures, Cambridge UK, July 1996. Ed. Page CL, Bamforth PB & Figg J W. SCI.

1997 Bamforth P. (1997) Probabilistic performance based durability design of concrete structures. Management of Concrete Structures for long term serviceability. Ed. Byars & McNulty. Telford, London. pp 33-44.

- Berra M, Castellani A, & Coronelli D. (1997) Bond in reinforced concrete and corrosion of bars. Proc. Conf. Structural Faults & Repair, Ed Forde M. Engineering Technics Press, Edinburgh UK. Vol 2. pp 349-356.
- Coronelli D. (1997) Bond of corroded bars in confined concrete: test results and mechanical modelling. Studi E Richerche, Vol 18, pp 137-211.
- Noghabai K. (1997) Environmental effects on bond between deformed bar and concrete - a fracture mechanics approach. Proceedings Fourth CANMET/ACI Conference on Durability of Concrete. Sydney, Australia. Aug. 1997.
- Stanish K. (1997) Corrosion effects on bond strength in reinforcement in concrete. MSc thesis, Dept. Of Civil Engineering, University of Toronto.

1998 Alonso C., Andrade C., Rodríguez J., Díez J.M.: Factors controlling cracking of concrete affected by reinforcement corrosion. Materials and Structures, Vol.31, Aug. Sept. 1998, pp. 435-441.

- Cairns J. (1998) Assessment of effects of reinforcement corrosion on residual strength of deteriorating concrete structures. Proceedings of the First International Conference on Behaviour of Damaged Structures, Rio de Janeiro, Brazil. Federal University of Fluminense, Niteroi, Rio de Janeiro. 1998. Also published at http://server.uff.br/damstruc/

Copyright fib, all rights reserved. This PDF copy of fib Bulletin 10 is intended for use and/or distribution only by National Member Groups of fib.

5 Bond of fusion bonded epoxy coated reinforcement

Working Party 5:

John Cairns (Convener, Heriot Watt University, Edinburgh, UK), **James O. Jirsa** (University of Texas at Austin, USA), **Steven McCabe** (University of Kansas, Lawrence, USA)

5.1 Background to fusion bonded epoxy coated reinforcement (FBECR) 219
5.1.1 Introduction 219
5.1.1 Development of FBECR 219
5.1.2 The problem of reinforcement corrosion 219
5.1.3 Manufacture of epoxy coated reinforcement 220
5.1.4 Effect of coating on reinforcement properties 220
5.1.5 Standards for FBECR 221

5.2 The importance of bond to structural performance 222
5.2.1 Bond : General 222
5.2.2 Modes of bond failure 222
5.2.3 Influence on design 222
5.2.4 Measurement of bond performance 223

5.3 Review of parameters influencing anchorage performance of FBECR 224
5.3.1 Introduction 224
5.3.2 Concrete strength 225
5.3.3 Coating type and thickness 225
5.3.4 Bar diameter 225
5.3.5 Confinement 226
5.3.6 Rib geometry 226
5.3.7 Casting position 228
5.3.8 Anchorage and lap length 228
5.3.9 Sustained and cyclic loading 229
5.3.10 Hooks and bends 229
5.3.11 Welded wire fabric 229
5.3.12 Fire resistance 229
5.3.13 Summary 230

5.4 Analytical models for bond strength of FBECR 230

5.5 Influence of FBECR on tension stiffening, deflection and cracking 231
5.5.1 Introduction 231
5.5.2 Tension stiffening and deflections 232
5.5.3 Crack control 232
5.5.4 Plastic rotation capacity 234
5.5.5 Summary 234

5.6 Review of existing code rules for design with FBECR 235

Copyright fib, all rights reserved. This PDF copy of fib Bulletin 10 is intended for use and/or distribution only by National Member Groups of fib.

5.7 Derivation of proposed additions to Model Code 90 for epoxy coated reinforcement **236**
5.7.1 General 236
5.7.2 Local bond stress-slip model 236
5.7.3 Tension stiffening effects 237
5.7.4 Moment curvature relationship 237
5.7.5 Rotation capacity 238
5.7.6 Ultimate strength of lapped joints and anchorages 239
5.7.7 Anchorage of stirrups 242
5.7.8 Limit state of cracking 242
5.7.9 Summary of proposed modifications to MC90 243

5.8 References **243**

Notation

$A_{tr}.f_{yt}/(s_t.\varphi)$ transverse reinforcement ratio
c : minimum cover or half bar spacing
f_{bs} : bond stress
f_{bu} : ultimate bond
l_b : lap or anchrage length
f_{cu} : concrete cube compressive strength
α_{sb}; relative rib area
β, : face angle of rib, bond coefficient
δf_s : change in stress along bar
δl_b : length of bar over which δf_s occurs
φ: nominal diameter of equivalent plain round bar
ψ: coefficient

Copyright fib, all rights reserved. This PDF copy of fib Bulletin 10 is intended for use and/or distribution only by National Member Groups of fib.

5.1 Background to Fusion Bonded Epoxy Coated Reinforcement (FBECR)

5.1.1 Introduction

Epoxy coated reinforcing bars were introduced to improve durability of concrete structures. The epoxy coating is impermeable and an electrical insulator, and resists corrosion of reinforcement by providing a physical barrier to the oxygen and moisture necessary for the corrosion reaction, and by interrupting electrical continuity of the corrosion cell. The surface texture of an epoxy coating is much smoother than the normal millscale surface of a hot rolled reinforcing bar, and affects the interaction, or bond, between reinforcement and concrete.

Bond of reinforcement influences structural performance at both serviceability and ultimate limit states. At the serviceability limit state, bond influences crack widths and deflection. At the ultimate limit state, strength of laps and anchorages depends on bond. In addition, bond characteristics of flexural reinforcement will influence rotation capacity of plastic hinges. Extreme loss of bond is also known to influence flexural and shear capacity of beams at the ultimate limit state, but changes of this degree lie beyond the change in bond that will arise as a result of epoxy coating, and are not considered further here.
The aim of this Chapter is to review the influence of an epoxy coating on bond and anchorage performance of reinforcement, and to develop recommendations for revisions to Model Code 90 to enable structures to be designed using epoxy coated bars to a margin of safety consistent with that for ordinary reinforcement.

5.1.1 Development of FBECR

Coating of reinforcement with a fusion bonded epoxy powder was originated in the USA in the 1960's, in response to widespread and severe deterioration of bridge decks due to corrosion of the steel. US practice was to use permanently exposed concrete wearing surfaces in bridge construction, and consequently deicing salts were spread directly onto the concrete deck. The salt easily penetrated the concrete cover, and led to serious corrosion of reinforcement and delamination of concrete cover, in some instances within only a few years of construction.

The huge scale of the problem prompted a major investigation by the American FHWA in the early 1970's into methods of resisting corrosion. One of the projects was concerned with use of non-metallic coatings [Clifton et al 1976]. Of 47 organic coating systems investigated, the only coatings to demonstrate adequate toughness and impermeability were the epoxy powder coatings originally developed to coat steel pipe. In 1973 the first bridge to use epoxy coated bars for deck reinforcement was constructed in Pennsylvania. An ASTM Standard for Epoxy Coated Reinforcement was first issued in 1981. Similar problems and further investigations in Canada resulted in 1978 in epoxy coated bars being specified for top steel in all bridge decks. By 1987, epoxy-coated bars accounted for around 5% of total reinforcement consumption in the USA. A British Standard for epoxy coated reinforcement was published in the latter part of 1990. Coated reinforcement is now widely specified in North America, and produced by 30 different plants. It is manufactured in the Middle East, the Far East, and Europe. Annual usage is reported as approximately 400,000 tonnes worldwide. Manning has provided an excellent review of the development of FBECR in North America (Manning 1996).

5.1.2 The problem of reinforcement corrosion

The alkaline environment surrounding reinforcement in sound fresh and uncontaminated concrete results in formation of a passivating layer on the surface of reinforcement which effectively prevents corrosion. It is only when the passivating layer is broken, either by carbonation of cover concrete, by penetration of chlorides through the cover, or by other less common mechanisms, that active corrosion may develop.

Corrosion is an electrochemical process. An electrochemical cell is set up with different areas on the bar surface acting as anodes and cathodes, Figure 5.1. Iron is lost (as iron ions) at the anode, and oxygen is reduced at the cathode to form hydroxyl ions. Electrons flow between anode and cathode through the steel bar, and the concrete assumes the role of the electrolyte, through which the hydroxyl ions migrate from cathode to anode. The essential requirements for dissolution of iron from reinforcement in a concrete structure are therefore [Schiessel 1988]:

breakdown of the passivating film at points on the bar surface.

Copyright fib, all rights reserved. This PDF copy of fib Bulletin 10 is intended for use and/or distribution only by National Member Groups of fib.

a difference in electrical potential at points on the surface of the bar.

moist concrete to act as an electrolyte

the availability of oxygen at the cathode

All four of the above factors must exist in order for corrosion to proceed, and the absence of any single factor will be sufficient to halt corrosion. If concrete is dry, for example, its resistivity will be very high, and it will be unable to function as an electrolyte. Corrosion therefore becomes insignificant in dry concrete. Organic coatings on reinforcement to prevent corrosion also function by interrupting continuity of the electrical circuit forming the corrosion cell, and also restrict the supply of oxygen to the cathode of the corrosion cell.

Considerable concern has been expressed about the vulnerability of a coated bar to flaws in the coating caused by damage during fabrication or construction [Davies 1990]. A number of studies of durability of concrete test specimens suggest that coating provides improved corrosion resistance even where the coating has been damaged [Treadaway & Davies 1989]. The well publicised corrosion damage to coated reinforcement of a bridge in a marine environment in Florida [Sagues et al 1990] fuelled doubts over durability and led to a ban on the use of epoxy coated bars in that state, but appears to have been attributable to faulty coating application and an absence of quality control. Other surveys of structures constructed with coated reinforcement show no problems of durability to date. It now appears to be generally accepted that although an epoxy coating cannot provide 100% protection against corrosion, it does enhance durability of reinforced concrete construction and is superior to galvanising.

Further discussion of durability aspects of FBECR lie outwith the scope of this report. For more information, the reader is referred to a recent CEB Bulletin [1992] on Protective Systems for Reinforcement.

5.1.3 Manufacture of epoxy coated reinforcement

Reinforcement for coating may be individual deformed bars, welded wire fabric, or prefabricated reinforcement cages. (Prestressing strand may also be coated, but is not considered further here) Although epoxy powder may be applied by spray or by fluidised bed dipping techniques, current national standards cover only electrostatic or tribostatic spray application to individual bars or to fabric. The process of coating individual bars comprises the following stages.

1. Cleaning by grit/shot blasting to SA 2.5 or better and (in some plants) chemical pre-treatment.
2. Heating to a temperature of around 240°C using a heating technique that does not impair cleanliness of the bar.
3. Application of the coating powder to the hot bar by a spray technique. (The electrically charged particles are attracted to the earthed bar)
4. Curing of the coating by the residual heat of the bar, followed by water quenching.

Fuller descriptions of manufacturing processes and technology are given by Read [1990] and by King [1990].

Prefabricated reinforcement cages are coated using the fluidised bed method. The cages are first fabricated by welding bars at all intersections before dipping in a tank containing a fluidised bed of epoxy powder. This method gives a greater thicker but less uniform coating thickness, which tends to smooth out bar deformations. Mechanical interlock of bar ribs with concrete can then not be relied on for transfer of force. Bond and anchorage are instead provided by welded transverse bars.

5.1.4 Effect of Coating on Reinforcement Properties

The consequences of each stage in the manufacturing process on mechanical properties of the reinforcement and on its interaction with concrete are now briefly examined to identify properties of coated reinforcement that may differ from those of non-coated bar.

Grit/shot blasting removes mill scale and any rust from the bar surface, and roughens the bar surface to provide a key to assist adhesion of the coating. The process will tend to smooth sharp re-entrant angles at the base of the ribs, where fatigue cracks tend to initiate, thus reducing stress concentrations. Hawkins

Copyright fib, all rights reserved. This PDF copy of fib Bulletin 10 is intended for use and/or distribution only by National Member Groups of fib.

[1976] has concluded that fatigue endurance of coated reinforcement is slightly better than that of black bars, and cyclic loading tests by Kobayashi and Takewaka[1984] have demonstrated that endurance of coated bars is satisfactory.

The increased strength of high yield reinforcement is obtained by alloying, cold working, quenching and tempering or by some combination of these. Reheating of the steel above a certain temperature may remove the effects of latter two processes. The temperature at which significant loss of residual strength will occur is of the order of 550°C [C&CA 1972, Rehm & Russwarm 1977], well above the temperature used in the coating process.

An epoxy coating is much smoother than the normal mill scale surface of a 'black' (i.e. non-coated) bar and is chemically inert. Chemical adhesion and friction between bar and concrete are therefore reduced by coating. Plain round bars, which rely on adhesion and friction for bond, are thus not suitable for coating, except where it is intended that bond be destroyed (for dowel bars in carriageway construction, for example) or where other means of force transfer are to be used (for example, by welded cross wires in fabric). As discussed later, Standards for coated reinforcement apply only to ribbed deformed bars and wire fabric. Subject to some restrictions on geometry of bar deformations, spray methods of coating are capable of providing a uniform coating thickness, and therefore do not significantly alter rib geometry. Changes in bond properties are then entirely attributable to the different surface texture of the coated bar.

The fluidised bed method provides less control over coating thickness than spray methods. It produces a thicker but less uniform coating, which tends to smooth out bar deformations. Bond is then affected by both the change in surface text and the change in rib geometry. The effectiveness of the interlock of bar ribs with surrounding concrete may be severely impaired. The fluidised bed method is more appropriate to prefabricated cages of reinforcement, where force is transferred by bearing of welded transverse bars, than to single bars.

5.1.5 Standards for FBECR

Coated reinforcing bars are manufactured to ASTM A775 [1989] or to ASTM A934 [1995] in the USA. ASTM A934 covers bars to be prefabricated prior to coating, ASTM A775 to bars that may be bent after coating. A specification for epoxy coated welded wire fabric is given in ASTM A884 [1991]. In the UK, BS7295 for coated reinforcement was published in 1990 [British Standards Institution 1990], and in Japan coated reinforcement is produced in conformity with Specifications of the Japan Society of Civil Engineers [1986a]. German and Norwegian Standards are also reported to be in preparation. Although epoxy powder may be applied by electrostatic or tribostatic spray or by fluidised bed dipping techniques, Standards apply only to spray methods of application.

It is now widely accepted that a coating thickness of 0.2mm provides an optimum compromise between durability and structural performance requirements, and this is reflected in product Standards. Results reviewed later in this paper are confined to coating thicknesses of this order, applied by spray methods.

Production Standards for coated bars specify tests for coating thickness, continuity and adhesion. Tests for hardness, impact resistance and abrasion resistance, bendability, chloride permeability and cathodic disbondment of the coating material may also be specified. Requirements of these Standards with regard to durability of coated bars have been discussed in some detail by Read [1989], and are not considered further here. Tests for mechanical properties of reinforcement specified in bar production Standards are not repeated on coated bars, but a bond classification test is specified. Both ASTM A775 and BS7295 utilise pullout type bond specimens. Such specimens generally preclude the splitting mode of failure found in lapped splices, and as a consequence, record bond strengths is considerably in excess of those normally attainable in a lapped joint, for example. The value of such tests for design purposes is questioned, [Cairns & Abdullah 1995b]. It is generally agreed that bond strength for design must be derived from tests that more closely represent practical situations.

Production Standards are material specifications and therefore do not cover structural design requirements, although all recognise that the smoother surface finish of the epoxy coating may adversely affect bond between reinforcement and concrete, and include a bond test requirement. Plain round bars, which rely on friction to transfer force between bar and concrete, are considered unsuitable for coating.

Copyright fib, all rights reserved. This PDF copy of fib Bulletin 10 is intended for use and/or distribution only by National Member Groups of fib.

5.2 The Importance of Bond to Structural Performance

5.2.1 Bond : General

Bond between reinforcement and concrete is necessary to ensure composite interaction of the two materials. The normal assumptions of plane section behaviour used in section analysis and design rely on composite interaction being achieved. Bond stress may conveniently be regarded as a shear stress over the surface of a bar, although, as discussed in more detail later, this representation is a considerable simplification. Bond stress is defined as the change in force in a bar divided by the area of bar surface over which the change in force takes place, Equation 5.1.

$$f_{bs} = \delta f_s.\varphi/4.\delta l_b \qquad \text{Equation 5.1.}$$

Bond strength initially comes from weak chemical bonds between steel and hardened cement, but this resistance is broken at a very low stress. Once slip occurs, friction contributes to bond, but with increasing slip between bar and concrete, bond comes to depend principally on the bearing, or mechanical interlock, of the ribs rolled on the surface of the bar with the concrete. In this stage, the reinforcing bar generates bursting forces which tend to split the surrounding concrete. The failure load may be limited by the resistance provided by concrete cover and confining reinforcement to these bursting forces.

When cured, an epoxy coating is chemically inert, and has a smooth surface. Both chemical adhesion and friction between bar and concrete will therefore be reduced by coating. Plain round bars, which rely on friction and adhesion for bond strength, are therefore unsuitable for use as normal reinforcement when coated.

5.2.2 Modes of Bond Failure

Three modes of bond failure of ribbed reinforcing bars may be identified, and are described in descending order of bond strength. The first, illustrated in Figure 5.2(a), is the pullout type failure. Concrete is sheared on a surface running across the tops of the bar ribs. This type of failure occurs where the resistance available to bursting forces, either through a thick cover or by heavy secondary reinforcement confining the bar, exceeds the bursting forces generated by bond. It is generally agreed that pullout failures occur where the minimum concrete cover is in excess of 3 times bar diameter.

Where concrete cover is less than twice the diameter of the bar, bond failure occurs by splitting of the surrounding concrete, Figure 5.3. Bond splitting failure can be divided into two types, as illustrated in Figure 5.2(b) and 5.2(c). Figure 5.2(b) shows the type of failure generally found with typical European non-coated bars. Bearing of the rib shears off a wedge of crushed concrete which remains adhering to the bearing face of the rib once the concrete splits.

The second type of splitting failure, Figure 5.2(c), may occur where the angle the rib face makes with the bar axis is relatively small, say less than 30°, or where the face of the rib is less rough than a normal mill scale finish. Here the inclined failure surface runs along the interface between rib and concrete, and not through the concrete, as in Figure 5.2(b). This is the failure mode in which the surface condition of a bar will influence failure strength most strongly.

Various researchers have observed that there appears to be a shift from the first to the second of the two splitting failure modes when coated bars are used. Jirsa and Treece[1989] and Choi et al [1991], for example, note that the wedges of crushed concrete found in front of the bearing face of the ribs on non-coated bars were absent on the coated bars.

Bars in compression are also able to transmit load by bearing of the end of a bar on the concrete [Arthur & Cairns 1978]. The higher design bond strengths allowed in some Codes for compression bars take account of the contribution of end bearing. End bearing also produces bursting forces which tend to split the concrete cover.

5.2.3 Influence on Design

For design purposes, bond is considered to be a factor in several aspects of the structural performance of reinforced concrete. At the serviceability limit state, bond characteristics of reinforcement influence cracking and deflection. At the ultimate limit state, strength of laps and anchorages depends on bond. The rotation capacity of plastic hinges is also influenced by the bond characteristics of the reinforcement. All

Copyright fib, all rights reserved. This PDF copy of fib Bulletin 10 is intended for use and/or distribution only by National Member Groups of fib.

the above aspects are dealt with in detail in the CEB-FIP Model Code 90[1993]. National Codes of Practice for design tend to take more or less explicit account of these factors through calculation or through 'deemed to satisfy' rules, although all major national codes do require explicit checks on anchorage capacity. In addition, section 3.1 of MC90 proposes a general bond stress - slip relationship for reinforced concrete. Parameters for both plain round and ribbed bars are presented. It is intended that the general relationship may in due course become an acceptable part of design procedures.

As coating the reinforcement with epoxy alters it's surface condition, it may therefore also affect the various aspects of structural performance mentioned above. Furthermore, as adhesion, friction and bearing are brought into play to varying degrees at different slips, coating may affect these various aspects of performance to differing degrees.

5.2.4 Measurement of bond performance

For the study of bond performance, two types of test may be carried out :

- anchorage type tests, in which a loading is applied to an individual bar in a manner that will cause the bar to be pulled out of the surrounding concrete. Anchorage bond stress is defined as the force applied to the bar divided by the surface area of the bar over the length of bar in bond.
- transfer type tests, in which a bar is stretched while embedded in concrete. Bar performance is generally assessed through deformation of the embedded bar in relation to that of a bare bar. Alternatively, if the test bar is instrumented with strain gauges, performance may be assessed through the difference in bar force at sections a known distance apart.

The former type is concerned with the ability of the concrete section to anchor the bar, and is relevant to anchorage/development lengths and to lapped joints. The second type of test measures the ability of the bar to share stress with the surrounding concrete, and is related to tension stiffening, and hence to beam deflections, to control of crack widths, and, if the bar is loaded beyond yield, to plastic rotation capacity.

Investigations into anchorage bond of FBECR may be further roughly subdivided into two main categories, namely investigations primarily concerned with the identification and quantification of the factors which affect bond behaviour, and investigations primarily concerned with the influence of bond behaviour on structural performance. The latter category include studies aimed at development of Code of Practice type rules.

Investigations in the former category generally use specialised bond test specimens such as axial pullout and beam end type specimens. Measurements are taken of slip and of bar force, from which bond stress may be derived. Comparison of performance in bond tests has been based on a variety of criteria, including failure load, limiting slip at a specified bond stress, and on bond stress developed at a specified slip, both at free and at loaded ends of test bars. In all studies, bond strength of coated bars has been compared with that of similar non-coated bars in an identical specimen.

Bond stresses from pullout type tests are often of little direct relevance to design, however [Cairns & Abdullah 1995b] . Strain conditions in a pullout specimen differ markedly from conditions in a beam under which crack width and deflection are checked. Bond strength depends on the resistance the section can provide to the bursting forces generated by bond action of ribbed bars, and pullout and beam end specimens typically provide significantly greater resistance than will be available at a lapped joint, for example. If bursting resistance is low, failure occurs by splitting of concrete cover along the line of the bar (splitting failure), but if resistance is high, failure occurs by the bar shearing the concrete across the tops of the ribs (pull-through failure), Figure 5.2. Bond strengths are substantially lower for splitting type failures, which therefore tend to be more critical for design. Pullout tests, on the other hand, typically fail in a pull-through mode. Bond strength measured in a pullout test is therefore not directly applicable to design, and, because of the different failure mechanisms, may not even provide a reliable comparison between different bars under conditions in which a splitting failure occurs [C&CA 1972]. For this reason, it is necessary to seek design guidance from tests more representative of practical construction.

Studies which deal with structural performance and which aim to develop design guidance use test specimens more representative of entire structural components such as beams, slabs or columns. Performance is assessed on the relevant aspect of performance. For example, at the serviceability limit state performance is assessed on measurements of deflection or crack width at working loads and performance at ultimate assessed on the maximum bar force developed in a lapped joint. Test specimens are generally larger (and more expensive to construct) than pullout type specimens.

Copyright fib, all rights reserved. This PDF copy of fib Bulletin 10 is intended for use and/or distribution only by National Member Groups of fib.

The variety of criteria used and the general absence of established relationships between bond strength as assessed in specialist (and somewhat arbitrary) bond tests and performance in a structural element does not make it easy to determine a unique 'bond reduction factor' for coated bars appropriate to practical design. Cairns & Abdullah[1994a] report that the ratio of bond stress developed by an epoxy coated bar to that developed by a nominally identical uncoated bar varies from approximately 0.55 to 1.1, depending on the slip at which comparison is made, Figure 5.4. Similarly, Cusens and Yu [1993] derived markedly different reduction factors depending on whether comparison was based on measured slip at specified bond stress or on failure strength. Jirsa and Treece[1989] concluded that reduction factors of 0.67 and 0.87 were appropriate to 'low' and 'high' cover situations respectively. The dependence of bond reduction on the conditions and criteria selected suggests that the search for a unique bond reduction factor for coated bar may be fruitless, and that different reduction factors may be appropriate to different aspects of bond performance and to different details.

5.3 Review of Parameters Influencing Anchorage Performance of FBECR

5.3.1 Introduction

This section of the report reviews the findings of research studies into the factors which affect anchorage bond performance of fusion bonded epoxy coated reinforcement. The format adopted is to compare performance of coated bars against that of equivalent non-coated bars under identical conditions. The objective is to identify those parameters which affect the relative bond strength of coated and non-coated bars. This form of assessment will be commented on critically in a later section of the report.

Several investigators comment on the different appearance of coated and non-coated bars after bond failure. The epoxy coated bars are reported to retain a smooth glassy surface with no adherent concrete particles, whereas mild steel bars with a mill scale surface generally had concrete particles adhering to the bar surface, and crushed concrete adhering to the bearing face of ribs. These observations provide evidence of reduced adhesion between concrete and coated bars.

Further evidence of adhesion loss was provided in a series of tests conducted by Cairns and Abdullah [1994a] to compare frictional properties of mill scale steel surfaces and a fusion bonded epoxy surface. They reported that for both types of surface friction was composed of an adhesion component, independent of normal stress, and a frictional component which varied in proportion to normal stress. The friction component differed little between coated and uncoated surfaces, but coating caused a significant loss in adhesion. At low normal stress, ultimate shear stress between coated steel and concrete was of the order of 60% of that between mill scale steel and concrete. The difference between surfaces, as expressed by the ratio of shear strength for coated to mill scale surfaces, reduced with increasing normal stress.

As outlined earlier, assessment of bond performance may be based on a variety of criteria. Only two are used here. Firstly and most widely, bond strength is used for comparison. Secondly, bond stiffness, generally measured as the bond stress at a defined value of slip, is also used.

Virtually all studies have concluded that bond strength may be reduced by an epoxy coating. Bond strength ratio, defined as the ratio of the measured bond strength of a coated bar to that of a similar non-coated bar under identical conditions, is generally reported to be in the range 0.75 to 0.9, although ratios in the range 0.65 to 1.10 have been reported in individual studies. The following sections review the various factors which may influence bond strength with a view to identification of those which influence bond strength ratio.

Bond stiffness is also generally reduced by coating, particularly at low slips, Figure 5.4. The reduction has a marked dependance on the slip at which the comparison is made. Differences in the precise criteria used, and the generally less comprehensive reporting of measurements of bond stiffness, preclude as detailed a review as is possible for bond strength. It may be noted that bond stiffness ratio varies more than does bond strength ratio. For example, Cairns and Abdullah[1994a] report that bond *stiffness ratio* increased from approximately 0.5 to 1.1 as slip increased from 0.01mm to 1.0mm. Cusens and Yu report bond stress ratios of 0.44 to 1.00 based on 'critical' bond stresses (lesser of bond stress at free end slip of 0.5mm and at loaded end slip of 0.25mm) measured in beam end[1993] and pullout [1992] tests. They also noted a lesser difference between loaded and free end slips where coated bars were used, which also points to a lesser bond stiffness for the coated bars.

Copyright fib, all rights reserved. This PDF copy of fib Bulletin 10 is intended for use and/or distribution only by National Member Groups of fib.

5.3.2 Concrete Strength

Jirsa and Treece[1989] tested lapped splices in beams constructed using concrete cylinder strengths over a range of 27MPa to 88MPa, but did not detect any influence of concrete strength on the ratio of bond strengths for coated to that for non-coated bars. Cleary and Ramirez [1991] found no difference in bond strength ratio between specimens manufactured using concrete strengths of 27.6MPa and 48.3MPa. Hamad & Jirsa [1993] reported concrete strengths in the range 35MPa to 65MPa to have only a minor influence on bond strength ratio.

5.3.3 Coating type and thickness

No evidence is reported which suggests that the proprietary brand of epoxy powder used to coat the bars has any effect on bond behaviour [Cairns & Abdullah 1994a,1994b].

Several studies using different types of bond test specimen have shown that variations in thickness of spray coatings within the range 0.13mm-0.30mm, the range permitted by ASTM A775, do not influence bond strength significantly[1][Jirsa & Treece 1989, King 1990]. Choi et al[1991] also agree that variations in coating thickness (within the allowable range) have an insignificant influence on bond strength ratio for no. 6 (19mm) and larger bars, but reported that bond strength ratio dropped from an average of around 0.93 to 0.84 with no. 5 (16mm) bars as coating thickness increased from 0.13mm to 0.30mm. Even with the thickest allowable coating of 0.30mm, however, the bond strength ratio for the no. 5 bars did not drop significantly below that for the larger bars. Hamad & Jirsa [1993] also concluded that variations in coating thickness within the range permitted by ASTM A775 had no influence on bond strength ratio for no.6 and no. 11 bars. In a short series of pullout tests, Kobayashi and Takewaka[1984] report a reduction of 0.04, half that measured by Choi et al, also for 16mm diameter bars.

Some studies report the shape of a rib to be altered by coating, that the rib becomes rounded over, and that the effective height of the rib is reduced. Measurements of rib geometry on UK produced reinforcement before and after coating showed size and shape of the ribs to be unaltered by coating [Cairns & Abdullah 1989]. It appears that the uniformity of coating thickness may vary according to the degree of control attainable at the coating plant. Non-uniformity of coating thickness will be greater on smaller diameter bars where the coating forms a greater proportion of bar diameter. With the relatively small influence measured, the effect of variations in coating thickness may be of little practical importance given the strength advantage conferred by high cover ratios where small bars are used.

5.3.4 Bar diameter

It is recognised that larger diameter bars develop less bond strength than smaller under otherwise constant conditions. This is at least in part because cover, as a proportion of bar diameter, is reduced as bar size increases. Analyses of bond strength are therefore based on the assumption that it is the ratio of cover to bar diameter which controls strength. This section follows the same practice, and the effect of bar diameter on bond strength is assessed under conditions of constant cover ratio.

Tests were conducted on three diameters of bars cast in the corners of beam end specimens at BCA [Clarke 1990]. Cover to bar diameter was maintained constant at 1.5. It has been established that the specimens give 'realistic' bond strengths for design purposes. The ratio of bond strengths for coated to non-coated bars was 0.80, 0.88 and 0.88 for bottom cast 10mm, 25mm and 40 mm diameter bars respectively. For top cast bars, corresponding ratios were 1.09, 0.98 and 1.0.

Choi et al[1991] also tested beam end specimens with bars sizes Nos. 5, 6, 8 and 11. (16mm, 19mm, 25mm and 38mm) with a range of coating thicknesses. All had a cover of 2 times bar diameter, and were bottom cast. Bond strength ratios averaged 0.88, 0.89, 0.83 and 0.86 respectively over three different rib patterns. A series of beam splice tests, conducted as part of the same study, produced similar conclusions, with an average bond ratio of 0.82 and no clear influence of bar diameter. Results from pullout test by Hamad & Jirsa [1993] and from splice tests conducted by Jirsa and Treece[1989] using No 6 and No. 11 bars also produce the same conclusion, although Treece and Jirsa reported a much reduced bond strength ratio of around 0.66. None of the studies conducted to date indicate a significant dependence of bond ratio on bar diameter.

---

[1] BS7295 imposes a tighter specification of 0.15mm-0.25mm on coating thickness.

Copyright fib, all rights reserved. This PDF copy of fib Bulletin 10 is intended for use and/or distribution only by National Member Groups of fib.

5.3.5 Confinement

Bond action of ribbed bars generates bursting stresses which tend to split the surrounding concrete. Bond strength in a splitting failure mode is considered to be limited by the splitting resistance of a concrete hoop around the bar, together with additional resistance from any confining reinforcement crossing the failure plane. Tensile capacity of the concrete hoop is assumed to be dependant on the lesser of minimum cover thickness or half the clear spacing between adjacent lapped joints. Semi-empirical regression analyses of test data demonstrate that bond strength of non-coated bars increases with confinement to the bars, either from increased cover, transverse reinforcement, or lateral pressure.

In tests using beam end type specimens, Choi et al[1991] demonstrated that the absolute increase in bond strength with concrete cover is similar for both coated and non-coated bars, and hence that the difference in bond strength between coated and uncoated bars (expressed as a ratio) reduces with increasing cover. The change in bond strength ratio depended on the precise basis on which the comparison was made, but averaged 0.88 to 0.93 as cover increased from 2 to 3 bar diameters. The change in bond ratio reported by Hamad & Jirsa [1993] for an increase in cover from 1 to 2 bar diameters was a more modest 0.72 to 0.74.

Hamad & Jirsa [1993] tested eccentric pullout tests in which one half of the bar was embedded in concrete, and a confining force could be applied directly to the other face. No very clear effect of confining force emerged from the study. This may have been attributable to the altered mode of failure as the 'top load' was increased. The confining force applied was probably somewhat greater than would be expected in a lapped joint, for example.

Hamad and Jirsa [1993] and Hester et al [1993] have both examined the influence of confining links on bond strength of coated reinforcement. In a series of 12 tests on beam laps, Hamad reported average increases in bond strength ratio from 0.74 where splices were unconfined by links to 0.81 and 0.84 where increasing amounts of confining reinforcement were provided for No. 11 bars. For No. 6 bars, bond strength ratio increased from 0.67 to 0.74 with the addition of links. However, when Hester et al analysed results from their own 65 test specimens along with the 12 of Hamad et al, they concluded there was no significant variation in bond strength ratio with varying amounts of confining reinforcement. Differences between these studies may have influenced measured bond ratios and their analysis. For example, the range of confining reinforcement investigated by Hester et al is greater than that used by Hamad and Jirsa, and extends beyond the limit, suggested by Orangun et al [1975], to which additional quantities of confining reinforcement increase bond strength. Nonetheless, the effect of increasing confinement on bond ratio remains rather unclear. Both increased cover and quantities of confining reinforcement would be expected to exert similar effects. However, results reported to date suggest that bond strength ratio increases with cover, but may not be increased by confining reinforcement.

5.3.6 Rib Geometry

Principle parameters used to quantify rib geometry of ribbed bars are :

- relative rib area, α_{sb}, a measure of the area of the ribs above the core of the bar, projected on a plane perpendicular to the bar axis, to the nominal surface area of the bar.
- the face angle of the rib, β, Figure 5.5.

The inclination of the rib to the bar axis has also been shown to exert a minor influence on bond strength.

In early studies, bond strengths of coated bars were generally reported as between 80% and 100% of strength of coated bars in pullout tests [Mathey & Clifton 1976, Kobayashi & Takewaka 1984, Salparanta 1989], although it is possible that coated and non-coated bars may not have been identical in some series. The basis of comparison was a limiting slip in some cases and a maximum load in others. However, one study by Swamy & Koyama [1988] noted the very different relative bond strengths of coated and non-coated bars obtained when testing bars with different rib shapes. Bars with three different rib patterns were tested, and reductions in bond strength when coated found to range between 3.9% and 31.6%. Precise details of rib geometry were not reported.

Beam end tests reported by Choi et al[1991] demonstrated that bond strength ratio varies considerably with the deformation pattern rolled on the bar. Of the three rib patterns examined, that with ribs perpendicular to the bar axis and designated type 'S' exhibited the greatest reduction on coating. The associated beam splice tests conducted as part of the same study do not show the same dependence on rib pattern, however, and the bar pattern exhibiting the greatest reduction in the beam end tests exhibited the smallest reduction in the splice tests. It is worth noting that the bond strengths attained in the beam end tests were around four times greater than those attained in the splice tests, and may have affected the

Copyright fib, all rights reserved. This PDF copy of fib Bulletin 10 is intended for use and/or distribution only by National Member Groups of fib.

failure mechanism. Although some details of rib geometry were given, relative rib area and rib face angle were not reported.

Cairns and Abdullah[1994a] report a series of pullout tests on machined bars of constant relative rib area and varying rib face angle, Figure 5.6. Rib face angle clearly influenced the bond stress ratio of coated to non-coated bars at low values of free end slip, but at high slips (of 1.0mm and beyond) the influence of rib face angle was minimal. Bond strengths in these specimens were high (>10MPa), and failure generally occurred in a pull-through mode, Figure 5.2(a). The dependence of the bond stress ratio on the slip at which it is measured probably reflects a difference in the location of the slip surface. At low slip, bar/concrete movement will occur at the bar concrete surface, as shown in Figure 5.2(b) or (c). At high slips, bar/concrete movement will occur on a surface running across the tops of the ribs, as indicated in Figure 5.2(a), and it is evident that the surface condition of the bar would then have a minimal influence on bond performance.

Hamad & Jirsa [1993] tested three different rolled bar patterns in an eccentric pullout test specimen. In some specimens, one side only of the bar was cast in concrete, and a variable confining 'top load' applied directly to the opposite side. They reported no difference in bond strength ratio of three different rib patterns, described as diamond, parallel and crescent shaped, under comparable conditions. Bond strength ratios ranged between 0.65 and 1.0, covering a range of test conditions. However, all bars had similar rib face angles of around 30°, and it appears that relative rib areas may not have been markedly different. Hamad and Jirsa also tested manufactured bars with rib face angles of 30°, 45° and 60°. The 30° bars exhibited the lowest bond strength ratio, as would be expected from earlier studies by Lutz and Gergely [1967], but the 45° bars exhibited a higher bond strength ratio than the 60° bars. Bond strengths were relatively high (>10MPa) and it is reported that the steeper rib face angles tended towards a pull-through failure mode, whereas the shallower ribs tended to fail by the ribs riding over the concrete keys, in a manner akin to a splitting failure.

In tests on specimens representing lapped joints, Cairns and Abdullah[1995a] demonstrated that bond strength of coated and non-coated bars was affected by both relative rib area and by rib face angle, and that the strongest epoxy coated bars could develop approximately the same strength as the weakest black bars. They derived regressions equations for their test specimen which showed that bond ratio would be expected to increase with increasing rib face angle, Figure 5.7. Darwin and Idun [1995] agree that greater reductions in bond strength are found where the rib face is at an acute angle to the bar axis, ie where the rib face angle β is low, Figure 5.5, but suggest an alternative form of relationship to the regression relationship proposed by Cairns & Abdullah, Figure 5.8. As most bars tested by Cairns and Abdullah had rib face angles below the value corresponding to the step in Figure 5.8, the results are not inconsistent. The form of relationship in Figure 5.8 is also consistent with that obtained through a theoretical model for bond splitting failures developed by Cairns & Abdullah [1996], Figure 5.9. Both suggest that there may be a rib face angle beyond which coated and non-coated bars would develop the same bond strength. In another set of tests in which enamel paint was used to simulate an epoxy coating, Hamad [1995] also demonstrated that the difference between coated and non-coated bars reduces with increases in rib face angle, and also provides evidence which could support the suggestion of a limiting rib face angle above which a coating would not reduce strength. Whether this angle lies within the range of bar face angles normally rolled or readily coated remains to be established.

In conditions corresponding to minimum confinement at a lapped joint, Cairns and Abdullah [1995a] found that bars with higher relative rib areas were stronger and exhibited larger bond strength reductions when coated. Darwin and Idun [1995], Hamad [1995], and Tan et al [1996] all arrived at the opposite conclusion, namely that bars with higher relative rib areas exhibit lesser bond strength reductions when coated. Cairns and Abdullah tested lapped joints confined by minimum links, whereas Hamad and Darwin and Idun both tested bars unconfined by links, which the latter suggest may be the cause of the difference. The greater bond strengths obtained in these studies (around 4 and 2 times greater than those measured by Cairns and Abdullah) may also be relevant, as it is possible that a different mechanism may have controlled failure in the two studies. Tan et al tested lapped splices of high rib area (α_{sb} >0.1) bars with and without stirrups, and reported that the ratio of coated/uncoated anchorage strength increased from around 0.7 to 0.9 with an increase in relative rib area from 0.07 to 0.14, although individual results showed an appreciable scatter. However, the difference between coated and non-coated bars measured by Cairns and Abdullah for standard relative rib areas ($\alpha_{sb} \approx 0.065$) was less than that measured by Tan et al under broadly similar conditions. There is therefore some uncertainty about the influence of relative rib area on bond strength reduction.

Copyright fib, all rights reserved. This PDF copy of fib Bulletin 10 is intended for use and/or distribution only by National Member Groups of fib.

The difference is important, as reduction factors for design with coated bars should be (conservatively) derived from strengths of the inherently weakest bars, used in the weakest section detail. It is recognised that bond strength increases with relative rib area, and comparisons should therefore be based on bars with relative rib areas close to the minimum allowable. According to Cairns and Abdullah, it is then the smallest bond strength reduction factors which are relevant, whereas according to Darwin and Idun's results, bond strength reduction factors for design should be based on the largest reduction factor measured. It also appears that bond strength ratios may be dependent on the degree of confinement available from the surrounding concrete, and also (as will be demonstrated later) on bond length. There remains a need to account for the opposing conclusions reached in these studies.

5.3.7 Casting position

Compaction of concrete tends to be poorer close to the top of a pour, and bleeding and settlement of fluid concrete may lead to formation of a weak layer below bars cast near the top of a pour. Bond strength is dependent on the quality and compaction of the surrounding concrete, and bars cast in locations near the top of a pour tend to be weaker in bond than those cast near the bottom. The effect is well established from tests on non-coated bars, and the CEB-FIP MC 90, for example, imposes a reduction factor of 0.7 on bond strength of 'top cast' bars.

In an extensive study employing beam end test specimens, Hadje-Ghaffari et al [1994] examined the interaction of slump, casting position and compaction. They found bond strength of coated bars to be affected less by 'poor' casting position than black bars, and suggested a reduced top bar factor. Top cast non-coated and coated bars were found to exhibit a similar reduction in low slump (<100mm) concretes, with a top cast factor (ratio of bond strength of bar when cast near top of pour to that of identical bar cast near base of pour) around 0.88. For high slump (>125mm) concretes, the top cast factor for non-coated bars reduced markedly to 0.78, while for coated bars it was 0.93, higher than the low slump value. They also noted that lack of compaction had a more detrimental effect on coated than non-coated bars.

Tests conducted at BCA [Clarke 1990] also showed the effect of a 'poor' casting position to have less effect on epoxy coated bars than on black bars. Top bar reduction factors of 0.67, 0.72 and 0.78 were measured for 10mm, 25mm and 40mm diameter non-coated bars respectively. For coated bars, the corresponding top bar factors were 0.91, 0.80 and 0.88. Details of concrete workability and compaction were not reported.

5.3.8 Anchorage and Lap Length

Little reliable test data is available on bond strength of coated bars over a range of anchorage or lap lengths. Many test series on lapped joints either contain only a very narrow range of lap length ratios (lap length expressed as a multiple of bar diameter) [Choi et al 1990, Hamad & Jirsa 1993] or simultaneously vary lap length ratio and another important factor [Jirsa & Treece 1989, Cleary & Ramirez 1991& 1993].

Three studies contain tests in which lap length has been varied independently [Clarke 1990, Cairns & Abdullah 1994b, Makhlouf et al 1994], and results are summarised in Figure 5.10. Note that the various studies all employed different lap details and quantities of confining reinforcement, and results are therefore not directly comparable. Bond strength was clearly reduced by the epoxy coating. The reduction varied from 30% for one of the shortest to 12% for the longest lap tested. In all cases average bond strength of non-coated bars was found to reduce with lap length, but lap length had little influence on average bond strength of coated bars. The difference between coated and non-coated bars therefore tended to reduce with increasing lap length. All three studies indicate that, unlike ordinary black bars, bond strength of epoxy coated laps is substantially independent of lap length. Beam end tests conducted by Cusens and Yu [1993] provide further supporting evidence, based on comparisons of bond stress at critical values of slip, that the difference in average bond strength between coated and non-coated bars reduces with increases in bonded length.

Results from pullout tests have demonstrated that an epoxy coating reduces bond/slip stiffness of reinforcement. Using a RILEM pullout type specimen, Cairns & Abdullah[1994a] showed bond stiffness to be reduced by an epoxy coating by around 20% at slips of 0.25mm, the slip at which bond failure of a lapped joint has been observed to occur. The influence of bond/slip stiffness on the distribution of bond stress along a lapped bar may be analysed using Modulus of Displacement Theory. The theory was first developed for analysis of distribution of loads amongst rivets in long lapped joints, and was subsequently developed by Tepfers for analysis of bond stresses along a lapped joint [1973]. Figure 5.11 plots variation in bond stress along the length of a single lapped bar for three lap length ratios as tested by Cairns & Abdullah[1994b]. Average bond stress is taken to be the same for all three lap lengths. A

Copyright fib, all rights reserved. This PDF copy of fib Bulletin 10 is intended for use and/or distribution only by National Member Groups of fib.

constant bond slip stiffness of 0.005N/mm^3 has been used in calculations, derived from measurements on lapped joint specimens [Cairns & Abdullah 1995a]. Tensile strength of concrete has been taken to be negligible in the analyses, allowing interaction between reinforcement and concrete to be ignored. The analytical results presented here are therefore based on considerable simplifying assumptions, and are intended to give a qualitative description only of behaviour. Similar calculations were carried out for bars with a reduced bond slip stiffness 0.004N/mm^3, representing behaviour of epoxy coated bars.

Bond failure occurs when splitting resistance of the concrete cover and any secondary reinforcement is exceeded. Clearly, bond failure will be initiated where bond stresses are highest. The plots in Figure 5.11 show bond stress to be highest close to the ends of the lapped joint. This is to be expected from observations of splitting cracks, which first form close to the ends of the lap. Judge, Scott & Gill [1990] have confirmed experimentally the presence of high peak bond stresses at ends of lapped joints. If bond failure is taken to be related to peak bond stress, it follows that mean bond stress at failure will decrease with increasing lap length. Equation 5.2, derived from statistical analysis of test data on strength of lapped joints [Orangun et al 1975], shows this to be the case.

$$f_{bu} = [0.09 + 0.24\, c/\varphi + 3.9\, \varphi/l_b + 0.022\, A_{tr}.f_{yt}/(s_t\, .\varphi)].\sqrt{f_{cu}} \qquad \text{Equation 5.2.}$$

Now consider the effect of bond stiffness on bond stress distribution. Figure 5.12 presents mean bond stresses calculated for "Stiff" and "Flexible" bond/slip characteristics, representing behaviour of non-coated and epoxy coated bars respectively. The force applied to the lapped joints has been adjusted to give the same peak bond stress for all lap lengths. Figure 5.12 shows the reduction in mean bond stress with increasing lap length to be less marked for bars with more flexible bond/slip characteristics. If it is taken that bond failure is related to peak bond stress, it follows that mean bond strength of epoxy coated bars will be less strongly influenced by lap length than that of non-coated bars, as has been observed.

5.3.9 Sustained and Cyclic Loading

Clifton and Mathey [1983] report that creep of epoxy coated bars in pullout specimens at tensile stresses of 103N/mm^2 and 206 N/mm^2, corresponding to average bond stresses of 1.61N/mm^2 and 3.22N/mm^2, is of the same order as that of black bars. Cusens and Yu [1993] conducted sustained load tests on 2 pairs of beam specimens, and measured free end and loaded end slips. The increase in measured slips under sustained load appears to be somewhat higher for coated bars, particularly at the free end, but rigorous conclusions cannot be drawn from the small number of specimens tested.

Similarly, Johnston and Zia [1982] concluded that behaviour of coated bars under cyclic loading was essentially similar to that of black bars, although a tendency for the differential to diminish as the number of cycles increased was noted. Cusens and Yu [1993] reported a similar or slightly reduced difference in slip at the loaded end of coated test bars when compared to that for non-coated bars. In a series of tests to failure of beams containing lapped splices, Cleary & Ramirez [1993] measured higher bond strength ratios in specimens previously subjected to repeated load applications. The differential between coated and non-coated specimens reduced with the number, although not with the cyclic stress range, of the repeated loading.

5.3.10 Hooks and bends

Hamad et al [1990, 1993] report that anchorage capacity of hooks and bends are reduced by coating, although the differential between coated and non-coated bars is slightly less than for straight bar anchorages. They recommended a 20% increase in the development length for epoxy coated bars over that for an uncoated bar.

5.3.11 Welded Wire Fabric

Bartoletti and Jirsa [1995] conducted pullout and one-way slab tests on both coated and uncoated welded wire fabric, from which they concluded that an epoxy coating has no appreciable effect on the development and anchorage of plain and deformed welded wire fabric.

5.3.12 Fire resistance

Both steel and concrete loose strength as they are heated to temperatures in excess of approximately 300°C. Fire resistance of a reinforced concrete member depends on ensuring that a sufficient period of time will elapse before the reinforcement and the core of the concrete reach such a temperature.

Fusion bonded epoxies are thermosetting polymers, that is they cannot be turned to a molten state by application of heat, although they may pyrolyse at higher temperatures. The material does soften around

Copyright fib, all rights reserved. This PDF copy of fib Bulletin 10 is intended for use and/or distribution only by National Member Groups of fib.

the glass transition temperature of approximately 110°C, however. Pullout tests conducted by Lin et al [1988] on coated and non-coated reinforcement cast into a reinforced concrete slab under fire conditions showed that all test bars were able to attain their yield strength in the test, and that the reduction in bond strength attributable to coating was not significantly affected by elevated temperature. Coated bars displayed markedly greater free end slip than companion non-coated bars at temperatures of 110°C and above. However, scatter in measured bar slips was considerable. Although it is evident that the coating material softened at temperatures above 110°C, and that bond behaviour was affected, it should not be concluded that fire resistance is lessened by use of epoxy coated bars. However, it is necessary to bear in mind the reservations concerning the relevance of pullout type tests to practical situations, set out above.

5.3.13 Summary

There is general agreement that bond strength and stiffness of coated bars is lower than that of nominally identical 'black' bars. The strength reduction is generally estimated at between 10% and 25%, although reductions of up to 40% have been reported.

From the foregoing review it can be seen that :

- there is no evidence that variations in concrete strength, coating type and thickness (within the range permitted in standards for coated rebar, or bar diameter (for a given cover/bar diameter ratio) need be given individual consideration when examining bond reduction factors for design.
- an assessment of bond performance based on performance of straight bars at ambient temperatures under monotonic short term loading should tend to give bond ratios which are reasonable or conservative for other circumstances.
- different bond strength factors are likely to be appropriate for top and bottom cast positions.
- the influence on bond strength ratio of rib geometry and confinement, whether from concrete cover, links or lateral pressure, remains unclear.

5.4 Analytical Models for Bond Strength of FBECR

Of the large number of models for bond which have been presented in recent years, the great majority deal principally with the resistance to splitting afforded by the concrete section. In contrast, hardly any attention has been paid to the relationship between bursting stresses and bond. As reported above, bond strength of an epoxy coated bar is less than that of a similar black bar in most circumstances, and the reduction is attributable to the greater bursting force developed by coated bars. There are, however, few analytical models which attempt to deal with the generation of bursting forces and which might help explain the difference in bond strength of black and coated bars.
Cairns and Abdullah [1996] advanced a model for bond strength in splitting condition failure modes which takes account of the different surface characteristics of epoxy coated and mill-scale surface bars. The model treats bond failure of ribbed bars as a bearing failure of the ribs. Two failure types are identified, a slip type failure along the rib face, and a shear failure through the concrete on the underside of the rib, as represented in Figure 5.2(c) and 5.2(b) respectively. (The pull-through type failure of Figure 5.2(a) was not included in the analysis). Theoretical expressions for bond strength were derived by developing expressions for the bursting force generated by bond and for the resistance of the concrete section (together with any confining reinforcement) to splitting, and equating these two quantities. The analysis was validated against test data for non-coated and coated bars. The resulting expressions were also used to evaluate the bond strength reduction attributable to epoxy coating of reinforcement, and to examine the factors which influence the magnitude of that reduction. The analysis indicates that relative rib area, rib face angle and confinement may influence the reduction in bond strength of coated reinforcement, but that the reduction is not greatly influenced by concrete strength, Figures 5.6, 5.13 and 5.14. Except where stated otherwise, Figures 5.6, 5.13 and 5.14 are derived for bars with a relative rib area of 0.065 and a face angle of 40°, a concrete cube strength of 30MPa, and an area of transverse steel ($100A_{tr}/n.s.d_b$) of 0.028.

Figure 5.6 shows the influence of rib face angle on bond strength of ribbed and of coated bars as estimated by the model. Below a face angle of approximately 43°, both types of bar fail by slip along the

Copyright fib, all rights reserved. This PDF copy of fib Bulletin 10 is intended for use and/or distribution only by National Member Groups of fib.

rib face, Figure 5.2(c), and bond strength increases with face angle. The effect of the coating is significant in this range. Above 50°, the face angle is steep enough for failure to occur by shear through the concrete below the bearing face whether the bar is coated or not, Figure 5.2(b), and failure occurs at the same stress for both types of bar. In the transition between face angles of 43° and 50°, bond capacity of the black bar is limited by the shear capacity of the concrete while bond strength of the coated bar continues to increase with face angle. The ratio of bond strength of coated bars to that of black bars changes rapidly in this zone. In reality, of course, the transition between the two failure modes may not be as abrupt as in Figure 5.6.

The model also suggests the transition angle between the two failure modes will be sensitive to variations in other parameters. For example, Figure 5.13 shows the influence of confinement on strength ratio determined using the model. An increase in confining pressure increases bond strength, and also tends to shift the mode of failure from the rib face mode towards the concrete shear mode, ie at greater confining pressures bond strength tends to be limited by the shear capacity of the concrete and the transition between failure modes occurs at lesser confining pressures. Figure 5.14 also indicates that concrete grade will cause a small shift in the rib face angle that marks the transition between the two failure modes.

European commercially produced bars generally have rib face angles of between 40° and 50°. The analysis in Figures 5.13 and 5.14 suggest that relatively small variations in rib face angle and in confining pressure might cause significant variations in bond strength ratio within this range, and might offer an explanation for the variations reported by various investigators for specimens that were not markedly dissimilar.

Hadje-Ghaffari, Darwin & McCabe [1991] independently derived an analytical model to take account of the influence of rib face angle on relative bond strength of coated and non-coated bars, Figure 5.8. The trend represented in Figure 5.8 is similar to that of Cairns & Abdullah, and is also consistent with experimental observations. The model takes account of the reduction in friction on the bar/concrete interface as a result of coating, but appears to take account of the failure mechanism in Figure 5.2(c) only. The jump in the coated/uncoated strength ratio at a face angle of around 40° is achieved by setting an empirical limit to the validity of the equation, and not, as in Cairns and Abdullah, by choosing the lesser strength from the two failure mechanisms. The strength ratio for rib face angles below 40° has a value of approximately 0.90, which fits results from highly ribbed bars but overestimates the strength ratio of bars with standard rib geometries.

The models are reported in greater detail in the 'Bond Models' Chapter of this report.

5.5 Influence of FBECR on Tension Stiffening, Deflection and Cracking

5.5.1 Introduction

In a "fully cracked" beam cross section, tension forces are carried by the steel only. However, concrete does possess some tensile strength, and between transverse cracks may carry some tensile force. Bond characteristics of reinforcement influence the transfer of force between bar and concrete, and may affect structural performance in two ways:

a) Between transverse cracks, reinforcement strains are reduced below the value that would be calculated if the section were fully cracked, Figure 5.15. The reduction in average bar strain is termed tension stiffening. Tension stiffening is influenced by the bond characteristics of the reinforcement, and affects beam deflections and crack widths.

b) The distance between successive transverse cracks is influenced by the rate at which tension in the longitudinal bars is transferred to the surrounding concrete. The stiffer the load/slip relationship, the more rapid the transfer of force, and the shorter the distance required to increase tensile stress in the concrete to the level at which a crack will form, Figure 5.13.

The reader is referred to an earlier CEB Bulletin [1983/84] for a more comprehensive description of these phenomena.

Although a number of studies report measurements to compare deflections and crack widths of similar specimens reinforced with non-coated and with epoxy coated bars, there have been relatively few studies

Copyright fib, all rights reserved. This PDF copy of fib Bulletin 10 is intended for use and/or distribution only by National Member Groups of fib.

devoted to the topic. In the majority of investigations, crack widths were measured in the constant moment zone of beam specimens designed primarily for measurement of splice strength. Consequently, the length of beam over which observations were made was fairly short, and individual series frequently contained little variation in beam section or cover, parameters known to influence crack spacing and crack widths. Lapped joint specimens have usually been relatively highly reinforced. Tension stiffening has less influence on deformations of highly reinforced sections, which are therefore relatively insensitive to variations in bond characteristics of reinforcement.

Because there are few studies devoted to this aspect of performance, because each study contains a relatively small number of specimens, and also because of the inherent variability of parameters such as crack spacing and crack widths, no attempt here has been made to identify the influence of the various parameters reviewed in Section 3. Only the generic difference in bar surface properties, whether coated or uncoated, is considered.

5.5.2 Tension Stiffening and Deflections

Cusens and Yu [1993] reported tests on black and epoxy coated bars axially embedded in concrete prisms. Two bar diameters, 25mm and 12mm were tested, embedded in concrete prisms 410mm and 200mm long respectively. Closely spaced electrical resistance strain gauges were fixed in a slot machined in the bars. Figure 5.16 compares the variation in steel strains along the bars measured in the two 25mm diameter specimens. At a force of 95kN, equivalent to a stress of 229N/mm^2, the force in the bar at midlength of the prism is reduced by around 43% and 36% below the value at the ends for black and coated bars respectively. End slips were also reported to be about 50% greater for the coated bars. Both observations point to a reduced bond stiffness as a result of coating. Lesser differences were reported in specimens reinforced with 12mm bar.

Cairns [1994] tested 7 pairs of reinforced beams, all having different cross sections. One specimen in each pair was reinforced with coated bars, the other with nominally identical black ribbed bars. The main variables were cover, which varied between 1.56 and 4.2 bar diameters, and percentage of reinforcement ($100A_s/bd$), which varied between 0.37% and 2.14%. Increases in mean strains in longitudinal reinforcement of between 2% and 26% were reported where coated bars were used, with an average increase of 17%. A similar increase in midspan deflection was also measured. Average strains were noted to be less affected by coating of reinforcement in more heavily reinforced sections.

Abrishami et al conducted short series of tests on beams [1995] and on flat slabs [1996] of normal and high strength concretes reinforced with black and coated bars. Epoxy coating thicknesses of around 0.18mm and of 0.28mm were used. Beams had a reinforcement ratio ($100A_s/bd$) of 0.92%. Deflections of FBECR reinforced beams were approximately 5% greater in specimens cast with high strength concrete. The difference was negligible in the normal strength beams. As subsequently pointed out by Cairns [1996a], however, the cross section of the beams tested in this study would have been relatively insensitive to variations in bond characteristics of the reinforcement. In a subsequent study of flat slabs reinforced with 0.48% steel, surface strains on the tension face of the slab were increased by an average of over 20%, greater increases being reported with a thicker epoxy coating and higher strength concrete. The conclusion in these studies that performance is influenced by coating thickness runs counter to the general trend reported, Section 3.3. Kobayashi & Takewaka[10] measured a 7% increase in deflections on beams reinforced with coated reinforcement. Their test specimens used beams with 1.6% tension reinforcement.

Deflection measurements are also reported in several studies primarily concerned with splice strength. For example, Jirsa and Treece[1989] measured deflections on beams containing reinforcement ratios of 0.6% and 1.6%, but did not find the coating to make a significant difference. Cleary and Ramirez[1991] and Choi et al[1991] report 'slight' or 'little' difference between pairs of specimens reinforced with coated and non-coated bar. In a later study, Cleary and Ramirez [1993] reported a 5.5% increase in deflection, although this reduced under cyclic loading to 2.9%. However, test specimens in these studies were all relatively heavily reinforced, (generally $100A_s/bd > 0.9\%$) and would not be expected to be sensitive to bond characteristics of reinforcement. The presence of a lapped joint may also have served to obscure any differences in tension stiffening. Thus, despite the negligible differences reported in several studies, it is evident that tension stiffening and deflections may be affected by use of coated reinforcement, and that there is a tendency for less heavily reinforced sections to be affected to a greater degree.

5.5.3 Crack Control

There is evidence that the load at which cracks first form is not significantly altered when coated bars

Copyright fib, all rights reserved. This PDF copy of fib Bulletin 10 is intended for use and/or distribution only by National Member Groups of fib.

are used [Kobayashi & Takewaka 1984, Cleary and Ramirez 1993]. Crack spacing and crack width are invariably greater in specimens reinforced with epoxy coated bars, although there are marked differences in the increase reported in individual studies. For example, a Japanese study reported an increase of 12%-34% in crack spacing and an increase of 3%-12% in crack widths when coated reinforcement was used. However, a US study by Treece & Jirsa [1987] reported average crack widths up to 200% greater in the coated bar specimens, although the average increase was around 60%. Crack spacings were up to 100% greater, with an average increase of 45%. The width of cracks did not exceed 0.3mm at the serviceability limit state in any of the beams reinforced with non-coated bars, but exceeded 0.3mm in 7 of the 12 coated bar specimens. Other studies on beams have reported average increases in crack widths of 3% to 62%[Choi et al 1991, Hamad et al 1990]. However, a study on axially loaded pavement slabs containing 0.61% and 0.73% reinforcement reported increases in crack width of only 5-10% [Zwernerman et al 1995], less than might be anticipated from the results for beams. The crack spacing in these studies was in excess of 1.0m, suggesting that a stabilised cracking pattern had not developed.

Cairns [1994] conducted measurements of crack width and spacing on seven pairs of beams, one of which was reinforced with epoxy coated bars and the other with non-coated bars. Specimens did not contain lapped joints, and a variety of section details and concrete covers were used. Crack spacings were between 7% and 48% higher in specimens reinforced with epoxy coated bars. The increase in crack widths (measured directly over the reinforcing bars) was somewhat greater, at 13% to 85%. Greater increases tended to be found in specimens with narrower cracks, which were in their turn associated with lesser covers. Specimens reinforced with black bars and with 20mm or 25mm cover had crack widths of around 0.10mm. In similar specimens reinforced with coated bars, cracks averaged around 70% wider over the bars. In specimens with 40mm or 50mm cover, crack widths were significantly greater, but increases averaged only 25%. Crack widths were greatest midway between longitudinal bars, but here measured increases were smaller.

The wide variation in measured crack width ratios has been explained by Cairns, making use of Equations 5.3 and 5.4 below, as originally set out by Beeby [1979]. Similar Equations formed the basis of the calculation model presented in MC78 [CEB 1978].

$$w_o = S_m \cdot \varepsilon_m \qquad \text{Equation. 5.3.}$$

$$S_m = \psi_1 \cdot c + \psi_2 \cdot \varphi / \rho_{s,ef} \qquad \text{Equation. 5.4.}$$

where
- w_o : average crack width over the bar
- ε_m : average tensile strain in reinforcement
- S_m : average crack spacing
- c : cover to bar
- φ : diameter of bar
- $\rho_{s,ef}$: effective area of concrete, calculated as the ratio of the area of a reinforcing bar to the area of concrete around the bar and with the same (vertical) centroid.
- ψ_1 : constant for a given probability of excedence

and
- ψ_2 : factor depending on ratio of the cover to the bar to the height of the crack (c/h_{cr}), and on probability of excedence.

In the estimation of average strain in reinforcement, ε_m, allowance should be made for the stiffening effect of surrounding concrete in tension. As discussed in the preceding section, tension stiffening is reduced, and hence mean reinforcement strain is increased, where epoxy coated bars are used. Thus, width of flexural cracks will be increased because of both the increase in the spacing between cracks and also the reduction in tension stiffening.

The first part of the term on the right hand side of Equation 5.4 represents the "no-slip" part of deformation at a crack. Bond behaviour of the bars will not influence this part of the expression. The second part of the right hand side of Equation 5.4, containing a factor ψ_2, is a "bond-slip" part, and is related to bond behaviour. ψ_2 is related to the inverse of bond stiffness, and is also a function of the effective reinforcement percentage ρ_{eff}. In members with large percentages of reinforcement or with high cover the part of Equation 5.4 containing ψ_1 predominates. Bond properties of the bar will exert a small effect on crack spacing under these circumstances. Conversely, bond will have a greater influence when the member is lightly reinforced and stressed in direct tension, or when cover is low, when the part of Equation 5.4 containing the factor ψ_2 predominates. Crack width increases and the influence of the bond characteristics of the reinforcement decreases with distance from the surface of the nearest reinforcing

Copyright fib, all rights reserved. This PDF copy of fib Bulletin 10 is intended for use and/or distribution only by National Member Groups of fib.

bar to the point on the member surface under consideration.

Cairns [1994] observed that the ratio of crack width in beams reinforced with coated bars to that in similar beams with black bars was greater in lightly reinforced specimens and in specimens with low cover. Using the above form of analysis, he used his test results to demonstrate that the variable increase in crack spacing and crack width was consistent with a 50% reduction in bond stiffness due to coating, Figure 5.17. The analysis was extended to results reported by others, and showed reasonable agreement, Figure 5.18, [Cairns 1996b]. The analysis was also used to show that increases in design crack width in beams reinforced with coated bars could range from a negligible amount to a doubling of the width found in a similar beam reinforced with non-coated ribbed bars, dependant on the cross section of the member. As a simplification for practical design purposes, Cairns suggested that crack spacing in beams be assumed to be 50% greater for coated bars. This ratio effectively averages the effect of 'slip' and 'no slip' components of Equation 5.4 for section geometries in which greater crack widths are likely to be observed.

Both Cleary and Ramirez [1993] and a study conducted at BCA by Clarke [1990] reported crack widths to increase with repeated load. Cleary and Ramirez reported a reduction in the difference in crack widths between specimens reinforced with coated and black bars under repeated applications of load, but results from the BCA study were inconclusive. Hasan et al [1996] report increases in total crack width, consistent with a reduction in tension stiffening, of 25% on initial loading and 12% after 1 million cycles in one set of specimens. Differences in deflection between specimens reinforced with coated and non-coated bars were also reduced by repeated applications of load.

5.5.4 Plastic Rotation Capacity

The ability of a structure to redistribute elastic moments is governed by the rotation capacity of the plastic hinges which form in regions where bending moments are at maximum values. Bond behaviour of reinforcement may affect the rotation capacity of plastic hinges in reinforced concrete members by affecting the rate at which strains are reduced by tension stiffening [Park & Paulay 1975].

Abrishami et al [1995], in what appears to be the only published study to report on ductility of beams containing epoxy coated bars, show a reduction in rotation capacity with epoxy coated bars. Beams contained 0.92% tension reinforcement. Load deflection plots to maximum load are shown in Figure 5.19. Member ductility, defined as the ratio of deflection at maximum load to that at first yield, averaged 3.4 for two specimens with non-coated bars constructed using normal and high strength concrete, against an estimated average of 2.7 for similar specimens containing coated bars. The lowest ductility for a coated bar specimen was 1.9. As the first yield loads for all specimens are similar, the differences are almost entirely attributable to differences in deflection at maximum load. The scope of the study was fairly restricted, as only a single loading arrangement and beam section were tested. The trend in the experimental data is therefore opposed to that predicted by the CEB-FIP Model Code [1990].

In an as yet unpublished report, Cairns and Carbaugh [1997] measured plastic rotation capacity of paired beam sections reinforced with black and with coated reinforcement. The sections were designed with 0.43% and 0.77% reinforcement in order that they would be sensitive to differences in bond characteristics. Three different spans were tested. The ratios of deflection at maximum load to that at first yield were around 6 and 3 respectively for the two reinforcement ratios. Rotation capacity was calculated as $2.\Delta_{plastic}$/span, Figure 5.20, where $\Delta_{plastic}$ was the difference between the deflection at first load and the deflection at maximum load. Results are summarised in Figure 5.21. As would be expected, the rotation capacity of the short span is less than that of the longer spans. The difference in rotation capacity between specimens reinforced with coated and black bars is not significant, however.

Conclusions from studies by Abrishami et al and by Cairns and Carbaugh conflict to some degree. It should be pointed out, however, that measurements of ductility may be imprecise, as it is difficult to accurately identify the deflection at the point maximum moment on the plateau of a load deflection curve. The point is also likely to be sensitive to variations in the loading or displacement rate used in the test. It may also be noted that the difference in local bond stress between coated and black bars reduces with increasing slip, and is little (<10%) different at slips of 0.3mm or more in confined concrete, Figure 5.4. As maximum crack widths are likely to exceed 1.0mm at ultimate load, little difference in bond, and hence in rotation capacity, would be expected.

5.5.5 Summary

There is ample evidence that under working loads tension stiffening may be redu ~d and crack widths

Copyright fib, all rights reserved. This PDF copy of fib Bulletin 10 is intended for use and/or distribution only by National Member Groups of fib.

and deflections increased by use of coated bars. Greater differences in tension stiffening and deflections are likely to be found with lightly reinforced sections. Crack widths are, in addition affected by concrete cover, the greatest differences in crack widths being found directly over bars with low covers. These differences tend to reduce under repeated loading. There is little evidence that coated reinforcement reduces plastic rotation capacity.

5.6 Review of Existing Code Rules for Design with FBECR

Coated bars have now been produced for around 30 years, but it is only within the past 10 years, following the introduction of product Standard specifications, that Codes of Practice have introduced guidance on design and detailing of concrete structures reinforced with epoxy coated bars. Reduction factors for bond strength at anchorages and lapped joints were first proposed for inclusion in the ACI Building Code in 1988 [ACI Committee 318 1988]. This section briefly reviews the rules introduced into National Codes of Practice to date and the bond tests specified in national Standards.

USA
The American Concrete Institute first introduced design rules for laps and anchorages of FBECR into the ACI Building Code in [1989] (Clause 12.2.4.3). The rules specify a 50% increase in lap length for coated reinforcement over requirements for non-coated bars where cover is less than 3 bar diameters and clear spacing between laps is less than 6 bar diameters, and an increase of 20% in lap length over requirements for non-coated bar in all other circumstances. These modification factors are derived largely from two studies, one on tension lapped splices conducted by Treece and Jirsa [1989]who reported an average reduction of 34%, the other of beam end specimens conducted by Johnston and Zia [1982]. The greater modification factor is equivalent to a bond strength reduction of 33%, and is associated with lesser covers. The lesser factor is associated with covers in excess of $3d_b$, but at the time of its introduction, had not, according to Hadje Ghaffari et al[1994], been validated by test.

The bond performance test in ASTM A775[1989] uses a pullout type specimen. Bond performance of coated bars is evaluated in comparison with performance of a similar non-coated bar. Bond stress of the coated bar has to exceed 80% of that of the non-coated bar at specified free or loaded end slips. A sustained load pullout test is also specified.

United Kingdom
At present, only the Code of Practice for Design of concrete structures for retaining aqueous liquids, BS 8007 [1987], makes provision for epoxy coated bars. It notes that no UK Standard for coated bars existed at the time of drafting, and recommends compliance with ASTM A775 as a minimum requirement. It is stated that bond strength of deformed bars may be assumed to be unaffected by epoxy coating.

Other UK Codes of Practice for structural design make no specific reference to epoxy coated reinforcement. However, it is probable that rules will shortly be introduced now that a Standard for coated reinforcement, BS 7295 [1990], has been published. Current UK practice is to apply a 20% or 25% increase in anchorage or lap lengths where coated bars are used.

The bond performance test in BS 7295 uses a pullout type specimen. A bar is deemed to satisfy requirements for classification as a high bond ribbed bar if free end slip is less than a limiting value of 0.2mm. Cairns and Abdullah [1995b] have shown the unsatisfactory nature of the test, and demonstrated that the classification criteria is too lax.

Japan
Guidelines of the Japanese Society of Civil Engineers [1986b] for use of epoxy coated reinforcement require a 25% increase in bond and lap lengths for coated bar over requirements for non-coated bars. It is pointed out that a greater increase may be necessary for small diameter bars, as the coating may smooth the rib profile. No mention is made of differences in crack control properties.

The bond performance test is similar to the US test.

Scandinavia
No requirements are yet established in Codes of Practice, but the Norwegian producer of coated reinforcement recommends an increase in bond and anchorage lengths of 25% over requirements for non-

Copyright fib, all rights reserved. This PDF copy of fib Bulletin 10 is intended for use and/or distribution only by National Member Groups of fib.

coated bars. No mention is made of differences in crack control properties.

FBECR is at present produced to ASTM A775, and utilises the bond test specification of that Standard.

In summary, there are at present wide variations in recommendations of national Codes for design of structures reinforced with fusion bonded epoxy coated reinforcement. At the ultimate limit state, different Codes recommend increases in lap length of between nil and 50%. The ACI reduction is significantly greater than that indicated in the majority of research studies, and the accuracy of the ACI factors, derived from results obtained in a single study, is debated. At the serviceability limit state, an epoxy coating is either taken to have no effect on serviceability behaviour, or any effect is ignored.

5.7 Derivation of Proposed Additions to Model Code 90 for Epoxy Coated Reinforcement

5.7.1 General

The objective of this section of the report is to derive design rules which will enable Model Code 90 to be used for structures reinforced with fusion bonded epoxy coated reinforcement. In deriving these proposals the format of the existing MC90 rules for ordinary black ribbed bars has been retained. The proposals developed here are therefore restricted to establishing values of coefficients applicable to FBECR for use in the established MC90 equations. Consideration of the safety margins to be assigned to design bond stresses lies outwith the scope of this report. Only bars produced in accordance with a recognised standard for fusion bonded epoxy coated reinforcement such as ASTM A775[1989] or BS7295[1990] are considered.

Curved brackets ( ) are used to denote relevant MC90 Clause numbers throughout the following sections.

For practical design, crack widths and deflections at the serviceability limit state are controlled through simple 'deemed to satisfy' rules and not by direct calculation. This is at least in part because serviceability is intrinsically less critical than the ultimate limit states, and the major calculation effort required for a detailed estimate is rarely justified. It also reflects the inherent difficulty in obtaining accurate estimates for these parameters at the design stage. Crack widths are controlled by limiting transverse spacing between longitudinal bars, and deflections controlled by limiting the span/depth ratio. Bond characteristics do not feature in such rules. These 'deemed to satisfy' rules are not considered in this review, which instead concentrates on adaptation of the rules provided for more detailed assessment of performance at the serviceability limit state. However, the approach evolved could subsequently be used in parametric studies for the development of simplified rules.

5.7.2 Local bond stress-slip model (3.1.1)

The Model Code provides an average 'local bond' vs. 'local slip' model for black ribbed reinforcing bars and for smooth bars, (Figure 3.1.1). The relationship is divided into 4 phases, defined by (Equations 3.1-1 to 3.1-4). Two states of confinement are considered. Bond failure occurs by shearing across the tops of the ribs where concrete is 'confined', and by splitting where concrete is 'unconfined'. For both confinement states, the form of the rising branch of the relationship is given by (Equation 3.1-1).

$$\tau = \tau_{max}(s/s_1)^{\alpha} \text{ for } 0 \le s \le s_1 \qquad \text{(Equation 3.1-1)}$$

Pullout tests by Cairns and Abdullah[1994a], Figure 5.4, may be used to derive bond-slip parameters for coated bars in well confined concrete. This study showed that :

a) bond slip stiffness of coated bars was approximately 50% of that of similar non-coated bars at low (0.01mm) slip.
b) at high slips (>0.7mm) coated bars attained similar or slightly greater stresses than similar non-coated bars.

From (b), the value of the peak stress τ_{max} for coated bars has been set 10% higher for coated bars under confined conditions. The value of α is set at 0.4 for ordinary ribbed bars in (Table 3.1.1). By setting α = 0.55 for coated bars, the bond stress of coated bars at a slip of 0.01mm is 55% of the corresponding value for ordinary ribbed bars. The relationship between bond stress of coated and non-coated bars

Copyright fib, all rights reserved. This PDF copy of fib Bulletin 10 is intended for use and/or distribution only by National Member Groups of fib.

obtained by use of the above factors may be compared with that measured by Cairns and Abdullah in Figure 5.22. The model gives a good representation of behaviour at slips above 0.005mm. The differences below this slip are attributable to the assumption in the model that slip starts from zero bond stress. In fact Cairns & Abdullah's results suggest that a finite bond stress {of around 1MPa} is required to break adhesion between concrete and the mill scale surface of an uncoated bar.

After peak stress, increasing slip occurs by shearing across the tops of the ribs. There is no evidence to suggest significant differences in post-peak behaviour between coated and non-coated bars, nor, in view of the failure mechanism, would any difference be expected. It is unlikely that the value of the parameters s_2, s_3, and τ_f (Table 3.1.1) needs be altered for coated bars.

Cusens and Yu[1992] carried out tests on coated bars in unconfined conditions (c/φ of 1.1 and 2.0 for 25mm and 12mm diameter bars respectively). At a loaded end slip of 0.05mm, the average ratio of the bond stress for coated bars to that for non-coated bars was 0.68 and 0.74 for 25mm and 12mm bar specimens respectively. Using α and τ_{max} values for coated and non-coated bars as above in (Equation 3.1-1) gives a bond stress ratio of 0.70, within the range of measured values.

Coated bars are recognised to be around 25% weaker than similar non-coated bars at failure in unconfined conditions, although the ratio is influenced by a number of factors which will be discussed in more detail in the derivation of design bond strength. In unconfined conditions, the value of the parameter τ_{max} should therefore be reduced by 25% below the corresponding value for non-coated bars. Taken in relation to the values given for non-coated values in (Table 3.1.1), τ_{max} for coated bars should be $1.5\sqrt{f_{ck}}$ and $0.75\sqrt{f_{ck}}$ for 'good' and 'other' bond conditions respectively.

In the absence of evidence to the contrary at the time of writing, no changes are proposed to other parameters in (Table 3.1.1).

5.7.3 Tension stiffening effects (3.2)

It is evident that tension stiffening is reduced where non-coated 'black' bars are replaced by epoxy coated bars. Cairns [1994] suggested that tension stiffening is reduced by around 50%, and noted the correlation between the reduction in tension stiffening and the bond strength ratio derived from pullout tests at corresponding values of slip. In Figure 5.23, comparison is made between the reduction measured in Cairns tests with that determined by application of the tension stiffening clauses of MC90 to Cairns test beams, and assuming the β factor for epoxy coated bars to be 50% of that for non-coated bars in (Equation 3.2-11). The effective reinforcement ratio has been determined in accordance with the method specified in (Figure 5.7.4.2), and the β factor has been taken as 0.6 for black ribbed bars tension under short term loading in accordance with (Table 7.4.2). The overall average ratio for strain in coated bars to that for black bars is 1.18, in good agreement with the average measured ratio of 1.17. The correlation between measured and calculated ratios for individual specimen pairs is not particularly strong, however.

A similar comparison based on results from the slab tests of Abrishami et al [1996], again assuming the β coefficient for coated bar to be half that for black bar, suggests that strains would be around 23% and 28% higher in specimens reinforced with coated bars for normal and high strength concretes respectively. Measured increases were 0% and 30% for normal strength concrete, and 15% and 40% for high strength concretes, the higher increases being associated with a thicker coating. The reduction in tension stiffening calculated by MC90 therefore lies within the (fairly broad) range of measured values.

It is evident both from the scatter in individual test results and from practical considerations that a fairly broad brush approach is required when proposing provisions for tension stiffening of coated bars. It is suggested that the β coefficients for black ribbed bars in Sections (3.2) and (7.4.3) be reduced by 50% for epoxy coated reinforcement. This reduction is commensurate with coated bars having tension stiffening characteristics equivalent to those of plain round bars.

Cracks at the bar surface are around 0.02-0.05mm wide at working loads [Yannopoulos 1989]. Bar/concrete slip will be half the crack width, and hence it is bond behaviour at slip values of 0.01-0.02mm which will influence crack width. The proposals for the local bond slip curve presented in the preceding section result in a coated/black bond stiffness ratio of 0.55 at a slip of 0.01mm. In view of the broad interpretation of results required here, the two proposals are consistent.

5.7.4 Moment Curvature relationship (3.6)

The different bond characteristics of coated and black reinforcement affects tension stiffening, as

Copyright fib, all rights reserved. This PDF copy of fib Bulletin 10 is intended for use and/or distribution only by National Member Groups of fib.

demonstrated earlier, and so it is to be expected that moment curvature relationships will be similarly affected. As discussed earlier, Cairns[1994] measurements showed a similar change in mean strains and in midspan deflections when coated bars were used in place of black bars.

MC90 contains models for both the average stress-strain relationship of steel embedded in concrete (discussed in the preceding section) and for moment curvature of beams. In both models, deformations are calculated by subtracting an amount related to the difference between cracked and uncracked deformations at the cracking load from the deformation that would be determined by ignoring the contribution of the concrete in tension. The difference between cracked and uncracked deformations is multiplied by a bond factor β to evaluate the contribution of tension stiffening. The model for the stress-average strain relationship for embedded reinforcement after cracking has stabilised, (Section 3.2.3), uses a constant value of tension stiffening, independent of the applied loading. However, in the model for moment-curvature relationship in (Section 3.6), tension stiffening is represented as reducing in proportion to the ratio of the cracking moment to the applied moment. A given difference in bond characteristics would be expected to exert a similar influence whichever model were used, ie the relationship between the β coefficients for the two types of bars would be the same in both models. However, it is evident that because tension stiffening is represented in different ways in the two models, the relative increase in deformations when coated bars are used calculated by the moment curvature model will differ from the relative increase obtained using the embedded steel model.

It was shown in the preceding section that the increase in deformations measured when coated bars were used was consistent with the predictions of the MC90 average strain model. It follows that good agreement cannot be expected with the moment curvature model, and this is indeed the case. The calculated difference in deflections for Cairns'[1994] beams averages 5%, considerably less than the measured difference of around 18%. The difference in deflections between beams reinforced with coated bars and those reinforced with black bars tested by Abrishami et al[1995] is calculated to be 3% using the provisions of section [7.5.2.1], modified as above for coated bars. The measured difference lies in the range 0-5%. Measurements on nominally identical beam specimens in Cairns study tend to show a fairly constant difference between coated and black bars. A similar conclusion is reached from inspection of strain plots from slabs presented by Abrishami et al. From this limited survey, it appears that the form of the tension stiffening model gives a better representation of the physical behaviour of reinforced concrete sections.

As stated earlier, it is not intended to undertake a detailed review of MC90 behavioural models. It is therefore proposed that the moment-curvature model be modified in a similar manner to the tension stiffening rules for use with coated bars. Thus, it is suggested that for coated reinforcement the coefficient β_1 used in the derivation of β_b, (Equation 3.6-2b), be taken as 0.5, equal to the value currently specified for plain bars.

The effect of the difference in bond characteristics between coated and black bars will in many cases have a negligible effect on member deformations. The influence of reinforcement percentage ($100A_s/bd$)on the increase in deflection attributable to use of coated reinforcement is plotted in Figure 5.24. The analysis was carried out by Cairns [1996a] for the beam cross section used by Abrishami et al in their tests using the CEB moment-curvature model, with tension stiffening reduced by 50% for coated bars. It can be seen that for reinforcement percentages in excess of 0.7%, the increase in deflection attributable to coating would not exceed 10%. Bearing in mind the difficulty in the accurate estimation of beam deflection at the design stage, a 10% error is almost negligible. By way of illustration, consider a rectangular beam with a span/effective depth ratio of 20 containing 1% reinforcement and with nominal dimensions of 400mm deep by 200mm wide. Deviations in overall section geometry within the tolerances set out in (Table 1.4.1) of MC90 could cause a difference of nearly 6% in calculated deflection. Further errors may be introduced through differences in materials properties and cover dimensions between assumed design values and 'as constructed' values, through errors in estimation of shrinkage strains through uncertainties in environmental service conditions, and errors in creep factors through uncertainties in the level of long term sustained loads. Thus it is only in lightly reinforced sections that the differing bond characteristics of black and coated bars is likely to have any significant influence.

5.7.5 Rotation Capacity (3.7)

In the absence of sufficient data to show that rotation capacity is affected to a significant degree by use of coated reinforcement, and as it would be expected from extrapolation of other tension stiffening results that coatings are likely to have the beneficial effect of increasing rotation capacity, it is proposed that the

Copyright fib, all rights reserved. This PDF copy of fib Bulletin 10 is intended for use and/or distribution only by National Member Groups of fib.

coefficients for black ribbed bars in Clause (3.2.3) be used also for coated bars. It is appreciated that the use of different values for β in the elastic and post-yield stages will give rise to a discontinuity in force-deformation relationships as reinforcement attains yield. However, test data to date does not permit a more accurate determination of the transition.

5.7.6 Ultimate strength of lapped joints and anchorages (6.9.3-6.9.6)

The objective of this section is to determine the value of bond coefficients for use in MC90 to enable structures to be designed using fusion bonded epoxy coated reinforcement to the same margin of safety as that currently used for ordinary (black) reinforcing bars. Consideration of the safety margins to be assigned to bond failure lies outwith the scope of this report.

Although there is widespread agreement on which parameters exert an influence on bond strength, the form of the various expressions that have been proposed to relate bond strength to these parameters show considerable variation. It is not the purpose of this review to consider the merits of the various expressions. The form of bond strength expressions used in MC90 is here accepted without reservation. The value of the coefficients used for black bars in these expressions have, however, been temporarily adjusted in some instances to provide a better fit to experimental data.

The approach adopted here is to first analyse individual results from 7 studies comprising around 200 tests on lapped joints. These studies have largely been carried out on paired sets of nominally identical specimens, one specimen of each pair reinforced with ordinary black bars, the other reinforced with FBECR. Lap lengths varied between 12.8 and 37.0, with an average of 17.8. Bond strengths measured on specimens reinforced with black bars have first been analysed to determine the margin of safety currently used in MC90 and the statistical precision of the MC90 design rules. Results from specimens reinforced with coated bars are then analysed, and coefficients in the MC90 expressions adjusted so that :

a) the ratio of measured to MC90 design strength is largely independent of the value of the various parameters previously identified as exerting an influence on the relative strength of coated and black bars.
b) a similar overall ratio of measured to MC90 design strength is obtained for coated and for black bars.

Proposals derived from the analysis of the strength of lapped joints are then validated against conclusions from anchorage tests.

MC90 rules for strength of lapped joints of black bars

Treece and Jirsa [1989], Choi et al[1991], Cleary and Ramirez[1991,1993], Hamad and Jirsa[1993], Hester et al [1993] and Cairns and Abdullah[1994b] have all reported experimental investigations in which the strength of lapped joints of epoxy coated bars has been compared with that of nominally identical lapped joints of black bars. Details of the specimens tested and the measured bond strengths are set out in Table A.1 of Appendix A for the black bar specimens. It should be noted that several test specimens did not comply with detailing requirements of MC90 for minimum cover or for minimum transverse reinforcement.

According to MC90, basic anchorage length is proportional to the characteristic strength of the reinforcement, and is also influenced by concrete strength, type of reinforcement, casting position and bar diameter (6.9.3 & 6.9.4). To obtain the design anchorage length, account must also be taken of the shape of the bar (straight, bent, hooked or with welded transverse bar) and confinement by cover and transverse reinforcement or transverse pressure (6.9.5). The design lap length of bars in tension is additionally affected by the percentage of main reinforcement lapped at a section (6.9.6).

The ratio of the measured strength of lapped joints of ordinary black ribbed bars to the design strength calculated from application of MC90 design rules was obtained, and results are set out in Table A.1. The influence of the various parameters listed in the preceding paragraph on this ratio was analysed where possible to verify that the safety margin embodied in the MC90 rules was consistent across the range of test data. Concrete strength, bar diameter, and the quantity of confining reinforcement did not exert a significant influence on the measured/design strength ratio within the range of available data, and are not considered further.

MC90 overestimated the adverse effect of poor casting position, and underestimated the beneficial

Copyright fib, all rights reserved. This PDF copy of fib Bulletin 10 is intended for use and/or distribution only by National Member Groups of fib.

influence of extra cover on joint strength. In order to improve the fit to experimental data, the casting position factor η_2 was taken as 0.90, and not as 0.7 as specified in MC90. Cover factor α_3 is derived from Equation 5.5, taken from (Table 6.9.1), using a value of k_α=0.15. To provide a better fit, MC90 design strength of black bars has instead been based on a value of k_α=0.21. (It is not suggested that the MC90 coefficients are wrong, merely that they do not provide the best fit to the experimental data here)

$$\alpha_3 = 1 - k_\alpha * (c_d - \varphi)/\varphi \qquad \text{Equation 5.5.}$$

The mean and the coefficient of variation of the ratio of measured to MC90 design bond strength so obtained were 2.47 and 0.17 respectively.

Strength of lapped joints of epoxy coated bars

The ratio of the bond strength of a lapped joint of epoxy coated bars to that of a companion specimen reinforced with black bars in the 8 studies ranged from 0.95 to 0.54, with an average of 0.77. Details of test specimens and the measured bond strengths are set out in Table A.2 of Appendix A for the coated bar specimens. The simplest approach to modifying MC90 rules for coated bars would be to reduce design bond stresses by 23%. The factor α_1 would then be reduced from a value of 2.25 for black ribbed bars to 1.75 for coated bars. However, such an approach ignores the influence of several factors including cover, lap length, and casting position on the differential between lap strength of coated and black bars.

Bond strength of epoxy coated bars has been found to be less severely affected by casting position than bond strength of black ribbed bars, as discussed earlier. Casting position was not a variable within any of the test programmes, however. Casting position would be classified as 'not good' in 2 of the 7 studies examined here, and as 'good' in the remaining 5 studies. (Although tension reinforcement was cast in the top face of the specimens in two of these five studies, the depth of concrete below the lapped bars fell within the 250mm limit specified in MC90 for bond strength to be classified as 'good'). A reasonable fit to the lap data was again obtained using a top cast factor η_2 of 0.9, as for the black bar tests. Within the analysis of lap test results, the value of η_2 has therefore been taken as 0.9 for both types of bar. The value of the coefficient η_2 for use with coated bars will be further considered in the analysis of anchorage tests later in this section.

The ratio of minimum concrete cover to bar diameter encompassed within the seven studies ranged from 0.35 to 3.16, with an average of 2.0. The best fit to experimental data was obtained using a value of 0.27 for coefficient k_α, Equation 5.4. This results in an increase in the value of cover factor α_3 for coated bars over that for black bars for concrete covers above the minimum of one bar diameter. The magnitude of the increase varies with cover/bar diameter ratio, greater differences being found at higher covers. The net effect is a reduction in the difference in bond strength between coated and black bars as cover thickness is increased. Trends observed in the grouped data are therefore consistent with those reported in individual studies.

Coefficient k_α was determined as 0.21 for black bars in the analysis reported here. The corresponding value for coated bars was around 25% greater, at 0.27. The value given in MC90 (for black bars) is 0.15. To maintain equivalence between coated and black bars, it is proposed that the value of coefficient k_α for coated bars also be set around 25% higher, at 0.20.

Splice lengths varied between 12.8 and 37.0, in tests, with an average of 17.8. In comparison, a full strength lap joint would typically be in the range 30-50 bar diameters. As reviewed earlier, average bond strength reduces more rapidly with increasing lap length for black bars than for coated bars. Relatively short laps are common in experimental studies in which it is desired to ensure bond failure, but results tend to overestimate the average bond strength that can be obtained in a full strength lap. Cairns and Abdullah's[1994b] results suggest that the average bond stress in a full strength black bar splice is around 92% of that of an equivalent joint of half the length, whereas for coated bars the proportion was 98%. Clarke [1990] and Makhlouf's [1994] results indicate greater differences. Taken as an average for the three studies suggests that, in order to develop the full strength of a bar, a half-length coated bar lap need develop only 90% of the strength of an equivalent black bar splice. The average ratio of MC90 design lap strength to measured strength in tests on black ribbed bars was 2.47, using best fit coefficients. To obtain an equivalent margin of safety for full strength laps of coated bars the corresponding ratio need only be 2.47 x 0.9 = 2.22. Assigning a value of 1.75 to factor η_1 for coated bars, and using 'best fit' coefficients derived earlier, gives an average ratio of MC90 design lap strength to measured strength of 2.20 with a coefficient of variation of 0.20.

Copyright fib, all rights reserved. This PDF copy of fib Bulletin 10 is intended for use and/or distribution only by National Member Groups of fib.

Figure 5.25 shows the frequency distributions of the ratio of measured to MC90 design bond strength for both coated and black bars. Measured black bar lap strengths have been multiplied by a factor of 0.90 to account for the extra bond strength obtained when short splice lengths are tested. The frequency distributions are similar for both types of bar.

Average ratios of measured to MC90 design bond strength from each of the seven investigations analysed here are plotted in Figure 5.26. Results reported by Hester et al have been divided into beam and slab specimens, giving a total of eight comparisons. Nearly 70% of results lie within the relatively narrow band between 1.95 and 2.20. The minimum margin of safety between measured and design bond strength in any series is 1.96 for the coated bars, compared to 1.98 for black bars. In only one set of results does the difference between the test/design strength ratio for coated and black bars exceed 8%, and there the margin of safety was higher for the coated bars. Despite the wide variations in bond strength ratio reported in the several studies, the minimum margin of safety (assessed against the provisions of MC90) is remarkably consistent. In particular, Figure 5.26 suggests that in the study by Treece and Jirsa[1989] (on which the ACI provisions are based) the detail employed may have accentuated differences between coated and black bars.

Anchorage tests

Having derived proposals for bond coefficients on the basis of lap test results, it is now necessary to verify that these coefficients are also satisfactory for anchorages.

Results of lap tests did not indicate any difference in the top cast bond strength reduction between coated and black bars, and the casting position bond strength reduction was not as severe as allowed for in MC90. As discussed earlier, however, casting position was not a controlled parameter in any of the lap studies. As reviewed earlier, more controlled studies suggest that the casting position reduction factor could be increased by 14%. In MC90, a casting position factor η_2 of 0.7 is currently specified for black bars. On the basis of the anchorage results, it is reasonable to increase factor η_2 to 0.8 for coated bars.

Hadje Ghaffari et al [1994] investigated the influence of coating, cover and casting position on anchorage bond strength. Results presented in Table 2 of their study show an average reduction in bond strength on coating of 11%. The average reduction in design bond stress obtained using the above proposals for amended values of η_1, η_2 and k_a is 5%. If allowance is made for the relatively short embedment lengths used in the tests, the difference is not significant. Measured and calculated design bond strength ratios follow similar trends, Figure 5.27.

In a related study, Choi et al[1991] reported bond strength reductions of between 26% to 9% for a range of rib patterns and bar diameters, with an overall average of 14%. Anchorage lengths were relatively short, in the range 5.6φ to 8φ. The average reduction in design bond stress obtained using the above proposals is22%.

Cusens and Yu[1993] tested beam end anchorages with covers of 1.1 and 2.0 bar diameters, and anchorage lengths of 16 to 28 bar diameters. Test bars were cast near the bottom face of the specimens. They recommended a 25% increase in anchorage lengths for coated bars. The present proposals represent an average 32% increase.

Anchorage tests were conducted by Clarke [1990]on bar diameters of 10mm, 25mm and 40mm cast both in top and bottom of the specimen. The average reduction in anchorage strength on coating was 6%. The MC90 proposals presented here represent a 20% reduction.

These comparisons indicate that the present proposals derived from tests on lapped joints would tend to be conservative for anchorages.

From the earlier discussion of the effects of repeated and sustained loading it was concluded that recommendations based on monotonic loading will be conservative under other circumstances. Similarly, recommendations based on straight bar anchorages will be conservative if applied to anchorage by hooks or bends. Tests have also demonstrated that the factor α_2 for laps and anchorage of welded wire fabric is equally applicable to coated fabric.

Insufficient evidence has been found to justify changes to any of the remaining bond factors.

Copyright fib, all rights reserved. This PDF copy of fib Bulletin 10 is intended for use and/or distribution only by National Member Groups of fib.

Effect of proposed modifications on lap and anchorage length

The net effect of the proposed factors on the increase in lap length required for coated reinforcement over that required for black bars depends on cover and casting position. The lap length factor for coated bars, ie the ratio of the required lap length for a coated bar to that required for a similar black bar, is plotted as a function of cover for 'good' and 'other' casting positions in Figure 5.28. The greatest increase, of 29%, is required for 'good' casting positions in which a minimum cover of 1 bar diameter is provided. (MC90 in particular and national Codes in general specify a minimum cover of one bar diameter for structural reasons). For a top cast bar with a minimum cover of 2.7 bar diameters, no increase is required.

FBECR will not generally be used with cover to bar diameter ratios as low as 1.0. FBECR is to be considered to provide an additional measure of corrosion protection for reinforcement. Specification of coated reinforcement is intended to supplement and not to not supplant existing cover requirements for durability[2]. As the extra cost of FBECR is generally justified only where there is risk of significant reinforcement corrosion, its use will be justified primarily in harsh environments, and it will not generally be specified for exposures less than Exposure Class 3, as defined in (Table 1.5.1). Concrete cover to reinforcement in structures subjected to such environments will be relatively high. By way of illustration, compare minimum concrete cover requirements for concrete of Grade 40. Grade 40 is commonly specified for reinforced concrete structures such as bridge decks in chloride contaminated environments. Nominal cover to reinforcement in Class 3 conditions is 50mm, as opposed to 20mm for a "Mild" exposure. The cover ratio (minimum cover expressed as a multiple of bar diameter) for a 32mm bar in a slab in a Class 3 environment is thus 1.56. In a beam element, minimum cover and requirements for links around main reinforcement means that cover ratio to lapped bars will be at least 1.45, even for 40mm diameter bars. In comparison, cover ratio for bars of size 20 or greater in a mild exposure need only be 1.0. The increase in lap or anchorage lengths required for a cover equal to 1.5 times bar diameter is 25% and 10% respectively for 'good' and 'poor' casting positions. The increase in lap or anchorage lengths required for a cover equal to 1.5 times bar over that required for a black bar with cover of 1 bar diameter are 16% and 1%. Thus increases in lap lengths for respective minimum covers are less than might be thought at first sight.

5.7.7 Anchorage of stirrups

Results from McGormley et al [1996] have demonstrated that coated No.3 (9.5mm) stirrup bars have adequate anchorage for shear, but caution against extrapolation to larger diameters. The BCA study also confirmed that shear capacity was not impaired by use of coated stirrups. Accordingly, no changes are proposed to 9.1.1.4 in respect of coated reinforcement.

5.7.8 Limit State of Cracking (7.4)

For practical purposes, design crack width w_k may be estimated as mean strain in reinforcement ε_m times the distance $l_{s,max}$ between cracks, (Equation 7.4.2). A variety of expressions have been proposed for estimating crack spacing and are generally similar in form, Equation 5.3. Coefficient k_1 takes account of bond properties, and is greater for bars with less stiff load-slip behaviour. The increase in k_1 is widely assumed to be inversely related to bond. A change in bond characteristics may thus have a twofold influence on crack widths, as crack spacing will be greater and tension stiffening less when bond stiffness is reduced.

$$w_k = l_{s,max} \cdot \varepsilon_m \qquad \text{Equation 7.4.2}$$

Modifications to MC90 procedures to allow for the effect of an the epoxy coating on mean reinforcement strain ε_m has already been discussed in Section 7.3. Crack spacing $l_{s,max}$ is set equal to double the distance required to transfer the difference in bar force at a crack and at a point midway between cracks by bond. This distance is influenced by several factors including bond characteristics of reinforcement, cover, and strain distribution across the section, as set out in Equations 5.3 and 5.4, Section 5.5.3. The equation is too complex for normal design use, and Cairns has shown that for practical purposes an upper bound to the crack spacing of coated bars can be taken as approximately 50% greater than that for black bars. It is therefore proposed that existing values of bond stresses τ_{bk} in (Table 7.4.2) be reduced by 33% for use with coated bars.

---

[2] Personal communication from J Hartley, Allied Bar Coaters, UK.

Copyright fib, all rights reserved. This PDF copy of fib Bulletin 10 is intended for use and/or distribution only by National Member Groups of fib.

5.7.9 Summary of proposed modifications to MC90 requirements for design bond stress

(2.2.3.2) ***Surface characteristics.*** New classification for epoxy coated bars to be introduced. Relevant production standards to be cited.

(3.1.1) ***Bond Stress-Slip Relationship.*** In Table 3.1.1, the value of α and τ_{max} for coated bars in confined concrete in good bond conditions should be taken as 0.55 and $2.75\sqrt{f_{ck}}$ respectively. Values of τ_{max} for coated bars for Unconfined Concrete should then be taken as $1.5\sqrt{f_{ck}}$ and $0.75\sqrt{f_{ck}}$ for 'good' and 'other' bond conditions respectively. The value of α should again be taken as 0.55. Other values are unchanged.

(3.2) ***Tension Stiffening***. β values in b) the crack formation phase and c) the stabilised cracking phase should be reduced by 50% where coated bars are used. β values need not be changed in the post-yield phase.

(3.6) ***Moment-Curvature Relationship***. β values should be reduced by 50% where coated bars are used.

(3.7) ***Rotation Capacity*** No additions/changes proposed.

(6.9.3) ***Design bond stress for reinforcing bars***. After "η_1 = 1.4 for indented bars", insert "η_1 = 1.75 for fusion bonded epoxy coated reinforcement"

After "η_2 = 0.7 ..... built with slip forms", insert "except that η_2 = 0.8 for epoxy coated bars in such locations"

(6.9.5) ***Design anchorage length***. In Table 6.9.1, add "for coated bars, $\alpha_3 = 1 - 0.20\,(c_d - \varphi)/\varphi$ $\{0.7 \leq \alpha_3 \leq 1.0\}$

(7.4.3) ***Verification of crack width***. Values of β in Table 7.4.2 to be reduced by 50% for coated bars. Values of τ_{bk} to be reduced by 33%.

(7.5) ***Limit States of Deformation***
The values of β in Equation 7.5-6b to be reduced by 50% for coated bars.
Values for the coefficient η in Equation 7.5-1b need to be re-evaluated, Table 7.5.1.

5.8 REFERENCES

1967 Lutz, L.A. & Gergely, P. Mechanics of bond and slip of deformed bars in concrete. Proceedings of the American Concrete Institute, Vol. 64, No. 11, Nov 1967. pp711-721

1972 Cement and Concrete Association. Handbook on the Unified Code for structural concrete. (CP110 : 1972).. London.

1973 Tepfers R. (1973) A theory of bond applied to overlapped tensile reinforcement splices for deformed bars. Publication 73:2, Division of Concrete Structures, Chalmers University of Technology. Göteborg, Sweden.

1975 Orangun C.O., Jirsa J.O., & Breen J.E. (1975) The strength of anchored bars ; a re-evaluation of test data on development length and splices. Research Report 154-3F, Center for Highway Research, The University of Texas at Austin. Austin. 78pp.

– Park, R. and Paulay, R. (1975) Reinforced Concrete Structures. Wiley. New York.

1976 Clifton, J R, Beeghley, H F and Mathey, R G. (1976) Non-metallic coatings for concrete reinforcing bars. US National Bureau of Standards.

– Hawkins, N.M. Fatigue Design Considerations for Reinforcement in Concrete Bridge Decks. Proceedings American Concrete Institute, Vol 73 No. 2. Feb 1976. pp104-115.

– Mathey, R.G. & Clifton J.R. Bond of coated bars in concrete. Proc ASCE V 102. ST1. Jan 1976. pp215-229.

1977 Rehm, G. & Russwarm, D. (1977) Assessment of Concrete Reinforcing Bars made by the Tempcore

Copyright fib, all rights reserved. This PDF copy of fib Bulletin 10 is intended for use and/or distribution only by National Member Groups of fib.

Process. Betonwerk + Fertigteil-Technik, No 6, pp300-307.

1978 Arthur, P. D. & Cairns, J. (1978) Compression laps of reinforcement in concrete columns. The Structural Engineer, Vol 56B, No.1.

– CEB-FIP (1978) Model Code for Concrete Structures. CEB-FIP. Lausanne.

1979 Beeby, A.W. The prediction of crack widths in hardened concrete. The Structural Engineer. Vol. 57A, No.1, January 1979. pp9-17.

– Johnston, D.W., and Zia, P. (1982) Bond characteristics of epoxy coated reinforcing bars. Department of Civil Engineering, North Carolina State University, Report No. FHWA/NC/82-002, August. 163p.

1983 CEB (1983/84) Design Manual Cracking and Deformations. CEB Bulletin 158. CEB. Lausanne.

– Clifton,J.R. & Mathey, R.G. Bond and Creep Characteristics of Coated Reinforcing Bars in Concrete. American Concrete Institute Journal. Vol 80, No.4. July/August 1983. pp288-293.

– Japan Society of Civil Engineers. (1986a) Standard Specification and test methods for epoxy-coated reinforcing steel bars. JSCE EP10-EP17.Tokyo.

– Japan Society of Civil Engineers. (1986b) Recommendation for Design & Construction of Concrete Structures Using Epoxy-Coated Reinforcing Steel Bars. JSCE. Tokyo.

1984 Kobayashi, K. & Takewaka, K. Experimental studies on epoxy coated reinforcing steel for corrosion protection. International Journal of Cement Composites and Lightweight Concrete, Vol 6, No. 2. May 1984. pp99-116.

1987 British Standard Institution British Standard Code of Practice BS8007:1987. Standard specification for design of concrete structures for retaining aqueous liquids. London.

– Treece, R.A. & Jirsa, J.O. (1987) Bond strength of epoxy coated reinforcing bars. PMFSEL Report No. 87-1, University of Texas, Austin, Jan. 85pp. (Summarised in American Concrete Institute Materials Journal, Vol. 86, No.2. Mar-Apr. 1989. pp 167-164)

1988 ACI Committee 318. Revisions to Building Code Requirements for Reinforced Concrete. Vol. 85, No. 6, Nov/Dec 1988. pp645-674.

– Lin, T.D. et al. Pullout tests of epoxy coated bars at high temperatures. ACI Materials Journal. Nov-Dec 1988. pp544-550.

– Schiessel P. (1988) (Ed) Corrosion of steel in concrete. RILEM Report of Technical Committee 60-CSC. 96pp.

– Swamy, R.N. & Koyama, S. (1988) Epoxy coated rebars - the panacea for steel corrosion in concrete. Proceedings, UK Corrosion '88 Conference, Brighton, Oct. pp197-209.

1989 ACI Committee 318. Building Code Requirements for Reinforced Concrete and Commentary (ACI 318-89/ACI 318 R-89). American Concrete Institute. Detroit. 1989. 353pp.

- ASTM Standard specification for epoxy coated reinforcing steel bars. ASTM A775/A775M-88a, 1989. Annual Book for ASTM Standards, Vol.1.04, Philadelphia, USA, pp548-552.

1989 Cairns, J. & Abdullah, R. (1989) Bond strength of epoxy coated reinforcement. Proc. 3rd International Conference on Deterioration & Repair of Reinforced Concrete in the Arabian Gulf. Vol. 1. Bahrain Society of Engineers. Bahrain. pp353-368.

– Jirsa, J.O. & Treece, R.A. Bond strength of epoxy-coated reinforcing bars. ACI Materials Journal, Vol 86, No. 2. March-April 1989. pp167-174.

– Read, J. (1989) FBECR - The Need for Correct Specification and Quality Control. Paper presented at Symposium on FBECR at Sheffield University. 23pp.

– Salparanta, L. Epoxy coated concrete reinforcement. Nordisk Betong. Vol 5 1989. pp27-30.

– Treadaway, K.W.J. & Davies, H. Performance of fusion bonded epoxy coated steel reinforcement. The Structural Engineer, Vol 67 No. 6. March 1989. pp99-108.

– Yannopoulos, P.J. Variation of concrete crack widths through the concrete cover to reinforcement. Magazine of Concrete Research. Vol 47, No. 147. June 1989. pp63-68.

1990 British Standard Institution. BS7295:1990. Fusion bonded epoxy coated carbon steel bars for the reinforcement of concrete. London. 7pp.

– Clarke, J L. (1990) Tests on fusion-bonded epoxy-coated steel. BCA Project Report RN1.025.01. Slough, UK. 23pp.

Copyright fib, all rights reserved. This PDF copy of fib Bulletin 10 is intended for use and/or distribution only by National Member Groups of fib.

- Davies, H. (1990) Studies of the performance of fusion bonded epoxy coated reinforcement during the construction process. Protection of Concrete, ed Dhir, R.K. and Green, J.W. Spon
- Hamad, B S, Jirsa, J O & d'Abreu d Paolo N. (1990) Effect of epoxy coating on bond and anchorage of reinforcement in concrete structures. Report 1181-1F. Center for Transportation Research, University of Texas at Austin.
- Judge, R.C.B., Scott R.A. & Gill P.A.T. Strain and bond stress distributions in tension lap joints in reinforced concrete. Magazine of Concrete Research, Vol. 42, No. 150. March 1990. pp5-14.
- King, E. (1990) Post-fabrication coating systems. Paper presented at Seminar on Durable Reinforcement for Aggressive Environments. Luton.
- Read, J. (1990) Specification and Standards for Epoxy Coated Bar. Paper presented at Seminar on Durable Reinforcement for Aggressive Environments. Luton.
- Sagues, A., Powers, R. & Zayed, A. (1990) Marine Environment Corrosion of Epoxy Coated Reinforcing Steel. Proceedings of Conference on Corrosion in Concrete, ed Page, C., Treadaway, K.W.J. & Bamforth, P., Birmingham. SCI.

1991 ASTM Standard specification for epoxy coated steel wire and welded wire fabric for reinforcement. ASTM A884/A884M-91b. Annual Book for ASTM Standards.

- Choi, O.C., Hossain, H-G., Darwin, D., & McCabe, S.L. Bond of epoxy coated reinforcement : bar parameters. American Concrete Institute, Materials Journal. Vol.88, No. 2. Mar-Apr 1991. pp 207-217.
- Cleary D.B. & Ramirez, J.A. Bond strength of epoxy-coated reinforcement. American Concrete Institute Materials Journal, Vol.88 No.2, Mar-Apr 1991. pp146-149.
- Hadje-Ghaffari H, Darwin D & McCabe S L. (1991) Effect of epoxy coating on bond of reinforcing steel to concrete. SM Report No. 28, University of Kansas. Lawrence, Kansas. 288 pp.

1992 CEB (1992). Protection systems for reinforcement. CEB Bulletin No. 211. CEB. Lausanne.

- Cusens A R & Yu Z. Pullout tests of epoxy-coated reinforcement in concrete. Cement and Concrete Composites. Vol 14, Pt 4 1992. pp 269-276.

1993 CEB-FIP Model Code 1990. Comite-Euro International du Beton/Federation Internationale de la Precontrainte. Thomas Telford, London. 437 pp.

- Cleary D B and Ramirez, J A. Epoxy coated reinforcement under repeated loading. ACI Structural Journal, Vol 90, No. 4, July-Aug 1993. pp451-458.
- Cusens A R, and Yu, Z. Bond strength and flexural behaviour of beams with epoxy coated reinforcement. The Structural Engineer, Vol 71, No. 7, April 1993. pp 117- 124.
- Hamad B.S. & Jirsa J.O. Strength of epoxy-coated reinforcing bar splices confined with transverse reinforcement. ACI Structural Journal Vol 90, No. 1 Jan/Feb 1993. pp77-88.
- Hester, C.J., Salamizavaregh, S., Darwin, D. and McCabe, S.L. Bond of epoxy-coated reinforcement: Splices. ACI Structural Journal, Vol. 90, No. 1, Jan-Feb 1993. pp89-102.

1994 Cairns, J. Performance of epoxy coated reinforcement at the serviceability limit state. Proceedings of the Institution of Civil Engineers, Structures & Buildings. Vol 104. Feb 1994. pp61-73

- Cairns, J., & Abdullah, R. (1994a) Fundamental tests on the effect of an epoxy coating on bond strength. American Concrete Institute Materials Journal. Vol. 91, No. 4. July/August pp 331-338.
- Cairns, J., & Abdullah, R. (1994b) Ultimate strength of lapped joints of epoxy coated reinforcement. Proceedings of the Institution of Civil Engineers, Structures & Buildings. Vol 104. Nov. pp391-400
- Hadje-Ghaffari H, Choi O C, Darwin D & McCabe, S L. Bond of epoxy coated reinforcement: cover, casting position slump and consolidation. ACI Structural Journal, Vol 91, No. 1, Jan-Feb 1994. pp59-68.
- Makhlouf H M, Al-Tamimi, A, Akbari, A H. (1994) Bond Carrying capacity of epoxy coated reinforcement. Proc. Conf. On Corrosion and Corrosion Protection of Steel in Concrete. Sheffield Academic Press. Sheffield. pp1218-1230.

1995 Abrishami, H H, Cook, W D, and Mitchell, D. Influence of epoxy coated reinforcement on response of normal and high strength concrete beams. ACI Structural Journal, Vol 92, No. 2. March-April 1995, pp157-166

- ASTM Standard specification for epoxy-coated prefabricated steel reinforcing bars. ASTM A934/A934M-95. Annual Book for ASTM Standards, Vol.1.04, Philadelphia, USA, 1995 pp504-516.

Copyright fib, all rights reserved. This PDF copy of fib Bulletin 10 is intended for use and/or distribution only by National Member Groups of fib.

- Bartoletti and Jirsa Effects of epoxy coating on anchorage and development of welded wire fabric. ACI Structural Journal, Vol 92, No.6. Nov-Dec. 1995. pp 757-764.
- Cairns, J., & Abdullah, R. (1995a) Influence of rib geometry on strength of epoxy coated reinforcement splices. American Concrete Institute Structural Journal. Vol 92, No. 1. Jan-Feb pp23-27.
- Cairns, J., & Abdullah, R. (1995b) An evaluation of bond pullout tests and their relevance to structural performance. The Structural Engineer, Journal of The Institution of Structural Engineers. Vol 73, No. 11. June. pp179-185.
- Darwin D & Idun E K. Discussion of Cairns & Abdullah(1995). American Concrete Institute Structural Journal, Vol 92, No. 6. Nov-Dec 1995. pp 782-784.
- Hamad, B S. Comparative bond strength of coated and uncoated bars with different rib geometries. American Concrete Institute Materials Journal, Vol 92, No. 6, Nov-Dec 1995. pp 579-590.
- Zwernerman, F., Donahey, R.C, Syed, H.S. & Gunna, S.R. Cracking of concrete pavement continuously reinforced with epoxy coated steel. ACI Materials Journal, Nov/Dec 1995. pp 678-685

1996 Abrishami, H H, Cook, W D, and Mitchell, D. The effect of epoxy-coated reinforcement and concrete quality on cracking of flat plate slab-column connections. ACI Materials Journal, Vol 93, No. 2, March-April 1996. pp 121-128.

- Cairns, J. Discussion of 'Influence of epoxy coated reinforcement on response of normal and high strength concrete beams', by Abrishami, H H, Cook, W D, and Mitchell, D. ACI Structural Journal, Jan-Feb 1996, pp140-141.
- Cairns, J., & Abdullah, R. Bond strength of black and epoxy coated reinforcement - a theoretical approach. American Concrete Institute Materials Journal, Vol. 93, No. 4. July-Aug 1996. pp 362-369.
- Hasan H O, Cleary D B, and Ramirez J A. Performance of concrete bridge decks and slabs reinforced with epoxy-coated steel under repeated loading. ACI Structural Journal, July-Aug 1996. pp397-403.
- McGormley, J C, Cleary, D B, and Ramirez, J A. The performance of epoxy-coated shear reinforcement. ACI Structural Journal, Vol. 93, No. 5. Sept/Oct 1996. pp. 531-537.
- Manning D G Corrosion performance of epoxy-coated reinforcing steel: North American experience. Construction & Building Materials, Vol 10 No. 5. 1996. pp 349-365.
- Tan C, Darwin D, Tholen M & Zuo J. (1996) Splice strength of epoxy-coated high relative rib area bars. Structural Engineering and Engineering Materials Report SL 96-2. University of Kansas. Lawrence, Kansas. 68 pp.

1997 Cairns J & Carbaugh C.(1997) Deformability of beams reinforced with epoxy coated bars. To be published.

Copyright fib, all rights reserved. This PDF copy of fib Bulletin 10 is intended for use and/or distribution only by National Member Groups of fib.

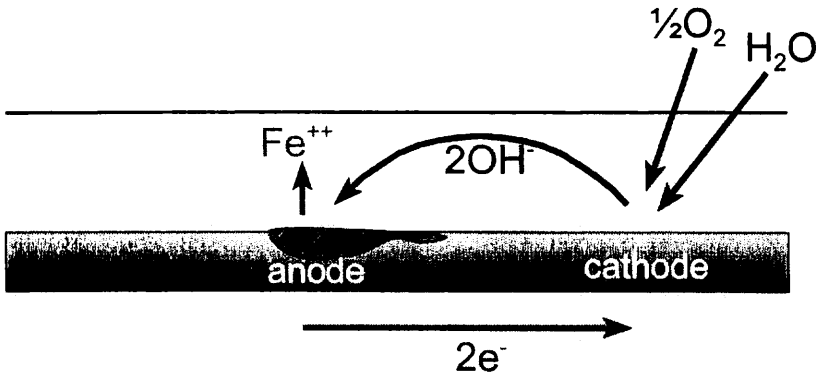

Figure 5.1 Formation of electrochemical corrosion cell on reinforcement.

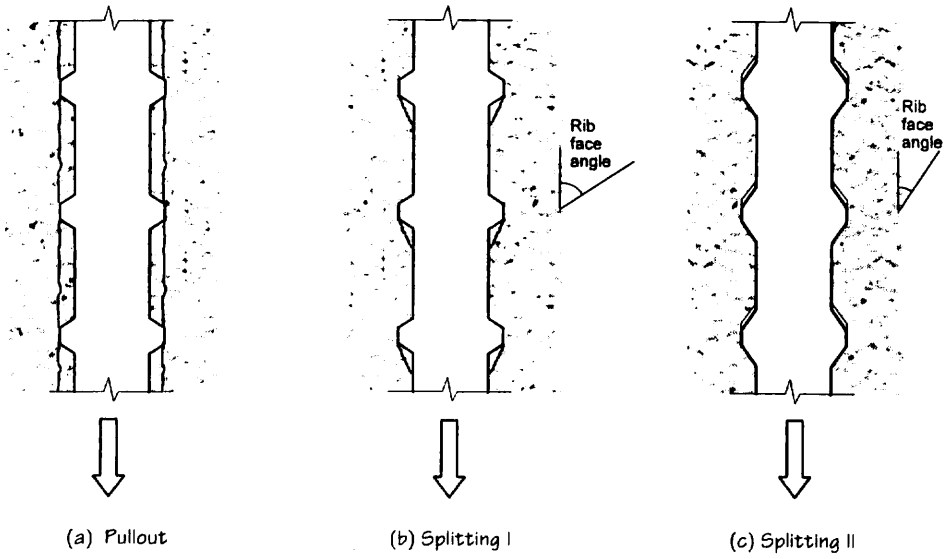

Figure 5.2 Modes of bond failure

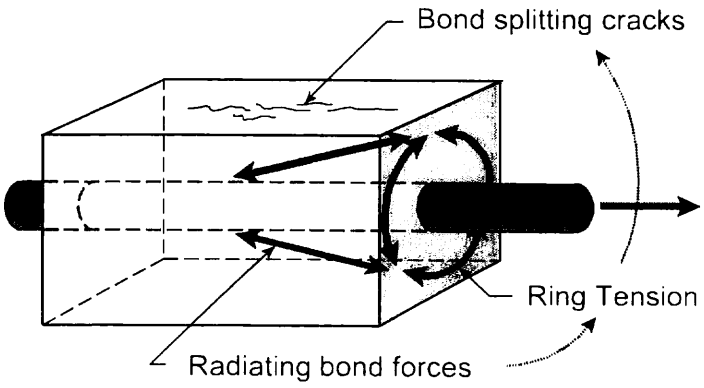

Figure 5.3 Splitting of concrete cover by bond action of ribbed reinforcing bar.

Copyright fib, all rights reserved. This PDF copy of fib Bulletin 10 is intended for use and/or distribution only by National Member Groups of fib.

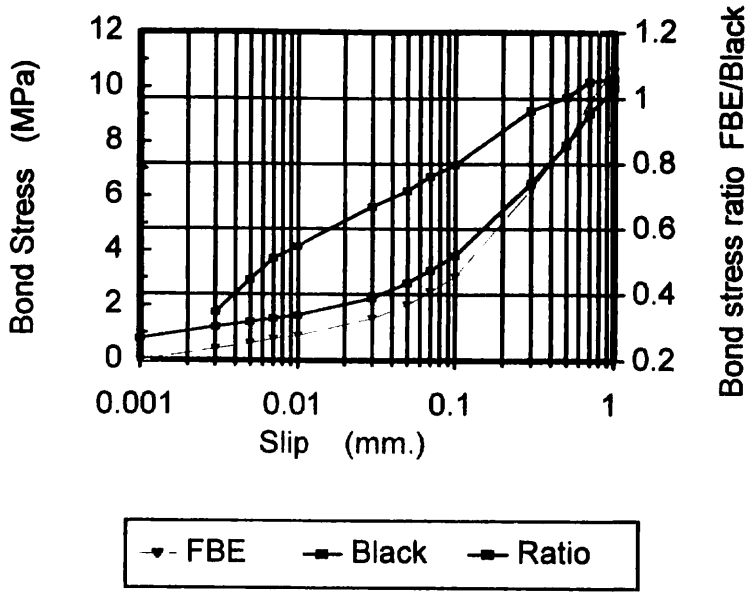

Figure 5.4 Variation in bond stress with slip for coated and non-coated (black) reinforcement, [Cairns & Abdullah 1994a].

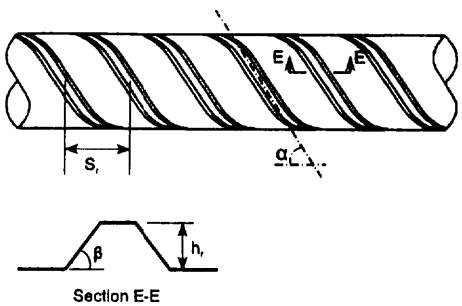

Figure 5.5 Rib face angle definition

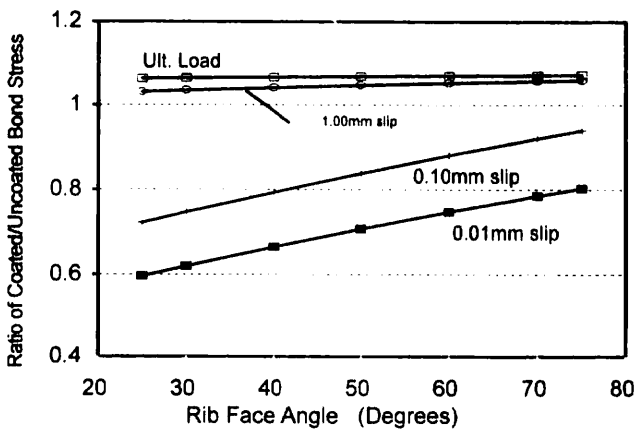

Figure 5.6 Influence of rib face angle on bond stress, measured using RILEM pullout specimen, [Cairns & Abdullah 1994a].

Copyright fib, all rights reserved. This PDF copy of fib Bulletin 10 is intended for use and/or distribution only by National Member Groups of fib.

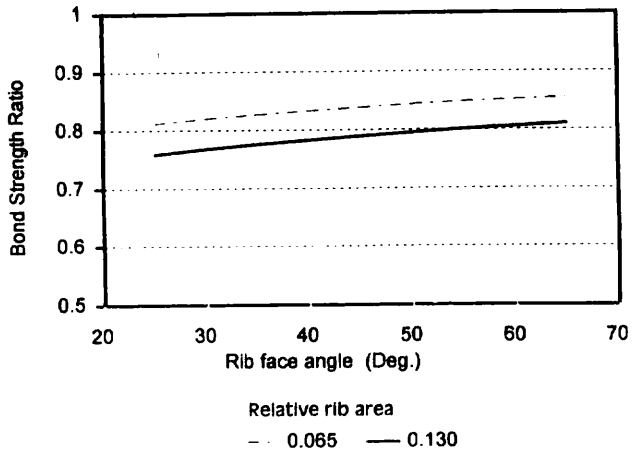

Figure 5.7 Measured variation in bond strength ratio with rib face angle, [Cairns & Abdullah 1995a]

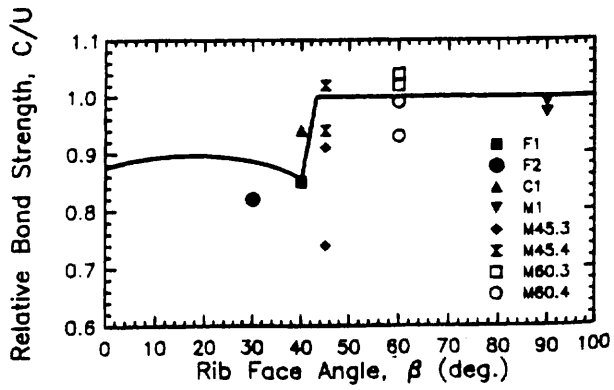

Figure 5.8 Calculated variation in bond strength with rib face angle, [Darwin & Idun 1995]

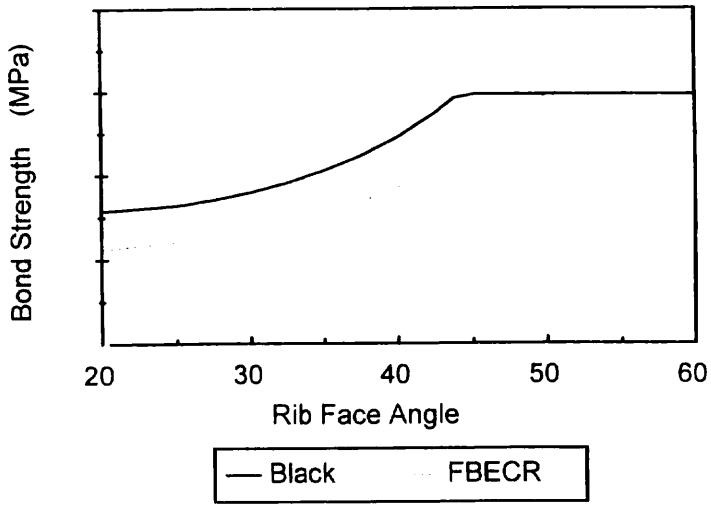

Figure 5.9 Calculated variation in bond strength with rib face angle, [Cairns & Abdullah 1996].

Copyright fib, all rights reserved. This PDF copy of fib Bulletin 10 is intended for use and/or distribution only by National Member Groups of fib.

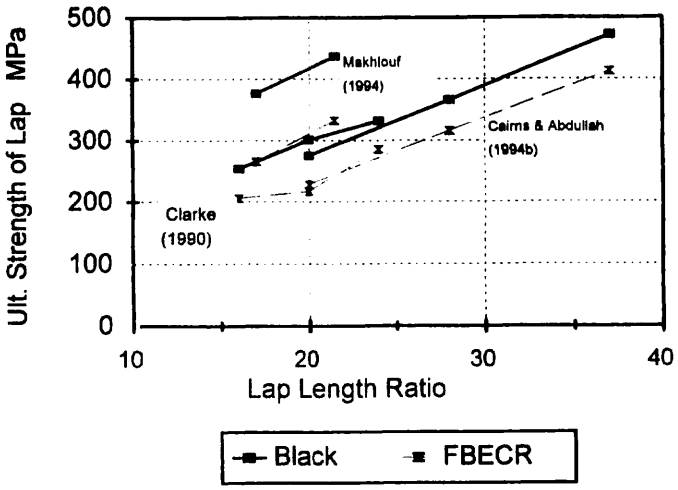

Figure 5.10 Influence of lap length on joint strength.

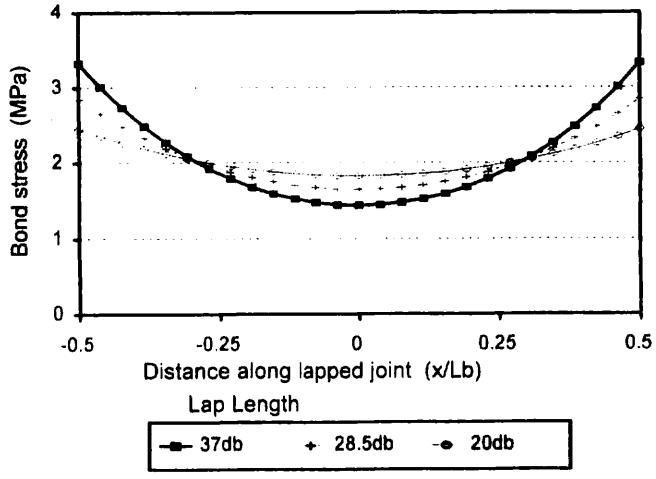

Figure 5.11 Distribution of bond stress along lap length, calculated using modulus of displacement theory.

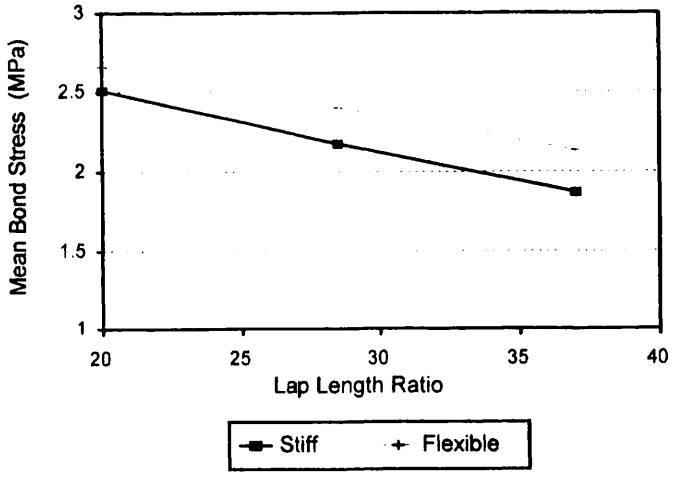

Figure 5.12 Average bond stress for calculated for specified peak bond stress : effect of bond stiffness.

Copyright fib, all rights reserved. This PDF copy of fib Bulletin 10 is intended for use and/or distribution only by National Member Groups of fib.

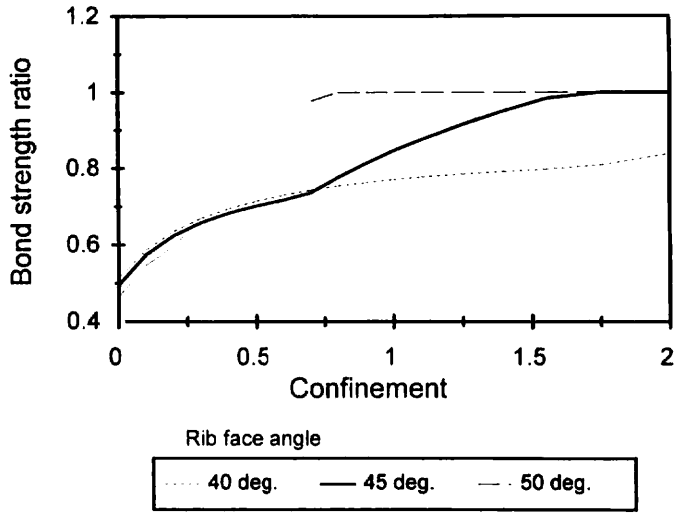

Figure 5.13 Influence of confinement on ratio of bond strength of coated bars to that of black bars. Cairns & Abdullah's model [1996]

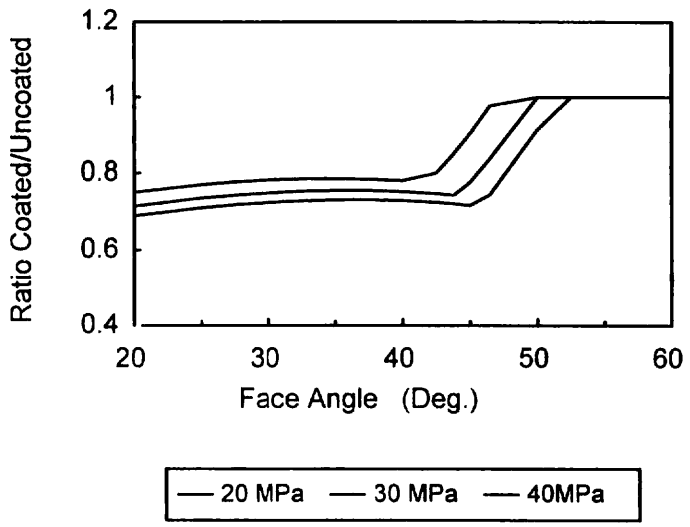

Figure 5.14 Influence of face angle and concrete strength on ratio of bond strength of coated bars to that of black bars. Cairns & Abdullah's model [1996]

Copyright fib, all rights reserved. This PDF copy of fib Bulletin 10 is intended for use and/or distribution only by National Member Groups of fib.

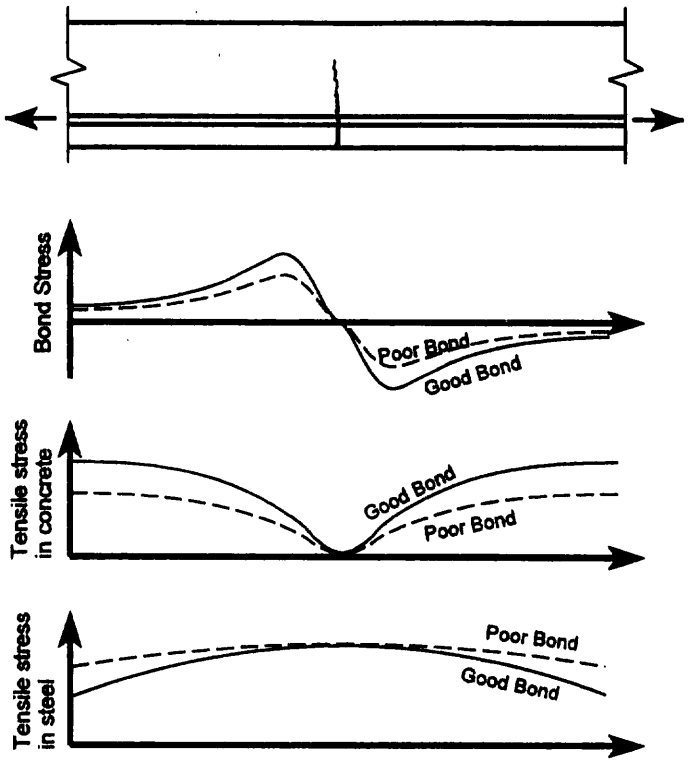

Figure 5.15 Influence of bond characteristics of reinforcement on cracking and on tension stiffening.

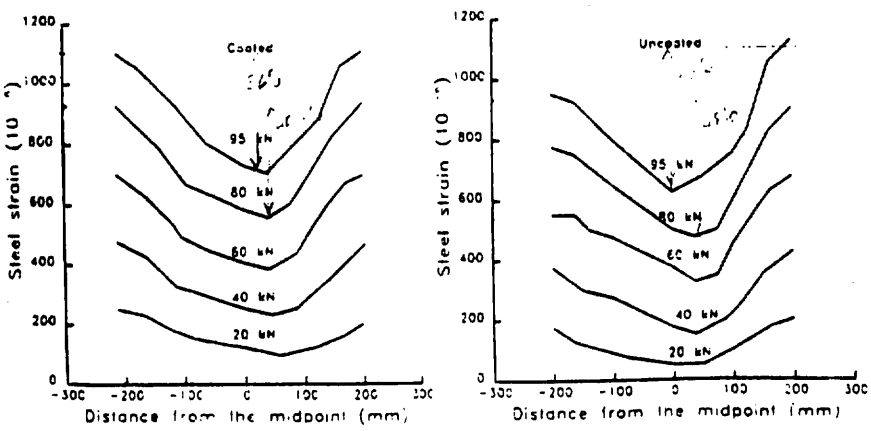

Figure 5.16 Variation of bar strain in double pullout test. [Cusens & Yu 1992]

Copyright fib, all rights reserved. This PDF copy of fib Bulletin 10 is intended for use and/or distribution only by National Member Groups of fib.

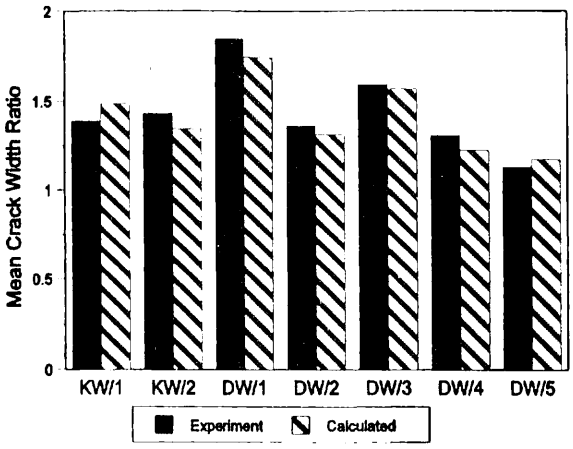

Figure 5.17 Influence of epoxy coating on crack widths : comparison of experimental and calculated ratios, [Cairns 1994]

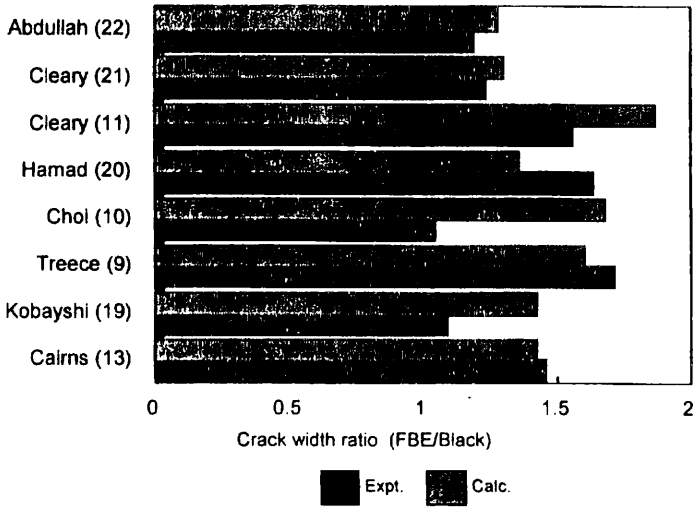

Figure 5.18 Comparison of measured and calculated crack width ratios, various studies. [Cairns 1996b]

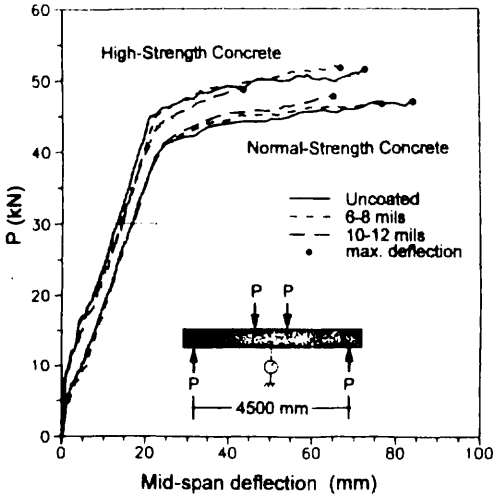

Figure 5.19 Comparison of load-midspan deflection relationships for beams reinforced with epoxy coated and non-coated bars. [Abrishami et al 1995]

Copyright fib, all rights reserved. This PDF copy of fib Bulletin 10 is intended for use and/or distribution only by National Member Groups of fib.

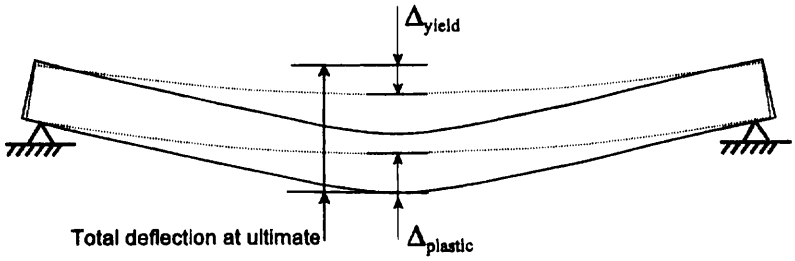

Figure 5.20 Determination of plastic hinge rotation.

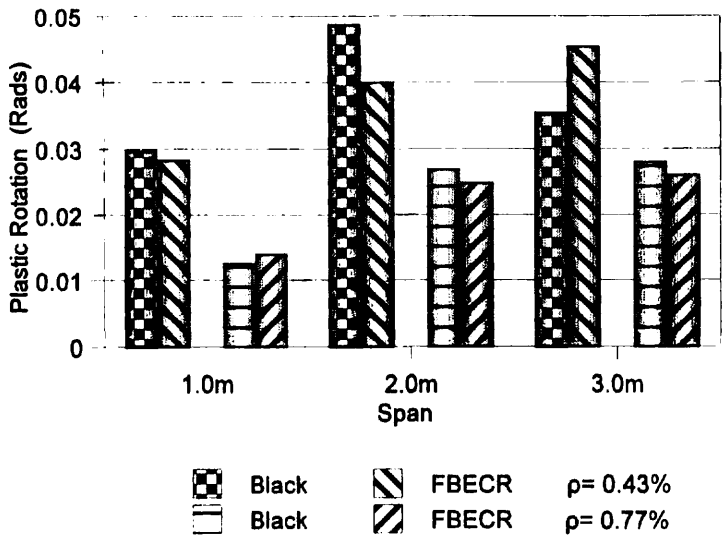

Figure 5.21 Influence of epoxy coating on rotation capacity. [Cairns & Carbaugh 1997]

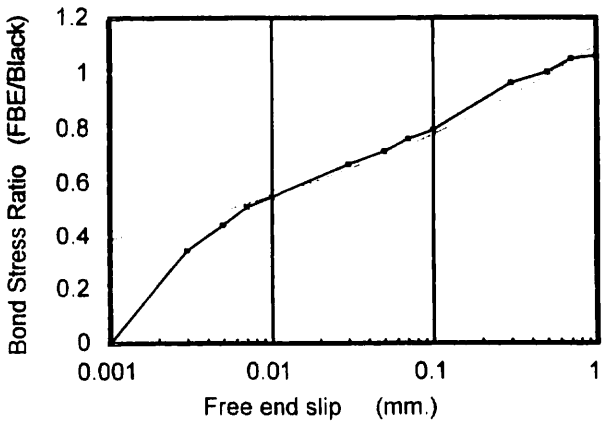

Figure 5.22 Comparison of proposed local bond slip relationships for black and coated bars.

Copyright fib, all rights reserved. This PDF copy of fib Bulletin 10 is intended for use and/or distribution only by National Member Groups of fib.

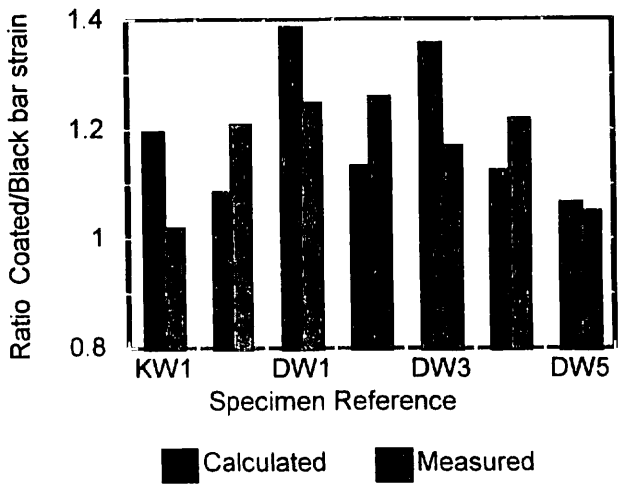

Figure 5.23 Comparison of average reinforcement strains, calculated assuming a 50% reduction in tension stiffening, with measured differences between coated and black bars.

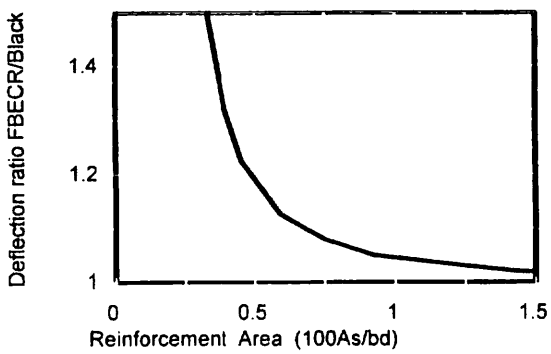

Figure 5.24 Sensitivity of increase in midspan deflection of beams reinforced with coated bars to geometric ratio of reinforcement

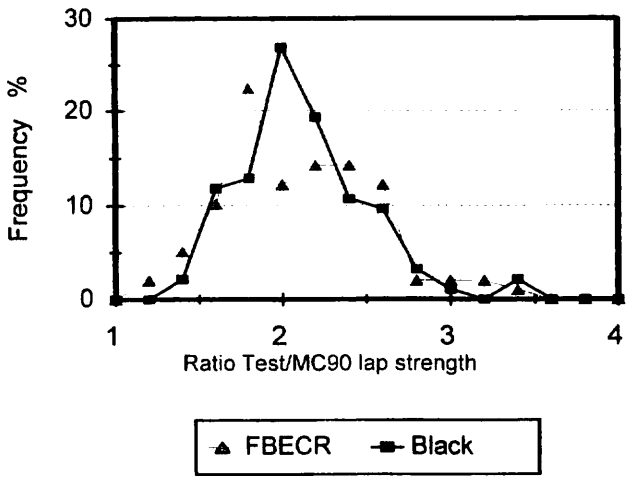

Figure 5.25 Frequency distributions for measured to design lap strength ratios

Copyright fib, all rights reserved. This PDF copy of fib Bulletin 10 is intended for use and/or distribution only by National Member Groups of fib.

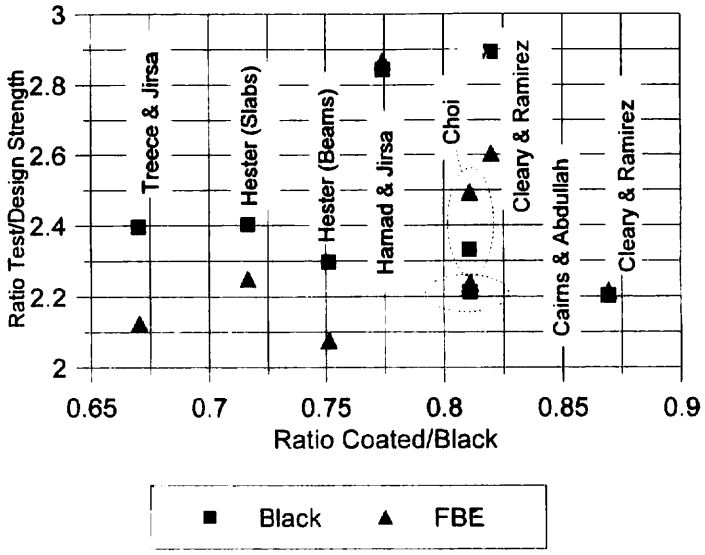

Figure 5.26 Comparison of measured and design lapped joint strengths: by test series.

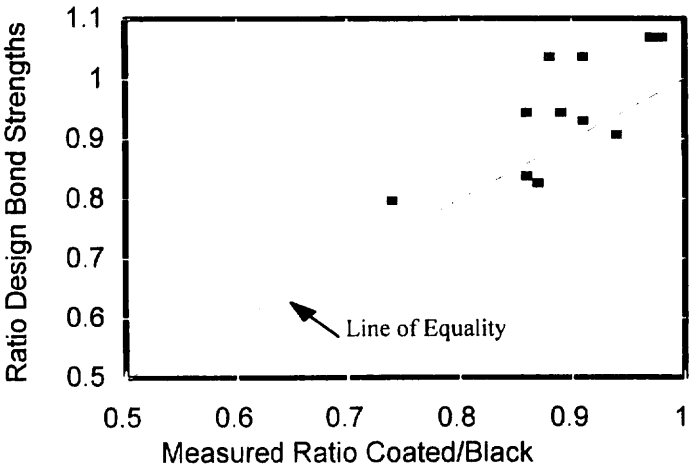

Figure 5.27 Influence of concrete cover on bond strength ratio : comparison of measurements by Hadje Ghaffari et al [1994] with proposed design rules.

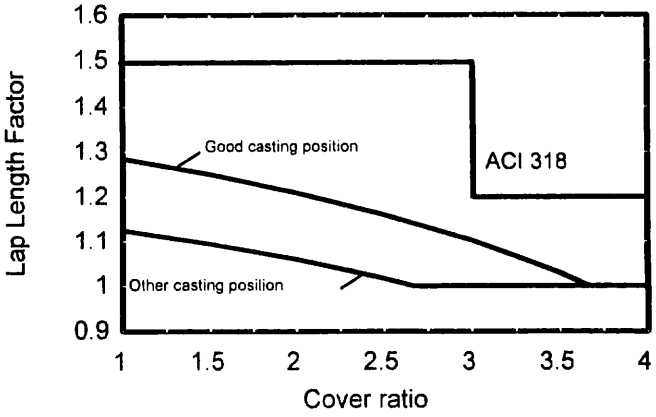

Figure 5.28 Effect of proposed modifications on lap length

Appendix 5.1 Analysis of Lap Strength Data for Black Bars

Study	Test Ref.	Concrete Strength f_{cu} N/mm²	Bar Dia. φ mm	Position Factor η_2	Bar Dia. Factor η_3	Design Anchor. Stress f_{bd}	Cover ratio	Cover factor α_3	Lapped %age α_6	Transv. Reinft. factor α_4	MC90 Design Lap Strength f_{bl} N/mm²	Expt Lap Strength f_{bexpt} N/mm²	Ratio f_{bexpt}/f_{bl}
T&J	0-6-4	36.7	19.2	0.9	1.0	2.62	2.66	0.65	2.0	1.00	2.01	5.73	2.85
T&J	10-6-4r	33.3	19.2	0.9	1.0	2.46	1.30	0.94	2.0	1.00	1.31	3.45	2.63
T&J	0-11-4	43.4	35.8	0.9	0.96	2.82	1.42	0.91	2.0	1.00	1.55	2.9	1.87
T&J	0-11-4b	37.0	35.8	0.9	0.96	2.53	1.42	0.91	2.0	1.00	1.39	3.1	2.23
T&J	0-6-8	69.3	19.2	0.9	1.0	4.00	1.15	0.97	2.0	1.00	2.06	5.1	2.47
T&J	0-11-8	71.4	35.8	0.9	0.96	3.93	1.51	0.89	2.0	1.00	2.20	5.45	2.48
T&J	0-6-12	108.7	19.2	0.9	1.0	5.40	0.99	1.00	2.0	1.00	2.70	5.11	1.90
T&J	0-11-12	90.6	35.8	0.9	0.96	4.60	1.42	0.91	2.0	1.00	2.53	6.35	2.51
T&J	0-11-12b	82.8	35.8	0.9	0.96	4.34	1.42	0.91	2.0	1.00	2.38	5.8	2.44
Choi	SP1N	46.2	15.9	1.0	1.0	3.39	1.57	0.88	2.0	1.00	1.93	5.27	2.73
Choi	SP1N	46.2	15.9	1.0	1.0	3.39	1.57	0.88	2.0	1.00	1.93	5.5	2.85
Choi	SP2S	51.8	19.1	1.0	1.0	3.66	1.31	0.94	2.0	1.00	1.96	4.66	2.38
Choi	SP2C	51.8	19.1	1.0	1.0	3.66	1.31	0.94	2.0	1.00	1.96	5.25	2.68
Choi	SP3S	51.6	25.4	1.0	1.0	3.65	1.48	0.90	2.0	1.00	2.03	4.32	2.13
Choi	SP3N	51.6	25.4	1.0	1.0	3.65	1.48	0.90	2.0	1.00	2.03	4.34	2.14
Choi	SP4S	50.4	34.9	1.0	0.97	3.49	1.43	0.91	2.0	1.00	1.92	3.71	1.93
Choi	SP4C	50.4	34.9	1.0	0.97	3.49	1.43	0.91	2.0	1.00	1.92	3.47	1.81

Copyright fib, all rights reserved. This PDF copy of fib Bulletin 10 is intended for use and/or distribution only by National Member Groups of fib.

Study	Test Ref.	Concrete Strength	Bar Dia.	Position Factor	Bar Dia. Factor	Design Anchor. Stress	Cover ratio	Cover factor	Lapped %age	Transv. Reinft. factor	MC90 Design Lap Strength	Expt Lap Strength	Ratio f_{bexpt}/f_{bl}
Cleary_1	16	48.5	19.2	1.0	1.0	3.51	2.66	0.65	2.0	1.00	2.69	5.25	1.95
Cleary_1	14	46.4	19.2	1.0	1.0	3.40	2.66	0.65	2.0	1.00	2.61	6.00	2.30
Cleary_1	12	34.4	19.2	1.0	1.0	2.79	2.66	0.65	2.0	1.00	2.14	5.00	2.34
Cleary_1	10	70.7	19.2	1.0	1.0	4.51	2.66	0.65	2.0	1.00	3.46	7.66	2.22
Cleary_2	U12410A	29.7	19	1.0	1.0	2.53	3.00	0.58	2.0	1.00	2.18	6.84	3.14
Cleary_2	U12410B	30.3	19	1.0	1.0	2.56	3.00	0.58	2.0	1.00	2.21	6.48	2.93
Cleary_2	U12415A	29.7	19	1.0	1.0	2.53	3.00	0.58	2.0	1.00	2.18	6.63	3.04
Cleary_2	U12415B	30.3	19	1.0	1.0	2.56	3.00	0.58	2.0	1.00	2.21	6.84	3.10
Cleary_2	U12410C	35.5	19	1.0	1.0	2.85	3.00	0.58	2.0	1.00	2.45	7.40	3.02
Cleary_2	U12415C	35.5	19	1.0	1.0	2.85	3.00	0.58	2.0	1.00	2.45	6.90	2.81
Cleary_2	U10710A	47.6	19	1.0	1.0	3.46	3.00	0.58	2.0	1.00	2.98	8.04	2.69
Cleary_2	U12710A	47.6	19	1.0	1.0	3.46	3.00	0.58	2.0	1.00	2.98	6.82	2.29
Cleary_2	U12715A	48.6	19	1.0	1.0	3.51	3.00	0.58	2.0	1.00	3.03	6.79	2.24
Cleary_2	U7241	20.7	22	1.0	1.0	1.99	2.91	0.60	2.0	1.00	1.66	4.85	2.93
Cleary_2	U7242	32.4	22	1.0	1.0	2.68	2.91	0.60	2.0	1.00	2.24	5.59	2.50
Cleary_2	U7361	35.9	22	1.0	1.0	2.87	2.91	0.60	2.0	1.00	2.39	7.16	2.99
Cleary_2	U7362	36.6	22	1.0	1.0	2.91	2.91	0.60	2.0	1.00	2.42	6.87	2.83
Cleary_2	U7363	27.6	22	1.0	1.0	2.41	2.91	0.60	2.0	1.00	2.01	7.07	3.52
Cleary_2	U7301	20.7	22	1.0	1.0	1.99	2.91	0.60	2.0	1.00	1.66	5.43	3.27
Cleary_2	U11241	20.7	35	1.0	0.97	1.93	1.83	0.83	2.0	1.00	1.17	3.57	3.06
Cleary_2	U11242	32.4	35	1.0	0.97	2.60	1.83	0.83	2.0	1.00	1.57	4.17	2.65
Cleary_2	U11243	20.7	35	1.0	0.97	1.93	1.83	0.83	2.0	1.00	1.17	3.83	3.28
Cleary_2	U11301	35.9	35	1.0	0.97	2.78	1.83	0.83	2.0	1.00	1.68	4.66	2.77
Cleary_2	U11302	36.6	35	1.0	0.97	2.82	1.83	0.83	2.0	1.00	1.71	4.43	2.60
Cleary_2	U11303	27.6	35	1.0	0.97	2.33	1.83	0.83	2.0	1.00	1.41	4.34	3.07

Appendix 5.1 : 2 of 6

Copyright fib, all rights reserved. This PDF copy of fib Bulletin 10 is intended for use and/or distribution only by National Member Groups of fib.

Study	Test Ref.	Concrete Strength	Bar Dia.	Position Factor	Bar Dia. Factor	Design Anchor. Stress	Cover ratio	Cover factor	Lapped %age	Transv. Reinft. factor	MC90 Design Lap Strength	Expt Lap Strength	Ratio f_{bexpt}/f_{bl}
Hamad	B1	31.9	35.8	0.9	0.96	2.30	1.42	0.91	2.0	1.00	1.26	2.82	2.24
Hamad	B3	31.9	35.8	0.9	0.96	2.30	1.42	0.91	2.0	1.02	1.24	3.06	2.48
Hamad	B5	34.5	35.8	0.9	0.96	2.42	1.42	0.91	2.0	0.96	1.39	3.24	2.34
Hamad	B7	34.5	35.8	0.9	0.96	2.42	0.35	1.14	2.0	0.94	1.13	2.68	2.36
Hamad	B9	32.3	19.1	0.9	1.0	2.41	0.83	1.04	2.0	1.00	1.16	4.47	3.85
Hamad	B11	32.3	19.1	0.9	1.0	2.41	0.83	1.04	2.0	0.89	1.30	4.94	3.79
Hester	B 1 / 8 N 3 - 16-0-U	51.7	25.4	1.0	1.0	3.66	1.50	0.90	2.0	1.08	1.89	5.43	2.88
Hester	B 1 / 8 N 3 - 16-2-U	51.7	25.4	1.0	1.0	3.66	1.50	0.90	2.0	1.01	2.02	6.09	3.02
Hester	B 2 / 8 C 3 - 16-0-U	53.5	25.4	1.0	1.0	3.74	1.50	0.90	2.0	1.00	2.09	5.01	2.40
Hester	B 2 / 8 C 3 - 16-2-U	53.5	25.4	1.0	1.0	3.74	1.50	0.90	2.0	1.01	2.06	4.77	2.31
Hester	B 3 / 8 S 3 - 16-0-C	51.9	25.4	1.0	1.0	3.67	1.50	0.90	2.0	1.00	2.05	5.07	2.48
Hester	B 3 / 8 S 3 - 16-2-U	51.9	25.4	1.0	1.0	3.67	1.50	0.90	2.0	1.01	2.02	5.02	2.48
		51.9	25.4	1.0	1.0	3.67	1.50	0.90	2.0	1.00	2.05	5.07	2.48
		51.9	25.4	1.0	1.0	3.67	1.50	0.90	2.0	1.01	2.02	5.02	2.48
Hester	B 4 / 8 S 3 - 16-0-U	55.6	25.4	1.0	1.0	3.84	1.50	0.90	2.0	1.00	2.14	4.6	2.15
Hester	B 4 / 8 S 3 - 16-2-U	55.6	25.4	1.0	1.0	3.84	1.50	0.90	2.0	1.01	2.11	5.11	2.42
Hester	B 4 / 8 S 3 - 16-3-U	55.6	25.4	1.0	1.0	3.84	1.50	0.90	2.0	0.98	2.18	5.43	2.49

Appendix 5.1 : 3 of 6

Copyright fib, all rights reserved. This PDF copy of fib Bulletin 10 is intended for use and/or distribution only by National Member Groups of fib.

Study	Test Ref.	Concrete Strength	Bar Dia.	Position Factor	Bar Dia. Factor	Design Anchor. Stress	Cover ratio	Cover factor	Lapped %age	Transv. Reinft. factor	MC90 Design Lap Strength	Expt Lap Strength	Ratio f_{bexpt}/f_{bl}
Hester	B5/8C3-16-0-U	47.4	25.4	1.0	1.0	3.45	1.50	0.90	2.0	1.00	1.93	4.28	2.22
Hester	B5/8C3-16-3-U	47.4	25.4	1.0	1.0	3.45	1.50	0.90	2.0	0.97	1.98	5.02	2.54
Hester	B6/8C3-22-0-U	50.5	25.4	1.0	1.0	3.60	1.50	0.90	2.0	1.00	2.01	3.91	1.95
Hester	B6/8C3-22-3-U	50.5	25.4	1.0	1.0	3.60	1.50	0.90	2.0	1.01	2.00	4.26	2.13
Hester	B6/8C3-22-4-U	50.5	25.4	1.0	1.0	3.60	1.50	0.90	2.0	0.98	2.04	4.22	2.06
Hester	B7/8C3-16-0-U	45.2	25.4	1.0	1.0	3.34	2.13	0.76	2.0	1.00	2.19	4.87	2.22
Hester	B7/8C3-16-3-C	45.2	25.4	1.0	1.0	3.34	2.09	0.77	2.0	0.99	2.19	5.55	2.54
Hester	S1/6C3-10-0-U	43.5	19.2	1.0	1.0	3.26	3.16	0.55	2.0	1.00	2.99	5.71	1.91
Hester	S2/6C3-10-0-U	46.3	19.2	1.0	1.0	3.40	2.90	0.60	2.0	1.00	2.82	6.13	2.17
Hester	S2/6C3-10-2-U	46.3	19.2	1.0	1.0	3.40	2.76	0.63	2.0	0.98	2.75	6.60	2.40
Hester	S3/6S3-10-0-U	43.4	19.2	1.0	1.0	3.26	2.70	0.64	2.0	1.00	2.53	5.99	2.37
Hester	S3/6S3-10-2-U	43.4	19.2	1.0	1.0	3.26	2.75	0.63	2.0	0.98	2.63	6.74	2.57
Hester	S4/6C5-10-0-U	45.6	19.2	1.0	1.0	3.36	2.78	0.63	2.0	1.00	2.68	6.07	2.26
Hester	S4/6C5-10-2-U	45.6	19.2	1.0	1.0	3.36	2.62	0.66	2.0	0.88	2.90	6.74	2.32

Appendix 5.1 : 4 of 6

Copyright fib, all rights reserved. This PDF copy of fib Bulletin 10 is intended for use and/or distribution only by National Member Groups of fib.

Study	Test Ref.	Concrete Strength	Bar Dia.	Position Factor	Bar Dia. Factor	Design Anchor. Stress	Cover ratio	Cover factor	Lapped %age	Transv. Reinft. factor	MC90 Design Lap Strength	Expt Lap Strength	Ratio f_{bexpt}/f_{bl}
Hester	S5/8C5-16-0-U	44.0	25.4	1.0	1.0	3.29	2.09	0.77	2.0	1.00	2.13	4.65	2.18
Hester	S5/8C5-16-2-U	44.0	25.4	1.0	1.0	3.29	2.05	0.78	2.0	0.94	2.24	4.16	1.86
Hester	S6/8C5-16-0-U	46.7	25.4	1.0	1.0	3.42	2.08	0.77	2.0	1.00	2.21	3.88	1.76
Hester	S6/8C5/16-4-U	46.7	25.4	1.0	1.0	3.42	2.04	0.78	2.0	0.86	2.53	4.41	1.74
Hester	S7/6C5-10-0-U	46.6	19.2	1.0	1.0	3.41	2.83	0.62	1.6	1.00	3.47	8.85	2.55
Hester	S7/6C5-10-2-U	46.6	19.2	1.0	1.0	3.41	2.73	0.64	1.6	0.91	3.67	8.72	2.38
Hester	S8/6C5-10-0-U	46.9	19.2	1.0	1.0	3.43	2.73	0.64	2.0	1.00	2.69	4.82	1.79
Hester	S8/6C5-10-2-U	46.9	19.2	1.0	1.0	3.43	2.71	0.64	2.0	0.89	3.02	6.88	2.28

Appendix 5.1 : 5 of 6

Copyright fib, all rights reserved. This PDF copy of fib Bulletin 10 is intended for use and/or distribution only by National Member Groups of fib.

Study	Test Ref.	Concrete Strength	Bar Dia.	Position Factor	Bar Dia. Factor	Design Anchor. Stress	Cover ratio	Cover factor	Lapped %age	Transv. Reinft. factor	MC90 Design Lap Strength	Expt Lap Strength	Ratio f_{bexpt}/f_{bl}
Abdullah	20	30.6	16	1.0	1.0	2.58	1.44	0.91	2.0	1.00	1.42	3.41	2.40
Abdullah	28.5	30.6	16	1.0	1.0	2.58	1.44	0.91	2.0	1.00	1.43	3.23	2.27
Abdullah	37	30.6	16	1.0	1.0	2.58	1.44	0.91	2.0	1.02	1.39	3.18	2.28
Abdullah	A20-1	29.5	20	1.0	1.0	2.52	1.65	0.86	2.0	0.98	1.49	2.94	1.98
Abdullah	A20-2	29.5	20	1.0	1.0	2.52	1.65	0.86	2.0	0.98	1.49	3.07	2.06
Abdullah	B20	29.5	20	1.0	1.0	2.52	1.65	0.86	2.0	0.98	1.49	3.53	2.37
Abdullah	C20	29.5	20	1.0	1.0	2.52	1.65	0.86	2.0	0.98	1.49	3.46	2.33
Abdullah	D20	29.5	20	1.0	1.0	2.52	1.65	0.86	2.0	0.98	1.49	3.2	2.15
Abdullah	E20	29.5	20	1.0	1.0	2.52	1.65	0.86	2.0	0.98	1.49	3.08	2.07

Notes

1 Concrete strengths based on cube results. Cube strength f_{cu} taken as 125% of cylinder compressive strength.
2 Derivation of transverse reinforcement factor α_4 based on equivalent area/unit length for full strength lap rather than on total quantity.
3 f_{bl} is equivalent design bond stress for full strength lap.

Copyright fib, all rights reserved. This PDF copy of fib Bulletin 10 is intended for use and/or distribution only by National Member Groups of fib.

Appendix 5.2 Analysis of Lap Strength Data for Coated Bars

Study	Test Ref.	Concrete Strength	Bar Dia.	Position Factor	Bar Dia. Factor	Design Anchor. Stress	Cover ratio	Cover factor	Lapped %age	Transv. Reinft. factor	MC90 Design Lap Strength	Expt Lap Strength	Ratio
		f_{cu}	φ	η_2	η_3	f_{bd}		α_3	α_6	α_4	f_{bl}	f_{bexpt}	f_{bexpt}/f_{bl}
		N/mm²	mm								N/mm²	N/mm²	
T&J	12-6-4	36.7	19.2	0.90	1.0	1.92	2.66	0.55	2.0	1.00	1.74	3.59	2.07
T&J	5-6-4	36.7	19.2	0.90	1.0	1.92	2.66	0.55	2.0	1.00	1.74	4.97	2.86
T&J	12-6-4r	33.3	19.2	0.90	1.0	1.80	1.15	0.96	2.0	1.00	0.94	2.42	2.58
T&J	5-6-4r	33.3	19.2	0.90	1.0	1.80	0.99	1.00	2.0	1.00	0.90	2.55	2.84
T&J	12-11-4	43.4	35.8	0.90	0.96	2.07	1.42	0.89	2.0	1.00	1.17	1.93	1.65
T&J	5-11-4	43.4	35.8	0.90	0.96	2.07	1.42	0.89	2.0	1.00	1.17	2.07	1.77
T&J	12-11-4b	37.0	35.8	0.90	0.96	1.86	1.42	0.89	2.0	1.00	1.05	1.66	1.58
T&J	12-6-8	69.3	19.2	0.90	1.0	2.94	0.99	1.00	2.0	1.00	1.46	2.83	1.93
T&J	12-11-8	71.4	35.8	0.90	0.96	2.88	1.59	0.84	2.0	1.00	1.71	3.45	2.01
T&J	12-6-12	108.7	19.2	0.90	1.0	3.96	0.83	1.05	2.0	1.00	1.90	3.31	1.75
T&J	12-11-12	90.6	35.8	0.90	0.96	3.38	1.42	0.89	2.0	1.00	1.91	4.55	2.39
T&J	12-11-12b	82.8	35.8	0.90	0.96	3.18	1.42	0.89	2.0	1.00	1.80	3.73	2.08
Choi	SP1N	46.2	15.9	1.0	1.0	2.49	1.57	0.85	2.0	1.00	1.47	4.09	2.78
Choi	SP2S	51.8	19.1	1.0	1.0	2.69	1.31	0.92	2.0	1.00	1.47	4.38	2.99
Choi	SP2C	51.8	19.1	1.0	1.0	2.69	1.31	0.92	2.0	1.00	1.47	3.98	2.72
Choi	SP3S	51.6	25.4	1.0	1.0	2.68	1.48	0.87	2.0	1.00	1.54	3.87	2.52
Choi	SP3N	51.6	25.4	1.0	1.0	2.68	1.48	0.87	2.0	1.00	1.54	3.71	2.41
Choi	SP4S	50.4	34.9	1.0	0.97	2.56	1.43	0.88	2.0	1.00	1.45	2.62	1.81
Choi	SP4C	50.4	34.9	1.0	0.97	2.56	1.43	0.88	2.0	1.00	1.45	2.82	1.94

Copyright fib, all rights reserved. This PDF copy of fib Bulletin 10 is intended for use and/or distribution only by National Member Groups of fib.

Study	Test Ref.	Concrete Strength	Bar Dia.	Position Factor	Bar Dia. Factor	Design Anchor. Stress	Cover ratio	Cover factor	Lapped %age	Transv. Reinft. factor	MC90 Design Lap Strength	Expt Lap Strength	Ratio f_{bexpt}/f_{bl}
Cleary_1	16	48.5	19.2	1.0	1.0	2.57	2.66	0.55	2.0	1.00	2.33	4.50	1.94
Cleary_1	14	46.4	19.2	1.0	1.0	2.50	2.66	0.55	2.0	1.00	2.26	4.93	2.18
Cleary_1	12	34.4	19.2	1.0	1.0	2.04	2.66	0.55	2.0	1.00	1.85	4.77	2.58
Cleary_1	10	70.7	19.2	1.0	1.0	3.31	2.66	0.55	2.0	1.00	2.99	6.47	2.16
Cleary_2	E12410A	29.7	19	1.0	1.0	1.85	3.00	0.46	2.0	1.00	2.01	5.59	2.77
Cleary_2	E12410B	30.3	19	1.0	1.0	1.88	3.00	0.46	2.0	1.00	2.04	5.62	2.75
Cleary_2	E12415A	29.7	19	1.0	1.0	1.85	3.00	0.46	2.0	1.00	2.01	5.68	2.82
Cleary_2	E12415B	30.3	19	1.0	1.0	1.88	3.00	0.46	2.0	1.00	2.04	5.96	2.92
Cleary_2	E12410C	35.5	19	1.0	1.0	2.09	3.00	0.46	2.0	1.00	2.27	6.72	2.96
Cleary_2	E12415C	35.5	19	1.0	1.0	2.09	3.00	0.46	2.0	1.00	2.27	6.41	2.82
Cleary_2	E10710A	47.6	19	1.0	1.0	2.54	3.00	0.46	2.0	1.00	2.76	6.66	2.41
Cleary_2	E12710A	47.6	19	1.0	1.0	2.54	3.00	0.46	2.0	1.00	2.76	6.46	2.34
Cleary_2	E12715A	48.6	19	1.0	1.0	2.57	3.00	0.46	2.0	1.00	2.80	5.68	2.03
Cleary_2	E124SA	30.3	19	1.0	1.0	1.88	3.00	0.46	2.0	1.00	2.04	5.30	2.60
Cleary_2	E107SA	46.2	19	1.0	1.0	2.49	3.00	0.46	2.0	1.00	2.71	5.62	2.08
Cleary_2	E107SB	51.0	19	1.0	1.0	2.66	3.00	0.46	2.0	1.00	2.89	5.47	1.89
Cleary_2	E127SA	48.6	19	1.0	1.0	2.57	3.00	0.46	2.0	1.00	2.80	5.82	2.08
Cleary_2	E127SB	48.8	19	1.0	1.0	2.58	3.00	0.46	2.0	1.00	2.81	6.44	2.30
Cleary_2	E7241	20.7	22	1.0	1.0	1.46	2.91	0.48	2.0	1.00	1.50	4.60	3.06
Cleary_2	E7242	32.4	22	1.0	1.0	1.96	2.91	0.48	2.0	1.00	2.03	4.60	2.27
Cleary_2	E7361	35.9	22	1.0	1.0	2.10	2.91	0.48	2.0	1.00	2.17	5.22	2.41
Cleary_2	E7362	36.6	22	1.0	1.0	2.13	2.91	0.48	2.0	1.00	2.20	4.46	2.03
Cleary_2	E7363	27.6	22	1.0	1.0	1.77	2.91	0.48	2.0	1.00	1.82	5.94	3.26
Cleary_2	E7301	20.7	22	1.0	1.0	1.46	2.91	0.48	2.0	1.00	1.50	4.39	2.92
Cleary_2	E11241	20.7	35	1.0	0.97	1.41	1.83	0.78	2.0	1.00	0.91	3.05	3.35

Appendix 5.2: 2 of 5

Copyright fib, all rights reserved. This PDF copy of fib Bulletin 10 is intended for use and/or distribution only by National Member Groups of fib.

Copyright fib, all rights reserved. This PDF copy of fib Bulletin 10 is intended for use and/or distribution only by National Member Groups of fib.

Study	Test Ref.	Concrete Strength	Bar Dia.	Position Factor	Bar Dia. Factor	Design Anchor. Stress	Cover ratio	Cover factor	Lapped %age	Transv. Reinft. factor	MC90 Design Lap Strength	Expt Lap Strength	Ratio f_{bexpt}/f_{bl}
Cleary_2	E11242	32.4	35	1.0	0.97	1.91	1.83	0.78	2.0	1.00	1.23	3.29	2.68
Cleary_2	E11243	20.7	35	1.0	0.97	1.41	1.83	0.78	2.0	1.00	0.91	3.13	3.44
Cleary_2	E11301	35.9	35	1.0	0.97	2.04	1.83	0.78	2.0	1.00	1.31	3.50	2.66
Cleary_2	E11302	36.6	35	1.0	0.97	2.07	1.83	0.78	2.0	1.00	1.33	3.37	2.53
Cleary_2	E11303	27.6	35	1.0	0.97	1.71	1.83	0.78	2.0	1.00	1.10	2.55	2.31
Hamad	B2	31.9	35.8	0.90	0.96	1.68	1.42	0.89	2.0	1.00	0.95	2.08	2.19
Hamad	B4	31.9	35.8	0.90	0.96	1.68	1.42	0.89	2.0	1.00	0.95	2.47	2.59
Hamad	B6	34.5	35.8	0.90	0.96	1.77	1.42	0.89	2.0	0.92	1.09	2.71	2.49
Hamad	B8	34.5	35.8	0.90	0.96	1.77	0.35	1.17	2.0	0.89	0.84	2.28	2.70
Hamad	B10	32.3	19.1	0.90	1.0	1.76	0.83	1.05	2.0	1.00	0.84	3.00	3.55
Hamad	B12	32.3	19.1	0.90	1.0	1.76	0.83	1.05	2.0	0.85	1.00	3.67	3.68
Hester	B1/8N3-16-1-C	51.7	25.4	1.0	1.0	2.68	1.50	0.87	2.0	1.03	1.50	4.12	2.75
Hester	B1/8N3-16-2-C	51.7	25.4	1.0	1.0	2.68	1.50	0.87	2.0	0.99	1.56	4.6	2.94
Hester	B2/8C3-16-0-C	53.5	25.4	1.0	1.0	2.74	1.50	0.87	2.0	1.00	1.58	4.15	2.62
Hester	B2/8C3-16-2-C	53.5	25.4	1.0	1.0	2.74	1.50	0.87	2.0	0.99	1.60	4.1	2.57
Hester	B3/8S3-16-0-C	51.9	25.4	1.0	1.0	2.69	1.50	0.87	2.0	1.00	1.55	3.33	2.14
Hester	B3/8S3-16-2-C	51.9	25.4	1.0	1.0	2.69	1.50	0.87	2.0	0.99	1.57	3.45	2.20
Hester	B3/8S3-16-0-C	51.9	25.4	1.0	1.0	2.69	1.02	0.99	2.0	1.00	1.35	2.86	2.11
Hester	B3/8S3-16-2-C	51.9	25.4	1.0	1.0	2.69	1.02	0.99	2.0	0.98	1.38	3.27	2.36
Hester	B4/8S3-16-0-C	55.6	25.4	1.0	1.0	2.82	1.50	0.87	2.0	1.00	1.63	3.32	2.04
Hester	B4/8S3-16-2-C	55.6	25.4	1.0	1.0	2.82	1.50	0.87	2.0	0.99	1.64	3.46	2.12
Hester	B4/8S3-16-3-C	55.6	25.4	1.0	1.0	2.82	1.50	0.87	2.0	0.96	1.70	3.32	1.95
Hester	B5/8C3-16-0-C	47.4	25.4	1.0	1.0	2.53	1.50	0.87	2.0	1.00	1.46	3.43	2.35
Hester	B5/8C3-16-3-C	47.4	25.4	1.0	1.0	2.53	1.50	0.87	2.0	0.94	1.55	3.74	2.42
Hester	B6/8C3-22-0-C	50.5	25.4	1.0	1.0	2.64	1.50	0.87	2.0	1.00	1.52	2.53	1.66

Appendix 5.2: 3 of 5

Study	Test Ref.	Concrete Strength	Bar Dia.	Position Factor	Bar Dia. Factor	Design Anchor. Stress	Cover ratio	Cover factor	Lapped %age	Transv. Reinft. factor	MC90 Design Lap Strength	Expt Lap Strength	Ratio f_{bexpt}/f_{bl}
Hester	B6/8C3-22-3-C	50.5	25.4	1.0	1.0	2.64	1.50	0.87	2.0	0.98	1.55	2.7	1.74
Hester	B6/8C3-22-4-C	50.5	25.4	1.0	1.0	2.64	1.50	0.87	2.0	0.96	1.60	2.92	1.83
Hester	B7/8C3-16-0-C	45.2	25.4	1.0	1.0	2.45	2.13	0.70	2.0	1.00	1.76	4.17	2.37
Hester	B7/8C3-16-3-C	45.2	25.4	1.0	1.0	2.45	2.09	0.71	2.0	0.98	1.78	4.17	2.35
Hester	S1/6C3-10-0-C	43.5	19.2	1.0	1.0	2.39	3.16	0.42	2.0	1.00	2.87	4.40	1.53
Hester	S2/6C3-10-0-C	46.3	19.2	1.0	1.0	2.49	2.90	0.49	2.0	1.00	2.55	4.75	1.86
Hester	S2/6C3-10-2-C	46.3	19.2	1.0	1.0	2.49	2.76	0.52	2.0	0.97	2.44	4.40	1.80
Hester	S3/6S3-10-0-C	43.4	19.2	1.0	1.0	2.39	2.70	0.54	2.0	1.00	2.20	4.59	2.08
Hester	S3/6S3-10-2-C	43.4	19.2	1.0	1.0	2.39	2.75	0.53	2.0	0.97	2.33	4.59	1.97
Hester	S4/6C5-10-0-C	45.6	19.2	1.0	1.0	2.47	2.78	0.52	2.0	1.00	2.37	4.14	1.74
Hester	S4/6C5-10-2-C	45.6	19.2	1.0	1.0	2.47	2.62	0.56	2.0	0.86	2.55	5.06	1.98
Hester	S5/8C5-16-0-C	44.0	25.4	1.0	1.0	2.41	2.09	0.71	2.0	1.00	1.71	3.23	1.89
Hester	S5/8C5-16-2-C	44.0	25.4	1.0	1.0	2.41	2.05	0.72	2.0	0.92	1.83	3.05	1.67
Hester	S6/8C5-16-0-C	46.7	25.4	1.0	1.0	2.51	2.08	0.71	2.0	1.00	1.77	2.49	1.41
Hester	S6/8C5/16-4-C	46.7	25.4	1.0	1.0	2.51	2.04	0.72	2.0	0.83	2.09	2.93	1.40
Hester	S7/6C5-10-0-C	46.6	19.2	1.0	1.0	2.50	2.83	0.51	1.6	1.00	3.09	7.36	2.38
Hester	S7/6C5-10-2-C	46.6	19.2	1.0	1.0	2.50	2.73	0.53	1.6	0.90	3.27	7.42	2.27
Hester	S8/6C5-10-0-C	46.9	19.2	1.0	1.0	2.51	2.73	0.53	2.0	1.00	2.35	4.50	1.91
Hester	S8/6C5-10-2-C	46.9	19.2	1.0	1.0	2.51	2.71	0.54	2.0	0.87	2.69	5.69	2.11

Appendix 5.2: 4 of 5

Copyright fib, all rights reserved. This PDF copy of fib Bulletin 10 is intended for use and/or distribution only by National Member Groups of fib.

Study	Test Ref.	Concrete Strength	Bar Dia.	Position Factor	Bar Dia. Factor	Design Anchor. Stress	Cover ratio	Cover factor	Lapped %age	Transv. Reinft. factor	MC90 Design Lap Strength	Expt Lap Strength	Ratio f_{bexpt}/f_{bl}
Abdullah	20	30.6	16	1.0	1.0	1.89	1.44	0.88	2.0	0.97	1.10	2.85	2.59
Abdullah	28.5	30.6	16	1.0	1.0	1.89	1.44	0.88	2.0	0.97	1.11	2.81	2.54
Abdullah	37	30.6	16	1.0	1.0	1.89	1.44	0.88	2.0	0.99	1.08	2.79	2.59
Abdullah	A20-1	29.5	20	1.0	1.0	1.85	1.75	0.80	2.0	0.95	1.21	2.5	2.06
Abdullah	A20-2	29.5	20	1.0	1.0	1.85	1.75	0.80	2.0	0.95	1.21	2.54	2.09
Abdullah	B20	29.5	20	1.0	1.0	1.85	1.75	0.80	2.0	0.95	1.21	2.32	1.91
Abdullah	C20	29.5	20	1.0	1.0	1.85	1.75	0.80	2.0	0.95	1.21	2.78	2.29
Abdullah	D20	29.5	20	1.0	1.0	1.85	1.75	0.80	2.0	0.95	1.21	2.4	1.98
Abdullah	E20	29.5	20	1.0	1.0	1.85	1.75	0.80	2.0	0.95	1.21	2.55	2.10
												Mean	2.33
												CoV	0.20

Notes

1 Concrete strengths based on cube results. Cube strength f_{cu} taken as 125% of cylinder compressive strength.
2 Derivation of transverse reinforcement factor α_4 based on equivalent area/unit length for full strength lap rather than on total quantity.
3 f_{bl} is equivalent design bond stress for full strength lap.

Copyright fib, all rights reserved. This PDF copy of fib Bulletin 10 is intended for use and/or distribution only by National Member Groups of fib.

Copyright fib, all rights reserved. This PDF copy of fib Bulletin 10 is intended for use and/or distribution only by National Member Groups of fib.

6 Bond of prestressing tendons

Working Party 6:

Joop den Uijl (Convener, Delft University of Technology, The Netherlands), **György Balázs** (Technical University of Budapest, Hungary), **Björn Engström** (Chalmers University of Technology, Göteborg, Sweden), **Koji Otsuka** (Tohoku Gakuin University, Chuo Tagajo, Japan), **Lucie Vandewalle** (Katholieke Universiteit Leuven, Heverlee, Belgium)

6.1 Introduction **270**
6.1.1 Scope 270
6.1.2 Aim 270
6.1.3 Terminology 270
6.2 Bond mechanism **272**
6.2.1 Plain wire 272
6.2.2 Plain seven-wire strand 273
6.2.3 Tendons with increased surface roughness 274
6.3 Modeling **275**
6.3.1 Elastic and plastic bond zone 275
6.3.2 Bond stress versus slip 275
6.3.3 Bond stress versus slip and steel stress change 276
6.3.4 Bond stress based on concrete confinement 279
6.3.5 Coefficient of friction versus slip 280
6.3.6 Interface model for bond of strand 281
6.3.7 Basic bond tests 282
6.4 Prestress transfer and anchorage of plain seven-wire strand **285**
6.4.1 Influence of concrete strength 285
6.4.2 Influence of concrete cover and spacing 289
6.4.3 Influence of strand geometry and surface condition 291
6.4.4 Influence of time on transmission length 291
6.4.5 Influence of initial steel stress 292
6.4.6 Relation between draw-in and transmission length 292
6.4.7 Standardized bond test 293
6.5 Prestress transfer and anchorage of wire and strand with increased surface roughness **296**
6.6 Prestress transfer and anchorage of epoxy coated strand **298**
6.6.1 Transmission length 298
6.6.2 Anchorage capacity 299
6.6.3 Effect of bond situation 300
6.6.4 Bond splitting 301
6.6.5 Influence of elevated temperature 302
6.7 Design rules for transmission length and anchorage length **303**
6.7.1 ACI 318 303
6.7.2 CEB-FIP Model Code 1990 304
6.7.3 Eurocode 2 306
6.7.4 Comparison of various codes 308
6.8 Summary and conclusions **309**
6.9 Notations **310**
6.10 References **311**

Copyright fib, all rights reserved. This PDF copy of fib Bulletin 10 is intended for use and/or distribution only by National Member Groups of fib.

6.1 Introduction

6.1.1 Scope

Compared to post-tensioned prestressing steel bond of pretensioned prestressing steel is studied much more intensively, because the prestress transfer and the anchorage capacity under flexural loading fully depend on the bond properties of the pretensioned tendons. This is reflected in the present chapter of this state-of-the-art report, which mainly deals with the bond of pretensioned prestressing tendons.

The type of tendon widely used is plain seven-wire strand. Besides, indented wire and indented strand are applied, but unfortunately there is very few published material about the bond characteristics of the latter. Relatively new developments are epoxy coated strand and non-metallic tendons. The latter is extensively discussed in Chapter 8 "Bond of non-metallic reinforcement". Therefore it is not treated here.

Central items related to the bond of prestressing tendons that will be discussed are the transmission length, the anchorage capacity and the detailing of the anchorage zone (concrete cover, tendon spacing, transverse reinforcement).

Worthwhile mentioning is the impact of a memorandum issued by the Federal Highway Administration (USA, October 1988), that restricted the use of pretensioned seven-wire strand in highway bridge applications, on the research efforts in this field, resulting in an intensive discussion on the anchorage length of pretensioned strand, that has not been finished yet.

The work presented here builds on the state-of-the-art reports published in CEB-Bulletin no. 151 (1982) and no. 181 (1987). It is strived to include in the bibliography all relevant material published since 1987. Earlier publications to which is referred in the text are included as well.

6.1.2 Aim

The aim of this part of the present state-of-the-art report is:

- to summarize and discuss the developments made during the last decade with respect to understanding and modelling of bond behaviour and calculation of transmission length and anchorage capacity of prestressing tendons,
- to compare design rules on transmission length, anchorage capacity and detailing of the anchorage zones in various codes and
- to identify inconsistencies and deficiencies in existing modelling and design rules.

6.1.3 Terminology

Terminology concerning anchorage of pretensioned tendons strongly differs in Europe and in the USA. To facilitate the discussion in this field, the principle differences are given hereafter. Throughout this chapter the terminology and notations from MC90 (CEB-FIP Model Code 1990) are used. In the list of notations the USA equivalent terms are mentioned as well.

The distance along which the prestress is built up in the tendon after prestress transfer is called transmission length (MC90) or transfer length (USA). The distance at which the prestress has just been linearly distributed over the concrete cross-section is called development length (MC90). In the USA this term is used to indicate the embedment length required to transfer the ultimate tendon force to the concrete. In case of a pretensioned tendon this development length (USA) is the sum of the transfer length (USA) and the flexural bond length (USA). The latter is that part of the embedment length where bond is only activated after a bending crack has originated. In Europe no such distinction is made and the equivalent of development length (USA) is anchorage length (MC90).

It is noticed that the bond test which is commonly denoted by "pull-out test" should rather be denoted by "pull-through test". The difference between both concerns the embedment length, which remains constant in a pull-through test but which diminishes in a pull-out test. Here the current

Copyright fib, all rights reserved. This PDF copy of fib Bulletin 10 is intended for use and/or distribution only by National Member Groups of fib.

wording is followed unless otherwise stated.

The average bond stress is defined as the bond force divided by the corresponding nominal bond surface, the latter being taken as the surface of a cylinder with a diameter equal to the nominal diameter of the tendon. Some researchers estimate the bond stress on the basis of the actual strand surface that is in contact with the concrete. For reasons of comparison those values are converted to the first mentioned definition by multiplication with the factor 1.33. This problem can be evaded by expressing the bond resistance as bond force per unit length instead of using bond stress.

Copyright fib, all rights reserved. This PDF copy of fib Bulletin 10 is intended for use and/or distribution only by National Member Groups of fib.

6.2 Bond mechanism

It is a generally accepted view that the transfer of forces between a reinforcing tendon and concrete is caused by adhesion, friction and (other) mechanical actions. The contribution of each of these three mechanisms strongly depends on the surface texture of the tendon. Therefore the various mechanisms are discussed in relation to the different types of prestressing tendons.

6.2.1 Plain wire

In case of plain wire bond can be attributed to adhesion and friction.

Adhesion

The designation adhesion stands for the contributions to elastic bond, which refers to the deformation of the cementitious layer around the tendon. It consists of both chemical and physical adhesion and interlocking between cement stone particles and the microscopically rough steel surface. Failure of adhesion bond occurs at a very small relative displacement and therefore adhesion will only play a minor part in practice. After breakage of the adhesion bond (debonding), force transfer is provided by dry friction.

Friction

The radial compressive stress connected to this friction is caused by shrinkage, roughness of the sliding plane and wedging of cement stone particles. The sliding plane is found to coincide with the steel-to-concrete interface for very smooth steel surfaces and to run through the cementitious layer around the tendon when a certain threshold value of the roughness is passed: R_a>1.2 μm [Stroeven & De Wind (1982)]. Due to wear of the sliding plane the radial compressive stress diminishes with increasing slip, and so does the bond stress.

When the pretensioning force in a tendon is released, the diameter of the tendon increases, which generates radial compressive stresses and, hence, contributes to the frictional bond resistance. This Poisson effect is proportional to the change in the longitudinal steel stress. As a consequence of this effect the bond resistance of plain wire is strongly reduced when the steel stress is increased.

Friction is the resistance against a parallel displacement between two surfaces that are kept in contact by a compressive force perpendicular to the contact plane. Friction between concrete and steel was rather occasionally studied, and the reported coefficient of friction varies highly. Baltay & Gjelsvik (1990), for example, found for similar tests values between 0.3 and 0.6. This variation will partly be caused by the test conditions, but also by factors playing a role in the processes by which friction is governed. Those processes are not fully understood and the following description should therefore be considered as a strong simplification.

In general, the real contact area is much smaller than the nominal contact area due to the roughness of the surfaces, which means that in the points of contact the "yield" stress is present. Hence, the real contact area is proportional to the normal stress. When parallel displacement occurs, the contact points are sheared off, or, in case of two materials that differ in hardness, the harder asperities are forced to plough through the softer material.

Baltay & Gjelsvik (1990) used this model representation to explain the different coefficient of friction between concrete and mild steel with or without mill scale. Some concrete particles are harder than a machined surface of mild steel, resulting in plastic deformation of the steel surface at relative movement. On the contrary, a steel surface with mill scale is not penetrated by the concrete particles and, as a consequence, the coefficient of friction is lower. At a higher level of normal stress the concrete starts to crush and concrete particles are not pressed into the steel surface anymore. Then the steel starts to plough through the concrete and the difference in coefficient of friction for both steel surfaces disappears.

Olofsson & Holmgren (1992) developed a test method to estimate the coefficient of friction with

Copyright fib, all rights reserved. This PDF copy of fib Bulletin 10 is intended for use and/or distribution only by National Member Groups of fib.

which the contact pressure and the sliding velocity could be kept constant measuring the torque required to turn a steel ring pressed against a concrete cube. The roughness of the hardened steel ring was maintained to R_a=0.4±0.1 μm, whereas the roughness of the concrete surface was R_a=2.3±0.38 μm (as cast) and R_a=25±4.8 μm (sand blasted), respectively. The sliding velocity and normal pressure were 0.1 or 1 μm/s and 2 or 6 MPa, respectively. The coefficient of friction was found to vary between 0.51 and 0.66 with an average of 0.59. Both a higher velocity and a rougher concrete surface resulted in a lower coefficient of friction, whereas a higher contact stress yielded a higher value.

Similar values were found by Rabbat & Russell (1985), who investigated the friction between hot-rolled steel plate and cast-in-place concrete or grout. The normal stress was varied (0.14, 0.41 and 0.69 MPa) as well as the condition of the interface (dry or wet). A wet interface was obtained by saturating it with water after the initial bond was broken. The coefficient of friction slightly decreased as the normal stress was higher. The effect of the condition of the interface was more pronounced. No significant difference was observed between concrete (f_c≈24 MPa) and grout (f_c≈55 MPa). The average coefficient of friction for wet interfaces was about 0.65, whereas for dry interfaces an average value of 0.57 was found.

In tests often a so-called *stick-slip effect* is observed from which it is concluded that the static coefficient of friction is higher than the kinematic one. This is mostly ascribed to an influence of the sliding velocity, assuming a decrease of the coefficient of friction as the sliding velocity increases. Martins & Oden (1985), however, quote several investigations in which the dynamic properties of the specimen are held responsible for the difference in the coefficient of friction. Due to elastic body waves generated by local failure in the contact plane, vibrations perpendicular to the contact plane occur and the normal compressive stress varies. Therefore the apparent reduction of the coefficient of friction depends on the dynamic properties of the bodies in contact together with the driving system.

6.2.2 Plain seven-wire strand

The bond stress-slip relations of plain wire and plain seven-wire strand are clearly different; see Fig. 6.2-1. In general, the bond resistance of a strand does not drop after a small slip, but it remains constant or even increases. This favourable behaviour is often ascribed to mechanical action without specifying its nature.

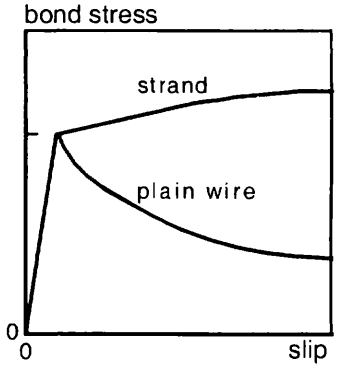

Fig. 6.2-1: Bond stress versus slip for plain wire and plain seven-wire strand

Mechanical action

In case of ribbed bars the mechanical action consists of *rib bearing* against the concrete keys that have been formed between the ribs, and if sufficient confinement is available these concrete keys are finally sheared off. Between the helical outer wires of a strand helical concrete ribs are formed as well. However, in general these ribs are not sheared off and a strand that is moved through the concrete follows the pre-shaped channel. Thus, rib bearing does not play a dominant role. Instead, other phenomena will contribute to the mechanical bond action of strand.

When a free strand is loaded its pitch will change, but this change is restricted when the strand is embedded. Due to this restraint deformation, a torsional moment develops in the strand that is

Copyright fib, all rights reserved. This PDF copy of fib Bulletin 10 is intended for use and/or distribution only by National Member Groups of fib.

equilibrated by contact stresses along the perimeter. According to Stocker & Sozen (1969) the contribution of these stresses to the frictional bond resistance is small because of the low torsional stiffness of the strand. They considered the wedge effect caused by irregularities in the shape of a strand as the most important reason for the different bond behaviour between plain wire and plain seven-wire strand. Variations in the pitch of the outer wires and non-similarity of subsequent cross-sections due to variations in the distribution of the space left between the outer wires because of the greater diameter of the centre wire are the causes of this *lack-of-fit effect*. Laldji & Young (1988) follow the same line describing bond of plain strand in mortar. They also point to the low torsional *stiffness* of a strand and from the observed influence of the embedment length on the shape of the bond stress-slip curve they argue that lack-of-fit is only developed if the embedment length is sufficiently long.

This explanation is contradicted by Russell & Burns (1993), who advocate the existence of a strong interaction between restraint twist and mechanical interlocking, arguing that Stocker & Sozen (1969) came to the opposite conclusion because of the boundary conditions in their pull-out tests with restrained twist. Due to the relatively long distance between the entrance plane and the strand section where the twist was restrained, the rotation of the strand corresponding to the slip at the entrance plane was smeared out over a much larger distance than what would happen near a bending crack, where this distance equals half the crack width. Thus, in the pull-out tests the torsional moment caused by restrained twist was much smaller than in a regular bending test. Unfortunately, the existence of such a restrained twist effect was only qualitatively indicated.

Besides the above-mentioned Poisson effect, which is proportional to the change in local steel stress, Den Uijl (1992b) takes into account a term proportional to the absolute value of the change in the local steel stress, which he denotes as *pitch effect*. By introducing this term, an empirical bond law was obtained, with which different bond situations could be simulated (Section 3.3), but no conclusive physical explanation of the pitch effect was given.

6.2.3 Tendons with increased surface roughness

When the roughness of the tendon surface is increased, e.g. by means of indents or lugs, a considerable amount of force is transferred through normal compressive stresses in the contact areas that can be projected to a plane perpendicular to the axis of the tendon. For ribbed bars the bond resistance was found to be a function of the roughness expressed as the ratio between the projected rib area and the surface area between two subsequent ribs, the so-called relative rib area.

Copyright fib, all rights reserved. This PDF copy of fib Bulletin 10 is intended for use and/or distribution only by National Member Groups of fib.

6.3 Modelling

In practice, design aspects related to bond of pretensioned tendons are solved taking into account a simplified bond stress distribution. However, for a better understanding of the influence of various parameters on transmission length and anchorage capacity, a realistic image of the bond stress distribution is required. To that end various models have been developed, which are described in this section. Some of these models explicitly take into account the confinement of the concrete around the tendon, which is often conceived as a partly cracked thick-walled cylinder.

6.3.1 Elastic and plastic bond zone

To describe the anchorage capacity of a pretensioned strand, Cousins et al. (1990c) use a model, which they ascribe to Guyon (1968), that takes into account a so-called elastic-plastic bond stress distribution. Along the elastic bond zone the bond stress distribution is considered to be linear, whereas along the plastic bond zone the bond stress is considered to be constant. Assuming that the strain distribution at the concrete surface is similar to the course of strain in the strand, Cousins derives the elastic bond stress slope and the plastic bond stress level from the concrete strain measurements along the transmission length. However, the accuracy of the latter can be debated. By means of 2D FEM analyses the strain distribution in a pretensioned prismatic member was analysed, simulating bond by axial compressive forces over a distance l_t along the longitudinal axis. It was found that even with a uniform bond stress distribution along the transmission length l_t, the course of the strain at the concrete surface is curved near the end of the transmission length; see Fig. 6.3-1 left (Den Uijl, 1995a). As consequence, the bond stress derived from the concrete surface strain shows the elastic-plastic distribution; Fig. 6.3-1 right..

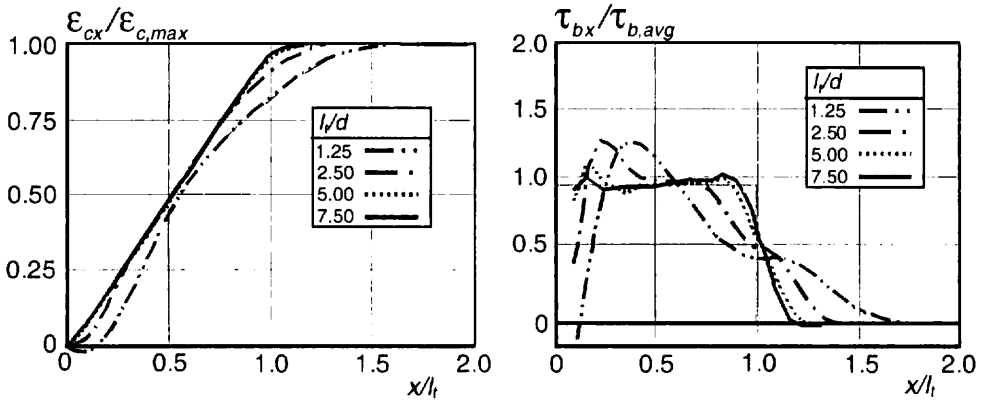

Fig. 6.3-1: Longitudinal strains at concrete surface for uniform bond stress from FEM calculation (left) and bond stress distribution derived from these strains (right), both for various transmission length over member depth ratios [Den Uijl (1995a)]

6.3.2 Bond stress versus slip

The slip distribution along an embedded tendon can be described by a second order differential equation considering equilibrium and compatibility and assuming linear elastic material behaviour and a bond stress that only depends on slip. An analytical solution of this differential equation for the bond situation along the transmission length has been derived by Balázs (1992) assuming a power function for this bond stress-slip relation:

$$\tau_b = \eta_1 \eta_2 f_{ci}^{0.5} \left(\frac{\delta}{\varnothing_p}\right)^{\eta_3} \tag{6.3-1}$$

with $\eta_1 = 1.35$, 1.0 and 0.65 for the upper bound, the mean and the lower bound value of the bond stress, respectively;
η_2 and η_3 are experimental constants; for $\varnothing_p = 12.8$ mm $\eta_2 = 2.055$ and $\eta_3 = 0.25$

Copyright fib, all rights reserved. This PDF copy of fib Bulletin 10 is intended for use and/or distribution only by National Member Groups of fib.

Eq. (6.3-1) shows that the bond stress was considered to be proportional to the square root of the concrete compressive strength at transfer. This approach results in expressions for the distribution along the transmission length of bond stress, steel stress and slip, see Fig. 6.3-2, and for relations between transmission length, initial steel stress, concrete strength, strand diameter and draw-in. In principle, this enables the estimation of the transmission length on the basis of the draw-in observed at transfer (Section 6.4.6).

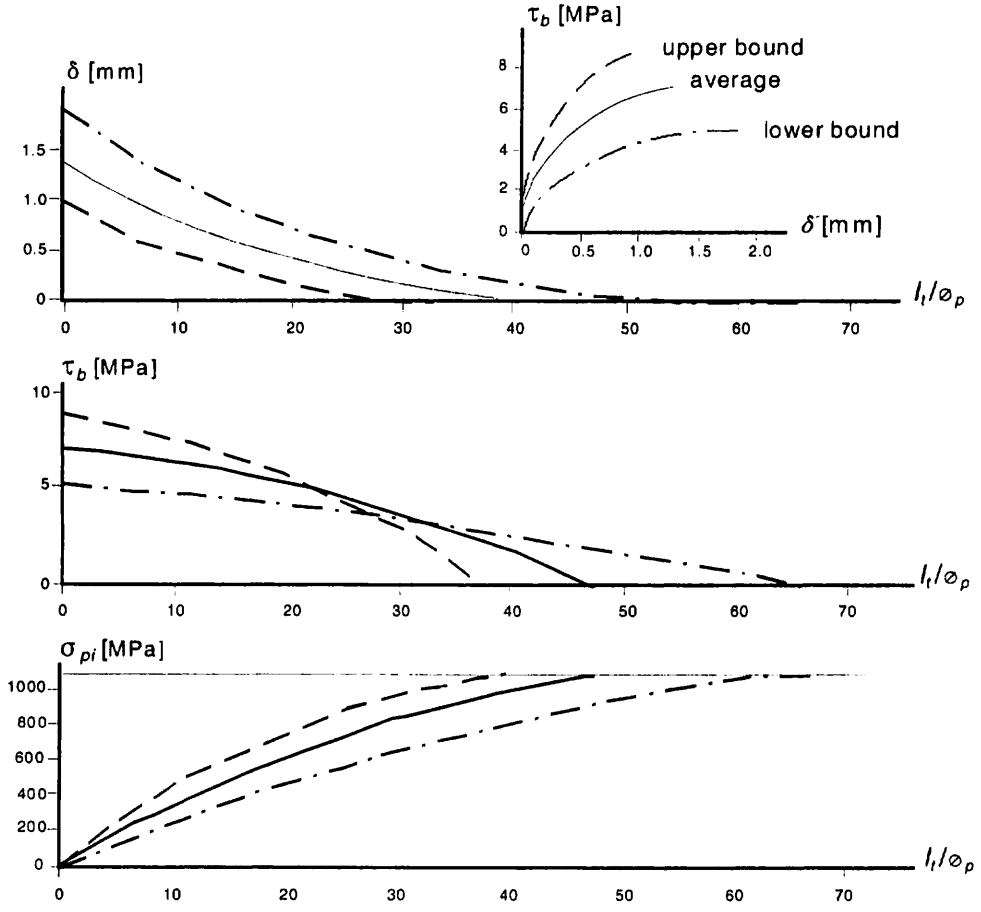

Fig. 6.3-2: Slip, bond stress and steel stress over transmission length for upper bound, average and lower bound of bond stress-slip relation expressed by power function in case of 12.8 mm diameter strand and f_{ci}=40 MPa [Balázs (1992)]

It is remarked that the description of the bond stress-slip relation with a power function, which results in a closed solution of the second order differential equation for bond, was first applied by Martin (1973) and Noakowski (1978) to ribbed bars and later by Bruggeling (1986) and Tassi et al. (1988) to pretensioned tendons.

6.3.3 Bond stress versus slip and steel stress change

The assumption of an invariable bond stress-slip relation along the transmission length implies that a possible influence of strand transverse deformation on bond stress (Poisson effect) is not taken into account. Den Uijl (1992b), however, concluded on the basis of bond stress-slip results from pull-out and push-in tests (9.3 mm strand diameter, 55 MPa cube strength, 50 and 88 mm embedded length, 46 mm clear cover) that the bond resistance is clearly influenced by the Poisson effect, see Fig. 6.3-3. This resulted in the following empirical relation:

$$\tau_b = 3 + 0.4\delta - 2.5\,10^{-3}\Delta\sigma_p + 1.5\,10^{-3}|\Delta\sigma_p| \qquad \text{[MPa]} \qquad (6.3\text{-}2)$$

Copyright fib, all rights reserved. This PDF copy of fib Bulletin 10 is intended for use and/or distribution only by National Member Groups of fib.

The terms at the right hand side of this equation are connected to adhesion, lack-of-fit effect, Poisson effect and pitch effect, respectively, see Section 6.2.2. The Poisson effect is shown to be proportional to the negative value of the change in steel stress, whereas the pitch effect is proportional to the absolute value of the change in steel stress.

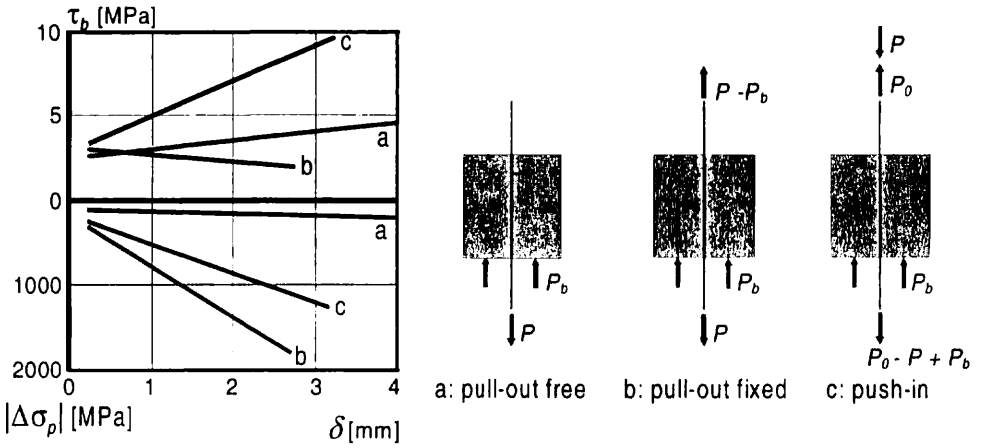

Fig. 6.3-3: Bond stress as a function of slip and steel stress change for plain seven-wire strand [Den Uijl (1992b)]

In Eq. (6.3-2) the relative deformation associated with adhesion has been neglected. This is justified if the reference point in the concrete were taken at the interface. However, in general this reference point is taken at some distance from the tendon surface, which means that at maximum adhesion the relative displacement consists of the elastic deformation of the concrete layer between the steel surface and the reference point. This aspect is taken into account in the following equation [Den Uijl (1994)]:

$$\tau_b = (\tau_{el} + 0.4\delta)\eta - 2.5\,10^{-3}\Delta\sigma_p + 1.5\,10^{-3}|\Delta\sigma_p| \quad \text{[MPa]} \tag{6.3-3}$$

with $\eta = \dfrac{\delta}{\delta_{el}}$ for $0 \le \delta \le \delta_{el}$

$\eta = 1$ for $\delta > \delta_{el}$

$\tau_{el} = 3$ MPa

$\delta_{el} = 0.2$ mm

This expression should be considered as indicative. First, the given constants depend on variables such as concrete strength and stiffness, shrinkage and steel roughness. Therefore they shall be estimated by means of experiments in a specific case. Second, the shapes of the experimental bond stress-slip curves are not always similar. For example, lightweight concrete showed stronger adhesion than gravel concrete of the same compressive strength. Furthermore, in lightweight concrete the bond stress dropped after debonding, as illustrated in Fig. 6.3-4 [Den Uijl (1986, 1992c)]. This behaviour may be attributed to the lower elastic modulus and the higher porosity of the lightweight aggregate, which yields more shrinkage and, hence, a stronger initial clamping of the tendon by the concrete.

In case of pretensioned tendons two different bond situations can be distinguished. Along the transmission length the steel stress is reduced at transfer, which causes an increase of the tendon diameter and, hence, contributes to the bond resistance. On the other hand, under flexural loading the steel stress in a cracked section is increased, which results in a reduction of the tendon diameter and a lower bond resistance. This is implicitly recognized in the ACI Building Code (ACI 318-89) and explicitly in MC90 [Den Uijl (1992c)] by considering a lower bond strength beyond the transmission

Copyright fib, all rights reserved. This PDF copy of fib Bulletin 10 is intended for use and/or distribution only by National Member Groups of fib.

length than within the transmission length (see Section 6.7.2). With the bond law according to Eq. (6.3-2) both bond situations are covered.

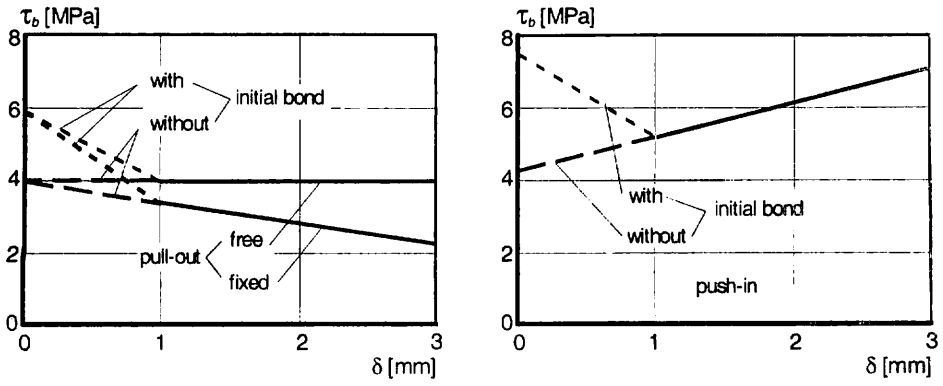

Fig. 6.3-4: Bond stress-slip curves in lightweight concrete [Den Uijl (1986)]

With increasing stress a strand contracts, which reduces its wedge action and thus the bond resistance. Beyond the yield stress the longitudinal strain increases rapidly and so does the strand contraction (Poisson effect). At a certain moment the strand contraction annuls the wedge action caused by steel surface roughness and lack-of-fit, leaving only the pitch effect to provide bond resistance. The strong reduction of the bond strength due to yielding will result in a considerable increase of the development length (USA terminology), as has been discerned by Buckner (1994).

To simulate the influence of yielding on the bond properties of strand the third term in Eq. (6.3-2), which represents the Poisson effect, can be rewritten as a function of strain instead of stress [Den Uijl (1998a)]:

$$\tau_b = 3 + 0.4\delta - 500\Delta\varepsilon_p + 1.5\,10^{-3}|\Delta\sigma_p| \quad \text{[MPa]} \tag{6.3-4}$$

with $\Delta\varepsilon_p$ change in longitudinal steel strain

Eq. (6.3-4) is followed until the sum of the first three terms at the right hand side becomes zero. Then, for negative values of this sum its contribution is neglected and only the term representing the pitch effect is considered. In Fig. 6.3-5 the anchorage capacity calculated with Eq. (6.3-4) is compared with existing codes and a proposal by Buckner (1994), in which the factor λ depends on the steel strain at compression zone failure. With a high reinforcement ratio the steel strain at compression failure is small and, hence, the reduction of the bond stress due to yielding is limited, thus $\lambda \rightarrow 1$. Reversely, a low reinforcement ratio is coupled with a large yielding strain and a considerable bond stress reduction, thus $\lambda \rightarrow 2$.

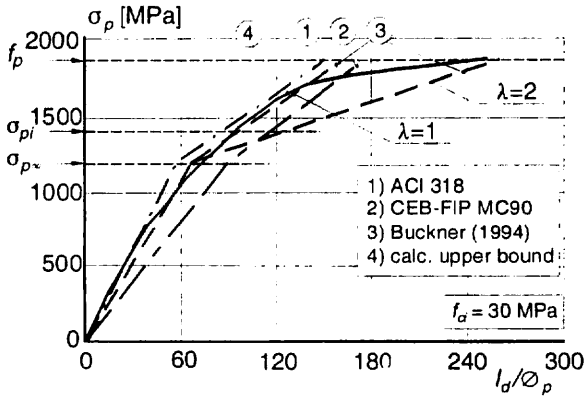

Fig. 6.3-5: Anchorage capacity of strand according to ACI 381, MC90, proposal by Buckner (1994) and calculated with Eq. (6.3-4) [Den Uijl (1998a)]

Copyright fib, all rights reserved. This PDF copy of fib Bulletin 10 is intended for use and/or distribution only by National Member Groups of fib.

6.3.4 Bond stress based on concrete confinement

The force transfer between a tendon and concrete is connected with radially directed compressive stresses, irrespective of the transfer mechanism. These stresses are equilibrated by circumferential tensile stresses that may initiate radial cracks starting at the steel-to-concrete interface. The confining capacity of the concrete, that is the maximum radial compressive stress that can be resisted, determines the bond resistance. To evaluate this confining capacity in case of lightly confined concrete, the concrete around the tendon is often conceived as a partly cracked thick-walled cylinder. Analytical solutions describing the internal pressure as a function of the crack penetration depth have been obtained by assuming a certain distribution of the circumferential stresses over the cracked part of the cylinder wall [Tepfers (1973)], and more recently by taking into account the softening behaviour of concrete loaded in tension. A survey of both analytical and numerical solution methods is given by Noghabai (1995).

In most cases the interest in the response of the thick-walled cylinder is restricted to the maximum value of the internal pressure, which then is connected with the maximum bond stress by assuming the angle between the tendon axis and the resultant of the radial stress and the bond stress. However, to include for example the Poisson contraction (or Hoyer effect) in a bond model based on concrete confinement, the relation between the radial displacement of the interface and the radial stress is required.

The fictitious crack model can be used to find the circumferential tensile stresses in the cracked part of the cylinder wall. Since the fictitious crack model gives the transmitted tensile stress as a function of the crack width, the resulting stress-strain relationship changes with the measuring length. Thus, for each circumferential fibre in the cracked part of the cylinder the stress-strain relation is different.

Weerasekera & Loov (1990) have derived an approximative solution for the stress distribution in the cracked part of the cylinder wall by using the same stress-strain relation for all circumferential fibres. This - hyperbolic - softening curve is described by three constants. It is used to define a stress level dependent elastic modulus, with which the radial and the circumferential stresses are described as a function of the radial and circumferential strain. Then a second order non-linear non-homogeneous differential equation follows from equilibrium in radial direction, which is numerically solved. An iterative solution is used to find the crack penetration depth that yields the required combination of radial displacement and radial compressive stress at the steel-to-concrete interface. Further, they assume that bond consists of dry friction, the coefficient of friction being the fourth constant, and that the thick-walled cylinder is only loaded by expansion of the tendon. With this model bond stresses and steel stresses along the transmission length are found using the finite difference method.

Den Uijl & Bigaj (1996) also used a thick-walled cylinder model to describe the bond behaviour of ribbed bars taking into account the wedge action of the ribs and the Poisson contraction, thus including the effect of bar yielding on bond. Concrete softening was simulated with the fictitious crack model using a bi-linear softening law. This - analytical - confinement model defines the radial stress at the interface as a function of the radial displacement of the interface. The bond stress follows from the radial stress under the assumption of dry friction in the sliding plane between bar and concrete.

Den Uijl (1998b) followed a similar approach to model bond of strand. Referring to the empirical relation given in Section 6.3.3, the radial displacement of the steel-to-concrete interface was taken as a function of both the Poisson effect and the wedge effect caused by the irregular shape of the strand and the pitch effect; see also Section 6.2.2.

With this model the influence on bond of concrete properties and detailing characteristics such as concrete cover and strand spacing can be investigated. An example of which is shown in Fig. 6.3-6, where the bond stress along the transmission length is given as a function of concrete cover and concrete strength. It is remarked that the drop in bond stress at the end of the transmission length reflects the adhesion strength that is taken into account in Eq. (6.3-2).

The confinement model was also used to explain the differences between NSC and HSC with regard to bond strength and bond splitting of strand [Den Uijl, 1996b], see Section 6.4.2.

Copyright fib, all rights reserved. This PDF copy of fib Bulletin 10 is intended for use and/or distribution only by National Member Groups of fib.

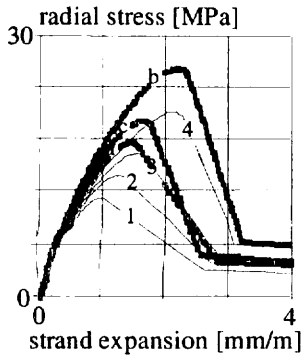

#	$c/\varnothing_p$	f_{cc} MPa	f_{ct} MPa	G_f N/m	l_{ch} mm	$l_t/\varnothing_p$
1	2.0	40	3.01	117	324	65
2	2.5	40	3.01	117	324	55
3	3.0	40	3.01	117	324	48
4	4.0	40	3.01	117	324	43
a	2.5	65	3.94	138	261	46
b	2.5	65	5.10	179	201	37
c	2.5	65	4.70	132	175	42

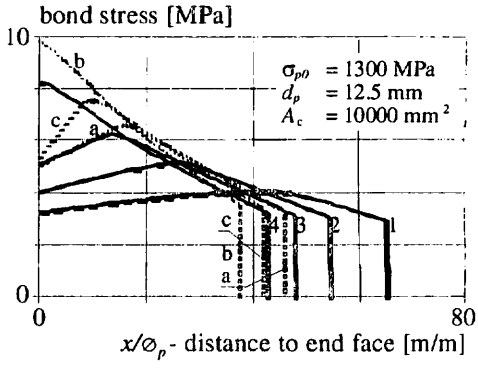

Fig. 6.3-6: Concrete confinement (left) and bond stress along transmission length (right) as a function of concrete cover and concrete quality [Den Uijl (1998b)]

6.3.5 Coefficient of friction versus slip

To describe the bond stress distribution along the transmission length, Van de Vondel & Kamoen (1992) and Bogaerts & Brosens (1995) assume the existence of a unique relationship between the coefficient of friction and the slip. This relation is supposed to be only influenced by the concrete quality and not by the geometry of the cross-section. It is found with the help of push-in tests, that give the bond stress as a function of slip and steel stress change. With these data the relation between the slip and the radial compressive stress at the interface is calculated, considering the response of the thick-walled concrete cylinder around the tendon to the radial displacement of the interface. This displacement follows from the change of the steel stress and the transverse deformation of the tendon caused by the radial compressive stress at the interface. Finally, the coefficient of friction follows from the ratio between the bond stress and the radial compressive stress.

The response of the thick-walled cylinder to the interface displacement was evaluated in various ways. First, Van de Vondel & Kamoen (1992) assumed the behaviour of concrete loaded in tension to be elasto-plastic, which overestimates the confining action of the concrete. Later Bogaerts & Brosens (1995) applied Van der Veen's (1990) approach to estimate the response of the partly cracked thick-walled cylinder, which uses the fictitious crack model to describe the softening behaviour of the cracked part.

In Fig. 6.3-7 the average coefficient of friction versus slip curve obtained from a push-in test with short embedment length is shown. A clear tendency can be observed. The highest coefficient of friction is found at debonding. With increasing slip it decreases until a constant value is reached after

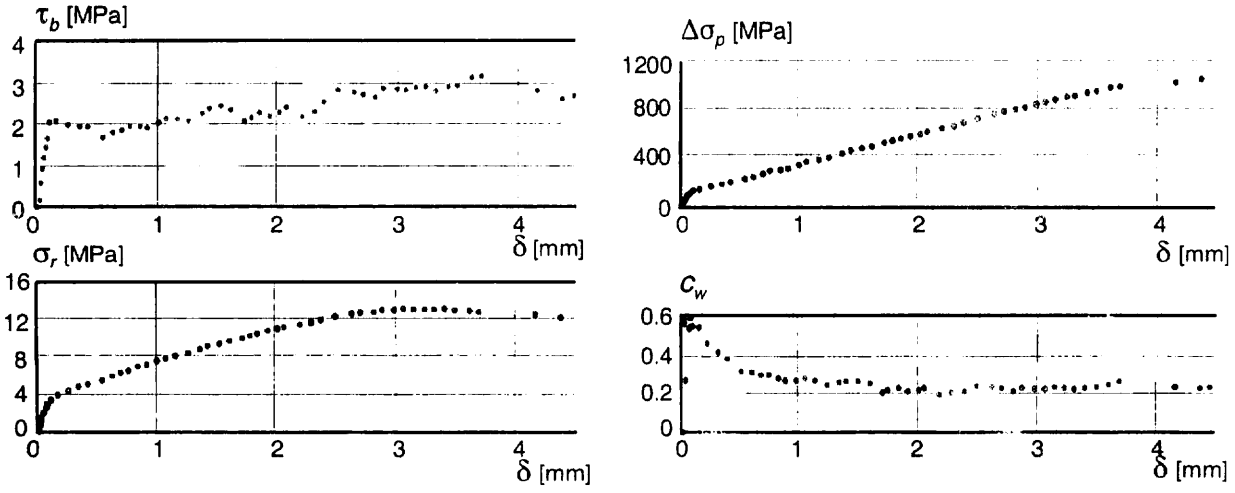

Fig. 6.3-7: Coefficient of friction (c_w) versus slip for seven-wire strand from push-in test results and assumed confinement relation [Bogaerts & Brosens (1995)]

Copyright fib, all rights reserved. This PDF copy of fib Bulletin 10 is intended for use and/or distribution only by National Member Groups of fib.

about 1 mm slip.

It is noticed that Bogaerts & Brosens put the radial displacement of the steel-to-concrete interface equal to the radial displacement of the interface between the cracked and uncracked parts of the thick-walled cylinder, thus neglecting the radial deformation of the cracked part. The resulting overestimation of the stiffness of the cylinder response increases with the penetration depth of the radial cracks.

As in the approach by Weerasekera & Loov (1990), mentioned in Section 6.3.4, here the displacement of the steel-to-concrete interface is only based on expansion of the tendon connected to the decrease of the longitudinal stress. Other phenomena such as wedge action of the strand and wear of the sliding plane are neglected. This limits the applicability of both methods to push-in bond situations.

6.3.6 Interface model for bond of strand

With the aim to analyse the anchorage zone of a pretensioned member at prestress transfer taking into account non-linear material behaviour, Åkesson (1993) developed a three-dimensional interface model that simulates the bond behaviour of prestressing strand. The model is based on friction and takes also into account adhesion. It defines the shear stress parallel to the tendon axis and the normal stress perpendicular to the steel-to-concrete interface. The other stress components are fixed at zero. An elastic-plastic material model is assumed that includes a Coulomb line as yield criterion, a non-associative flow rule (yielding due to shear deformation only affects the shear stress) and a linear softening behaviour for the shear component delivered by adhesion (as a function of the plastic shear strain). After the adhesion strength has been reduced to zero, the plastic shear strain is interpreted as slip. An important feature of the element is that for fixed boundary conditions shear deformation generates a normal stress according to a so-called expansion curve, see Fig. 6.3-8. This represents the wedge action of a strand and the subsequent wear of the sliding plane.

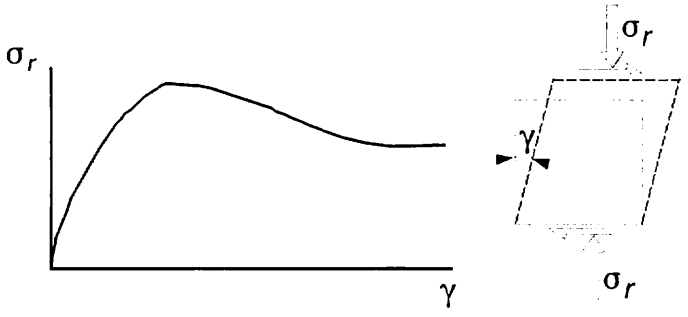

Fig. 6.3-8: Radial compressive stress at interface as a function of shear displacement of slip layer [Åkesson (1993)]

The interface model has been implemented in ABACUS, a non-linear finite element code, and it has been calibrated against pull-out test results ($\varnothing_p$=3 mm, f_{cc}=55.4 MPa, l_b=30 and 400 mm, c=93 mm) and transmission length tests ($\varnothing_p$=12.8 mm, f_{cc}=48 and 62 MPa, σ_{pi}=1200 MPa). With this numerical tool various experiments have been simulated and hollow core slab ribs have been analysed for prestress transfer.

The simulation of pull-out and push-in tests, that were reported by Den Uijl (1992b), shows a reasonable agreement for the pull-out tests with free non-loaded end and the push-in tests, but the agreement for the pull-out tests with fixed non-loaded end, for which the model was not intended, is less good; see Fig. 6.3-9.

Copyright fib, all rights reserved. This PDF copy of fib Bulletin 10 is intended for use and/or distribution only by National Member Groups of fib.

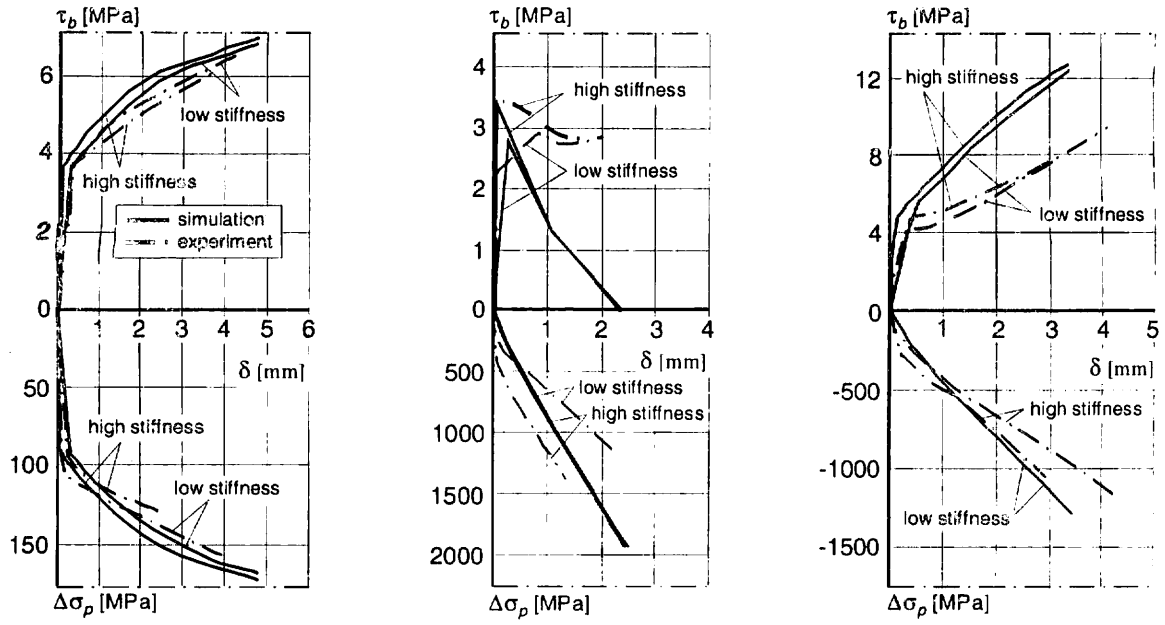

Fig. 6.3-9: Simulation with interface model of pull-out test with non-loaded end free (left), pull-out test with non-loaded end fixed (middle) and push-in test (right) (stiffness refers to test set-up) [Åkesson, (1993)]

6.3.7 Basic bond tests

This section deals with some experimental aspects in connection with the above-mentioned bond models. Therefore only test set-ups are discussed from which basic bond properties are found. Experiments meant to estimate the transmission length and the anchorage capacity are treated in the sections pertinent to the matter in question.

Pull-out test with short embedment length

To study the bond characteristics of reinforcing tendons pull-out tests with short embedment length are often used. The idea behind this set-up is that bond stresses are not uniformly distributed along the embedment length. As a result the difference between the maximum and the average value of the bond stress increases with the bonded length. Hence, to obtain the presumed unique bond stress-slip relation, the embedment length shall be as short as possible. For reasons such as scatter of results due to inhomogenity of concrete and rib spacing, a practical length of three to five times the tendon diameter is often used. Stocker & Sozen (1969) have shown that in case of seven-wire strand the average value of the bond stress increases with the embedment length until a maximum value is reached. To their opinion this is due to the lack-of-fit effect (Section 6.2.2), which is connected to irregularities in both the cross-sectional and longitudinal shape of a strand. Hence, a certain length is required to develop this effect. Den Uijl (1978) found a maximum average bond stress for an embedment length of three times the strand diameter. Laldji & Young (1988) reported about pull-out tests with 2, 4 and 6 strand diameters embedment length. Adhesion was highest with the shortest embedment length, the highest bond stress after debonding was found for $4\varnothing_p$ embedment length.

It is recognized that the pull-out test with short embedment length is useful in comparative studies, when bond is dominated by pull-out rather than by splitting, but the bond strength found with it is of limited value because the boundary conditions in the specimen have a poor resemblance with those in practical bond situations. However, by modifying the set-up some of the real boundary conditions can be taken into consideration as well.

Copyright fib, all rights reserved. This PDF copy of fib Bulletin 10 is intended for use and/or distribution only by National Member Groups of fib.

Push-in versus pull-out

The importance of the transverse expansion of the tendon for the development of the radial compressive stress at the interface and, hence, the frictional resistance has been discerned since the early development of pretensioning (Hoyer effect). This influence is implicitly studied by estimating either the transmission length or the anchorage length, which are governed by the push-in and the pull-out bond situation, respectively. The influence of strand expansion can also be studied more explicitly by means of a so-called push-in test; see Fig. 6.3-10 [Keuning et al. (1962)]. In this test the strand is pretensioned first between A and B and then the concrete is cast. After hardening the prestressing force is gradually released at A, causing a movement of the strand into the direction of B. Since the concrete is supported at C, this strand movement generates bond stresses between concrete and strand (the designation "push-in" refers to the fact that a similar loading condition can be created by applying a compressive force at A).

Guyon (1968) referred to the push-in experiments by Keuning et al. (1962) without making a comparison with the results of pull-out tests. According to Stocker & Sozen (1969) the differences observed by Keuning at all between both types of tests were small. Moreover, Stocker & Sozen found good agreement between the transmission length that was observed in experiments and calculated on the basis of pull-out tests with $2.3\varnothing_p$ embedment length. Therefore they believed that in case of plain seven-wire strand the contribution of the transverse deformations to the bond resistance is small compared to the wedge action caused by the lack-of-fit effect. It is remarked that the maximum steel stress reached in the pull-out tests was about 100 MPa.

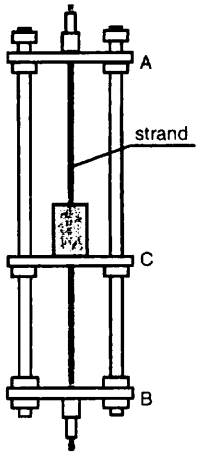

Fig. 6.3-10: Principles of push-in test [Keuning et al. (1962)]

Den Uijl (1992b) came to the opposite conclusion after evaluation of pull-out and push-in tests with short ($5.4\varnothing_p$ and $9.5\varnothing_p$) embedment length, in which the maximum steel stress change amounted to more than 1200 MPa. To obtain this value in a pull-out test with short embedment length, the non-loaded end of the strand was anchored as well. The influence of transverse deformation on the bond resistance of strand is clearly shown in Fig. 6.3-3, where the bond stress is given as a function of the slip and the steel stress change.

Abrishami & Mitchell (1993) followed a similar approach using specimens with 300 mm embedment length to estimate the bond characteristics of pretensioned strand under the two distinct bond situations. They also found a clear difference between the bond stress-slip curves in pull-out and push-in tests. However, their results for the push-in bond situations that are depicted in Fig. 6.3-11 for 13 mm strand, considerably differ from those reported by Den Uijl (1992b); see Fig. 6.3-3. In the latter case the bond stress continuously increased with slip, whereas the present results show a steep drop of the bond stress after having reached the peak value. This peak value coincides with the slip initiation at the bottom side of the concrete cylinder. For this phenomenon no explanation was given, but it might be attributed to a strong drop of the bond stress at breaking of the adhesion bond. Such a drop was also observed in similar tests with lightweight concrete, see Fig. 6.3-4 [Den Uijl (1986)]. Another reason might be bursting of the concrete, but this is not very likely because of the 150 mm diameter of the concrete cylinder.

Copyright fib, all rights reserved. This PDF copy of fib Bulletin 10 is intended for use and/or distribution only by National Member Groups of fib.

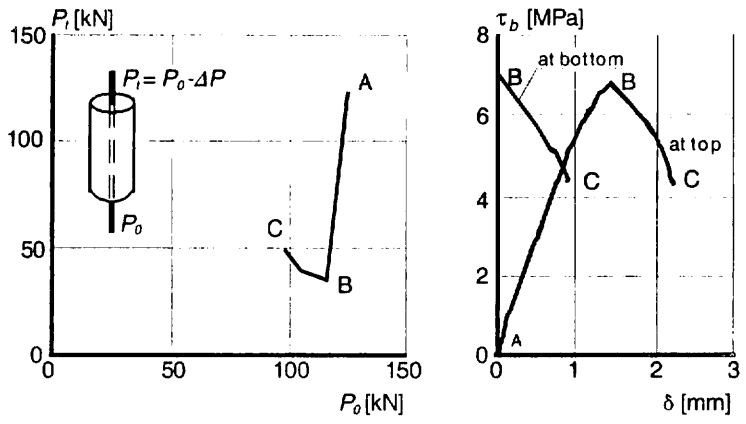

Fig. 6.3-11: Results of push-in tests: force at top and bottom (left) and bond stress versus slip at top and bottom (right) [Abrishami et al. (1993)]

It is noticed that the relatively long bonded length in these tests is coupled with a strong variation of the slip, the local steel stress change and probably also the local bond stress along the embedment length. Therefore the reported results can not be directly converted into a relation that gives the bond stress as a function of the slip and the local steel stress change.

Leskelä (1990) suggested a push-out test for quality control in hollow-core slab production. The specimen is taken from a slice sawn from the slab and the strand is loaded as shown in Fig. 6.3-12. Variation of the embedment length, which corresponds to the slice width, between 50 and 110 mm ($\varnothing_p$ =9.3 mm) yielded similar results. Therefore and to prevent yielding of the indenter, an embedment length smaller than or equal to 70 mm was recommended. It was noted that sufficient cover is required to prevent splitting cracks.

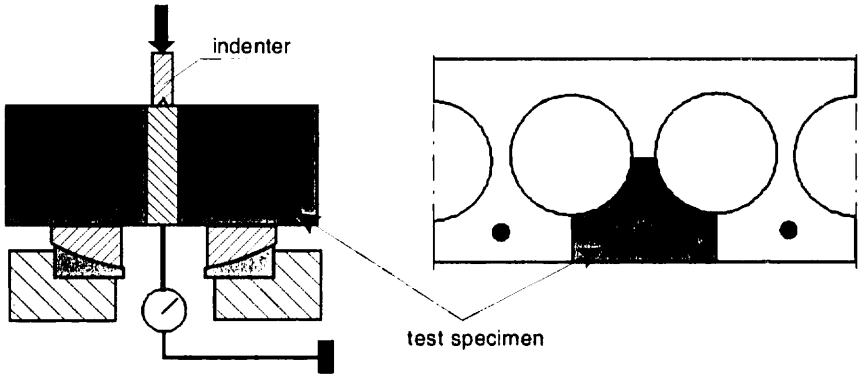

Fig. 6.3-12: Push-in test for quality control of hollow core slabs [Leskelä (1990)]

Copyright fib, all rights reserved. This PDF copy of fib Bulletin 10 is intended for use and/or distribution only by National Member Groups of fib.

6.4 Prestress transfer and anchorage of plain seven-wire strand

Although plain seven-wire strand is the most widespread prestressing tendon, other types are also used, such as wire and strand with ribs or indents. Besides, epoxy coated strand is gaining attention as well as non-metallic prestressing tendons. In this chapter recent developments concerning prestress transfer and anchorage capacity of plain seven-wire strand are discussed. Developments related to other types of tendons are treated in subsequent chapters.

6.4.1 Influence of concrete strength

Early studies into the influence of concrete strength on bond resistance of strand resulted in contradictory conclusions. Stocker & Sozen (1969) found other factors, such as shrinkage, having a stronger effect on bond resistance than concrete strength, especially for small slip values. On the other hand, Zia et al. (1977) derived from published data connected to a concrete strength between 14 and 56 MPa for the average transmission length after gradual prestress transfer:

$$l_t = 1.3 \frac{\sigma_{pi}}{f_{ci}} \varnothing_p - 58 \quad \text{[mm]} \tag{6.4-1}$$

Oleśniewicz (1975) found from a statistical evaluation of field measurements and laboratory tests with 20 to 50 MPa cube strength at transfer a less pronounced influence of the concrete strength at gradual prestress transfer:

$$l_t = \psi \varnothing_p \sqrt{\frac{\sigma_{pi}}{f_{cci}}} \tag{6.4-2}$$

with $\psi = 7$, 10 and 13 for the characteristic lower bound, the average and the characteristic upper bound value, respectively.

The same relation between cube strength and bond strength was reported by Laldji et al. (1988), who tested bond of strand in mortar with 40, 46 and 57 MPa cube strength.

More recently, Mitchell et al. (1993) investigated 22 rectangular beams eccentrically pretensioned with one strand. Variables were strand diameter (slightly rusted 9.5 mm, smooth 12.7 and 15.7 mm) and concrete strength (at prestress transfer $f_{ci} = 21$ to 50 MPa, at bending test $f_c = 31$ to 89 MPa). Three different concrete mixes were used, two of which with a high content of cement blended with 7% silica fume, superplasticizer and a low water-cement ratio. The distance from the centre of the strand to the bottom fibre was always 50 mm, thus $c/\varnothing_p \geq 2.63$. The strands were provided with 200 mm spaced strain gauges.

The concrete strength at transfer (gradual release) was found to have a clear influence on the transmission length, similar to that suggested by Oleśniewizc. The average of the experimental values could reasonably be described with:

$$l_t = \frac{\sigma_{pi} \varnothing_p}{21} \sqrt{\frac{20}{f_{ci}}} \tag{6.4-3}$$

The anchorage capacity was determined by a three- or four-point-bending test, thus varying the distance from the load point to the nearest beam end. Only when considerable slip preceded flexural crushing or shear failure, the failure mode was classified as bond failure. From the strand strain measurements yielding of the steel was clearly observed; Fig. 6.4-1. Den Uijl (1998a) could simulate this behaviour with the help of Eq. (6.3-4).

A conservative description of the observed anchorage lengths was given by:

Copyright fib, all rights reserved. This PDF copy of fib Bulletin 10 is intended for use and/or distribution only by National Member Groups of fib.

$$l_b = \frac{\sigma_{pi} \varnothing_p}{21} \sqrt{\frac{20}{f_{ci}}} + \frac{f_{pd} - \sigma_{p\infty}}{7} \sqrt{\frac{30}{f_c}} \tag{6.4-4}$$

This expression consists of a part that represents the transmission length calculated with the concrete strength and steel stress at prestress transfer and a part that counts for the contribution of the bonded length beyond the transmission length. For the latter the design values of the concrete strength and the steel stress, including all losses, are considered.

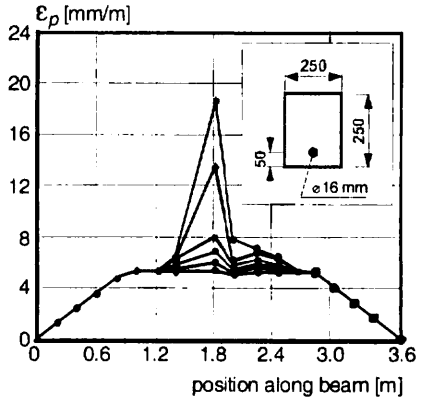

Fig. 6.4-1: Steel strain along beam during bending test at yielding of strand [Mitchell et al. (1993)]

Cousins et al. (1994a) tested 12 T-shaped beams pretensioned with nine 12.7 mm diameter strands, Fig. 6.4-2. The principal goal was to investigate the influence of strand spacing (centre-to-centre spacing $s_{ctc}/\varnothing_p = 3.5$ and 4, see Section 6.4.2), but also two concrete mixes were applied (NSC: $f_{ci} = 37$ MPa, $f_c = 44$-55 MPa and HSC: $f_{ci} = 55$ MPa, $f_c = 69$-80 MPa). Steel stress before and after transfer was 1490 and 1397 MPa, respectively. Prestress transfer was effectuated by subsequent flame cutting of the strands. Concrete strain measurements were used to estimate the transmission length. The anchorage length was determined in three-point-bending tests, the embedment length varying between 2400 and 4500 mm.

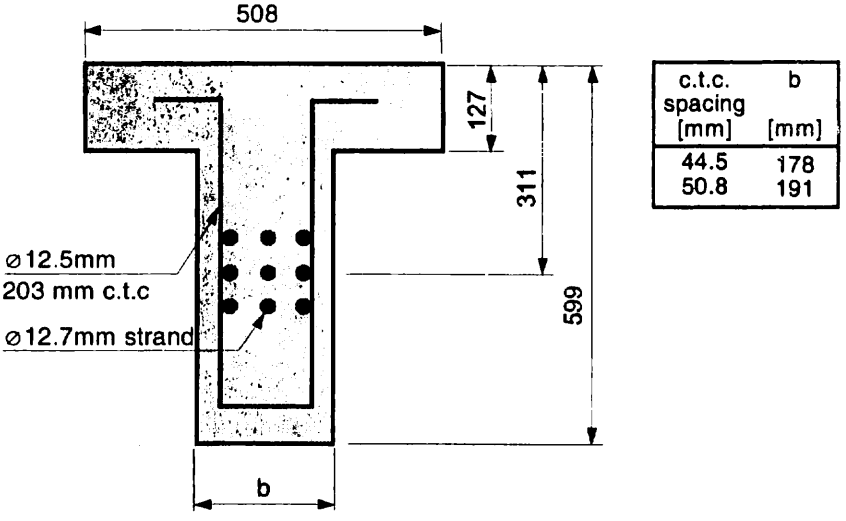

Fig. 6.4-2: Cross-section tested beams [Cousins et al. (1994a)]

The transmission length measurements showed considerable scatter, as illustrated by the ratio between the maximum and minimum value of the transmission length observed under similar conditions. For HSC and $s_{ctc}/\varnothing_p = 4$ this ratio amounted to 1.6.

Copyright fib, all rights reserved. This PDF copy of fib Bulletin 10 is intended for use and/or distribution only by National Member Groups of fib.

No influence of spacing on the transmission length was found. The average transmission length amounted to 1422 and 944 mm for NSC and HSC, respectively ($l_t/\varnothing_p$ = 112 and 74). Compared to the ACI-recommendations, the transmission lengths in NSC were 1.7 times longer, for which no explanation was given. One reason might be the position of the strands. Since this was more than 200 mm above the bottom side of the cross-section, bond strength might have been reduced due to sedimentation with a factor of 0.7 according to MC90.

The ratio between the average transmission length in NSC and HSC was 1.5. Thus also HSC presented a somewhat greater transmission length than predicted by ACI, which does not take into account the concrete strength. The ratio between the two compressive strengths amounted to 1.49, which indicates that the transmission length was inversely proportional to the concrete compressive strength.

The anchorage capacity was tested on 18 beam ends. Only in four cases a clear bond failure was observed (NSC, $l_b/\varnothing_p$ = 192 and 228). All other tests failed in flexure, which was sometimes connected to some slip. When this occurred, the strands in the top row showed more slip than the others. The smallest embedment length in HSC amounted to $216\varnothing_p$. Since this did not result in bond failure it was concluded that bond in HSC was better than in NSC. No differences were found between the failure behaviour of tests with similar concrete and embedment length and different strand spacing.

Den Uijl (1995a) used test results of Vossen (1994) to evaluate the influence of concrete strength at release on the transmission length. As a basis for comparison eq. (6.4-2) was used, considering the ψ-value as the transmission length normalized for concrete strength and steel stress just after release. From Fig. 6.4-3 it can be learned, however, that a stronger influence of the concrete strength should be taken into account to obtain a constant ψ-value. For Vossen's tests this would have required $f_{cc}^{0.8}$ instead of $f_{cc}^{0.5}$ in the denominator of Eq. (6.4-2), which lays between the findings of Oleśniewicz (1975) and Mitchell et al. (1993) on the one side and those of Zia et al. (1977) and Cousins et al. (1994) on the other side.

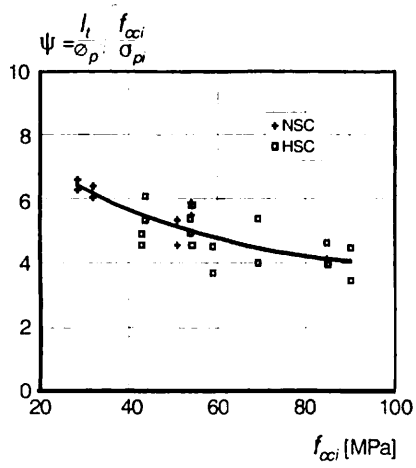

Fig. 6.4-3: Influence of concrete strength at transfer on transmission length derived from Vossen (1994)

The anchorage capacity in HSC was measured on eight beams pretensioned with three 12.5 mm diameter strands according to two patterns, see Fig. 6.4-4 [Den Uijl (1995d, 1996)]. Besides crushed gravel limestone was used as coarse aggregate. The cube strength at prestress transfer and at testing was 65 and 110 MPa, respectively. Compared to gravel concrete, limestone concrete was more susceptible to bond cracking and yielded longer transmission lengths; see Fig. 6.4-8. Fig. 6.4-5 gives the maximum steel stress at the loading point normalized to the effective prestress as a function of the effective embedment length normalized to the transmission length. The effective embedment length is defined as the distance from the end of the member to the loading point minus the distance from the loading point to the inclined bending crack that is closest to the loading point. This effective embedment length was marked by a bond splitting crack in the bottom cover. The solid line in Fig. 6.4-5 indicates the theoretical anchorage capacity assuming that:

- within the transmission length the anchorage capacity corresponds to the effective prestress;

Copyright fib, all rights reserved. This PDF copy of fib Bulletin 10 is intended for use and/or distribution only by National Member Groups of fib.

- beyond the transmission length the bond strength is half the value present within the transmission length.

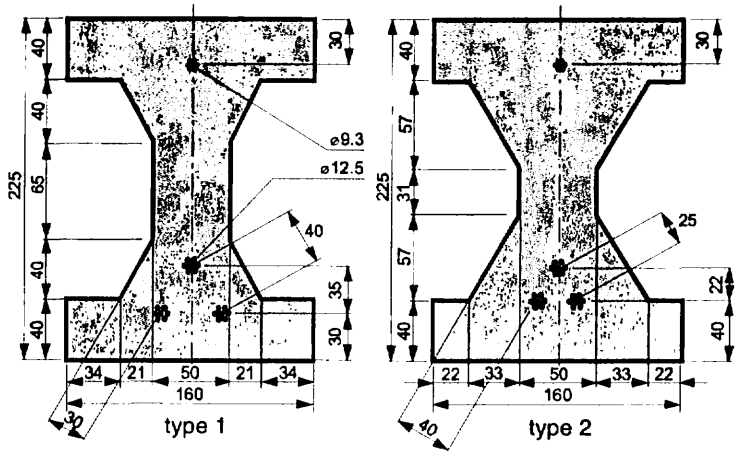

Fig. 6.4-4: Cross-sections of tested beams; at one end I-shaped, at other end rectangular [Den Uijl (1996a)]

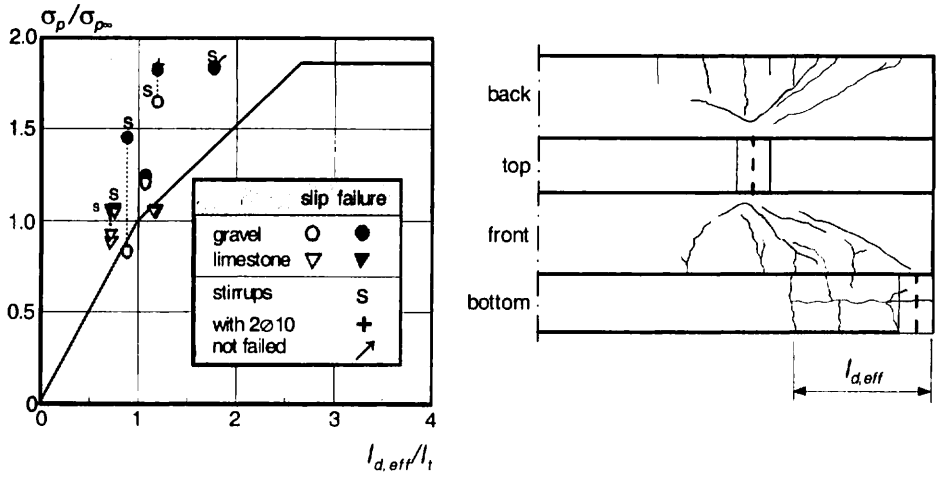

Fig. 6.4-5: Anchorage capacity measured at rectangular end of beams [Den Uijl (1996a)]

In a review of recent test results on transfer and anchorage length Buckner, (1994) discussed the influence of concrete strength at prestress transfer on transmission length. Whereas the correlation between transmission length and concrete strength was poor, he found a reasonable correlation between the transmission length and the apparent elastic modulus, see Fig. 6.4-6, which he derived from the concrete strain measurements in the region with a constant strain level:

$$l_t = \frac{1250\,\sigma_{pi}}{E_c}\,\varnothing_p \tag{6.4-5}$$

Often the elastic modulus of hardened concrete is considered to be proportional to the square root of the compressive strength. Assuming that the same proportionality holds for hardening concrete, it can be concluded that the transmission length is inversely proportional to the square root of the compressive strength. This agrees with the findings of Oleśniewicz (1975), Laldji & Young (1988) and Mitchell et al. (1993).

Copyright fib, all rights reserved. This PDF copy of fib Bulletin 10 is intended for use and/or distribution only by National Member Groups of fib.

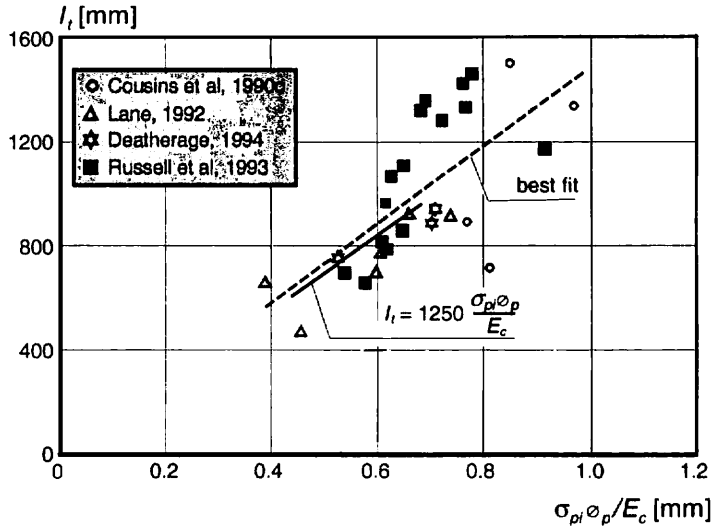

Fig. 6.4-6: Transmission length as a function of apparent elastic modulus [Buckner (1994)]

6.4.2 Influence of concrete cover and spacing

In the test programme conducted by Deatherage & Burdette (1994) on full-scale bridge girders, clear strand spacing of 3 and 2.5 times the strand diameter did not yield different results as far as transmission length and anchorage capacity were concerned. Four strand diameters were used (13, 13.3, 14 and 15 mm) in different patterns, see Fig. 6.4-7. The beam ends were provided with shear and confinement reinforcement. Cylinder strength at release amounted to 23 to 38 MPa and at the three-point-bending test it was 35 to 54 MPa. Steel stress before release measured 1400 MPa. In one series of eight beams 13 mm diameter strand from four suppliers was used without showing systematic differences in bond resistance.

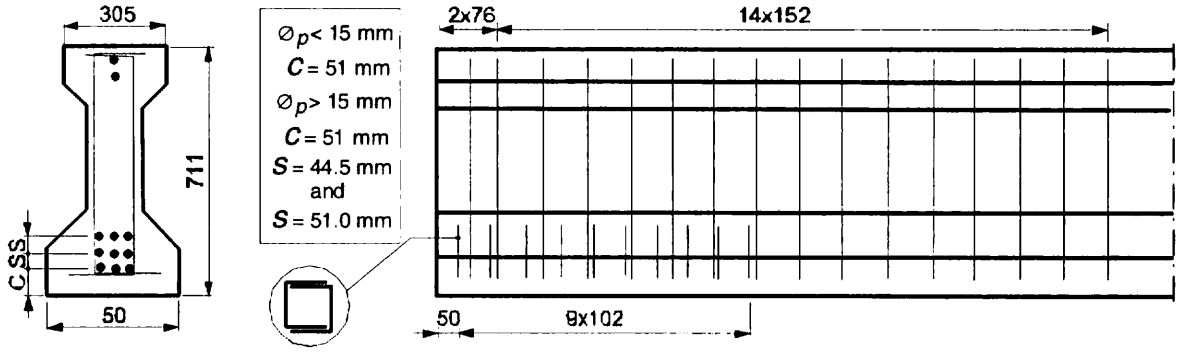

Fig. 6.4-7: Cross-section and transverse reinforcement of tested beams [Deatherage et al. (1994)]

Cousins et al. (1994) carried out a similar experimental study to verify the ACI-requirement concerning strand spacing, the details of which have been given in Section 6.4.1. They concluded that a reduction of the clear spacing from 3 to 2.5 times the strand diameter did not affect the transmission length nor the anchorage length.

Den Uijl investigated the transmission length (1995a, 1995c) in HSC. A principle goal was to estimate the cover required to prevent bond splitting. The transmission length was measured on 13 rectangular prisms, which contained one or two 9.3 mm or 12.5 mm diameter strands. The concrete mix contained gravel, silica fume and plasticizer and had a low water-cement ratio. Prestress was transferred after 12 and 19 hours at 40 and 70 MPa cube strength, respectively (f_{ct}=4.1 and 5.2 MPa). Clear cover and clear spacing were varied as follows: $c/\varnothing_p$=1.36 to 3.0, $s/\varnothing_p$=0.40 and 1.23. For comparison of various cover and spacing combinations, an effective cover is defined assuming that the concrete between the tendons can resist more effectively the circumferential tensile stresses than the concrete in the cover. To that end an effectiveness factor of 1.5 had arbitrarily been chosen.

Copyright fib, all rights reserved. This PDF copy of fib Bulletin 10 is intended for use and/or distribution only by National Member Groups of fib.

Fig. 6.4-8 shows the observed reduction of the relative transmission length as the effective cover increases. This influence is explained by the non-linear response of the concrete to the wedge effect of the strand, see also Section 6.3.7. A larger cover is connected to a more linear response and beyond $c_{eff}/\varnothing_p = 3$ to 4 no further reduction of the transmission length is to be expected.

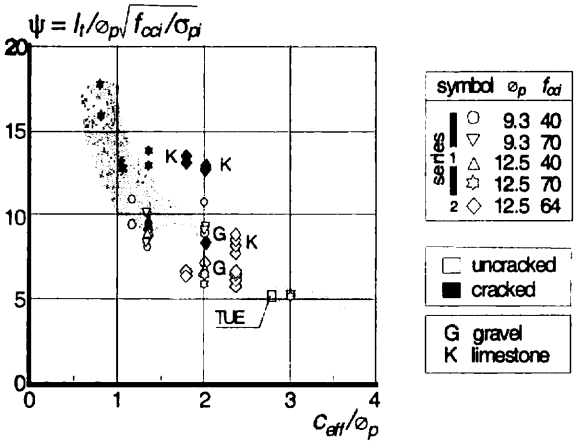

Fig. 6.4-8: Relative transmission length as a function of effective concrete cover [Den Uijl (1995c)]; TUE refers to average of experiments carried out by Vossen (1994)

The occurrence of bond splitting cracks as a function of cover and spacing is shown in Fig. 6.4-9. HSC was clearly less sensible to bond splitting than NSC. This was explained from the fact that, compared to NSC, in HSC the tensile strength is raised more than the elastic modulus, which results in a higher strain at reaching the concrete tensile strength. Hence, the radial interface displacement at which the cover cracks is greater in HSC than in NSC. In the case of HSC more pronounced bond splitting cracks were observed when the concrete strength at prestress transfer was higher. This was ascribed to the increased brittleness of the stronger concrete.

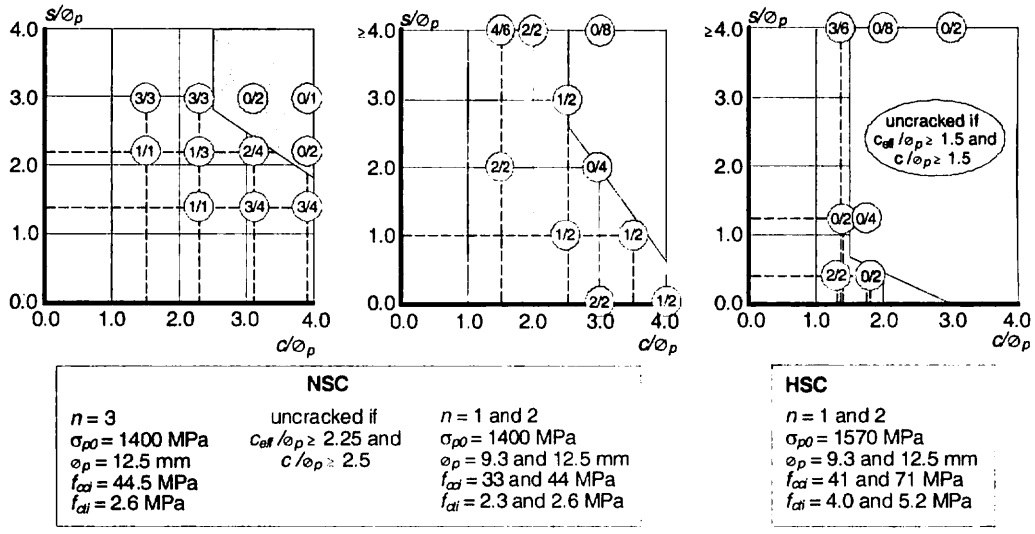

Fig. 6.4-9: Occurrence of bond splitting cracks in NSC and HSC as a function of strand spacing and concrete cover [Den Uijl (1995a and 1996a)] (i/j means i out of j tests showed bond splitting cracks)

Russell & Burns (1996) investigated the transmission length of 12.7 and 15.2 mm diameter strand in single and multi-strand specimens. The clear cover measured 63.5-0.5$\varnothing_p$ mm and the centre-to-centre spacing was 50.8 or 63.5 mm. This resulted for 12.7 mm diameter strand in $c/\varnothing_p = 4.5$ and $s/\varnothing_p = 3.0$ and 3.5 and for 15.2 mm strand in $c/\varnothing_p = 3.7$ and $s/\varnothing_p = 2.3$ and 2.75. The steel stress before release amounted to 1396 MPa and the cylinder strength at release varied between 26 and 38 MPa. Some specimens were provided with confining transverse reinforcement. It was concluded that a

Copyright fib, all rights reserved. This PDF copy of fib Bulletin 10 is intended for use and/or distribution only by National Member Groups of fib.

centre-to-centre spacing of 50.8 mm was sufficient to fulfill the requirements with respect to transmission length also in the case of 15.2 mm diameter strand. Confinement reinforcement had no systematic influence on the transmission length.

6.4.3 Influence of strand geometry and surface condition

The prime geometrical parameter of a strand is the diameter. Under the assumption of a uniform bond stress along the transmission length and a bond stress magnitude independent of the strand diameter, the transmission length is proportional to the strand diameter. Russell & Burns (1996), however, found the transmission length to be proportional to the strand diameter raised to the power 1.68. In their tests the effective cover for the 15.2 mm diameter strands was $c_{eff}/\varnothing_p$=2.71 and 2.88, which was clearly smaller than for the 12.7 mm diameter strand for which held $c_{eff}/\varnothing_p$=3.37 and 3.56. This difference may partly explain the longer transmission length observed; see also Fig. 6.4-8.

The frictional bond resistance of seven-wire strand is thought to be enhanced by geometrical properties that contribute to the wedge effect and by the pitch effect; see Section 6.2.2. The geometrical characteristics involved are the ratio between the diameter of the outer wires $\varnothing_e$ and the diameter of the centre wire $\varnothing_i$ and the pitch p with which the outer wires are laid around the centre wire. According to NEN 3868 (Dutch code for prestressing steel) the diameter ratio $\varnothing_i/\varnothing_e$ should be between 1.02 and 1.05 and the pitch p should lay between $12\varnothing_p$ and $18\varnothing_p$. Den Uijl (1995a, 1996b) found a higher bond strength value for 12.5 mm diameter strand than for 9.3 mm diameter strand, which might be caused by the observed differences in geometry:

$\varnothing$9.3	- $\varnothing_i/\varnothing_e$	= 1.026
	- $p/\varnothing_p$	= 19.0
$\varnothing$12.5	- $\varnothing_i/\varnothing_e$	= 1.037
	- $p/\varnothing_p$	= 16.8

Transmission length tests on 9.3 mm diameter strand with 130, 140 and 160 mm pitch did not show a systematical influence of the pitch on bond strength. This might be ascribed to the fact that also variations were observed in the diameter ratio (1.03 to 1.04) and surface roughness (R_a=0.13 to 0.40 μm) [Den Uijl (1987)].

Deatherage et al. (1994) investigated the influence of weathering on the transmission length and the anchorage length of seven-wire strand. To that end beams were made without weathering the strands and after 1 and 3 days of weathering. The weathered strands did not show visible rust, but the microscopical roughness was reported to be increased. The transmission length was reduced with 30 and 40% after weathering for one and three days, respectively. This result was ascribed to the effect of weathering on the residual surface lubricants, which would have resulted in an increase of both adhesion and coefficient of friction.

6.4.4 Influence of time on transmission length

Bond of prestressing tendons is strongly dependent on the confinement by the surrounding concrete, which is activated as a consequence of radial displacement of the interface. The high local stresses and strains involved will be reduced due to creep and relaxation and may result in transmission length increase. On the other hand, prestress is mostly transferred when the concrete strength has not yet obtained its design value. Thus, strength increase and possible self-healing of initially originated cracks may counteract the above effect. Besides, the coefficient of friction is supposed to be higher for standing friction than for sliding friction. This explains why, in general, some increase of the transmission length is observed only during the first days after prestress transfer. However, some studies seem to show diverging results in this respect.

Tassi et al. (1984) reported an increase of transmission length of 10 to 25% within 7 to 14 days after prestress transfer in beams with one 12.5 mm diameter strand (σ_{pi}=1290 MPa). The smallest increase was observed for beams with transverse reinforcement, whereas beams without transverse reinforcement yielded the largest increase. It should be noted, however, that the clear concrete cover amounted to $2.7\varnothing_p$ and that prestress transfer was effectuated when the concrete had reached its design strength (f'_{cc}=40-54 MPa). The relatively small cover probably involved substantial radial

Copyright fib, all rights reserved. This PDF copy of fib Bulletin 10 is intended for use and/or distribution only by National Member Groups of fib.

cracking, on the one hand, see Section 6.4.2, whereas the late prestress transfer did not allow for compensation due to further hydration.

In a comparative bond study of uncoated strand and epoxy coated grit impregnated strand Dorsten et al. (1984), see Section 6.6.1, found an initial transmission length of $54\varnothing_p$ for uncoated and $63\varnothing_p$ for coated strand, which in 14 months increased with 20 and 3%, respectively.

Cousins et al. (1990a) also compared bond of uncoated and epoxy coated strand, see Section 6.6.1. They found after one year the transmission length to be increased with 5% and up to 16% for uncoated strand and epoxy coated grit impregnated strand, respectively. The time-dependent increase of epoxy coated strand was smaller as the grit density was increased.

Lane (1992) described the transmission length changes observed after one year in concentrically pretensioned members with 1 or 4 strands (9.5, 12.7 and 15.2 mm diameter, f_{ci}=29.8 MPa, f_c=40.7 MPa, $\sigma_{pi}=0.75f_p$, $\sigma_{ci}=0.6f_{ci}$, $c/\varnothing_p \geq 4.8$, $s_{ch}/\varnothing_p \geq 4.0$). Both uncoated and epoxy coated grit impregnated strands were applied. Prestress transfer was effectuated by means of flame cutting. The results were not unambiguous: both increase and decrease of the transmission length was observed. The average final transmission length for the three strand diameters amounted to $70\varnothing_p$, $>90\varnothing_p$, $43\varnothing_p$ and $51\varnothing_p$ for one uncoated, four uncoated, one coated and four coated strands, respectively.

6.4.5 Influence of initial steel stress

By assuming a uniform bond stress distribution along the transmission length and neglecting the influence of the transverse strain of the tendon on the bond strength, the transmission length becomes linearly proportional to the initial steel stress. However, the maximum bond stress is also influenced by the transverse deformation of the strand (Poisson effect) and the resulting bond stress is not uniformly distributed, as also follows from the shape factor for the steel stress distribution along the transmission length, see Section 6.4.6. This explains why e.g. Oleśniewicz (1975) found the transmission length to be proportional to the square root of the initial prestress.

It is remarked that the practical meaning of a possible non-linear correlation between transmission length and initial prestress is small because of the limited range of initial stresses used in pretensioned concrete applications.

6.4.6 Relation between draw-in and transmission length

It can easily be shown that the transmission length is related to the slip of the tendon at the end face, the so-called draw-in, according to:

$$l_t = \alpha \frac{A_p E_p}{P_0} \delta_e = \alpha \frac{E_p}{\sigma_{p0}} \delta_e \qquad (6.4\text{-}6)$$

with
- α shape factor for steel stress distribution, which is connected to the bond stress distribution: a linear ascending, uniform and linear descending bond stress yield for α the values 1.5, 2.0 and 3.0, respectively
- δ_e draw-in
- P_0 force in tendon before prestress transfer

This relationship can be used to estimate the transmission length by measuring the draw-in, assuming a value for α. It has also been suggested as an assurance criterion in the production of pretensioned concrete members, such as hollow-core slabs. However, Den Uijl (1992a) has shown that when end faces are obtained by sawing as in the case of hollow-core slabs, the transmission length can considerably be underestimated due to a different width of the saw-cut in concrete and tendon, which is caused by oscillations of the saw blade.

Balázs (1993) generalized Eq. (6.4-6) for any kind of bond stress distribution and type of tendon:

Copyright fib, all rights reserved. This PDF copy of fib Bulletin 10 is intended for use and/or distribution only by National Member Groups of fib.

$$l_t = \frac{2}{1-\eta_3}\frac{E_p}{\sigma_{p0}}\delta_e \tag{6.4-7}$$

where η_3 is the power of the bond stress-slip relationship given by Eq. (6.3-1). With $\eta_3 = 0.33$ the bond stress distribution is linear descending and the $2/(1-\eta_3)$ coefficient is 3. For $\eta_3 \to 0$, the bond stress distribution becomes uniform with the coefficient equal to 2. Other η_3 values are also possible. For 12.8 mm diameter plain seven-wire strand $\eta_3 = 0.25$, which results in a coefficient of 2.67 [Balázs (1993)].

In addition to the above modification of Eq. (6.4-6), Balázs (1993) derived two non-linear equations providing alternative methods for evaluating the transmission length. For 12.8 mm diameter strand these equations are:

$$l_t = 3.47\frac{\sigma_{p0}}{f_{ci}^{0.5}\,\delta_e^{0.25}} \tag{6.4-8}$$

$$l_t = 111\frac{\delta_e^{0.625}}{f_{ci}^{0.15}\,\varepsilon_{p0}^{0.4}} \tag{6.4-9}$$

For equal initial prestress and draw-in values these equations give the same transmission length. However, Eq. (6.4-8) and also Eq. (6.4-7), follow better the variation in draw-in, whereas Eq. (6.4-9) follows better the variation in initial prestress if inaccuracies are considered.

By measuring both transmission length and draw-in the shape factor α can be estimated. From the data reported by Oleśniewicz (1975), who carried out a statistical evaluation of both laboratory and field measurements, a characteristic upper bound value of 2.86 and an average of about 2.30 can be deduced. The confining conditions, concrete cover, strand spacing and transverse reinforcement, if any, were within practical limits. Similar values of the shape factor were found by Den Uijl (1996a), who estimated them at each step during stepwise release of the prestressing force. Notwithstanding a considerable scatter, which could partly be ascribed to errors in the estimation of the transmission length, the shape factor tended to decrease as the prestressing force transferred became higher, thus showing that the bond stress distribution gradually changed from descending to more uniform. When bond splitting cracks were observed, the shape factor had become considerably smaller, which indicated that the bond stress near the entrance plane had been reduced, resulting in an ascending bond stress distribution. In these tests the concrete cover and strand spacing, which defined the confining conditions, were varied as shown in Fig. 6.4-9.

An explanation for the abovementioned changing bond stress distribution can be found by considering the confining action of the surrounding concrete, which is activated by the radial displacement of the tendon-to-concrete interface, see Section 6.3.7. For small radial displacements the concrete response will be linear with a descending bond stress distribution as result, but for larger values of the radial displacement the top of the response curve may be passed and, as a consequence, the bond stress will not increase anymore and may even become smaller. Hence, the distribution of the bond stress is flattened. This process will proceed faster as the concrete cover is smaller. It has been shown in Section 6.4.2 Fig. 6.4-8 that a smaller cover is connected to a longer transmission length. However, no such a clear relation could be established for the relation between cover and shape factor, which might be caused by the large scatter observed in the shape factor.

6.4.7 Standardized bond test

Under apparently similar conditions bond properties generally show great variations. The influence of some parameters, such as compaction of the concrete around the tendon or sedimentation of the mortar below the tendon are qualitatively understood but hard to quantify. Other influencing factors, which might be dominant, are not yet understood. Logan (1997), for example, reports about

Copyright fib, all rights reserved. This PDF copy of fib Bulletin 10 is intended for use and/or distribution only by National Member Groups of fib.

the results of pull-out tests with 13 mm diameter strands from various producers. The average pull-out force of strands from four producers compared well with the results of similar tests that had been executed 20 years earlier, but strands of two other producers only yielded about 25% of the pull-out force obtained in the other tests. Possible influencing factors, such as a shiny surface versus a lightly rusted weathered surface, the amount of removable residues on the strand surface or the pitch with which the outer wires are layed around the centre wire, proved not to be decisive, and no explanation was found for the enormous difference observed. This example shows the need for a robust bond test that can de used to judge whether a tendon is suitable for use in pretensioned applications.

The bond strength in an experiment is influenced by the test conditions, whereby i.a. embedment length, position during casting, degree of confinement, bond situation (pull-out or push-in) and supporting conditions play a role. To be able to judge the bond strength of a specific tendon, a generally accepted way of testing has to be used. The conditions with which such a standardized test should comply, depend on the objectives of the test. With the goal to verify if the bond strength is not lower than an accepted limit value, a simple pull-out test suffices. However, when the test results should reflect the bond strength for a specific bond situation, either along the transmission length or along the anchorage length of a pretensioned tendon, the test conditions must be in accordance with this specific situation.

The pull-out test with short embedment length (3 to 5 times the tendon diameter), originally developed for ribbed bars, has often been used for strands as well. This test is relatively simple to perform. Due to the short embedment length, the pull-out force is small, and, as a consequence, influences connected to the steel stress, or rather the change of the steel stress (Hoyer effect, pitch effect), cannot be investigated with this type of test; see also Section 6.3.7.

Logan (1997) and Rose & Russell (1997) investigated the relationship between the bond strength measured in pull-out tests with long embedment length and the bond strength along the transmission length and the anchorage length of a pretensioned tendon. The pull-out test, which was first used by Moustafa in 1974, has the following characteristics:

- a number of strand samples is vertically embedded over 457 mm in a concrete block;
- the concrete cover and spacing between the strands is sufficient to provide good confinement;
- bond is prevented over 51 mm at the loaded end;
- each strand is individually pulled out, whereby the spacing between the legs of the jack support and the strand is about 100 mm.

Logan compared the results of the pull-out tests with transmission length and anchorage capacity measurements on beams (section 165×305) with one strand at 51 mm from the bottom. Strands from various providers were used. Logan concluded that strands with a pull-out capacity over 160 kN had a shorter transmission length and a better anchorage capacity than required in ACI 318-95. On the other hand, with a pull-out capacity below 53.3 kN, the transmission length and anchorage capacity did not comply with the ACI requirements. It was recognized that a more refined judgement could only be made on the basis of draw-in measurements after 21 days and measurement of anchorage capacity in bending tests.

Rose and Russell investigated with which type of test the transmission length is predicted best. To that end they used a slightly modified Moustafa test, tensioned pull-out tests and draw-in measurements. The tensioned pull-out test was similar to what in Section 6.3.3 has been called a push-in test and the set-up resembles that shown in Fig. 6.3-10. In this case the loading frame was in horizontal position and the concrete prism measured 140×140×305 mm. Draw-ins and transmission lengths were measured on beams (section 152×305 mm) with two 12.7 mm diameter strands at 51 mm from the bottom. An important variable in these tests was the surface condition (as received, weathered, cleaned and silane treated). In general, a lower bond strength in both the Moustafa tests and in the tensioned pull-out tests corresponded with a longer transmission length. However, in both cases the correlation was quite poor. On the other hand, the correlation between draw-in and transmission length was very strong.

Of course, the latter is not surprising. As long as the strands are sufficiently confined to prevent the occurrence of visible splitting cracks, the bond stress distribution along the transmission length will be similar, which results in a linear relationship between the draw-in and the transmission length. It is noticed, however, that under seemingly identical circumstances the ratio between the characteris-

Copyright fib, all rights reserved. This PDF copy of fib Bulletin 10 is intended for use and/or distribution only by National Member Groups of fib.

tic upper bound value and lower bound value of the transmission length is already about 2 (COV 20%). In practice the scatter will be considerably larger due to many variations that may occur (materials, boundary conditions, execution). Therefore, an ample safety margin is required, that can be reduced when in the production the bond quality is checked, e.g. by draw-in measurement in case of hollow core slabs; see also Section 6.4.6.

The difficulty to correlate the bond properties measured in a pull-out tests to the bond properties of a pretensioned tendon was the reasons that FIP recommended to determine the bond properties of prestressing tendons by measuring the draw-in and concrete surface strains on concentrically pretensioned members.

In conclusion it can be said that:

- there is a clear need for a standardized test to judge the bond properties of prestressing tendons for pretensioned applications;
- there should be a could correlation between the bond strength measured in the standardized test and the bond of the pretensioned tendon (transmission length, anchorage capacity);
- the understanding of the mechanisms that govern the bond of a pretensioned tendon has to be improved to be able to distinguish better between the factors that are responsible for the variations in bond properties;
- for better comparison of test results, test characteristics (dimensions, materials, execution) shall be harmonized;
- the tendon used shall be better documented (e.g for strand: diameters of outer wire and centre wire, surface condition: roughness of wire surface and amount of residues on surface, pitch, longitudinal and torsional stiffness, production process).

Copyright fib, all rights reserved. This PDF copy of fib Bulletin 10 is intended for use and/or distribution only by National Member Groups of fib.

6.5 Prestress transfer and anchorage of wire and strand with increased surface roughness

The bond resistance of wire and strand can be increased by indenting the surface or providing it with ribs. This results into a reduction of the transmission length, but also into an increase of the splitting action and higher bursting and spalling stresses in the end block. Little information is found in recent literature about the bond properties and splitting action of wire and strand with increased surface roughness.

Karlsson (1985) reported about centric pull-out tests on horizontally casted specimens and eccentric pull-out tests on extruded hollow core slabs, with 150 mm and 300 mm embedment length, respectively. Plain seven-wire strand and two types of indented seven-wire strand were used. The bond stress-slip curve was steeper and the maximum bond stress was higher as the indentation was deeper, see Fig.6.5-1. In the hollow-core slabs the bond quality near the longitudinal slab sides was clearly less than in the middle part of the slabs, which was ascribed to different compaction.

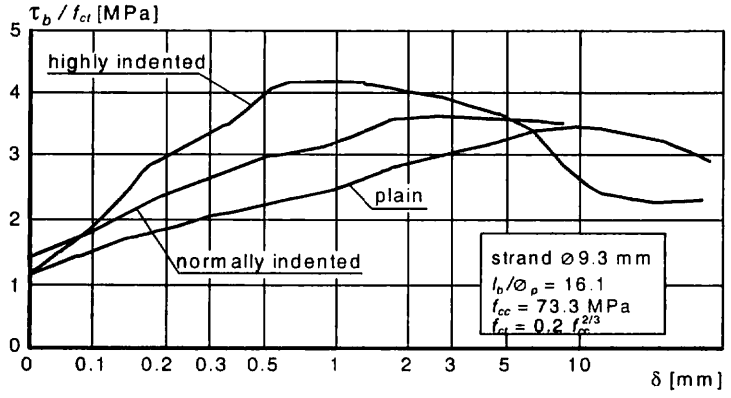

Fig. 6.5-1: Bond stress versus slip of plain and indented strand [Karlsson (1985)]

Den Uijl (1985) concluded from pull-out tests on 5 mm diameter indented wire with 25 mm embedment length that there is a clear relationship between the bond resistance and the relative rib area f_r; see Fig. 6.5-2. The relative rib area is the ratio between the area of the projections of the indents on a plane perpendicular to the axis and the area of the tendon surface between the indents. In these tests only pull-out failure ware observed.

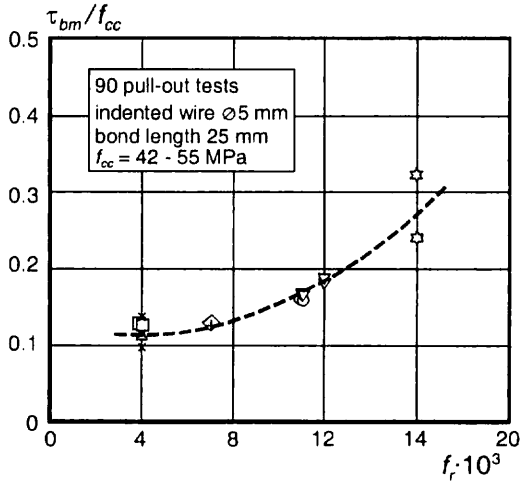

Fig. 6.5-2: Average bond strength versus relative rib area for indented wire [Den Uijl (1985)]

Laldji and Young (1988) compared the bond of 12.9 mm diameter plain strand, 12.7 mm diameter Dyform strand and 12.5 mm diameter indented strand by means of pull-out tests ($2\varnothing_p$ bond length in

Copyright fib, all rights reserved. This PDF copy of fib Bulletin 10 is intended for use and/or distribution only by National Member Groups of fib.

100 mm mortar cubes, cube strength 40-57 MPa) with 0 to 15 MPa biaxial lateral pressure. After debonding, the bond resistance of plain strand and Dyform strand decreased with increasing slip, whereas the bond stress of indented strand increased first, reaching a top at about 2 mm slip. Bond stresses increased proportionally to lateral pressure. The proportion between the maximum bond stresses at all lateral stress levels was 1.0(plain):0.9(Dyform):1.2(indented).

Transmission length measurements carried out at the University of Luttich (NDI, 1994) clearly showed the increased splitting action of indented strand (no details given about indents) compared to plain strand, as can be seen in Fig. 6.5-3, which gives the occurrence of splitting cracks as a function of the concrete cover and clear strand spacing after Den Uijl (1995). The transmission length, which was estimated on the basis of the draw-in values, showed a strong variation, also if no splitting cracks were observed.

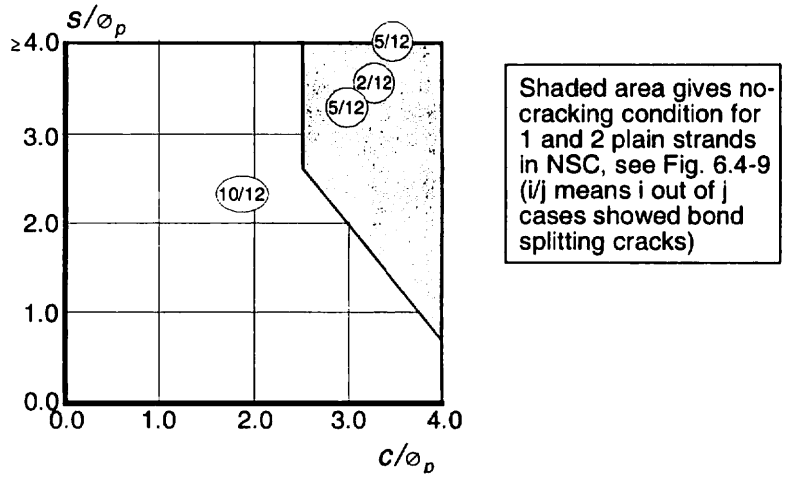

Fig. 6.5-3: Bond splitting of indented strand as a function of concrete cover and strand spacing [NDI (1994)]

Preuveneers and Walgraeve (1996) executed a limited number of push-in tests with short embedment length and transmission length tests on half-beam specimens, comparing the bond behaviour of plain and indented wires. The evaluation of the test results was done according to the method described in Section 6.3.5. Due to the large scatter and the small number of tests no definite conclusions could be drawn.

As far as the bond mechanism of indented wire and strand is considered, a transition between the frictional mechanism of plain wire and strand and the rib bearing mechanism of ribbed bars can be assumed. The latter seems to be less sensible to the influence of transverse contraction of the steel than the former one, at least before yielding of the steel has started. Therefore it has to be investigated whether a distinction should be made between different bond situations in case of indented wire and strand.

Different indent shapes are used in practice. Some have a flat bottom and a steep edge, others have a circular longitudinal cross-section, resulting in a small slope of the edge. No information was found about the influence of the shape of indents on bond strength and bond splitting of indented tendons.

Copyright fib, all rights reserved. This PDF copy of fib Bulletin 10 is intended for use and/or distribution only by National Member Groups of fib.

6.6 Prestress transfer and anchorage of epoxy coated strand

Epoxy coated seven-wire prestressing strand was developed to be used in bridge decks, where the risk of chloride induced corrosion exists. By applying grit (e.g. aluminium oxide) to the epoxy the bond properties can be enhanced. The minimum thickness of the epoxy layer t_c is present at the crown of the outer wires and amounts to about 0.8 to 1.0 mm. A great part of the space between the outer wires is filled up with epoxy, thus changing the initial cross-sectional shape of the strand, Fig 6.6-1. The space between the centre wire and the outer wires is not filled.

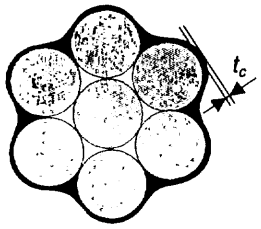

Fig. 6.6-1: Cross-section of epoxy coated strand

A clear difference between uncoated and grit impregnated epoxy coated strand is observed with respect to the interface after the occurrence of slip. While the concrete face is smooth in the case of uncoated strand, it is scratched when coated strand is used, thus showing that the harder grit particles plough through the mortar layer near the interface. This can be interpreted in terms of a higher coefficient of friction.

6.6.1 Transmission length

Dorsten et al. (1984) are the first who report about comparative pull-out and transmission length tests with grit impregnated epoxy coated and uncoated 12.7 mm diameter strand. Immediately after prestress transfer, the coated strand showed a 16% longer transmission length than the uncoated one, but the time-dependent increase of the latter amounted to 20% after 14 months, while the transmission length of the coated strand only increased with 3% (f_{ci}=28 MPa, σ_{p0}=1395 MPa, $l_{ti,un}$=683 mm, $l_{ti,c}$=796 mm). The average unit bond force in pull-out tests with 457 mm embedment length and 28 MPa cylinder strength amounted to 102 and 139 N/mm for uncoated and coated strand, respectively. These values are lower than the average unit bond force in the transmission length tests, which were about 186 and 159 N/mm for uncoated and coated strand, respectively. From the fact that the difference between the average unit bond force in both tests is greater for uncoated strand than for grit impregnated coated strand, the conclusion can be drawn that the latter is less susceptible to the Poisson effect than the former, which can be ascribed to the interlocking action of the grit particles.

Cousins et al. studied the transmission length of epoxy coated strand (1990a). Variables were strand diameter (9.5, 12.7 and 15.2 mm) and strand surface condition: UN-uncoated, CP-coated without grit and coated with various grit densities (CL, CM and CH, for low middle and high density, respectively; t_c=1.1 mm). The specimens contained one strand concentrically placed in members with a square cross-section to measure the transmission length and eccentrically positioned in members with a rectangular cross-section to estimate the anchorage length, see Section 6.6.2 ($c/\varnothing_p$=3.5-4.8, σ_{p0}=1490 MPa, σ_{pi}=1192-1266 MPa, f_{ci}=30 MPa, f_c=34.5 MPa). At prestress release the steel stress got lost in two CP-specimens, showing that there was virtually no bond. UN had a longer transmission length than CL. Increasing grit density resulted in a shorter transmission length. The average results are shown in Table 6.6-1.

Cousins observed that the measured transmission length of uncoated strand was much longer than what would be expected. For this he found no definite explanation, but he underlined the need to understand possible effects of drawing lubricants and corrosion inhibitors that remain on the strand. The transmission length reducing influence of the grit density can clearly be seen in this table. Long-term observation showed that in case of coated strand the transmission length increased more than in case of uncoated strand, but after one year coated strand still had a shorter transmission length than uncoated strand. Similar results were found by Lane (1992), see Section 6.4.4.

Copyright fib, all rights reserved. This PDF copy of fib Bulletin 10 is intended for use and/or distribution only by National Member Groups of fib.

diameter [mm]	coating type[1)]	$l_t/\varnothing_p$	coefficient of variation [%]	number of samples	increase after 1 year [%]
9.5	UN CM	9137	1416	1612	5.4 15.4
12.7	UN CL CM CH	100563834	21 21 21 15	208168	-[2)] 13.9 15.6 9.7
15.2	UN CM	9553	13 17	10 12	-[2)] 4.1

1) UN-uncoated, CL-coated light, CM-coated medium, CH-coated high
2) not measured

Table 6.6-1: Transmission length of uncoated and epoxy-coated strand [Cousins et al. (1990a)]

6.6.2 Anchorage capacity

The above-mentioned single-strand specimens with rectangular cross-section were used to estimate the anchorage length [Cousins et al. (1990b)]. To that end the pretensioned beams were subjected to a three-point-bending load (f_{ci}=32 MPa, f_c=42 MPa). Besides clear bond failures also flexural and shear failures were observed and combinations in which, for example, crushing of the compression zone was accompanied by considerable draw-in. When bond failure was observed, the distance from the loading point to the nearest beam end was increased in the next test. In the case of a flexural failure this distance was decreased. This iterative test procedure was continued until the anchorage length was determined.

A survey of the anchorage lengths found is given in Table 6.6-2. Besides the experimental values $l_{b,exp}$, the required values according to ACI 318-83, $l_{b,ACI}$, are included. The observed moment at failure was about 25% greater than the calculated one according to ACI 318-83. The last column shows the anchorage length associated with this latter moment. As with the transmission length tests, the uncoated strands yielded results that are much higher than expected and that are far beyond the required values according to the ACI-code. On the contrary, the anchorage length of grit impregnated epoxy coated strand is shorter than required. There is a clear tendency that it reduces with increasing grit density. The inconsistencies observed in this respect are ascribed to non-uniformity of the grit density.

diameter [mm]	coating type[1)]	$l_{b,exp}$ [mm]	$l_{b,ACI}$ [mm]	M_{fail}/M_{ACI}	$l_{b,eff}$[2)] [mm]
9.5	UN CM	1448 610	1229 1232	1.15 1.32	1270 483
12.7	UN CL CM CH	3023 1626 762 762	1577 1582 1605 1580	1.33 1.35 1.08 1.33	2311 1245 711 584
15.2	UN CM	3353 1626	1948 1933	1.26 1.25	2692 1321

1) UN-uncoated, CL-coated light, CM-coated medium, CH-coated high
2) $l_{b,eff}$ is the embedment length that in the present cases would have yielded M_{ACI}

Table 6.6-2: Anchorage length of uncoated and epoxy-coated strand [Cousins et al (1990b)]

Besides these static loading tests a series of repeated loading tests was executed on pretensioned

Copyright fib, all rights reserved. This PDF copy of fib Bulletin 10 is intended for use and/or distribution only by National Member Groups of fib.

beams that were cracked during the first load cycle. The position of the loading point for the different strand diameters and surface conditions corresponded to the measured anchorage lengths shown in Table 6.6-2. Under maximum load the calculated tensile strength in the bottom fibre was equal to $0.5f_c^{0.5}$ [MPa], which corresponds to the allowable stress in a precompressed tensile zone according to ACI 318-83. The minimum load amounted to 10% of the maximum load. After 1.5 million load cycles no increase of the transmission length was observed. Subsequent static loading until failure did not reveal any harmful effect of the load history.

6.6.3 Effect of bond situation

Simultaneously to the above-mentioned transmission length tests [Cousins et al. (1990a)] and anchorage capacity tests [Cousins et al. (1990b)] concentric pull-out tests were executed, about which Brearley & Johnston (1990) reported. The specimens consisted of concrete prisms (203x203x305 mm, f_c=32-59 MPa) with a concentrically placed strand bonded over the entire length. Strand diameter and surface conditions were varied as described in Section 6.6.1. Two characteristic bond strength values were obtained from the pull-out tests. The first one marks the initiation of slip at the free end and the second one gives the ultimate bond stress. The average values per group divided by $f_c^{0.5}$ are summarized in Table 6.6-3.

diameter [mm]	coating type[1)]	$\tau_{b,ini}/f_c^{0.5}$ 2) [$N^{0.5}$/mm]	$\tau_{b,max}/f_c^{0.5}$ 3) [$N^{0.5}$/mm]	$\tau_{b,anc}/f_c^{0.5}$ 4) [$N^{0.5}$/mm]	$\tau_{b,trd}/f_c^{0.5}$ 5) [$N^{0.5}$/mm]
9.5	UN	0.55	0.62	0.11	0.56
	CM	0.75	0.99	0.53	1.37
12.7	UN	0.30	0.32	0.11	0.56
	CL	0.41	0.55	0.38	0.88
	CM	0.80	1.03	0.53	1.37
	CH	0.92	1.05	0.53	1.37
15.2	UN	0.27	0.28	0.11	0.56
	CM	0.33	0.49	0.38	0.88

1) UN-uncoated, CL-coated light, CM-coated medium, CH-coated high
2) bond stress at initiation of free end slip
3) ultimate bond stress
4) bond strength in anchorage length tests
5) bond strength in transmission length tests

Table 6.6-3: Pull-out resistance of uncoated and epoxy-coated strand [Brearley & Johnston (1990)]

Besides the normalized bond strength values from the pull-out tests, Table 6.6-3 gives similar data derived from the anchorage length tests and transmission length tests discussed above. The latter were averages of the following combinations of test variables, for which no systematic differences in the results could be observed:

- all diameters UN
- 12.7 mm CL and 15.2 mm CM
- 9.3 mm CM, 12.7 mm CM and 12.7 CH

Again, grit impregnated epoxy coated strands show a higher bond resistance than uncoated strand and the bond stress increase from first free end slip to the ultimate value is higher for coated strand than for uncoated strand. From the differences between the results of the three loading conditions considered it can be concluded that the pull-out test does not reflect the push-in condition (transmission length) nor the pull-out condition as found along the anchorage length. The results clearly show that also in case of grit impregnated epoxy coated strand, the bond condition has a considerable influence on the bond resistance. However, the ratio between push-in bond stress and pull-out bond stress is significantly greater for uncoated strand than for grit impregnated epoxy coated strand. Apparently, the contribution of the grit interlock to bond is relatively stronger than the influence of the Poisson effect.

Copyright fib, all rights reserved. This PDF copy of fib Bulletin 10 is intended for use and/or distribution only by National Member Groups of fib.

6.6.4 Bond splitting

Dorsten et al. (1984) suggested that a grit impregnated epoxy coated strand may require more cover than an uncoated strand. In some of the transmission length tests on moist cured specimens bond splitting cracks were observed at prestress transfer (f_{ci}=28 MPa, σ_{p0}= 1395 MPa, $c/\varnothing_p$=3). However, similar tests on steam cured specimens did not show visible splitting cracks.

Cousins et al. (1990a) reported about two transmission length tests on single-strand members (epoxy coated grit impregnated) with a square cross-section that failed due to bond splitting at prestress release ($c/\varnothing_p$=3.5).

The required strand spacing and concrete cover for epoxy-coated strand ($\varnothing_p$=12.7 mm, t_c=0.9 mm) were investigated by Cousins et al. (1994b). To that end prismatic members with different strand arrangements were investigated, see Fig. 6.6-2 (f_{ci}=30-36 MPa, σ_{p0}=1400 MPa, σ_{ci}=15-17 MPa). Moreover, nine control specimens with uncoated strand were tested. The prestressing force was released by flame cutting the strand(s) at one end of the prestressing bed, which resulted in an average transmission length at these ends of 965 mm, while the average value at the opposite ends amounted to 787 mm. The average transmission length at the ends that did not show splitting cracks was 610 mm, whereas it amounted to 945 mm at the cracked ends. Without giving details, it was mentioned that the average transmission length of uncoated strand was more than what was observed in case of uncracked and cracked members with epoxy coated strand. This meant that the transmission length of the uncoated strand was more than 50 times the strand diameter, which can be considered as a rough estimate of the average value.

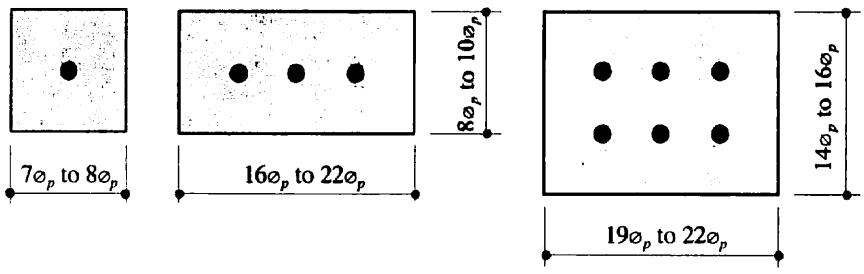

Fig. 6.6-2: Cross-sections of transmission length test specimens [Cousins (1994b)]

Three out of six single-strand members cracked for the full length. Only one out of 16 three-strand members did not present one or more splitting cracks, but none out of seven six-strand specimens showed visible splitting cracks. The control members with uncoated strand had no visible splitting cracks. In all but one case both spacing and cover cracks were experienced, the cover crack mostly being an extension of the spacing crack. In some cases the cover crack ran to an outer face parallel to the plane through the strands. One member end had only a spacing crack. The maximum crack length tended to be shorter as the spacing and cover were larger. A survey of the cracking tendency of epoxy-coated strand as a function of strand spacing and concrete cover can be found in Fig. 6.6-3, where the dashed area indicates the crack free conditions for uncoated strand according to Den Uijl (1995). Grit impregnated epoxy coated strand clearly shows a greater tendency to cause bond splitting cracks than uncoated strand does. It can also be seen that the six-strand specimens were somewhat less sensitive to cracking than the three-strand members. For this phenomenon no explanation was given.

Copyright fib, all rights reserved. This PDF copy of fib Bulletin 10 is intended for use and/or distribution only by National Member Groups of fib.

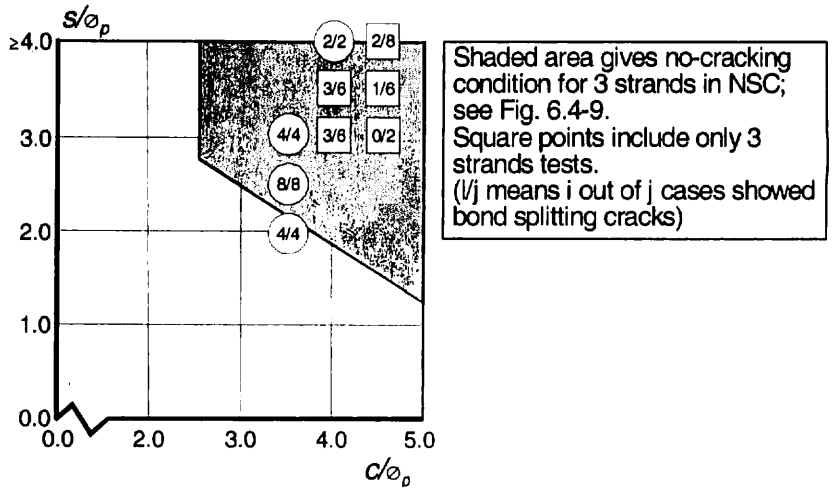

Fig. 6.6-3: Occurrence of bond splitting cracks with epoxy coated strand [Cousins (1994b)]

6.6.5 Influence of elevated temperature

Pull-out tests on epoxy coated strand at elevated temperature showed bond strength deterioration starting at about 40°C and bond strength was reduced with 33 and 85% at 70 and 90°C, respectively [LeClaire & Shaikh (1996)]; see Fig. 6.6-4. The specimens consisted of concrete cubes (f_c=35 MPa) in which a 13 mm diameter strand was embedded over 76 mm. Both 20 grit impregnated epoxy coated strands and 4 uncoated strands were tested. At 21°C the average unit bond force for both types of strand amounted to 373 N/mm. At 93°C the uncoated strand showed a unit bond force of 332 N/mm, while for epoxy coated strand the unit bond force was reduced to 53 N/mm. In the latter case failure occurred at the epoxy-to-steel interface. It is recommended that prestress transfer shall not be performed at internal concrete temperature greater than 70°C.

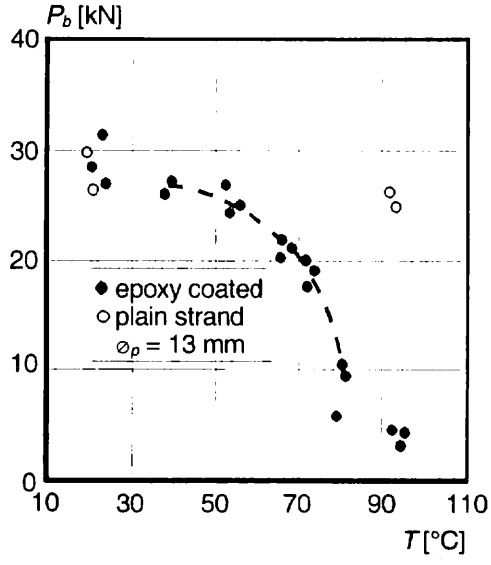

Fig. 6.6-4: Pull-out force of epoxy coated and uncoated strand as a function of temperature [LeClaire & Skaikh (1996)]

Copyright fib, all rights reserved. This PDF copy of fib Bulletin 10 is intended for use and/or distribution only by National Member Groups of fib.

6.7 Design rules for transmission length and anchorage length

In design codes for concrete structures a variety of rules on transmission length and anchorage capacity is found. Here three codes are quoted and compared with each other. In the USA and Canada the current code provisions are intensively discussed at the moment, to which is referred to in Section 6.7.1.

6.7.1 ACI 318

In a historical overview Tabatabai & Dickson (1993) give the background of the current ACI Building Code requirements on transmission length and anchorage length of prestressing strand, which first appeared in 1963 in ACI 318. The anchorage length is defined as:

$$l_b = \frac{\sigma_{p\infty}}{21} \varnothing_p + \frac{f_{pd} - \sigma_{p\infty}}{7} \varnothing_p \tag{6.7-1}$$

with $\sigma_{p\infty}$ prestress including all losses
f_{pd} tendon tensile strength
and constants in [MPa]

The first term at the right-hand side of Eq. (6.7-1) represents the transmission length and was found to give an average value of recent test results. For verification of the shear resistance ACI 318 defines the transmission length as:

$$l_t = 50 \varnothing_p \tag{6.7-2}$$

This expression yields values lower than the average transmission length found in recent tests. The anchorage capacity described by Eq. (6.7-1) was considered to give a reasonable mean of the available data.

The October 1988 FHWA-memorandum that restricted the use of pretensioned strand in bridges was based on two considerations [Lane (1990)]. First, currently used strand differs from that applied in the sixties (larger diameter, higher tensile strength, lower relaxation) and, second, experiments by Cousins et al. (1990) showed much larger anchorage lengths than predicted by Eq. (6.7-1).

As a result of this memorandum, research projects were initiated at various places. In 1993 Buckner (1994, 1995) reviewed the results available at that time and proposed a modification for Eq. (6.7-1). He pointed to the fact that the current ACI provision is unconservative, especially for large embedment length. With respect to the transmission length, Buckner followed Shahawy et al. (1992), who suggested to change the effective prestress into the steel stress just after release:

$$l_t = \frac{\sigma_{pi}}{21} \varnothing_p \tag{6.7-3}$$

where dimension of constant is [MPa].

To count for the increased steel stress at release Buckner suggested to modify Eq. (6.7-2) into:

$$l_t = 60 \varnothing_p \tag{6.7-4}$$

The proposal by Mitchell et al. (1993) to introduce the concrete compressive strength at prestress transfer into Eq. (6.7-3) - and into the expression for the anchorage length - was not followed by

Copyright fib, all rights reserved. This PDF copy of fib Bulletin 10 is intended for use and/or distribution only by National Member Groups of fib.

Buckner, because he found that Mitchell's expression strongly underestimated the transmission length measured by Brearly & Johnston (1990), Deatherage & Burdette (1994) and Russell & Burns (1993). However, this anomaly might be ascribed to deviations of the actual concrete strength from the supposed value, as can be concluded from the good correlation between the transmission length and the apparent elastic modulus found by Buckner for these tests, see Section 6.4.1.

The proposal by Russell et al. (1993) to define an upper bound limit for the transmission length, which was connected to an alternative verification method for the anchorage capacity that aimed at excluding the transfer zone from cracking, was also not followed by Buckner. First, he found the proposed method did not yield a conservative solution for all applications and, second, he pointed to the fact that the current code provisions are in agreement with the approach of "attainable average bond stress over the length of embedment", which is also followed for non-prestressed reinforcement. To adopt the alternative method would mean that this approach is abandoned and it would require a set of equations specific to support conditions and loadings.

To obtain a conservative expression for the anchorage length, Buckner proposed to introduce a multiplier λ, which depends on the steel strain at failure:

$$l_b = \frac{\sigma_{pi}}{21} \varnothing_p + \lambda \frac{f_{pd} - \sigma_{p\infty}}{7} \varnothing_p \tag{6.7-5}$$

with $1.0 \leq \left[\lambda = 0.6 + 40\varepsilon_{pd}\right] \leq 2.0$

and ε_{pd} corresponding to f_{pd}

This multiplier takes into account the reduction of bond strength caused by the transverse tendon deformation that occurs when the longitudinal tendon strain is increased, especially after initiation of yielding.

Buckner further proposed to multiply the transmission length according to Eq. (6.7-3) and the anchorage length according to Eq. (6.7-5) with a factor of 1.3 for strands that end in the upper one-third of a member and having 305 mm or more of concrete cast beneath.

6.7.2 CEB-FIP Model Code 1990

A rationale of the clauses on prestress transfer and anchorage of pretensioned tendons in MC90 was given by Den Uijl (1992c). Fig. 6.7-1 shows the various items involved in the calculation of transmission length and anchorage capacity.

The basic anchorage length, l_{bp}, which can be considered as the length required to anchor a non-pretensioned tendon, follows from:

$$l_{bp} = \frac{A_p}{\pi \varnothing_p} \frac{f_{pd}}{f_{bpd}} \tag{6.7-6}$$

with A_p cross-sectional area: wire $\frac{1}{4}\pi \varnothing_p^2$, strand $\frac{7}{36}\pi \varnothing_p^2$

f_{pd} design strength of tendon

f_{bpd} design bond strength

$\pi \varnothing_p$ nominal tendon perimeter, irrespective type of tendon

The design bond strength is proportional to the design tensile strength and takes into account type of tendon and position during casting:

Copyright fib, all rights reserved. This PDF copy of fib Bulletin 10 is intended for use and/or distribution only by National Member Groups of fib.

$$f_{bpd} = \eta_{p1}\,\eta_{p2} f_{ctd} \tag{6.7-7}$$

with
η_{p1} type of tendon: indented wire and crimped wire 1.4, plain strand 1.2
η_{p2} casting position: inclined and at top 0.7, at bottom 1.0
f_{ctd} design value of concrete tensile strength

It is remarked that in MC90 the relation between tensile strength and compressive strength is taken as:

$$f_{ctk} = \eta f_{ck}^{0.67} \tag{6.7-8}$$

with
η=0.2 for characteristic lower bound value
η=0.3 for characteristic upper bound value

Thus, implicitly the bond stress is taken proportional to $f_c^{0.67}$ as well.

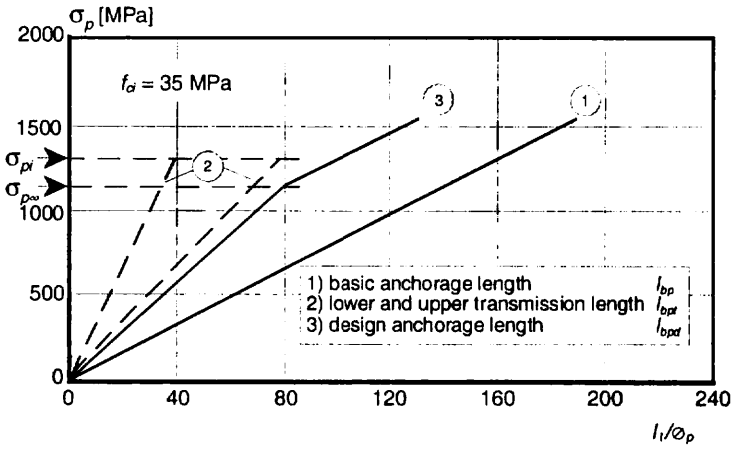

Fig. 6.7-1: Definitions for transmission length and anchorage capacity of pretensioned tendon according to MC90

The transmission length is calculated taking into account way of release, effect to be verified and bond condition. An upper bound value is estimated for moment and shear capacity verification, a lower bound value for analysis of tensile stresses in the anchorage zone. The bond condition refers to push-in situation, where bond is enhanced by transverse deformation of tendon at prestress release (Poisson effect):

$$l_{bpt} = \alpha_8 \alpha_9 \alpha_{10} l_{bp} \frac{\sigma_{pi}}{f_{pd}} \tag{6.7-9}$$

with
α_8 gradual release 1.0, sudden release 1.25
α_9 moment and shear verification 1.0, tensile stresses in anchorage zone 0.5
α_{10} Poisson effect: strand 0.5, indented wire and crimped wire 0.7
σ_{pi} steel stress just after release

The design anchorage length is found assuming that along the transmission length the present steel stress (prestress after losses) can be anchored and that beyond the transmission length the design bond stress is available:

Copyright fib, all rights reserved. This PDF copy of fib Bulletin 10 is intended for use and/or distribution only by National Member Groups of fib.

$$l_{bpd} = l_{bpt} + l_{bp}\frac{\sigma_{pd} - \sigma_{pcs}}{f_{pd}} \tag{6.7-10}$$

with l_{bpt} characteristic upper bound value of transmission length
σ_{pd} design steel stress
σ_{pcs} prestress after all losses

The development length equals:

$$l_p = \sqrt{h^2 + (0.6 l_{bpt})^2} > l_{bpt} \tag{6.7-11}$$

with h total depth of concrete cross-section

6.7.3 Eurocode 2

In Eurocode 2 "Design of concrete structures" prestress transfer and anchorage of pretensioned tendons is treated in Part 1-1 "General rules and rules for buildings" and in Part 1-3 "General rules. Precast concrete elements and structures". In Part 1-1 (ENV 1992-1-1, June 1995) the transfer length follows from:

$$l_{bpm} = \beta_b \varnothing_p \tag{6.7-12}$$

with l_{bpm} average transmission length (notice: EC2 uses l_{bp} instead of l_{bpm})
β_b coefficient depending on concrete strength and type of tendon, see Table 6.4-1

The design value l_{bpt} of the transmission length is given by $0.8 l_{bpm}$ or $1.2 l_{bpm}$, whichever is less favourable for the effect considered (notice: EC2 uses l_{bpd} instead of l_{bpt}). Only in case of sudden release a bond neutralized zone $l_{bp,0}$, which has not been quantified, should be taken into account. It is noted that β_b is inversely proportional to about the square root of the concrete strength.

In Eurocode 2 the development length, which is the distance from the end of the member to the first section where the strain distribution over the concrete cross-section is linear, is called the dispersion length and is defined by:

$$l_{p,eff} = \sqrt{l_{bpt}^2 + d^2} \tag{6.7-13}$$

with d effective depth of concrete cross-section

type of tendon	concrete strength at prestress transfer [MPa]					
	25	30	35	40	45	50
strand, indented wire[1)]	75	70	65	60	55	50
ribbed wire	55	50	45	40	35	30

1) for strand $A_p \leq 100$ mm^2, for indented wire $\varnothing_p \leq 8$ mm

Table 6.7-1: Bond coefficient β_b for pretensioned tendons

Copyright fib, all rights reserved. This PDF copy of fib Bulletin 10 is intended for use and/or distribution only by National Member Groups of fib.

Verification of the anchorage capacity of pretensioned tendons in flexural members at ULS is only required if the concrete tensile stress (flexural and principal) exceeds the design tensile strength. The anchorage capacity is given by:

$$F_{px} = \frac{x}{l_{bpt}} P_i \leq \frac{A_p f_{p0.1k}}{\gamma_s} \tag{6.7-14}$$

with P_i force in tendon just after prestress release.

It is noticed that here P_i has been used instead of P_0. The latter refers to the force in the tendon before prestress transfer. In ENV 1992-1-1 P_0 is given in the corresponding formula, but P_i is shown in a figure to which is referred first.

In addition to Part 1-1, Part 1-3 gives an expression of the tensile force that should be anchored:

$$T_{dx} = \frac{M_{Sd}(x)}{z} + V_{Sd}(x) \cdot \cot\theta \tag{6.7-15}$$

with
- $M_{Sd}(x)$ bending moment in section x
- z internal lever arm
- $V_{Sd}(x)$ shear force in section x
- x distance from centre of support
- θ angle of compression strut with member axis. For member without shear reinforcement, $\cot\theta$ should be taken as 1.

Besides the linear steel stress built up in the anchorage zone, a parabolic distribution is given as "an alternative for more accurate calculations". To that end the transmission length has to be taken as:

$$l_{bpl} = 1.25\, l_{bpm} \tag{6.7-16}$$

The limit envelop for the anchorage capacity is found in a similar way as shown in Fig. 6.7-2.

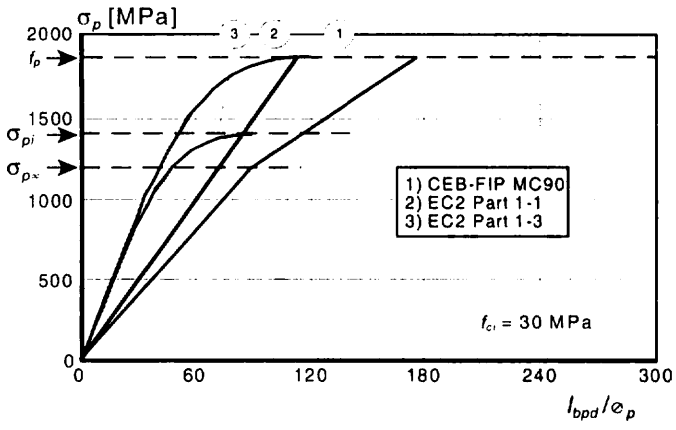

Fig. 6.7-2: Prestress building up and limit envelop for anchorage capacity according to EC2 (linear and parabolic steel stress distribution) and according to MC90

With respect to this approach several remarks can be made. In Eq. (6.7-16) l_{bpm} is used, but one may wonder whether this should be l_{bpt}, which would have resulted in a 20% increase of both transmission and anchorage length. In Fig. 6.7-2 σ_{pi} has been used again instead of σ_{p0}, which was mentioned in EC2. Further, by adopting the parabolic stress course it is suggested that within the transmission length the steel stress that can be anchored is more than the initial steel stress. This is in contradiction with the starting point adopted in ACI 318 and MC90, which says that within the

Copyright fib, all rights reserved. This PDF copy of fib Bulletin 10 is intended for use and/or distribution only by National Member Groups of fib.

transmission length the anchorage capacity corresponds to the initial steel stress, eventually including long-term losses. Finally, the parabolic stress building up would involve a linear descending bond stress along the transmission length. Although a certain gradient of the bond stress profile is not to be excluded, there is no proof for the linear descending distribution.

6.7.4 Comparison of various codes

The above-mentioned code provisions on anchorage capacity are summarized in Fig. 6.7-3. To that end the following values have been taken into account: f_p=1860 MPa, σ_{pi}=0.75f_p=1395 MPa and $\sigma_{p\infty}$=0.85σ_{pi}=1186 MPa. Further, MC90 has the possibility to use the 28-days concrete strength for estimating the course of the second branch. This would result in a somewhat steeper course of the second branch, because of the strength increase after prestress transfer. However, this has not been taken into consideration here. A higher concrete strength at prestress transfer would have resulted in shorter anchorage length according to both EC2 and MC90, but not according to ACI. A strength increase at prestress transfer from 30 to 40 MPa results in a reduction with 15% and 21% according to EC2 and MC90, respectively.

Both EC2 and MC90 aim at estimating the characteristic upper bound value of transmission and anchorage length, whereas the ACI provisions are supposed to give a reasonable mean value of these lengths. For a usual concrete strength at transfer both transmission length and anchorage length are longer according to MC90 than according to ACI. This also holds for the transmission length according to EC2, but not for the anchorage capacity according to this code. For higher concrete qualities, the MC90-envelop for the anchorage capacity will approach the ACI-envelop. Compared to these codes the EC2 estimation becomes highly unconservative.

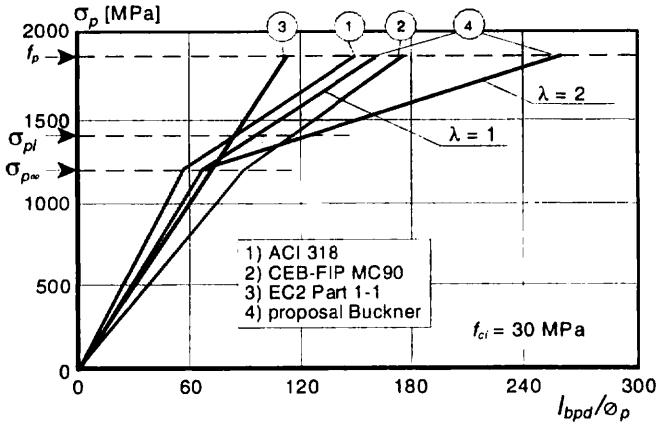

Fig. 6.7-3: Summary of code provisions on anchorage capacity for f_{ci}=30 MPa

In Fig. 6.7-3 it can also be seen that the proposal by Buckner (1994, 1995) yields more conservative values than the present ACI-provisions. It is also more conservative than the MC90-provisions, especially for members where a large yield strain occurs before the concrete compression zone fails (λ>2).

It is remarked that both MC90 and EC2 consider characteristic values. For the transmission length both an upper and a lower boundary value are given. The ratio between these two boundary values amounts to 2 in MC90 and to 1.5 in EC2. Due to the stochastic nature of the transmission length, the scatter of the average transmission length in members with two or more tendons will be smaller than with a single tendon. This is not explicitly taken into account.

Copyright fib, all rights reserved. This PDF copy of fib Bulletin 10 is intended for use and/or distribution only by National Member Groups of fib.

6.8 Summary and Conclusions

In this Chapter of the state-of-the-art report on Bond Models, bond of prestressing tendons is treated. In Section 6.2 the mechanisms which play a role in the force transfer between reinforcement and concrete are discussed in relation to the surface texture of the type of tendon considered. Besides adhesion, friction plays a main role in the bond of plain tendons, whereas other mechanical actions are activated when the surface roughness is increased, e.g. wedging and rib bearing. Although it is recognized that the typical shape of strand caused by the helical course of the outer wires contributes to its bond resistance, the mechanism behind it is not yet fully understood.

In Section 6.3 a review is presented of models used to analyse the bond stresses along a bond activated zone of a strand. The complexity of these models varies from a simple straight forward assumption of a uniform bond stress distribution to confinement based approaches that take into account the non-linear behaviour of concrete loaded in tension. Most models are directed towards the estimation of the transmission length and can not be used to calculate the anchorage capacity since they do not distinguish between push-in and pull-out. These two bond situations differ with respect to the transverse deformation of the tendon, which is directly related to the confining stress acting at the interface and, hence, to the frictional resistance. However, when the transverse deformation would only depend on the Poisson effect, the increasing steel stress in a pull-out situation soon resulted in a complete loss of bond, which is observed with plain wire but not with plain seven-wire strand. Therefore other aspects shall be considered in the models, e.g. wedging due to lack of fit and pitch effect.

Prestress transfer and anchorage capacity of plain seven-wire strand are treated in Section 6.4. Notwithstanding the considerable scatter connected to it, the transmission length was found to be inversely proportional to a power function of the concrete strength at prestress transfer, the exponent of the power function laying between 0.5 and 1. Although not explicitly investigated, the influences of variables such as roughness of the steel surface, position of the strands during casting and way of prestress release were found to follow earlier established tendencies. In some cases unusual large transmission length values were measured, which initiated much research. Some investigators suggested that the poor bond might be caused by drawing lubricants and corrosion inhibitors that remain on the strand surface, but this was not confirmed by experimental results. In general, the time-dependent change of the transmission length is found to be small, but in some cases an increase with 25% after one year has been reported.

Concrete cover and strand spacing required to prevent bond splitting are often estimated on the basis of the so-called thick-walled-cylinder model, where the radial compressive stress at the interface is linked to the circumferential tensile stresses. By not only considering the maximum confinement stress but also the radial deformations involved, the influence of concrete strength on bond splitting could be explained.

It is not always recognized that in case of inclined bending cracks the distance from the end of the member to the position of the load should be the sum of the anchorage length and the "shift of the moment line", which goes with the inclined cracking. Further, it has been shown that the anchorage length increases more than proportionally with the steel stress when the strand starts to yield. This effect, which reflects a diminution of the bond strength, can be attributed to the Poisson contraction. It has been suggested to take this phenomenon into account by relating the anchorage length to the steel strain at failure of the compression zone.

About the bond of indented wire and indented strand very few has been published, as can be found in Section 6.5. However, it has clearly been shown that increased surface roughness results in a shorter transmission length, but that it is also connected to an increased bond splitting action.

In Section 6.6 epoxy coated strand is discussed. It has been shown that plain epoxy coated strand does not present reliable bond properties, but grit impregnated epoxy coated strand has a higher bond resistance than plain seven-wire strand. Consequently, the bond splitting action of the grit impregnated epoxy coated strand is also greater than that of plain strand. The difference between the push-in and the pull-out bond situation was found to be smaller for the grit impregnated epoxy coated strand than for plain strand.

Copyright fib, all rights reserved. This PDF copy of fib Bulletin 10 is intended for use and/or distribution only by National Member Groups of fib.

Finally, design rules for transmission length and anchorage capacity are compared in Section 6.7. The provisions in CEB-FIP MC90 are more conservative than those given by ACI 318 and EC2. However, a recent proposal for a modification of ACI 318 yields more conservative anchorage length values, especially when the steel strain at ultimate load is high. It is noted that the two European codes take into account the concrete strength at prestress release, whereas the ACI and also the new proposal is independent from the concrete strength at release.

6.9 Notations

Abbreviation

cov	*coefficient of variation*
c.t.c.	*centre-to-centre spacing*

Subscript

avg	average
c	concrete
d	design value
m	average
p	prestressing tendon
0	before release of prestressing force
i	just after release of prestressing force
∞	after all prestress losses

Lower case Roman

a	shear span
b	width of section
c	clear concrete cover
c_{eff}	effective concrete cover (average of cover in four directions; each $\geq 4\varnothing_p$)
d	effective depth of section
h	total depth of section
f_{bpd}	design bond strength
f_c	concrete compressive strength (cylinder)
f_{cc}	concrete compressive strength (cube)
f_{ct}	concrete tensile strength
f_p	tensile strength of prestressing tendon
l_b	embedment length
l_{bp}	basic anchorage length
l_{bpd}	design anchorage length (USA: development length)
l_{bpt}	transmission length (USA: transfer length)
l_d	anchorage length
l_t	transmission length
p	pitch of outer wires of strand
s	clear spacing
z	internal lever arm

Capital Roman

A	cross-sectional area
F	normal force
M	bending moment
P	force, load
R_a	surface roughness
T	shear force

Greek

$\Delta\sigma_p$	change of stress in prestressing tendon
δ	slip
δ_e	draw-in, end slip
ε	strain
σ	normal stress
τ_b	bond stress
$\varnothing_p$	tendon diameter

Copyright fib, all rights reserved. This PDF copy of fib Bulletin 10 is intended for use and/or distribution only by National Member Groups of fib.

6.10 References

1958 Kajfasz S.: Technical problems with the use of glass fibres as reinforcement for prestressed concrete (in German). FIP, Berlin, Session II , paper No. 15, pp. 436-450.

1962 Keuning R.W., Sozen M.A., Siess C.P.: A Study of Anchorage Bond in Prestressed Concrete. University of Illinois. Structural Research Series NO. 251.

1963 Somes N.F.: Resin-bonded glass-fibre tendons for prestressed concrete. Magazine of Concret Research: Vol. 15, N0. 45: November 1963, pp.151-158.

1968 Guyon Y.: Construction en Béton Précontraint. Tome 2: Étude de la Poutre. Éditions Eyrolles, 351 pp.

1969 Stocker M.F., Sozen M.A.: Investigation of Prestressed Reinforced Concrete for Highway Bridges. Part VI: Bond Characteristics of Prestressing Strand. University of Illinois. Structural Research Series NO. 344, 363 pp.

1973 Martin H.: Zusammenhang zwischen Oberflächenbeschaffenkeit, Verbund und Sprengwirkung von Bewehrungsstählen unter Kurzzeitbelastung. Deutscher Ausschuss für Stahlbeton, Heft 228.

– Tepfers R.: A theory of bond applied to overlapped tensile reinforcement splices for deformed bars. PhD thesis Chalmers University of Technology, Göteborg, Sweden, 328 pp.

1975 Oleśniewicz A.: Statistical evaluation of transmission length of strand. Research and Design Centre for Industrial Building "BISTYP", Warsaw.

1977 Zia P., Mostafa T.: Development Length of Prestressing Strands. PCI Journal, September-October, pp.. 54-65 (see also discussion in PCI Journal, July-August 1978, pp. 97-107).

1978 Noakowski P.: Die Bewehrung von Stahlbetonteilen bei Zwangsbeanspruchung infolge Temperatur. Deutscher Ausschuss für Stahlbeton, Heft 296, 144 pp.

1981 Jokela J., Lukkariniemi I., Tepfers R.: Bond of bundled prestressing steel strands. Chalmers University of Technology. Publication 81:15, Nr. 501, 23 pp.

1982 Bond Action and Bond Behaviour of Reinforcement. State-of-the-Art Report. CEB Bulletin d'Information N° 151, 153 pp.

– FIP 7: Report on prestressing steel - Test for the determination of the tendon transmission length under static conditions.

– Stroeven P., De Wind G.: Structural and Mechanical Aspects of Debonding of a Steel Bar from a Cementitious Matrix. Bond in Concrete, ed. P. Bartos, Applied Science Publishers, pp. 40-50.

1984 Dorsten V., Hunt F.H., Preston H.K.: Epoxy-Coated Seven-Wire Strand for Prestressed Concrete. PCI Journal, July-August, pp. 120-129.

– Tassi G., Erdélyi L.: The Time-Dependent Change of the Transmission Length in Prestressed Pre-Tensioned Members. Rilem Symposium on Long-Term Observation of Concrete Structures, Boedapest.

1985 Den Uijl, J.A.: Comparative study of bond properties of different types of indented wire. TU Delft, Stevin Report 5-85-10, 28 pp.

– Karlsson D.: Bond between strands and concrete in hollow-core slabs. Nordic Seminar: Bond and Anchorage of Reinforcement in Concrete. Chalmers University, October 23, pp. 68-81.

– Martins J.A.C., Oden J.T.: Interface Models, Variational Principles and Numerical Solutions for Dynamic Friction Problems. Mechanics of Material Interfaces. Proc. of ASCE/ASME Mechanics Conference, Albuquerque, June 23-26, pp. 3-23.

– Rabbat B.G., Russell H.G.: Friction Coefficient of Steel on Concrete and Grout. ASCE, Journal of Structural Engineering, Vol. 111, No. 3, pp. 505-515.

1986 Bruggeling A.S.G.: The transmission length of prestressing steel (in Dutch). Cement XXXVI nr. 7, pp. 447-455.

– Den Uijl, J.A.: Properties of lightweight concrete with sinterized fly ash as aggregate. Part 4. Transmission length of prestressing strand (in Dutch). TU Delft, 53 pp.

1987 "Anchorage Zones of Prestressed Concrete Members", State-of-the-Art Report. CEB Bulletin d'Information N° 181, 137 pp.

– Ghosh S.K., Fintel M.: Development Length of Prestressing Strands, Including Debonded Strands, and Allowable Concrete Stresses in Pretensioned Members. PCI Journal, Vol. 31, No. 5, pp. 38-57.

– Lakatos O., Madarász L.: Development and production of a new concrete stressing staple in the "4th December" Wire Works. Quality and Reliability, pp. 38-40.

1988 Abdie J.L., Mattock A.H.: Transfer of Force Between Reinforcing Bars and Pretensioned Strand. PCI Journal, May-June, pp. 90-106.

– Brooks M.D., Gerstle K.H., Logan D.R.: Effect of Initial Strand Slip on the Strength of Hollow-Core Slabs. PCI Journal, January-February, pp. 90-111.

– Laldji S., Young A.G.: Bond between steel strand and cement grout in ground anchorages. Magazine of Concrete Research: Vol. 40, No. 143, June, pp. 90-98.

– Tassi G., Balázs G., Bodi I.: Bond Properties of Prestressing strands. Proc. of FIP Symposium, Jeruzalem, September 4-9, pp. 121-128.

1990 Baltay P., Gjelsvik A.: Coefficient of Friction for Steel on Concrete at High Normal Stress. Journal of Materials in Civil Engineering, Vol. 2, N0. 1, February, pp. 46-49.

– Brearley L.M., Johnston D.W.: Pull-Out Bond Tests of Epoxy-Coated Prestressing Strand. Journal of Structural Engineering, Vol. 116, No. 8, August, pp. 2236-2252.

– a Cousins T.E., Johnston D.W., Zia P.: Transfer Length of Epoxy-Coated Prestressing Strand. ACI

Copyright fib, all rights reserved. This PDF copy of fib Bulletin 10 is intended for use and/or distribution only by National Member Groups of fib.

Materials Journal / May-June, pp. 193-203.
- b Cousins T.E., Johnston D.W., Zia P.: Development Length of Epoxy-Coated Prestressing Strand. ACI Materials Journal / July-August, pp. 309-318.
- c Cousins T.E., Johnston D.W., Zia P.: Transfer and Development Length of Epoxy Coated and Uncoated Prestressing Strand. PCI Journal, July-August, pp. 92-103.
- Lane S.: Development Length of Prestressing Strand. PUBLIC ROADS, September, pp. 200-205.
- Leskelä M.V.: Push-out test for assessing the bond strength of prestressing tendons. Nordic Concrete Research, Publ. No. 9, pp. 81-96.
- Plähn J.: Report on the RILEM Draft Recommendation "Determination of the modulus of elasticity of prestressing steel strands". Materials and Structures, 23, pp. 131-138 (Draft Recommendation: pp. 139-141).
- Weerasekera R., Loov R.E.: Prestress Transfer Length Predicted By Cohesive Crack Model. In: Micromechanics of Failure of Quasi-Brittle Materials. Ed. Shah, S.P., Swartz, S.E., Wang M.L. Elsevier Applied Science, London, pp. 417-426.

1992 Abrishami H.H., Mitchell D.: A new approach for studying bond characteristics. International Conference BOND IN CONCRETE, Riga, October 15-17, pp. 1/28-1/37.
- Åkesson M., Gylltoft K.: Anchorage of strands in precast concrete elements of the type hollow core. International Conference BOND IN CONCRETE, Riga, October 15-17, pp. 2/1-2/9.
- Balázs G.L.: Transfer Control of Prestressing Strands. PCI Journal, November-December, pp. 60-71.
- Balogh T.: Statistical distribution of draw-in of seven-wire strands. International Conference BOND IN CONCRETE, Riga, October 15-17, pp. 2/10-2/19.
- Burnett E.F.P., Marefat M.S.: Anchorage bond for seven-wire strand. International Conference BOND IN CONCRETE, Riga, October 15-17, pp. 2/68-2/78.
- a Cousins T.E., Badeaux M.H., Moustafa S.: Proposed Test for Determining Bond Characteristics of Prestressing Strand. PCI Journal, January-February, pp. 66-73.
- b Cousins T.E., Francis L.H., Gopu V.: Spacing and concrete cover requirement for epoxy coated prestressing strand. International Conference BOND IN CONCRETE, Riga, October 15-17, pp. 5/81-5/90.
- a Den Uijl J.A.: Relation between draw-in and transmission length in pretensioned concrete members cut off by sawing. TU Delft, Faculty of Civil Engineering. Progress in Concrete Research, Vol. 3, pp. 89-107.
- b Den Uijl J.A.:Bond and splitting action of prestressing strand. International Conference BOND IN CONCRETE, Riga, October 15-17, pp. 2/79-2/88.
- c Den Uijl J.A.: Background of the CEB-FIP MC90 clauses on anchorage and transverse tensile actions in the anchorage zone of prestressed concrete members. CEB Bulletin d'Information No. 212, pp. 71-94.
- De Sitter W.R., Vonk R.A.: Splitting forces in FRPR pretensioned concrete. Fiber-Reinforced-Plastic Reinforcement for Concrete Structures. International Symposium. ACI SP-138, pp. 1-14.
- Jonsson E.: Anchorage of strands in prestressed extruded hollow-core slabs. International Conference BOND IN CONCRETE, Riga, October 15-17, pp. 2/20-2/28.
- Lane S.N.: Transfer length of uncoated and epoxy-coated strands in rectangular prestressed concrete specimens. International Conference BOND IN CONCRETE, Riga, October 15-17, pp. 5/62-5/70.
- Nanni A., Tanigaki M.: Pretensioned prestressed concrete members with bonded fiber reinforced plastic tendons: development and flexural bond lengths (static). ACI Structural Journal, July/August, pp. 433-441.
- Olofsson U., Holmgren M.: Friction measurement at low sliding speed using a servo-hydraulic tension-torsion machine. Swedish National Testing Institute, Building Structures Section, Report SP AR 1992:51, 18 pp.
- a Shahawy M.A., Issa M., Batchelor B.: Strand Transfer Lengths in Full Scale AASHTO Prestessed Concrete Girders. PCI Journal, May-June, pp. 84-96.
- b Shahawy M.A., Issa M.: Effect of Pile Embedment on the Development Length of Prestressing Strands. PCI Journal, November-December, pp. 44-59.
- Tassi G.: Contribution to the components of bond between prestressing wire and concrete. International Conference BOND IN CONCRETE, Riga, October 15-17, pp. 2/107-2/212.
- Tassios T.P., Bonataki E.: Experimental analysis of the bond behaviour of prestressed tendons. International Conference BOND IN CONCRETE, Riga, October 15-17, pp. 2/29-2/37.
- a Tertea I., Onet T., Popa P., Magureanu C.: The anchorage length of pre-tensioned strands in leightweight and normal weight concrete elements. International Conference BOND IN CONCRETE, Riga, October 15-17, pp. 2/38-2/46.
- b Tertera I., Magureanu C., Onet T.: The effect of long term and repeated loading upon bonding properties of pre-tensioned strands. International Conference BOND IN CONCRETE, Riga, October 15-17, pp. 7/69-7/76.
- Valente G.: Bond stresses in pretensioned lightweight hollow core slabs. International Conference BOND IN CONCRETE, Riga, October 15-17, pp. 3/10-3/19.

1993 Abrishami H.H., Mitchell D.: Bond Characteristics of Pretensioned Strand. ACI Materials Journal / May-June, pp. 228-235.
- Åkesson M.: Fracture Mechanics Analysis of the Transmission Zone in Prestressed Hollow Core Slabs. Chalmers University of Technology, Division of Concrete Structures, Licentiate thesis, Publication

Copyright fib, all rights reserved. This PDF copy of fib Bulletin 10 is intended for use and/or distribution only by National Member Groups of fib.

93:5, 62 pp.
- Balázs G.L.: Transfer Length of Prestressing Strand as a Function of Draw-in and Initial Prestress. PCI Journal, March-April, pp. 86-93.
- König G., Tue N.: Method to Solve Bond Differential-Equation System in Prestressed Concrete. Journal of Engineering Mechanics, Vol. 119, No. 10, October, pp. 2194-2206.
- Mitchell D., Cook W.D., Khan A.A.: Influence of High Strength Concrete on Transfer and Development Length of Pretensioned Strand. PCI Journal, May-June, pp. 52-66.
- Russell B.W., Burns N.H.: Design Guidelines for Transfer, Development and Debonding of Large Diameter Seven Wire Strands in Pretensioned Concrete Girders. The University of Texas at Austin, Center for Transportation Research, Reserch Report 1210-5F, 300 pp.
- Tabatabai H., Dickson T.J.: The History of the Prestressing Strand Development Length Equation. PCI Journal, November-December, pp. 64-75.

1994 Buckner C.D.: An Analysis of Transfer and Development Lengths for Pretensioned Concrete Structures. U.S. Department of Transportation, Federal Highway Administration, Publication No. FHWA-RD-94-049, December, 108 pp.
- a Cousins T.E., Stallings J.M., Simmons M.B.: Reduced Strand Spacing in Pretensioned Prestressed Members. ACI Structural Journal / May-June, pp. 277-286.
- b Cousins T.E., Francis L.H., Stallings J.M., Gopu V.: Spacing and Concrete Cover Requirements for Epoxy-Coated Prestressing Strand in Unconfined Sections. PCI Journal, July/August, pp. 76-84.
- Den Uijl J.A.: Das Verbundverhalten von Spannlitzen im Rahmen der Bruchmechanik. Beiträge zum 29. Forschungskolloquium am 24. und 25. März 1994 an der TU Delft, Deutscher Ausschuss für Stahlbeton, pp. 81-88.
- Deatherage J.H., Burdette E.G.: Development Length and Lateral Spacing Requirements of Prestressing Strand for Prestressed Concrete Bridge Girders. PCI Journal, January-February, pp. 70-83.
- Ibell T.J., Burgoyne C.J.: A generalized lower-bound analysis of anchorage zones. Magazine of Concrete Research, 46, No. 167, June, pp. 133-143.
- Mejia-McMaster J.C., Park R.: Tests on Special Reinforcement for the End Support of Hollow-Core Slabs. PCI Journal, September-October, pp. 90-105.
- NVN-ENV 1992-1-3. Eurocode 2. Design of Concrete Structures. Part 1-3: General rules. Precast concrete elements and structures.
- Russell B.W., Burns, N.H., ZumBrunnen, L.G.: Predicting the Bond Behaviour of Prestressed Concrete Beams Containing Debonded Strands. PCI Journal, September-October, pp. 60-77.
- Vandewalle I., Mortelmans F.: Anchorage of Strands. FIP congres Washington,
- Vossen P.F.: Prestressed members of high strength concrete (in Dutch). Graduate thesis TU Eindhoven.

1995 Bogaerts B., Brosens K.: Ankering van voorspanstrengen in holle vloerplaten. Graduate thesis Katholieke Unversiteit Leuven, 120 pp.
- Buckner C.D.: A Review of Strand Development Length for Pretensioned Concrete Members. State-of-the-Art Report. PCI Journal, March-April, pp. 84-99.
- a Den Uijl J.A.: High performance concrete in the prefab industry. Part 3: Transmission length of prestressing strand (in Dutch). TU Delft, Stevin Report 25.5-95-3, 65 pp.
- b Den Uijl J.A.: High performance concrete in the prefab industry. Part 4: Draw-in of prestessing strand (in Dutch). TU Delft, Stevin Report 25.5-95-4, 21 pp.
- c Den Uijl J.A.: Transfer Length of Prestressing Strand in HPC. TU Delft, Faculty of Civil Engineering. Progress in Concrete Research, Vol. 4, pp. 75-90.
- d Den Uijl J.A.: High performance concrete in the prefab industry. Part 5: Anchorage capacity of prestressing strand (in Dutch). TU Delft, Stevin Report 25.5-95-5, 79 pp.
- NVN-ENV 1992-1-1. Eurocode 2. Design of concrete structures. Part 1-1: General rules and rules for buildings.
- Noghabai K.: Splitting of Concrete in the Anchorage Zone of deformed bars. Licenciate Thesis 1995:26, Luleå University of Technology, Sweden, 131 pp + app.
- a Otsuka K.: Bond Properties of Prestressing Wire Strand. Tohoku Gakuin University, Tagajo Miyagi 985, Japan, Abstract of Experimental Study, 16 pp.
- b Otsuka K.: Bond Properties of "After-Bond" Prestressing Steel. Tohoku Gakuin University, Tagajo Miyagi 985, Japan, Abstract of Experimental Study, 8 pp.
- Sanders D.H., Breen J.E.: Post-Tensioned Anchorage Zones - A Survey and a Solution. Concrete International, August, pp. 65-70.

1996 Den Uijl J.A., Bigaj A.J.: A bond model for ribbed bars based on concrete confinement. HERON, Vol. 41, No. 3, pp. 201-226.
- Den Uijl J.A.: Bond of strands in high performance concrete. Fourth International Symposium on Utilization of High Strength/High Performance Concrete, 29-31 May, Paris, pp. 1175-1184.
- LeClaire P.J., Shaikh A.F.: Effect of Elevated Temperature on the Bond Strength of Epoxy-Coated Prestressing Strand. PCI Journal, July-August, pp. 54-61.
- Logan D.R.: Discussion of "A Review for Strand Development Length for Pretensioned Concreet Members", PCI Journal,March-April, pp. 112-116.
- Preuveneers I., Walgraeve B.: Anchorage of prestressing tendons in pretensioned slabs (in Dutch). Graduate thesis Katholieke Universiteit Leuven, 112 pp.
- Russell B.W., Burns N.H.: Measured Transfer Lengths of 0.5 and 0.6 in. Strands in Pretensioned

Copyright fib, all rights reserved. This PDF copy of fib Bulletin 10 is intended for use and/or distribution only by National Member Groups of fib.

Concrete. PCI Journal, September-October, pp. 44-65.
1997 Cook R.A., Fagundo F.E., Richardson D.: Effect of External Elevated Temperatures on the Bond Performance of Epoxy-Coated Prestressing Strands. PCI Journal, January-February, pp. 68-75.
– Logan D.R.: Acceptance Criteria for Bond Quality of Strand for Pretensioned Prestressed Concrete Applications. PCI Journal, March-April, pp. 52-90.
– Rose D.R., Russell B.W.: Investigation of Standardized Tests to Measure the Bond Performance of Prestressing Strand. PCI Journal, July-August, pp. 56-80.
– Ehsani M.R., Saadatmanesh H., Thomson Nelson C.: Transfer and Flexural Bond Performance of Aramid and Carbon FRP Tendons. PCI Journal, January-February, pp. 76-86.
1998a Den Uijl J.A.: Bond modelling of prestressing strand. ACI Spring Convention, Seattle, Washington, USA, April 5-10. ACI SP-180, pp. 145-169.
– b Den Uijl J.A.: Connection between concrete properties and bond of prestressing strand. Proc. of the XIIIth FIP Congress, Amsterdam, 23-29 May, pp. 129-130.

Copyright fib, all rights reserved. This PDF copy of fib Bulletin 10 is intended for use and/or distribution only by National Member Groups of fib.

7 Bond of non-metallic reinforcement

Working Party 7:

Ralejs Tepfers (Convener, Chalmers University of Technology, Göteborg, Sweden), **Edoardo Cosenza** (Università di Napoli Federico II, Naples, Italy), **Janis Modniks** (Institute of Polymer Mechanics, Riga, Latvia), **Stavroula Pantazopoulou** (Demokritos University of Thrace, Xanthi, Greece), **Kypros Pilakoutas** (University of Sheffield, UK), **Roberto Realfonzo** (Università di Napoli Federico II, Naples, Italy), **Hiroshi Shima** (Kochi University of Technology, Japan), **Luc Taerwe** (University of Ghent, Belgium), **Vitauts Tamuzs** (Institute of Polymer Mechanics, Riga, Latvia), **Tamon Ueda** (Hokkaido University, Sapporo, Japan)

7.1 Characteristics of materials **317**
7.1.1 Introduction 317
7.1.2 Fibers 317
7.1.3 Resins 319
7.1.4 Basic mechanical properties of reinforcing units 319
7.1.4.1 Basic mechanical properties of unidirectional composites 319
7.1.4.2 Effects of loading direction on the tensile strength 320
7.1.4.3 Thermal characteristics 320
7.1.4.4 Creep characteristics 321
7.1.4.5 Long term strength 321
7.1.4.6 Relaxation characteristics 321
7.1.4.7 Fatigue 321
7.2 Bond and anchorage of FRP reinforcing materials **322**
7.2.1 Introduction 322
7.2.2 Bond action 322
7.2.2.1 Plain bars 322
7.2.2.2 Deformed or surface treated bars 322
7.2.2.3 Spliced bars 324
7.2.3 Parameters affecting bond of FRP reinforcement 325
7.2.3.1 Shape of the bar cross section 326
7.2.3.2 Bar deformations 326
7.2.3.3 Low elastic modulus in the axial direction 326
7.2.3.4 Elastic modulus of the bar in the transverse direction 327
7.2.3.5 Transverse pressure 327
7.2.3.6 Poisson effect 327
7.2.3.7 Position of the bar in the cross-section 327
7.2.3.8 Wedging effect 327
7.2.3.9 Bends in anchored bars 327
7.2.3.10 Concrete cover and distances between parallel bars 328
7.2.3.11 Thermal expansion 328
7.2.3.12 Environmental influence on bond 328
7.2.3.13 Bar diameter 328
7.2.3.14 Concrete strength 329
7.2.3.15 Transverse reinforcement 329
7.2.4 Testing of bond performance of FRP bars/rods/strands 329
7.2.4.1 Determination of local bond slip relationship 330
7.2.4.2 Tests to determine bond performance in practice 333
7.2.5 Conclusions 335
7.3 Local bond stress-slip relationship **337**
7.3.1 Research on bond behavior 337
7.3.1.1 Bond strength and characteristics for bars with different surface texture 337
7.3.1.2 Effect of concrete strength and other parameters on bond strength 341
7.3.1.3 Long term performance of bond 343
7.3.2 Bond splitting tendency of FRP bars 344
7.3.3 Analytical modeling of bond between FRP bars and concrete 347
7.3.3.1 Local bond modeling 347
7.3.3.2 General bond modeling 349
7.3.4 Other parameters affecting bond 352
7.3.4.1 Bond under sustained load - creep tests 352

Copyright fib, all rights reserved. This PDF copy of fib Bulletin 10 is intended for use and/or distribution only by National Member Groups of fib.

7.3.4.2 Temperature effects 352
7.3.4.3 Crack widths and shrinkage 353
7.3.4.4 Ductility 353
7.3.4.5 Fatigue and fretting of bonded FRP rods 354
7.3.4.6 Environmental influence on bond 354
7.3.5 Other types of bonded reinforcing devices 355
7.3.5.1 Bond of grid type FRP in concrete 355
7.3.5.2 Bond performance of woven fabrics in cementitious composites 356
7.3.5.3 Composite beams of fiber reinforced plastic profile and concrete 357
7.3.6 Conclusions 357
7.4 Anchorage of continuous fiber tendons for prestressing 359
7.4.1 Anchorage of PC tendons for prestressing systems 359
7.4.2 Anchorage of prestressing tendons in concrete and rock 361
7.4.3 Anchorage of PC tendons for post-tensioning systems 361
7.4.4 Fatigue of anchoring systems 362
7.4.5 Summary 362
7.5 Joints 363
7.5.1 Direct joints 363
7.5.2 Lap splice 363
7.5.3 Connecting of precast members 364
7.5.4 Summary 365
7.6 Bond of continuous fiber sheets and plates 366
7.6.1 Introduction 366
7.6.2 Materials and techniques used for external bonding 366
7.6.2.1 Epoxy adhesives 366
7.6.2.2 Strengthening materials 367
7.6.2.3 Surface preparation of external bonding technique 369
7.6.3 Types of bond - related failures 369
7.6.3.1 Resin interface failure 369
7.6.3.2 Concrete interface failure 369
7.6.3.3 End anchorages to enhance concrete bond strength 371
7.6.3.4 Bond strength of tensile reinforcement 372
7.6.3.5 Bond strength of shear reinforcement 372
7.6.4 Analytical predictive methods for bond stress distribution, bond strength and anchorage lengths 373
7.6.5 Environmental and time-dependent effects on bond strength 377
7.6.6 Design and testing recommendations 378
7.6.7 Instrumentation for bond tests 378
7.6.8 Producers 378
7.6.9 Summary 379
7.7 Conclusions 380
7.8 Design rules 381
7.8.1 Existing bond clauses 381
7.8.2 Canadian Standards Association recommendation, CSA 381
7.8.3 Canadian Highway Bridge Design Code, CHBDC 381
7.8.4 Japan Society for Civil Engineering, JSCE recommendation 383
7.8.5 American Concrete Institute Design recommendations 385
7.9 References 387

Terminology

AFRP	Aramid fibre reinforced plastics
CFRM	Carbon fibre reinforced materials
FRP	Fibre reinforced plastics
GFRP	Glass fibre reinforced plastics
HM	High modulus
HT	High tension
UD	Unidirectional fibre composite

Copyright fib, all rights reserved. This PDF copy of fib Bulletin 10 is intended for use and/or distribution only by National Member Groups of fib.

7.1 Characteristics of materials

7.1.1 Introduction

Due to their corrosion resistance, fiber reinforced polymer (FRP) materials gain increasingly more attention as a reinforcing option for concrete. FRP reinforcement has a high tensile strength with moderate modulus of elasticity and is elastic up to failure. It is non-magnetic and some types are electrically neutral. However, it should not be treated in the same way as steel reinforcement since its qualities and performance are quite different to that of steel reinforcement.

FRP rods are built up of continuous fibers arranged in different ways and impregnated with resin. There are many different ways to manufacture FRP bars. The most common manufacturing process involves the fibers being pulled and impregnated in the pultrusion process. Different fibers can be mixed to form a hybrid bar. Special bar constructions can also be made, for instance to improve the ductility of the bar just before failure. The bar surface can be specially reinforced with extra hard corrosion resistant resin reinforced with chopped mineral fibers and the bond friction increased with siliceous grains or a rough surface. The bars could be produced with in-built optical sensors and other more sophisticated systems, since the temperatures at which the FRP bars are normally manufactured are around 200°C.

FRP reinforcement for concrete does not need to have the same shape as steel reinforcement. The reinforcement could be shaped in the form of bars, rods, cables, profiles and even as the formwork or mould for the concrete. Due to good corrosion resistance, the FRP does not need the cover protection of the concrete and it can be exposed in many cases to the environment. However, the resin used for impregnation limits its fire resistance.

As with all new developments, the introduction of FRP reinforcement into construction started with imitating the use of steel reinforcement in concrete. In due time it can be expected that FRP will find its right application in civil engineering and the necessary guidelines will be developed. In Japan, the Japanese Society of Civil Engineers (JSCE) has produced a code for FRP reinforced concrete structures. The base for this code is the State-of-the-Art-Report written by JSCE, Second Research Committee on CFRM. This report written in 1993 gives a good survey of existing knowledge. This section dealing with bond of FRP in concrete refers to the JSCE report and presents new known developments, completed with new results and conclusions. In Canada the Canadian Highway and Bridge Authority has also produced a code for use of FRP reinforcement, the "Canadian Highway Bridge Design Code", CHBDC, 1996. In USA, the American Concrete Institute has elaborated a proposal for design of concrete members reinforced with FRP reinforcing bars. A European research project (EUROCRETE) also produced design guidelines in the form of modifications to existing European codes.

FRP materials are currently new to most civil engineers. In addition, the bond performance of FRP rods, unlike that of steel, is very dependent on their design, manufacture and mechanical properties. Hence, to enhance the understanding of subsequent sections, the constituent materials of FRP are briefly introduced in the first part of this chapter.

7.1.2 Fibers

Currently the most common fibers used to make FRP rods are carbon, aramid and glass. All these fibers have tensile strength higher than that of steel and are elastic up to tensile failure without showing any yield.

Carbon fiber

Carbon fiber is made from either petroleum or coal pitch and poly acrylic nitrile (PAN). The fibers are an aggregate of imperfect fine graphite crystals. Carbon fibers conduct electricity and, therefore, direct contact with steel might give corrosion problems. The composition and orientation of the crystals determine the characteristics of the fibers. There are two types of fibers: pitch and PAN. Both are made

Copyright fib, all rights reserved. This PDF copy of fib Bulletin 10 is intended for use and/or distribution only by National Member Groups of fib.

of HT-fibers (HT means high tension) with high strength and lower modulus of elasticity than HM-fibers (HM means high modulus) which have higher modulus of elasticity but lower strength. Typical properties are given in table 7.1 The pitch fibers have generally 20% lower qualities than the PAN fibers. Carbon fibers show excellent resistance against alkali, water and seawater. However, they are currently the most expensive fibers.

	PAN HT	PAN HM	Pitch Ordinary	Pitch HM
Tensile strength MPa	3500	2500-4000	780-1000	3000-3500
Modulus of elasticity GPa	200-240	350-650	38-40	400-800
Ultimate elongation %	1.3-1.8	0.4-0.8	2.1-2.5	0.4-1.5
Density kg/m^3	1700-1800	1800-2000	1600-1700	1900-2100
Diameter μm	5-8	5-8	9-18	9-18

Table 7.1. Properties of carbon fibers.

Aramid fiber

Four types of aramid fibers are available, with commercial names Kevlar, Twaron, Technora and Russian aramid fibers SVM. Their typical characteristics are given in Table 7.2 The aramid fibers tend to weaken under ultraviolet rays, however, this fact may not be a serious problem when the fiber is embedded in concrete.

	Kevlar 49 and Twaron	Technora	Russian aramid SVM
Tensile strength MPa	3600	3500	3800 - 4200
Modulus of elasticity GPa	130	74	130
Ultimate elongation %	2.7-3.5	4.6	3.5
Density kg/m^3	1450	1390	1430
Diameter μm	12	12	15

Table 7.2. Properties of aramid fibers.

Glass fiber

Two types of glass fiber are commercially available for use in continuous FRP materials. These are E-glass and alkali-resistant glass fiber. Typical properties are given in table 7.3 The E-glass fiber contains large amounts of boric acid and aluminate. The alkali-resistant glass fiber contains an amount of zirconia, which serves to prevent corrosion by alkali attacks from cement matrices. Glass fibers are also sensitive to exposure to water.

	E-glass	Alkali resistant glass	Polyvinyl alcohol fiber
Tensile strength MPa	3500-3600	1800-3500	2300
Modulus of elasticity GPa	74-75	70-76	61
Ultimate elongation %	4.8	2-3	5.0
Density kg/m^3	2600	2270	1300
Diameter μm	8-12	8-12	14

Table 7.3. Properties of glass and polyvinyl alcohol fibers.

Copyright fib, all rights reserved. This PDF copy of fib Bulletin 10 is intended for use and/or distribution only by National Member Groups of fib.

Polyvinyl alcohol fiber

The high strength polyvinyl alcohol fiber used as continuous fiber material is spun by a wet process using polyvinyl alcohol of a high degree of polymerization and rolled to provide added strength and elasticity to conventional fibers. The fiber also remains stable in alkaline surrounding. This fiber however has relatively low strength and modulus of elasticity, as shown in table 7.3.

7.1.3 Resins

Resins used to impregnate and hold together the fibers include epoxy, polyester, vinyl ester, polyamide, modified urethane and polyethylene.

	Epoxy	Polyester	Vinyl ester	Polyamide
E, GPa room temperature	2-3.5	3.5	3.2	2.8
Strength at tension, MPa	70-90	40-60	80-90	70-80
Ultimate elongation, %	5-6	5-6	4-5	50-60
Density, kg/m^3	1200-1300	1380	1120	1150

Table 7.4. Properties of some resins

7.1.4 Basic mechanical properties of reinforcing units

7.1.4.1 Basic mechanical properties of unidirectional composites

FRP rods are essential is unidirectional composites (UD) and, hence, they arte anisotropic. UD have very different elastic moduli and strength characteristics in the fiber and transverse directions. The modulus in fiber direction can be easily estimated by the rule of mixtures:

$$E = \sum E_i v_i \qquad \ldots\ldots (7.1)$$

where E_i are the elastic moduli of constituents (fibers and resin), v_i the corresponding volume content of constituents ($\Sigma v_i = 1$) . The strength of UD in fiber direction (if only one type of fibers is used) can be roughly estimated as:

$$\sigma_c = \sigma_f v_f \qquad \ldots\ldots (7.2)$$

where σ_f is strength of fiber, v_f - fibers volume content.

The stress-strain behavior is linear till the failure. By mixing several types of fibers the stress strain characteristics of hybrid composite becomes nonlinear, and the properties, performence and ultimate strength depend on the ratio of fiber volume contents and compatibility of fiber types.

The transverse modulus and strength of UD depend mainly on resin properties. The transverse modulus can be roughly estimated as $E_{tr} = E_m / v_m$, where E_m and v_m are modulus and volume content of matrix.

Copyright fib, all rights reserved. This PDF copy of fib Bulletin 10 is intended for use and/or distribution only by National Member Groups of fib.

Typical characteristics of some unidirectional composites are given in table 7.5. The testing of flat coupons of unidirectional composites is standardized (i.e. tensile testing ISO 527).

	Glass polyester $v_f = 0.6$	Carbon epoxy $v_f = 0.6$	Aramid epoxy
Longitudinal modulus E_1, GPa	45	143	78-95
Transverse modulus E_2, GPa	13	8-9.5	4.1-5.5
Longitudinal tensile σ_1, MPa	1600	1400-1600	1400-2200
Transverse tensile σ_2, MPa	15-25	3	12-28
Shear modulus G_{12}, GPa	3.5	5.5	2.1
Shear strength σ_{12}, MPa	20-40	75	20-40
Thermal expansion coefficient $\alpha * 10^6 K^{-1}$ longitudinal	6 to 10	-1 to 0	-6 to +4
Transverse	21 to 23	22 to 23	35 to 80
Density kg/m^3	2000	1550	1350

Table 7.5. Properties of unidirectional composites

7.1.4.2 Effects of loading direction on the tensile strength

The tensile strength is highest in the direction of fibers. When FRP reinforcement is used as stirrups or prestressing tendons, the strength in an inclined direction to the bar axis (direction of fibers must be determined. Tests indicate that, at 30° to the fiber direction, bars with fibers wound around them register about 30% of the tensile strength for carbon fibers, about 45% for aramid fibers, and 65% for glass fiber bars. Twisted carbon fiber materials register about 50% of the fiber strength in the direction of load. A comparison can be done with wood, which is also a fiber composite. When the direction of load is inclined more than 15° to the direction of fibers, a drastic fall of tensile strength is registered. When FRP bars are bent before a thermoset resin hardens, the fibers on the compressive side of bend become buckled and on tensile side stretched - some of them to failure, hence, the strength in a bend is reduced. The transverse shear strength and modulus of the FRP bar is also considerably lower than that of steel bars.

7.1.4.3 Thermal characteristics

Since the expansion coefficients of both steel and concrete are nearly identical at $10*10^{-6}$/°C, the effect of the materials on each other may be ignored. The expansion coefficient for continuous fiber materials varies and for carbon fibers is about $1*10^{-6}$/°C, for aramid fibers -6 to $-2*10^{-6}$/°C (negative!), for glass fibers about $10*10^{-6}$/°C and for polyvinyl alcohol fibers about $4.4*10^{-6}$/°C.

Copyright fib, all rights reserved. This PDF copy of fib Bulletin 10 is intended for use and/or distribution only by National Member Groups of fib.

The coefficient of radial thermal expansion of an FRP bar is governed by the thermal expansion of the resin. This coefficient of thermal expansion can be 5 to 8 times higher than the corresponding value for concrete.

The strength and modulus of elasticity of the fibers is also temperature dependent. In the temperature range 0°C to 60°C each increase of 10°C lowers the tensile strength by 50 to 100 MPa and the modulus of elasticity by 1 to 2 GPa. This behavior should be considered when determining safety factors.

When fibers are impregnated with resin, the resin determines the temperature resistance of the FRP rod, since resins soften, melt or start to deteriorate at about 200°C.

7.1.4.4 Creep characteristics

It has been reported that cable carbon fiber reinforcing materials can be subjected to a creep strain of 0.0068% after a time lapse of 1000 hours under stress equal to 65% of the tensile strength, Machida (1993). In the case of braided aramid fiber bars the ratio of creep strain to elastic strain under a stress equal to 50% and 60% of the tensile strength is 9.5% to 10% after a time lapse of 1000 hours. Glass fiber rods may be used only to about 25% of their tensile strength because of the risk of stress corrosion/rupture. At this stress level, the creep is very small for GFRP bars/rods.

FRP rods in general have a lower modulus of elasticity than steel reinforcement. This fact makes the use FRP as reinforcement in unprestressed concrete elements as active load-taking reinforcement more difficult. If a high bar strain (and stress) is developed cracks will become visible and deflections excessive. Hence, FRP bars are best used as secondary reinforcement or in secondary elements. The FRPs with their lower modulus of elasticity are well suited as prestressing reinforcement, because creep of concrete will not affect the prestressing force as much. It is very important that the FRP materials have very small creep to achieve this objective.

7.1.4.5 Long term strength

Glass fiber bars/rods are sensitive to high stress levels and may show reduced long term strength. The long-term strength is influenced by aggressive environments and by stress corrosion. For carbon FRP the creep failure load for 1 million hours is estimated to be about 50% of the static short term load. At least the same must be accounted for aramid FRP and glass FRP. Glass fiber rods should not be used as prestressing reinforcement because of stress corrosion/rupture. When used as unprestressed reinforcement the low modulus of elasticity and the deformations of structure limit the stress level to not more than 30% of the tensile strength.

7.1.4.6 Relaxation characteristics

For carbon, aramid and glass fibers, it can be noted that the relationship between pure relaxation rate and time in logarithmic terms is linear for a load level of 0.8 of the tensile failure load. When the relaxation is computed for the 30 years point the relaxation is about 14% for all three materials at 20°C, Machida (1993). It is nearly identical to that of prestressing steel wires and two times that of prestressing steel bars. When the temperature is raised to 60°C the relaxation increases to 17%. Further studies are needed to clarify the relaxation behavior of these materials.

7.1.4.7 Fatigue

Fatigue of composites has been investigated comprehensively since they are widely used in mechanical engineering applications. Carbon fiber composites have excellent fatigue properties (0.8 from static strength and full amplitude at 10^6 cycles). The glass epoxy and glass polyester UD composites have the fatigue limit at 10^6 cycles about 0.4-0.5 of static tensile strength. The influence of moisture to fatigue resistance is crucial and can reduce the fatigue limit significantly (up to 2 times).

Copyright fib, all rights reserved. This PDF copy of fib Bulletin 10 is intended for use and/or distribution only by National Member Groups of fib.

7.2 Bond and anchorage of FRP reinforcing materials

7.2.1 Introduction

Bond between concrete and FRP reinforcing bars is the key to understanding the composite action of FRP reinforced concrete and ought to be adequately understood before FRP materials can be accepted widely in the construction industry. To secure composite action, sufficient bond must be mobilised between reinforcement and concrete for successful transfer of forces from one to the other. Particular areas of attention include splices and end anchorage regions, since hook anchorages (by bending of the bar) are not always possible with FRP bars.

The bond behaviour of FRP bars to concrete is expected to vary from that of conventional steel bars, since various key parameters that influence bond performance are different. Such parameters include (Achillides, Pilakoutas & Waldron, 1997):

- the modulus of elasticity of the material is lower than that of steel, both in the lateral and the longitudinal directions,
- the shear stiffness of FRP is also much lower than that of steel,
- the resin matrix has lower shear strength than steel, a factor that is expected to limit the strength of the surface deformations of the bar
- the FRP coefficient of thermal expansion is different from that of steel or concrete.

The large number of possible combinations of fibres, resins and shapes of reinforcement may create difficulties in the development of general and consistent codes for the bond performance of FRP materials. To avoid restraining future innovation by excessive standardisation, this report limits itself to FRP materials made of E-glass, carbon and aramid fibres and epoxy, polyester and vinyl ester resins.

7.2.2 Bond action

The bond performance between bar and concrete along the anchorage length can be described as follows:

7.2.2.1 Plain bars

Bond of plain bars is mainly governed either, by the adhesion between the bar surface and the surrounding concrete, or by the inter-laminar shear strength between successive layers of fibres at the surface of the bar. Bond failure occurs along the perimeter of the bar as the bar is being pulled out from the concrete. Since no tensile cracking is likely to occur along the bar, splitting bond forces are unlikely to develop. The bond strength in plain bars is normally very low and with a large variability. Hence, plain bars (not wires) may be used as reinforcement only if they are used together with other anchoring devices such as bends, hooks and transverse bars.

7.2.2.2 Deformed or surface treated bars

The FRP bar to concrete interaction is best described by using the bond versus loaded end slip response curve of a short embedment length subjected to pullout, as shown in Fig. 7.2-1.

Section OA: At the beginning of loading, the main mechanism that resists the external load is the chemical adhesion between the two materials. No measurable slip is observed at this stage.

Section AB: As the load increases, adhesion breaks down and the bond mechanism changes. The slip at the loaded end of the bar gradually increases and the deformations of the bar develop bearing stresses due to reaction against the surrounding concrete. The principal tensile stress caused by bond stresses reaches the tensile strength of concrete and microcracks initiate at the tips of the bar deformations (Fig. 7.2-2), which allow the bar to slip. However, since the surface deformations of FRP bars are much "softer" than the deformations of steel bars, it is believed that the initiation of

Copyright fib, all rights reserved. This PDF copy of fib Bulletin 10 is intended for use and/or distribution only by National Member Groups of fib.

transverse microcracks is relatively delayed. Tepfers (1997) even suggests that the bond behaviour of FRP bars, at this stage, is better than that of steel deformed bars.

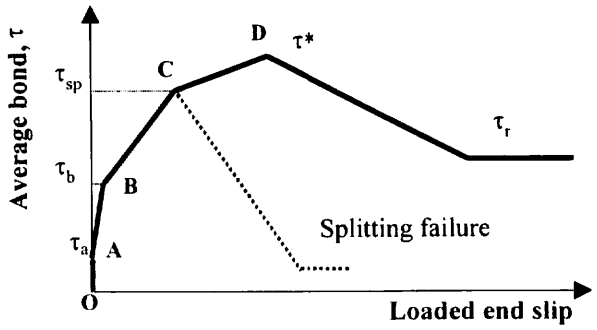

Fig. 7.2-1: Typical average bond stress versus loaded end slip curve of an FRP short embedment, Achillides (1998)

Section BC: At this stage, the bearing stresses from the bar deformations to the surrounding concrete increase considerably, as the slip of the bar increases. The principle direction of these stresses is assumed to subtend an angle α to the horizontal (see Fig 7.2-3). The value of angle α is believed to depend on the value of the elastic modulus of the bar, the shear strength of concrete at the location of the microcracks, Achillides (1998) and the type of the bar surface, Tepfers (1997). The radial component from the bond forces is balanced against rings of tensile stresses developed in the surrounding concrete (Fig 7.2-3).

The splitting resistance of the concrete surrounding the bar is decisive at this stage. The possible ultimate crack pattern giving minimum splitting resistance against the radial pressure generated by bond force determines the anchorage capacity. Confinement by the surrounding concrete mass, transverse reinforcement and pressure, applied externally to the anchorage zone, influence the splitting resistance.

If the bar is not adequately confined and the value of the tensile hoop stress exceeds the tensile strength of concrete, splitting cracks may develop along the length of the reinforcing bar as shown in Fig 7.2-4. When the splitting crack propagates through the entire cover of the embedment, the displacement between the bar and the concrete increases considerably and results in evenly distributed bond stresses along the anchorage length (see Fig 7.2-5). The radiating bond forces are now resisted by the tensile strength of the surrounding concrete in an ultimate failure crack pattern. The ultimate crack pattern is determined by the geometry of the concrete member section and depends upon the location of the crack (Fig 7.2-6).

Section CD: If sufficient resistance to splitting can be provided by the surrounding concrete, as for example in the case of short embedments in pullout cube tests, then the bond stress can reach the maximum bond strength, τ^*. At this stage, both the loaded and unloaded ends of the bar are slipping and bond stiffness is significantly decreased. Depending on the relative magnitude of concrete strength as compared to the shear strength of the surface bar deformations, four modes of bond failure are identified as:

1. *Shearing off part of or all the surface deformations of the bar* - The bond strength of FRP bars in this case is not controlled by the concrete strength, but appears to be governed either by the interlaminar shear strength between successive layers of fibres or by the shear strength of bar deformations. Therefore, unlike steel bars, an increase in concrete strength will not be accompanied with a corresponding noticeable increase in the bond strength of the FRP bar. This type of bond failure will yield the highest possible bond resistance from a bar.

2. *Concrete shear failure* - With failure occurring in the concrete this mode of failure is similar to that of deformed steel bars. The concrete is crushed in front of the bar deformations and the bond strength is controlled mainly by the shear strength of concrete.

Copyright fib, all rights reserved. This PDF copy of fib Bulletin 10 is intended for use and/or distribution only by National Member Groups of fib.

3. *Combined mode* - A combined mode of the above failures is likely to develop for intermediate levels of concrete strength.

4. *Squeeze through* - The bar could "squeeze through" the concrete due to its low stiffness in the radial direction. Bond resistance is provided by friction through wedging of the bar deformations on the surrounding concrete. The bond is much more ductile in this case and the maximum bond strength developed can be quite significant depending on the geometry of the bar deformations, the radial stiffness of the bar and the amount of concrete confinement provided.

Section DE: After attaining the maximum bond stress, the bearing mechanism between bar deformations and concrete corbels breaks down and the bond stress decreases considerably. The residual bond strength mainly depends on the frictional resistance, τ_r, at the failure interface. The roughness of this interface determines the magnitude of 'τ_r'.

7.2.2.3 Spliced bars

The bond resistance of spliced bars is influenced by the same parameters as anchorage. Side by side lapped bars, however, are thought to lead to increased side pressure due to "double slip" between bars.

It is recommended that the confining reinforcement along the lap length be concentrated at the lap ends to discourage development of longitudinal cracking, since those are locations of maximum bond demand at the serviceability stage. For bars in compression, confinement is recommended just outside the lap, because the bearing pressure from the tip of the bar will induce splitting forces in front of the bar end, Cairns (1979). However, it should be noted that FRP bars are not as efficient in compression, since the magnitude of potential compressive strains in concrete is relatively low compared to strains that develop under tension.

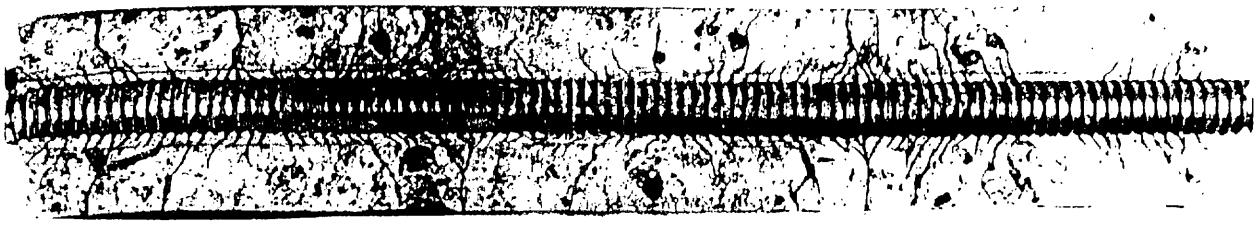

Fig. 7.2-2: Internal cracking around a bar due to bond forces surpassing the principal tensile stress of concrete. Courtesy Y. Goto (1971)

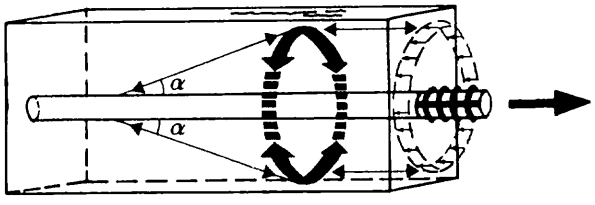

Fig. 7.2-3. Schematic representation of how the radial components of the bond forces are balanced against tensile stress rings in the concrete in the anchorage zone, Tepfers (1973)

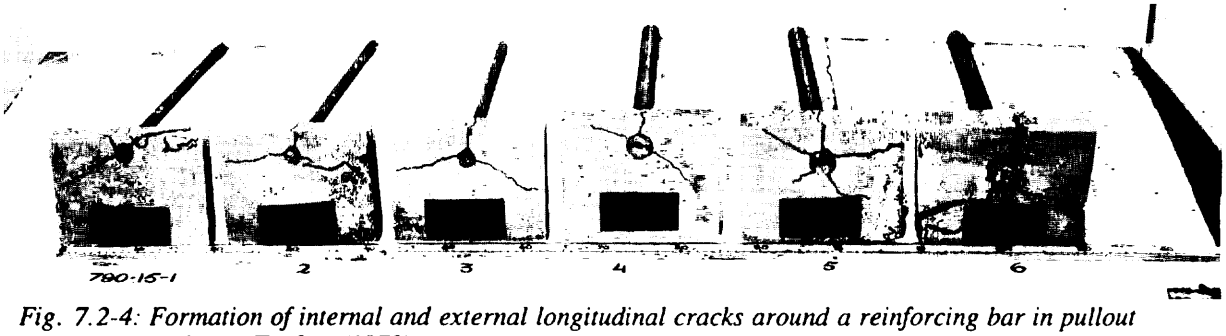

Fig. 7.2-4: Formation of internal and external longitudinal cracks around a reinforcing bar in pullout specimen, Tepfers (1973)

Copyright fib, all rights reserved. This PDF copy of fib Bulletin 10 is intended for use and/or distribution only by National Member Groups of fib.

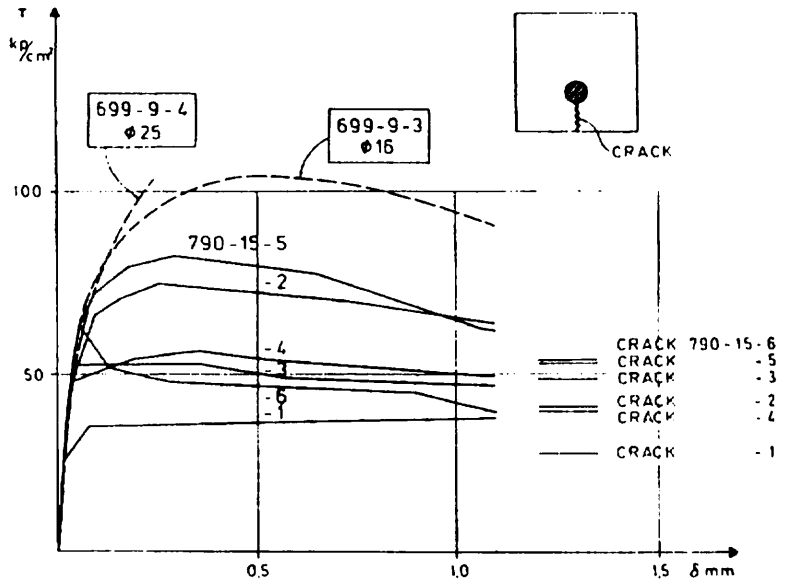

Figure 7.2-5: Bond stress-free reinforcing bar end slip in pullout specimens. The bond stress levels for cracking of the concrete cover are marked for the specimens in the diagram, Tepfers (1993)

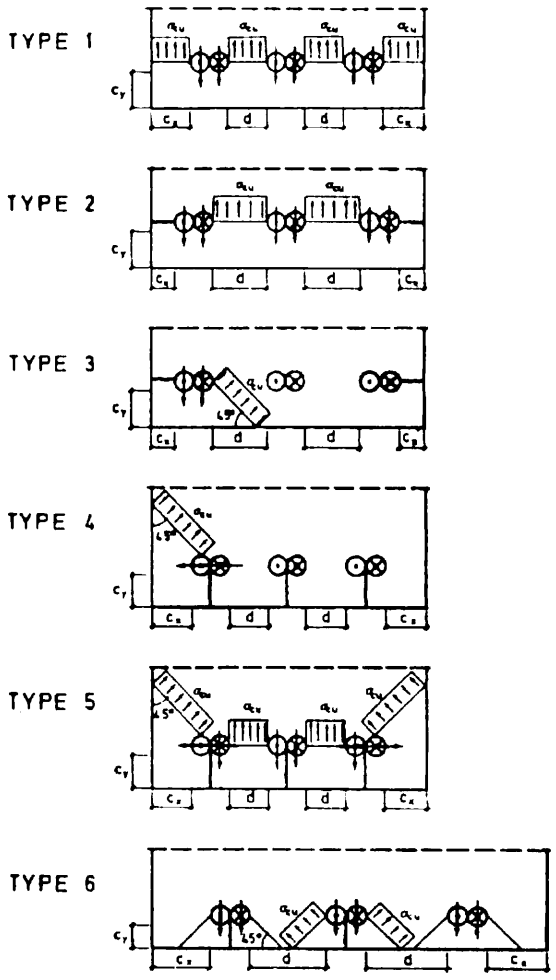

Figure 7.2-6. Possible ultimate splitting failure crack patterns for overlapped reinforcing bars, Tepfers (1973).

7.2.3 Parameters affecting bond of FRP reinforcement

The bond behaviour of steel bars depends on many parameters that influence the strength and ductility of anchorages in concrete. Those parameters are expected to have a different effect on the

Copyright fib, all rights reserved. This PDF copy of fib Bulletin 10 is intended for use and/or distribution only by National Member Groups of fib.

bond behaviour of FRP bars, since FRP materials are strongly anisotropic and have different mechanical properties compared to steel. A proper evaluation of the influence of these factors on bond development is crucial to the understanding of bond behaviour and in determining the required anchorage lengths. The most important of those parameters are presented below.

7.2.3.1 Shape of the bar cross section

The shape of the cross section determines the bonded area and, hence, affects the bond behaviour. Achillides, Pilakoutas and Waldron (1997) reported that square bars develop higher bond strength than round bars under full confinement conditions. This is due to their edgy cross section which enhances the wedging effect and, hence, their bond resistance to concrete. However, in comparison to circular bar sections, flat bars might exert increased splitting forces from the flat surfaces on concrete in anchorage zones. When splitting cracks occur, slip increases and the ultimate bond resistance is affected. Shapes with flat surfaces can be provided with shear connectors and FRP strings for improved anchorage in concrete, Kettil (1995).

7.2.3.2 Bar deformations

Surface deformations are the source of surface roughness for the FRP bar and, thus, are important in developing mechanical anchorage and in mobilising lateral pressure. Surface deformations could consist of just resin, fibre-reinforced resins, or resin containing longitudinal continuous fibres. The latter type is achieved by braiding the fibres or by winding the rod with a separate fibre filament. However, when the longitudinal fibres are brought out of the direction of the bar axis by braiding or by press-deforming the longitudinal fibre (for example, this occurs when winding a fibre bundle), the axial stiffness of the rod decreases.

Small dense surface deformations give a very intense bond transfer at low loads. However, at higher loads, the bar becomes thinner due to the Poisson effect and splitting cracks may develop in the concrete cover along the reinforcing bar. Under these circumstances, small deformations may suddenly lose their grip in concrete resulting in bond failure, while bigger ribs may still be active. To avoid such problems, Malvar (1995) suggested that surface deformations of about 5.4% of the bar diameter are sufficient to provide adequate bond behaviour to concrete.

If the shear resistance of surface deformations determines the bond strength, an increase of the deformation depth should increase the shear resistance. Because the spaces between deformations or lugs are filled up with concrete that takes up the lug pressure, shear failure (local compression) of the concrete corbels could be encouraged, if these spaces become too small. Moreover, due to the smaller perimeter, it is expected that bond shear stresses at the base of the deformations are higher than at the top, where the concrete bond shear failure is expected to take place.

The size and inclination of surface deformations, not only determines the magnitude of mechanical lock, but also the magnitude of splitting forces. For example, although bars with large deformations supply high bond resistance under fully confined conditions, they show a much higher tendency for causing splitting failure and, hence, have a lower bond resistance to splitting than sand-coated bars.

The roughness of bars is another parameter that appears to affect splitting resistance. Rough surfaces appear to resist the splitting movement and enhance splitting resistance, whereas smooth surfaces appear to encourage splitting. This was also observed in epoxy-coated bars.

Depending on the materials used, there is an optimum deformation shape for maximum bond, which should be pursued by the bar manufacturers.

7.2.3.3 Low elastic modulus in the axial direction

Achillides (1998) suggested that the elastic modulus of reinforcing bars plays an important role in their bond splitting strength. The deformability of the reinforcement determines the crack geometry, spacing and crack-width and, consequently, affects the concrete shear transfer along cracks. These factors were demonstrated analytically to influence the ultimate splitting tendency of

Copyright fib, all rights reserved. This PDF copy of fib Bulletin 10 is intended for use and/or distribution only by National Member Groups of fib.

the bars. Bars with lower elastic modulus (e.g. GFRP, E=45GPa) were also found to develop higher splitting stresses and, consequently, lower bond strength than bars with a higher elastic modulus (e.g. CFRP, E=115 GPa).

7.2.3.4 Elastic modulus of the bar in the transverse direction

The elastic modulus of the bar in the transverse direction also appears to influence the bond splitting tendency of FRP bars. It has been observed that certain types of FRP bar give higher bond cracking resistance than corresponding steel bars ,Tepfers (1997). This is probably due to the fact that FRP bars have transverse modulus of elasticity similar or even less to that of concrete. *Since* FRP bars are much more "squeezable" than steel bars, the FRP bar deformations do not create as intense stress concentrations in concrete as steel bars do. As a result, certain FRP bars may show a lower cover splitting tendency and, thus, higher splitting strength than steel bars. However, as mentioned above, this may depend on the surface texture as well.

7.2.3.5 Transverse pressure

It is known that transverse pressure improves the anchorage capacity of steel rebars. Even though the same is expected for FRP bars, Achillides (1998) suggests that any transverse pressure applied, either externally or internally, is less efficient for anchoring FRP bars than for steel bars before any splitting cracks are initiated in the concrete. This may be attributed to the lower modulus of elasticity in the transverse direction of FRP bars, which means that the transverse pressure is dissipated near the bar surface.

7.2.3.6 Poisson effect

For most FRP materials, the Poisson ratio is about the same as for steel. Hence, at high longitudinal strains, the transverse deformation of FRP bars is expected to be higher than that of similar steel bars and may affect bond. Clearly, the pullout or push-in conditions (for example at development of a pre-stressing force) will affect bond differently. Push in conditions are favoured by the Hoyer effect, which is more pronounced for FRP bars.

Hence, for pre-tensioned reinforcement, the development length could be estimated by using an accepted force-spreading model. Confinement against the splitting tendency may be quantified based on general recommendations, whereas confinement against bursting may be based on the symmetric prism method. The required confinement to preclude spalling should be estimated from analysis of the "loaded prism model".

7.2.3.7 Position of the bar in the cross-section

The position of bar during casting in concrete (top or bottom bar position, and horizontal, inclined or vertical bar position) influences the bond interaction between concrete and bar. This influence should be determined for each type of FRP bar.

7.2.3.8 Wedging effect

It has been observed that the wedging effect increases the anchorage capacity of seven wire steel strands above that of deformed bar with increasing slip, Jokela & Tepfers (1982). This wedging effect does not appear in FRP strands due to the considerably lower surface hardness and the Poisson effect. However, Achillides, Pilakoutas and Waldron (1996), observed a significant increase in the bond strength of EUROCRETE FRP bars embedded in a concrete slab, due to artificially mobilised wedging action.

7.2.3.9 Bends in anchored bars

Anchorage of bent bars is affected by the change of direction of the fibres at the bend, which leads to lateral stress concentrations and, hence, lower axial strength. The strength of the bar at the bend is also dependent on the way the bend is made. In twisted thermoplastic bars, it is possible that the fibres are buckled on the inner side of the bend and broken on the outside (tension face).

Copyright fib, all rights reserved. This PDF copy of fib Bulletin 10 is intended for use and/or distribution only by National Member Groups of fib.

7.2.3.10 Concrete cover and distances between parallel bars

Concrete cover is an important design consideration to prevent bond splitting. Although the required concrete cover for steel bars is rather controlled by the requirement to protect the bar from aggressive environmental conditions, the structural role of concrete cover appears to be the more critical for FRP bars. Since certain FRP bars generate higher splitting forces in concrete than the respective steel bars, the need for greater concrete covers is evident. Sufficient concrete covers should also be determined for environmental and fire protection of the FRP bars. Indications exist that covers with thickness greater than 4 diameters are satisfactory for anchorage of prestressed FRP strands.

7.2.3.11 Thermal expansion

Differences in thermal expansion between the FRP unit and concrete, especially in the transverse direction, might influence bond. Too high transverse thermal expansion of the bar might give rise to splitting cracks in concrete surrounding the bar. However, FRP rods are transversally flexible enough not to cause splitting of the concrete cover when trying to expand. The lateral thermal expansion may also be counteracted by the Poisson contraction of tensioned rods. If the surface of bar deformations or lugs is of sufficient size, the difference in thermal elongation between concrete and FRP rod is not expected to affect bond.

7.2.3.12 Environmental influence on bond

Environmental influence on bond between FRP bar and concrete should also be taken into consideration. Absorption of water leading to strength and modulus deterioration as well as expansion of the rod, might influence the bond resistance. The highly alkaline environment in concrete (pH-values 12-13.5), might degrade the rod surface or fibres, especially in warm and wet environments. Sometimes less resistant fibres are protected by resistant, thick resin layers. Hence, it is important to identify the level at which bond transfer becomes critical and to develop degradation models for both resin and fibres. The environmental conditions during construction, transportation and handling should also be considered. Finally, it is important to note that FRP materials might need protection against exposure to UV radiation.

7.2.3.13 Bar diameter

The bar diameter appears to play an important role in the bond behaviour of FRP bars to concrete. It is reported that larger diameter bars develop lower average bond strength than smaller diameter bars, Achillides, Pilakoutas and Waldron (1997). Bond development in FRP bars is affected by the diameter, due to their low shear stiffness in the axial direction. The value of the shear stiffness of FRP bars depends mainly on the shear stiffness of the bar resin and the shear strength capacity at the resin-fibre interface. When an FRP bar is pulled in tension through the surface, there can be a differential movement between the core and the surface fibres, which results in a non-uniform distribution of normal stresses through the cross section of the bar. This point is illustrated by the idealised stress distribution of Fig. 7.2-7.

The actual developed bond strength between the bar and the concrete is directly related to the value of the normal stress that occurs close to the surface of the bar (σ_{max}). On the other hand, the calculated bond strength that the user anticipates as the "real" bond strength, is proportional to the value of the average normal stress over the whole cross section of the bar (σ_{av}). As the diameter of the bar increases, the difference between σ_{max} and σ_{av} is also expected to increase, especially when the axial shear stiffness of the bar is relatively low as in the case of FRP bars, and the "real" bond strength of the bar decreases. This effect, known in the literature as the "shear lag effect", appears to be more significant for higher normal bar stresses which usually happen at greater embedment lengths. For steel bars, this effect is less important, since the shear strength of steel is significantly higher.

Copyright fib, all rights reserved. This PDF copy of fib Bulletin 10 is intended for use and/or distribution only by National Member Groups of fib.

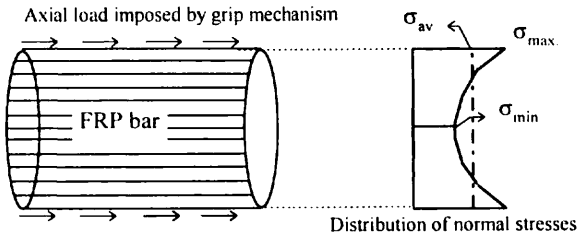

Fig. 7.2-7: Indicative distribution of normal stresses on a FRP bar cross-section subjected to axial load, Achillides (1998)

7.2.3.14 Concrete strength

Results in the literature showed that the strength of the surrounding concrete is directly related to the actual mode of bond failure of the bar during pullout. As explained earlier, the value of concrete strength relatively to the shear strength of the surface bar deformation affects the mode of bond failure of FRP bars. Fig. 7.2-8 shows the effect of concrete strength on the bond strength of EUROCRETE bars. For concretes with compressive strengths greater than 30 MPa, the bond failure interface occurs in the surface of an FRP bar. Consequently, the bond strength of FRP bars does not depend on the value of concrete strength, as far as the concrete strength is greater than 30 MPa. However, for lower concrete strengths (around 15 MPa) the bond failure mode changes. In this case, the failure interface occurs in the concrete matrix and the bond behaviour of the bar is directly related to the bond strength.

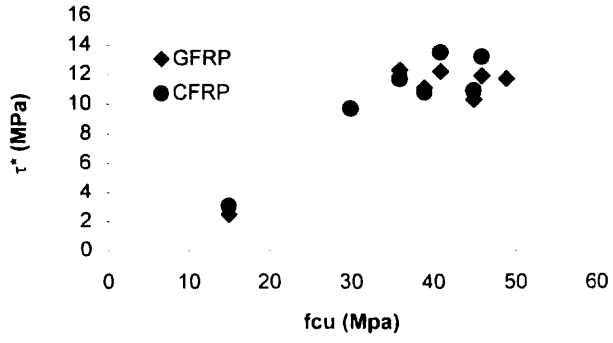

Fig. 7.2-8: Influence of concrete strength on the bond strength of EUROCRETE FRP bars, Achillides, (1998)

7.2.3.15 Transverse reinforcement

Achillides (1998) investigated the influence of transverse reinforcement on the bond splitting strength of FRP anchorages and splice regions. It was found that shear links (transverse reinforcement) could enhance the splitting resistance of the concrete surrounding the bar, only when these have already been stressed (for example, when they are located in the shear zone of the beam). Otherwise, the initiation of splitting cracks does not seem to be influenced by the presence of shear links due to the low strain at which tension cracks form in concrete. However, after the initiation of splitting cracks, the transverse reinforcement arrests the crack propagation and restrains further opening of the crack, thereby contributing to the splitting bond strength of the reinforcing bar.

7.2.4 Testing of bond performance of FRP bars/rods/strands

A framework of testing procedures is presented below for the estimation of bond performance of FRP bars/rods/strands in concrete, taking into account the parameters affecting bond as discussed in the preceding section.

In the JSCE (Japan Society for Civil Engineering) recommendations for design using FRP materials, JSCE (1997), a pullout bond test, with short bond length using a relatively small concrete cube specimen, is proposed. To avoid splitting failure, the cylinder is reinforced with spiral

Copyright fib, all rights reserved. This PDF copy of fib Bulletin 10 is intended for use and/or distribution only by National Member Groups of fib.

reinforcement. However, the recommendations make it clear that bond performance obtained from this test can only be used for relative comparisons. Other tests, such as push-out, double sliding testing and beam tests, have advantages and disadvantages and should be used for more complete information on bond.

7.2.4.1 Determination of local bond slip relationship

1) Pullout tests with concentric bar placement

Pullout tests with concentric bar placement in concrete can be used for experimental determination of the local bond slip relation between bar and concrete. The confining action provided by the surrounding concrete mass or reinforcement should be adequate so as to mitigate the risk of splitting the concrete by bond forces. The bond length should be such that the bond stresses are evenly distributed in all loading stages. In most cases, this means that the anchored length should be between 3 and 5 bar diameters. The experimentally measured bond strength by this test represents the greatest value possible between bar and unconfined concrete. The type of bond failure, such as, concrete shear failure, shearing off of the surface deformations of the bar, or squeezing out the bar from the concrete, should be recorded.

For the pull-out test, the bond length is normally situated in the central part of the concrete body. Fig. 7.2.9 shows the two main types of tests used for evaluating the bond strength of steel bars. Their main difference is the location of the embedment length inside the concrete cube. Various views are expressed in the literature as to which test is more appropriate for deformed steel bars. Nevertheless, it is widely accepted that only minor differences exist among the results of those tests. No significant change is expected for the values of the maximum bond strength, τ^*, or the residual bond strength, τ_r.

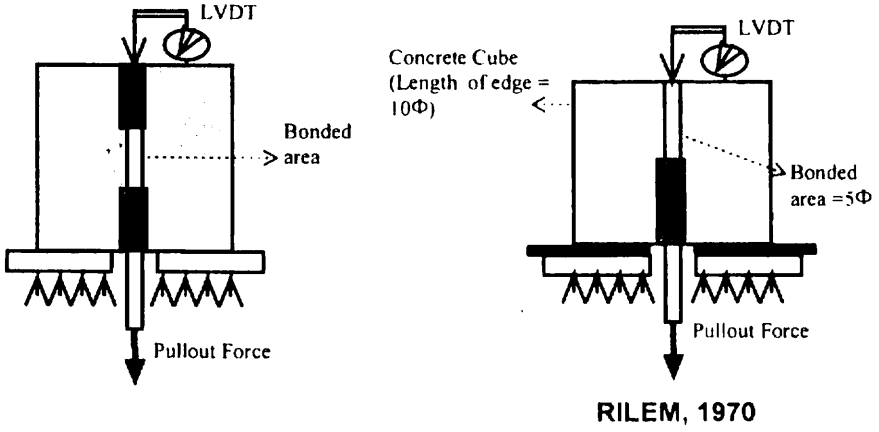

Fig 7.2-9: Two types of common pull-out tests used for steel bars

With FRP bars, however, things appear to be different. Their different mode of failure renders the measured bond strength dependent on the experimental arrangement used. For example, the experimental arrangement by Rehm (1961) and Losberg (1962), overestimates the bond strength during pullout. This is because bond failure occurs most frequently at the bar surface and as the undamaged part of the bar, that follows the embedded part, encounters the embedment length zone, it adds resistance to the pullout load. This results in an erroneous increase in the recorded bond values, which does not reflect the real bond characteristics of the bar (Achillides, Pilakoutas and Waldron, 1998). So, in the case of FRP bars, an experimental arrangement with the embedded part of the bar lying at the very end of the cube, similar to RILEM test, is more likely to lead to reliable pullout bond results. In this case, no part of the bar should protrude from the cube.

Fig. 7.2-10, shows typical bond stress-slip characteristics obtained from pull-out tests on the following bars: 15 mm GFRP (Hughes Brothers), 15 mm C-BAR, Hedlund and Rosinski (1997), 15 mm C-BAR, Karlsson (1997), 16 mm Swedish Ks400 and Ks600 steel bars, Berggren (1965), Tepfers (1973), 7 wire 12.5 mm steel strand Jokela and Tepfers (1982), CFCC (Carbon Fibre Composite Cable) 12.5 mm cable and an Arapree 2x20 mm strip, Tepfers, Molander & Thalenius (1992). The

Copyright fib, all rights reserved. This PDF copy of fib Bulletin 10 is intended for use and/or distribution only by National Member Groups of fib.

bonded lengths were in the range of 45 to 50 mm. The concrete compressive strengths for the specimens were in the range of 43-48 MPa. It can be seen from the figure, that at the beginning of loading, the GFRP bar appears to have a stiff behaviour. However, at increased loads, the GFRP bar shows considerable slip and ductility. The behaviour of the GFRP bar is similar to that of the Arapree strip in the early stages of loading. The GFRP bar specimen reached its ultimate bond strength at a slip of 4 mm. The bond strength level was similar to that of a CFCC strand. The C-BAR had the same bond stress-slip relation as the Ks600 steel bar in a pullout test with full concrete confinement, despite the fact that the steel bar had a higher relative rib area according to DIN 488 (0.13) than the C-BAR (0.08). The CFCC cable and the Arapree strip, shown in the figure as scatter bands from several tests, indicate a stiff initial response but their stiffness reduces substantially after initial slip.

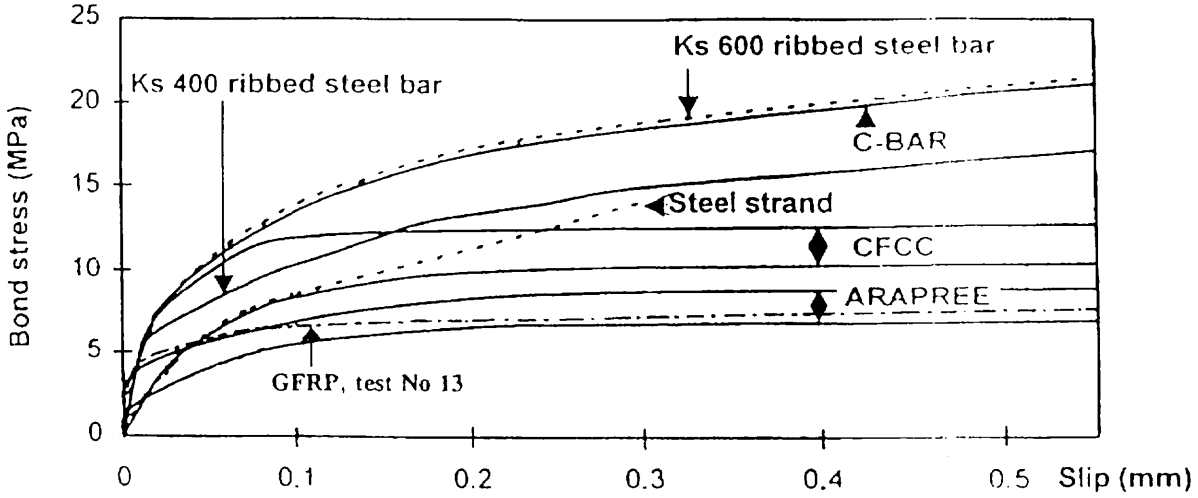

Fig 7.2-10: Bond stress-slip relation of GFRP, Ks400, Ks600 steel reinforcing bar, C-BAR all diameter 15-16 mm, 12.5 mm CFCC cable and 7-wire steel strand and Arapree 2x20 mm2 strip. fcc = 43-48 MPa.

2) Pullout tests with eccentric placement of bar

For the estimation of the concrete splitting tendency due to bond forces, a pullout test with eccentric placement of bar can be used, as illustrated in Fig. 7.2-11. The cover thickness is usually 1.5 bar diameters. The bond length should be between 3 and 5 bar diameters, such that the bond stresses are evenly distributed at all loading stages. The height of the pullout specimen should be the same as the bond length. For the determination of the local bond slip relation, the load should be registered at characteristic points, such as, when the concrete cover cracks along the bar and when the concrete surrounding the bar is pushed off. Performance should be compared to that of standard steel rebars, which provide a well-established point of reference.

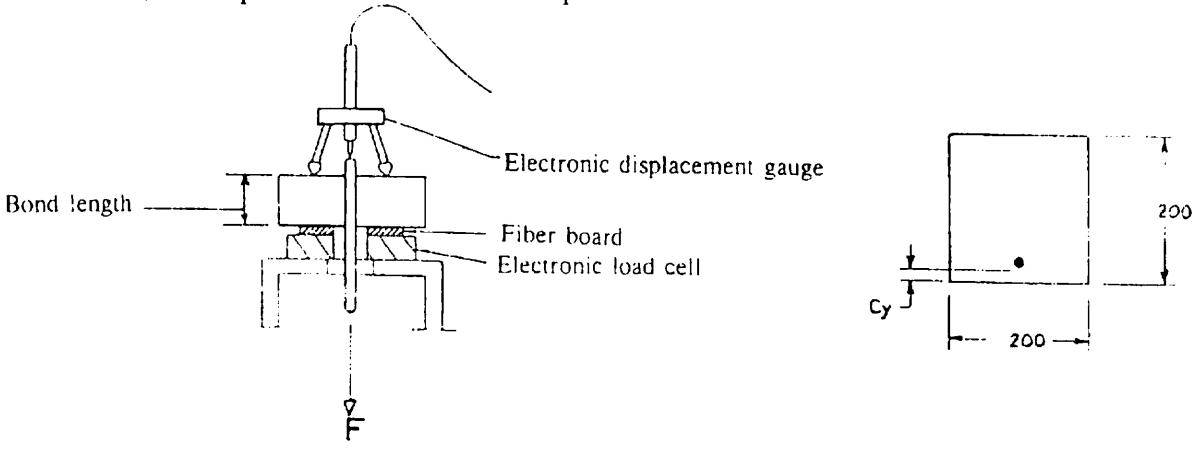

Fig 7.2-11: Pullout test with short bond length and eccentric placement of bar, Tepfers (1997)

Fig. 7.2-12 shows the relation between bond stress, f_{cbc}, at cover cracking along the bar, and concrete tensile stress, f_{ct}, as a function of concrete cover thickness, c_y, normalised with respect to the bar diameter. Tepfers (1973, 1979) developed predictive equations for f_{cbc} at the elastic stage,

Copyright fib, all rights reserved. This PDF copy of fib Bulletin 10 is intended for use and/or distribution only by National Member Groups of fib.

partly cracked elastic stage and plastic stage for the reaction force at an angle α = 45°, as illustrated in Fig 7.2-3. Results from tests with Swedish Ks600 steel bars and C-BARs, fall between the partly cracked elastic and plastic stages, Karlsson (1997). However, the C-BAR results are closer to the plastic stage. Results from tests by Hedlund and Rosinski (1997) on the GFRP bar are grouped above the line that corresponds to the plastic stage. However, good agreement is achieved if, for the plastic stage, angle α is changed to 30°, as shown by the dotted line. Therefore, it may be concluded that these particular GFRP bars with a sand coated surface exert a lower lateral splitting pressure against the surrounding concrete than the bars with a large indentations.

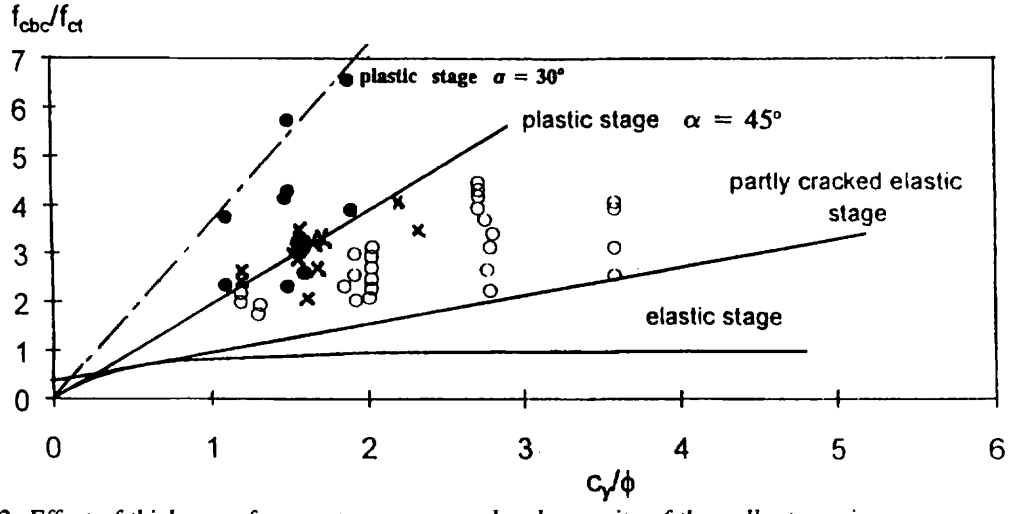

Fig 7.2-12: Effect of thickness of concrete cover upon bond capacity of the pullout specimens on occurrence of concrete cover crack along the bar. Open circles Ks600 steel reinforcing bars, closed circles GFRP bars (Hughes Brothers) and cross marks C-BARs ,Tepfers (1997)

3) Ring pullout test

The angle, α, of the bond forces, at different stages of loading, can be estimated using the "Ring Pullout Test", Tepfers and Olsson (1992). The ring pullout test comprises of a small cylindrical concrete body confined by a thin steel cylindrical shell, with an axially placed bar, as illustrated in Fig. 10. The bond length is short and the height of the concrete cylinder is equal to the bond length. The circumferencial strain on the steel cylinder is measured with strain gauges. During loading, the pullout specimen is supported close to the bar by a ring support with several teflon sheet layers in between the concrete and the supporting steel ring. To have a well-established reference, comparison of performance should be done against standard steel reinforcing bars. The load-displacement curve for a "Ring Test" is shown schematically in Fig. 7.2-13. At load 'F_r', there is an increase in displacement due to the radial cracking of the concrete specimen. This displacement increment, , mobilises the confinement mechanism of the steel ring. Once the steel ring is stressed, the pull-out specimen recovers its stiffness.

The angle, α is evaluated from the measurements by using the following procedure. The bond stress, τ, in the direction of the bar can be found by:

$$\tau = F/\pi\phi h \qquad (7.2\text{-}1)$$

The lateral bond stress component orthogonal to the bar axis, can be found by the resolution of forces as $\tau \tan \alpha$. If it is assumed that the lateral bond forces act as hydraulic pressure through the concrete against the steel ring, then:

$$\tau \tan \alpha \; \phi \; h = 2\varepsilon_{rs} \, E \, h \, t \qquad (7.2\text{-}2)$$

Hence, solving for α:

$$\alpha = \arctan (2\varepsilon_{rs} \, E \, t / \tau\phi) = \arctan (2E \, t \, h \, \pi/F) \qquad (7.2\text{-}3)$$

Copyright fib, all rights reserved. This PDF copy of fib Bulletin 10 is intended for use and/or distribution only by National Member Groups of fib.

where, E = Modulus of elasticity of steel,
ε^{rs} = Tangential strain of steel ring,
t = Thickness of steel ring,
h = Height of steel ring,
φ = Diameter of reinforcing bar,
F = Pulling force in direction of bar.

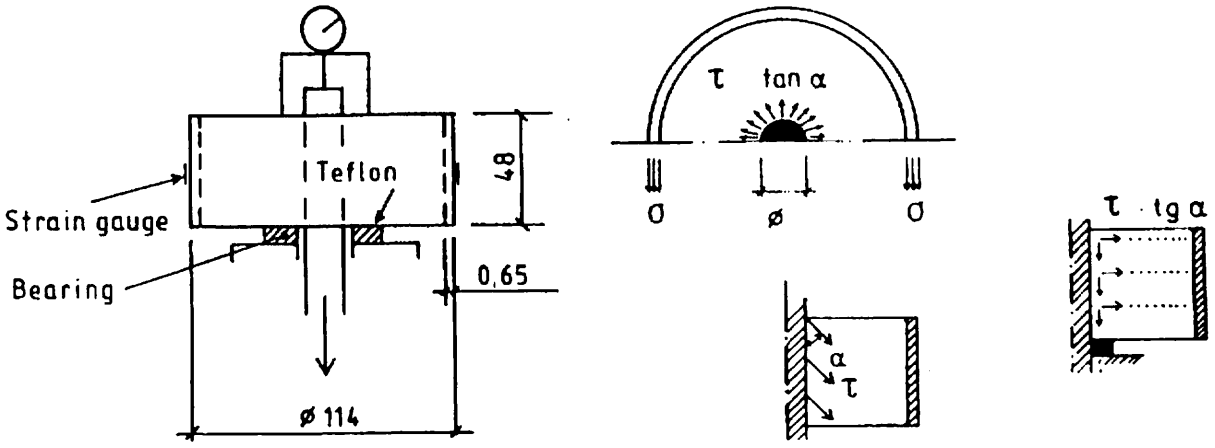

Fig 7.2-13: The "Ring Test" specimen and arrangement, Tepfers and Olsson (1992)

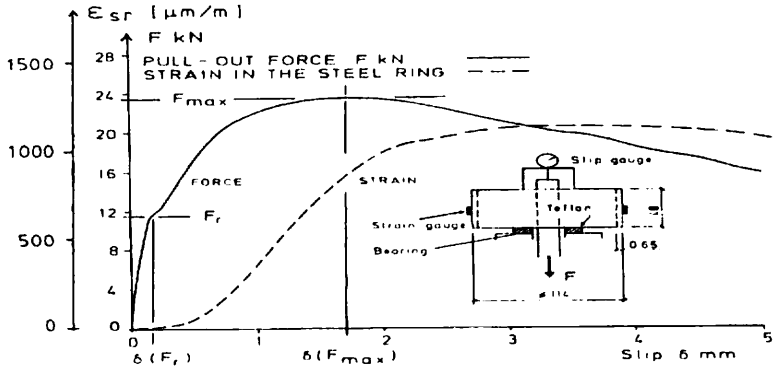

Fig 7.2-14: The load-displacement curve for a "Ring Test", Tepfers and Olsson (1992)

7.2.4.2 Tests to determine bond performance in practice

1) Overlap splice tests

Tensile overlap splice tests are normally performed on four point loaded concrete beams. The lap splices are situated in the constant moment zone, between symmetrically applied point loads. It is preferable for the beam to be loaded upside down, since the disturbing influence of self-weight can be practically ignored and the moment along the lap length becomes almost constant. In addition, it is easier to study the development of flexural and concrete cover cracks. Again, comparison of performance should be done with standard steel reinforcing bars.

Copyright fib, all rights reserved. This PDF copy of fib Bulletin 10 is intended for use and/or distribution only by National Member Groups of fib.

With this test, it would be possible to determine the splitting tendency of bars, since it is reported that bars with lower pull-out bond strengths can still behave better under these conditions than bars with higher pull-out strengths. Fig. 7.2-15 shows the failure stress in the lapped Swedish Ks600 tensile reinforcement for 520 mm long overlaps, tested using concrete of different compressive strengths, Tepfers (1973). The vertical concrete cover varied between 16 and 24 mm and the horizontal between 26 and 37 mm. The results from the tests with C-Bar overlaps are made with splice lengths of 0.40, 0.60 and 0.80 m and are also shown in the diagram, Karlsson (1997). At a splice length of about 0.52 m, the C-Bar developed only 70% of the corresponding stress level in Ks600 bars. Decreasing bond stress levels for Ks600 bars with concrete strength exceeding 100 MPa depend on high cement content in concrete and by this caused ring shrinkage stresses. These stresses add to bond splitting stresses and decrease the bond resistance.

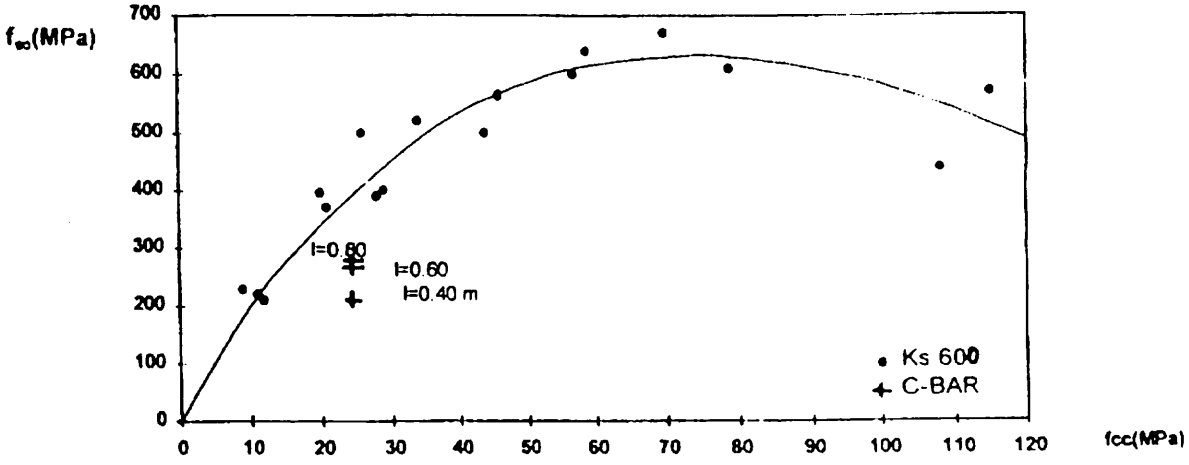

Fig 7.2-15: Ultimate stress in lapped tensile reinforcement versus concrete compressive strength for Swedish Ks600 reinforcing bars and for C-BARs, Tepfers (1997)

2) Tension stiffening performance of bars/rods

The tension stiffening effect can be estimated by embedding bars in a square concrete block. The dimensions of the block should be at least 7 ϕ x 21ϕ x 1500 mm, where ϕ is the bar diameter. The protruding ends of the bar are clamped in the pulling machine. The concrete crack development, distances and width may be studied when the bar ends are pulled up to the ultimate load and conclusions can be drawn concerning the tension stiffening effect.

3) Bond in region of support - transverse compression

Simply supported beam-ends with reinforcing bars anchored just above the supports can be used for the determination of bond under transverse compression, as illustrated in Fig. 7.2-16, Magnusson, (1997). The bars are totally free between the anchorage regions. The beam is split into two equal parts, to allow for the exact determination of the compressive force. This statically determinate construction is loaded in a symmetric four-point load system. Bar bending in the anchorage zone should be avoided by a distance holder or hinges. This test could also facilitate the study of several layers of anchorage bars.

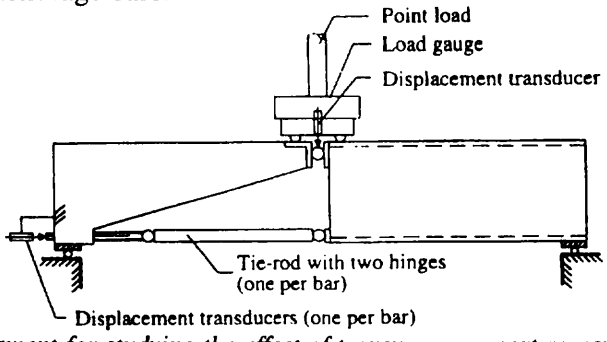

Fig 7.2-16: Testing arrangement for studying the effect of transverse support pressure on the anchorage f tensile bars, Magnusson (1997)

Copyright fib, all rights reserved. This PDF copy of fib Bulletin 10 is intended for use and/or distribution only by National Member Groups of fib.

4) Transfer length for prestressing force

The transfer length can be estimated by embedding the prestressing strand in a square concrete block. The dimensions of the block should be at least 7φ x 7φ x 2000 mm, where is the diameter of the strand. The strand should be prestressed to about 65% of the fracture load with a jacking device and then locked before casting the surrounding concrete. After hardening of the concrete, strain gauges are placed on both ends of the specimen at 50 mm spacing along the line of the strand for a length of at least 70 . Strain measurements taken before and after release of prestress can be used to estimate the transfer length.

Tepfers, Molander and Thalenius (1992) performed tests on such specimen. The rods were axially prestressed with one 12,5 mm CFCC cable. The concrete compressive strength was f_{cc} = 39.4 MPa. At the ends of the concrete rod, the CFCC cable was surrounded by spiral confining steel of ϕ6 Ss260 over a 700 mm long segment. The prestressing force was 83.0 kN (59% of ultimate capacity). Concrete strains were measured along the end 700 mm of the specimen during the release of the prestressing force. It was concluded that 400 mm are needed to transfer the full prestressing force to the concrete from a 12.5 mm CFCC strand (Fig. 7.2-17).

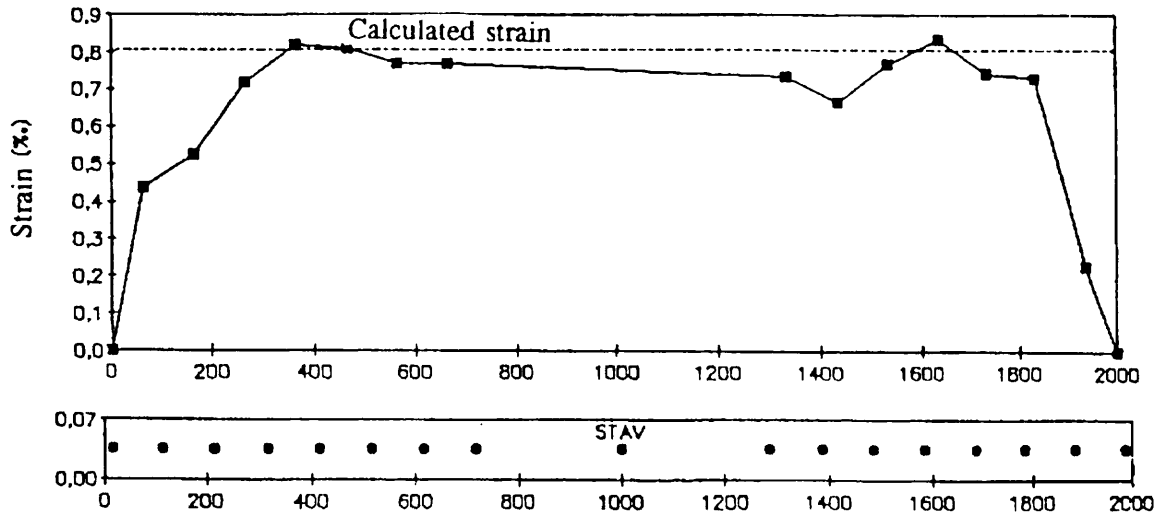

Fig 7.2-17: Specimen for determination of transfer length for prestressed FRP strand, Tepfers, Molander and Thalenius (1992)

7.2.5 Conclusions

The main conclusions from chapter 7.2 are given below.

1. The bond behaviour of FRP bars/rods in concrete is expected to differ from that of steel due to the different mechanical characteristics of the materials.
2. Different failure modes are possible with FRP materials, which may lead to lower direct pull-out bond strengths.
3. The splitting tendency of bars appears to be influenced both by the surface texture of the bar and the lateral and longitudinal stiffness of the materials. Some FRP bars show a lower splitting tendency than steel bars, whereas smooth bars with large surface deformations demonstrate higher splitting tendencies.

Different tests may be used in order to estimate and better understand the bond performance of FRP bars/rods in concrete, such as given below.

1. Concentric pullout tests with short bond length and adequate concrete confinement generally give optimum bond resistance.
2. Eccentric pullout tests can be used to estimate the concrete cover splitting tendency.
3. The "Ring test" can be used to estimate the lateral pressure on the surrounding concrete from the bond forces at different load levels.

Copyright fib, all rights reserved. This PDF copy of fib Bulletin 10 is intended for use and/or distribution only by National Member Groups of fib.

4. Splice tests can be used to investigate the performance and anchoring capacity of the FRP bars/rods in beams.
5. The influence of bond on tension stiffening can be estimated by studying crack width and crack spacing, using centrally reinforced concrete specimen in tension.
6. The hinged beam test can be used to study the bond in the region of supports, where transverse pressure is available.
7. The transfer length of bonded prestressing FRP cables can be measured on the surface of axially prestressed concrete rods by measuring the concrete strain before and after the release of prestress.

Copyright fib, all rights reserved. This PDF copy of fib Bulletin 10 is intended for use and/or distribution only by National Member Groups of fib.

7.3 Local bond stress-slip relationship

Most current design guide-lines and design oriented research, have adopted and extended the methodologies developed for steel reinforced concrete structures to those reinforced with FRP rebars. However, many experimental studies have demonstrated that some key properties of the physical and mechanical behaviour of FRP rebars are qualitatively and quantitatively different from the well-known properties of steel rebars. Such differences originate either from the significant variations in the material properties or from the difference in the interaction mechanism between the reinforcement and concrete. Therefore, a rational design approach for FRP reinforced structures should be developed based on theories derived for FRP materials. Hence, a better understanding of physical behaviour is needed to assess correctly the dominating factors and their quantitative influence. This should lead to the development of analytical models and new predictive design equations.

Bond between concrete and reinforcing bars is one of the main characteristics determining the behaviour of both reinforced and prestressed concrete structures. In the former case, both at the serviceability and at the ultimate state, the transfer of stresses between the two materials is strongly dependent on the quality of bond. Resisting mechanisms such as bending, shear and torsion are all related to the development of adequate bond. Moreover, many serviceability checks, such as the control of crack width and structural deformation, involve the evaluation of the effects of tension stiffening, which is a phenomenon directly arising from the bond between the two materials. When designing prestressed concrete structures, a key issue to be examined is the transfer of stress from the tendons to the concrete, which is governed by bond mechanisms.

Steel and FRP reinforcement fail in a fundamentally different manner. The philosophy of steel reinforced concrete design is entirely based on the ductile properties of steel, which means the main objective to achieve a ductile flexural failure by suppressing all other possible failure modes. With FRP reinforcement, however, a ductile flexural failure can not be achieved through reinforcement yield. Consequently, the preferred failure mode may be different for different elements. This means that controlled bond failure may be preferable to bar fracture. Clearly, a different philosophy of design is required which requires a more precise understanding of all possible failure modes. Hence, the modification of conventional design practice is not adequate when dealing with FRP reinforcement and this is particularly true when dealing with bond.

In recent years many experimental studies have been conducted to investigate bond between FRP rebars and concrete. Such studies aimed either at understanding the resisting mechanisms activated in pull-out tests or at determining bond-slip constitutive laws. A state-of-the-art review of this research on bond behaviour of FRP rebars with different surface texture is presented in the next section, following a historical sequence. Other parameters affecting the bond characteristics are also examined. Research examining the splitting mode of failure is then examined, followed by a review of local and global analytical bond models. After that, research is presented covering a number of other important topics affecting bond and bond of non-continuous fibre products. At the end follows a general discussion.

7.3.1 Research on bond behaviour

7.3.1.1 Bond strength and characteristics for bars with different surface texture

Itoh, Maruyama & Nishiyama (1989) conducted several experimental tests on aluminum oxide grain covered rebars made of epoxy resin and of different types of fibre (carbon, aramid and glass). Those rebars initially showed good bond performance reaching high values of the peak bond strength (over 11 MPa), but a brittle behaviour was observed as a result of a sudden detachment of the interface between grains and bars.

Daniali (1992) examined the behaviour of E-glass fibre deformed rebars made of vinyl ester resin. The surface deformations of the rebars were made by wrapping a fibreglass strand in a 45° helical pattern. A total of 30 beam specimens were tested and tension and pull-out failure modes

Copyright fib, all rights reserved. This PDF copy of fib Bulletin 10 is intended for use and/or distribution only by National Member Groups of fib.

were observed. In case of pull-out failure, the concrete sheared off the ribs on the surface of the FRP bars, causing large slippage and bond failure.

Tepfers, Molander & Thalenius (1992), performed pull-out tests with short bond length aiming to estimate the maximum bond strength between FRP rods and surrounding concrete and to study the bond-slip relationship. The tests were done on a 7-wire Carbon Fibre Composite Cable (CFCC) and Arapree 2x20 mm^2 strip, both impregnated with epoxy. The concrete used had compressive strength of 48 MPa. The bond-slip relations obtained were compared with those for a ribbed reinforcing bar and a 7-wire steel strand. It was observed that at low loads, the slip of the FRP rods was smaller than that of the steel bars, but for higher loads it increases and surpasses that of steel bars and strands. The authors expected the FRP rods to have larger transverse deformation due to their lower modulus of elasticity combined with a similar Poisson's ratio as steel. This was given as an explanation for the lower ultimate bond strength obtained by the FRP bars.

Faoro (1992) performed several pull-out tests with short embedment lengths to compare the bond behaviour of GFRP sanded rebars with that of GFRP rebars obtained with some different external surface processes (i.e. bars with epoxy powder coating, bars with polyamide sheeting). The following conclusions were reported:

1) Chemical bond (adhesion) is not negligible but, bond resistance is higher in the case of grain covered rods,
2) Peak bond stresses are obtained at higher slip values compared to conventional steel bars,
3) Bond-slip curves of sanded rebars are similar to those obtained for deformed steel rods.

Machida (1993), in the JSCE (Japan Society of Civil Engineers) State-of-art-report, summarized results from Japan on pull-out tests using FRP rods in concrete. The tests were performed in accordance with JSCE standards.For bars with winded spiral fibres as deformation on the surface of bar it was reported that:

1) The free end slip of deformed continuous fibre bars is larger than that of deformed steel bars,
2) If appropriately processed with deformations, continuous fibre bars may be able to provide bond strength of 10 MPa or more,
3) The bond strength of twisted continuous fibre bars is identical or higher than that of PC steel strands,
4) Sand covered continuous fibre bars show good bond performance at the initial stage, but the interface between the sand grains and the bars detaches abruptly, eliminating bond all together,
5) Deformed continuous fibre bars with spiral fibre show different degrees of bond depending on the way the spiral fibres are wound and shaped; however, the detachment of the interface between the bars and the spiral fibres eliminates bond all together.

It was also concluded that, the design bond stress should not be evaluated based on the bond stress occurring at a small slip of 0.002φ or 0.005φ, as in the case of steel bars, since the slip of continuous fibre bars is higher. The bond stress-slip relationship for twisted carbon fibre bars (CFCC) varied with the bond length, but the difference was smaller than that of deformed steel bars. Work was also reported on braided continuous fibre bars with and without sand cover. The results indicated that the sand-covered bars initially had bond resistance identical or greater than that of steel, but the bond stress did not increase with larger deformations. Bars without sand cover registered increased bond stress as deformation increased and the stress ultimately reached higher values than that of sand covered bars.

When three different resins were used (1. rigid epoxy, 2. soft epoxy and 3. Poly para phenelen sulphide) to attach sand grains to the surfaces of continuous fibre bars made from thermoplastic resin reinforced by glass fibres or carbon fibres, the bond strength increased in the order $2 < 1 < 3$. When examined against the absence of sand grains, the advantage of attaching sand grains was found to be significant.

Flat FRP bars were also used to increase the bond area and by providing surfaces with small irregularities to improve bond performance. The flat shape was reported to favour splitting of surrounding concrete by bond forces in the plane of the strip. The many small shallow irregularities are thought to provide a very stiff bond connection, which results in high peak bond stresses

Copyright fib, all rights reserved. This PDF copy of fib Bulletin 10 is intended for use and/or distribution only by National Member Groups of fib.

favouring progressive concrete splitting. When the splitting crack develops the bond resistance drops due to the small surface irregularities, which lead to a loss of grip.

Makitani, Irisawa & Nishiura (1993) performed bond tests by beam specimens to study the bond behaviour of FRP rebars in concrete members. Different types of deformed and sanded rebars were examined made of continuous fibres such as carbon, aramid and glass embedded in a epoxy resin matrix. According to the authors, sanding leads to an increase of chemical bond, resulting in increased bond strength. However, the maximum bond stress develops at very small slip values.

The bond behaviour of deformed rebars was found to be strongly dependent on the activation of the interlocking interaction. The rebar geometry, the concrete properties and the rebar mechanical characteristics, all influence mechanical interlocking. In some cases, FRP deformed rebars do not develop such type of interaction and the bond behaviour only depends on friction and adhesion. A friction type bond behaviour was noticed by Kanakubo et al. (1993) in case of pull-out tests of braided rebars and by Larralde & Silva Rodriguez (1993), in case of GFRP rebars with a spiral indentation. In the latter case, the authors found a slight cracking of the concrete matrix only and, then, concluded that adhesion and friction are the primary component of bond of FRP rebars to concrete.

Malvar (1994, 1995) analysed experimentally the bond characteristics of different types of GFRP rebars with the following different surface deformations:

Type A bars had an external helicoidal tow, which provided both a protruding deformation and a small indentation on the bar surface. An outer layer consisting of exclusively of matrix material (polyester or vinyl ester) was provided around the fibres for additional protection. The deformation width was about 3.2 mm, yielding a clear deformation spacing of 15 mm.

Type B bars had a surface tow stressed during fabrication so indentations were obtained instead of deformations. These bars had large variations in the surface indentations and variation in mechanical properties.

Type C bars had the surface tow glued to the exterior of the bar to provide only surface deformations. Fibres in the bar itself were perfectly straight.

Type D had similar indentation as the bar Type B. The bars have an outer veil to protect the fibres.

Local bond stress-slip data, as well as bond stress-radial deformation data, needed for constitutive modelling of the interface mechanics, were obtained for varying levels of confining pressure. In addition to bond stress and slip, radial stress and radial deformation were considered fundamental variables needed to derive configuration-independent relationships.

Each test specimen consisted of a 19 mm (#6) GFRP rebar embedded in a 76 mm diameter, 102 mm long pre-cracked concrete cylinder, with compressive concrete strength 29 MPa, subjected to a controlled, constant amount of confining axi-symmetric radial pressure. Only 67 mm (i.e. the equivalent of 5 steel bar lugs) of contact was allowed between the bar and the concrete. For each rebar type, bond stress-radial deformation relationships were obtained for five levels of confining axi-symmetric radial pressure. The following conclusions were reported:

1) Deep indentations and the resulting kinks in the longitudinal fibres reduce bar strength. For the 19 mm diameter bars tested, the ultimate strengths varied from 448 to 710 MPa and the moduli of elasticity from 28 to 48 MPa.
2) A bond mechanism involving both friction and mechanical interlock has been found for Type A, Type B and Type D rebars. In these cases, the study of specimens after the tests revealed both damage on the outer surface of the bars and wide diffusion of cracks in the concrete matrix. Such cracking implies that a bearing type mechanism (interlocking) was activated.
3) Small surface deformations, about 5.4% of the nominal bar diameter (i.e. similar to that of steel), are sufficient to yield maximum bond stresses up to five times the concrete tensile strength, similar to that obtained with steel bars. Either surface deformations or indentations obtained by stressing an external helicoidal strand are acceptable for bond purposes.
4) For the same amount of confinement, the bond strength for a steel bar is, on average, 1.2 to 1.5 times greater than the bond strength for a FRP bar.
5) Large variations in the indentation depths resulted in large variations in bond strength.
6) Bond strength can usually be increased threefold by increasing confining pressure.

Copyright fib, all rights reserved. This PDF copy of fib Bulletin 10 is intended for use and/or distribution only by National Member Groups of fib.

7) Deformations just glued to the surface are not recommended, since they may become unbonded and thereafter fail to provide any bond. In fact, in case of Type C deformed rebars it was found that the bond behaviour was similar to that of smooth rebars with no mechanical interlock. Tests showed a bond collapse due to the detachment of the spiral, whereas the concrete remains uncrushed. In this case, bond performance was independent both from concrete compressive strength and from confinement pressure.

A similar behaviour was reported by Hattori et al. (1995) for twisted CFRP cables (ϕ7.5 mm). The study of the interface after pull-out tests indicated that the concrete surface remains undamaged whereas the bar outer surface was damaged. Nevertheless, in case of spirally wounded aramid bars (ϕ6 mm), there was an apparent dependence of the maximum bond stress on the concrete compressive strength. It was also concluded that the pull-out behaviour is greatly influenced by the properties of both the binding material (resin) and concrete.

Al-Zahrani (1995) studied experimentally the behaviour of smooth glass-vinyl ester rods after removing the resin rich layer. The results showed an increase in the bond strength (5 times higher than unaltered smooth rods) due to the "skin removed effect", proving that the rod surface condition (composition of the resin rich surface layer and its smoothness) clearly affects the adhesion and friction components of the bond strength.

Jerret & Ahmad (1995) performed short-term pull-out tests on 8 mm diameter CFRP "Leadline". The bars of embedment length 152 mm, 305 mm and 457 mm were cast vertically in concrete slabs. Smooth and deformed rods were tested. The concrete strength was 44.8 MPa. The results for the smooth CFRP rod bond tests showed that the average bond strength of 0.417 MPa was very low compared with the ultimate strength of the rod. The maximum bond resistance increased with the bond length. There was no free end displacement before the rods reached their maximum pull-out loads. The performance of the deformed CFRP rods was significantly better, with 2 to 5 times higher loads. However, there was an initial free-end displacement as compared to the smooth rods followed by a significant increase in loads. The load at initial free-end displacement and the maximum load increased almost linearly with the increase in embedment lengths. The average bond strength of the deformed rods at initial free-end displacement was 1.63 MPa, and the average bond stress associated with the maximum load was 7.44 MPa.

Tamuzs et.al. (1995) investigated the bond between FRP bars and concrete by short bond length pull-out tests. The tests were performed with a specially designed ductile type of bar with central cylindrical hollow core shell with glass fibre braids around. The surface comprised of the braids covered with polyester resin. The concrete had compressive strength of 48 MPa. Failures were caused by shearing off the resin irregularities and partly the braid deformations. After the peak load deformation was exceeded, the bond exhibited plastic behaviour. The bond shear failure resistance of the resin and the sliding friction in the resin concrete interface are though to be easier to control than the bond resistance of concrete. This can lead to control of the concrete member ductility by limiting the maximum bond resistance of the rod provided the bond ductility can be ensured.

Al-Zahrani, Nanni, Al Dulaijan & Bakis (1996) used the direct pull-out test to study the behavior of machined glass/vinylester (GV), carbon/vinylester (CV), and carbon/epoxy (CE) FRP reinforcement rods with axisymmetric lugs. Loaded and free end slips of the FRP rod and internal stress distribution along the rod (axial and hoop directions) were measured. Glass/vinylester rods with five and ten lugs, and different lug widths and heights were studied. Increasing the embedment length did not increase the pull-out load linearly due to the progressive nature of failure of the lugs. Bond between the machined FRP rods and concrete was controlled by mechanical interlock and shear strength of the lugs until the failure of lugs. After shearing off of the lugs, friction between rod and concrete dominated the bond mechanism. The FRP rods (G/V, C/V and C/E) had comparable shear stress-slip diagrams and experienced the same failure mode (shearing off the lugs). The resin types rather than the fibre type appeared to control bond strength. G/V and C/V rods had similar shear strength values, which were 60 to 70% of that of C/E rods. When adequate concrete cover was used to prevent concrete splitting, the mechanism of failure was independent of the concrete compressive strength, since failure was controlled by the FRP surface. The embedment lengths and lug heights investigated had no effect on the failure mode. Doubling the embedment length and number of lugs reduced the nominal shear strength.

Copyright fib, all rights reserved. This PDF copy of fib Bulletin 10 is intended for use and/or distribution only by National Member Groups of fib.

Gowripalan & Chiang (1996) studied specimen from pull-out tests with the SEM technique. CFCC, Fibra, Leadline and steel for comparison were investigated. Concrete with silica fume was also used, since silica fume can fill up the pores close to the surface of reinforcement. CFCC provided the highest bond strength due to the external layer with cross fibres and the even distribution of longitudinal fibres. It was concluded that the bond characteristics of FRP tendons are superior to the bond of steel tendons with concrete.

Freimanis, Bakis, Nanni & Gremel (1998) investigated experimentally and analytically GFRP (Hughes Brothers) rods to determine the effect of rod geometry on concrete bond strength. The rods had well-controlled variations in depth and pitch of their indented helical wrappings. The maximum bond stress increased with increasing indent depth, but did not display any particular dependence on indent pitch. It was reported that a heavier application of the sand coating significantly increased the bond strength. Loaded-end slip at the onset of free-end slip increased with increasing embedment length and decreasing rod diameter and was relatively constant for rods with similar embedment length to diameter ratios.

Larralde, Mueller-Rochholz, Schneider & Willmann (1998) have used pull-out and beam end specimens to investigate the bond capacity of glass and aramid (Arapree) FRP rods and compare it with that of steel rebar. The concrete compressive strength varied between 27-41 MPa. The Arapree rods, which have a relatively straight surface with only a sandpaper-like texture, exhibited the lowest bond strength. The GFRP bars exhibited only slight increase in the bond strength in spite of the indentations produced by the fibre wrapping around the bars. Unlike for steel, it appears that there was a positive influence of the transverse beam support pressure on the bond capacity of GFRP and AFRP rods.

7.3.1.2 Effect of concrete strength and other parameters on bond strength

Shima, Suga & Honma (1993) used braided aramid fibre bars, carbon fibre seven-wire strand and conventional seven-wire steel strand in one-sided pull bond tests. Local bond stress-local slip relationships were obtained from the strain distribution along the embedded bar. The embedded length was made long enough not to cause free end slip. Experimental variables included type of bar material (braided aramid fibre, 7-wire CFRP strand, 7 wire steel strand), bar diameter (12-16 mm) and concrete strength (38-84 MPa). The following conclusions were reported:

1) The local bond stress-slip relationships of a braided aramid fibre bar and a carbon fibre strand obtained from the pull test with long embedded length were independent of the location along the bar, excluding the loaded end region.
2) The shape of local bond stress-slip curves differed with bar type. The bond stress-slip curve of a braided aramid fibre bar showed low initial stiffness and no slip softening, however, the CFRP strand and steel strand showed a high initial stiffness and slip softening.
3) The bond stress of the CFRP and steel strands was proportional to between 1/2 to 2/3 power of concrete compressive strength. For a braided aramid fibre, there was a quite small effect of concrete strength on the bond stress.
4) The local slip was proportional to the bar diameter in the local bond-slip relationship of braided aramid fibre bars.

Shima & Suga (1993) investigated by pretensioned bond tests the local bond stress-slip relationship of braided aramid fibre bar. Local bond stress-local slip relationships were obtained from the strain distribution along the embedded bar. The embedded length was made long enough not to cause a strain change at the centre of the specimen. The concrete strength was the main experimental variable. It was concluded that:

1) The local bond stress-slip relationship of braided aramid fibre bar varied with the test method. The bond stress obtained from the pretensioned bond test is much larger than that obtained from the pull bond test with long embedment. The bond stress obtained from the pullout test with short embedment is intermediate between these bond stresses.
2) The effect of concrete strength on the local bond stress-slip relationship of braided aramid fibre bar also differs with the test method. The bond stress at a given slip increases remarkably with concrete strength in the pretensioned bond test, although the effect of concrete strength on the bond stress is little in the pull bond test with long embedment.

Copyright fib, all rights reserved. This PDF copy of fib Bulletin 10 is intended for use and/or distribution only by National Member Groups of fib.

In Canada, researchers at Sherbrooke University, conducted two experimental series investigating the bond behaviour of GFRP bars, firstly in direct pullout and then in beam tests. The GFRP bars, supplied by a Canadian manufacturer (Pultrall Inc.), had a smooth surface on which deformations were added by helically winding the same kind of fibres and by sand coating particles. Their tensile strength was around 700 MPa and the elastic modulus around 45 GPa. Normal and high strength concrete (f_{cy}=30 and 80 MPa) were used in both series.

In the first series Chaallal & Benmokrane (1993), the GFRP bars were embedded vertically in 150 x 300 mm concrete cylinders having anchorage lengths 5 or 10 times the bar diameter. Three bar diameters were tested (12.7 mm, 15.9 mm, 19.1 mm) in a large number of tests. The main conclusions from the tests were:

1) The bond strength of GFRP deformed rods embedded in high strength concrete is similar to that obtained when such rods were embedded in normal strength concrete. The bond strength of glass-fibre rods in normal strength concrete varied from 11.1 to 15.1 MPa with average 12.9 MPa, which is 62% to 84% of that of steel deformed bars.
2) The bond strength of FRP bars did not depend on the concrete strength in the same way as steel (for concrete strengths 30, 80 MPa). According to the authors, such difference between FRP and steel rebars is due to the fact that the surface deformations of the GFRP rod appear not to be able to provide enough lateral confinement through rib bearing.
3) An anchorage length of 20d is necessary for reaching the ultimate tensile capacity of GFRP bars.

In the second series (Benmokrane, Chaallal & Tighiouart, 1996), 20 beam tests were prepared according to RILEM/CEB (1978) specifications. Four different reinforcing bars diameters (12.7, 15.9, 19.1 and 25.4 mm) were considered and the embedment length in all the specimens was kept equal to 10d. All GFRP specimens failed by pullout and in some of them, there was some evidence that the deformations of the reinforcing bars either sheared or were damaged. The main conclusions from this series were:

1) The maximum bond strength of GFRP reinforcing bars, varied between 6.4 to 10.6 MPa, which is lower than that of steel bars, approximately 60 to 90%, depending on the bar diameter.
2) The bond strength observed from pullout tests was 5 to 80% higher than that obtained from beam tests, depending on the bar diameter.
3) The distribution of bond stresses along the anchorage length of GFRP bars was found to be non-linear and similar to that of steel. The maximum bond stress moved progressively towards the free and of the reinforcing bar with increasing load.

Alunno, Rossetti, Galeota & Giammatteo (1995) investigated the local bond stress-slip relationships of glass fibre reinforced plastic bars embedded in concrete. The results obtained were used to develop a model of the stress-slip relationship and to estimate the anchorage lengths needed to embed these bars in concrete casts.

Benmokrane & Masmoudi (1996) investigated the bond strength and top-cast modification factor for the C-bars. Concrete of compressive strength f_{cc} = 52 MPa was used in pull-out tests with bond embedment length 5 bar diameters. It was concluded that the average bond strength was about 15.8 MPa and the top cast modification factor was 1.1. After the maximum resistance was achieved the bar sliding resistance stabilised at a level of about 55% of maximum resistance.

Achillides, Pilakoutas & Waldron (1997) reported an experimental series where more than 100 specimens were tested in direct pullout with short embedment lengths to investigate the bond behaviour of the EUROCRETE FRP bars. The EUROCRETE bars utilise both Glass and Carbon, have a rough surface produced by a peel ply and are manufactured in different diameters and shapes. All the specimens failed in a pull-through failure. It was reported that the mode of bond failure of FRP bars differed substantially from the respective mode of bond failure of steel deformed bars. For concrete strengths greater than 30 MPa, the failure occurred on the surface of the bar, by peeling part of the surface layer of the bar. For concrete strengths less than 15 MPa, the concrete was crushed in front of the bar deformations and the bond strength was controlled mainly by the shear strength of concrete. The series of the pullout cube tests highlighted some of the factors that influence the bond strength of FRP bars. The influence of these factors is summarised in the following:

Copyright fib, all rights reserved. This PDF copy of fib Bulletin 10 is intended for use and/or distribution only by National Member Groups of fib.

1) Type of bar fibres: No significant difference was found between the bond strengths developed by GFRP and CFRP bars. CFRP and GFRP bars can develop bond strength 80% of that developed by steel deformed bars.
2) Embedment length: An increase in the embedment length is accompanied with a decrease in bond strength.
3) Concrete strength: The concrete strength influences the bond strength only when the bond failure takes place in the concrete matrix.
4) Bar diameter: Smaller diameter bars (8.5 mm) develop higher bond strength than larger diameter bars (13.5 mm). This difference is believed to be more significant in FRP than in steel bars, due to their low axial shear stiffness.
5) Cross sectional shape of bar: Square bars develop higher bond strength than round bars. The "wedging effect" due to the edgy cross section shape seems to be responsible for this difference.
6) Surface deformations: A minimum height of deformations is necessary to develop satisfactory bond behaviour to concrete.

Takagi, Kojima, Iwamoto & Inoue (1997) studied bond of FRP rods with the RILEM beam type specimen under static and fatigue loading. Braided aramid and stranded carbon fibre rods were used. The concrete compressive strength was 65 MPa and rod diameters 7.2 - 7.5 mm. The bond characteristics were influenced by the introduction of prestress, loading methods, embedment length and type of rod. These influences were more pronounced for the braided rods.

Kono, Inazumi & Kaku (1997) studied confinement obtained from carbon fibre sheet to resist bond concrete splitting. The compressive concrete strength increase was determined for differently wrapped cylinders to be up to 3 times that of unwrapped (~35 MPa) for three sheet layer wrapped. One layer of CFRP sheet increased the bond strength by about 80%. Bond tests were performed on "Schmidt-Thrö" specimens and beams. The CFRP sheet suppressed the brittle bond splitting failure and increased the load carrying capacities. Half-wrapped beam specimens suffered sheet bond failure. Fully wrapped beams gave better confinement.

Kachlakev & Lundy (1998) evaluated the bond of hollow GFRP bars with similar geometry, but different microstructure, in concrete with compressive strengths 17.9-22.4, 35.0-39.2 and 48-53 MPa. Pull-out specimens with axial and off-axis placement of bar were used. Different embedment lengths were used. Concrete strength appeared to have no influence on bond strength, which means that the bar surface deformations peeled off. The axisymmetric bond strength was 200% higher than that of off-axis pull-out specimens. The off-axis specimens were not analysed by taking into consideration the splitting resistance of the concrete cover.

Tighiouart, Benmokrane & Gao (1998) tested concrete beams of RILEM type and pull-out specimen with different casting positions. Comparisons were made with bond of steel rebars. It was concluded that for GFRP bars adhesion and friction control the bond strength. The top effect modification factor varied from 1.26 to 1.32 and increased as the diameter of the bar decreased.

Greco, Manfredi, Pecce & Realfonzo (1998) conducted an investigation on the bond properties C-BAR by using prismatic concrete specimens. The GFRP rebar had a 4/8" (≅12.7 mm) diameter and the embedment length L ranged from 5 to 20 times the bar diameter d_b. The main conclusions reported were the following:
1) In case of small embedment length (5 times the bar diameter) a pull-out failure, without splitting, was obtained; with values of bond strength over 11 MPa (with some scatter) similar to that of steel rebars.
2) Low slip values were measured but with a large difference between the free end and loaded end. This difference is due to the low elastic modulus and makes difficult the development of simple bond-slip constitutive laws.
3) In case of larger embedment lengths (10 to 20 d_b) tension failure occurred.

7.3.1.3 Long term performance of bond

Nanni et.al. (1995) conducted an investigation aiming to develop test methods relating long-term degradation of the bond strength of FRP rods to elastic parameters, embrittlement and strength of the FRP material. Direct pull-out tests with embedment length of 5 bar diameters were used. Two

Copyright fib, all rights reserved. This PDF copy of fib Bulletin 10 is intended for use and/or distribution only by National Member Groups of fib.

groups of FRP rods of different composition and surface configuration were used. The first group (benchmark) consisted of smooth or machined (axi-symmetric grooves) FRP rods. The benchmark rods were made of the following matrix systems: glass-vinyl ester (GV), carbon-vinyl ester (CV), and carbon-epoxy (CE). The second group consisted of commercially available FRP rods (CFCC with diameter 12.7 mm and Leadline with diameter 8 mm) and conventional deformed steel bars (diameter 9.5 and 12.7 mm). The strain distribution within the bonded length of the FRP rod was measured. The main conclusions were:

1) For smooth rebars the bond strength is not dependent on concrete strength. Friction appears to play a major part in pull-out resistance, since adhesion vanishes as soon as the rod slips relative to the concrete. Therefore, the finish and composition of the resin-rich surface layer of an FRP rod affect the development of bond strength due to adhesion and friction.
2) The strength of concrete appears to have an insignificant influence on bond strength and failure mechanism of FRP rods. Unlike in steel re-bars, concrete failure was not experienced in any case of FRP rod pull-out
3) All machined FRP rods failed by shearing off of the rings (lugs) followed by sliding. This failure mechanism was controlled by resin (epoxy based systems are stronger than vinyl ester-based systems). The height of rings was not important, provided the failure mode did not change.
4) Steel reinforcing bars develop higher bond strength than commercially available FRP rods, but not higher than the machined CE system.
5) Smaller diameter rods have higher pull-out strength than larger diameter rods.
6) The use of a strain probe inside the FRP rod shows promise in the monitoring of the strain field during the pull-out process. The influence of resin cracking must be considered.

Den Uijl (1995) performed pull-out tests under monotonic and repeated loading to study the fatigue and bond properties of the aramid based tendon Arapree strips (35 kN rupture load). Embedment lengths of 50, 100 and 150 mm were used. Relatively large cross-sectional dimensions of the concrete body (f_{cu} = 50Mpa) were chosen to prevent the concrete from splitting. The loading rate of static tests was 10 kN/min. In the dynamic tests a sinusoidal load with frequency 50 Hz was applied. The tendon the slip was measured both at the loaded and at the free end. The results showed that:

1) Under monotonic loading, bond failure only occurred in case of 50 mm embedment length, whilst for the longer embedment lengths rupture of the Arapree strips took place. The maximum average bond stress was 14.25 MPa.
2) Under repeated loading between 5 and 15 to 22 kN, bond gradually deteriorated and the activated bond zone shifted from the loaded end away.
3) The number of load cycles to bond failure increased with increased embedment and lower maximum load. At 150 mm bond length and loading 5 and 20 kN more than 2.8 million load cycles could be resisted without failure.
4) Pull-out tests with repeated loading that did not present bond failure, showed a fatigue behaviour comparable to that found in tests on bare Arapree samples.
5) The slip versus number of load cycles measured under repeated load showed curvatures in accordance with what is normally found in concrete under repeated compressive load.

Hattori, Kawasaki, Miyagawa & Fuiji (1997) performed pull-out tests with several bond lengths including under sustained load. The FRP bars tested were carbon fibre strand (CFCC) and aramid fibre deformed bar (Technora). Both rebar types showed similar relationships between the ratio of bond length to nominal diameter and the ratio of pull-out load at initial free-end slip to tensile capacity. The loaded end of the FRP rebars showed a tendency of getting settled within a year, when subjected to 20% of their tensile capacity.

7.3.2 Bond splitting tendency of FRP bars

Faza & GangaRao (1990) at West Virginia University conducted a series of beam type pullout tests (see Figure 7.3.1) in order to investigate the bond behaviour of Glass FRP bars (σ_t = 900 MPa, E_G = 48 GPa) in "high" strength concrete (f_{cy} = 45-52 MPa). Rough surface bars with diameters 9.5 mm (#3) and 25.4 mm (#8) were tested. Longitudinal and transverse reinforcement was provided to the beam specimen.

Copyright fib, all rights reserved. This PDF copy of fib Bulletin 10 is intended for use and/or distribution only by National Member Groups of fib.

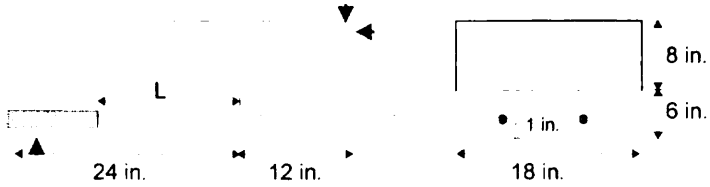

Figure 7.3.1: Beam type bond test arrangement by Faza and GangaRao (1990)

The results showed that the #8 bars, having embedment lengths 406 mm (16d) and 610 mm (24d), developed maximum average bond strength values of 3.2 and 2.8 MPa respectively. The #3 bars failed in tension, so their ultimate bond capacity was not possible to be measured. Nevertheless, it was suggested that the #3 bars could develop more than 2.7 MPa bond strength in the worst case of 610 mm (64d) embedment length. The authors did not mention in their report the mode of failure of the #8 bars, but this is expected to be due to bond splitting.

Kanakubo, et. al (1993) investigated the bond splitting strength of concrete members reinforced with a variety of FRP bars in two series of tests. In the first series, a simple bond test was used and in the other a cantilever type bond test. Both confined and unconfined specimens were used. The results showed that in both cases the bond strength is influenced by the elastic modulus of longitudinal bar. The following formula to predict the bond splitting strength for FRP bars was proposed:

$$T_{bu}=T_{co}+T_{st} \tag{7.3.1}$$

where, T_{bu}: bond splitting strength
T_{co}: bond splitting strength without lateral reinforcement
T_{st}: increment of bond splitting strength caused by lateral reinforcement

$$T_{co}=0.313K_{co}(0.4b_i+0.5)f_c^{(1/2)} \tag{7.3.2}$$
$$T_{st}=K_{st}(b/d_b)p_w f'^{(1/2)}_c \tag{7.3.3}$$
$$K_{co}=0.26E_{ma}^{(0.29)} \text{ for } E_{ma}<10^2 \text{ and } K_{co}=1 \text{ for } E_{ma}>10^2 \tag{7.3.4}$$
$$K_{st}=15.8E_{ma}^{-0.52} \tag{7.3.5}$$

where, E_{ma}: elastic modulus of longitudinal bar (GPa)
f'_c: concrete compressive strength (MPa)
b: width of member
b_i: normalised length of failure line ($=(b-N_t d_b)/N_t$)
d_b: diameter of longitudinal bar
p_w: lateral reinforcement ratio ($=a_w/bs$)
N_t: number of longitudinal bars
a_w: sectional area of a pair of lateral reinforcements
s: spacing of lateral reinforcement
h/d = relative lug/diameter relation

It was concluded that:

1) In the case of no lateral reinforcement, the bond splitting strength of the cantilever type specimen can be evaluated by using the result obtained for the simple type specimen.
2) Bond splitting strength without lateral reinforcement (T_{co}) can be evaluated using the reduction factor (K_{co}), which is a function of the elastic modulus of longitudinal bar (E_{ma}).
3) The difference in the bond splitting strength between corner and centre bars can not be observed in specimen with FRP longitudinal bars. The increment of bond splitting strength (T_{st}) is also given as a function of elastic modulus of longitudinal bar.

Faoro (1996) studied bond between FRP bars and concrete and concluded that relatively high bond forces can be developed in the concrete within a relatively short development length, which result in splitting of the concrete cover. The lower modulus of elasticity and the higher deformability of the FRP bar in the transverse direction play a role in splitting mechanism. FRP

Copyright fib, all rights reserved. This PDF copy of fib Bulletin 10 is intended for use and/or distribution only by National Member Groups of fib.

tendons in the market are available with a variety of surface shapes and contours, which leads to different bond characteristics. FRP bars and tendons display higher bond strengths in concrete than conventional prestressing steels. This means that higher bond forces can be developed in the concrete over a shorter development length. The splitting forces increase and should be met by thicker concrete covers. If mixed reinforcement is used the stiffer reinforcing elements could be overloaded.

An experimental series investigating the bond splitting behaviour of spliced GFRP bars was conducted in Norway by SINTEF (1996), under the EUROCRETE Project, Clarke & Waldron (1996). Three medium scale concrete beams (2.85 x 0.25 x 0.15m) were reinforced with 13.5 mm GFRP bars (σ_t = 1000 MPa, E_G = 45 GPa) and Plytron links (σ_t =520 MPa, E_G = 23.4 GPa). The beams were tested in four-point bending. All the specimens were cast using normal density concrete C35 of high workability and the bottom and side concrete cover to the spliced bars was 22.5 mm. The only variable in the test program was the splice length, which was lying entirely in the constant moment zone. The results showed that the average bond strength developed in splices decreased as the splice length increased. For splice length (L) 18.5d, 26d and 37d, the bond stresses developed were 4.0, 3.3 and 2.9 MPa respectively. The authors suggested that if a full utilisation of the tensile strength of FRP bars was requested, the development length should be around 80 bar diameters.

Tepfers & Karlsson (1997) tested the bond between GFRP C-BARs and concrete using pull-out tests with central and eccentric placement of bar. Three overlap splice tests for tensile reinforcement in bent beams have been performed. C-BARs have a surface shape similar to that of steel rebar with inclined ribs. Comparison were done with the bond properties of Swedish Ks600 steel rebar which has a higher relative rib area than that of C-BAR. It was concluded that when there is enough confinement to prevent splitting, C-BAR has the same stress-slip relationship as steel rebar. The cover splitting tendency along the bar is lower for C-BAR than for steel bar. This is probably because the C-BAR has a softer surface than steel and gives rise to less stress concentrations in concrete and less micro cracks. However, when the cover is split along the bar, the radial pressure increase from the C-BAR and the final ultimate splitting crack pattern is formed and the cover is split off for a rupture load, which is about 30% lower than that of steel reinforcing bar. The glossy surface of C-BAR causes increased slip, when concrete resistance decreases after cover cracking and results in greater splitting forces.

Tepfers, Hedlund & Rosinski (1998) investigated the bond between GFRP bars produced by Hughes Brothers, Inc. and concrete, using pull-out tests with central and eccentric placement of bar. Three overlap splice tests for tensile reinforcement in bent beams were performed with different lap lengths. Comparisons were done with the bond properties of Swedish Ks600 and Ks400 steel rebars and other types of FRP rods. It was concluded that the tested GFRP bars have a stress-slip relationship similar to that of other FRP rods with relatively soft surface and small deformations. For low loads, the bond resistance demonstrated high stiffness due to the coarse sand coating. For higher loads, the slip increased and when the confinement was good, the bond resistance become ductile retaining about 50% of the maximum bond resistance at a slip of 20 mm. If cracking of the concrete cover along the anchored bar takes place, the bond resistance is limited and happens at a considerably smaller slip. The cover splitting tendency along the bar is considerably lower than that of Swedish Ks600 steel rebar and C-BAR.

Achillides (1998) tested beams with lapped bars and short anchorages, using GFRP and CFRP Eurocrete bars and GFRP shear links. It was concluded that spliced bars and single anchorages develop similar bond strengths. The shear links were found to enhance the splitting resistance of concrete only in the shear span, when they were already stressed. Transverse pressure due to supports was also found to be beneficial in reducing splitting problems. GFRP bars showed a higher splitting tendency than CFRP bars, despite the fact that both bars show the similar pull-out bond strengths. This casts doubt over the use only of pull-out tests for comparison of different bars.

Copyright fib, all rights reserved. This PDF copy of fib Bulletin 10 is intended for use and/or distribution only by National Member Groups of fib.

7.3.3 Analytical modelling of bond between FRP bars and concrete

Analytical models of bond-slip are essential for the determination of structural performance of FRP reinforced concrete structures by means of numerical analysis. Even though many experimental programs have been conducted world-wide examining the bond characteristics of FRP bars, very little work has been published on analytical modelling. In the following, a review of these works is reported.

7.3.3.1 Local bond modelling

Malvar (1994) proposed a refined model of the overall bond behaviour depending on two empirical constants. These constants are to be determined by curve-fitting the experimental τ-s curves. Malvar's model is represented by the following relationship:

$$\frac{\tau}{\tau_m} = \frac{F \cdot (s/s_m) + (G-1) \cdot (s/s_m)^2}{1 + (F-2) \cdot (s/s_m) + G \cdot (s/s_m)^2} \tag{7.3.6}$$

where, τ_m, s_m = peak bond stress, slip at peak bond stress;
F, G = empirical constants determined for each rebar type.
F = 11 for FRP rebars with an external helicoidal tow which provides both a protruding deformation and a small indentation of the bar surface (named Type A rebars);
F = 13 for FRP rebars with indentations given by stressing the outer surface during fabrication (named Type D rebars);
G = 1.2 for Type A rebars;
G = 0.5 for Type D rebars.

Faoro (1992), Alunno Rosetti, Galeota & Giammatteo (1995) and Cosenza, Manfredi & Realfonzo (1995) have successfully applied the well-known model for deformed steel rebars by Eligehausen, Popov & Bertero (1983) to FRP rebars. The ascending branch of this bond-slip ($s \leq s_m$) relationship is given by:

$$\frac{\tau}{\tau_m} = \left(\frac{s}{s_m}\right)^{\alpha} \tag{7.3.7}$$

where, α is a curve-fitting parameter that must be not larger than 1 to be physically meaningful (α = 0.40 in case of steel reinforcements).

Furthermore, the Eligehausen et al. (1983) model is given by the following:
1) A second branch of constant bond ($\tau = \tau_m$) up to a slip $s = s_2$
2) A linearly descending branch from (s_2, τ_m) to (s_3, τ_3)
3) A horizontal branch for $s > s_3$, with a value of τ due to the development of friction ($\tau = \tau_3$).

Values of s_2, s_3 and τ_3 have to be calibrated on the basis of experimental results. Cosenza, Manfredi & Realfonzo (1995) proposed a modified version of such model (called "double branch model") in order to model FRP-concrete bond (Figure 7.3.2). In fact, by comparing experimental and analytical curves using the original model by Eligehausen et al. (called B.P.E. model) the Authors found there was no second branch in case of FRP rebars. The ascending branch is the same as in the original model, while the softening branch is given by:

$$\tau / \tau_m = 1 - p\,(s - s_m) / s_m \tag{7.3.8}$$

where, τ_m is the peak bond stress
s_m the respective slip, as shown below
α and p are parameters based on available experimental data.

Copyright fib, all rights reserved. This PDF copy of fib Bulletin 10 is intended for use and/or distribution only by National Member Groups of fib.

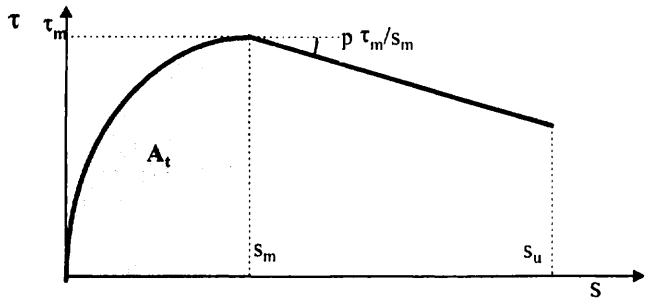

Figure 7.3.2: Modified BEP constitutive law, Cosenza, Manfredi & Realfonzo (1995)

The value of parameter α, which determines the ascending branch, is derived by equating the area, A_τ, under the ascending branch of the experimental curve to the area corresponding to the analytical curve:

$$A_\tau = \tau_m s_m / (1 + \alpha) \tag{7.3.9}$$

The value 'p', which determines the descending branch, is evaluated by a similar philosophy for the area underneath the experimental and analytical curves within the softening range. Moreover, Cosenza, Manfredi & Realfonzo (1995) proposed a law to model the first branch of the τ-s curve (C.M.R. model):

$$\frac{\tau}{\tau_m} = \left(1 - e^{-s/s_r}\right)^\beta \tag{7.3.10}$$

where, s_r and β are parameters based on curve-fitting of experimental data.

In an investigation by Cosenza, Manfredi & Realfonzo (1995, 1996) the Malvar model, the modified B.P.E. model and the C.M.R. model were compared. The three models were evaluated against experimental results gathered from various research projects. The analysis of the experimental data showed that:

1) The bond performance of FRP bars depends on the characteristics of the outer surface and, for the same type of surface, depends on the manufacturing process,
2) It is generally possible to obtain bond strengths in FRP bars of similar or greater magnitude than from steel,
3) Indented and grain covered bars seem to provide the best results in terms of bond strength.

The authors suggested that the Malvar model was able to reproduce the entire constitutive bond-slip curve by means of a single equation, but it seemed to be less reliable than the modified version of the B.P.E. model. Meanwhile, the C.M.R. model seemed to be the most suitable in the modelling of the ascending branch. As an illustrative example, a comparison between the B.P.E. model, the C.M.R. model and two experimental bond-slip curves are presented in Figure 7.3.3.

The authors also introduced the following analytical expression for calculating the anchorage length l, based on the B.P.E. model:

$$l = l_0 \cdot \left(\frac{\sigma_l}{\sigma}\right)^{\frac{2\alpha}{1+\alpha}} \cdot \frac{1+\alpha}{1-\alpha} = \frac{\phi \cdot \sigma}{4 \cdot \tau_m} \cdot \left(\frac{\sigma_l}{\sigma}\right)^{\frac{2\alpha}{1+\alpha}} \cdot \frac{1+\alpha}{1-\alpha} \tag{7.3.11}$$

where, l_0 is the embedment length at a given value of σ in case of $\tau = \cos t = \tau_m$
σ_l is the maximum tensile stress that can be carried by the bar using only the ascending branch of the bond-slip relationship:

Copyright fib, all rights reserved. This PDF copy of fib Bulletin 10 is intended for use and/or distribution only by National Member Groups of fib.

$$\sigma_l = \sqrt{\frac{8 \cdot E}{\phi} \cdot A_\tau} = \sqrt{\frac{8 \cdot E}{\phi} \cdot \frac{\tau_m \cdot s_m}{1+\alpha}} \qquad (7.3.12)$$

The value of 'l' obtained with such equation requires only the ascending branch of the bond-slip law to be utilised in the range σ less than or equal to σ_l. Since $(1+\alpha)/(1-\alpha)$ is less than 1, l is greater than l_0.

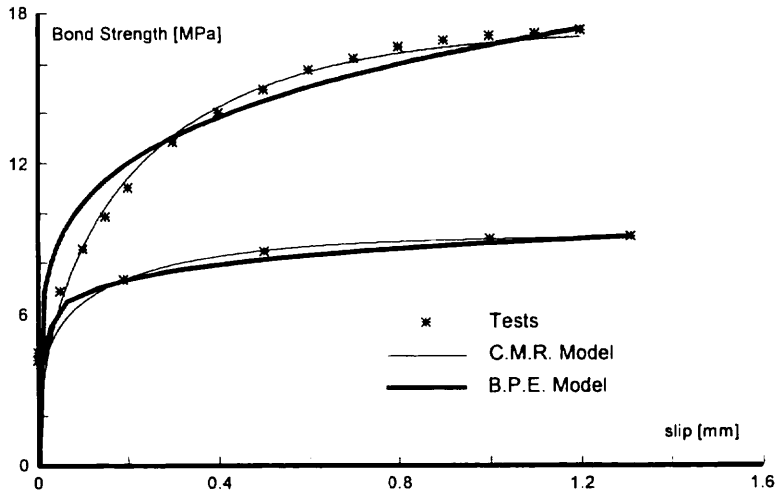

Figure 7.3.3- Experimental data versus Analytical Models (Cosenza, Manfredi & Realfonzo, 1996)

7.3.3.2 General bond modelling

Achillides (1998) introduced a method of modelling the pullout bond behaviour of FRP bars. The FRP-concrete cube specimens were modelled by using 2-dimensional elements. Bar and concrete were linked together with non-linear spring elements at a spacing of 27 mm (27 mm = 2 times the bar diameter). In order to model the different sizes of embedment length used in the experiments, identical cube models were developed differing only in the number of connecting springs, Figure 7.3.4. Every spring was assumed to represent the bond contribution of a 27 mm bar length to the overall bond behaviour of the embedment length.

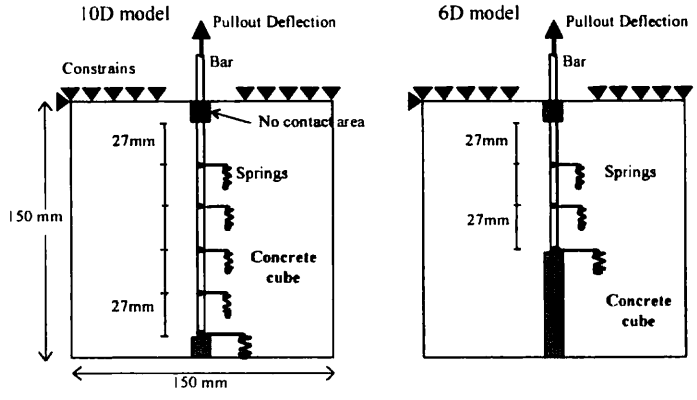

Figure 7.3.4 Model of 10D and 6D specimens

The required input data that define the behaviour of the springs are the spring extension values and the corresponding force levels applied on the spring. In the case of this model, the spring extension was identified by the bond slip of the bar and the corresponding force was a function of the bond strength of the bar. In order to define the input load-bond slip curve, selected experimental data from the pullout cube tests were used.

Copyright fib, all rights reserved. This PDF copy of fib Bulletin 10 is intended for use and/or distribution only by National Member Groups of fib.

For example, the load versus unloaded end slip curves of the specimens with embedment lengths 4D and 2D are considered in more detail. The 4D embedment length is assumed to be identical to two 2D lengths as shown in Figure 7.3.5.

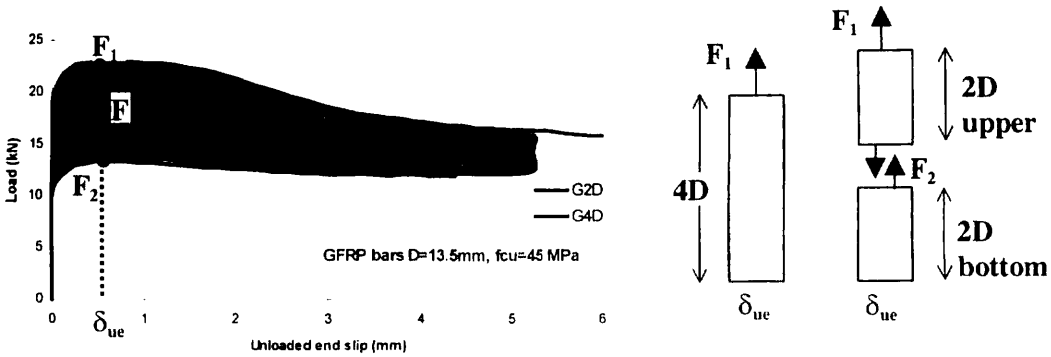

Figure 7.3.5 Contribution of the upper 2D bar length to the bond behaviour of the bar

The unloaded end slip, δ_{ue}, is a function of the load F_1, which corresponds to the 4D embedment length, but is also a function of the internal load F_2 which corresponds to the bottom 2D embedment length. Since the load values F_1 and F_2 correspond to the same δ_{ue}, the difference between F_1 and F_2 will give a load value F that represents the contribution of the upper 2D length at that certain slip. The contribution of the upper 2D embedment to the load versus unloaded end slip curve of the whole 4D embedment, is the shaded area between the 4D and 2D curves. The resultant curve of F versus δ_{ue} is introduced in the springs except the very last one, where the F-δ_{ue} curve of the 2D specimen was used.

The analytical results were compared with the corresponding experimental ones. In Figure 7.3.6, the load-slip curves at the loaded (LE) and unloaded end (UE) of one of the models are presented together with the respective experimental curves. The results show a very good correlation with the respective experimental, both at the ascending and descending branches of the bond-slip curve.

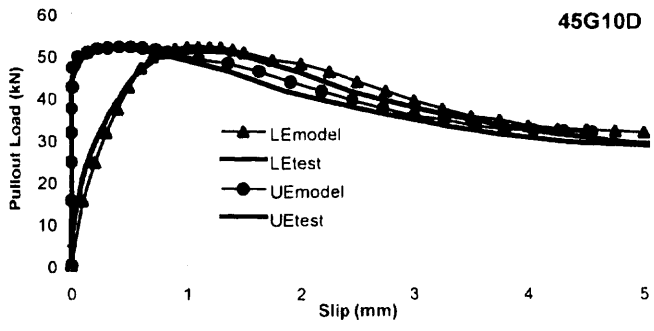

Figure 7.3.6 Load - slip curves of model and experimental tests

To investigate the effect of the elastic modulus on the bond splitting strength of reinforcing bars, Achillides (1998) considered the following simplified FE models. A square concrete block constrained at its top edge and having a reinforcing bar attached on its matrix was used, as shown in Figure 7.3.7. This model was assumed to simulate the behaviour of an end bar-concrete "system" between successive flexural cracks. This kind of "system" can be found in concrete beam elements reinforced with a single bar anchorage or even it can be identified with the bar-concrete system between successive microcracks. The bar was loaded axially in the horizontal direction and the distribution of vertical stresses developed along the bottom side of the bar was monitored. These stresses were assumed to be the splitting stresses induced by the bar to the bottom concrete cover.

Two solutions were obtained by using model 1. In the first one, the bar had the Young's modulus of EUROCRETE GFRP bars (45 GPa), whereas in the second solution the bar had the modulus of CFRP bars (115 GPa). The applied load had the same value in both cases. The distribution of vertical stresses induced in the bottom concrete cover had the same shape in both solutions, as

Copyright fib, all rights reserved. This PDF copy of fib Bulletin 10 is intended for use and/or distribution only by National Member Groups of fib.

shown in Figure 7.3.8. The peak stress, however, had different values for each material. The peak stress value which controls the bond splitting strength of the bar, was greater in the GFRP bar which suggested that GFRP bars tend to split more than CFRP bars under identical pullout load.

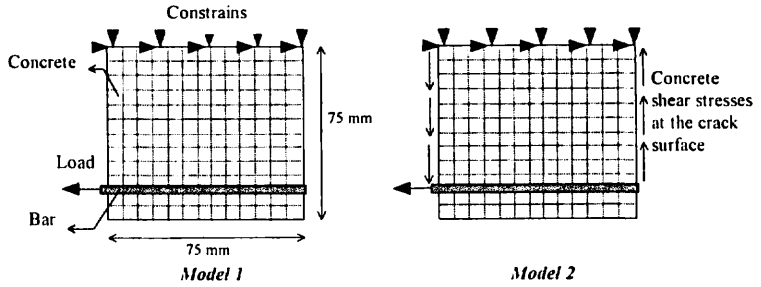

Figure 7.3.7 FE models for the investigation of the effect of Young's modulus on bond splitting strength

A similar model was also used to evaluate the effect of the shear stress along the cracks, on the bond splitting tendency of reinforcing bars. Shear stresses were added to the two sides of the model, as shown in model 2 in Figure 7.3.7. These stresses simulate the shear resistance of the concrete, which mainly depends on the geometry of the cracks. Before the formulation of the cracks, full shear concrete resistance is assumed, whereas as the crack develops, the shear resistance decreases.

A series of solutions were performed at different values of shear stress by using the same type of bar. The results showed that as the concrete shear stress reduces, the peak splitting stress increases resulting to a higher splitting tendency. This was an important observation also related to the deformability of the reinforcing bar. The concrete shear strength at the crack location depends mainly on the geometric characteristics of the crack (width and length). The crack geometry, however, depends on the elongation of the bar just outside the concrete block, which is proportional to the elastic modulus of the bar. So, for example, GFRP bars having lower elastic modulus than CFRP bars are expected to create larger cracks and consequently the concrete shear strength at the crack position will be less. As a result, the splitting tendency of the GFRP bars is higher than CFRP bars.

From the results of the above two modelling studies, it was concluded that the value of the Young's modulus of reinforcing bars plays an important role in their bond splitting strength. It influences the deformability of the bars inside the concrete and in parallel, it affects the crack geometry and consequently the concrete shear strength at the location of the crack. Both factors influence the splitting tendency of the bars, as it was shown above. The author suggested that GFRP bars are expected to develop less than 80% of the bond splitting strength of CFRP bars due to the combined effect of the above factors. The experimental results of the series of beam tests conducted by Achillides, Pilakoutas and Waldron (1998) confirmed the above findings.

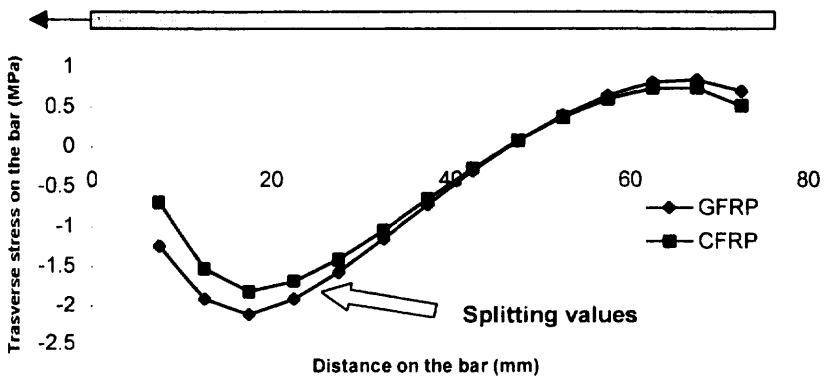

Figure 7.3.8 Splitting stress distribution along the bar

Copyright fib, all rights reserved. This PDF copy of fib Bulletin 10 is intended for use and/or distribution only by National Member Groups of fib.

7.3.4 Other parameters affecting bond

7.3.4.1 Bond under sustained load - creep tests

Hattori, Inue, Miyagawa, Fujii (1995) investigated bond creep behaviour of two kinds of FRP rebars embedded in concrete by conducting pull-out creep test using concrete cube specimens and measuring the increase in the free end slip up to 8000 hours. The effect of bond creep on the long-term deflection of reinforced concrete beams using FRP reinforcing bars also was investigated. They concluded the following:

1) The mechanical properties of resins used for the binding materials affect the bond slip behaviour of the twisted carbon fibre cable ($\varepsilon=7.5$ mm) and deformed aramid fibre bar ($\varepsilon=6$ mm) especially in the preliminary stage of pulling out, when bond stress is rather small.
2) The deformed aramid fibre bar showed a larger free end slip than the deformed mild steel bar (D10) under the same conditions of average bond stress with a bond length of 64 mm in the pull-out test.
3) The effect of bond creep on the long-term deflection of a cracked reinforced concrete beam using a twisted carbon fibre cable or a deformed aramid fibre bar had less significance. Compressive creep of concrete in compression zone mainly controlled the development of the deflection, as is the case of the deformed steel bar. The results indicate that the bond stress developed further along the FRP rebars in the beams than is the for the deformed steel bar, which consequently reduced the local bond stress on the FRP rebars enough to cause similar bond creep to the deformed steel bar.

Wang, Goto & Joh (1997) investigated the bond characteristics of FRP rods and effect on long term deflection of concrete beams. The bond stress-slip determined in pull-out tests were affected significantly by the type of fibre material, modulus of elasticity and the surface shape of the rods. The slip at peak load differed even though the peak load was approximately the same. The long term testing of FRP reinforced beams showed that their deflections varied and in average was 2.85 times that of steel reinforced beams. The FRP reinforced beams had a rapid increase of deflection at the beginning, which then stabilised and became the same as for beams with steel reinforcement, with the same rate of deflection. The long-term deflection of beams was less for GFRP rods than for CFRP and AFRP.

Non-destructive test methods, modal analysis, acoustic emission analysis and electromagnetic reflection (radar) analysis were applied by Reinhardt, Gollas, Weiler, Grosse & Eberle (1997) to three point bending and pull-out tests using aramid-vinyl ester resin bars. The modal analysis could detect bond deterioration qualitatively, but could not relate results to the degree of deterioration. Acoustic emission proved a sensitive means of locating the process of bond deterioration in terms of space and time. Radar did not detect changes in bond between aramid and concrete.

7.3.4.2 Temperature effects

The thermal incompatibility of FRP reinforcement and concrete may disturb the bond between rebar and concrete causing splitting type stresses and degrades the bond strength. Gentry & Hudak (1996) studied the heat effect on FRP bars with uni-directional fibres which had considerable transverse thermal movements caused by the resin. Wrapping fibres in the transverse direction may restrict the transverse movements

Honma & Maruyama (1989) investigated the effect of temperature on CFRP rods, by performing tests at room temperature after maintaining the specimens for 3 hours at different pre-set temperatures (from +20°C to +100°C). They found that the high temperature has a very detrimental effect on bond, probably as a result of lower shear stiffness of the matrix of FRP rods.

Al-Zaharani (1995) investigated the effect of temperature changes on the pull-out resistance of smooth rods. The author performed pull-out tests at different thermal conditions. In particular, three conditions were considered, characterised by different curing and testing temperatures, but the same absolute difference in temperature ($\Delta t=40$°C) between curing and testing. The results showed a much lower bond resistance when reducing the temperature between curing and testing by Δt than when increasing it. This effect is due to the bar contraction and expansion, caused by the

Copyright fib, all rights reserved. This PDF copy of fib Bulletin 10 is intended for use and/or distribution only by National Member Groups of fib.

temperature reduction and increases respectively, since both phenomena significantly influence the friction component of the bond mechanism. Therefore, besides the surface roughness, the coefficient of thermal expansion of FRP rods is an important parameter for determining bond behaviour of smooth rods, since it is responsible of a change in radial pressure on the rod when thermal conditions vary.

7.3.4.3 Crack widths and shrinkage

Zhao, Pilakoutas and Waldron (1997) studied the behaviour of concrete beams reinforced with steel and EUROCRETE GFRP rebars and investigated crack widths and the development of cracks. The concrete covers used were 25 mm. The BS 8110 equation for crack width prediction was used to predict the crack widths of FRP reinforced beams. The results were slightly un-conservative. It was concluded that the code approaches do not take into consideration the concrete characteristics, the effect of different surfaces on bond development and the large strains likely to be developed in FRP reinforced elements. The effect of shrinkage on FRP reinforced elements was thought not likely to be more pronounced than that for steel reinforcement.

7.3.4.4 Ductility

Malvar (1994) studied analytically a hybrid FRP bar made of two types of fibres with different modulus of elasticity. The conclusions were that it is possible to engineer hybrid FRP reinforcing bars, which would offer high initial stiffness, pseudo-ductility and hardening, and high strains to failure. Their high initial stiffness would ensure lower deflections and better concrete utilisation. Their potential for pseudo-ductility and hardening would allow for the redistribution of forces and prevention of a sudden structural collapse. The high strain to failure would serve as a precursor to failure. Hence, the properties of these hybrid FRP bars could potentially be very similar to those of steel bars.

Experimental tests with hybrid fibre bars by Tamuzs, et.al (1994) indicated that there might be problems to obtain bar ductility. These is because when the bond between the fibres is good, the impact of the breaking bundles of the stiffer fibres tears off neighbouring softer fibres and thereby destroys the hybrid ductility effect. However, if the bond in between the fibres is limited, the spreading of fracture from rupturing stiff fibres to softer ones is limited and hybrid ductility effect could be obtained. The ductile rod behaviour may be developed with braided fibre strands around a specially-made hollow core, Tamuzs et al (1995, Apinis et al (1998) and Apinis et al (1999). When unidirectional carbon fibers are mixed in certain proportion with aramide or glass fibers the FRP rods get a stress strain relation like cold formed steel. At critical strain level of about 1.2% the carbon fibers break and successively transfer the load to aramid or glass fibers with breaking elongation of about 3%. The fiber mix proportion, resin impregnation procedure and size effect of filaments and rods are very important to achieve desirable pseudo-ductile performance, Apinis et al (1999).

In an investigation on rotation capacity Lees & Burgoyne (1996) prepared a series of small-scale beams using two types of AFRP tendons or steel tendons. The influence of bond was investigated by testing beams with bonded tendons, unbonded tendons (the central length of the tendon in the beam had no bond) or partially bonded tendons (the bond was intermittent with staggered bonded and unbonded lengths of tendon or by coating tendon with a resin with known low shear strength). It was found that, unlike the bonded and unbonded beams, the beams with partially bonded tendons achieved both a high rotation capacity and a high ultimate load. It was concluded that the extent and distribution of bond along the length of FRP tendon has a significant influence on the flexural response of a beam. A good crack distribution and high ultimate moment capacity characterised the beams with bonded FRP tendons. Failure was due to tendon rupture with a limited rotation capacity. In the beams with unbonded tendons, there was only one major crack and failure occurred due to concrete crushing after a significant rotation had taken place. The ultimate capacity was lower than that of the bonded beams. In several of the partially bonded beams, the combination of a high rotation capacity and a high ultimate load was realised. Multiple cracks formed during testing.

Copyright fib, all rights reserved. This PDF copy of fib Bulletin 10 is intended for use and/or distribution only by National Member Groups of fib.

7.3.4.5 Fatigue and fretting of bonded FRP rods

In concrete beams loaded by repeated loads, slip of prestressed FRP cables at deviators might cause friction fretting of the rod surface with successive destruction of the rod. The same might take place close to flexure-induced cracks where bond stresses are high and cause a certain amount of slip. There are no known results about FRP fretting close to concrete cracks. This problem deserves further investigation.

In their investigation Sippel & Mayer (1996) concluded that an 0.35 mm thick epoxy-based powder coating mixed with sand and hardened under thermal conditions on GFRP strand can protect the fibres from damaging abrasive slip during load cycling. Reversed cyclic loading (with minimum load 0 kN) did not affect the ultimate static bond stress. The loading and unloading lead to an increased slip and to remaining relative displacement after each load step. With the new coating, the number of sustainable load cycles particularly in the service load range increased by a factor of 10.

Shield, French & Retika (1997) investigated the effect of thermal and mechanical fatigue on bond between GFRP rebar with helical deformations and concrete with compressive strength 55 MPa. The embedment lengths were chosen so that splitting failure resulted in all specimens. Out of 30 specimens, six were mechanically tension-tension cycled between 20-50% of static F_u 10^5 cycles, twelve specimens were thermally cycled 20 times between -20 and +25°C and twelve specimens were used as control specimens. During thermal fatigue, the rebars were also subjected to a constant tensile load of 5% F_u. The GFRP specimens showed no reduction in bond strength due to mechanical fatigue while the steel ones showed a 13% reduction. The thermal fatigue showed a 12% reduction of bond strength for GFRP and only 3% for steel. Despite this, GFRP bars are acceptable for reinforcement in concrete structures because the percentage of bond reduction in GFRP specimens due to thermal fatigue was similar to that of steel specimens due to mechanical fatigue.

7.3.5.5 Environmental influence on bond

Mashima & Iwamoto (1993) studied the bond characteristics of FRP rebars in concrete due to repeated freeze and thaw actions. The authors performed bond tests on 100 mm cubes with an FRP rod embedded at the centre of the specimen cube. Carbon, vinylon, glass and aramid FRP rods were used. After numerous freezing and thawing cycles, they observed that in case of GFRP, CFRP and VFRP rebars the bond strength was not changed appreciably, while bond resistance of AFRP rods reduced gradually with the progress of freezing and thawing.

Uppuluri et. al. (1996) developed analytical and experimental techniques to predict the effect on bond between FRP reinforcement and concrete in the presence of an accelerated service history. They presented an experimental verification of a finite element model on bond with and without accelerated environmental exposure. Agreement between the theoretical and measured bond stress development and load slip behaviour was shown, enabling the prediction of the effect of separately-measured environmental degradation of FRP materials on long term bond behaviour. It was concluded that the pull-out behaviour of chemically conditioned commercial rods can be predicted by conducting a simple experiment on a stand-alone rod to determine the percentage matrix degradation and then using normalised load versus normalised slip curves which have the percent matrix degradation as a parameter. Thus, the models provide a means to circumvent the necessity to conduct actual direct pull-out tests to determine the corrosion resistance and bond of degraded rods, where rough predictions are sufficient.

Al-Dulaijan & Nanni, Al-Zahrani, Bakis & Boothby (1996) performed FRP/concrete direct pull-out tests, FRP sonic resonance tests and FRP short beam shear strength tests aiming to establish the effect of accelerated environmental conditioning on the bond behaviour of GFRP rods. Three glass/vinylester rod types with different shapes of the outer surface were used: "machined glass-vinylester rod" (MGV) and two "commercially available GFRP rods" (CP and IG). The conditioning consisted of immersing for 28 days the FRP/concrete specimens in a saturated calcium hydroxide solution with high pH and temperature (at 60°C).

It was concluded that environmentally conditioned specimens showed degraded bond in comparison with control specimens. For MGV rods with axisymmetric lugs bond failure occurred

Copyright fib, all rights reserved. This PDF copy of fib Bulletin 10 is intended for use and/or distribution only by National Member Groups of fib.

by shearing off the lugs and at 14% lower load level for environmentally affected specimens. The reduction was due to the degradation of the resin. The reduction of the longitudinal modulus of elasticity of the rods was stated to be 9% and was due to fibre degradation. CP rods had 65% less bond strength. The degradation of bond strength was related to a 12% reduction in longitudinal modulus and 30% reduction in shear strength of the rod. The bond mechanism for this rod type is controlled by the resin rich surface. IG rods had a reduction of 38% of the bond strength. The reduction occurred simultaneously with a 17% reduction in the longitudinal modulus and an 11% reduction in the shear strength of the rod. No numerical correlation of pull-out load with shear strength or elastic modulus was possible since the bond mechanism is controlled by the resin coating that covers the FRP rod.

Bank, Puterman & Katz (1997) found similar results. They tested FRP rebars, conditioned in aqueous solution for 14 and 84 days at temperature of 80°C, which showed appreciable material degradation due to the polymer resin degradation. The authors found a good correlation between material degradation and the decay in bond strength and stiffness properties of FRP rebars.

Sen, Shahawy, Sukumar & Rosas (1998) studied the effect of tidal exposure on bond of CFRP rods using pull-out and beam specimens. The specimens were exposed for 18 months to three identical environments - wet in tanks outdoor, simulated tidal cycles with high humidity when out of water and combined tidal/thermal cycles. The water in the tanks was heated to 60°C with a cooling period out of water. The results from pull-out specimens indicated a significant increase in the maximum average bond stress during the first twelve months under both wet/dry cycles and the combined effect of vet/dry and thermal cycles. The rods absorbed water and swelled. Such improvement in bond was not, however, observed in the beam specimens tested where bond degradation was found to affect both the failure mode and ultimate capacity over the same time frame. The increase in bond resistance obtained from pull-out tests is believed to be largely due to moisture absorption by both the embedded and protruding part of the CFRP rod that lead to significant increase in the frictional component of bond. As this bond increase was especially noticeable over the first twelve months of exposure, the results indicate that it will be unwise to use pull-out specimens in accelerated durability tests. Such tests are unlikely to provide a realistic measure of the true bond in exposed flexural members. The lack of confinement in beams, compared with the pull-out tests, was probably the cause for the observations. After 18 months, a reduction in bond was observed.

Extensive research has been carried out by one of the Task groups of the EUROCRETE project into durability of fibre reinforced composites in alkaline and reinforced concrete environments, Sheard (1997). The main objective was to develop reliable test methods and data from which the long term performance of non-ferrous rebars in the concrete environment could be extrapolated. To achieve this objective a major test programme was initiated. By evaluating the effects of accelerating ageing against in service performance and assessing the long-term bond behaviour in concrete it was concluded that:

1. The concrete environment proved to be less severe than the simulated pore fluid solution, used for accelerated ageing.
2. The manufacturing process needs to be very carefully controlled to achieve desirable levels of durability in the fibre reinforced polymers field.
3. The matrix has more influence on the durability and the bond characteristics of a fibre reinforced composite rebar, than does the rebar.
4. There is no evidence to support that specially designed glass fibre reinforced rebars are not suitable for use in reinforced concrete.

7.3.5 Other types of bonded reinforcing devices

7.3.5.1 Bond of grid type FRP in concrete

Mochizuki & Udagawa (1995) investigated anchorage properties of two-dimensional FRP grid in concrete using pull-out tests. The grids were made of carbon fibres or carbon and glass fibres impregnated with vinyl ester. The specimens consisted of a concrete block 300 mm in width, 200 mm in depth and 650 to 750 mm length, with a slit inducing the crack. A part of the grid was

Copyright fib, all rights reserved. This PDF copy of fib Bulletin 10 is intended for use and/or distribution only by National Member Groups of fib.

embedded in each half specimen The concrete compressive strength of the specimens was 28 to 38 MPa. The test variables included the type of fibre, the number of longitudinal bars and the number of transverse bars. The test results indicated that the bond and anchorage of two-dimensional FRP grid depends mainly on the resistance of the transverse bars at the grid intersections. For carbon FRP grids, at least three transverse bars were required to obtain enough anchorage, while for hybrid grids (made of glass and carbon fibre), two transverse bars were required. During initial loading, a crack appeared at the location of the first transverse bar. Immediately after the appearance of this crack, the transverse bar nearest to the crack attracted load. As the load increased, the force at each cracked intersection became equal. The bending moment distribution in the projected area of the transverse bar is thought to be analogous to that of a laterally loaded restrained pile in soil and that in the area between the intersections is analogous to that of a beam fixed at both ends.

Kobayashi, Rahman & Fujisaki (1997) proposed a formula for crack width determination after studying the stress transfer mechanism of NEFMAC-RC strip slabs. It appears that the crack width w, is mainly a function of the grid spacing and reinforcement ratio.

$$w = C_f \beta (\varepsilon_s + \varepsilon_{cs}) \tag{7.3.13}$$

where,

$$C_f = k + l L + m f_{ct}/(\rho_t f_u) \tag{7.3.14}$$

with β = ratio of distance between the neutral axis and the extreme tension fibre to that between the neutral axis and the centroid of the main reinforcement.
ε_s = strain in NEFMAC reinforcement
ε_{cs} = shrinkage of concrete
L = grid spacing of NEFMAC reinforcement
k, l, m = numerical constants respectively 4.956, 1.006 and 5.03.
f_{ct} = tensile strength of concrete
ρ_t = geometrical percentage of reinforcement
f_u = NEFMAC tensile strength

The above equation is a further development of the Gergely & Lutz equation. The predicted crack widths agree well with the measured ones. For low reinforcement ratios, crack widths reached 0.3 to 0.5 mm immediately after first crack.

FRP (carbon, vinylester) grids with various designs were placed as reinforcement in concrete beams and tested for flexural performance. The grids transmit anchoring loads via the transverse members, which provide mechanical interlocking with concrete. The following grid designs were used: (i) weaves with fibre connectivity between adjacent layers, (ii) cross-plies without layer fibre connectivity, (iii) a combination of cross-piles and fibres (33% and 67%) that turn the corners. Fibres passing straight through the joint have a primary influence on "beam" stiffness (anchorage), whereas the interlocking fibres due to weaving have a secondary influence on beam stiffness.

7.3.5.2 Bond performance of woven fabrics in cementitious composites

Woven fabrics have a great potential in reinforcing thin elements to produce high performance cementitious composites. The weaving process and the interlacing of yarns cause a crimped shape both in fill and warp yarns. Peled, Yankelevsky & Bentur (1995) presented a study on the bond between monofilament polyethylene yarns and the cement matrix. The study was performed on curved yarns, which were made from different woven fabrics. The woven fabrics were plain weave with varied yarn density. Straight yarns were also examined for comparison. Pull-out tests were carried out to investigate the bond mechanisms. It was found that the yarn structures geometrical characteristics have a pronounced effect on the bond resistance parameters. The crimped structure is responsible for load cycling while pulling out. The following were concluded:

1) The crimped structure of the yarns improved the bond capacity between polyethylene monofilament yarns and the cement matrix compared to a straight yarn.

Copyright fib, all rights reserved. This PDF copy of fib Bulletin 10 is intended for use and/or distribution only by National Member Groups of fib.

2) The pull-out resistance of a crimped yarn depends significantly on the yarn wavy structure: amplitude decrease affects a reduced anchoring resistance whereas wave length decrease contributes to an enhanced resistance.
3) Fabric density affects the wavy structure of fills and warps, both in wave length and wave amplitude. These geometrical characteristics have an important influence on bond performance.
4) The crimped structure is responsible to load cycling while pulling out, due to phase changes between the yarn-crimped structure and the matrix crimped groove structure.

7.3.5.3 Composite beams of fibre reinforced plastic profile and concrete.

Kettil (1995) studied composite beams of concrete and structural profiles of fibre-reinforced plastic (FRP). FRP profiles have a low stiffness to strength ratio, making deflection and buckling critical. Adding concrete to FRP profiles improves stiffness, prevents buckling and may increase the shear capacity. The study resulted in formulas for flexural stiffness and strength, and tentative models for shear strength and deformation were presented. Detailing for bond was found to be crucial for composite action. The bond strength, when sand was glued to the GFRP shape, was at least 3 MPa. No slip occurred between concrete and GFRP. Bond failure did not occur at all when shear connectors were added. The observed behaviour was in reasonable correlation with theoretical predictions, but a larger number of tests were deemed necessary for validation purposes.

7.3.6 Conclusions

From the research on pull-out tests on FRP bars/rods the following can be concluded:
1) The surface characteristics of the FRP bar/rod (braided, strand, sanded, having ribs) influence considerably the bond strength and slip behaviour. For good concrete, the resin type, rather than the fibre type, controls the bond strength. If shearing off of the lugs takes place, the height of the lugs has no significant influence on the bond strength.
2) FRP rods with well-bonded deformations appear to have better bond than steel at low loads, but later have an increased slip due to their lower modulus of elasticity and the Poisson effect. Bond strengths are in general comparable with those of steel re-bars, even though for normal concrete strengths bond failure is more likely to be due to damage in the FRP concrete interface. As a result, concrete strength does not appear to have as significant effect as in the case of steel. Nonetheless, for low concrete strengths, bond failure occurs in the concrete.
3) Sand covering of the bar surface also provides a stiff bond at low loads, but at higher loads, the surface layer may peel off. This happens for concrete compressive strengths in excess of f_{cc} = 30 to 40 MPa. After peeling a ductile sliding friction bond may develop, which can retain 50% of the ultimate bond strength. This friction bond can be of importance for long bond lengths and can be used to improve the ductility of concrete members. Indentations in the bar surface also increase the bond. Sand coated bars appear to have a lower splitting tendency than smooth deformed bars.
4) Spirally wound bars shows very scattered bond strength.
5) Smaller bar diameters give higher bond strength.
6) Flat or square section bars may have a higher bond strength than round bars, but may lead to increased splitting forces in the surrounding concrete.
7) Top-cast bars have about 10 to 30 % lower bond resistance if the failure is due to concrete and not peeling off of the anchored bar surface.
8) Confinement of the rods appears to increase bond resistance. Transverse beam support pressure seems to have a positive influence on anchorage of FRP bars. This, however, may depend of the type of rod. FRP rods are easy to squeeze and, hence, the effect of confinement may be limited.
9) Confinement by wrapping the concrete member with carbon fibre sheet to prevent concrete splitting increases the bond strength of embedded FRP bars.
10) The splitting tendency of FRP bars can be studied by using eccentric pull-out tests and evaluating the results by the theory for a thick-walled ring around the bar.
11) Embedment length affects the average bond stress due to progressive nature of failure of bond. Loaded-end slip at the onset of free-end slip increases with increasing embedment length and decreasing load diameter and is relatively constant for rods with similar embedment length to diameter ratios.
12) Pretensioning of the FRP rod may increase bond strength.

Copyright fib, all rights reserved. This PDF copy of fib Bulletin 10 is intended for use and/or distribution only by National Member Groups of fib.

13) The resin properties appear to influence creep of FRP at low loads. At higher loads the creep of concrete in compression is expected to have a dominating effect on the element deformations.
14) Mechanical fatigue reduced the bond strength of steel bar by 13%, but not for GFRP bars.
15) A thin epoxy-based powder coating mixed with sand can decrease fatigue fretting of fibres.
16) GFRP bars exposed to thermal cycling in concrete show a 12% reduction in bond strength, as against to 3% in steel.
17) Using FRP bars with intermittent lengths of debonded bars can increase rotation capacity of concrete beams. Hybrid fibre bars designed with initial high stiffness, pseudo-ductility and hardening could allow for redistribution of forces and prevention of sudden structural collapse as in the case of steel.
18) The environmental effects on the degradation of bond can be predicted by using accelerated immersion tests and suitable modelling.
19) Tests with grid FRPs in concrete show that anchorage is enhanced by the transverse FRP bars. When load increases the shared force for each transverse bar along the anchorage length equalises. Crack widths are mainly dependent on the grid spacing.
20) Woven fabrics have a potential for reinforcing thin elements. Bond studies on polyethylene yarns in cementitious matrix have concluded that the geometrical characteristics have a great influence on bond and a crimped structure is favourable.
21) Pulltruded FRP sections can be used as reinforcement in concrete members as well as provide the mould for casting. The shapes could have shear connectors or sanded surface for improved bond.

Copyright fib, all rights reserved. This PDF copy of fib Bulletin 10 is intended for use and/or distribution only by National Member Groups of fib.

7.4 Anchorage of continuous fiber tendons for prestressing

7.4.1 Anchorage of PC tendons for prestressing systems

A summary of published results on anchorage of continuous fiber tendons for pretensioning systems is given in the JSCE (Japan Society of Civil Engineers) State-of-the-art-report, Machida (1993).

The bond between the FRP tendon and concrete must be adequate and stable for very long time. The shape of the tendon surface can have either twisted form, braided form, spiral fiber, indented form, flat bar with irregularities, or it may be shaped as a grid and rope.

The twisted carbon fiber tendons show a bond at least as good as that of PC steel tendon of the same diameter (12.5 mm). The transfer length is about 35 diameters.

Braided continuous aramid fiber rods with sanded surface require a transfer length of about 20 rod diameters while rods without sand cover register about 35 diameters. Carbon fiber rods register somewhat shorter transfer lengths.

Deformed continuous fiber tendons (ϕ6) with spiral fiber obtained by winding and setting aramid fibers in a spiral around the tendon while this is treated by pultrusion process required a transfer length of 42 and 58 diameters for the force levels of 55% and 76% of the tensile capacity respectively.

Carbon FRP tendons (ϕ8) with indentations needed 100 diameters to transfer the prestressing force and this length did not change during a 2 month period.

Flat aramid fiber strip (1.5x20 mm^2) with irregularities needed only 60 mm for prestressing load transfer. The shape of the strip and the intense force transfer resulted in high splitting stresses.

Plain grid continuous fiber tendons (ϕ8) anchor mainly with the transverse bars. The transfer length was found to be two transverse bar distances (150 mm between the transverse bars). As the grid crossings are dependent of the strength of the resin, however the transfer length may change with time.

Aramid fiber rope tendons consisting of eight braids needed about 280 mm to transfer the prestressing force.

The factors influencing the transfer length are: the kind of fibre, surface configuration, diameter, introduced prestressing force, concrete strength and type, cross sectional area, prestress, arrangements of tendons, method of releasing prestress and passage of time. Because of the many existing variables a standard method for determination of transfer length should be developed.

With the aim to determine the development length for the prestressing force prestressed concrete rods 2.00 m long with a section of 70x70 mm^2 were made, Tepfers et. al. (1992). Three rods were axially prestressed with Arapree strips (2x20 mm^2) and three with CFCC (ϕ12.5 mm). The concrete strength was f_{cc} = 43.2 MPa for those with Arapree strips and f_{cc} = 39.4 MPa for those with CFCC. At the ends of the rods the Arapree strips were surrounded by spirals of steel ϕ3 Ss260 (Swedish standard), 100 mm long and the CFCC were surrounded by spirals of steel ϕ6 Ss260, 700 mm long. The Arapree prestressing force was 36.5 kN and that of CFCC 83.0 kN.

The registration of the introduction of the prestressing force into the concrete rods was done at releasing of prestress by measuring the concrete strain along the center line on two opposite sides of the concrete rods. The measurements were taken from the ends of the rods 700 mm towards the center. The tests with Arapree resulted in appearance of splitting cracks along the prestressing strips opening from the ends towards the middle of the rods. The splitting forces from the flat sides of the strips together with little confinement from conclusively the small spirals at the ends of the rods resulted in this progressive splitting failure. The development length could not be stated. However it was found that 400 mm are needed to transfer the full prestressing force to the concrete from 12.5 mm CFCC rod.

Copyright fib, all rights reserved. This PDF copy of fib Bulletin 10 is intended for use and/or distribution only by National Member Groups of fib.

Fiber composite bars containing aramid fibers can be used as prestressing elements. Up to now research and practical applications mainly focussed on the pretensioning system. Hence it is important to have information about the transmission length of this type of bars. Force transfer of AFRP Twaron bars in concrete prisms has been investigated by Taerwe and Pallemans (1995). Tests have been performed with the aim to determine the transmission length and the critical concrete cover of several available bar types. The aramid FRP bars have nominal diameters of 7.5 and 5.3 mm with sanded surface. For the latter type bars with compressible "expancel" coating with and without sand were also tested. For the sanded bars without coating, it is tentatively suggested to determine the transmission length by the relationship $l_{bpt} = 16\ \phi$ with ϕ the nominal diameter.

The critical concrete cover for the sanded bars is about 2.8 ϕ. The compressible "expancel" coating reduces the Hoyer effect and thereby this value to 2.3 ϕ. Also the use of high strength concrete and the addition of synthetic fibers reduces the critical concrete cover.

In order to investigate possible cracking due to thermal expansion (5 to 8 times that of concrete) in transverse direction of the AFRP rods temperature cycles with a rate of 15°C/hour between 20°C and 50°C did not result in cracking of the concrete cover of the prisms prestressed with AFRP bars without compressible coating.

Monitoring of bond deterioration in aramid prestressed elements by non-destructive testing is reported by Krüger et. al (1996). The coefficient of thermal expansion of concrete and aramid does not match, which may cause differential movement and deterioration of bond between concrete and aramid. Tests are carried out in order to quantify this effect by means of modal analysis and acoustic emission.

Transfer and development lengths for 8 mm Leadline bars and 10.5, 12,5 and 15,2 mm CFCC strand have been investigated by Zaki & Rizkalla (1996) testing pretensioned concrete beams using different shear span values. The proposed transfer length is:

$$L_t = f_{pi}\ d/(\alpha_t\ f'^{0.67}_{ci});$$

and proposed flexural bond length is:

$$L_{fb} = (f_{pu} - f_{pe})/(\alpha_f\ f'^{0.67}_{c}).$$

The development length is $L_d = L_t + L_{fb}$.

Where

d	tendon diameter (m)
f_{pi}	initial prestress (MPa)
f'_{ci}	concrete strength (MPa)
f_{pu}	ultimate tensile strength (MPa)
f_{pe}	effective prestress level (MPa)
α_t	coefficient determined by regression analysis for Leadline 1.9 and for CFCC 4.8.
α_f	coefficient determined by regression analysis for Leadline 1.0 and for CFCC 2.8.

Conclusions:

* Both transfer length and flexural bond length are proportional to the tendon diameter of CFRP tendons.
* The average transfer bond strength for CFCC is not affected by changes in the strand diameter.
* The average flexural bond strength for CFCC increases with the increase of strand diameter.
* The transfer length is proportional to the prestress level while the transfer bond strength was not affected by the prestress level.
* Concrete cover 4d was enough to prevent splitting at the beam ends.
* Transfer length of 8 mm Leadline bar is about 12% more than ACI prediction for equivalent steel strand for concrete strength of 30 MPa at transfer.
* Transfer length of CFCC strand is about 50% of ACI prediction for equivalent steel strand for concrete strength of 30 MPa at transfer.

Copyright fib, all rights reserved. This PDF copy of fib Bulletin 10 is intended for use and/or distribution only by National Member Groups of fib.

* Flexural bond length of Leadline is about 20% less than ACI prediction for steel strands for concrete strength of 35 MPa.
* Flexural bond length of CFCC strands is about 25% of the ACI prediction for steel strands for concrete strength of 35 MPa.

7.4.2 Anchorage of prestressing tendons in concrete and rock

Bond strength of fiber reinforced plastic (FRP) cement grouted anchor bolts has been investigated by Xu, Bellavance & Benmokrane (1995). The tests have been performed as laboratory tests with GFRP (E-glass fibers impregnated with thermoset polyester resin in pulltrusion process) installed in concrete blocks and field tests with FRP anchored in rock mass. A total of 68 GFRP and 26 steel anchors with the same diameters, 25.4 mm, three bond lengths were tested. The bond lengths were in laboratory 63.5, 127 and 190.5 mm and in field 150, 450 and 900 mm. The bond strength, bond stress-slip behavior, critical length of cement grouted GFRP anchors are examined in comparison with conventional steel anchors. The grout had a compressive strength of 52 MPa.

Type A of the GFRP bar has a deformed surface created by fibers wound around the GFRP in a spiral shape and Type B has a surface, which also is sand coated. Type C has a smooth sand coated surface. The fibers on the smooth surface of Type D is loose. Type E has the surface taws stressed so that indentations are obtained.

A critical bond length is defined as the minimum bond length required to develop the ultimate tensile strength of the anchor, and depends on the bond strength and the tensile strength of the tendon, Table 7.4.1.

The following conclusions in the comparative study are obtained from the tests on five types of GFRP anchors:

* The bond resistance of GFRP anchors installed in concrete blocks is higher than that in rock mass.
* The bond strength of GFRP A and E anchors is lower than that of steel bar anchors, and is slightly higher than that of Dywidag bar anchors. GFRP C and D anchors with a smooth surface have a significantly lower bond strength than steel and Dywidag bar anchors.
* The critical bond length of GFRP anchors varies considerably. GFRP anchors have a much longer critical bond length than steel bar anchors due to their higher tensile strength and lower bond strength. GFRP A and E anchors have similar critical bond length to, and GFRP B, C and D anchors with smooth surface have a longer critical bond length than, Dywidag anchors.
* GFRP anchors have similar load-slip behavior to that of steel and Dywidag bar anchors, except GFRP D anchors with the smooth surface. The slip at failure of GFRP anchors is greater than that of steel anchors mainly due to their low modulus of elasticity.

Anchor type	Rock mass L_c (mm)	L_c/d	Concrete block L_c (mm)	L_c/d
GFRP A	471	18.6	364	14.3
GFRP B	996	39.2	859	33.8
GFRP C	2624	103.3	1369	53.9
GFRP D	2519	99.2	1303	51.3
GFRP E	922	36.3	577	22.7
Steel bar	-	-	194	7.6
Dywidag bar	800	31.5	504	19.9

Table 7.4.1. Average critical bond length L_c of GFRP and steel anchors. Diameter d.

7.4.3 Anchorage of PC tendons for post-tensioning systems

The following is stated in the JCCE State-of-the-art-report, Machida (1993).

Copyright fib, all rights reserved. This PDF copy of fib Bulletin 10 is intended for use and/or distribution only by National Member Groups of fib.

Continuous fiber tendons are reinforced in one direction only. When pulling them by a jack using blocking devices for steel would cause compressive stresses in transverse direction simultaneously as tensile stress occurs, resulting in shearing stress and causing the tendon to fracture under a stress smaller than the actual strength. Therefore several special types of devices, which may be put into practical use, have been developed.

Some requirements for anchorage device for continuous fiber tendons are:

* The device should be easy to operate when prestressing and the time of work should not be very different from that spent on PC steel.
* The device must have a simple system and take small space in relation to overall anchorage areas.
* The device must be corrosion resistant.
* The device effect should be time stable.

There can be wedge type devices made of metal or FRP, mold type devices where resins or expanding cement mortars fix the tendon inside a sleeve. Threaded anchorages with nuts have not been used, because the tensile strength is lower of the threaded section of the tendon. There can be single or multiple type of wedge anchorages. The wedge anchorages tend to be longer than those used for PC steel. It is difficult to anchor the same force in all tendons with multiple type anchorages, why the rupture load of these tendons becomes lower. Carbon FRP tendons are also die-cast to enable the use of wedges intended for PC steel strands. Anchorage devices of mold type are somewhat longer than wedge type anchorages and usually delivered after being especially adapted to the site. This not always favors the productivity.

When anchoring devices made of steel come into direct contact with carbon FRP tendons, electrical corrosion might occur. FRP wedge devices are therefore preferable.

7.4.4 Fatigue of anchoring systems

The fatigue resistance of the tendons in the anchoring zone should be studied.

7.4.5 Summary

The bond of prestressing rods/strands has to be stable and adequate for very long time. The bond transfer length has been determined for different types of FRP rods/strands and varies between 35 to 100 bar diameters. Flat rod shapes have intense bond transfer, but high splitting forces from the flat surfaces. In certain cases it seems to be advisable to reduce the intensity of bond transfer from rod/strand to limit splitting, spalling and bursting forces in the end of concrete member. Concrete cover thickness, concrete strength and confining reinforcement determines the splitting resistance. The splitting forces depend on the type of FRP rod/strand.

The coefficient of thermal expansion of concrete and aramid does not match, which may cause deterioration of bond. Test with temperature cycles between 20 and 50°C however did not result in cracking of concrete cover and deterioration of bond.

GFRP grouted anchor bolts in rock have been tested and need longer anchorage lengths than steel anchor bolts. The slip is greater for GFRP due to lower modulus of elasticity than for steel.

Different types of wedging systems have been developed for different FRP rods/cables. The main problem is the limited transverse compression resistance of the rods/cables to the wedge pressing. Carbon FRP should not be in direct contact with steel wedging systems doe to risk for corrosion. The device should have simple system, take small space and be easy to operate.

Copyright fib, all rights reserved. This PDF copy of fib Bulletin 10 is intended for use and/or distribution only by National Member Groups of fib.

7.5 Joints

7.5.1 Direct joints

Direct joints of FRP can be classified into the mechanical joint type which uses rivets and screws and the adhesive connecting type which uses adhesives, Machida (1993). Most of the methods so far tried consist of connecting a rope-shaped exterior cable with a sleeve for linking members. However there is little data about these methods. The FRP tendons are usually made such that joining is not needed.

7.5.2 Lap splice

Results from tests of continuous carbon fiber bars (ϕ7.5) of seven twisted wires with sleeve joints conducted according to JSCE Recommendations for evaluation of joints in reinforcing bars suggest that the splice must be about 800 mm (107ϕ) long to fail by rupture of the continuous fiber bar, Machida (1993).

Makitani, Irisawa & Nishiura (1993) performed eight tests of lap splice joints. The truss type of beam specimen with two anchoring ends and CFRP rebars as main reinforcement was tested to evaluate the effect of lap splice length on the bond characteristics of the bars. The FRP rebars were positioned in the central of two chord members and the length of lapped splice was ranging from 10 to 60 times the bar diameter. CFRP rebars were 8 mm in diameter and their surface was processed into crossed spiral ribs in order to improve bond behavior. The tensile strength of rebars was equal to 1860 N/mm^2 while the compressive concrete strength was 31 N/mm^2.

Conclusions:

* With the length of lap splice more than 40 times the bar diameter the full tensile force could be transferred;
* The unit bond strength increased by increasing the lap splice length; however, it decreased for length ranging from 40 to 60 times the bar diameter.

There is a special type of bars, C-bars, manufactured in limited lengths as steel bars usually are. C-bars are deformed FRP bars for use in non-prestressed concrete. The bars are made of glass fibers with a hybrid pulltrusion/ compression molding process using alkaline resistant resin (Urethane modified vinyl ester) mixed with chopped ceramic fibers forming the lugs. (According to other source the surface layer made of PPS (Poly para phenelen sulphide, Ryton) with high melting point 290°C, is hard and very resistant to strong alkalis and weak acids). The interior of the rebar incorporates a less expensive unsaturated polyester resin made from recycled P.E.T. The bars are available with glass, aramid or carbon fibers. The bars are delivered in 6 m lengths and have to be lap spliced if necessary. The nominal bond strength is for #12 bar 17 MPa and for #15 bar 18 MPa and is determined by the shear strength of the lugs. The lap lengths are determined from these bond strengths.

Tepfers & Karlsson (1997) performed several tests in order to study the bond behavior of such rebars in different conditions. The test program included: pull-out tests with central and eccentric placement of bar; splice tests. Test results indicate that the splitting anchoring forces and the available confinement determine the bond transfer and the splice lengths. Due to ribbed glossy surface of the C-Bars the splitting forces become more pronounced than for steel reinforcing bar. Pull-out tests with central placement of bar were conducted by using three different bond length (3, 5 and 7 times the bar diameter) and three types of concrete (compressive strength equal to 25, 40 and 55 MPa).

Independently on the bond length, in case of diameter 15 mm C-BAR positioned in concrete with compressive strength 29 MPa the obtained maximum bond stress was about 14 MPa, which is on the level of a good steel reinforcing bar.

The overlaps were tested in almost constant moment zone of bent symmetrically two points loaded isostatic beams. Three beams were tested (splice length 0.4, 0.6 and 0.8 m). Concrete compressive

Copyright fib, all rights reserved. This PDF copy of fib Bulletin 10 is intended for use and/or distribution only by National Member Groups of fib.

strength was 29 MPa.

It was stated that diameter 15 mm C-BAR lapped with 0.80 m overlap splice and cover 30 mm is able to transfer about 300 MPa tensile stress. The bond stress is then 1.3 MPa.

A similar investigation was performed by Tepfers, Hedlund & Rosinski (1998) using sand covered GFRP bars made of continuous glass fibers impregnated with polyester resin (Hughes Brothers, Inc - USA). In order to improve bond behavior, the continuous fibers are surrounded by a spirally wound fiber filament.

Results from splice tests show that diameter 25 mm bars, lapped with overlap length 0.80 m in concrete with compressive strength 29 MPa and cover 30 mm, are able to transfer 400 MPa tensile stress. The bond stress is then 3.1 MPa.

Pull-out tests show that when confinement is good (bar in central position) the maximum bond stress is between 3 and 6 MPa.

From the investigations above it can be concluded that the C-BARs give better anchorage when confinement is good (i.e. in case of pull-out tests with central placement of bar) but the GFRP bar gives better anchorage when confinement is limited. (i.e. in case of splice tests). This is due to the lower splitting tendency of the GFRP bar.

Benmokrane, Tighiouart & Thériault (1997) have investigated the strength of GFRP overlap splices. The effects of bar size (12.7 and 15.9 mm) and lap length (0.6, 0.7, 0.9, 1.3 and 1.6 l_d, where l_d is the development length according to ACI 1994 Building Code) were studied. Test results indicate that a modification factor 1.3 is necessary for the development length of GFRP bars. At 1.6 l_d the bond stress permits the development of the complete GFRP rebar tensile strength. Compressive strength of concrete was 30 MPa. All splice failures were concrete cover splitting failures. The bars had two opposite helical fiber filaments wound around as surface deformations.

Achillides, Pilakoutas & Waldron (1998) have conducted an experimental series in order to investigate the splitting bond strength of C and GFRP EUROCRETE bars. Various types of reinforcement configurations were tested in order to examine the bond splitting behaviour of G and CFRP bars in splices and as single anchorages. The beams were tested in four-point bending. Two types of concrete strengths were used (f_c = 35, 45 MPa). The following conclusions were drawn:

* GFRP bars developed only 70% of the bond splitting strength of CFRP bars under identical experimental conditions, which contradicted the results of the pull-out cube tests that suggested similar bond behaviour between G and CFRP bars. This was attributed to the large difference in the modulus of elasticity between G and CFRP bars. The modulus of elasticity is believed to play an important role to the bond splitting behaviour of reinforcing bars. In order to justify this, the authors applied an analytical approach that is described in Section 7.3.3.
* Spliced bars appeared to develop similar bond strength values to single bar anchorages.

Grids made of glass or carbon FRP with 100 mm spacing were tested in bending of one way slabs with lap splice in the middle span, Machida (1993). The results showed that it was necessary to provide a joint length of at least one grid spacing. It should be noted that the strength of the joint is dependent on the strength of the points of crossing, the grid spacing and the strength of the concrete. The obtained result yields only for certain parameter combinations.

7.5.3 Connecting of precast members

Due to their good corrosion resistance it is favorable to use FRP as connectors. However, the dowel action and shear resistance of the FRP connectors is limited. Therefore, FRP connectors should be used as a system for post-tensioning.

Copyright fib, all rights reserved. This PDF copy of fib Bulletin 10 is intended for use and/or distribution only by National Member Groups of fib.

7.5.4 Summary

Continuous fiber bars provide a higher tensile strength than steel bars and consequently need longer lap splices than steel bars. Necessary design tensile FRP reinforcement overlap lengths have to be stated in beam tests for every type of FRP reinforcement.

GFRP with ribs like those of steel bar lugs (C-BAR) demonstrates the same bond resistance as steel, if confinement is good. The C-BAR gives better anchorage, when confinement is good, but the indented sand covered GFRP bar gives better anchorage, when confinement is limited.

Glossy ribbed bar surface provides high splitting bond forces and sand covered surface not.

The strength of lapped grid reinforcement is dependent on the points of crossing, the grid spacing and strength of concrete. The overlap should be at least one grid.

Future work should include development of sleeve joints. If metals are used, the risk of corrosion should be accounted for.

Copyright fib, all rights reserved. This PDF copy of fib Bulletin 10 is intended for use and/or distribution only by National Member Groups of fib.

7.6 Bond of continuous fibre sheets and plates

7.6.1 Introduction

Continuous fibre sheets (or laminates) and plates (also known as *External continuous Fibre Reinforced Plastics*, ExFRP's) are composite materials of continuous fibres bonded with polymers. The lightness and flexibility of this reinforcement enables easy handling during construction. Although the fibres possess much higher tensile strength than steel (here considering only carbon, aramid and glass), they are brittle and do not possess any ability for plastic deformation.

The bonding mechanism of ExFRP is different from those of ordinary steel reinforcing bars and continuous fibre reinforcing bars. Steel and continuous fibre reinforcing bars are embedded in concrete and usually have indentations on their surface for better bonding. ExFRP's, however, are externally attached to the concrete surface and have no indentations for anchorage on their surface. Therefore, the main source of bonding resistance for continuous fibre sheets and plates is only the layer of adhesive that is used to bond the surface of the ExFRP on concrete. In some cases, special mechanical anchorage devices (such as clamping hardware) are used to supplement the bond between concrete and continuous fibre reinforcement.

In comparison with steel plates currently used for external strengthening, ExFRP´s not only have a much higher strength to weight ratio but also are more practical to use and are more resistant to corrosion. Surface preparation, which is an additional cost when using steel plates (achieved by shot blasting), is not necessary if thin sheets or a peel ply is used. In fact, if the peel ply is only removed just prior to bonding, then the extensive cleaning operation is also avoided. Hence, despite the higher cost of the raw strengthening materials, the total cost of the operation can be lower when ExFRP is used.

It is well established that the flexural capacity of ExFRP reinforced elements will only be achieved if bond or shear failures are avoided. Many investigators have developed models for predicting the flexural capacity based on the classical beam theory. Even though it is known that inadequate shear strength will lead to problems in applications where flexural strengthening is the primary objective, this topic is beyond the scope of this report, which will concentrate mainly on issues relating to bond.

The following section presents techniques for material characterisation and outlines the basic material properties. It then discusses the various types of bond failure observed either in experiments or in field applications. This will be followed by a report on analytical work and design guidelines in this field.

7.6.2 Materials and techniques used for external bonding

A successful plate strengthening project depends mainly on the materials and techniques used in the bonding processes. A brief review of this subject is presented in this part.

7.6.2.1 Epoxy adhesives

Epoxy resins have been used in the highway and construction fields as early as 1955 (Nordby *et al*, 1962) and since then, many applications of epoxy-resin adhesives in construction are known (Iino and Otokawa, 1981). Epoxies have favourable characteristics for repair applications, such as good adhesion, versatility, inertness, low shrinkage, rapid hardening and moisture resistance. They make excellent structural adhesives for bonding concrete to concrete and concrete to steel and after proper curing, possess five to eight times higher tensile and shear strength than Ordinary Portland Cement (OPC) concrete, but much reduced Young's and shear moduli. As a result, bond failures are not generally expected to take place within the adhesive layer.

Copyright fib, all rights reserved. This PDF copy of fib Bulletin 10 is intended for use and/or distribution only by National Member Groups of fib.

Epoxy resins used in civil engineering usually comprise two components. One is the resin itself and the other component is a hardening system. The manufacturers often supply adhesives by giving the resin and hardener components in substances of distinct colours. Mixing of the resin and hardener must be done thoroughly with a power mixer and carried out at an appropriate time in accordance with the manufacturer's instructions. Normally, colour contrast is not apparent when mixing is completed. Power mixing should be operated at low speed to prevent excessive temperature increase and air entrainment during the mixing operation. In addition, small batch mixing is recommended because the curing process is rapidly accelerated by the exothermic reaction, causing rapid hardening in larger batches.

In order to achieve successful bonding, surfaces that are to be attached must be strong, sound, dry and clean. Injection under pressure, vacuum, or coating and adhering under pressure are some of the techniques used for bonding. Bonding of fibre fabrics by direct application of resin is also possible with FRP. The main objective is to eliminate or minimise the formation of air bubbles, since those create discontinuities in the glue joint and weaken the bond strength by reducing the area of adhesive. When using plates, the bonded surfaces should be flat and compatible with each other. In the injection process, the flatness of a concrete substratum is not so severely required as in the press bonding process.

A monolithic body of concrete and adherent bonded with epoxy resin can transmit stress efficiently. However, since the elastic modulus of epoxy resin is much lower than that of the adherent and concrete, the thickness of the epoxy resin layer should be minimised as far as possible.

The strength of adhesive joints made with epoxies depends on the degree of curing before opening the concrete to service. The time required for curing relies on the hardening rate of the epoxy resin at various temperatures, and can be obtained from the manufacturer. During curing, the joint must not be moved, otherwise cracks might develop at the interface, which could lead to loss of bonding by the ingress of moisture.

7.6.2.2 Strengthening materials

1) Steel plates

From a structural and economic point of view, mild steel can be a very good choice for externally strengthening structural elements, due to its stiffness, strength and low cost. Both short and long-term experience, however, suggests that the steel plate bonding method often suffers from a number of disadvantages:

a) difficult handling in the construction site, due to the heavy weight of the steel plates,
b) frequent joints, due to the limited delivery lengths of the steel plates,
c) intensive scaffolding to meet the requirement of labour safety,
d) deterioration of the bond at the interface of steel and concrete, due to electrochemical corrosion of the steel plates, and
e) the magnetic and electrical characteristics of steel plates also limit their use in certain 'sensitive' structures.

Although stainless steel is appropriate for enhancing the durability of structural members, it is not generally recommended for use, since adequate surface preparation for bonding is more difficult to be correctly and effectively executed.

2) FRP sheets and plates

Although some of the above mentioned disadvantages of the steel plates can be overcome with careful planning, concrete structures are found in many complex and severe environments, therefore, great care must be taken to ensure their durability. Mitigating the electrochemical corrosion problem of the steel plates has been acknowledged recently as a major concern in structural repairing activities. Therefore, this problem and the disadvantages mentioned in the preceding, have motivated alternative technologies, that replace entirely the steel plates with non-metallic advanced composite materials.

Copyright fib, all rights reserved. This PDF copy of fib Bulletin 10 is intended for use and/or distribution only by National Member Groups of fib.

Currently, the most important alternative materials considered are, glass fibre reinforced polymers (GFRP), carbon fibre reinforced polymers (CFRP) and aramid fibre reinforced polymers (AFRP).

Meier (1992) states that these materials are not only free from corrosion even under aggressive environments, but also offer very positive properties for use as structural materials, such as outstanding fatigue performance and lighter weight, coupled with reasonably high stiffness and a very high strength. Meier (1995) gave a qualitative comparison between GFRP, AFRP and CFRP, as illustrated in Table 7.6-1.

Table 7.6-1: Qualitative comparison between E-glass, Aramid and H-T carbon fibres (Meier, 1995)

	Fibre composite laminates made of		
Criterion	Carbon	Aramid	E-glass
Tensile strength	Very good	very good	very good
Compressive strength	Very good	Inadequate	good
Modulus of elasticity	Very good	Good	adequate
Long term behaviour	Very good	Good	adequate
Fatigue behaviour	Excellent	Good	adequate
Bulk density	Good	excellent	adequate
Alkaline resistance	Very good	Good	inadequate
Price	Adequate	Adequate	very good

3) CFRP sheets and plates

CFRP composites have the highest tensile modulus of elasticity amongst the various types of FRP reinforcement (typically, 50- 70% of the modulus of steel) and appear to be the most suitable for strengthening applications. The properties of CFRP composites depend on the constituents of carbon fibres and resin matrix system used. Gill (1972) gave a detailed description of properties of CFRP composites in his book, ''Carbon Fibres in Composite Materials''. Some typical data obtained from this book regarding properties of CFRP composites are presented in the following.

Temperature resistance of CFRP plates depends mainly on the resin matrix, since carbon fibres could retain their full mechanical strength up to at least 1000° C. However, Gill (1972) pointed out that temperatures above 350° C are sufficiently high to cause loss of mechanical properties even in the most advanced resin systems.

Hoshijima and Yagi (1996) concluded that the maximum fire resistant temperature for the CFRP sheets was 260° C for 2 hours. This conclusion was based on the observation that the strength of the CFRP sheet was not affected after the sheet had cooled down to environmental temperature from a 2 hour-long exposure to 260° C. However, according to the test results, the maximum usable temperature for the CFRP sheets was 80° C because at that temperature the CFRP strength had been lowered to 80% of its normal-temperature value.

Gill (1972) showed that the mechanical properties of carbon fibres themselves are not affected by immersion in water. The mechanical properties of carbon fibre composites are, therefore, not significantly changed by immersion in water at ambient temperatures, where the resin matrix is also unaffected. With some resins, however, a slight loss in strength, up to 5%, may occur particularly at elevated temperatures, but the stiffness will remain unchanged.

Electrical resistance along the fibre direction is proportional to the length of the fibres and inversely proportional to the total cross sectional area of CFRP composites. The electrical resistance of CFRP composites along their axis lies in the range of 750 - 800 cm at 25 ° C, depending on the graphitising temperature used. Generally, the resistance falls at higher temperatures and is about 650 at 200 ° C.

Copyright fib, all rights reserved. This PDF copy of fib Bulletin 10 is intended for use and/or distribution only by National Member Groups of fib.

7.6.2.3 Surface preparation of external bonding technique

Surface preparation is a key step in the process of bonding two materials since the success of the external bonding technique depends primarily on the degree of composite action that can be achieved between the external sheet/plate and concrete. A poorly prepared surface becomes the weak link in the system, regardless of how good or bad the adhesive might be. Cleanliness, roughness and flatness are the primary factors that govern the surface conditions required on the concrete and plate for the application of the adhesive. In general, a satisfactory surface for bonding is achieved through effective surface treatment preparation.

There are several types of systems available to properly prepare a surface, by removing any contaminated or loose material and leaving the surface in a roughened condition. These systems are either mechanical or chemical. Mechanical systems include: shot blasting, sand blasting, scabbing, scarifying, grinding or using high pressure water jets. Chemical systems are used first to roughen by reacting with the cement paste and then to clean.

A combination of mechanical and chemical methods may also be used. Whatever the method used, the dust and debris must be removed by jetting with compressed air. The result should be a surface abraded to the extent that large aggregate particles are exposed and are free from dust and contaminants.

The surfaces of FRP plates need to be made more conforming to the mating surface by sanding. They should be devoid of contaminants and degreased using solvents. However, if a suitable peel ply is used during manufacture, then the surface could be ready for bonding simply by peeling the ply prior to bonding.

7.6.3 Types of bond - related failures

7.6.3.1 Resin interface failure

For normal strength concrete, the correct application of ExFRP should prevent bond failure at the resin interface. Currently, structural adhesives have a much higher tensile strength than concrete, and despite their low shear modulus, will transfer the shear stress to concrete effectively. For a lap joint in which two sheets are bonded by resin, however, shearing off of the bonding resin may occur if the lap length is not long enough. Ueda et al (1997) indicates that a minimum lap length of 100 to 300 mm is required by the Japanese design guidelines in the state-of -art report of the Japan Concrete Institute.

7.6.3.2 Concrete interface failure

Wu (1998) indicated three modes of debonding failure:
1. propagation of interface crack induced by a flexural crack,
2. peeling-off induced by relative displacement of the faces of a shear crack,
3. shearing-off of surface concrete.

Blaschko et al (1998) presented five failure modes depending on the location of debonding. Wang (1998) included two additional modes, that of shear failure in the anchorage zone, and the so-called "tooth peeling failure".

In an experiment conducted by Asano (1998) it was found that if a sheet is subjected to eccentric tension, de-bonding initiates at the location of maximum tensile stress. Once debonding begins, it propagates through the sheet very quickly. The sheet stress at debonding is the same as that in the case of uniform tension. The bond strength at the concrete/ sheet interface can be increased by wrapping over another sheet in a direction perpendicular to the existing sheet, due to confinement of the concrete surface.

Copyright fib, all rights reserved. This PDF copy of fib Bulletin 10 is intended for use and/or distribution only by National Member Groups of fib.

Takeo et al (1997) found that the concrete surface treatment affects the interface strength of bonded carbon fibre sheets. Treatment with hydro-jet resulted in higher bond strength than surface treatment with a disk grinder. Kishi et al (1998) observed in a test using aramid fibre sheets that treatment with deep chipping also outperformed the treatment by grinding. However hydrojet treatment may result in microcracks in concrete surface due to pressurized water penetration in concrete pores.

1) Effect of bonded length

Experimental results in previous studies indicate that the average bond strength of continuous fibre sheets and plates decreases with increasing development lengths. This result is similar to what is observed with regards bond strength Bleich (1924) and Granholm (1958) and is consistent with the experimental observations of Maeda et al (1997) and Sekijima (1998) namely that local bond failure initiates at the loaded end and gradually propagates towards the free end. During this progressive bond failure, the length over which bond stress is acting is observed to be almost the same. This length is called *the effective bond length*, L_e, Figure 7.6-1. Within the effective bond length, the strain gradient in the longitudinal direction does not change much although the number of sheet layers change. Based on the experimental results, Maeda et al (1997) proposed equations for determining the effective bond length, L_e and bond strength, f_{bu}.

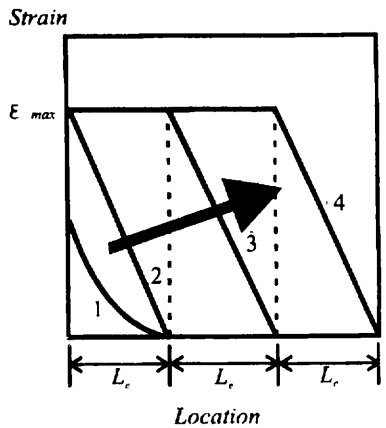

Figure 7.6-1 Effective bond length

The effective bond length ranged between 20 and 90 mm in the study by Maeda (1997) and was approximately 100 mm in the study by Takeo et al (1997). Brosens et al. (1997) pointed out that the effective bond length was longer than 275 mm. Furthermore, Sato at al (1998) found that the Maeda equation for the effective bond length can be applied to both carbon and aramid fibre sheets. He (1998) at the University of Sheffield demonstrated experimentally the effect of bond length on the normalised bond stress of pull-out specimens. This relationship implies that different anchorage lengths are required to develop the strength of different types of plates, Figure 7.2-6.

2) Effect of bonded sheet width, thickness and stiffness

The width of the sheet also affects the average bond strength. In the experiment by Asano (1998) it was found that a narrower sheet gives greater bond strength if the width is less than 50 mm. The reason might be that the resisting area against peeling-off of the concrete surface is wider than the width of sheet because the failure zone includes concrete outside the sheet. The relative significance of this effect becomes negligible for sheets wider than 50 mm. Another likely reason for the width effect might be defects at the interface between sheet and concrete, caused by poor construction, which could trigger overall bond failure of the sheet.

Copyright fib, all rights reserved. This PDF copy of fib Bulletin 10 is intended for use and/or distribution only by National Member Groups of fib.

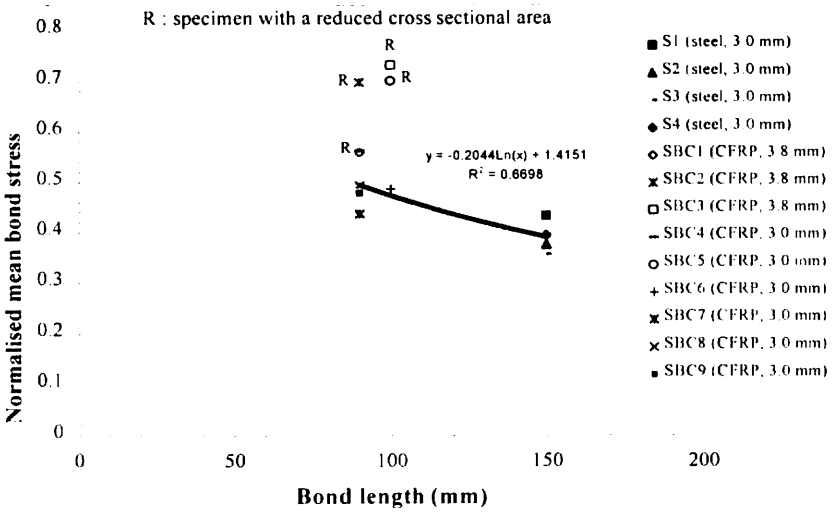

Figure 7.6-2 Normalised mean bond stress ($\frac{\tau}{\sqrt{f_{cu}}}$) versus bond length, He (1998)

In many studies, including one done by Maeda et al (1997), the bond strength of one sheet layer is usually greater than that of more than two layers. By assuming the same sheet width and applied tensile force, it is concluded that whereas the shear force between the sheet and concrete remains constant in these two examples, the tensile strain in the single-sheet case is lower. It may be said that less strain in the sheet gives greater average bond strength. This is also found when dealing with bar reinforcement, since the greater bar size gives less average bond strength.

Experimental work by He (1998) indicated that the normalised moment capacity of strengthened beams reduces slightly with increased plate thickness, due to the peeling off of the plate at the beam ends. This finding applied to beams reinforced with steel or CFRP plates and motivated examination of alternative techniques for enhancing the beam performance by reducing the stiffness of the plate in the anchorage zone. Feathered plates gave a better performance and a new technique was developed which could delay or totally eliminate peeling-off of the plate. Similar performance was observed in beams strengthened with CFRP sheets tested by Maeda (1998).

7.6.3.3 End anchorages to enhance concrete bond strength

Anchorage failure occurs usually after bond failure due to the shearing-off of the concrete surface at the reinforcement interface. Therefore, the anchorage strength of the sheet and plate depends purely on the bond strength of the concrete failure surface.

There are various types of anchorage. The most typical one is the anchorage with bolts. The area of the sheet surrounding the holes is very susceptible to local rupture and should be specially reinforced. Using a metal plate lapped with the sheet can provide the necessary protection against local failure of the sheet, as it prevents direct contact between the bolt and the sheet. Sato et al (1997b) found that the frictional force between the steel plate and the sheet reduces the intensity of bond stress that develops between the sheet and concrete. This was considered the main reason for the increase of the bond strength at the anchorage. However, as in the case of steel plates, bolts only have the potential for enhancing the strength marginally, since failure can migrate further in. The compatibility between glue and bolt functions have to be taken into account.

Wraps of continuous fibre sheets in directions orthogonal to the main longitudinal reinforcement are also used for anchorage purposes. These can be placed in different configurations. Takahashi et al

Copyright fib, all rights reserved. This PDF copy of fib Bulletin 10 is intended for use and/or distribution only by National Member Groups of fib.

(1997) and Mikami et al (1998) used U-jacketing instead of just placing the sheet on the bottom face of beams. In the U-jacketing, apart from the confining effect, a larger contact area is available to develop bond. The efficiency of the wraps depends to a large extend on the surface area available on the sides of the beams (i.e. whether they can be extended to reach the compression zone of the beam) and on the stiffness of the sheet. Stressing the wraps or straps on the beam is thought to be the best way of avoiding anchorage failure and this is the subject of patents by Meier at EMPA and Pilakoutas at Sheffield.

7.6.3.4 Bond strength of tensile reinforcement

For an ordinary reinforcement bar, the development length for the full strength of the reinforcement can be calculated by using the average bond strength or is simply given as a full development length. For a continuous fibre sheet, however, a long enough length for full development may not be possible. In many cases, sheets attached to the concrete surface as tensile reinforcement are likely to delaminate due to premature bond failure before sheet fracture.

Van Gemert (1980 and 1982) investigated the bond shear strengths of externally bonded steel plates, using concrete beams or slab specimens under "pure shear" and "shear-and-bending" tests. The thickness of the plates used was 5 mm. Based on the results from the "pure-shear" tests a physical model was developed to interpret the mechanism of force transfer at the interface between steel and concrete. It was estimated that the maximum bond shear stress was 2.5 MPa at the free end of the anchoring zone. In addition, the author suggested that, in pure shear, a safe design could be based on a bond shear stress in the initial bond zone of less than 1.5 MPa.

By carrying out a number of pull-out tests, and single and double lap tests, Swamy, Jones and Charif (1986) assessed the shear strength of steel plates bonded onto concrete by means of epoxy resin. From the test results it was concluded that both pull-out and double lap tests may be used to determine the interface bond shear strength. The bond shear strength obviously varied with the concrete strength. For the range of concrete strengths used in the pull-out tests (from 25 to 70 MPa), measured values for the bond shear strength varied from 6.0 to 8.3 MPa. Furthermore, different thicknesses of the adhesive layer were considered (ranging from 0.5 mm to 0.3 mm) with the corresponding values of bond shear strength varying from 6.7 to 6.9 MPa suggesting that the influence of the thickness of the epoxy resin on bond strength of the plate is negligible.

Wu (1998) pointed out that flexural and shear cracks in concrete may damage bond in the vicinity of cracks in different ways and reduce the average bond strength. Horiguchi et al (1997) presented experimental results that indicate that the bond strength obtained by bending tests is greater than that by pull-out tests. This implies that results of pull-out tests may not be used for sheets in a manner similar to that used for tensile reinforcement.

Resin used between the sheet and concrete does not allow any slip, unless local bond failure occurs. Cracking of concrete, therefore, may easily cause localised tensile strains in the sheet. Due to lack of ductility, this localised strain may result in earlier fracture of the sheet in tension. Hence, due this effect, Ueda et al (1997) introduced design guidelines, intended to reduce the allowable design strength of sheets used for flexural strengthening. For unbonded sheets, however, which are anchored well by mechanical means, it is possible to develop higher fracture strengths.

7.6.3.5 Bond strength of shear reinforcement

Bond failure of continuous fibre sheet that is used as shear reinforcement is an other major issue. The sheet acting as shear reinforcement is normally attached to the side faces of the concrete member. Unless the sheet is extended to the bottom and top face of the member, a sufficient development length cannot be provided. In particular, in the case of T or I beams the sheet cannot be extended even to the compression end of the side face because of the upper flange. In the case of I-sections the situation is even worse because of the lower flange, which prevents extending the sheets to the tension end of the

Copyright fib, all rights reserved. This PDF copy of fib Bulletin 10 is intended for use and/or distribution only by National Member Groups of fib.

side face. In these cases, mechanical anchorage may be the only solution for better bonding as indicated in the study by Sato et al (1997b). Sato et al (1997a) also compared cases where the sheet was attached only on the side faces of the beam web, with similar specimens having the sheet attached on the bottom face as well. The debonded zone in the former case was smaller than in the latter case as shown in Fig.7.6-3, which indicates that the average of the effective bond length is shorter in the former case. This is the reason why the bond strength in the former case is smaller.

Kamiharako et al (1998) compared the experimentally observed debonded length at shear failure of beams with that calculated by a cut-off type of shear force-slip relationship with encouraging results.

In the study by Asano (1998) it was observed that the ultimate shear strength of a beam retrofitted with smaller shear reinforcement ratio of stripe-like sheet is almost the same as that with a greater shear reinforcement ratio of monolithic sheet. This implies that the bond strength of narrow strips is greater than that of widely spread monolithic sheet. One explanation for this may be the fact that in monolithic sheets once local bond failure occurs, failure spreads quickly over the whole sheet. However, in the case of striped sheets bond failure does not spread immediately to other strips.

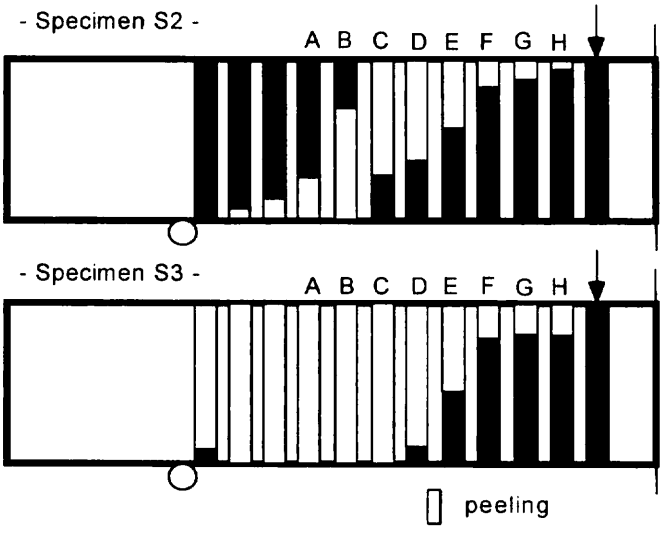

Figure 7.6-3 Debonding of sheet attached on side face as shear reinforcement

If a concrete member is wrapped around by the sheet or strips completely, by using adequate lap lengths, a much better reinforcing effect can be expected.

7.6.4 Analytical predictive methods for bond stress distribution, bond strength and anchorage lengths

The determination of the stress distribution along the bonding length and the maximum peeling off stresses of ExFRP can be determined if the displacement along the bonded surface is known. The bond stress distribution can be calculated, by using a theory based on the modulus of displacement, K (MN/m^3), first reported by Bleich (1924). Bleich used the theory to determine the individual rivet loads in long riveted joints. In this calculation, the rivets are replaced by a continuous medium. The shear deformations in the medium are characterised by the modulus of displacement. The tangent or secant modulus for the relationship between bond stress and slip in a pull-separation test with short bond length constitutes the modulus of displacement. The modulus of displacement depends on the resin deformation characteristics, roughness of the concrete surface and concrete strength. The determination of stress distribution is rather insensitive to changes in the modulus of displacement. However, the stress calculations give stress peaks close to the plate ends. The calculated high stress gradients appear only along very short lengths at the ends. However, the intense stress gradients will be somewhat reduced by the non-linear behavior of resin and concrete. Granholm (1949) applied the theory to

Copyright fib, all rights reserved. This PDF copy of fib Bulletin 10 is intended for use and/or distribution only by National Member Groups of fib.

connections in nailed timber structures and this was extended to reinforced concrete, by Granholm (1958), Losberg (1962 and 1963) and Tepfers (1973 and 1980).

The classical lamination theory can also be used to calculate the stress distribution at the free end of the ExFRP, and the concrete cover can be considered to be a layer of the composite material.

Triantafillou and Plevris (1992) investigated the FRP plate debonding failure and proposed three different mechanisms to describe this type of failure:

1. Interface Crack Propagation - the debonding of the FRP plate is caused by the disastrous propagation of a crack along the concrete/FRP interface. This type of failure occurs in a sudden and brittle manner;
2. FRP Peeling Off - it is suggested that horizontal and vertical openings associated with shear cracks in concrete beams cause FRP peeling off;
3. Concrete Shear Delamination - shear stress concentrations at the ends of the FRP sheet (anchorage zones) cause the FRP to peel off from the strengthened beam. This kind of failure initiates near the ends of the FRP sheet, the concrete cover being finally ripped away at the internal main reinforcement level. It was recommended that the flexural failure load be estimated according to the analytical model of Kaiser (Thesis in German, 1989). Although the bond shear strength depends on the concrete strength, it was suggested that a limiting value of about 8.0 MPa be used for the bond shear stress of normal strength concrete.

Triantafillou et al (1991 and 1992) also presented an analytical model to describe the maximum achievable prestress level in ExFRP. Linear-elastic material characteristics were adopted and it was assumed that the shear deformation governs the behaviour of the adhesive layer. However, tests have shown that unless special end anchorage details have been provided, CFRP sheets shear off at the end zones immediately with a prestress of just over 5% of their failure strength.

There are various failure criteria for debonding. For the bi-linear shear force-slip relationship, yield stress and ultimate slip must be provided, while only yield criteria is needed for cut-off types of shear force-slip relationship. The Mohr-Coulomb yield criterion is sometimes applied. In the study by Malek et al (1998) an experimentally obtained failure criterion for concrete under bi-axial stress, which was presented by Kupfer et al. (1973), is used, while the discrete crack with a tension softening model is applied in the study by Jansze (1997). Another modelling approach is based on fracture mechanics. Yoshizawa et al. (1997) and Fukuzawa et al. (1997) defined the critical strain energy release rate as the debonding fracture energy and demonstrate how this property may be obtained by experiment. Brosens et al. (1997) presented a similar model based on fracture energy concepts and gave equations for determining the maximum force for mode II failure mode of adhesive, based on non-linear fracture mechanics.

It was established that peeling-off tension stresses develop normal to the plate at the cut-off points of plates. Sano et al. (1995) studied the problem with linear finite element analysis. Malek et al. (1998) used closed form solutions from the theory of elasticity in order to calculate the stress distributions in the neighbourhood of the cut-off points. Equations for the maximum shear stress τ_{max} and normal peeling stress $f_{n,\,max}$ at the cut off point are presented.

Ranisch and Rostasy (1986) discussed the feasibility of reducing fatigue stresses of coupled tendons in multispan bridges by externally bonding mild steel plates as additional reinforcement to the members. An example of this application was given in their paper. They pointed out that the key aspect of design for such strengthening is the determination of the anchorage length. In their paper, they proposed an equation for the required anchorage length of the steel plate. In this equation, the authors defined the global safety factor against bond failure, γ to be 1.45. In addition, the authors pointed out that the peak value of bond shear stress, τ_p, depends on the "tear-off" strength of the concrete. Therefore, the partial transmission of the load by shear friction could only be warranted when the adhesive comes into contact with the coarse aggregate (up to 8 mm). This point highlights the need for sandblasting the concrete surface before plating.

Copyright fib, all rights reserved. This PDF copy of fib Bulletin 10 is intended for use and/or distribution only by National Member Groups of fib.

However, their theoretical and experimental findings proved that there was a limiting value of an effective anchorage length in metal to metal bonding. They also found that debonding of the external steel plate is due to high interface shear stresses and the debonding failure occurred when the peak value of the interface shear stress reached its limiting value. The double lap steel to concrete bond tests showed that the limiting value of the interface shear stresses depends on the strength of concrete and it is approximately 8 MPa for normal concrete strength.

Jones, Swamy and Charif (1988) studied the interface force system between the external plate/glue and strengthened RC beam based on the simple elastic theory. They proposed two equations to assess the demand of interface bond stress for a given load in regions unaffected and affected by the plate cut-off respectively. However, the equations depend on determining the anchorage length, an issue that is inherently difficult.

The peak value of the interface bond stress is found from experiments to be in the range of 1.4 times the concrete tensile splitting strength of the beams. Bond stresses in strengthened beams, predicted by these equations were compared with experimental results by He (1998) and found to be very conservative and were thought to ignore the effect of plate cut-off.

Roberts and Haji-Kazemi (1989) presented a theoretical investigation that was based on Newmark's partial interaction theory Newmark et al (1951). The basic principle of the theory can be expressed in that the basic equilibrium and compatibility equations for an element of the beam are reduced to a single second-order differential equation, in terms of the resultant axial force in the concrete, or the interface slip. Solutions for the axial force, or slip, are substituted back into the basic equilibrium and compatibility equations, which are then solved to determine displacements and strains throughout the beam.

The solution was obtained for the displacements, strains and stresses in RC beams, and for the shear and normal stresses within and adjacent to the adhesive layers. The results showed that the shear and normal stresses increased rapidly towards the ends of the plates. Their magnitude depended on many parameters, such as the stiffness of concrete, the material moduli of plates and adhesives, the cross sectional geometry and the points of termination of the steel plates. The theoretical solution has been correlated successfully with the experimental results of Jones et al (1988). However, this method is too complex for use in design.

Roberts (1989) also proposed a simple and approximate theoretical model to quantify the shear and normal stress concentrations in the adhesive layer of plated RC beams. Comparisons between available test data from plated RC beam tests and results obtained from rigorous theoretical analyses based on the partial interaction theory correlated successfully with results obtained from the simplified theoretical model. It was concluded that for a simply supported beam the stress concentrations can be reduced significantly by, (a) terminating the plate as close to the supports as possible, (b) by reducing the thickness of the plate, and (c) by using a more flexible adhesive.

Though simple, the solutions obtained by the Roberts' approximate model are not rigorous. The author also admitted that the stresses may be underestimated by up to 30% when comparing with the rigorous solutions of Newmark's partial interaction theory. This is because the solution suggested by Roberts for calculating interface shear and normal stresses was based on the linear behaviour of materials, including concrete, internal steel reinforcement, external steel plate, and the adhesive layer or interface between the steel plate and concrete.

Sharif et al (1994) pointed that this solution could be employed to predict the plate peeling off load by rearranging the equations of Jones, Swamy and Charif (1988), provided that the maximum bond shear stress (τ) was known. He (1998) examined the above two techniques and found out that they do not predict well the results of experiments on CFRP plates.

Copyright fib, all rights reserved. This PDF copy of fib Bulletin 10 is intended for use and/or distribution only by National Member Groups of fib.

Hamoush and Ahmad (1990), introduced the linear elastic fracture mechanics approach through finite element analysis to investigate the debonding failure of RC beams strengthened with steel plates. It was concluded that the debonding load is relatively insensitive to the thickness of the adhesive layer. This is consistent with the conclusion obtained by other researchers.

Oehlers and Moran (1990) classified plate peel-off failures of plated RC beams into two categories, on the basis of several experiments (57 beams in total). *Shear* peeling is induced by the formation of diagonal shear cracks and results in the rapid separation of the plate, whereas *flexural* peeling is induced by increasing curvature and results in a gradual separation of the plate. For the flexural peeling failure case, they proposed an empirically derived expression for calculation of the ultimate peeling strength. The authors reported that flexural peeling failure occurred at a curvature of $f_t/(0.474E_p t_p)$ thereby suggesting that limiting the strain in the plate is not an effective means of preventing flexural peeling failure. The effect of precracking was also examined in this study but it was not found to affect the ultimate strength of plated beams.

Oehlers (1992) later concluded that "there is a very strong interaction between flexural and shear peeling" and proposed a moment shear interaction equation. In a recent study, He (1998) reported that the above techniques were not as successful in predicting the actual strength (failure loads) of beams reinforced with CFRP plates

Muravljov and Krasulja (1994) investigated the shear strength of steel/concrete bonded joints with two different models using both experimental data and finite element analysis. It was demonstrated that finite element modelling can be used to effectively solve the steel/concrete bonding problems. However, the non-linear behaviour of concrete and adhesive should be considered in order to obtain a more accurate solution.

From shear tests conducted on double overlap of FRP on concrete specimens, Ghaleb (1992), the lower value of maximum bond shear stress obtained was 3.5 MPa. In order to avoid the effect of complex stresses in double lap specimens, Sharif et al (1994) proposed a value of $\tau_0 = 3.5$ MPa as the maximum bond shear stress in estimating the failure load with the approximate model for plate separation by Roberts (1989). By comparing the results calculated with experimental values, it was shown that this approximate analytical solution was more accurate for beams that had failed from plate separation in a flexural manner rather than for beams that had failed in a brittle manner. Hussain et al (1995) confirmed this conclusion when comparing experimental values with theoretical ultimate loads calculated by Roberts' solution (1989).

Zhang et al (1995) used Kani's tooth model to idealise the behaviour of the concrete cover between two adjacent cracks. As illustrated in Figure 7.6-4, the cover is assumed to act as a cantilever having a lever arm of h' which is carrying the bond shear force between the RC beam and the steel plate. A further assumption of this model was that the concrete teeth did not interact with each other and that the critical strength of the teeth root (point A) corresponded to the tensile strength of concrete. Thus, lower and upper bounds of the tensile stresses in the steel plate were derived

A comparison of the analytical and the test results reported by Oehlers (1992) showed that this model was reasonable for predicting the upper and lower bounds of the peeling moment. However, it should be noted that the accuracy of the analytical results depends strongly on the assumed crack spacing.

By using the analytical method presented by Roberts (1989), Quantrill, Hollaway and Thorne (1996) investigated the parametric sensitivity of the maximum bond shear stress and normal stress at the free ends of the external plates for the beams tested. It was concluded that the stress *concentration* factor, which is equal to the theoretical maximum shear and normal stresses divided by the ultimate elastic shear stress, appeared to be independent of concrete strength and provision of anchorage, but vary with adhesive thickness and plate aspect ratio. In addition, the levels of both bond shear and

Copyright fib, all rights reserved. This PDF copy of fib Bulletin 10 is intended for use and/or distribution only by National Member Groups of fib.

normal stress at the free ends of the plate provided by the FRP plates are higher than those of the corresponding steel plates before the plate peeling off failure has occurred.

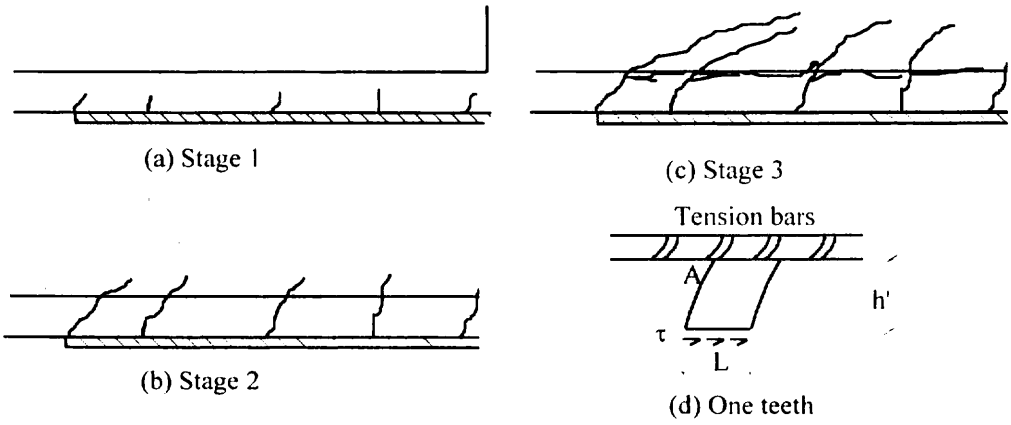

(a)-(c) Various stages of crack propagation(d) Behaviour of concrete tooth between two adjacent flexural cracks

Figure 7.6-4 Assumed mode of plate peeling failure, Zhang et al (1995)

Considering the great importance of interface stresses and force transfer between concrete and plate, Chajes et al (1994) studied this issue in detail through a series of single lap shear test specimens. The aim of the tests carried out was to investigate the effect of surface preparation, type of adhesive and concrete strength on average bond strength. The material used for the plates was a composite of carbon/epoxy having 1.016 mm thickness. Four types of epoxy were used in the tests. The mechanically abraded surface preparation provided the highest bond strength amongst the three different surface preparation methods, and the combination of mechanically abraded surface preparation with a silane surface primer (Chemglae) improved the bond strength as well. The test results showed that all specimens failed due to the shearing of concrete beneath the bond surface, except those bonded with epoxy - Tyrite. Considering this failure mode, the bond strength certainly increased as the strength of concrete increased. In addition, a number of tests were carried out to study the anchorage bonding length to fully develop the joint. An idealised linear model was recommended to calculate the bond resistance based on the rate of strain reduction in the plate along the bond length.

Due to a linear strain rate of 1140 $\mu\varepsilon$/in obtained from tests, an average shear stress of 4.95 MPa was obtained considering the elastic modulus of the plate and the cross area of the plate. According to this model, 95.25 mm of the length was taken as the effective bond length for the given material properties and geometry of the plate. However, the feasibility of this model for other bond conditions and requirements needs to be verified.

Malek, Saadatmanesh and Ehsani (1998) published a theoretical study based on linear elastic behaviour of materials. In this research particular emphasis was placed on estimating shear and normal stress concentrations at the cut-off point of the plate. The effect of large flexural cracks along the beam as locations of potential peeling failure has also been investigated with this model. The authors proposed equations for the tensile stress the interfacial shear stress and normal stress in the plate.

7.6.5 Environmental and time-dependent effects on bond strength

The required service life of civil engineering structures is typically much longer than other fields where FRP sheets and plates find application. For this reason durability considerations are important in the design of repair/ strengthening solutions of structural members with these products. Although composite materials do not corrode through the same chemical reactions as conventional reinforcement, they too are susceptible to degradation from contact with a number of chemical and physical reactants. Durability concerns arise

Copyright fib, all rights reserved. This PDF copy of fib Bulletin 10 is intended for use and/or distribution only by National Member Groups of fib.

from exposure to UV radiation, low-cycle fatigue, freeze-thaw cycles, moisture, etc., as exposure to any of these conditions might severely affect the service life of the composite itself, or of the adhesive layer.

In a study by Hayes et al (1998) the effect of moisture on the fatigue response of a commercial glass/vinyl ester composite plate system was studied for the case of quasistatic tension. An irrecoverable strength loss in the order of 25% was found for a moisture concentration of 95% suggesting permanent damage in the material structure perpetrated by the effects of water on the surface of the glass fibres. Hisabe et al. (1997) presented experimental results indicating that bond strength of continuous fibre sheets that are attached while the specimens are subject to vibration (small fatigue loading) is almost the same as that of sheets attached in normal conditions. Juvandes (1998) found that deterioration of surface concrete causes poor bond behaviour, which is consistent with earlier finding that the strength of the concrete surface affects the bond strength of the sheet. Hattori et al. (1998) conducted accelerated durability tests with sulphuric acid solution (of a month-long duration) and found some deterioration on tha bond properties of sheet. Mitsui et al. (1998) presented experimental results indicating almost no deterioration of bond strength after a year-long field-exposure test. Kawasaki et al. (1998) conducted development and bending tests on pre-stressing reinforcement at one and three months and found out that bond properties were consistent in both cases.

Under dense layers of FRP sheet moisture may concentrate in concrete due to unfavourable temperature gradients. This moisture concentration may cause freeze-taw deterioration of concrete underneath the FRP layer and result in loss of bond.

7.6.6 Design and testing recommendations

In the Japanese design guidelines for continuous fibre sheets, Ueda et al (1997), typical values for design bond strength are in the range from 0.40 MPa to 0.45 MPa for carbon fibre externally bonded sheets and 0.70 MPa for aramid fibre sheets. The minimum lap lengths range from 100 mm to 200 mm for carbon fibre sheets and from 200 to 300 mm for aramid fibre sheets.

The JCI Committee (1998) recommends standardised pull-out tests to assess bond strength of sheet products. The specimen should be a concrete prism with sheets attached symmetrically on two opposite faces, which are then subject to pull-out. This test gives a reference value for the average bond strength that can be used in design provided that anchorage details such as length, width and number of sheet layers are similar in the application as in the reference test. An additional requirement is that during application of the composite the concrete surface is free of cracks and flexural deformations.

7.6.7 Instrumentation for bond test

The typical way to measure bond stress and to detect debonding is the use of strain gages mounted on the continuous fibre sheet. Several alternative techniques have also been used by researchers. For example, Nanni et al (1997) showed the applicability of Moiré interferometry and photoelasticity in detecting crack propagation beneath the continuous fibre sheet. Wu et al (1997) used piezo-sensors sensing small vibrations in experiments to detect debonding. Iwanami et al (1998) used thermography in his studies to study the fact that energy is dissipated into the debonded zone. Hattori et al (1998) and Iwanami et al (1998) used acoustic emission. The latter observed that AE events were still counted after debonding because of friction between sheet and concrete.

7.6.8 Producers

The following systems are commercially available and may be used for strengthening and repair of columns and beams by jacketing:

Copyright fib, all rights reserved. This PDF copy of fib Bulletin 10 is intended for use and/or distribution only by National Member Groups of fib.

Replark system developed by Mitsubishi Chemical Company, Tokyo;
Forca Towsheet, Tonen Corporation,Tokyo;
Towpreg system by XXsys Technologies, San Diego;
Inc, Fiberwrap, Tyfo S system by Hexcel Fyfe Co, San Diego;
Sika Carbodur system by SIKA AG, Zürich.
Wrapping materials also are produced by
Fibre e Tessuti Speciali Srl Como, Italy,
Toray, Japan
Toho Rayon, Japan,
Nippon Sekiyu, Japan,
Mitsubishi Rayon, Japan,
Fybex, Japan and
Teijin, Japan.

The JCI Committee (1997 and 1998) provides a detailed list of producers in Japan.

7.6.9 Summary

Bond stress distributions along continuous fibre sheets, strips, and plates can be estimated using the theory of modulus of displacement that was originally developed for long riveted joints, (Bleich 1924, Granholm (1949 and 1958), Losberg (1962 and 1963) and Tepfers (1973 and 1980). The rivets in the theory are replaced by a continuum with a predefined modulus of displacement K (MN/m^3). The variable K represents the resistance of the laminate-glue system to deformation. Another alternative method is to use finite element modelling with appropriate constitutive laws to represent the properties of the interface between sheet and concrete.

Bond strength of the sheets depends not only on sheet length but also on sheet width. Because in actual circumstances it may not be possible to provide the continuous lengths required by the design calculations, and hence it might be impossible to fully develop the capacity of the sheets. This is why it is important to assess anchorage requirements and to evaluate the performance of the repair in case of sheet delamination at the critical locations

Copyright fib, all rights reserved. This PDF copy of fib Bulletin 10 is intended for use and/or distribution only by National Member Groups of fib.

7.7 Conclusions

There are at least three types of fibers, glass, aramid and carbon impregnated with either epoxy, polyester or vinyl ester. There can be hybrid combinations of fibers and other types of resins added. This means that only a general statement can be provided for what should be considered concerning bond of FRP reinforcement in concrete. Every type of available FRP reinforcement should be investigated concerning bond-slip relationship, tendency to split surrounding concrete, effect of confinement by surrounding concrete, reinforcement and support pressure, bond transmission length, lap length, tension stiffening effect and distribution of cracks in tensioned and bent members. Influence of fatigue, varying temperatures and environmental effects on bond should also be considered. This indicates that as a design code for bond and anchorage for FRP reinforcement the structure of Model Code 90 could be used, but the coefficients should have boxed values for the different available types of FRP reinforcing bars, rods, strands and cables. Some special precautions should also be given if necessary for each type of FRP reinforcement. The use of fiber sheet and strip externally bonded for strengthening (or retrofitting) should also have special rules related to the type of sheet and strip.

Consequently there is a necessity to develop reliable test methods for determination of the boxed values for different types of FRP reinforcements. In many cases a contribution of information from different tests is required for estimation of boxed values.

Copyright fib, all rights reserved. This PDF copy of fib Bulletin 10 is intended for use and/or distribution only by National Member Groups of fib.

7.8 Design rules

7.8.1 Existing bond clauses

For bond of FRP reinforcement in concrete elements some code proposals have been recently formulated:

- Based on the experimental results of many theoretical and experimental studies on FRP reinforced concrete in Japan: the Japan Society of Civil Engineers (JSCE, 1997) code and the Guidelines of the Building Research Institute (BRI, 1995);
- in Canada: the Canadian Highway Bridge Design Code (CHBDC, Technical Subcommittee No. 16, 1996), in which section 16 is dedicated to "Structures with fibre reinforcement" and the CSA code (Canadian Standard Association, 1995).
- in USA: the Code by Subcommittee 440H of the American Concrete Institute (ACI, 1998);

In formulating new design methods two approaches are possible:

* The first is to develop completely new methods;
* The second is to adapt the existing ones.

From the design point of view, the study of concrete structures reinforced using FRP rebars has been initially developed by extending to such structures the wide body of informations gathered in a century of use of steel reinforced concrete. Therefore, studies have been often developed by comparing performances obtained by using steel rebars and by using FRP rods while the production technologies have been oriented towards the fabrication of composite rebars that, at least in shape and dimensions, were similar to deformed steel rebars.

In many cases test results have shown that a critical review of the classical theories and changes in the design methodology are needed in order to adopt this new type of rebars as reinforcement for concrete structures. In fact, in some cases differences between steel and FRP rebars shown by tests are rather strong, so that simple application of the existing design rules for steel reinforced concrete is unsafe. However, some attempts have been performed in order to extend, with some minor modifications, the general design rules reported in the codes traditionally used for steel reinforced concrete to such new materials; this is the case of the relationships adopted in the evaluation of the embedment length clearly derived by extension of the formulation used for steel rebars.

Provisions by some of the above-mentioned international codes are reported in the following.

7.8.2 Canadian Standards Association Recommendation, CSA

Draft 1 (revised) - May 29/30, 1995.

This standard covers requirements for the determination of engineering properties and design of building components reinforced with FRP bars, tendons, etc.

Definitions
Development length: length of embedded reinforcement required to develop the design strength of reinforcement;
Embedment length: length of embedded reinforcement provided beyond a critical section.

Only CFRP and AFRP reinforcing bars and grids are covered by this code. GFRP reinforcement is permitted as reinforcement in non-structural components (partition walls, claddings, slabs-on-ground, and linings of floors and walls).

7.8.3 Canadian Highway Bridge Design Code, CHBDC

Section 16, Fiber reinforced structures, final draft - July 6, 1996.

Copyright fib, all rights reserved. This PDF copy of fib Bulletin 10 is intended for use and/or distribution only by National Member Groups of fib.

Definitions:
Bar - a non-prestressed FRP element, with nearly rectangular or circular cross section, used to reinforce a structural concrete component.
Critical fiber length - the minimum length required to develop the full tensile strength of the fibre in a matrix.
Equivalent diameter - a diameter of a circular cross-section having the same cross-sectional area as that of the non-circular section.

CFRP and AFRP are permitted as pretensioned, posttensioned and primary reinforcement.
GFRP is permitted as posttensioned reinforcement, when the grout is non-alkaline nor cement based.
For FRP bars and grids, the minimum cover shall be 25 mm.
For an FRP tendon, the clear cover shall be 40 mm, but not less than the equivalent diameter of the tendon.
Anchors for aramid fiber ropes and FRP tendons in concrete shall be of suitably durable materials, such as stainless steel and certain FRPs.
The maximum stress in FRP bars shall not exceed ϕ_{FRP} F f_{pu}, where the resistance factor ϕ_{FRP} is equal to 0,9 and f_{pu} is the tensile strength of the FRP bar. The factor F is dependent on R (see table 7.8.1), which is the ratio of the stresses due to factored dead loads to the stresses due to factored live loads in the FRP bars or grids.

Table 7.8.1 - Values of F

R	0.5	1.0	2.0 or more
F for GFRP	1.0	0.8	0.7
F for CFRP	1.0	0.9	0.9
F for AFRP	1.0	0.6	0.5

Development length l_d of FRP bars in tension shall be:

$$l_d = 0.45 \frac{k_1 k_4}{d_{cs} + K_{tr} \frac{E_{FRP}}{E_s}} \frac{F f_{pu}}{f_{cr}} A$$

Where:

k_1 the bar location factor.
k_4 the bar surface factor, being the ratio of the bond strength of the FRP bar to that of an equivalent ordinary steel deformed bar, but not greater than 1.0.
d_{cs} the smallest of the distance from the closest concrete surface to the centre of the bar being developed, or two-thirds of the centre-to-centre spacing of the bars being developed, mm.
K_{tr} the transverse reinforcement index (specified in Clause 8.15.2.2), mm.
E_s the modulus of elasticity of steel, MPa.
f_{cr} the cracking strength of concrete, MPa.
E_{FRP} the modulus of elasticity of the FRP bar, MPa.

For FRP grids in which the intersecting orthogonal bars have been demonstrated to be fully anchored, the development length shall be such as to include at least two transverse bars of the grid lying perpendicular to the direction of the force under consideration.

Capacity of anchors shall be designed such that the FRP tendon can develop 90% of its specified tensile strength.

The end zones of pre-tensioned concrete components shall be reinforced against splitting, unless it can be demonstrated that such reinforcement is not necessary.
Commentary: Some parts in this code concerning bond are missing here.

Copyright fib, all rights reserved. This PDF copy of fib Bulletin 10 is intended for use and/or distribution only by National Member Groups of fib.

7.8.4 Japan Society for Civil Engineering, JSCE Recommendation

The following is the contents relating to bond of continuous fiber reinforcement (non-metallic reinforcement) in the JSCE code on concrete structures with continuous fiber reinforcement which was published in September 1997.

Basic development length

(1) As a rule, basic development length of continuous fiber tension reinforcement is to be obtained by appropriate experiment.

(2) The basic development length may be calculated by Eq.(1) for cases of reinforcement with bond splitting type of failure, but not less than 20ϕ.

$$l_d = \alpha_1 \times [f_d/(4\times f_{bod})]\times\phi \qquad (1)$$

where ϕ: diameter of tension reinforcement
f_d: design tensile strength
f_{bod}: design bond strength of concrete.
α_1 = 1.0 (for $k_c \leq 1.0$)
0.9 (for $1.0 < k_c \leq 1.5$)
0.8 (for $1.5 < k_c \leq 2.0$)
0.7 (for $2.0 < k_c \leq 2.5$)
0.6 (for $2.5 < k_c$)

and $k_c = c/\phi + (15\times A_t)/(s\times\phi)\times(E_t/E_o)$
c: lesser between concrete cover for tension reinforcement and a half of its spacing
A_t: cross-sectional area of transverse reinforcement normal to assumed splitting plane
s: center-to-center spacing of transverse reinforcement
E_t: Young's modulus of transverse reinforcement
E_o: Basic value for Young's modulus (=200 kN/mm^2)

The design bond strength of concrete is given by:

$$f_{bod} = \alpha_2 \times (0.28\times f'_{ck}{}^{2/3}/\gamma_c) \quad \text{[but not more than 3.2 N/mm}^2\text{]} \qquad (2)$$

where α_2 is a modification factor for bond strength of continuous fiber reinforcement
α_2 is equal to 1 when the bond strength is equivalent or greater than that of deformed steel bars
α_2 is less than 1 when the bond strength is poor.
γ_c is a material factor for concrete (safety factor), [$\gamma_c = 1.3$ when $f'_{ck} < 50$ N/mm^2 otherwise $\gamma_c = 1.5$]
f'_{ck} is the characteristic value for concrete compressive strength.

(3) When reinforcement is placed above the level which is 30 cm below top surface of concreting and in direction with an angle less than 45 degree to horizontal direction, basic development length shall be 1.3 times l_d obtained by equation (1).

(4) Basic development length for compression reinforcement may be 0.8 times l_d obtained following all the previous provisions [sections (1),(2) and (3)].

Commentary

(1) Development length for continuous fiber reinforcement depends on kind of reinforcement, concrete strength, concrete cover and transverse reinforcement. Experiment needs to be conducted considering this fact. In order to obtain the development length experimentally, it

Copyright fib, all rights reserved. This PDF copy of fib Bulletin 10 is intended for use and/or distribution only by National Member Groups of fib.

is preferable to take methods with which actual bond characteristics in members is reflected such as method with beam specimens or lap splices.

"Test Method for Bond Strength of Continuous Fiber Reinforcing Materials by Pull-Out Testing (JSCE-E 53)" does not reflect bond characteristics in actual members, and thus overestimates bond strength generally. It should be avoided to calculate the basic development length by using the bond strength f_{bod} obtained by this method.

(2) JSCE Standard Specification for Concrete Structures provides development length for steel reinforcement with transverse reinforcement by Eq.(C1).

$$l_o = [f_{yd}/(1.25\times\sqrt{f'_{cd}})-13.3]\times\phi/\{0.318 + 0.795\times[c/\phi + (15\times A_t)/(s\times\phi)]\} \qquad \text{(C1)}$$

where f_{yd}: design value for tensile yielding strength of steel reinforcement (N/mm^2)
f'_{cd}: design value for compressive strength of concrete (N/mm^2)
$c/\phi \leq 2.5$

After simplifying this equation, the code provides an equation which is identical to Eq.(1) introducing the factor α_1.

For continuous fiber reinforcement with deformation on its surface which fail by bond splitting, the experimental bond strength is compared with that calculated by Eq.(C2) inFig.C1.

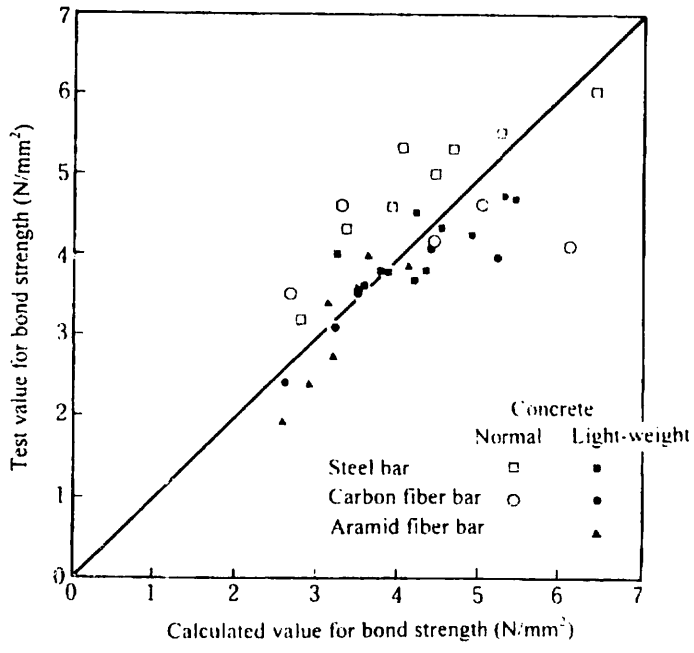

Figure 7.8.1 Comparison of bond strength Eq. (C2) with test results, JSCE (1997).

Equation (C2) is derived from Eq.(C1) considering ratio of Young's modulus of continuous fiber reinforcement, $E_t(=E_f)$ to standard Young's modulus $E_o(=E_o)$ which is Young's modulus of steel.

$$f_{bod}=\{0.318+0.795\times[c/\phi+(15\times A_t)/(s\times\phi)\times E_t/E_o]\}/\{1/\sqrt{f'_{cd}}-(1.25\times 13.3)/f_y\}\times 4/1.25 \qquad \text{(C2)}$$

In the above equation, 1.25, 4 and 13.3 are the constants appearing in Eq.(C1).
Eq. (C2) can be rewritten as follows:

$$f_{bod}=\{0.318+0.795\times[c/\phi+(15\times A_t)/(s\times\phi)\times E_t/E_o]\}/\{1/\sqrt{f'_{cd}}-16.6/f_y\}\times 3.2 \qquad \text{(C2')}$$

Copyright fib, all rights reserved. This PDF copy of fib Bulletin 10 is intended for use and/or distribution only by National Member Groups of fib.

Figure 7.8.1 indicates that Eq.(C2) may be used for the cases of continuous fiber reinforcement with bond splitting failure. However, continuous fiber reinforcement with deformation which causes bond splitting failure may possess bond strength less than that of steel deformed bar. For this type of the reinforcement the modification factor α_2 ($\leq$ 1.0) needs to be multiplied for calculating bond strength by Eq.(2). The value of α_2 is generally obtained by experiment since there is not sufficient data at present.

For reinforcement, whose bond failure is pull-out type basic development length needs to be obtained by appropriate experiment.

By considering the following equation, Eq.(C2) can be derived from Eq.(C1).

$$f_{bod} \times \pi \times \phi \times l_o = f_{yd} \times \pi \times \phi^2/4$$

As seen in Eq.(C2) the effect of the difference in Young's modulus is considered by introducing the term of E_t/E_o, which is the Young's modulus ratio between continuous fiber reinforcement and steel. The term of $15 \times A_t/(s \times \phi)$ represents the effect of transverse reinforcement. The smaller the Young's modulus is, the less effect on the bond splitting strength is.

7.8.5 American Concrete Institute Design Recommendations

(ACI Committee 440 - Draft 2 – September 1998)

The design of structural concrete utilising Fiber Reinforced Plastic (FRP) bars is presented as an extension of the current ACI code requirements for steel reinforced structures (ACI 318-95). Thus the proposed code requirements are analogous to current provisions but appropriate changes to accommodate the differences in the algorithms and the structural behavior between the FRP and the steel reinforced elements are presented.

Only non-prestressed FRP reinforcementa are considered.

<u>Development and splices of reinforcement (Chapter F12)</u>

Development length of FRP reinforcing bars in tension

The basic development length l_{df} for FRP bars in tension can be obtained by:

$$l_{df} = \frac{1}{17} \times \frac{A_{f.bar}}{\sqrt{f_c'}} \times f_{fu} \quad \text{[inches]}$$

where $A_{f,bar}$ is the FRP bar area and f_{fu} is the ultimate design strength of FRP.

The basic development length shall not be taken less than 20 times the bar diamater d_b nor less than 15 inches. A minimum value of l_{df} is needed to account for the inherent properties and the variable bond strengths of FRP bars.

The development length l_d in inches is given by:

$$l_d = l_{df} \times (\text{applicable modification factor})$$

The factors for use in the expression for development of FRP bars in tension are:
α = reinforcement location factor
α = 1.4 horizontal reinforcement so placed that more than 12 inches of fresh concrete is cast in the member below the development length or splice
α = 1.0 other reinforcement

Copyright fib, all rights reserved. This PDF copy of fib Bulletin 10 is intended for use and/or distribution only by National Member Groups of fib.

c = spacing or cover dimension, in.
c = 1.5 when the concrete cover is less than or equal to d_b or when the spacing of FRP reinforcement is less than or equal to d_b

Commentary

The constant 1/17 is about 50% more than the ACI provisions for steel rebars. This constant is a conservative value that is based on the available data.

Experimental results from pull-out tests showed that this constant can as low as 1/50 but until more data becomes available and a better understanding of the bond effect on the development length a value of 1/17 will be maintained.

Factor α accounts for the position of the reinforcement in freshly placed concrete. Value of 1.4 was based on research results.

The concrete cover has significant effect on the failure mechanisms. If the cover is less or equal d_b, a splitting failure may occur; if c is larger than d_b a pull-out failur may occur.

Experimental tests indicated that the ratio of the evaluated bond strength in the specimens with cover of $2d_b$ to those of d_b varied between 1.2 and 1.5 being 1.5 conservative.

Copyright fib, all rights reserved. This PDF copy of fib Bulletin 10 is intended for use and/or distribution only by National Member Groups of fib.

7.9 References

1924 Bleich Fr.: Theorie und Berechnung der Eisernen Brücken. (Theory and design of steel bridges). Verlag von Julius Springer, Berlin 1924. p. 306-314.

1949 Granholm Hj.: Om sammansatta balkar och pelare med särskild hänsyn till spikade träkonstruktioner. (On composite beams and columns with particular regard to nailed timber structures). Transactions of Chalmers University of Technology. No 88. Göteborg, Sweden 1949. p. 214.

1958 Granholm Hj.: Sprickbildning i armerad betong. (Cracking in Reinforced Concrete). Compendium. Chalmers University of Technology, Department of Building Technology, p. 28. Göteborg 1958.

1951 Newmark, N.M., Siess, C.P. and Viest, I.M.: Tests and Analysis of Composite Beams with Incomplete Interaction. Proceedings of the Society for Experimental Stress Analysis, USA, Vol. 9, No. 1, 1951, pp. 75-92.

1961 Rehm G.: Ueber die Grundlagen des Verbundes zwischen Stahl und Beton. (About the fundaments of bond between steel and concrete). Deutscher Ausschuss für Stahlbeton. Heft 138, Berlin 1961. p. 59.

1962 Losberg A.: Sprickbildning i kontinuerliga betongbeläggningar och andra betongkonstruktioner, låsta mot rörelser av temperature och krympning. (Cracks in continuous concrete road slabs and other concrete structures restrained against movements from temperature and shrinkage). Chalmers University of Technology, Department of Building Technology, No 607, p. 45. Göteborg 1962.

- Nordby, G.M. et al.: Guide for Use of Epoxy Compounds with Concrete, Journal of the American Concrete Institute, Proceedings, Vol. 59, No. 9, September 1962, pp 1121-1142.

1963 Losberg A.: Kraftöverföring och spänningsfördelning vid förankring och avslutning av armering. (Force transfer and stress distribution at anchorage and curtailment of reinforcement). Chalmers University of Technology, Department of Building Technology, No 608, p. 49, Göteborg 1963.

1965 Berggren, L.: Utdragsprov med kort vidhäftningslängd. (Pullout tests with short bond length). Chalmers University of Technology, Department of Concrete Structures. Nr 686. Göteborg, 1965. p. 84.

1971 Goto Y.: Cracks formed in concrete around deformed tension bars. Journal of the American Concrete Institute, Vol. 68, pp. 244-251

1972 Gill, R.M.: Carbon Fibres in Composite Materials, The Plastics Institute, 1972.

1973 Kupfer, H.B. and Gerstle, K.H.: Behavior of Concrete Under Biaxial Stresses. Journal of Engineering Mechanics Division, ASCE, Vol.99(EM4), pp.853-866.

- Tepfers, R.: A Theory of Bond Applied to Overlapped Tensile Reinforcement Splices for Deformed Bars. Publ 73:2. Department of Concrete Structures, Chalmers University of Technology, Göteborg, May 1973, p. 328.

1979 Cairns J.: Analysis of the ultimate strength of lapped joints of compression reinforcement. Magazine of Concrete Research, Vol 31, No 106. pp 19-27.

- Tepfers, R.: Cracking of concrete cover along anchored deformed reinforcing bars. Magazine of Concrete Research Vol. 31, No 106, March 1979, pp. 3-12.

1980 Tepfers, R.: Bond stress along lapped reinforcing bars. Magazine of Concrete Research, Vol. 32, No 112. September 1980. pp. 3-12.

- Van Gemert, D.: Force Transfer in Epoxy Bonded Steel/Concrete Joints. International Journal of Adhesion and Adhesives, nr. 2, 1980, pp. 67-73.

1981 Iino, T. and Otokawa, K.: Application of Epoxy Resins in Strengthening of Concrete Structures, Proceedings Third International Congress on Polymers in Concrete, Koriyama, Japan, May 1981, Vol. 11, pp 997-1011.

1982 Jokela J., Tepfers R.: Bond of bundled prestressing steel strands. Nordic Concrete Research, Publication No 1. The Nordic Concrete Federation. Oslo 1982. pp. 12.1-12.19.

- Tepfers, R.: Lapped tensile reinforcement splices. American Society of Civil Engineers, Journal of the Structural Division, January 1982, New York. pp. 283-301.

- Van Gemert, D.A.: Repairing of Concrete Structures by Externally BondedSteel Plates. Proc. ICP/RILEM/IBK Internat. Symposium on Plastics in Material and Structural Engineering, Prague, June 1981, Elsevier Scientific Publishing Co., 1982, pp. 519-526.

1983 Eligehausen R., Popov E.P. , Bertero V.V., Local Bond Stress-Slip Relationships of Deformed Bars Under Generalized Excitations, Report n°.83/23, EERC, University of California, Berkeley.

1986 Ranisch, E.H. and Rostasy, F.S.: Bonded Steel Plates for the Reduction of Fatigue Stresses of Coupled Tendons in Multispan Bridges. Adhesion between Polymers and Concrete (Bonding • Protection • Repair), Proceeding of an International Symposium Organized by RILEM Technical Committee 52-Resin Adherence to Concrete and Laboratoire Central des Ponts et Chaussées, Paris France, September 16-19, 1986, pp. 561-570.

- Swamy, R.N., Jones. R., and Charif, A.: Shear Adhesion Properties of Epoxy Resin Adhesives. Proceedings of an international symposium organised by RILEM Technical Committee 52, Adhesion between polymers and concrete: bonding, protection, repair, Ed. H.R. Sasse, Chapman and Hall, London New York, September, 1986, pp 741-755.

1988 Faoro M.: Zum Tragverhalten kunstharzgebundener Glasfaserstäbe im bereich von Endverankerungen und Rissen im beton. Dissertation Universität Stuttgart, 1988.

Copyright fib, all rights reserved. This PDF copy of fib Bulletin 10 is intended for use and/or distribution only by National Member Groups of fib.

1988 Jones. R., Swamy, R.N. and Charif, A.: Plate Separation and Anchorage of Reinforced Concrete Beams Strengthened by Epoxy-Bonded Steel Plates. The Structural Engineer, Vol. 66, No. 5, 1 March 1988, pp. 85-94.

- Faoro M.: Zum Tragverhalten kunstharzgebundener Glasfaserstäbe im bereich von Endverankerungen und Rissen im beton. Dissertation Universität Stuttgart, 1988.

1989 Honma M., Maruyama T.: Bond Properties of Carbon Fibre Reinforced Plastic rods at Elevated Temperatures, Architectural Institute of Japan Convention, Vol.C (in Japanese).

- Itoh S., Maruyama T.: Nishiyama H., Study of Bond Characteristics of Deformed Fibre Reinforced Plastic Rods, Proceedings of the Japan Concrete Institute, Vol.11, No.1 (in Japanese).
- Kaiser, H.P.: Strengthening of Reinforced Concrete with Epoxy-Bonded Carbon-Fiber Plastics. Doctoral Thesis, Diss. ETH Nr. 8918, ETH Zürich, CH-8092 Zürich/Switzerland, 1989 (in German).
- Roberts, T.M. and Haji-Kazemi, H.: Theoretical study of the behaviour of Reinforced Concrete Beams Strengthened by Externally Bonded Steel Plates. Proc. Institution Civil Engineers, Part 2, 87, March 1989, pp. 39-55.

1990 CEB-FIP Model Code: Bulletin d'information No 213/214. Thomas Telford, London 1993. p. 437.

- Hamoush, S.A. and Ahmad, S.H.: Debonding of Steel Plate-Strengthened Concrete Beams. Journal of Structural Engineering, Vol. 116, No. 2, August, 1990, pp. 356-371.
- Handbook: Kompozicionnije materiali. Moscow Mashinostrojenije, 1990.
- Oehlers, D.J. and Moran, J.P.: Premature Failure of Externally Plated Reinforced Concrete Beams. Journal of Structural Engineering, Vol. 116, No. 4, April, 1990, pp. 978-995.

1991 Faza S. S., GangaRao H. V. S.: Bending Response of Concrete Beams Reinforced with Fiber Reinforced Plastic Rebars for varying concrete strengths. Advanced Composite Materials, ASCE, 1991.

- Triantafillou, T.C., Deskovic, N.: Innovative Prestressing with FRP Sheets: Mechanics of Short-Term Behavior. Journal of Engineering Mechanics, Vol. 117, No. 7, July, 1991, pp. 1652-1672.

1992 Daniali S.: Development Length for Fibre-Reinforced Plastic Bars. Proceedings of the 1st International Conference on Advanced Composite Materials in Bridge & Structures, Sherbrooke, Québec, Canada.

- Faza S., GangaRao H.: Bending and bond behaviour of beams reinforced with plastic rebars. Transportation Research Record 1290, pp. 185-193.
- Ghaleb, B.N.: Strengthening of Damaged Reinforced Concrete Beams by External Fiberglass Plates. MSc thesis, King Fahd University of Petroleum and Minerals, 1992.
- Meier, U.: Carbon Fibre-Reinforced Polymers: Modern Materials in Bridge Engineering, Structural Engineering International, 1992, pp. 7-12.
- Molander I., Thalenius K.: Icke metallisk armering i betong. (Non metallic reinforcement in concrete) Examensarbete. Chalmers University of Technology, Division of building Technology, Work No. 770. Göteborg, January 1992. p. 71.
- Oehlers, D.J.: Reinforced Concrete Beams with Plates Glued to Their Soffits. Journal of Structural Engineering, Vol. 118, No. 8, August, 1992, pp 2023-2038.
- Plevris, N. and Triantafillou, T.C.: FRP-Reinforced Wood as Structural Material. Journal of Materials in Civil Engineering, Vol. 4, No. 3, August, 1992, pp. 300-317.
- Sippel T.M.: Design, testing and modelling of an anchorage system for resin bonded fibreglass rods used as prestressing tendons.ACMBS I, K.W. Neale and P. Labossiere, Editors; Canadian Society for Civil Engineering, Montreal 1922.
- Tepfers R., Molander I., Thalenius K.: Experience from testing of concrete reinforced with carbon fibre and aramid fibre strands. XIV. Nordic Concrete Congress & Nordic Concrete Industry Meeting, 6.-8. August 1992. Icelandic Concrete Association, Reykjavik. pp. 337-347.
- Tepfers R., Olsson P-Å.: Ring Test for Evaluation of Bond Properties of Reinforcing Bars. International Conference "Bond in Concrete - From Research to Practice", Riga, Latvia, October 1992. pp. 1-89 - 1-99.
- Triantafillou, T.C. and Plevris, N.: Strengthening of RC Beams with Epoxy-Bonded Fibre-Composite Materials. Materials and Structures, 1992, 25, pp. 201-211.

1993 CEB-FIP Model Code 1990. Design Code. Comité Euro-International du Béton. Thomas Telford Services Ltd, London 1993. p. 437.

- Chaallal O., Benmokrane B., Pullout and bond of glass-fibre rods embedded in concrete and cement grout, Materials and Structures, Vol 26, pp 167-175
- Kanakubo T., Yonemaru K., Fukuyama H., Yasuhisa S.: Bond splitting strength of concrete members reinforced with FRP bars. Transactions of the Japan Concrete Institute, Vol. 15, pp.305-318.
- Kanakubo T., Yonemaru K., Fukuyama H., Fujisawa M., Sonobe Y.: Bond Performance of Concrete Members Reinforced with FRP Bars, Proceedings of the International Symposium on Fibre Reinforced Plastic Reinforcement for Concrete Structures, ACI SP-138, (Edited by Nanni A. and Dolan C.W.), Vancouver, Canada.
- Larralde J., Silva Rodriguez R., Bond and Slip of FRP Rebars in Concrete, Journal of Materials in Civil Engineering, ASCE, Vol.5, No.1.
- Machida A. (Editor), Second Research Committee on CFRM, Japan Society of Civil Engineers. State-of the Art Report on Continuous Fibre Reinforcing Materials. Concrete Engineering Series 3.Tokyo, October 1993. pp. 15-26.

Copyright fib, all rights reserved. This PDF copy of fib Bulletin 10 is intended for use and/or distribution only by National Member Groups of fib.

1993 Makitani E., Irisawa I., Nishiura N., Investigation of Bond in Concrete Member with Fibre Reinforced Plastic Bars, Proceedings of the International Symposium on Fibre Reinforced Plastic Reinforcement for Concrete Structures, ACI SP-138, (Edited by Nanni A. and Dolan C.W.), Vancouver, Canada.

- Machida Atshiko (Editor), Second Research Committee on CFRM, Japan Society of Civil Engineers. State-of the Art Report on Continuous Fiber Reinforcing Materials. Concrete Engineering Series 3. Tokyo, October 1993. pp. 15-26.
- Mashima M., Iwamoto K.: Bond Characteristics of FRP Rod and Concrete after Freezing and Thawing Deterioration, International Symposium on Fibre-Reinforced-Plastic Reinforcement for Concrete Structures, ACI SP-138, (Edited by Nanni A. and Dolan C.W.), Vancouver, Canada.
- Shima H., Suga T., Honma M.: Local bond stress-slip relationship of continuous fibre reinforcing materials obtained by pull bond test with long embedment. Transactions of the Japan Concrete Institute, 1993, Vol. 15, pp. 297-304.
- Tepfers R. (Editor), Fibre Composites as Nonmetallic Reinforcement in Concrete. Seminar March 15-16, 1993 at Chalmers University of Technology, Göteborg. Chalmers University of Technology, Department of Building Materials P-93:3, Work No 539. Göteborg 1993. p.199.

1994 Al-Zaharani M.M., Bond Behaviour of Fibre Reinforced Plastic (FRP) Reinforcements with Concrete, Thesis submitted in partial fulfilment of the requirements for the degree of Doctor of philosophy, The Pennsylvania State University, USA. 1994.

- Chajes, M.J. et al: Flexural Strengthening of Concrete Beams Using Externally Bonded Composite Materials. Construction and Building Materials, Vol. 8, No. 3, 1994, pp. 191-201.
- Malvar L.J.: Bond stress-slip characteristics of FRP rebars, Naval Facilities Engineering Service Center, Port Hueneme, CA 93043-4328. Technical Report TR-2013-SHR. February 1994. p. 45.
- Muravljov, M. and Krasulja, M.: Physical and Numerical Models for the Shear Load-Carrying Capacity Testing of Steel-Concrete Bonded Joints. Materials and Structures, January/February, Vol. 27, No. 165, 1994, pp. 40-53.
- Sharif, A., Al-Sulaimani, G.J., Basunbul, I.A., Baluch, M.H. and Ghaleb, B.N.: Strengthening of Initially Loaded Reinforced Concrete Beams Using FRP Plates. ACI Structural Journal, Vol. 91, No. 2, March-April, 1994, pp. 160-168.
- Shima H., Suga T.: Local bond stress-slip relationship of braided aramid fibre bar obtained from pretensioned bond test. Transactions of the Japan Concrete Institute, 1994, Vol. 16, pp. 191-196.
- Tamuzs V., Tepfers R., Olsson M., Svensson D.: Hybrid fibre composites as non-metallic reinforcement in concrete. Chalmers University of Technology, Department of Building Materials, Publication 94:3, Work No 560. Göteborg, April 1994. p.10. "First Slovak Conference on Concrete Structures, Bratislava, September 13-14, 1994 . pp.26-35.

1995 Cosenza E., Manfredi G., Realfonzo R.: Analytical modelling of bond between FRP reinforcing bars and concrete. Proceedings of the Second International RILEM Symposium (FRPRCS-S), Ghent 23-25 August 1995, edited by L. Taerwe. E & FN Spoon, London 1995. pp. 164-171.

- Den Uijl J.A.: Bond and fatigue properties of arapree. Proceedings of the Second International RILEM Symposium (FRPRCS-S), Ghent 23-25 August 1995, edited by L. Taerwe. E & FN Spoon, London 1995. pp. 146-153.
- Hattori A., Inoue S., Miyagawa T., Fujii M.: A study on bond creep behavior of FRP rebars embedded in concrete. Proceedings of the Second International RILEM Symposium (FRPRCS-S), Ghent 23-25 August 1995, edited by L. Taerwe. E & FN Spoon, London 1995. pp. 172-179.
- Hussain, M., Sharif, A. and Basunbul, I.A. et al.: Flexural Behavior of Precracked Reinforced Concrete Beams Strengthened Externally by Steel Plates. ACI Structural Journal, Vol. 92, No. 1, January-February 1995, pp. 14-22.
- Jerrett C.V., Ahmad S.H.: Bond tests of carbon fibre reinforced plastic (CFRP) rods. Proceedings of the Second International RILEM Symposium (FRPRCS-S), Ghent 23-25 August 1995, edited by L. Taerwe. E & FN Spoon, London 1995. pp. 180-191.
- Kettil P.: Composite beams of fibre reinforced plastic profile and concrete. Chalmers University of Technology, Division of Building Technology, Work No 8. Graduation thesis: E-95:1. Göteborg, September 1995. p. 80.
- Meier, U.: Strengthening of Structures Using Carbon Fibre/Epoxy Composites. Construction and Building Materials, Vol. 9, No. 6, 1995, pp. 341-351.
- Malvar L.J.: Tensile and bond properties of GFRP rebars. ACI Materials Journal, Vol. 92, No. 3, May-June 1995. pp. 276-285.
- Mochizuki S., Udagawa T.: On bond and anchorage of two dimensional grid type FRP. Proceedings of the Second International RILEM Symposium (FRPRCS-S), Ghent 23-25 August 1995, edited by L. Taerwe. E & FN Spoon, London 1995. pp. 192-199.
- Nanni A., Al-Zaharani M.M., Al-Dulaijan S.U., Bakia C.E., Boothby T.E.: Bond of FRP reinforcement to concrete - experimental results. Proceedings of the Second International RILEM Symposium (FRPRCS-S), Ghent 23-25 August 1995, edited by L. Taerwe. E & FN Spoon, London 1995. pp. 135-145.
- Nanni, A., Bakis, C.E., Boothby, T.E.: Test methods for FRP-concrete systems subjected to mechanical loads: state-of-the-art report. Journal of Reinforced Plastics and Composites.

Copyright fib, all rights reserved. This PDF copy of fib Bulletin 10 is intended for use and/or distribution only by National Member Groups of fib.

1995 Peled A., Yankelevsky D., Bentur A.: Influences of yarns shape in woven fabric on bonding performance of cementitious composites. Proceedings of the Second International RILEM Symposium (FRPRCS-S), Ghent 23-25 August 1995, edited by L. Taerwe. E & FN Spoon, London 1995. pp. 192-199.

- Rosetti A., V., Galeota D., Giammatteo M. M.: Local bond stress-slip relationships of glass fibre reinforced plastic bars embedded in concrete. Materials and Structures, 1995, 28, pp. 340-344.
- Sano, M. and Miura, T.: Behavior of steel plate bonded part of RC members strengthened by steel plate bonding. Proceedings of the 3rd Symposium on Research and Application of Composite Constructions, Japan Society of Civil Engineers (JSCE), pp. 137-142 (in Japanese).
- Taerwe L., Pallemans I.: Force transfer of AFRP bars in concrete prisms. Proceedings of the Second International RILEM Symposium (FRPRCS-S), Ghent 23-25 August 1995, edited by L. Taerwe. E & FN Spoon, London 1995. pp. 154-163.
- Tamuzs V., Apinis R., Vilks U., Modniks J., Tepfers R.: Ductility of nonmetallic hybrid fibre composite reinforcement for concrete. Chalmers University of Technology, Division of Building Technology, Publication No 95:4, Work No 6. Göteborg, 1995-09-01. p. 9.
- Tamuzs V., Apinis R., Vilks U., Tepfers R.: Bond between glass fibre composite reinforcement and concrete in pullout tests. Chalmers University of Technology, Division of Building Technology, Work No 7. Göteborg, 1995-10-25. p. 12.
- Xu H., Bellavance E., Benmokrane.: Bond strength of fiber reinforced plastic (FRP) cement grouted anchor bolts. Proceedings of the Second International RILEM Symposium (FRPRCS-S), Ghent 23-25 August 1995, edited by L. Taerwe. E & FN Spoon, London 1995. pp. 209-216.
- Zhang, S., Raoof, M. and Wood, L.A.: Prediction of Peeling Failure of Reinforced Concrete Beams with Externally Bonded Steel Plates. Proceedings of Institution of Civil Engineers Structures and Buildings, No. 110, August, 1995, pp. 257-268.

1996 Achillides Z., Pilakoutas K., Waldron P.: Anchorage Systems - Bond Improvement, EUROCRETE Report No CCC/96, Centre for Cement and Concrete, The University of Sheffield, Oct. 1996.

- Al-Dulaijan S. U. and Nanni A., Al-Zahrani M. M., Bakis C. E. and Boothby T. E.: Bond evaluation of environmentally conditioned GFRP/concrete systems. Advanced Composite Materials in Bridges and Structures, M. M. El-Badry, Editor, Canadian Society for Civil Engineering, Montreal, Quebec 1996. pp. 845-851.
- Al-Zaharani M.M., Bond Behaviour of Fibre Reinforced Plastic (FRP) Reinforcements with Concrete, Thesis submitted in partial fulfilment of the requirements for the degree of Doctor of philosophy, The Pennsylvania State University, USA.
- Al-Zahrani M. M., Nanni A., Al-Dulaijan S. U., Bakis C. E.: Bond of FRP to concrete in reinforcement rods with axisymmetric deformations. Advanced Composite Materials in Bridges and Structures, M. M. El-Badry, Editor, Canadian Society for Civil Engineering, Montreal, Quebec 1996. pp. 853-859.
- Bank L.C., Puterman M., Katz A.: The effect of material degradation on bond properties of FRP reinforcing bars in concrete, ACI Material Journal, 1996.
- Benmokrane B., Masmoudi R.: FRP C-bar reinforcing rod for concrete structures. Advanced Composite Materials in Bridges and Structures, M. M. El-Badry, Editor, Canadian Society for Civil Engineering, Montreal, Quebec 1996. pp. 181-187.
- Benmokrane B., Tighiouart B., Chaallal O.: Bond strength and load distribution of composite GFRP reinforcing bars in concrete. ACI Materials Journal, Vol. 93, No. 3, May-June 1996, pp. 246-253.
- Clarke J., Waldron P.: The reinforcement of concrete structures with advanced composites. The Structural Engineer, Vol. 74, No. 17, Sep. 1996.
- Cosenza E., Manfredi G., Realfonzo R.: Bond characteristics and anchorage length of FRP rebars. Advanced Composite Materials in Bridges and Structures, M. M. El-Badry, Editor, Canadian Society for Civil Engineering, Montreal, Quebec 1996. pp. 181-187.
- Cosenza E., Manfredi G., Realfonzo R.: Bond Characteristics and Anchorage length of FRP Rebars. Advanced Composite Materials in Bridges and Structures. 2nd International Conference. Montréal, Québec, Canada, August 11-14, 1996. pp. 909-916.
- Ehsani M. R., Saadatmanesh H., Tao S.: Design Recommendations for Bond of GFRP Rebars to Concrete. Journal of Structural Engineering, Vol 122, No 3, March 1996.
- Faoro M.: The Influence of Stiffness and bond of FRP Bars and Tendons on the Structural Behavior of Reinforced Concrete members. Advanced Composite Materials in Bridges and Structures. 2nd International Conference. Montréal, Québec, Canada, August 11-14, 1996. pp. 885-892.
- Gentry T. R., Hudak C. E.: Thermal compatibility of plastic composite reinforcement and concrete. Advanced Composite Materials in Bridges and Structures, M. M. El-Badry, Editor, Canadian Society for Civil Engineering, Montreal, Quebec 1996. pp. 149-156.
- Gowripalan N., Chiang Y.K.: The Influence of Surface Characteristics of FRP and Hydration Products on the Bond of Tendons in Pretensioned Beams. Advanced Composite Materials in Bridges and Structures. 2nd International Conference. Montréal, Québec, Canada, August 11-14, 1996. pp. 869-876.

Copyright fib, all rights reserved. This PDF copy of fib Bulletin 10 is intended for use and/or distribution only by National Member Groups of fib.

1996 Hoshijima, T. and Yagi, K.: Properties of CFRP Composites for Concrete Structures. Fibre Composites in Infrastructure, First International Conference on Composites in Infrastructure, ICCI´96, Tucson, Arizona, USA, 15-17 January, 1996, pp. 227-241.

- Hughes Brothers, Corrosion Proof Products: Fibre Reinforced Plastic (FRP) Rebar Catalog. 308 Tequesta Drive, Suite 14, FL 33469, USA (1996).
- Krüger L., Reinhardt H. W., Eberle K., Hensel K., Grosse C., Weiler B.: Monitoring of bond deterioration in aramid prestressed elements by non-destructive testing. Advanced Composite Materials in Bridges and Structures, M. M. El-Badry, Editor. Canadian Society for Civil Engineering, Montreal, Quebec 1996. pp. 861-867.
- Lee, H.S., Tomosawa, F., Noguchi and T., Kage, T.: Finite element analysis of effect of CFRP sheet on the flexural performance of RC beams. Proceeding of the Japan Concrete Institute, Vol.18, No.1. pp.1065-1070 (in Japanese).
- Lees J.M., Burgoyne C.J.: Influence of bond on Rotation Capacity of Concrete Pre-Tensioned with AFRP. Advanced Composite Materials in Bridges and Structures. 2nd International Conference. Montréal, Québec, Canada, August 11-14, 1996. pp. 901-908.
- Machida A.: Designing Concrete structures with continuous fiber reinforcing materials. Dept. of Civil and environmental Engineering, Saitama University, Urawa, Saitama 338, Japan. First International Conference on Composites in Infrastructure, ICCI'96, 15-17 January 1996, Tucson Arizona, USA. Department of Civil Engineering and Engineering Mechanics, University of Arizona, Tucson, Arizona 85721, USA. Tucson 1996. p. 13.
- Mahmoud Z.I., Rizkalla S.H.: Bond of CFRP Prestressing Reinforcement. Advanced Composite Materials in Bridges and Structures. 2nd International Conference. Montréal, Québec, Canada, August 11-14, 1996. pp. 877-884.
- Marshall Industries Composites Inc: C-bar reinforcing rods for concrete reinforcement. Information brochure. Jacksonville, FL 32217, USA, 1996.
- Quantrill, R.J., Hollaway, L.C. and Thorne, A.M.: Predictions of the Maximum Plate End Stresses of FRP Strengthened Beams: Part II. Magazine of Concrete Research, Vol. 48, No. 177, December, 1996, pp. 343-351.
- SINTEF-EUROCRETE: Non-ferrous reinforcement for concrete structures, Small beam test-Bond splice length. Restricted report STF22 F96828, Aug. 1996.
- Sippel T.M., Mayer U.: Bond behavior of FRP-strands under short-term, reversed and cyclic loading. Advanced Composite Materials in Bridges and Structures, M. M. El-Badry, Editor, Canadian Society for Civil Engineering, Montreal, Quebec 1996. pp. 837-844.
- Uppuluri V. S., Bakis C. E., Al-Dulaijan S. U., Nanni A., Boothby T. E.: Analysis of the bond mechanism in FRP reinforcement rods: The effect of rod design and properties. Advanced Composite Materials in Bridges and Structures, M. M. El-Badry, Editor, Canadian Society for Civil Engineering, Montreal, Quebec 1996. pp. 893-900.
- Zaki I. M., Rizkalla S. H.: Bond of CFRP prestressing reinforcement. Advanced Composite Materials in Bridges and Structures, M. M. El-Badry, Editor, Canadian Society for Civil Engineering, Montreal, Quebec 1996. pp. 877-884.

1997 Achillides Z., Pilakoutas K., Waldron P.: Bond Behaviour of FRP Bars to Concrete. Non-Metallic (FRP) Reinforcement for Concrete Structures. Proceedings of the International Symposium, Vol. 2, Sapporo, Oct. 1997. pp. 341-348.

- Benmokrane B., Tighiouart B., Thériault M.: Bond Strength of FRP Rebar Splices. Non-Metallic (FRP) Reinforcement for Concrete Structures. Proceedings of the International Symposium, Vol. 2, Sapporo, Oct. 1997. pp. 405-412.
- Brosens K., Van Gemert D.: Anchoring Stresses Between Concrete and Carbon Fibre Reinforced Laminates. Non-Metallic (FRP) Reinforcement for Concrete Structures. Proceedings of the International Symposium, Vol. 1, Sapporo, Oct. 1997. pp. 271-278.
- Cosenza E., Manfredi G., Realfonzo R., Behaviour and Modelling of Bond of FRP Rebars to Concrete, Journal of Composite for Construction, ASCE, Vol.1, No.2.
- El-Nawawy O.A.: The Use of Reinforced Plastic Rebars in Concrete Buildings in the Arab World. Non-Metallic (FRP) Reinforcement for Concrete Structures. Proceedings of the International Symposium, Vol. 2, Sapporo, Oct. 1997. pp. 413-422.
- Fukuzawa K., Numao T., Wu Z., Yoshizawa H., Mitsui M.: Critical Strain Energy Release Rate of Interface Debonding Between Carbon Fibre Sheet and Mortar. Non-Metallic (FRP) Reinforcement for Concrete Structures. Proceedings of the International Symposium, Vol. 1, Sapporo, Oct. 1997. pp. 295-302.
- Hattori A., Kawasaki K., Miyagava T., Fujii M.: Bond Behaviours of Carbon Fibre Strand and Fibre Deformed Bar. Non-Metallic (FRP) Reinforcement for Concrete Structures. Proceedings of the International Symposium, Vol. 2, Sapporo, Oct. 1997. pp. 349-356.
- He J.H., Pilakoutas K., Waldron P.: Strengthening of Reinforced Concrete beams with CFRP Plates. Non-Metallic (FRP) Reinforcement for Concrete Structures. Proceedings of the International Symposium, Vol. 1, Sapporo, Oct. 1997. pp. 343-350.

Copyright fib, all rights reserved. This PDF copy of fib Bulletin 10 is intended for use and/or distribution only by National Member Groups of fib.

1997 Hedlund G., Rosinski B.: Pullout Tensile Reinforcement Splice Tests with GFRP Bars. Chalmers University of Technology, Division of Building Technology, Work No: 18. Graduation thesis: E-72:2, Göteborg, September 1997. p. 72.

- Hisabe N., Sakai H., Otaguro H., Yagi K.: Flexural Reinforcing Effect of Reinforced Concrete Slab Strengthened with Carbon Fibre Sheet under Oscillation Loading. Non-Metallic (FRP) Reinforcement for Concrete Structures. Proceedings of the International Symposium, Vol. 1, Sapporo, Oct. 1997. pp. 335-342.
- Horiguchi T., Saeki N.: Effect of Test Methods and Quality of Concrete on Bond strength of CFRP Sheet. Non-Metallic (FRP) Reinforcement for Concrete Structures. Proceedings of the International Symposium, Vol. 1, Sapporo, Oct. 1997. pp. 265-270.
- Jansze, W.: Strengthening of reinforced concrete members in bending by externally bonded steel plates - Design for beam shear and plate anchorage. Ph.D thesis, Delft University. Delft 1997.
- Japan Society of Civil Engineers, JSCE: Recommendation for design and construction of concrete structures using continuous fiber reinforcing materials. Concrete Engineering Series 23. Tokyo 1997. p. 325.
- JCI Committee on Continuous Fibre Reinforced Concrete: Committee Report. Japan Concrete Institute (in Japanese). Tokyo 1997.
- Joh O., Wang Z., Goto Y.: Experimental Study on Bond Cracking performance of FRP Reinforced Concrete. Non-Metallic (FRP) Reinforcement for Concrete Structures. Proceedings of the International Symposium, Vol. 2, Sapporo, Oct. 1997. pp. 431-438.
- Karlsson M.: Bond between C-BAR FRP reinforcement and concrete. Chalmers University of Technology, Division of Building Technology, Work No 13. Graduation thesis: E-97:1. Göteborg, 1997-03-27. p. 71.
- Kobayashi K., Rahman H., Fujisaki T.: Crack Width Prediction for NEFMAC - Reinforced Flexural Members. Non-Metallic (FRP) Reinforcement for Concrete Structures. Proceedings of the International Symposium, Vol. 2, Sapporo, Oct. 1997. pp. 447-454.
- Kono S., Inazumi M., Kaku T.: Bond Splitting Behavior of Reinforced Concrete Members Confined with CFRP Sheets. Non-Metallic (FRP) Reinforcement for Concrete Structures. Proceedings of the International Symposium, Vol. 2, Sapporo, Oct. 1997. pp. 373-380.
- Maeda T., Asano Y., Sato Y., Ueda T., Kakuta Y.: A Study on Bond Mechanism of Carbon Fibre Sheet. Non-Metallic (FRP) Reinforcement for Concrete Structures. Proceedings of the International Symposium, Vol. 1, Sapporo, Oct. 1997. pp. 279-286.
- Magnusson J.: Bond and Anchorage of Deformed Bars in High-Strength Concrete. Chalmers University of Technology, Division of Concrete Structures, Licentiate thesis, Work No. 1113, Publication 97:1, Göteborg, November 1997. p. 234.
- Nanni A., Bakis C.E., Boothby T.E.: Externally Bonded FRP Composites for Repair of RC Structures. Non-Metallic (FRP) Reinforcement for Concrete Structures. Proceedings of the International Symposium, Vol. 1, Sapporo, Oct. 1997. pp. 303-310.
- Reinhardt W., Gollas L., Weiler B., Grosse Ch., Eberle K.: Non-Destructive Assessment of Bond Deterioration of Aramid in Reinforced and Prestressed Concrete. Proceedings of the International Symposium, Vol. 2, Sapporo, Oct. 1997. pp. 397-404.
- Saadatmanesh H., Malek A.M.: Prediction of Shear and Peeling Stresses at the Plate Ends of Beams Strengthened with FRP Plates. Non-Metallic (FRP) Reinforcement for Concrete Structures. Proceedings of the International Symposium, Vol. 1, Sapporo, Oct. 1997. pp. 311-318.
- Sato, Y., Ueda, T., Kakuta, Y. and Ono, S.: Ultimate shear capacity of reinforced concrete beams with carbon fibre sheet. Non-Metallic (FRP) Reinforcement for Concrete Structures, Proceedings of the Third International Symposium, October 1997, Sapporo. pp. 499-506.
- Sato, Y., Kimura, K. and Kobatake, Y.: Bond behavior between CFRP sheet and concrete (Part 1). Journal of Structural and Construction Engineering, Architectural Institute of Japan, No.500, pp. 75-82 (in Japanese).
- Sato, Y., Tanaka, T., Ueda, T. and Ono, S.: Shear behavior of RC beams reinforced with carbon fibre sheet. Transactions of Japan Concrete Institute, Vol.18. pp. 137-142.
- Sekijima, K. and Ohtsuka, Y.: Study on bond behavior of GFRP plate adherent to concrete. Proceeding of the Japan Concrete Institute, Vol.19, No.2. pp. 1581-1586 (in Japanese).
- Sheard P. A.: The development of non-ferrous reinforcement for concrete structures. Eurocrete Final Report to its sponsors.
- Shield C., French C., Retika A.: Thermal and Mechanical Fatigue Effects on GFRP Rebar-Concrete Bond. Non-Metallic (FRP) Reinforcement for Concrete Structures. Proceedings of the International Symposium, Vol. 2, Sapporo, Oct. 1997. pp. 381-388.
- Takagi N., Kojima T., Iwamoto K., Inoue S.: A Study of continuous Fibre rods Embedded in Beam Specimen. Non-Metallic (FRP) Reinforcement for Concrete Structures. Proceedings of the International Symposium, Vol. 2, Sapporo, Oct. 1997. pp. 365-372.
- Takahashi Y., Sato Y., Ueda T., Maeda T., Kobayashi A.: Flexural Behavior of RC Beams with Externally Bonded Carbon Fibre Sheet. Non-Metallic (FRP) Reinforcement for Concrete Structures. Proceedings of the International Symposium, Vol. 1, Sapporo, Oct. 1997. pp. 327-334.

Copyright fib, all rights reserved. This PDF copy of fib Bulletin 10 is intended for use and/or distribution only by National Member Groups of fib.

1997 Takeo, K., Matsushita, H., Makizumi, T. and Nagashima, G.: Adhesive characteristic of carbon fibre sheet on CFRP adhesive method. Proceeding of the Japan Concrete Institute, Vol.19, No.2. pp. 1599-1604 (in Japanese).

- Tepfers R.: Bond of FRP Reinforcement in Concrete. A State-of-the-Art in preparation. Chalmers University of Technology, Division of Building Technology. Work No 15. Göteborg, January 1997. p. 16. American Concrete Institute (ACI), Bond and Development of Reinforcement, SP-180. Farmington Hills, Michigan 1998. pp. 493-508.
- Tepfers R., Karlsson M.: Pull-out and tensile reinforcement splice tests using FRP C-BARs. FRPRCS-3 Third International Symposium on Non-Metallic (FRP) Reinforcement for Concrete Structures in Sapporo 14-16 October 1997. pp. 357-364.
- Ueda, T., Nakai, H. and Tottori, S.: JCI State-of-the-art report on retrofitting by CFRM - guidelines for design, construction and testing -. Non-Metallic (FRP) Reinforcement for Concrete Structures, Proceedings of the Third International Symposium, October 1997, Sapporo. pp.621-628.
- Wang Z., Goto Y., Yoh O.: Bond Characteristic of FRP Rods and Effect on Long Term Deflection of Concrete Beams. Non-Metallic (FRP) Reinforcement for Concrete Structures. Proceedings of the International Symposium, Vol. 2, Sapporo, Oct. 1997. pp. 389-396.
- Wu Z., Matsuzaki T., Tanabe K.: Interface Crack Propagation in FRP-Strengthened Concrete Structures. Non-Metallic (FRP) Reinforcement for Concrete Structures. Proceedings of the International Symposium, Vol. 1, Sapporo, Oct. 1997. pp. 319-326.
- Yoshizava H., Zhishen W.: Analysis of Debonding Fracture Properties of CFS Strengthening RC Member Subject to Tension. Non-Metallic (FRP) Reinforcement for Concrete Structures. Proceedings of the International Symposium, Vol. 1, Sapporo, Oct. 1997. pp. 287-294.
- Zhao W., Pilakoutas K., Waldron P.: FRP Reinforced Concrete: Cracking Behavior and Determination. Non-Metallic (FRP) Reinforcement for Concrete Structures. Proceedings of the International Symposium, Vol. 2, Sapporo, Oct. 1997. pp. 439-446.

1998 Achillides Z.: Bond behaviour of FRP bars in concrete (PhD Thesis), Centre for Cement and Concrete, Dept. of Civil and Structural Eng., The University of Sheffield, July 1998.

- Achillides Z., Pilakoutas K., Waldron P.: Bond of FRP anchorages and splices in concrete beams. 8th European Conference of Composite Materials, Naples, Italy, June 1998. pp. 277-284.
- Apinis R., Modniks J., Tamuzs V., Tepfers R.: Ductility of Hybrid Fibre Composite Reinforcement FRP for Concrete. Institute of Polymer Mechanics, Riga, Latvia. Chalmers University of Technology, Division of Building Technology, Work No 23. Riga, 1998. p. 16.
- Asano, Y.: A study on bond mechanism of carbon fibre sheet. Master thesis submitted to Hokkaido University (in Japanese).
- Blaschko M., Niedremeier R., Zilch K.: Bond Failure Modes of Flexural Members Strengthened with FRP. Proceedings of the Second International Conference on Composites in Infrastructure, ICCI´98. Department of Civil Engineering and Engineering Mechanics, University of Arizona. Tucson 1998. Vol. I. pp. 315-327.
- Freimanis A.J., Bakis C.E., Nanni A., Gremel D.: A Comparison of Pullout and Tensile Behaviors of FRP Reinforcement for Concrete. Proceedings of the ICCI´98, Second International Conference on Composites in Infrastructure, January 3-4, 1998, Tucson, Arizona, Vol. II. pp. 52-65.
- Greco C., Manfredi G., Pecce M., Realfonzo R.: Experimental analysis of bond between GFRP deformed rebars and concrete, 8th European Conference of Composite Materials, June 1998, Naples, Italy.
- Hattori, A., Etoh, Y., Ohnishi, Y. and Miyagawa, T.: Influence of degradation on strengthening by FRP sheet. Proceedings of JCI Symposium on Continuous Fibre Reinforced Concrete, May 21, 1998, Tokyo. pp.1-6 (in Japanese).
- He, J. H.: Behaviour of reinforced concrete beams strengthened with epoxy bonded CFRP plates. PhD Thesis, University of Sheffield, 1998.
- Iwanami, M., Matsumoto, A., Tomita, Y. and Otsuki, N.: Evaluation of bond failure between CFRP sheet and concrete. Proceedings of JCI Symposium on Continuous Fibre Reinforced Concrete, May 21, 1998, Tokyo. pp.21-26 (in Japanese).
- JCI Committee on Continuous Fibre Reinforced Concrete: Committee Report (II). Japan Concrete Institute (in Japanese). 1998.
- JSCE Committee on Retrofitting Design (Wu, Z.S.): Towards rational design method for delamination in retrofitting with wrap. Future for Design and Construction for Retrofitting Concrete Structures, Concrete Engineering Series, No.28, Japan Society for Civil Engineers. pp. I-249-I-258 (in Japanese).
- Kachlakev D.I., Lundy J.R.: Bond strength Study of hollow Composite Rebars with Different Micro Structure. Proceedings of the Second International Conference on Composites in Infrastructure, ICCI´98. Department of Civil Engineering and Engineering Mechanics, University of Arizona. Tucson 1998. Vol. II. pp. 1-14.
- Kamiharako A., Shimomura, T. and Maruyama, K.: Evaluation of shear capacity of RC members retrofitted with CFR sheets based on bond-peeling constitutive model. Proceedings of JCI Symposium on Continuous Fibre Reinforced Concrete, May 21, 1998, Tokyo. pp.7-14 (in Japanese).

Copyright fib, all rights reserved. This PDF copy of fib Bulletin 10 is intended for use and/or distribution only by National Member Groups of fib.

1998 Kawasaki, K., Hattori, A. and Miyagawa, T.: Long-term bond behavior of FRP tendon for pre-tension member. Proceedings of JCI Symposium on Continuous Fibre Reinforced Concrete, May 21, 1998, Tokyo. pp.27-32 (in Japanese).

- Kishi, N., Mikami, H., Sato, M. and Matsuoka, K.: Influence of concrete surface treatment on flexural bonding property of AFRP sheet glued to RC beams. Proceedings of JCI Symposium on Continuous Fibre Reinforced Concrete, May 21, 1998, Tokyo. pp.45-50 (in Japanese).
- Larrelde J., Mueller-Rochholz J., Schneider T., Willmann J.: Bond Strength of Steel, AFRP and GFRP Bars in Concrete. Proceedings of the ICCI´98, Second International Conference on Composites in Infrastructure, January 3-4, 1998, Tucson, Arizona, Vol. II. pp. 92-101.
- Maeda, T. : Fundamental Study on Maintenance of Concrete Structures. Doctoral Dissertation, Hokkaido University, 1998 (in Japanese).
- Malek A.M., Saadatmanesh H.: Design Equations and guidelines for Reinforced concrete beams Strengthened with FRP Plates. Proceedings of the Second International Conference on Composites in Infrastructure, ICCI´98. Department of Civil Engineering and Engineering Mechanics, University of Arizona. Tucson 1998. Vol. I. pp. 603-617.
- Mikami, H., Kishi, N., Sato, M. and Matsuoka, K.: Flexural bonding property of axially glued RC beams wrapped with U-shaped FRP sheets. Proceedings of JCI Symposium on Continuous Fibre Reinforced Concrete, May 21, 1998, Tokyo. pp.55-60 (in Japanese).
- Mitsui, M., Fukuzawa, K., Numao, T. and Kagawa, K.: Effect of various factors on bonding behavior between CFRP sheet and mortar. Proceedings of JCI Symposium on Continuous Fibre Reinforced Concrete, May 21, 1998, Tokyo. pp.15-20 (in Japanese).
- Mullins G., Sen R., Spain J.: Testing of CFRP/Concrete bond. Proceedings of the ICCI´98, Second International Conference on Composites in Infrastructure, ICCI´98. Department of Civil Engineering and Engineering Mechanics, University of Arizona. Tucson 1998. Vol. I. pp. .
- Sato, Y., Asano, Y., Maeda, T., Kobayashi, A., Ueda, T. and Kakuta, Y.: A study on bond strength of continuous fibre sheet. Structural Engineering and Construction: Tradition, Present and Future, Proceedings of the Sixth East Asia-Pacific Conference on Structural Engineering & Construction, January 1998. pp.1319-1324.
- Sen R., Shahawy M., Sukumar S., Rosas J.: Effect of tidal Exposure on Bond of CFRP Rods. Proceedings of the ICCI´98, Second International Conference on Composites in Infrastructure, January 3-4, 1998, Tucson, Arizona, Vol. II. pp. 512-523.
- Tepfers R.: Bond Between FRP-bars and Concrete. Chalmers University of Technology, Division of Building Technology, Work No 22. Publication 98:3. Göteborg, 1998-03-03. p. 16. Contribution to the Tenth International Conference on Mechanics of Composite Materials, Micro Symposia " Bond of FRP Reinforcement in Concrete", April 20-23 1998, Riga, Latvia.
- Tepfers R., Hedlund G., Rosinski B.: Pull-out and tensile reinforcement. Splice tests with GFRP bars. Proceedings of the ICCI´98, Second International Conference on Composites in Infrastructure, January 3-4, 1998, Tucson, Arizona, Vol. II pp. 37-51.
- Tighiouart B., Benmokrane B., Gao D.: Investigation on the Bond of Fibre Reinforced Polymer (FRP) Rebars in Concrete. Proceedings of the ICCI´98, Second International Conference on Composites in Infrastructure, January 3-4, 1998, Tucson, Arizona, Vol. II. pp. 102-112.
- Wang C. Y., Ling F. S.: Prediction Model for the Debonding failure of Cracked RC Beams with Externally bonded FRP Sheets. Proceedings of the Second International Conference on Composites in Infrastructure, ICCI´98. Department of Civil Engineering and Engineering Mechanics, University of Arizona. Tucson 1998. Vol. I. pp. 548-562.

1999 Apinis R., Dejke V., Modniks J., Tamuzs V., Tepfers R.: Rotation capacity of Concrete Beams with Ductile Hybrid CFRP+GFRP and Elastic CFRP Tensile Reinforcement. Chalmers University of Technology, Division of Building Technology, Work No 29. Publication 99:1. Göteborg, 1999. p. 10. Forth International Symposium on Fiber Reinforced Polymer for Reinforced Concrete Structures (FRPRCS-4), Baltimore, October 31-November 5, 1999.

Copyright fib, all rights reserved. This PDF copy of fib Bulletin 10 is intended for use and/or distribution only by National Member Groups of fib.

8 Innovative developments in the light of bond philosophy

Working Party 8:

Steven McCabe (Convener, University of Kansas, Lawrence, USA), **John Cairns** (Heriot, Watt University, Edinburgh, UK), **Joop den Uijl** (Delft University of Technology, The Netherlands), **Utz Mayer** (Stuttgart University, Germany),**Stavroula Pantazopoulou** (Demokritos University of Thrace, Xanthi, Greece), **Ralejs Tepfers** (Chalmers University of Technology, Göteborg, Sweden)

8.1 Introduction **396**

8.2 History of developments in bond **396**
8.2.1 Early development 396
8.2.2 Anchorages of plain bars 397
8.2.3 Anchorage of deformed bars - early investigations 397
8.2.4 Mechanical anchors 398
8.2.5 Anchorage of deformed bars - parameter investigations 398
8.2.6 Pull-out tests 400
8.2.7 Analysis of bond stress distribution 400
8.2.8 Splitting bond failures 401
8.2.9 Completing investigations 402
8.2.10 Bond of compressive reinforcement 402
8.2.11 Fatigue of bond 403
8.2.12 Analytical theory of bond 403
8.2.13 Summing up 404
8.2.14 Beginning of fracture mechanics 404
8.2.15 Investigations for code purposes 404
8.2.16 Conclusion 405

8.3 Codes: Where do we stand? **405**

8.4 Lessons from and benefits of bond research **410**
8.4.1 Bond in general 410
8.4.2 Bond in current practice 410
8.4.3 Bond research 413
8.4.4 Methods of bond testing 415
8.4.5 Developments in analysis and modelling 417
8.4.6 Design Philosophies 418

8.5 Current needs and future directions **419**

8.6 References **422**

Copyright fib, all rights reserved. This PDF copy of fib Bulletin 10 is intended for use and/or distribution only by National Member Groups of fib.

8.1 Introduction

The need for innovation in the design and analysis of reinforced concrete structures is essential to the continuing health of this vital structural technology. As with any area of modern engineering, there is a consistent need for evaluation of existing methods and the state of the art to assess where the technology is and where new ideas, methods and philosophies are needed to propel the application of reinforced concrete technology to the next level. The bond of reinforcement in concrete is the critical feature of reinforced concrete that makes the use of concrete as a structural material possible. Thus attention to this critical aspect of reinforced concrete is central to the development of new technologies and the use of advanced materials in reinforced concrete. Furthermore the development of improved methods for the analysis and design of RC structures will require more accurate bond modeling and design philosophies than what are now available to achieve greater structural efficiencies and safety.

As has been discussed in this report, important strides have been made in the depiction of bond processes. These improvements have made greater use of computer-based models and more detailed examinations of bond -- the *process* of anchoring a reinforcing bar in concrete -- than is now generally performed in design. This chapter is devoted to examining what has led us to this point in time and to view what developments are needed to move the bond technology and the analysis of bond to the levels needed to support these new technologies.

The chapter contains a historical discussion of the development of bond and the supporting analysis techniques as well as the codes that control design around the world. These sections are followed by a critical assessment of where the state-of-the-art is at this time and where the essential needs are in bond technology and analysis to support developments in the coming years. Thus, it may be said that this chapter evaluates the past and forecasts the future developments in the field of bond. It also is important to understand how and why the analysis and design of bond for reinforced concrete structures is performed as it is in current design codes -- remarkably similar from continent to continent. It also is important to view where the analysis methods in particular need to be developed to support many of the new design concepts and construction methods that are now in place or under research as this time.

8.2 History of developments in bond

The survey of history is mainly devoted to early developments in bond research extending up to 1970's - this section is intended to give an understanding of how research on bond evolved through the years, including the definition of the various issues relating to bond and the solution approaches that prevailed. From the early 1970's to the beginning of the 1980's, developments in bond - related research are covered by State of the Art reports published as CEB Bulletins d'Information No 151 (1982) and No 181 (1987). ACI Committee 408 (1990) published a state of the art report that summarized bond research and the Committee's recommendations as of the late 1980's. More recent developments in bond, extending from the beginning of the 1980's up to the present are covered in the preceding chapters in this "*fib*" Bulletin.

8.2.1 Early development

The issue of bond arose as soon as reinforcement was introduced in concrete. The first attempts in using what resembles modern reinforcement in concrete were made by Josef Monier in 1849, when he introduced reinforcement in flower pots and boxes and further

Copyright fib, all rights reserved. This PDF copy of fib Bulletin 10 is intended for use and/or distribution only by National Member Groups of fib.

improved his reinforcing system. This is the starting point in the development of many alternative reinforcing techniques. William Boutland Wilkinson in 1854 patented his reinforcing systems for buildings. Joseph Louis Lamboth in 1855 introduced a wire system as reinforcement in concrete boats. Several engineers thereafter patented various specialized reinforcing systems. The remaining years to the century change may be regarded as time for development of reinforcing systems. However, plain bars for general use as concrete reinforcement were introduced during the latest years of the 19th century. The limited anchorage capacity that could be obtained by the chemical adhesion between smooth lateral surface of the reinforcing bar and concrete was noted. End hooks for anchorage became necessary. At about the year 1900 the bars with surface deformations were introduced, first in America and then in Europe and gave rise to a whole new class of bond problems.

8.2.2 Anchorage of plain bars

Bach & Graf (1909), (1910), (1911), reported an extensive series of anchorage tests and tests with hook anchorages. Further tests were performed by the same authors on beam specimens that experienced anchorage failures in combination with shear failures (Bach & Graf, 1911). Splitting as a predominant failure mode was observed in the early bond tests. However the main motivation was to determine the necessary anchorage lengths for use in the design practice, rather than to seek sophisticated mechanistic interpretations of test observations through design models. As concrete structures became larger in size and more complex splicing of bars became necessary. Early systematic beam-tests were performed by Scheit & Wawrziniok (1912) and by Amos (1917) in order to improve knowledge with regards to splicing of tensile reinforcement. They worked both with hand mixed and machine mixed concrete (f_{cc}=7–28 MPa) and plain steel bars (f_{sy} = 258 MPa) with and without Considère hooks. The primary results were as follows:

1. The strength of concrete is a very important parameter with regards the occurrence of slip in plain bars.
2. Machine mixing and working gives better concrete than hand mixing.
3. The ultimate bond stress, as resolved from experimental data using the assumption of an even distribution of bond stress, drops when the lap length of the splice increases.
4. Splices without hooks are not recommended, however, at good working conditions a lap length of 1.25 m seems sufficient to replace an unspliced bar.
5. Splices with hooks are superior to those without hooks.
6. If the spliced bars are bundled with steel wire the strength of the splice increases. However, there are difficulties in placing the concrete in the neighborhood of the splice arrangement. Connection of two bars by hooking them in each other gives bad results because an initial displacement is required in order for the hooks to engage and start resisting load. It is stated that spliced bars with hooks and diameters of approximately ö10 mm can fully replace an unspliced bar. For bigger bar diameters especially ö > 20 mm this is no longer possible, not even with lap lengths s > 40ö.

8.2.3 Anchorage of deformed bars - early investigations

Another group of bond-tests that may be considered a classical example were performed by Abrams (1913). He analyzed in detail the bonding properties of different types of steel bars including deformed bars and end anchorages, but he did not carry out splice tests on beams. These tests produced many important results for the time, and they were considered state of the art for about two decades. Very little research concerning splicing of tensile reinforcement

Copyright fib, all rights reserved. This PDF copy of fib Bulletin 10 is intended for use and/or distribution only by National Member Groups of fib.

bars seems to be reported in the literature until 1937.

8.2.4 Mechanical anchors

In a paper Lucan (1925) presented an interlocking splicing system for tensile reinforcement. Forssell (1937) tested mechanical splices where the reinforcing bars in tension were connected to each other by means of special jointing sleeves. Bars are butted end to end and gripped by a crimped sleeve. This type of sleeve is of interest, because it is in point of principle the same as the sleeves investigated by Eriksson (1960), Segner (1965), Hahn & Fastenau (1968), Ivey (1968), Sozen & Gamble (1969) and Fastenau, Leonhardt & Hahn (1970). Despite the encouraging test-results, the Forssell sleeves did not become popular at the time whereas sleeves that were developed later were eagerly adopted in the construction practice. These were specially suitable for large diameter deformed bars. Forssell was of the opinion that ordinary overlap splices are not safe.

Spiral sockets for splicing tensile reinforcement with lugs were developed by Efsen (1957). However, these sockets were not economical in spite of their being a logical solution for a splice where the concrete is the medium transferring the stress from steel bar to steel bar. These types of splice could be so strong that rupture of the spliced bars would occur outside the splice.

Forssell (1960) suggested a type of splice in which "Forssell-rings" act as anchors at the ends of the spliced bars. These anchors are held together by means of screwed splicing equipment. High cost has limited the use of this splice construction.

Mechanical splicing performance has received a great deal of attention recently, especially by ACI in the context of seismic applications. A summary of options and concepts widely available can be found in the ACI Committee 439 report on mechanical splices (1990).

8.2.5 Anchorage of deformed bars - parameter investigations

A renewed interest in bond research, evidenced by increased publication activity started in the late thirties. Deformed bars were introduced to an increasing extent and the quality of the steel rose. The old results were no longer applicable.

The influence of different types of bar - deformations (ribs) on the bond strength of steel bars was investigated by Wernisch (1937), Tengvik (1941), Clark (1946) and (1949), Reese (1950), Bernander (1952), Efsen (1958), Lutz (1970) and Goto (1971). With the exception of some contradictory results, the tests performed indicate that surface deformations having small rib spacing and high ribs improve both the resistance to slip and the ultimate bond strength. The issue of optimal roughness of the reinforcing bar surface is also discussed by Östlund (1967). Generally speaking, bond strength increases with the roughness of the reinforcement but the splitting resistance of the surrounding concrete limits the anchorage capacity. At this stage there is not much point in increasing the roughness of the steel bars unless additional confinement is provided.

The inclination of the face of deformations is an important factor. Slip occurs almost entirely by crushing of concrete in front of the rib if the angle between the rib face and the bar axis is greater than 45 degrees. Slip (i.e., relative sliding between the steel and adjacent concrete) is encouraged by smaller rib-face angles. For good results the deformations must be spaced uniformly along the bar and the included angle with respect to the longitudinal axis should not

Copyright fib, all rights reserved. This PDF copy of fib Bulletin 10 is intended for use and/or distribution only by National Member Groups of fib.

be less than 45 degrees. It is not stated directly that as the bond capacity of the steel bars becomes higher the tendency of the surrounding concrete to split also increases. Transverse reinforcement must be used to prevent the progress of splitting cracks otherwise the improved bond resistance of the bar cannot be utilized. This observation is very important for reinforcement splices.

Gilkey, Chamberlin & Beal (1938) followed up the tests of Abrams (1913) concerning bond for concrete mixes currently in use.

Hoyer & Friedrich (1939) illustrated the bond improvement owing to the Hoyer-effect for steel bars of small diameter. This observation, very important in prestressing techniques, can not be used for anchoring and splicing ordinary non-prestressed reinforcing bars.

Welded tensile reinforcement splices were investigated by Landberg (1939), Teske (1956), Brede (1957) and Walls, Sanders & Munse (1965). It was shown that many alternative welding techniques can be used successfully for extending bars. However, the method is uneconomical for ordinary structures because of the need of highly trained workmen and the necessary quality control.

Overlap splices both of plain and of deformed bars were tested by Tengvik (1942). Deformed bar splices proved superior over those of plain bars even when the latter have hooks. Bending upwards the ends of overlapped bars to about 30 degrees gave no advantage in comparison with straight bars. These tests were followed up by Blankenburg (1944) and by Örbom (1948). Blankenburg reported overlap splice beam-tests with plain steel bars. Concrete of stiffer consistency (higher VB) appeared to give somewhat stronger splices.

Kluge and Tuma (1945) recorded strain distributions along the reinforcing bars in a tension splice. Their specimens were beams with single bar splices flanked by two continuous bars. The tensile stress and the bond stress along the spliced bars were evaluated from the strain measurements. It was found that the actual stress in the continuous bars may be about 8 to 10% higher than the normal stress obtained when all tensile bars in the beam have the same load. The authors reported that these differences in stress for static loads are evened out by yielding, but may have influence on the fatigue of the reinforcement because of the stress peaks in the continuous bars. It was further observed that there is no difference in the strength of the lap when the lapped bars are spaced 1.5 diameters clear as compared to the case where they are in contact. Chamberlin (1952) tested the influence of clear spacing of spliced bars in tension using pull-out specimens and found an increase in the deformation of concrete between spliced bars and a slight decrease in splice strength for increased clear spacing. These findings were confirmed by the experimental results of Chinn, Ferguson and Thompson (1955) obtained from beam-tests with spliced deformed bars in tension. The authors also made observations regarding the effect on splice strength and mode of failure of concrete cover, concrete strength, overlap length, bar size, ties around the splice and the level where the splice is cast in the beam. Splices cast at the top of the beam are 3 to 8% weaker than bottom bar splices.

The bond of bundled bars in groups of two and three was studied by Tepfers (1964) and equivalent bond areas were proposed. Bond of deformed bundled bars is stronger than that of round bars with the same transverse steel area as the bundle. This because the bonded perimeter is greater for bundled bars compared to that of a round bar with the same cross sectional area as the bundle.

The effect of settlement and bleeding of concrete on bond strength was also studied by Welch

Copyright fib, all rights reserved. This PDF copy of fib Bulletin 10 is intended for use and/or distribution only by National Member Groups of fib.

& Patten (1965). Pull-out specimens with horizontal bars rigidly positioned at different levels were cast. Differences in measured bond strength of about 50% were observed when using deformed bars with concretes of similar strengths but different settlements. Concretes with large settlement and bleeding characteristics experienced loss of bond strength even for horizontal bars with small depths of concrete beneath them. However, such results obtained from small pull-out specimens should be treated with caution because in practice the degree of rigidity of horizontal bars varies and concretes of high cement content have reduced settlement and bleeding.

The effect of entrained air on reinforcement-to-concrete bond was investigated by Hognestad & Siess (1950). Entrainment of air in concrete lowers the compressive strength of the concrete and also the bond strength in about the same proportion. Increasing the bearing area of the bar deformations raises the bond strength. The height of ribs is important from the point of view of the bond strength if the bar is cast horizontally. The authors also state that bond stress decreases with increased depth of concrete underneath the bars.

Peattie & Pope (1956) investigated the effect of the age of concrete on bond resistance. They observed that bond resistance increased more rapidly than concrete strength. The gain in bond resistance depends on shrinkage and exothermic effects during hardening of concrete which contribute in addition to the inherent growth that results from the progressive gain in strength of the concrete. However, shrinkage gives rise to tensile stresses in concrete around the bars, which may lead to cracking along the bars thereby causing a reduction in bond resistance, Tepfers (1973).

8.2.6 Pull-out tests

Pull-out tests have been a usual way in studying bond between concrete and reinforcing steel. The bars have been embedded in prismatic concrete specimens with fairly long embedment lengths. As Wattstein (1947), Bernander (1952), (1955) and Swida (1952) point out, distribution of bond stress along the embedded bar length is non-uniform. To achieve a uniform bond stress distribution, it is necessary to study pull-out specimens with very short embedment lengths. Rehm (1961), Losberg (1962), (1963), (1964) and Lutz (1970) have investigated bond using such specimens. Rehm, in particular, studied the bearing properties of different types of ribs and the stresses around them. He was the first to define a local bond-slip law. The mechanics of bond and slip of deformed bars in concrete have also been investigated by Lutz and Gergely (1967) and by means of finite element analysis by Lutz (1970).

8.2.7 Analysis of bond stress distribution

Osterman (1951) analyzed the state of stress in pull-out specimens using the theory of elasticity. He calculated the bond stress distribution between the reinforcing bar and the concrete and pointed out that the radial and circumferential stresses in the concrete are of importance for the anchorage of the steel bar. Anderson (1953) analyzed the bond in a pulled reinforced concrete specimen with several bars situated beside each other using Airy's stress function for a plane stress distribution. Granholm (1958), (1965) used the modulus of displacement (K-value), introduced by Bleich (1924) for long riveted steel plate joints, to calculate the bond stress distribution between reinforcement and concrete. The K-value theory is based on the hypothesis that the bond stress is directly proportional to the displacement between steel and concrete. The bond stress distribution was also calculated by Rehm (1961) in the same way as by Osterman (1951) but adapted to the spacing of the ribs. Losberg (1962),

Copyright fib, all rights reserved. This PDF copy of fib Bulletin 10 is intended for use and/or distribution only by National Member Groups of fib.

(1963), (1964) used the modulus of displacement (K-value) theory to treat the anchorage of reinforcement in concrete, to calculate stress distributions and the crack spacing and to study tension stiffening. He pointed out that the bond stress distributions along a reinforcing bar due to anchorage and concrete cracking respectively have no influence on each other and therefore can be superimposed. The distribution of stresses is studied with both constant and variable K-values. Tepfers (1973), (1980), (1982) used the K-value theory for calculation of bond stress distributions along overlapped bars and by combining these with the adequate local bond laws, determined the splice strengths.

Rieve (1970) examined theoretically the mechanics of pull-out specimen - a reinforcing bar embedded in a semi-infinite concrete body. An existing continuum mechanics solution for a point load on a semi-infinite body was used in order to solve for line loads acting at different levels in the body. The requirement of compatibility of deformations at the different levels produces the equations needed in order to calculate the bond and steel stress distribution along the embedded bar.

Empirical formulae for bond of deformed bars based on test results are given by Lutz (1970). To calculate the bond strength, the effect of concrete is added to the effect of the transverse reinforcement. Parameters such as width of beam, number of bars in a layer and so on are taken into consideration.

8.2.8 Splitting bond failures

Östlund (1963) investigated using beam specimens the effect of bending radius and concrete cover on the anchorage of deformed bars and stated that bond failure is a concrete splitting failure. He analyzed possible splitting failure patterns in the concrete and observed a linear dependency of the anchorage capacity on the $(f_{cc})^{1/2}$, i.e. the tensile strength of the concrete.

Ferguson, Breen and Thompson (1965) tested eccentric pull-out specimens. Observations were made of the splitting of concrete cover along the embedded steel bar. The effect of spiral reinforcement around the embedded bars was studied. Earlier, Ferguson, Turpin & Thompson (1954) had studied tensile bar spacing as a function of bond whereas Ferguson & Thompson (1962) had investigated the development length for reinforcement in beams. These tests confirm that splitting of the concrete cover is an important failure mechanism limiting bond strength. These bond tests were followed by tests of lapped splices in beams by Ferguson & Breen (1965). Lap lengths with and without stirrups were investigated. It was shown that the strength of a splice could be increased by as much as 50% if confined heavily by stirrups. Failure occurs by splitting of the concrete cover. Splitting builds up prior to failure developing gradually from the ends of the splice. If the splice is sufficiently long the central region remains intact until final failure which occurs in a violent, brittle manner. Ferguson & Briceno (1968) made a successful analysis of splice splitting failures by considering the free body diagram of each splitting pattern subjected to the stress interaction forces between the reinforcing bars and the concrete. These are assumed to be formed by uniform cone vectors oriented at 45° angles with respect the bar axis. Linear correlation is obtained between the calculated tensile stress at failure and the split cylinder strength.

Goto (1971) investigated crack formation in concrete around deformed tension bars by means of indicating ink. The method makes visible crack propagation and the existence of internal cracks when the specimen is split open after load test. Inclined (conical) cracks develop parallel to the direction of the principal compressive stress when the principal tensile stress exceeds the tensile strength of the concrete, and the bond forces obtain splitting force components. This

Copyright fib, all rights reserved. This PDF copy of fib Bulletin 10 is intended for use and/or distribution only by National Member Groups of fib.

conclusion is very important in interpreting the mechanics of bond in reinforced concrete.

8.2.9 Completing investigations

Hribar & Vasko (1969) investigated the end anchorage strength of deformed bars in pull-out specimens. The end anchorages were straight bars, right-angle hooks and semi-circular hooks. The 180 degree hook performed better than the 90 degree hook for the ultimate load but not for the displacement at lower loads.

Splicing by overlapping reinforcement loops was first mentioned by Leonhardt (1965) whereas the use of this splicing method especially in the precast concrete industry was pointed out by Rehm (1970).

An investigation of the anchorage of plain and indented (deformed) steel bar mesh was performed by Cederwall (1960). Lloyd & Kesler (1970) investigated deformed wire fabric splices. Important parameters for the anchorage strength of the splice were concrete strength, weld strength and bond strength. Calculation formulae were given for the splice length of deformed wire and deformed wire fabric.

Stocker & Sozen (1969) investigated the nature of bond between strand and concrete. This investigation comprised pull-out tests and prestressed beam tests and has observations relevant to studies of the bond of reinforcing bars. It was postulated that bond is provided by two mechanisms namely that of interlocking and that of friction after the interlocks have sheared off. The effects of shrinkage, concrete settlement and lateral pressure etc, on bond are studied. Stress distribution in a concrete key, which is interlocked with a microscopically rough steel surface, is calculated by the finite element method. The bond between the strand and the concrete as a function of the twist angle of the strand is investigated.

Stöckl (1968) found that displacing the splices over half the splice length applicable to the individual bars gave the best conditions of transverse strain in the concrete. If the splices are displaced by a whole splice length, the transverse strain peaks near the bar ends are superimposed, causing premature splitting of concrete at quite low loads.

Bond of reinforcement in lightweight aggregate concrete was studied with pull-out specimens by Baldwin (1965). The bond behavior in lightweight concrete was found to be about the same as that in normal-weight concrete. For a given compressive strength the bond strength in light-weight concrete is about 2/3 to 3/4 as great as that for normal-weight concrete depending on whether ultimate bond or bond at 0.01 inch slip is considered.

8.2.10 Bond of compressive reinforcement

Note that only few experimental investigations have been conducted on splices of compressive reinforcement and that very little has been achieved to that end, with the exception of the G-lock splices developed in the USA, an investigation by Pfister and Mattock (1963) and the investigation "Drucküberbergreifungsstösse" (1967). A more comprehensive investigation of reinforcement lap splices under compression was done by Cairns (1976). The end bearing of the bars was taken into account.

Copyright fib, all rights reserved. This PDF copy of fib Bulletin 10 is intended for use and/or distribution only by National Member Groups of fib.

8.2.11 Fatigue of bond

The concepts of fatigue of anchorages and splices in the mid 1970's are as follows. Under static loading failures usually occur by splitting of the surrounding concrete. The reinforcement surrounding the overlaps may yield or even rupture in some of the ultimate splitting failure pattern cracks. Of the two components, concrete and the reinforcement surrounding the splice, concrete is the weakest in fatigue. This statement is based on the observation that of the tested splices no fatigue failure has been reported to occur in the surrounding reinforcement, whereas invariably the surrounding concrete would split-off. The first loading cycles at high upper stress limits are more destructive for concrete than for steel. The fatigue analysis of splices with surrounding reinforcement should therefore be based on concrete as the weaker component. The tensile stresses in the concrete are critical for the fatigue resistance and can be analyzed in the same way as for splices without surrounding reinforcement. According to Soretz (1965) and Tepfers (1973) the same fatigue relations may be assumed for concrete in compression as in tension. Independence of the concrete strength is obtained by working with stress ratios of the max type $f_{c,max}/f_{cu}$ in Wöhler diagrams and in Smith diagrams according to Gaede (1962), Soretz (1965), Aas-Jakobsen (1970), Freitag (1970) and Holzapfel (1972). The main determining factors for fatigue are considered to be the maximum pulsating stress limit, the stress amplitude and the number of load cycles. Strain distribution measurements along the spliced bars indicate that the pulsating load tends to make the bond stress evenly distributed along the lap. The measurements show no noticeable difference in strain distribution or bond stress distribution for splices with and without surrounding reinforcement. Further information about fatigue of bond is given in CEB, Bulletin d'Information No 188, (1988).

The state of the art of bond performance under cyclic loading was compiled by ACI Committee (1992) and summarizes the information available on this topic. The report indicates that there is relatively limited information about bond deterioration under cyclic loading and that research is critically needed in this area.

8.2.12 Analytical theory of bond

The splicing problem for deformed bars was mainly regarded as a problem of splitting of the concrete cover and attempts were made to solve the problem of the real nature of bond. There was a lack of experimental research results in this field. Little work was done with regard to the influence of the thickness of concrete cover and many of the published tests omitted reporting important data that might be used for continued investigations based on new hypotheses.

An analytical theory for bond was presented by Tepfers (1973), (1979), (1980), (1982). He proposed a solution for the propagation of cracks along anchored bars using a concrete ring model. A lower bound solution corresponding to the partly cracked elastic stage and an upper bound solution corresponding to the plastic stage were used to estimate the failure loads. The stress distribution along the lap length was analyzed with the modulus of slip theory for different bond stages. The final bond failure by splitting of the cover according to minimum stressed failure patterns was analyzed taking into account the bond stress distribution along the bars. The effect of confining reinforcement was discussed and theoretically treated. Methods for calculation of bond resistance in lap splices were proposed and compared with tests.

Copyright fib, all rights reserved. This PDF copy of fib Bulletin 10 is intended for use and/or distribution only by National Member Groups of fib.

8.2.13 Summing up

At that stage it may be said that bond was understood and quantified as a resistance mechanism with properties that depended on bar size, arrangement and surface configuration. Other aspects such as the geometry of the surrounding concrete, concrete strength and the sequence of cracking were also important. The first cracks to appear are those identified and illustrated by Goto (1971). When these cracks appear, bond forces become organized as radial splitting components. The radial forces from the bar apply an internal pressure on surrounding concrete "rings", which crack, where these are thinnest in the cover along the anchored bar. A redistribution of stress at that stage causes the pressure to be resisted by tensile stresses in the remaining uncracked concrete. Upon further load increase, the concrete splits off due to the internal bar pressure according to a minimum resistance ultimate failure crack pattern. This crack pattern is dependent on the concrete geometry and the location where the longitudinal crack along the bar has appeared. The surrounding reinforcement and external transverse pressure or tension can be introduced in the bond resistance of the minimum ultimate failure crack patterns. The bond stress distribution along the anchorage length and the resulting splitting cracks caused by bond should be considered when determining the magnitude of minimum bond resistance, Tepfers (1973).

8.2.14 Beginning of fracture mechanics

Hillerborg et.al. (1976) formulated stress-strain and stress-crack opening relations for concrete under uniaxial tension, which are relevant in FEM modeling of bond between reinforcing bars and concrete. This modelling approach has been followed by many researchers and relevant research is ongoing to date.

8.2.15 Investigations for code purposes

Tassios (1979) made a comprehensive and important follow up of bond research and interpreted the bond performance under seismic actions.

Rehm & Eligehausen (1974) investigated welded deformed bar meshes. These investigations completed earlier investigations regarding proper lapping of meshes and resolved the necessary number of crossbars for successful anchorage.

Orangun, Jirsa & Breen (1975) reevaluated the strength of anchored bars and proposed empirical formulae that formed the basis for the subsequent ACI design requirements for anchorage of deformed bars in concrete. This was a landmark study of bond and addressed the effects of cover, spacing and confinement, among other factors.

A theoretical and statistical approach was presented by Eligehausen (1979). He calculated the distribution of bond stresses and splitting forces along the splice length by numerically solving the differential equation of bond for splices using local bond stress-slip-laws. FEM was used to estimate the concrete stresses caused by splitting forces. By varying the geometrical model parameters and by comparing the tensile stresses in the maximum stressed section averaged over a length equal to 0,5 times the bar diameter with the concrete tensile strength the influence of the investigated parameters was found and expressed analytically by fitting curves. Equations were obtained for calculating the splice strength and were checked against 390 tests. As the coefficient of variation was only 14%, these results were mainly used to derive the Model Code 1990 clauses, Eligehausen (1980).

Copyright fib, all rights reserved. This PDF copy of fib Bulletin 10 is intended for use and/or distribution only by National Member Groups of fib.

A summary of the ACI and Model Code 90 philosophies as well as a commentary on the performance of code relationships in light of bond research is presented by Mc Cabe and Pantazopoulou (1998).

8.2.16 Conclusion

At this point the review of historical evolution of bond research has outlined the state of the art leading up to the previous CEB Bulletins d'Information No 151 (1982) and No 181 (1987). Here the reader is referred to the next phase in bond research as described in those bulletins prior to returning to the comprehensive presentation of latest developments given in the preceding chapters.

A conclusion from the historical information about the buildup of knowledge in the area of bond is that the necessary know-how for practice has always been produced for the available materials. When materials changed and the practice was provided with an increased spectrum of either new reinforcement products or materials with improved mechanical properties, additional tests were performed. Currently, extensive research is being performed, while the results cannot be introduced in the code clauses, because code users are not prepared to accept increased complexity in the design. The present ongoing sophisticated research gives results for the possible future codes whether those be a computerized medium based on fracture mechanics and including durability considerations and life time predictions, or whether they represent a turn in the prevalent design philosophy (e.g. displacement based seismic design).

8.3 Codes: Where do we stand?

The development of reinforced concrete into a reliable, economical structural system has in part been based on the development of design codes. These codes are typically national documents that are developed based on the expertise of the research community, designers, contractors and the code writing bodies themselves. The codes provide an implicit limit as to the level of design that has been collectively determined to be acceptable or safe. In this context, the level of design refers to the design loads and the induced moments, shears and structural deformation or rotation responses when subjected to these loads.

The basic fact is that whatever the form of the rules, strain compatibility between the reinforcing elements and the concrete must be maintained, so that the constituent parts act together as a composite. The designer has been charged with providing an environment in which the reinforcement can indeed be bonded - anchored - to the surrounding concrete in such as way that the strain compatibility between the concrete and steel can be maintained under all loading conditions. The task of the research community has been to provide information in the form of test data, equations and recommendations that the designer can follow to ensure that the conditions are right for the bond to be maintained. Code writing bodies, such as *fib* (CEB-FIP), ACI and the EN (European standards) among others have had the task of synthesizing these data and recommendations into a set of rules for designers to utilize in structural design.

Yet *perfect* bond is not achievable nor is always required. A case in point is unbonded prestressed concrete construction where bond to maintain strain compatibility is not required, but anchorage of the strands is. Other examples are headed reinforcing bars where much, if

Copyright fib, all rights reserved. This PDF copy of fib Bulletin 10 is intended for use and/or distribution only by National Member Groups of fib.

not all, of the anchorage is provided by the head, and bond via the deformations is not a critical aspect of the attachment. The point is that understanding of the fundamental mechanisms is needed and accurate rules are essential to provide the designer with the tools necessary to manage the bond required by *their* design.

The research community, code writing bodies and designers have provided essential expertise and information in the development of accurate design rules. In particular recent research results from around the world provide the basis for improved understanding of the effects on bond performance of critical parameters such as confinement, spacing, and material properties. Much of this work has been empirical in nature and the applicability of empirical design expressions in calculations is limited. More importantly newer forms of analysis now being employed including nonlinear finite element calculations and other sophisticated analysis requires more information as to how the bond failure proceeds than simply an upper limit.

In the world today there are many different code bodies in place. The CEB-FIP Model Code 90 represents one of the few multinational consensus codes that has been developed based on collective experience of designers and researchers throughout the world. The EuroCodes, a more recent development, also are multinational in nature, albeit European only, but still represent a large effort and many different points of view. There also are national design codes that represent a particular national opinion and philosophy. These include standards such as the German Industry Norm (DIN), the British Standards (BS), the Japanese Society of Civil Engineers (JSCE) code and the American Concrete Institute (ACI) among many others. These national codes may or may not take input from the CEB-FIP Model Code 90 or other codes but are intended to provide designers under their jurisdiction with a safe economical set of rules for the design of reinforced concrete structures. Thus it is realistic to say that the CEB-FIP Model Code 90 is prepared to be a more thorough and scientific form of building code than a national code since there are a wider variety of opinions represented in the CEB-FIP process.

The question arises as to how does bond and the anchorage of reinforcement fit into this code system? The answer is that there are similarities and differences of approach when one considers the philosophy that is present today versus the needs of the future.

The present design technology represented by most national building codes, such as the ACI 318 for example, have utilized a traditional capacity design approach where designing for bond was considered to be a question of providing adequate strength along the bar anchorage for development of the bar yield force. In earlier code versions, average values of the actual bond stresses were computed and compared against an allowable bond stress. Therefore, bond, as well as all other tension-failure controlled problems such as shear, were dealt with in design by establishing allowable stress limits for concrete, with stresses calculated from an admissible state of equilibrium without consideration of deformations.

These rules have matured in recent years to be generally capacity based calculations using Load and Resistance Factor Design (LRFD) concepts where actual bond stresses are not computed; rather the designer must compute an anchorage length required, typically to yield the bar, given the particular material and geometric properties of the anchorage. These empirical relations based on experimental data for bond strength attempted to describe the parametric dependence of bond strength on an array of important design variables. Yet the underlying assumption is still that the bond stresses are uniformly distributed along the bar. The result is typically *a yes or no* decision: is the anchorage sufficient to yield the bar under load? If not then the design is altered until an adequate anchorage necessary to yield the bar is provided.

Copyright fib, all rights reserved. This PDF copy of fib Bulletin 10 is intended for use and/or distribution only by National Member Groups of fib.

It must be said that in some cases, the designer is not intending to yield the bar, but rather to develop a specific force in the bar that is less than yield. Many codes, the Model Code included, allow designers to reduce the anchorage length required if the bar area provided is greater than that required. Thus, the designer has the option to adjust the anchorage length by increasing the bar area. In these cases the anchorage check is made to ascertain if the bar is anchored sufficiently to develop the force required by the design. However, it is instructive to note that in these situations that the designer adjusts the design by implicitly adjusting the bond stress, pointing again to the central importance on bond to the design and detailing of the structural system.

Note that whereas deformation (slip) was universally acknowledged by researchers in the reported tests that formed the basis of current design requirements for bond, no systematic attempt had been made to process the available information in a manner analogous to the efforts placed on the side of strength. The bar slippage under load is ignored and assumed not to occur in these anchorage calculations - there is no need to consider it since the bar is either anchored or not. However the *yes or no* rules indirectly consider slippage and cracking, so the designer is saved from having to deal with them in detail. However, this convenience removes from the designer the ability to control these parameters

One might conclude that these rules are simple in form requiring generally only a hand calculation. The rules found in typical national codes have to be general in nature and widely applicable because these must work in many different scenarios, they must be simple, easy to apply and relatively conservative and robust. Therefore, the sophistication of the rules is sacrificed for a readily applicable design framework that can be applied in a range of situations.

These straightforward anchorage-type calculations also are found in the MC90 where an LRFD-style calculation is provided for designers. As with the national codes, the designer applying the MC90 can compute the length required to potentially develop the yield strength of the bar-- or the design strength required-- and to produce similar results to those from other codes.

Therefore, at this point in time designers are computing anchorage lengths and evaluating the effects of material properties and geometry on these required lengths solely based on a set of hand calculations that provide only an assessment of the anchorage length. There is no information provided as to the actual load-deformation behavior of the anchorage under load. Moreover the design community has been generally satisfied with this approach. More complex rules and procedures are not desired in these national codes because the complexity requires more time to compute an anchorage length that may differ from current estimates only slightly.

The point must be made that code rules found in the Model Code and other national codes do incorporate rules that attempt to provide ductility under load. That is, the rules are such that designers are encouraged to provide transverse confining reinforcement, or additional cover, or both, that can greatly increase the robustness of the structural element. A minimum amount of transverse steel is required to ensure that the steel being developed, or spliced, is confined and able to maintain load capacity even under significant amounts of deformation response. This added degree of ductility may not provide any increase in load capacity, it simply adds more deformation capacity to the system. The designer, however, may or may not be aware of these aspects of the rules and the behavior that the code writers are attempting to ensure.

Copyright fib, all rights reserved. This PDF copy of fib Bulletin 10 is intended for use and/or distribution only by National Member Groups of fib.

However, there is emerging a significant need for a more sophisticated approach to the evaluation and design of anchorages. Economics and the need to evaluate complex problems where simple decisions as to adequacy of anchorage lengths are not enough are in part driving this evolution. Instead, the actual behavior under load is needed. Scenarios where this is the case include the evaluation of bond performance under loading and deformation demands from blast or earthquake loading. Here computer calculations typically are performed using Direct Stiffness or Finite Element Methods that permit the designer to view the structural behavior well into the nonlinear regime. Stress-strain rules for the constituent materials are required for this type of analysis to model the behavior through the range of linear and nonlinear response. Moreover some depiction of the load-slip relationship for a reinforcing bar anchored in concrete is needed since the assumption of perfect bond without any significant slippage under load is inconsistent with experimental results and produces analytical results that are not generally completely valid.

What is required to support this more complex evaluation of structural performance is the ability to actually model not only the constituent materials of the structural element but also the bond of the reinforcement to concrete. The CEB-FIP Model Code 90 already has a simplified bond model in place that shows how such a set of parameters could be formulated. Actual application of this model in practice is very limited if at all. However, the use of the various bond models reported elsewhere in this report clearly point towards the future needs that the *fib* will necessarily have to address in future Model Code editions. Providing designers with additional guidance for evaluating the bond processes that develop as the load increases will be required as will providing modeling tools to be used with the relevant computer software in order to perform this evaluation.

Moreover, the designer also may need to be aware of where the nonlinearity is occurring. Nonlinear behavior that is distributed along a deformed bar as the bar gradually moves relative to the surrounding concrete can have different consequences for a structure than nonlinearity that occurs locally in a concentrated region at a mechanical anchorage. The bond failure in an anchorage is potentially more significant than a bond failure along a portion of a deformed bar and must be addressed by the designer. The combination of load capacity and ductility may force the designer into limiting slip at anchorages and to adding transverse confinement to maintain the anchorage. In contrast in a deformed bar, the degree of bond and how the bar slips under load may become yet another design parameter to be set.

An additional consideration is the emergence of new performance-based design approaches that have refocused the problem of bond. At the heart of these approaches lie considerations about overall structural deformation demand and supply, which inevitably bring forth questions about the compatibility of deformations between concrete and the anchored bar throughout the various stages of response. For the design to meet performance requirements, it may no longer be adequate to simply assess the strength of a given anchorage without also knowing the levels of deformation that would have to develop in order for the given strength to be realized, and whether these deformations can develop in the structure without completely altering the assumed load path through redistribution of internal forces and moments. For this reason, code writing bodies which have already explicitly adopted performance-based design approaches, such as the CEB-FIP, require modeling of the complete load deformation envelope of the bond-slip response of a given anchorage as reference for design purposes.

Thus the role of the *fib* in the future will be to provide leadership as to how to address these new issues driven by evaluation of structural performance using computer software and by

Copyright fib, all rights reserved. This PDF copy of fib Bulletin 10 is intended for use and/or distribution only by National Member Groups of fib.

taking the structural performance well into the nonlinear regime. The future *fib* Model Codes also will be able to address not only the general case of "typical" anchorage problems but also a narrower more precise class of calculation than will the various national codes. Here the rules will be developed to reflect the latest research and practice developments and will be more complex - and more accurate - in nature providing the designer with an alternative to general rules.

The equally important role of future *fib* work will be to synthesize the various bond philosophies and viewpoints into a consistent set of guidelines that will enable the designer not only to evaluate an anchorage for its development capacity, but also to evaluate how the bar-concrete interface performs under load. Monotonic loading into the post yield regime, where significant member cracking and changes in material properties occur is evaluated today by designer with the aid of computer models. *fib* must take the lead in proposing robust bond models to support these needs of practice to enable accurate performance of such evaluation using state of the art information.

The situation is even more urgent in the case of cyclic loading. Earthquake performance of reinforced concrete structures is an international concern. The role of bond deterioration and bar slippage is central to the development of displacements and stiffness loss in members. Designers are faced with the question of how to analyze structures under these loadings and to capture the bar-concrete interface in such a way that is realistic. At the present time most design rules for earthquake resistance are empirically derived and though it is generally acknowledged that bond will deteriorate under cyclic load reversals, there is no consensus as to the proper modeling the bond loss. This is a critical need.

The possibility of *oversupply* of bond resistance has become recently an important consideration of performance-based design. In the past, it was generally assumed that improvements in bond through changes in the bar geometry itself or trough other factors, will only improve the performance of the structure. However, this is not supported by theory or experiment. If bond is improved beyond the ability of the member to sustain it, the mode of failure will change from pullout to splitting. In such circumstances there is too much pullout resistance for the member as detailed. To remedy this situation additional transverse reinforcement would be necessary in order to confine the bars and thereby increase the splitting bond capacity. This may mean additional cost that must be weighed against the gains in performance. It may indeed be the case that the additional bond is not needed and that the structural performance is acceptable if the bar slips, provided that the slippage is controlled and accounted for in the design. Thus the bar slippage may become yet another parameter that the designer can control and optimize based on the overall needs of the structure. However increased sophistication in design has to be met by improved precision in production process, so there is a need for balance in the development as well.

The role of future *fib* Model Codes as well as the various national codes will be to provide designers with the design limits that are needed to produce safe structures. At the same time there are emerging critical needs for a higher level of guidelines and rules to give the designer greater control of how the structure responds to load. These limits will be controlled through material properties, detailing, perhaps reinforcing bar geometries and other properties. *fib* has a central role in providing designers with these tools so that the developments in practice and the needs of the international community are met by these rules.

Copyright fib, all rights reserved. This PDF copy of fib Bulletin 10 is intended for use and/or distribution only by National Member Groups of fib.

8.4 Lessons from and benefits of bond research

8.4.1 Bond in general

In an extensive study of methods of test for bond conducted in 1970, Snowdon wrote that "Bond ... is an intrinsic property of the bar itself", (Snowdon 1970). A major proportion of research into bond since that time has been devoted to factors which disprove his statement, and the influence of splitting behaviour associated with bond of ribbed bars and the contribution of concrete cover and confining reinforcement to resist bursting forces is now widely recognised. In current Codes of Practice, parameters associated with geometry of the element may determine design bond strength as much as does bar type. Many factors besides the surface characteristics of the bar will determine the bond strength that can be developed, and Snowdon's statement would today be recognised as wholly invalid.

This section attempts to identify the positive benefits of research on bond models, what has been learnt about bond to date, and the issues that have yet to be resolved. It is hoped that this will help to indicate to the research community how best to ensure that their work makes a worthwhile contribution for the future. In attempting to summarise the lessons from history, we recognise the risk that our views may be regarded by the future generations as heretical as those of Snowdon appear now. Despite this, the Task Group felt it important to attempt to stand back from the detailed reviews presented earlier and to attempt a broad overview of the progress that has been achieved through bond research.

A review of this nature can only attempt to cover the major trends in the topic, and there is no doubt that others will be able to point to individual studies which do not conform to the general trends described here, or which have attempted to resolve some of the issues regarded here as unresolved. The Authors apologise to any researchers who feel their work should not share criticisms advanced in this section, and commend those who have questioned the conventional wisdom of their day, but point out that space is too limited to allow everyone's contribution to be cited - the place for that is in the preceding chapters of this report.

8.4.2 Bond in current practice

Bond is not a single phenomenon, but serves a range of structural functions in reinforced concrete. At the serviceability limit state, bond serves to control crack widths and deflection. At the ultimate limit state, strength of laps and anchorages depends on bond. In addition, bond characteristics of flexural reinforcement will influence rotation capacity of plastic hinges. Extreme reductions in bond stiffness would affect the composite interaction between reinforcement and concrete and negate the usual assumptions of plane section behaviour, but changes of this degree will lie outwith beyond the change in bond that will arise as a result of epoxy coating, and are not considered further here. The range of functions is summarised in Table 8.4.1. In most national Codes, only anchorage of reinforcement is explicitly dealt with in detailing calculations, other aspects of performance usually frequently being covered implicitly within deemed to satisfy rules.

Bond between reinforcement and concrete can be considered to be of importance in three aspects of structural performance:

1 Bond is used to anchor the ends of the bar.
2 Bond serves to transfer force into concrete under tension, reducing the average strain

Copyright fib, all rights reserved. This PDF copy of fib Bulletin 10 is intended for use and/or distribution only by National Member Groups of fib.

in flexural reinforcement and enhancing member stiffness.

3 Bond is used to maintain composite interaction between bar and concrete.

While these functions cannot be entirely separated, it is evident that function (1) will tend to occur at the ends of a bar while functions (2) and (3) will be developed away from the ends. It is clearly essential that function (1) is maintained throughout, as without it no stress can be developed in the bar and concrete becomes unreinforced. Provided function (1) is maintained, functions (2) and (3) might be allowed to degrade to some extent without impairing element strength.

Serviceability Limit State	*Ultimate Limit State*
Control of flexural cracking.	Anchorage of reinforcement.
Control of member deformations.	Control of hinge rotations in flexural members
	Maintenance of composite interaction

Table 8.4.1 Functions performed by bond in reinforced concrete.

For all practical (and most research) purposes, the conceptual model used for anchorage bond, and hence for all bond matters explicitly dealt with in most national Codes, bond is assumed to be a uniform shear stress over the nominal surface of an equivalent plane round bar. The principal result parameter is the maximum bond stress averaged over a length of bar sufficient to develop its design strength, although other parameters including bar/concrete slip and (less commonly) splitting crack opening also may be considered. This model is deficient in several ways. Firstly, bond stress (as so defined) varies along the bond length, being higher close to the ends. The variation is greater in long than in short bond lengths. Secondly, in ribbed bars the transfer of load between bar and concrete near ultimate is achieved principally through bearing of the ribs, not through shear on the bar surface. Concrete in the vicinity of the ribs is in a complex triaxial state of stress, and may be cracked radially and conically. Thirdly, bearing of the bar itself (or of welded transverse bars) may assist in anchorage through bends and hooks or through end bearing of bars in compression. The model is, however, simple, reasonably convenient and certainly widely understood, and is unlikely to be overtaken in a significant way in the foreseeable future.

Significant revisions to bond detailing rules in Codes of Practice for reinforced concrete were implemented in the 1980's. These revisions reflect the progress made in the preceding two decades in the understanding of the role of casting position and confinement to ribbed bars by cover and transverse reinforcement on anchorage and in the quantification of their effects. The revisions came about through a) a major conceptual shift in understanding of the mechanics of bond action of ribbed bars and failure mechanisms, and the appreciation that bond was not simply a function of bar type (and of concrete strength) as had been assumed earlier by Snowdon and others, and b) a sufficient body of test data on specimens that related fairly closely to practical situations. That work now enables laps and anchorages of

Copyright fib, all rights reserved. This PDF copy of fib Bulletin 10 is intended for use and/or distribution only by National Member Groups of fib.

current Standardised reinforcing materials to be detailed with confidence that the design strength of the bar can be developed and without undue convenience of excessive length. The revisions introduced into Code procedures a number of design parameters which designers had not previously had to consider, and hence were regarded as increasing the complexity of design.

The 1980's revisions to anchorage and splice length provisions were therefore agreed with some reluctance by practitioners. Anchorage and lap lengths exert only a minor influence on the economics of construction, and hence there is perceived to be little benefit in refinement of Code of Practice rules. Should excessive lap lengths prove to be a problem, for example, it is usually possible to replace laps with mechanical splices. The profession perceives little benefit from research dedicated to refinement of anchorage rules for new design using existing materials (although it must be pointed out that the profession held this view before the 1980's revisions as well), and is unlikely to support further research in this area. Given the current view that surface width of transverse cracks is of little relevance to durability, there seems little to be gained from refinement of detailing rules for crack control.

It is important to appreciate that the recent advances in Code detailing rules for laps and anchorages have come about principally through semi-empirical statistical analysis of large quantities of test data, rather than through analyses derived from fundamental understanding of material properties and structural mechanics. Only a qualitative understanding of the phenomena is necessary in order to set up appropriate expressions for this approach, but a considerable body of test data is required for derivation of statistical coefficients. While this approach requires a lesser depth of understanding than does a truly fundamental analysis, it can, with care, produce usable results for practice. One matter for concern is the number of different expressions which have been proposed to fit test data. Although there is a general consensus on the parameters which are to be included, the manner in which they are combined by different investigators varies considerably. With only a few exceptions, investigators have limited their attempts to develop best-fit expressions to data generated solely within their own investigation.

Another deficiency in this approach is that whenever a new reinforcing material is introduced, a completely new set of test data has to be generated before statistical techniques can be deployed. There may thus be some time lag between the introduction of new materials and the development of reliable detailing rules. Epoxy coated reinforcement provides a case in point. FBECR was introduced in the US in the 1970's, but early tests were confined to pullout specimens in which splitting modes of failure were unlikely. Curiously at the time, the ASTM specification for coating qualification allowed epoxy coated bars to be deemed to have adequate bond strength provided they achieved 80% of the bond strength of the equivalent non-coated bar. Specific rules for detailing structures with FBECR were not introduced in the ACI Building Code until 1987, although prior to this it was common practice to increase anchorage lengths by 25%. The rules introduced in 1987 required substantial increases in development and splice length of 20% or 50%, dependent on cover, but were based on a set of only 12 coated bar specimens, several of which did not conform to Standards for coating thickness. Many researchers now believe the penalties imposed on anchorage of FBECR in the ACI Building Code to be excessive, and the proposals presented in Chapter 5 of this Review, based on a substantially larger and more diverse set of tests, will provide a more reliable basis for design. Over 30 years will have elapsed since the introduction of FBECR before Code implementation of these rules can be achieved, however. The profession must ask why it took so long to introduce modifications to design rules when an inferior standard of performance could be deemed acceptable in a standard test.

Copyright fib, all rights reserved. This PDF copy of fib Bulletin 10 is intended for use and/or distribution only by National Member Groups of fib.

While a rigorous, comprehensive and more fundamental bond model might enable bond properties of new reinforcing materials to be predicted prior to their introduction into practice, the present generation of models are not sufficiently comprehensive for such an approach. Bond research has been essentially retroactive - it has been limited to simulation of behaviour of existing materials. Consequently, existing analytical models are of little use for the prediction of performance of new materials, although it is possible to adapt existing models to new materials by adjusting empirical coefficients. As will be discussed later, the majority of bond models have concentrated on splitting resistance of the concrete section, and are of little value, for example, in predicting the effect of a smooth epoxy coating on a bar.

Tentative attempts have been made to develop specialised forms of mild steel reinforcement. Although research has established that it would be feasible to produce altered forms of ribbed bars with shorter development and splice lengths, commercial production has been restrained by inertia to change in the profession, by lack of commercial benefits, and possibly because of concerns over adverse effects on rotation capacity of plastic hinges. Transverse cracking at the serviceability limit state is another area where bond exerts an influence on structural performance. Specialised bar geometries for enhancement of crack width control have been investigated, but not taken to commercial production. The present generation of bar geometries appears to be regarded as adequate by practitioners.

It will be evident from perusal of earlier chapters of this review that much research in bond in recent years has been spurred principally by the introduction of new materials and products such as HSC (Chapter 2), FBECR (Chapter 5), fibre composite reinforcing materials (Chapter 7) and headed bars. Corroded bars could almost be regarded as a new material, as it is only in recent years that the demands of structural assessment have led to the need to estimate the residual strength of deteriorating structures. The demand from practice is mainly for development of safe, reliable and simple rules for detailing of structural elements using these novel products with an approach and margins of safety consistent with those for established reinforcing materials - practice has little desire for a more fundamental understanding. This may alter to some degree if performance oriented design techniques become established. The present generation of detailing rules are intended to ensure that reinforcement is able to develop the design strength of the bar (which will not exceed a specified lower characteristic yield strength). Design philosophies under development may generate a requirement to model behaviour of anchorages as the bar goes beyond yield. Performance models for bond will have to be related to the functions set out earlier. Opinions are likely to vary as to the degree of refinement required for this purpose, and indeed on whether performance modeling is required for end anchorage. In reviewing bond, it was our view that it is preferable to have a comprehensive, if, to the taste of some, a somewhat crude representation of overall behaviour, rather than a model in which particular facets of behaviour are highly refined but others are ignored.

8.4.3 Bond research

The simplicity of the common conceptual model for bond of a uniform shear strength has already been mentioned. Bond is a highly complex phenomenon, influenced by many parameters. Researchers have therefore attempted to simplify the development of bond models through elimination of some aspects of the problem. Thus short bond lengths have become favoured by researchers to limit the variations in bond and bar/concrete slip along the bonded length, and to eliminate the zipper effect, where splitting develops first at the ends of anchorages or lapped splices where bond stresses are highest - even single rib tests

Copyright fib, all rights reserved. This PDF copy of fib Bulletin 10 is intended for use and/or distribution only by National Member Groups of fib.

were in vogue for a short time. Large covers have been used to avoid the need to consider splitting of the concrete surrounding the bar. Concentrically embedded bars have been used to so that axisymmetry can be used to facilitate modeling. The convenience of pullout tests has led to a bond test arrangement where reinforcement is in tension but concrete in compression, a condition that would be exceptional in practice. Even in tests on lapped joints, there has been a preference for testing tension splices (which can be placed away from points of maximum moment in continuous beams) over compression splices (which usually have to be positioned where moments are at a maximum). Numerical modeling also tends to have been split into two areas, one concerned with variations of bond and slip along the bar, the other with circumferential stresses and deformations around the bar.

Probably because of these simplifications, the topic of bond behaviour and strength has been bedeviled by a number of misunderstandings arising from too narrow an approach to the topic. Some examples:

A belief that heavily ribbed bars produce greater bursting forces developed in the 1970's as a result of tests on pullout specimens where bars were relatively highly confined by a thick cover. Splitting failures occurred more frequently in these tests when more heavily ribbed bars were used. Thus it was considered that more heavily ribbed bars produced more splitting, and hence that too heavy a rib pattern was a bad thing. Wider recognition of the importance of splitting led to tests being conducted with lower covers and confinement, and here more heavily ribbed bars were found to develop the same or higher bond stresses. It is now apparent that highly ribbed bars developed higher bursting forces because they developed higher bond strengths and not because the bars generated intrinsically higher splitting forces. The greater splitting with more highly ribbed bars was actually caused by the higher bond strengths of these bars.

Early analyses of bond strength in splitting failure modes treated the bursting stresses generated by bond as a hydraulic pressure. In this model the bursting forces generated by bond are considered to act as a uniform radial pressure equal in magnitude to the bond stress. This led to a belief that, for similar cover, confinement and bond length, a lapped splice would generate twice the splitting force in an equivalent single bar anchorage, and hence that the stress developed in the spliced bars would be half that of the single bar anchorage. Statistical analysis of test results has demonstrated that this is far from being the case: splices are variously estimated to develop between 80% and 100% of the strength of single bar anchorages.

These two examples illustrate how misconceptions can arise when research studies examine only a part of the overall problem of bond strength. The first of these two illustrations has now been understood, but conflicting explanations for the cause of the second have yet to be reconciled (Reynolds & Beeby 1982, Cairns, den Uijl 1996). The hydraulic pressure analogy is still fairly widely used in numerical modeling of the splitting resistance of concrete cover, despite having been discredited in the view of many, however.

Analysis of splitting bond failures is based on equating the bursting forces generated by bond action of a bar to the confinement provided by the surrounding concrete, confining reinforcement and lateral pressure. The limit state to be satisfied can be represented by Equation 8.1.

Bursting forces generated by bond action $\leq$
Confinement from surrounding cover, reinforcement etc. Eq. 8.1

Copyright fib, all rights reserved. This PDF copy of fib Bulletin 10 is intended for use and/or distribution only by National Member Groups of fib.

In a comprehensive treatment of splitting bond capacity, both sides of the inequality of Equation 8.1 would receive equal attention. Modeling effort tends to have concentrated on the right hand side, however, and it is fair to say that the great majority of work on splitting aspects of bond has been devoted to evaluation of the resistance to splitting of the concrete cover and sophisticated numerical analysis based on refined constitutive models for cracked concrete cover have been developed. Chapter 1 of this Review is written primarily from this standpoint. In contrast, the contribution of confining reinforcement and the magnitude of the bursting forces have received relatively little attention.

The statistical analyses on which Code rules are derived has treated the contribution of confining reinforcement as additional to that of the cover. It is evident, however, that stirrup strains will be small if cover remains uncracked, but that once the concrete has cracked then the contribution of the concrete will reduce sharply. The situation is analogous to Code treatments of shear strength, where the contribution of transverse reinforcement is added to that of the concrete despite the concrete having to crack before the stirrups can develop appreciable stress. However, a number of studies of the strength of anchored bars confined by cover and reinforcement have shown that bond strength is barely reduced if the tensile strength of the concrete cover is pre-split in some way. There are also conflicting views on the stress that will develop in confining reinforcement at peak bond stress. Several researchers have expressed the opinion that stirrups will develop a stress of around 80MPa, while others believe that stirrups will be stressed beyond yield. Given these different views and the fact that laps and anchorages are invariably confined by stirrups in members of structural significance, it is surprising the confinement provided by transverse bars has not received more attention.

8.4.4 Methods of bond test

Most major reinforcement Standards / Codes of Practice for Design include specifications on how to conduct a bond test. Many of these test methods were designed over 30 years ago. Understanding of the bond phenomenon has altered markedly since that time. The importance of splitting failures in practical details is now widely recognised, but many Standard bond tests were developed at a time when bond was seen principally as a property of the reinforcement. Splitting was regarded (by the steel producers involved in the drafting of these standards) as an inconvenient side effect of the higher bond strength ribbed bars, and many of the various bond test specifications thus included heavy confining reinforcement to obviate this problem. That bond strengths measured in such tests are much greater than attainable in practice where a splitting mode of failure occurs was never in doubt. However, the fact that any comparison between bond strength of different bars is invalidated by the difference between a pullout and a splitting mode of failure has taken many years to be recognised. With the advent of European Codes, there is an opportunity to re-define the purpose of bond tests and the measures of performance required, and to develop an up to date bond test specification.

The principal choices in bond tests are between short and long bonded lengths, between specimens with high confinement in which failure occurs by pullout and those with lesser confinement where a splitting failure mode results, and between anchorage (bar loaded at one end only) and transfer type (same load applied at both ends of bar). In addition tests on bond may be carried out within structural elements representative of normal construction practice.

Copyright fib, all rights reserved. This PDF copy of fib Bulletin 10 is intended for use and/or distribution only by National Member Groups of fib.

- Short specimens are smaller and more convenient to test, and provide upper bound values for bond strength. They are thus preferred by reinforcement manufacturers, whose see their product shown in the best light. On the other hand, boundary effects will be more significant than for long bond lengths, and it is only through use of long bond test regions that it is possible to see how the bond process really works when significant strains develop. There is now an appreciation that for deformation based design we really need information on behaviour of the bond region when bar strains go beyond yield. This is a new area to be checked and scaled up results from short specimens are not adequate. Tests on long anchorage lengths are thus essential for the development of practical design guidance, which should be the long term goal of all research studies.

- Different failure mechanisms occur in confined and unconfined tests. Bond strengths are lower for splitting failures, which therefore tend to be more critical for design. Confined tests provide the highest strength results, but failure occurs in a pullout mode. Because of the different failure modes, it is unwise to use even a comparative evaluation of unconfined bond strength from pullout test results.

- Anchorage tests provide a measure of the ability of bond to develop the stress in the bar, and hence tend to be relevant to laps and anchorages at the ultimate limit state. Transfer tests, on the other hand, provide a measure of the ability of the bar to control cracking and overall deformations, and are relevant to serviceability behaviour under working loads and post yield. Pullout test specimens are widely used in the assessment of anchorage bond performance. There are, however, several objections to the form of such tests, particularly where ribbed bars are concerned. The two principal objections are firstly, that loading of the bar places concrete in compression and the bar in tension, a situation that will rarely be encountered in practical circumstances. The absence of transverse cracking affects the average bond stress which can be developed, and the type of cracking illustrated by Goto's tests is suppressed. Secondly, standard pullout tests are frequently associated with high confinement. Friction at the bearing end of the pullout specimen also resists bursting forces locally. All these objections may be overcome by eccentric pullout specimens. The reasons for the widespread adoption of pullout type specimens lies principally in their being economical to manufacture and test, and because they clearly represent the concept of anchoring a bar.

In the future we will require more comprehensive measures of bond performance, as a single strength result will clearly be inadequate. However, even a complete bond/slip record obtained under specific test conditions would be of little value without an understanding of how to interpret it in relation to the various bond functions described earlier - there is a need to explore correlations between bond performance in convenient standardised tests and structural performance in components representative of practical situations - unfortunately, there appears to be little information available on this topic. It will be necessary to decide the purpose of the test, for example whether bond testing is to be conducted as a comparative measure of the performance of different bar types, in order to generate data for numerical modeling, or for some other purpose. It will also be necessary to decide which of the various bond functions are to be addressed. A major question to be

Copyright fib, all rights reserved. This PDF copy of fib Bulletin 10 is intended for use and/or distribution only by National Member Groups of fib.

resolved is whether a range of measures in a single standard test specimen can provide the necessary information, or whether a separate test will be required to measure aspects of bond performance related to each performance function. One appraisal of bond test methods suggested that even the Standard RILEM pullout test could be useful for comparative evaluation of bar performance relevant to a range of functions, with crack control performance assessed through a correlation with bond stress at a free end slip of 0.01mm, bond strength in a splitting failure mode assessed through a correlation with bond stress at a free end slip of 0.1mm, and pullout strength of ribbed bars assessed through a correlation with bond stress at a free end slip of 1.0mm (Cairns and Abdullah 1995). For the time being, standard bond tests must be considered of limited value, and any new reinforcing materials need to be tested for bond performance in structural elements under conditions representative of practice. It is essential that approval organisations be made aware of this in order that sound design guidance be provided when a new material is introduced into practice, and not, as with FBECR, nearly 30 years later.

The need for more comprehensive measures of bond performance is implicitly recognised by the research community, as demonstrated by the wide variety of testing arrangements reviewed in earlier sections. It is, however, this diversity which itself makes comparisons between various studies so difficult. While many would (rightly) decry the idea of a single test measure for bond, the present situation in which each new investigation produces a variant on existing test methods is equally to be deplored.

8.4.5 Developments in analysis and modeling

Models seek to describe physical behaviour, usually in a mathematical form. Models of bond may act at various levels, Chapter 1.1.8. A variety of forms of model have been proposed and are discussed in detail in Chapter 1. Models vary in level at which they approach the topic, in their scope and in their degree of refinement. Models themselves may be formulated in various ways and for different purposes:

- To concisely describe a set of individual results.
- To simulate part of a physical phenomenon.
- To build a means of predicting behaviour of a system based on the characteristics of its components (characteristics of the components may themselves be modeled in any of these three ways)

The overall research trend during the period covered by this review has been towards micro-level models based on constitutive formulations of material behaviour and away from the macro-level models from which Code rules are derived. As discussed earlier, Code design rules are simplified versions of the first type of model, based on a statistically derived description of sets of physical test data, with the parameters for inclusion selected from a conceptual understanding of the problem and from inspection of test data. Such models are only loosely based on an understanding of the physical phenomena being modeled, and should not be extrapolated beyond the limits of experience. The models do not explain the phenomena, although they may assist in interpretation of data.

Finite element (FE) modeling techniques have greatly extended our ability to formulate models of physical phenomena associated with bond, and now eclipse more traditional mathematical approaches. FE models may fit into either of the latter two model formulations. Bond stress-slip models, for example, allow simulations of bar displacements to be carried out and estimates of bond stress distribution to be obtained. Such models have

Copyright fib, all rights reserved. This PDF copy of fib Bulletin 10 is intended for use and/or distribution only by National Member Groups of fib.

been based on empirically derived best-fit coefficients to test data, however. A similar situation holds with models for tension stiffening.

The third class of models are derived from more fundamental representations of materials behaviour. The contribution of concrete cover to splitting resistance can be analysed using more fundamental constitutive formulations for stress-strain relationships, and a major part of the effort in modeling of bond has been devoted to the evaluation of the tension field in the concrete around a bar. The work recognises that concrete in tension contributes greatly to bond (as well as other facets of structural strength including shear), contrary to assumptions frequently made with regard to behaviour at the ultimate limit state in Design Codes. The finite element method has become the major tool in this aspect of modeling.

However, and as stated earlier in the context of testing, major simplifications have been introduced into simulations and to more fundamental analyses in order to examine particular aspects of behaviour, but always with corresponding loss of generality. Many modeling studies have been limited to 2-dimensional analyses of particular aspects of bond phenomena, and thus ignore other important facets of behaviour. For example 2-D models of stress-slip variation along a bar do not consider formation of radial cracking around the bar, and 2-D models of a section perpendicular to the bar axis to model splitting resistance ignore the variations that occur along the anchorage length. A smeared cracking representation is commonly used, although splitting bond failure occurs through development of discrete cracks - the inner softening band approach (ISB) appears to offer advantages here. The hydraulic pressure analogy is commonly used to represent the radial pressures exerted by bond, despite evidence that it is inaccurate. Consequently models developed to investigate one specific aspect of bond have not been adequate for the analysis of other aspects. The restricted scope of existing models means that they cannot predict differences between bond of ordinary black bars and that of epoxy coated bars or of non-metallic reinforcement, for example. Where attempts have been made to predict behaviour in novel circumstances (see Chapter 4 on effects of corrosion) models have generally been unsuccessful.

The FE modeling work that has been carried out to date appears to have been largely retrospective, i.e. numerical investigations have attempted to simulate observed test behaviour rather than to predict effects of innovations. Most models attempt to refine representation of behaviour which is already conceptually well understood. A major item of concern is that models are proposed without indication of their limitations. A model which gives good agreement with one set of test results is frequently hopelessly inaccurate when applied to a different set. The impact of such bond models on practical construction has therefore been negligible so far.

8.4.6 Design Philosophies

Current Code guidance for detailing of anchorage and lap lengths is based on the assumption that the anchored bar must be able to develop its full design strength, i.e. its characteristic yield strength reduced by the appropriate partial safety factor, taken as 1.15 in MC90. The anchorage or lap length is then increased by a factor to provide a margin of safety. The approach requires that an adequate margin of safety be provided such that the reinforcement can attain a specified design stress which is less than the yield strength of the bar.

Displacement based design methodologies are currently under development. This approach requires knowledge on the behaviour of the structure through to collapse, when

Copyright fib, all rights reserved. This PDF copy of fib Bulletin 10 is intended for use and/or distribution only by National Member Groups of fib.

reinforcement will be strained above yield. This approach is of particular relevance to seismic design and to robustness, both of which require the provision of adequate post yield structural deformability.

The great majority of even long anchorage or lapped joint tests have been designed to ensure that failure will occur in bond prior to yielding of reinforcement. These tests have provided an adequate body of data from which empirical sets of rules can be derived for the current design methodology. They will not be adequate for displacement based methodologies, however.

The ductility of bond resistance is strongly dependent on the joint detail considered. Available data on anchorages and lapped joints confined by minimum shear links shows that sudden rupture may occur when the slip at the unstressed end of the bonded length is small (<0.1mm). A more ductile response may be obtained in other locations, for example where beam reinforcement is anchored within a column. In the first case, acceptable free end slip will be so small as to be treated as zero for design purposes. In the latter, free end slip of a few millimeters might be acceptable. However, it is more likely to be slip behaviour at the loaded end of the anchorage, particularly once bar strains exceed yield, which will influence structural behaviour. (Note that a post yield zone might be considered to lie outwith the 'anchorage length' according to its traditional definition as the length required to develop the yield force in the bar). To exploit such aspects of behaviour a move away from traditional bond force concepts towards that of a development length to attain a specified deformation related performance, expressed either in strain or in force terms but also in robustness, will have to be developed.

It seems likely that good detailing practice will continue to lead to anchorages and laps being positioned away from points where large inelastic deformations are required. If this is so, the main requirement for bond models in displacement based design is likely to lie away from ends of anchorages, and to be more concerned with tension stiffening effects, particularly post-yield behaviour in the vicinity of hinge locations. The preceding review on modeling suggests there is some way to go before developing fundamental FE models for this purpose. A change in emphasis in testing from anchorage type towards transfer type bond tests also appears likely.

8.5 Current Needs and Future Directions

From the foregoing discussion it is evident that the CEB-FIP Model Code 90 as well as the EuroCode and other national codes provide a comprehensive set of straightforward rules that govern the design of reinforced concrete structural systems. These rules typically require hand calculations for anchorages and define the required anchorage lengths for development of the ultimate bar force. The objective of this requirement is to ensure that given the detailing and the specific section geometry, the engagement of the bar deformations in concrete is sufficient to anchor the bar when it develops its full force capacity.

In determining the anchorage status the basic question is stated in the form of empirical equations developed over the years from experimental studies of bond. Whereas the equations are simple, the behavior certainly is not. More importantly the equations give the sense that the reinforcing bars truly are anchored in every sense of the word so that there is no movement of the bar under load. Though the concept of a perfectly bonded bar in concrete is convenient in design, it is not representative of the true behavior. As the load increases bond-slip occurs,

Copyright fib, all rights reserved. This PDF copy of fib Bulletin 10 is intended for use and/or distribution only by National Member Groups of fib.

which may become large enough to push the bar deformations (ribs) into the surrounding material causing dilation of concrete and a resulting tensile stress field. If the slippage continues then at some point fracture initiates as a result of stress concentration near the first loaded rib. The fracture energy is released instantaneously (brittle response) whereas the fracture surface grows through the thickness and along the bar. The splitting crack develops along a minimum energy path in concrete, from the bar surface to the nearest free surface of concrete, through the cover.

* Thus, the checks that are made by the designer using anchorage code equations are an effort to preclude large enough bond slippage to cause a splitting fracture of the cover over the reinforcement. The code equations are an attempt to deter this slippage by providing a long enough bar embedment, or large enough confinement through cover or transverse steel. Experience has shown that these equations generally lead to reasonable designs and that a correct assessment of the state of stress of the bars is being developed. However, several issues are becoming increasingly important and include the following.

* The data that were used in deriving these equations were obtained from specimens of low to moderate strength concrete whereas high strength concrete is more widely used today. Bond in high strength concrete has been shown to be quite different in that less redistribution of load occurs in that case from one deformation (rib) to another. The result is less ductile bond performance and a greater tendency to "unzip" the bar from the concrete as the bond failure begins.

* Many new reinforcing systems are becoming important such as welded wire, high strength bars, headed bars; all these products behave differently from the classical deformed bars with well defined 350-600 MPa yield strengths that were used in the past for much of the supporting experimental work.

* Nonmetallic reinforcements are being used worldwide and are poised to become significant alternatives to traditional metallic reinforcement. These new materials will require new experimental data to help develop and calibrate bond models to depict their bonding behavior under load.

* The existing equations are truly only applicable when designing new structures under conventional loads. The checks provided by the code equations may not be sufficient in assessing existing structures that have been significantly modified for some new use or subjected to an unforeseen overload such as from accidental damage, blast or earthquake.

* Application of the Finite Element Method (FEM) or other computer-based structural models to assess how systems behave under load can provide essential information as to how the system respond to and redistributes load. The modeling of the nonlinearity that occurs as yielding of the steel and cracking of the concrete occurs is the key feature of the analysis. It is apparent that nonlinear FEM may be the best practical alternative when evaluating structures that have been overloaded, or loaded in a manner unforeseen in the original design. However, a great deal of additional work is needed to provide straightforward, practical tools for use by designers.

* The slippage of the bar relative to the concrete as it is loaded is generally not provided by building codes today even though it is well known that bar slip is an important phenomenon in generating member rotations and displacements as well as damage to

Copyright fib, all rights reserved. This PDF copy of fib Bulletin 10 is intended for use and/or distribution only by National Member Groups of fib.

members. Moreover, the assumption of perfect bond, in essence the lack of a bond model, produces unconservative results.

* The environmental influence on bond in the form of corrosion and other degradation effects becomes an important issue. Attempts should be made to formulate code requirements and develop a design process for control of deteriorating bond and anchoring resistance.

As can be seen there are several significant issues in this brief list that belie the fact that we have at best a basic understanding of the bond of reinforcement in concrete but are still seeking how best capture the behavior for design. While the simple anchorage equations appear to work well within the range of parameters that govern them, the more complex question of the load - displacement is still open. A major problem is lack of consensus of how exactly to model bond. As can be seen in earlier chapters of this report there are many bond models that are capable of providing good results within limits. In some cases the model must be calibrated against experimental data and essentially tuned to produce good results. While this approach may be an acceptable step in the process of developing new modeling techniques, it is not proper for design or in the evaluation of structural performance where, in theory, there is a single correct answer for any particular situation.

One particular example is the assessment of structural performance using nonlinear FEM. Future application of the various finite element codes that are available will depend in part on removing much of the guesswork that exists at the present time in modeling of bond. This particular need is one that can be filled by organizations like *fib* and national organizations. There is a clear need for guidance developed from a consensus process and for clear concise modeling rules for bond. The need will increase as more structural engineers turn to nonlinear analysis methods to determine the adequacy of members and structures under load. At the present time, designers may choose between utilizing the present CEB-FIP Model Code 90 bond model which is over a decade old and developing case-specific models consistent with their own interpretation of the literature. Those using national codes will find no guidance on modeling. For example ACI provides no guidelines for bond modeling in the Building Code and will find only passing reference to the concept in the various reports of ACI Committee 408 on bond.

Another issue that must be addressed is the fact that most bond testing is conducted at stress levels that are well below the yield stress of the reinforcing bar so as to obtain reliable bar load values that are not as readily obtained in the post yield regime. However, the designer may be working at the yield level and perhaps at even higher loads. Thus the question can be raised as to how well these low stress bond relationship can be extrapolated significantly higher strains. This question becomes even more important when high strength steels or nonmetallic reinforcement is used resulting in significantly higher bond stresses than the data may support.

The possibility of oversupply of bond resistance has become recently an important consideration of performance based design. While it has long been thought that increases in bond are always good, there may in fact be a case for optimizing bond along with the other properties of the design. Studies in Europe and in the US regarding reinforcing bar geometries and the bar deformations suggest that there may in fact be ways to increase, or decrease, the bond performance. However, changes in the bond may result in changes in splitting forces within the section or other deleterious results.

With regards to the performance of plastic hinges, it has been suggested that increases in

Copyright fib, all rights reserved. This PDF copy of fib Bulletin 10 is intended for use and/or distribution only by National Member Groups of fib.

bond may lead to decreases in plastic hinge rotation (referred to in the literature as rotational capacity). Load redistribution in structures subjected to severe excitations occurs because of ductile performance of those hinges. Thus, any loss of ductility resulting from increases in bond may be counterproductive and may lead to premature failure. This topic is in need of systematic investigation, because of the many types of reinforcing steels and non-metallic *FRP* bars available. Existing data is not sufficient to determine whether with North American and European steels there is a potential upper limit to the bond that is advisable with all steels or if a limit exists for only certain types of steels, if at all.

The conclusion is that we are moving into a new era of practice. There are many new tools for the design and construction of structures including new materials such as high strength concrete and new types of reinforcing systems, both of which may be outside the bounds of the data used to develop the existing bond relationships. Moreover, new analysis tools principally include computer-based methods. While linear elastic models used to determine behavior under normal loads may continue to represent the vast majority of applications, it will become more and more commonplace for practicing engineers to rely on nonlinear methods for assessing structural behavior. A key ingredient will be the accurate modeling of all aspects of structural response, including bond and slippage under load. It is incumbent on the code writing organizations including *fib* to provide a unified consensus approach for bond modeling in these applications to ensure accuracy and safety in the analysis.

The question can be asked whether any form of bond modeling in large scale analysis is practical for design. At this time, the practicality is limited to those situations where detailed determination of post yield behavior is needed. Also, the practicality is limited by the analysis platform that the model is analyzed on as well as the software. Certainly, using analytical bond models in structural design is not a practical alternative for typical applications. However through ongoing research, it is likely that the application of bond models to performance determination will become a reasonable alternative for designers even for typical structures. The future will no doubt include design and analysis software that will enable designers to predict accurately bond stresses and bar- slip in an easy and straightforward manner.

8.6 References

1909 Bach C., Graf O.: Versuche mit Eisenbetonbalken namentlich zur Bestimmung des Gleitwiederstandes. (Tests with reinforced concrete beams namely for determination of slip resistance). Deutscher Aussuss für Eisenbeton, Heft 1-3 , Berlin 1909.

1910 Bach C., Graf O.: Versuche mit Eisenbetonbalken namentlich zur Bestimmung des Gleitwiederstandes. (Tests with reinforced concrete beams namely for determination of slip resistance). Deutscher Aussuss für Eisenbeton, Heft 4, Berlin 1910.

1911 Bach C., Graf O.: Versuche mit Eisenbeton-Balken zur bestimmung des Einflusses der Hakenform der Eiseneinlagen. (Tests with reinforced concrete beams for determination of the influences of the form of reinforcement hooks). Deutscher Aussuss für Eisenbeton, Heft 9 , Berlin 1911. p. 86.

- Bach C., Graf O.: Versuche mit Eisenbeton-Balken zur ermittlung der Widerstandsfähigheit Verschidener Bewehrung gegen Schubkräfte. (Tests with reinforced concrete beams for estimation of the resistance of different shear reinforcements). Deutscher Aussuss für Eisenbeton, Heft 12 , Berlin 1911.

1912 Scheit H., Wawrziniok O.: Versuche mit Eisenbeton Balken zur Ermittlung der Widerstandsfähigkeit von Stossverbindungen der Eiseneinlagen. (Tests with reinforced concrete beams to determine the lap strength). Deutscher Ausschuss für Eisenbeton. Heft 14, p. 54. Berlin 1912.

1913 Abrams Duff A.: Tests of bond between concrete and steel. University of Illinois, Engineering Experiment Station, Bulletin No 71, p. 238. Urbana 1913.

Copyright fib, all rights reserved. This PDF copy of fib Bulletin 10 is intended for use and/or distribution only by National Member Groups of fib.

1917 Scheit H., Wawrziniok O., Amos H.: Versuche mit Eisenbetonbalken zur Ermittlung der Widerstandsfähigkeit von Stossverbindungen der Eiseneinlagen (Ergänzungsversuche). (Tests with reinforced concrete beams to determine the lap strength. Completing tests). Deutscher Ausschuss für Eisenbeton, p. 24. Berlin 1917.

1924 Bleich Fr.: Theorie und Berechnung der Eisernen Brucken. (Theory and design of steel bridges). Verlag von Julius Springer, pp. 306-314, Berlin 1924

1925 Lucan E.: Eine neue Stossdeckung fur Bewehrungseisen. (New type of overlap for reinforcement). Beton und Eisen. Heft 11, pp. 174-176, Berlin 1925.

1926 Rausch E.: Maschinenfundamente. Der Bauingenieur, Heft 45, pp. 877-883. Berlin 1926.

1937 Forssell C.: Skarvning och förankring av armeringsjärn. (Splicing and anchoring of reinforcing bars). Betong, pp. 32-78. Stockholm 1937.

- Wernisch G R.: Bond Studies of Different Types of Reinforcing Bars. ACI-Journal, pp. 145-164. Detroit 1937.

1938 Gilkey H J., Chamberlin S J., Beal R W.: The Bond between Concrete and Steel. ACI-Journal, pp. 1-20. Detroit 1938.

1939 Graf O., Brenner E., 1939. Versuche zur Ermittlung des Gleitwiderstandes von Eiseneinlagen im Beton bei stetig steigender und oftmals wiederholter Belastung. (Tests for determination of the slip resistance of reinforcement in concrete at steady rising and often repeated load). Deutscher Ausschuss für Eisenbeton, Heft 93, p. 28, Berlin 1939.

- Hoyer E., Friedrich E.: Beitrag zur Frage der Haftspannung in Eisenbetonbauteilen. (Contribution to the question of bond in concrete elements). Beton und Eisen, pp. 107-110. Berlin 1939.

- Landberg E.: Svetsning av armeringsjärn. (Welding of reinforcing bars). Betong, pp. 189-202. Stockholm 1939.

1941 Tengvik N.: Jämförande undersökningar av s.k. kamjärn och rundjärn av högvärdigt stål. (Comparing tests of deformed and plain bars of high strength steel). Betong, pp. 285-303. Stockholm 1941.

1942 Tengvik N.: Skarvning av armeringsjärn av högvärdigt stål. (Splicing of reinforcement of high strength steel). Betong, pp. 301-308. Stockholm 1942.

1944 Blankenburg C H.: Undersökning av skarvar med armeringsjärn av ST 52. (Investigation of splices od ST52 reinforcement). Betong, pp. 179-189. Stockholm 1944.

1945 Kluge R W., Tuma Ed. C.: Lapped Bar Splices in Concrete Beams. ACI-Journal, pp. 13-33. Detroit 1945.

- Muhlenbruch C. W.: The Effect of Repeated Loading on the Bond Strength of Concrete. Proceedings ASTM, pp. 824-845.

1946 Clark A. P.: Comparative Bond Efficiency of Deformed Concrete Reinforcing Bars. ACI-Journal, pp. 381-400. Detroit 1946.

1947 Watstein D.: Distribution of Bond Stress in Concrete Pull-Out Specimens. ACI-Journal, pp. 1041-1052. Detroit 1947.

1948 Muhlenbruch C W.: The Effect of Repeated Loading on the Bond Strength of Concrete – II. Proceedings ASTM, pp. 977-985. 1948.

- Örbom B.: Högvärdigt stål som armering i betongbalkar. Förankring, skarvning, sprickbildning. (high strength steel as reinforcement in concrete. Anchorage, splicing, cracking). Betong, pp. 75-120. Stockholm 1948.

1949 Clark A. P.: Bond of Concrete Reinforcing Bars. ACI-Journal, pp. 161-183. Detroit 1949.

- Granholm Hj.: Om sammansatta balkar och pelare med särskild hänsyn till spikade träkonstruktioner. (About laminated beams and columns with special aspect to nailed wooden structures). Chalmers Tekniska Högskolas Handlingar No. 88, p. 214. Göteborg 1949.

1950 Hognestad E., Siess C. P.: Effect of Entrained Air on Bond between Concrete and Reinforcing Steel. ACI-Journal, pp. 649-667. Detroit 1950.

- Reese R. C.: New-Style Deformed Reinforcing Bars. ACI-Journal, pp. 681-688. Detroit 1950.

- Report of ACI-Committee 208 on Bond Stress, 1950. ACI-Journal, pp. 677-678. Detroit 1950.

1951 Osterman J.: Utdragsprovet. (Pull-out test). Betong, pp. 1-8. Stockholm 1951.

Proposed Revisions to Manual of Standard Practice for Detailing Reinforced Concrete Structures (ACI 315-48). ACI-Journal, pp. 349-351. Detroit 1951.

1952 Swida W.: Zum Problem der Haftspannungen. (About bond problem). Beton- und Stahlbetonbau, pp. 293-294. Berlin 1952.

1952 Bernander K-G.: Vidhäftningens beroende av kamarea och kamavstånd hos armeringsstål. (The dependence of bond of lug area and lug distance for reinforcing bars). Betong, pp. 1- 17. Stockholm 1952.

Copyright fib, all rights reserved. This PDF copy of fib Bulletin 10 is intended for use and/or distribution only by National Member Groups of fib.

1952 Chamberlin S. J.: Spacing of Spliced Bars in Tension Pull-Out Specimens. ACI-Journal, pp. 261-274. Detroit 1952.

1953 Andersson S. E.: Spänningsfördelning mellan armering och betong vid plant spänningstillstånd. (Stress distribution between reinforcement and concrete at plain stresses). Betong, pp. 111-118. Stockholm 1953.

1954 Ferguson P. M., Turpin R. D., Thompson J. N.: Minimum Bar Spacing as a Function of Bond and Shear Strength. ACI-Journal, pp. 869-887. Detroit 1954.

1955 Bernander K-G.: Något om samverkan mellan högvärdig armering och betong. (Something about cooperation between high strength reinforcement and concrete). Chalmers University of Technology, Department of Building Technology, p. 167. Göteborg 1955.

- Chinn J., Ferguson P. M., Thompson J. N.: Lapped Splices in Reinforced Concrete Beams. ACI-Journal, pp. 201-213. Detroit 1955.

1956 Paettie K. R., Pope J. A.: Effect of Age of Concrete on Bond Resistance. ACI-Journal, pp. 661-6y72. Detroit 1956.

- Teske K.: Geschweisste Bewehrungsstösse. (Welded reinforcement splices). Beton- und Stahlbetonbau, pp. 246-248. Berlin 1956.

1957 Brede Ch.: Schweissen von Torstahl, Betonstahl IIIb. (Welding of Tor-steel, Concrete steel IIIb). Beton- und Stahlbetonbau, pp. 182-187. Berlin 1957.

- Efsen A.: Spiral Socket Splices for Deformed Bars. Laboratoriet for Bygningsteknik, Danmarks Tekniske Höjskole, Meddelelse Nr. 8, p. 13. Köbenhavn 1957.

1958 Chang T. S., Kesler C. E.: Fatigue Behaviour of Reinforced Concrete Beams. ACI-Journal, pp. 245-254. Detroit 1958.

- Efsen A.: Adhaesionsevnen for armeringsjern med overflade deformation. (Bonded surface of reinforcing bars with surface deformations). Nordisk Betong, pp. 321-324. Stockholm 1958.

- Granholm Hj.: Sprickbildning i armerad betong. (Cracking in reinforced concrete). Kompendium. Chalmers University of Technology, Department of Building Technolgy, p. 28. Göteborg 1958.

- Mc Call J. T.: Probability of Fatigue Failure of Plain Concrete. ACI-Journal, pp. 233-240.Detroit 1958.

- Murdock J. W., Kesler C. E.: Effect of Range of Stress on Fatigue Strength of Plain Concrete Beams. ACI-Journal, pp. 221-231. Detroit 1958.

- Nordby G. M.: Fatigue of Concrete – A Review of Research. ACI-Journal, pp. 191-219. Detroit 1958.

- Stelson T. E., Cernica J. N.: Fatigue Properties of Concrete Beams. ACI-Journal, pp. 255-259. Detroit 1958.

1959 Mavis F. T., Stewart J. J.: Further Tests of Dynamically Loaded Beams. ACI-Journal, pp. 1215-1223. Detroit 1959.

1960 Cederwall K.: Försök med armeringsnät av slät och profilerad tråd. (Tests with reinforcing meshes of plain and indented bars). Chalmers University of Technology, Department of Building Technolgy, No 198. Göteborg, 1960.

- Eriksson O.: The Sleeve Method of Splicing Reinforcing Bars. Ingeniören - International Edition. Volume 4. pp. 136-147. Copenhagen 1960.

- Forssell C.: Skarvning av HJS 70 med Forssell-ringar. (Splicing of HJS 70 with Forsell rings). Nordisk Betong, pp. 47-50. Stockholm 1960.

- Rehm G.: Beitrag zur Frage der Ermüdungsfestigkeit von Bewehrungsstählen. (Contribution to the question of fatigue strength of reinforcing bars). Sixth Congress of the IABSE, Final Report, pp. 35-46. Stockholm 1960.

1961 Rehm G.: Ueber die Grundlagen des Verbundes zwischen Stahl und Beton. (About the fundaments of bond between steel and concrete). Deutscher Ausschuss für Stahlbeton. Heft 138, Berlin 1961. p. 59.

1962 Ferguson P. M., Thompson J. N.: Development Length of High Strength Reinforcing Bars in Bond. ACI-Journal, pp. 887-922. Detroit 1962.

- Gaede K.: Versuche über die Festigkeit und die Verformung von Beton bei Druck-Schwell-Beanspruchung. (Tests of concrete strength and deformation at compressive fatigue loading). Deutscher Ausschuss für Stahlbeton, Heft 144, p. 48. Berlin 1962.

- Hansen R. J., Liepins A. A.: Behaviour of Bond Under Dynamic Loading. ACI-Journal, pp. 563-582. Detroit 1962.

- Losberg A.: Sprickbildning i kontinuerliga betongbeläggningar och andra betongkonstruktioner, låsta mot rörelser av temperatur och krympning. (Cracks in continuous concrete road slabs and other concrete structures locked against movements from temperature and shrinkage). Chalmers University of Technology, Department of Building Technology, No 607, p. 45. Göteborg 1962.

Copyright fib, all rights reserved. This PDF copy of fib Bulletin 10 is intended for use and/or distribution only by National Member Groups of fib.

1962 Mehmel A., Kern E.: Elastische und Plastische Stauchungen von Beton infolge Druckschwell- und Standbelastung. (Elastic and plastic strain of concrete due to sustained load). Deutscher Ausschuss für Stahlbeton, Heft 153, p. 74. Berlin 1962.

- Tepfers R.: Studium av förankrings- och sprickproblem hos balkar armerade med Ks 60. (A study of anchorage and cracking problems for beams reinforced with Ks60). Chalmers University of Technology, Department of Building Technology, Nr. 626, p. 99, Göteborg 1962.
- Verna J. R., Stelson T. E.: Failure of Small Reinforced Concrete Beams under Repeated Loads. ACI-Journal, pp. 1489-1504. Detroit 1962.

1963 Losberg A.: Kraftöverföring och spänningsfördelning vid förankring och avslutning av armering. (Force transfer and stress distribution at anchorage and curtailment of reinforcement). Chalmers University of Technology, Department of Building Technology, p. 49, Göteborg 1963.

- Pfister J. S., Mattock A. H.: Lapped Splices in Concentrically Loaded Columns. Journal of the PCA Research and Development Laboratory, pp. 27-40. Skokie, Illinois. 1963.
- Verna J. R., Stelson T. E.: Repeated Loading Effect on Ultimate Static Strength of Concrete Beams. ACI-Journal, pp. 743-750. Detroit 1963.
- Östlund L.: Inverkan av bockningsradier och täckande betongskikt hos kamstål på spjälkningsrisken för armerade betongkonstruktioner. (Influence of bending radii and concrete cover for the splitting risk for reinforced concrete structures). Internal publication. The Royal Institute of Technology (KTH), 92 p. Stockholm 1963.

1964 Losberg A.: Anchorage of Beam Reinforcement Shortened According to the Moment Distribution Curve. Seventh Congress of the IABSE, Final Report, pp. 383-392. Rio de Janeiro 1964.

- Tepfers, R.: Buntad armering. (Bundled reinforcement). Chalmers University of Technology, Department of Building Technology, Work No 679. Göteborg, June 1964. p. 28.

1965 Baldwin J. W.: Bond of Reinforcement in Light-weight Aggregate Concrete. University of Missouri, p. 10. Columbia, Missouri 1965.

- Berggren L.: Utdragsprov med kort vidhäftningslängd. (Pull-out tests with short bond length). Chalmers University of Technology, Department of Building Technology, Nr 686, p. 85. Göteborg 1965.
- Ferguson P. M., Breen J. E.: Lapped Splices for High Strength Reinforcing Bars. ACI-Journal, p. 1063-1078. Detroit 1965.
- Ferguson .P M., Breen J. E., Thompson J. N.: Pull-Out Tests on High Strength Reinforcing Bars. ACI-Journal, pp. 933-950. Detroit 1965.
- Granholm Hj.: Nya rön beträffande användningen av kamjärn. (New information concerning the use of deformed bars). Chalmers Tekniska Högskolas Handlingar, Nr. 305, p. 36. Göteborg 1965.
- Leonhardt F.: Ueber die Kunst des Bewehrens von Stahlbetontragwerken. (About the art of reinforcing of reinforced concrete structures). Beton- und Stahlbetonbau, pp. 181-191. Berlin 1965.
- Leonhardt F., Reimann H.: Betongelenke. Versuchsbericht, Vorschläge zur Bemessung und konstruktiven Ausbildung. (Concrete joints. Test report, suggestions for design and structural form). Deutscher Ausschuss für Stahlbeton. Heft 175, p. 34. Berlin 1965.
- Neal J. A.: Some aspects of the fatigue of concrete. Thesis. University of Illinois, p. 61. Urbana 1965.
- Segner E. P. Jr.: Splices in Tensile Reinforcing Bars. The University of Oklahoma Research Institute. Project No. 1468, p. 59. Norman, Oklahoma 1965.
- Soretz S.: Ermüdungseinfluss im Stahlbeton. (The influence of fatigue on reinforced concrete). Zement und Beton, Nr. 31, pp. 1-19. Wien 1965.
- Walls J. C., Sanders W. W., Munse W. H.: Fatigue Behaviour of Butt-Welded Reinforcing Bars in Reinforced Concrete Beams. ACI-Journal, pp. 169-192. Detroit 1965.
- Welch G. B., Patten B. J. F.: Bond Strength of Reinforcement Affected by Concrete Sedimentation. ACI-Journal, pp. 251-264. Detroit 1965.

1966 Tepfers R.: Undersökning av den efter momentkurvan avkortade dragarmeringens förankrings egenskaper. (Investigation of curtailed reinforcement according the moment curve). Chalmers University of Technology, Department of Concrete Structures, Rapport 66:4, p. 212. Göteborg 1966.

1967 Bennett E. W., Muir S. E. St. J.: Some fatigue tests of high-strength concrete in axial compression. Magazine of Concrete Research, Volume 19, No. 59, June 1967, pp. 113-117. Wexham Springs.

- Druckubergreifungsstösse. (Compressive lap splices). Otto Graf-Institut an der Technischen Hochschule, Stuttgart. Auftrag S 10618, p. 167, Stuttgart 1967.
- Lutz L. A., Gergeley P.: Mechanics of Bond and Slip of Deformed Bars in Concrete. ACI-Journal, pp. 711 –721. Detroit 1967.

Copyright fib, all rights reserved. This PDF copy of fib Bulletin 10 is intended for use and/or distribution only by National Member Groups of fib.

1968 Ferguson P. M., Briceno E.: Bond Stress Development Length for Lapped Splices in Reinforced Concrete Beams and Walls. Progress Summary. The University of Texas at Austin, p. 27. Austin, Texas 1968.
- Hahn V., Fastenau W.: Der Thermit-Muffenstoss. (The thermit-sleeve splice). Beton- und Stahlbetonbau, pp. 77-82. Berlin 1968.
- Ivey D. L.: Fatigue of Grouted Sleeve Reinforcing Bar Splices. ASCE – Proceedings, pp. 199-210. 1968.
- Stöckl S.: Zwischenbericht über Versuchsprogramm "Ueberlappungsstösse von Zugbeanspruchten Rippenstählen". (In-between report on tensile deformed reinforcement overlap splices). Technische Hochschule München, Lehrstuhl für Massivbau, p. 11. München 1968.
1969 Hribar J, A., Vasko R, C.: End Anchorage of High Strength Steel Reinforcing Bars. ACI-Journal, pp. 875–883. Detroit 1969.
- Perry S E., Jundi N.: Pull-Out Bond Stress Distribution under Static and Dynamic Repeated Loadings. ACI-Journal, pp. 377-380. Detroit 1969.
- Stocker M. F., Sozen M. A.: Investigation of Prestressed Reinforced Concrete for Highway Bridges. Part VI: Bond Characteristics of Prestressing Strand. University of Illinois, Urbana 1969. p. 363.
- Sozen M. A., Gamble W. L.: Strength and Cracking Characteristics of Beams with #14 and #18 Bars Spliced with Mechanical Splices. ACI-Journal, pp. 949 – 956. Detroit 1969.
1970 Aas–Jakobsen K.: Fatigue of Concrete Beams and Columns. Norges Tekniske Högskole, Institutt for Betongkonstruksjoner. Bulletin No. 70-1, p. 148. Trondheim 1970.
- Fastenau W., Leonhardt F., Hahn V.: Der Pressmuffenstoss für gerippte Bewehrungsstäbe. (The compressed sleeve splice for deformed reinforcement). Beton- und Stahlbetonbau, pp. 168- 171. Berlin 1970.
- Freitag W.: Das Ermüdungsverhalten des Betons. (Fatigue behaviour of concrete). Beton (Deutscher Zementindustrie), p. 192- 194, pp. 247–252. 1970.
- Goto Y.: Cracks Formed in Concrete Around Deformed Tension Bars. ACI-Journal, pp. 244-251. Detroit 1971.
- Lloyd J. P., Kesler C. E.: Splices and Anchorages in One-Way Slabs Reinforced Deformed Wire Fabric. ACI-Journal, pp. 636-641. Detroit 1970.
- Lutz L.A.: Analysis of Stresses in Concrete near a Reinforcing Bar due to Bond and Transverse Cracking. ACI-Journal, pp. 778-787. Detroit 1970.
- Lutz L. A.: Information on the Bond of Deformed Bars from Special Pull-Out Tests. ACI-Journal, pp. 885-887. Detroit 1970.
- Proposed Revision of ACI 318-63: Building Code Requirements for Reinforced Concrete, 1970. ACI-Journal, pp. 91-94. Detroit 1970.
- Rehm G., 1970. Möglichkeiten der konstruktiven Gestaltung von Stössen in vorgefertigten Stahlbetonbauteilen. (Possibilities for structural design of splices in precast concrete members). Betonstein-Zeitung, pp. 75-84. Wiesbaden 1970.
- Rehm G., Martin H.: Biegefeste Verbindung von Stahlbetonfertigteilen. (Moment stiff connections between precast concrete members). Betonstein-Zeitung, pp. 447-453. Wiesbaden 1970.
- Rieve S. J.: Der Haftverbund zwischen Stahl und Beton. (Bond between steel and concrete). Memoires de l'Association Internationale des Ponts et Charpentes. Bd. 29, pp. 163–172. Zürich 1970.
- Snowdon, L.C.: Classifying reinforcing bars by bond strength. Building Research Station, Garston. p. 40. CP36/70.
1972 Holzapfel F.: Das Verhalten von Zementstein unter dynamischer Beanspruchung. (The behavior of cement stone under dynamic load). Westdeutscher Verlag, Opladen, p. 98. 1972.
- Stöckl S.: Uebergreifungsstösse von Zugbeanspruchten Bewehrungsstäben. (Overlapsplices for tensile reinforcing bars). Beton- und Stahlbetonbau Nr. 10, p. 229-234. Berlin 1972.
- Tepfers, R., Görlin, J., Samuelsson, T.: Concrete subjected to pulsating load and pulsating deformation of different wave forms. Nordisk Betong 4:1973. pp. 27-36.
1973 Tepfers, R.: A Theory of Bond Applied to Overlapped Tensile Reinforcement Splices for Deformed Bars. Publ 73:2. Division of Concrete Structures, Chalmers University of Technology, Göteborg, May 1973, p. 328.
1976 Hillerborg A., Modéer M., Petersson P.E.: Analysis of crack formation and crack growth in concrete by means of fracture mechanics and finite elements. Cement and Concrete. Res. Vol. 7. 1976. pp. 773-782.
1979 Eligehausen, R.: Übergreifungsstösse zugbeanspruchter Rippenstäbe mit geraden Stabenden. (Overlap splices for tensile deformed bars with straight ends). Deutscher Ausschuss für Stahlbeton. Heft 301. Berlin 1979.Wilhelm Ernst & Sohn. p. 118.

Copyright fib, all rights reserved. This PDF copy of fib Bulletin 10 is intended for use and/or distribution only by National Member Groups of fib.

1979 Tassios, T.P.: Properties of bond between Concrete and Steel under Load Cycles Idealizing Seismic Actions. AICAP-CEB Symposium, Vol 1 - State of Art Reports, CEB Bulletin d'Information No 131, Rome 1979. pp. 67-122.

- Tepfers, R.: Cracking of concrete cover along anchored deformed reinforcing bars. Magazine of Concrete Research Vol. 31, No 106, March 1979, pp. 3-12.

1980 Eligehausen, R.: Anchorage and splice regulations in the CEB-FIP Model Code and the German Code DIN 1045. Paper presented at the ACI-Fall Convention, September 1980, San Juan, Puerto Rico.

- Tepfers, R.: Bond stress along lapped reinforcing bars. Magazine of Concrete Research, Vol. 32, No 112. September 1980. pp. 3-12.

- Tepfers, R.: The Design of Anchorages and Splices. Presented at the 1980 Fall Convention 23-26/9 1980, ACI-Fall Convention, September 1980, San Juan, Puerto Rico.

1982 Tepfers, R.: Lapped tensile reinforcement splices. American Society of Civil Engineers, Journal of the Structural Division, January 1982, New York. pp.283-301.

- Tepfers, R.: Tensile lap splices with confining reinforcement. Bond in Concrete. Edited by P. Bartos Applied Science Publishers, London 1982. pp. 318-330.

- CEB Bulletin d'Information, No 151. Bond Action and bond behaviour of reinforcement. State of the art report. Comité Euro-International du Béton, Paris, April 1982. p. 153.

- Reynolds G C & Beeby A W. Bond strength of deformed bars. Bond in Concrete, Ed Bartos. Applied Science Publishers, London. pp 434-445.

1987 CEB Bulletin d'Information, No 181. Anchorage zones of prestressed concrete members. State of the art report. Comité Euro-International du Béton, Lausanne, April 1987. p. 137.

CEB Bulletin d'Information, No 188. Fatigue of concrete structures. State of the art report. Comité Euro-International du Béton, Lausanne, June 1988. p. 300.

1990 Committee 439: Mechanical Connections of Reinforcing Bars, "ACI 439.4R-90", American Concrete Institute, Farmington Hills, Michigan.

Committee 408: Suggested Development, Splice and Standard Hook Provisions for Deformed Bars in Tension, "ACI 408.1R-90" American Concrete Institute, Farmington Hills, Michigan.

1992 Committee 408: State of the Art report on Bond under Cyclic Loads, "ACI 408.2R-92" American Concrete Institute, Farmington Hills, Michigan.

1995 Cairns, J., & Abdullah, R.: An evaluation of bond pullout tests and their relevance to structural performance. The Structural Engineer, Journal of The Institution of Structural Engineers. Vol 73, No. 11. pp. 179-185.

1995 Cairns, J., & Jones, K.: The splitting forces generated by bond. Magazine of Concrete Research, Vol. 47, No. 171, June 1995. pp. 153-165, & Discussion by den Uijl J.

1998 Mc Cabe S., Pantazopoulou S.J.: Evaluation of bond performance in reinforced concrete structures. ACI SP-180 "Bond and Development of Reinforcement", A tribute to Dr. Peter Gergely. Farmington Hills, Michigan 1998. pp. 1-21.

ISSN-1562-3610
ISBN 2-88394-050-9

Bond of reinforcement in concrete

Contents

1 Bond mechanics including pull-out and splitting failures

2 Anchorage and bond in high strength concrete

3 Bond under repeated loading

4 Bond of corroded reinforcement

5 Bond of fusion bonded epoxy coated reinforcement

6 Bond of prestressing tendons

7 Bond of non-metallic reinforcement

8 Innovative developments in the light of bond philosophy

fib CEB-FIP

fédération internationale du béton
the international federation for structural concrete
created from the merger of CEB and FIP